COASTAL PROTECTION

A Pile Buck® Production

COASTAL PROTECTION

A Pile Buck® Production

NOTICE

"The information, including technical and engineering data, figures, tables, designs, drawings, details, procedures and specifications, presented in this publication has been prepared in accordance with recognized contracting and/or engineering principles, and are for general information only. While every effort has been made to insure its accuracy, this information should not be used or relied upon for any specific application without independent competent professional examination and verification of its accuracy, suitability and applicability, by a licensed professional.

This handbook is provided without warranty of any kind. Pile Buck®, Inc. hereby disclaims any and all express or implied warranties or merchantibility, fitness for any general or particular purpose or freedom from infringement of any patent, trademark, or copyright in regard to information or products contained or referred to herein. Nothing herein contained shall be construed as granting a license, express or implied, under any patents. Anyone making use of this material does so at his own risk and assumes any and all liability resulting from such use. The entire risk as to quality or useability of the material contained within is with the reader. In no event will Pile Buck®, Inc. be held liable for any damages including lost profits, lost savings or other incidental or consequential damages arising from the use or inability to use the information contained within. Pile Buck®, Inc. does not insure anyone utilizing this Handbook against liability arising from the use of this information and hereby will not be held liable for "consequential damages," resulting from such use.

All advertising contained within is the exclusive representation of those registered herein. Pile Buck®, Inc. makes no representation as to the accuracy, performance, design, specifications and/or any such "claims" made by advertisers, contained within. Anyone making use of these products does so at his own risk and assumes any and all liability resulting from such use. In no event will Pile Buck®, Inc. be held liable for any damages including lost profits, lost savings or other incidental or consequential damages arising from the use or inability to use the products advertised within. Pile Buck®, Inc. does not insure anyone from liability arising from the use of these products and hereby, will not be held liable for "consequential damages," resulting from such use.

Published By:
Pile Buck® Inc.
P.O. Box 1056
Jupiter, FL 33468-1056
PH: 407-744-8780
FAX: 407-575-9748

CREDITS/REFERENCES

PUBLICATION ONE:

Title	Coastal Protection
Publication Date	April, 1982
Document/Report Number	Navfac DM-26.2
Author(s)	Anonymous
Courtesy of	Department of the Navy, Naval Facilities Engineering Command

PUBLICATION TWO:

Title	Coastal Sedimentation and Dredging
Publication Date	December, 1981
Document/Report Number	Navfac Design Manual 26.3
Author(s)	Anonymous
Courtesy of	Department of the Navy, Naval Facilities Engineering Command

PUBLICATION THREE:

Title	Tidal Hydraulics
Publication Date	March, 1991
Document/Report Number	EM 1110-2-1607
Author(s)	Anonymous
Courtesy of	Department of the Army, U.S. Army Corps of Engineers

PUBLICATION FOUR:

Title	Storm Surge Analysis
Publication Date	April, 1986
Document/Report Number	EM 1110-2-1412
Author(s)	Anonymous
Courtesy of	Department of the Army, U.S. Army Corps of Engineers

MANUFACTURERS, SUPPLIERS, CONTRACTING AND ENGINEERING SERVICES

Customer Number	Company Name	Ad Location (Page No.)
1	Canadian Metal Rolling Mills	45
2	Central Plastics Company	83
3	Commercial Diving Service, Inc.	129
4	Commercial Forged Products, Inc.	63
5	CSA Marine Services, Inc.	157
6	Gator Dock & Marine, Inc.	53
7	Group Delta Consultants, Inc.	113
8	H & M Vibro, Inc.	35
9	Materials International	93
10	Nestor/Merrick Materials, Inc.	19
11	Norfolk Dredging Company	135
12	Ravens Marine, Inc.	73
13	Robishaw Engineering, Inc.	147
14	Southern Forest Products Association	103
15	Syro Steel Company	9
16	Jon Guerry Taylor, P.E., Inc.	27

CUSTOMER #1

CANADIAN METAL ROLLING MILLS
(A Division of Samuel Manu-Tech Inc.)
950 Industrial Road
Cambridge, Ontario
CANADA N3H 4W1
PH: 519/650-2222
FAX: 519/650-2223

CUSTOMER #2

CENTRAL PLASTICS COMPANY
1901 W. Independence
P.O. Box 3129
Shawnee, OK 74801
PH: 405/273-6302
U.S.: 800/654-3872
FAX: 405/273-5993
U.S. 800/733-5993

CUSTOMER #3

COMMERCIAL DIVING SERVICE, INC.
1120 Rarig Avenue
Columbus, OH 43219
P.O. Box 360568
Columbus, OH 43236
PH: 614/258-2000
U.S. 800/969-6169
FAX: 614/258-2047

CUSTOMER #4

COMMERCIAL FORGED PRODUCTS COMPANY
(A Wozniak Industries, Inc. Co.)
5757 West 65th Street
Bedford Park, IL 60638
PH: 312/767-8500
FAX: 708/458-9346

CUSTOMER #5

CSA MARINE SERVICES, INC.
759 Parkway Street
Jupiter, FL 33477
PH: 407/746-8998
FAX: 407/747-2954

CUSTOMER #6

GATOR DOCK & MARINE, INC.
2880 Mellonville Avenue
Sanford, FL 32773
PH: 407/323-0190
U.S. 800/621-2207
FAX: 407/322-6574

CUSTOMER #7

GROUP DELTA CONSULTANTS, INC.
4455 Murphy Canyon Road
Suite 100
San Diego, CA 92123
PH: 619/573-1777
FAX: 619/573-0069

CUSTOMER #8

H & M VIBRO INC.
3715 28th Street
P.O. Box 224
Grandville, MI 49418
PH: 616/538-4150
FAX: 616/532-8505

CUSTOMER #9

MATERIALS INTERNATIONAL
P.O. Box 1484
Lake Charles, LA 70602

PH: 318/439-8042
U.S. 800/256-8857
FAX: 318/439-8043

CUSTOMER #10

NESTOR/MERRICK MATERIALS, INC.
P.O. Box 95
1745 Merrick Ave., Suite 7
Merrick, N.Y. 11566

PH: 516/546-7900
FAX: 516/546-7992

CUSTOMER #11

NORFOLK DREDGING COMPANY
110 N. Centerville Turnpike
P.O. Box 1706
Chesapeake, VA 23327

PH: 804/547-9391
FAX: 804/547-2833

ADDITIONAL OFFICE:
3415 S.W. 96th Street
Stuart, FL 33497

PH: 407/287-2557

CUSTOMER #12

RAVENS MARINE, INC.
2255 N. Orange Blossom Trail
Orlando, FL 32804

PH: 407/649-3023
U.S. 800/676-3023
FAX: 407/649-4829

CUSTOMER #13

ROBISHAW ENGINEERING INC.
P.O. Box 19246
Houston, TX 77224

PH: 713/468-1706
FAX: 713/468-5822

CUSTOMER #14

SOUTHERN FOREST PRODUCTS ASSOCIATION
P.O. Box 641700
Kenner, LA 70064-1700

PH: 504/443-4464
FAX: 504/433-6612

CUSTOMER #15

SYRO STEEL COMPANY
1170 N. State Street
Girard, OH 44420

PH: 216/545-4373
Outside OH: 800/321-2755
In OH: 800/321-0779
FAX: 216/545-3718

ADDITIONAL OFFICES:
P.O. Box 99
950 West 400 South
Centerville, UT 84014

PH: 801/292-4461
Outside UT: 800/772-7976
In UT: 800/262-6228
FAX: 801/292-2145

2703 Austin Rose Lane
Orange Park, FL 32073

U.S. 800/247-4117
FAX: 904/272-7852

CUSTOMER #16

JON GUERRY TAYLOR, P.E., INC.
802 A Coleman Boulevard
P.O. Box 1082
Mt. Pleasant, S.C. 29464

PH: 803/884-6415
FAX: 803/884-4026

SERVICES AND SERVICES # IN ADDITION TO THE CORRESPONDING NUMBERS OF THE COMPANIES THAT SUPPLY THE SERVICE

SERVICE # AND SERVICE	ENGR./CONTRACTING SERVICE #
Barge, Workboat Services	
Barge Stability Analysis	
Blasting	3
Breakwater/Jetty, Constr.	3
Breakwater/Jetty, Design	7
Bridge Constr.	
Bridge Design	
Bulkhead/Seawall, Constr.	3,5
Bulkhead/Seawall, Design	7,12,16
Cathodic Protection Studies	
Coastal Studies	7,16
Cofferdam Constr.	3
Cofferdam Design	7
Concrete Repair	3,5
Construction Claims Assistance	7
Crane Services	
Demolition	3
Diving/Underwater Constr.	3,5
Dock/Pier Constr.	3,5
Dock/Pier Design	7,12,16
Dolphin Constr.	3
Dolphin Design	7
Dredging	3,11
Dredging Studies	7,16
Environmental Design	7,16
Environmental Studies	7,16
Feasibility Studies	7
Floating Dock Constr.	3
Floating Dock Design	12
Foundation Analysis	7
Grouting	3,5
Harbor Design	16
Hydraulic Studies	7,16
Hydrographic Surveys	3,5,7
Load Testing	7
Marina Constr.	3,5,7
Marina Design	16
Marine Structure Constr.	3,5
Marine Structure Design	16
Mooring System Constr.	3
Mooring System Design	16
Permitting	16
Pile Driving	3
Pile Driving Studies	7
Pile Restoration	3,5
Pile Testing	7
Piling Constr.	3,4
Piling Design	7
Pipeline Constr.	3
Pre-Bid Studies	
Pressure Grouting	3,5
Salvage	3,5
Sheet Piling Constr.	3
Sheet Piling Design	7,12
Site Investigations	3,7,16
Structure Integrity Studies	
Underpinning Constr.	3
Underpinning Design	7
Underwater Constr.	3,5
Underwater Inspections/Surveys	3,5
Underwater Photography	3,5,7
Underwater Welding & Burning	3,5
Vibration/Noise Monitoring	7
Wetland Studies	16

PRODUCT AND PRODUCT # IN ADDITION TO THE CORRESPONDING MFR./SUPPLIER NUMBERS OF THE COMPANIES THAT SUPPLY THE PRODUCT

PRODUCT # AND PRODUCT	MFR./SUPPLIER #
Admixtures, Concrete	
Air Compressors	
Air Hoists/Winches	
Air Hose & Access.	
Air/Steam Pile Hammers	15
Air Tuggers	
Aluminum Channels, Bar & Plate	
Aluminum Decking	6,12
Aluminum Dock Systems	6,12
Aluminum Gangways	6,12
Aluminum Ladders	6,12
Aluminum Sheet Piling	6,12
Amphibious Work Vehicles	
Anchor Chain	
Anchor/Mooring Systems	
Anchors, Barge, Boat, etc.	
Anchors, Bulkhead	
Anchors, Earth	
Anchor Winches/Hoists	
Auger Cutterheads & Tools	

PRODUCT # AND PRODUCT	MFR./SUPPLIER #
Auger Flighting & Accessories	
Auger Teeth	
Augers, Augered Piles	
Augers, Test/Soil Boring	
Augers, Truckmounted	
Banding, Timber Pile	
Barge Fittings	
Barge Mats	
Barge Movers, Winches	
Barges, Crane	13
Barges, Deck	13
Barges, Derrick	13
Barges, Hopper	13
Barges, Pontoon	13
Barges, Sectional	13
Batch Plants	
Beams, Aluminum	
Beams, Concrete	
Beams, Fiberglass	
Beams, Steel	1,10,15
Beams, Timber	
Bentonite	
Bentonite Pumps & Accessories	
Bits, Drill	4
Bits, Pilot	
Blocks, Sheaves & Tackle	
Boat Hoists	
Boat Lifts/Davits	
Boat Ramps	
Bollards	
Bolts, Washers, etc.	1
Boring & Sounding Equip.	
Bottom Braces/Spotters	
Breakwaters	1,12
Bridges, Floating	12,13
Bridges, Portable	12,13
Bridges, Pre-Fab. Concrete	
Bridges, Pre-Fab. Misc.	
Bridges, Pre-Fab. Steel	10
Bridges, Pre-Fab. Timber	
Buckets, Clamshell, Dragline, Grapples. etc.	
Bumpers/Fenders, Barge	
Bumpers/Fenders, Boat	
Bumpers/Fenders, Bow & Stern	
Bumpers/Fenders, Bulkhead	9,12
Bumpers/Fenders, Camels	
Bumpers/Fenders, Dock	9,12
Bumpers/Fenders, Dolphin	
Bumpers/Fenders, Foam	
Bumpers/Fenders, Marina	9,10,12
Bumpers/Fenders, Pier	9,10,12
Bumpers/Fenders, Pneumatic	
Bumpers/Fenders, Pushboat	
Bumpers/Fenders, Rubber	12
Bumpers/Fenders, Timber	12
Bumpers/Fenders, Tugboat	
Buoys	
Caisson Pipe	1,10
Caissons	1,10
Camels	
Capstans	
Car Floats	
Casing	
Cathodic Protection Systems	1,2
C.C.A. Piling	12,14
C.C.A. Timbers	12,14
Centrifical Pumps	
Chain, Anchor/Mooring	
Chain, Crawler	

PRODUCT # AND PRODUCT	MFR./SUPPLIER #
Channel Caps	1,15
Channel, Aluminum	12
Channel, F.R.P.	
Channel, Steel	1
Cherry Pickers	
Clamshell Buckets	
Cleats	
Clevis Assemblies	
Coal Tar Epoxy	1,15
Coatings/Coaters, Corrosion Control	1,2,15
Composite Piles	1
Compressors, Air	
Column/Pier Forms	1
Composite Piles	1
Compressors, Air	
Computer Software	
Concrete Admixtures	
Concrete Batch Plans	
Concrete Cribbing	
Concrete Decking	
Concrete Forms	1
Concrete Hose & Accessories	
Concrete Pile Cutters	
Concrete Pile Splicers	
Concrete Piling	
Concrete, Pre-cast/Prestressed	
Concrete Pumps	
Concrete Sheet Piling	2
Containment Systems, Floats	
Corrosion Protection	1
Couplings, Dredge Pipe	
Couplings, Hose	
Couplings, Pile	1,10
Couplings, Pipe	2
Crane Barges	13
Crane Booms, Jibs, etc.	
Crane Mats	
Crane Parts & Access.	
Cranes, Crawler	
Cranes, Derrick	
Cranes, Hydraulic	
Cranes, Truck	
Creosoted Piling	
Creosoted Timbers	
Crewboats/Supply Boats	
Cushion Material, Pile Hammer	
Cushion Material, Piling	
Cutterheads, Augers	
Cutterheads, Dredge	
Davits/Boat Lifts	
Deck Fittings	
Deck Winches	
Decking, Aluminum	6,12
Decking, Concrete	
Decking, Fiberglass	
Decking, Treated Timber	12,14
Decking, Untreated Timber	12,14
Derricks	
Dewatering Pumps & Equip.	
Diesel Pile Hammers	15
Diving Equip./Supplies	
Dock Boxes	
Dock Fingers	12
Dock Hardware	
Dock Lockers	
Dock Power Units	
Docks, Fixed/Stationary	12
Docks, Floating	12,13
Dock Washers	

PRODUCT # AND PRODUCT	MFR./SUPPLIER #
Docking/Boarding Systems	12
Dolphins	
Dragline Buckets	
Draglines	
Drainage Fabrics	
Drainage Pipes	15
Dredge Frames	
Dredge Pipe	
Dredge Pipe Couplings/ Connections	
Dredge Pipe Flotation	
Dredge Pumps	
Dredges, Bucket	
Dredges, Cutterhead	
Dredges, Hydraulic	
Dredges, Portable	13
Dredges, Suction	
Drill Bits & Access.	
Drill Rigs, Crawler Mounted	
Drill Rigs, Soil Testing	
Drill Rigs, Truck Mounted	
Drop Hammers	
Dry Docks	
Dry Stack Storage Systems	
Earth, Rock, Soil Anchors	1
Electrical Dock Components	
Electric Winches/Hoists	
Epoxy Products	10
Erosion Control Blocks	
Erosion Control Fabrics	
Excavators	10
Excavators, Amphibious	
Extractors, Pile	8,10
Fabrics, Geotechnical	
Fairleads	
Fasteners, Hardware	4
Fenders/Bumpers, Barge	
Fenders/Bumpers, Boat	
Fenders/Bumpers, Bow & Stern	
Fenders/Bumpers, Bulkhead	9,12
Fenders/Bumpers, Camels	
Fenders/Bumpers, Dock	9,12
Fenders/Bumpers, Dolphin	
Fenders/Bumpers, Foam	
Fenders/Bumpers, Marina	9,10,12
Fenders/Bumpers, Pier	9,12
Fenders/Bumpers, Pneumatic	
Fenders/Bumpers, Pushboat	
Fenders/Bumpers, Rubber	12
Fenders/Bumpers, Timber	12,14
Fenders/Bumpers, Tugboat	
Fiberglass Beams	
Fiberglass Decking	
Fiberglass Piling	
Fiberglass Reinforced Products (F.R.P.)	
Filter Cloth	
Finger Docks/Piers	1,6,12
Fixed (Stationary) Dock Systems	6,12,13
Flap Gates	6,12
Flighting, Auger	
Float Balls	
Float Drums	
Floating Dry Docks	
Floats	12,13
Floats, Containment	
Floats, Pipe Line	
Floating Breakwaters	12,13
Floating Bridges	12,13
Floating Dock Systems	6,12,13

PRODUCT # AND PRODUCT	MFR./SUPPLIER #
Foam Flotation	
Foundation Testing Equip.	
Gabion Wire	
Gabions	
Gangways	6,12
Generators	
Geotextile Fabrics	
Grapples	
Greenheart Piling	12
Grout	
Grout Hose & Accessories	
Group Pumps	
H-Piling	1,10,15
HZ-Sheet Piling	10
Hairpins	10
Handrail Hardware	
Handrails	12
Handrails, Aluminum	6,12
Hardware, Galvanized	
Hardware, Marine	
Headsheaves	
Hoists/Winches, Air	
Hoists/Winches, Electric	
Hoists/Winches, Hydraulic	
Hoists/Winches, Mechanical	
Hoists/Winches, Mooring	
Hoists/Winches, Spud	
Hydraulic Jacks	
Hydraulic Power Packs	
Jacks	
Jacking Equipment	
Jet Pumps, Dewatering Pumps	
Ladders	9
Ladders, Aluminum	6,12
Leads & Accessories	
Line Pipe	
Load Cells	
Load Testing Equipment	
Lubricators	
Lumber, Treated	12,14
Lumber, Tropical	12
Lumber, Untreated	12,14
Mandrels, Pile	
Marine Electronic Equip.	
Marine Engines	
Marine Generators	
Marine Hardware, Bolts, Tie-rods, etc.	
Marine Propellers & Units	
Marine P.T.O. Assemblies, etc.	
Marsh Buggies	
Mats, Crane	
Metal Docks	1,6,12
Mooring/Anchor Systems	
Mooring Arms	
Mooring Buoys	
Mooring Docks/Piers	
Mooring Hooks	
Mooring Lines	
Noise Monitoring Equipment	
OCTG Pipe	
OGee Washers	
Penta Piling	
Pile Analyzers	
Pile Beavers, Concrete Pile Cutters	
Pile Caps	15
Pile Clamp Assemblies	
Pile Coatings/Coaters	2
Pile Cushion Material	

PRODUCT # AND PRODUCT	MFR./SUPPLIER #
Pile Cutters	
Pile Driving Analyzers	10
Pile Extractors	15
Pile Forming Equipment	
Pile Guides, Floating Dock	6
Pile Guides, Lead Systems	
Pile Hammer Analyzers	
Pile Hammer Cushion Material	
Pile Hammer Leads & Access.	
Pile Hammers, Air/Steam	15
Pile Hammers, Diesel	10,15
Pile Hammers, Drop	10
Pile Hammers, Extractors	10,15
Pile Hammers, Hairpin	10
Pile Hammers, Hydraulic	15
Pile Hammers, Underwater	
Pile Hammers, Vibratory	8,15
Pile Jackets	
Pile Mandrels	10
Pile Points, Splicers & Accessories	1,10,15
Pile Restoration Materials	
Pile Shackles & Threaders	15
Pile Splicers, Points & Accessories	1,15
Pile Testing Equipment	
Pile Threaders	15
Pile Wraps	2
Piling, Aluminum Sheet	6,12
Piling, CCA	
Piling, Concrete	
Piling, Creosoted	
Piling, F.R.P.	
Piling, Greenheart	
Piling, HZ	10
Piling, H-Pile	1,10,15
Piling, Penta	
Piling, Plastic	9,12
Piling, Pipe	1,15
Piling, Spiral Weld	1,10
Piling, Steel Sheet	1,10,15
Piling, Treated Timber	
Piling, Tropical	12
Piling, Untreated Timber	
Piling, Vinyl	9,12
Pipe, Aluminum	
Pipe, Concrete	
Pipe, Plastic	
Pipe, Steel	1,10,15
Pipe Couplings, Dredge	2
Pipe Couplings, Piling	1,2,15
Pipe Line Floats	
Pipe Struts	10
Plastic Piling	12
Plastic Sheet Piling	2,9,12
Plate, Aluminum	
Plate, Stainless Steel	
Plate, Steel	1,10,15
Points, Pile	1,10,15
Polyurethane Coated Piling	
Pontoons	6,13
Pontoon Barges	13
Post Tensioning Equip.	
Post Tensioning Jacks	
Power Lifts, Boat	
Power Units, Dock	
Pre-cast/Prestressed Concrete	
Pre-cast/Prestressed Concrete	
Prestressed Concrete Piling	
Pumpout Systems	
Pumps, Concrete	
Pumps, Dewatering	
Pumps, Grout	
Pumps, Jet	
Pumps, Sludge	
Punch, "Star"	
Pushboats/Workboats	
Rigging, Shackles, etc.	
Rock & Soil Anchors	
Rock Drilling Equipment	
Rough Terrain Cranes	
Sectional Barges	13
Seismographs	
Shackles	
Sheaves, Blocks & Rigging	
Sheet Pile Shackles	10
Sheet Pile Threaders	10,15
Sheet Piling, Aluminum	2,6,12
Sheet Piling, Concrete	2
Sheet Piling, F.R.P.	2
Sheet Piling, HZ	2,10
Sheet Piling, Lightweight Steel	1,2,10
Sheet Piling, Plastic	2,9,12
Sheet Piling, Steel	1,2,10,15
Sheet Piling, Timber	2
Sheet Piling, Vinyl	2,9,12
Shoring	1,10,12
Sluice Gates	6
Software, Computer	
Soil/Rock Anchors	1
Soil Stabilization Fabrics	
Soil Testing Equipment	
Splicers, Pile	1,10,15
Spotters, Bottom Braces	
Spike Grids	
Spuds, Barge	10,13
"Star" Punch	
Steam Hose	
Steel, Drill	
Steel Fabricators	10,15
Steel H-Piling	1,10,15
Steel Pipe	1,10,15
Steel Plate	1,10,15
Steel Sheet Piling	1,10,15
Step Taper® Piling	10
Structural Steel, Plate, Wide Flange, etc.	1,10,15
Submersible Pumps	
Swamp Buggies	
Swivels, Air, Water & Grout	
Tampers, Vibratory Compactors	
Test/Soil Boring Equipment	
Testing Equipment	
Threaders, Pile	15
Throttle Valves	
Tie Rods, Earth Anchors	1,4
Tieback Machines	
Timber Billets	
Timber Pile Banding	
Timber Piling (See Piling)	
Timbers, CCA	12,14
Timbers, Creosoted	
Timbers, Greenheart	12
Timbers, Penta	
Timbers, Treated	12,14
Timbers, Tropical	12
Timbers, Untreated	12
Tongs, Log	
Tongs, Rock	
Trench Boxes	
Tropical Lumber	12
Tropical Piling	12

PRODUCT # AND PRODUCT	MFR./SUPPLIER #
Turnbuckles	
Tugboats	
Tunneling Equipment	10
U-Bolts	
Underpinning Equipment	10
Underreamers	
Underwater Const. Equip.	13
Utility Boxes, Dock	
Vibration Monitoring Equipment	
Vibratory Pile Drivers/Extractors	8,15
Vinyl Sheet Piling	9,12
Wale Systems	1,4,10
Washers, Bolts etc.	
Wave Attentuators	6
Wave Equation Analysis	
Welding Materials/Equipment	
Well Point Equipment	
Wide Flange Beams, F.R.P.	10
Wide Flange Beams, Steel	1,10,15
Winches/Hoists, Air	
Winches/Hoists, Electric	
Winches/Hoists, Hydraulic	
Winches/Hoists, Mechanical	
Winches/Hoists, Mooring	
Winches/Hoists, Spud	
Windlesses	
Wire Rope & Accessories	1
Wire Rope & Accessories	
Wire Rope Pullers	
Wire Rope Tension Monitoring Equip.	
Workboats/Pushboats	

TABLE OF CONTENTS

COASTAL PROTECTION

COASTAL SEDIMENTATION AND DREDGING

TIDAL HYDRAULICS

Page

STORM SURGE ANALYSIS

Page

EDITORS NOTE

Coastal Engineering is a highly specialized field which includes the study of wind, waves, currents, tides, storms, drift and other environmental forces which affect our coasts. Because of the public interest, government agencies at both the federal and state level have assumed the leadership in seeking ways in which people can live and work in what can be a hostile environment.

Many of the procedures for analyzing coastal problems and planning solutions have been formulated by the Army Corps of Engineers and the Navy's Facilities Engineering Command. Some of the technical publications issued by these agencies, i.e. the Shore Protection Manual, are virtual textbooks for coastal engineering.

These organizations have also developed a number of excellent technical manuals dealing with specific subjects in certain fields including coastal engineering. We have chosen four of these for re-printing and consolidation into our Volume III-Coastal Protection series. They cover subject matter for which an interest from the private sector exists, but which is not well covered in available literature.

Coastal Protection is a U.S. Navy publication which deals specifically with waves and their characteristics. Wave forces are the principal loads imposed on most coastal structures. In order to prepare safe designs, the normal and extreme waves which will act against the structure must be evaluated so that a design wave can be selected. This manual takes the user through this phase into the application of data to actual design of breakwaters and seawalls. The text is well illustrated with drawings and sample problems.

Coastal Sedimentation and Dredging is another Navy Facilities Engineering Command guide manual. Littoral transport of soil is the principal natural cause for shoaling in harbors and channels. This text examines this process, provides methods for estimating transport rates and offers some control methods. Since dredging is the ultimate solution to these problems, the manual also covers the subjects of dredging equipment and methods.

Tidal Hydraulics is based on a Corps of Engineers technical manual. This text deals with estuaries which are bodies of water affected by ocean tides, and which generally contain both salt and fresh water. The section discusses questions of tidal hydraulics and its influence on salinity, sedimentation, water quality, shore protection and other environmental considerations. These general subjects continue to be important and sometimes controversial subjects for public and private interests along the coasts. This discussion is illustrated by a number of case histories.

Storm Surge Analysis is another Corps of Engineers guide manual. High tides and wind-generated waves combine to provide a potential for abnormally high water levels and flooding during hurricanes or other serious storms. An understanding of this phenomena is essential in order to plan control structures or design others. This chapter discusses methods for predicting storm surge affects and offers criteria for design water level determinations.

COASTAL PROTECTION

Department of the Navy
Naval Facilities Engineering Command
April 1982

EDITORS NOTE

This is a re-print of a U.S. Navy publication DM 26.2 issued in 1982. Wind-generated waves are the origin of the principal forces acting upon many types of coastal structures including those designed and operated by the Navy. Over a period of years, coastal engineers have developed a good deal of scientific theory involving waves which has become the basis for criteria used for design. This manual does not attempt to duplicate the Shore Protection Manual series published by the Corps of Engineers which offer broad coverage of coastal engineering subjects. Instead, the Navy text focuses only on waves and their properties for design.

The design of breakwaters and seawalls in particular, requires an accurate assessment of wave forces since these structures are installed only for the purpose of controlling waves. Waves breaking against vertical surfaces such as cells or bulkhead walls are reflective, creating pressure conditions which are quite different from those associated with absorbed waves. Forces exerted by waves against free-standing walls and single piles are among other questions which engineers must resolve from time to time.

This publication provides a means for resolving many of these questions while creating a basis for designing the eventual coastal structure.

ABSTRACT

Design criteria and planning guidelines for qualified engineers are presented for design of coastal structures. Section 1 is a presentation of applicable wave theory and wave transformations. Section 2 includes criteria for the selection of design waves. Section 3 gives general planning and structural design principles. Section 4 presents design procedures for rubble-mound structures. Section 5 is a discussion on wave forces on walls and wall design procedures. Section 6 includes applications of floating breakwaters. Section 7 is a discussion of wave forces on cylindrical piles.

SECTION 1
INTRODUCTION

1. SCOPE. This manual presents basic information required for the design of coastal protective structures.

2. CANCELLATIONS. This manual, NAVFAC DM-26.2, Coastal Protection, cancels and supersedes Chapter 2 of the basic Design Manual 26, Harbor and Coastal Facilities, dated July 1968, and Change 1, dated December 1968.

3. RELATED CRITERIA. Certain criteria related to coastal protection appear elsewhere in the design manual series. See the following sources:

Subject	Source
Cargo Handling Facilities	DM-25.3, DM-38
Channel Layout	DM-26.1
Clear Width of Slips Between Piers, Length of Berth, and Width of Piers	DM-25.1
Coastal Sedimentation and Dredging	DM-26.3
Harbors	DM-26.1
Operational Structures	
Piers and wharves	DM-25.1
Ferry slips, degaussing and deperming facilities, and small-craft berths	DM-25.5
Port Control Offices	DM-23
Quayage Requirements	DM-25.1
Seawalls, Bulkheads, and Quaywalls	DM-25.4
Soil Mechanics, Foundations, and Earth Structures	DM-7
Utilities	DM-3, DM-4, DM-5, DM-25.2

4. GENERAL.

a. **Approaches**. Waves can be described by deterministic or by spectral theories. In the deterministic approach, the properties of a single wave are used for design. In the spectral approach, the random nature of waves is taken into account. The state-of-the-art of incorporating the spectral approach into engineering is rapidly developing. However, the deterministic approach is presently in widest use in the United States and is the approach which will be followed in the manual. Methods are presented to take into account some of the random properties of wave systems.

b. Wave Classifications. Gravity waves are primarily classified as seas or swell. Seas are waves caused by the wind at the place and time of observation. Swell are waves that have traveled out of the area in which they were generated. Other wave classifications include ship-generated waves, astronomical tides, storm surges, harbor seiches, tsunamis, capillary waves, and internal waves. However, the primary wave considered in the design of coastal structures is the wind-generated gravity wave having a period ranging from about 1 to 30 seconds.

5. WAVE THEORY. Most coastal engineering design procedures rely on the application of the linear, or "Airy," wave theory, aided by empirically developed procedures for specific design applications. Linear or "Airy" theory provides a first-order approximation to the complete mathematical description of a wave, whereas nonlinear wave theory provides a higher order of approximation. Unfortunately, the higher order of approximation requires a significantly larger mathematical and computational effort. Hence, linear wave theory is often used to the limit of its accuracy. In certain cases, such as wave forces on piles, more sophisticated wave theories are used to account for nonlinear properties of water waves.

6. WAVE PARAMETERS.

a. **Definitions**. The wave height, H, is the vertical distance between the crest and trough. The wavelength, L, is the distance between two successive wave crests. Wave period, T, is the elapsed time required for two successive wave crests to pass a given point. Wave celerity, or phase velocity, C, is given by L/T. The group velocity, C_g, is the velocity at which the wave group propagates. η is the water-surface elevation at a given point relative to the still water level (SWL), and a is

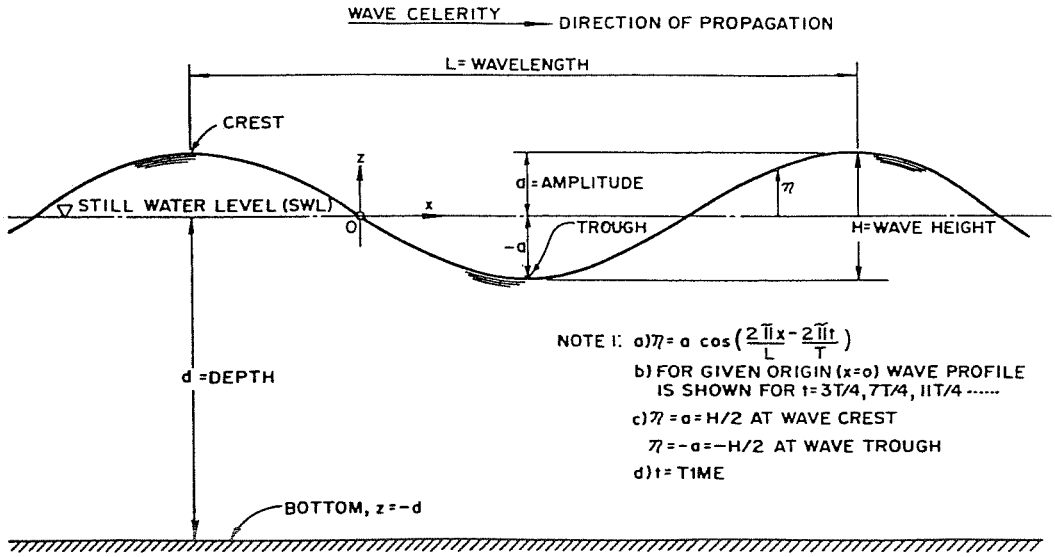

(AFTER SHORE PROTECTION MANUAL, 1977)

FIGURE 1
Wave Terminology

TABLE 1
Mathematical Expressions, Categorized by Relative Depth, for Various Wave Parameters -- Linear (Airy) Wave theory

RELATIVE DEPTH.....	SHALLOW WATER $\frac{d}{L} < \frac{1}{25}$	TRANSITIONAL WATER $\frac{1}{25} < \frac{d}{L} < \frac{1}{2}$	DEEP WATER $\frac{d}{L} > \frac{1}{2}$
WAVE PARAMETER 1. Wave Profile	Same As →	$\eta = \frac{H}{2}\cos\left[\frac{2\pi x}{L} - \frac{2\pi t}{T}\right] = \frac{H}{2}\cos\theta$	← Same As
2. Wave Celerity	$C = \frac{L}{T} = \sqrt{gd}$	$C = \frac{L}{T} = \frac{gT}{2\pi}\tanh\left(\frac{2\pi d}{L}\right)$	$C = C_o = \frac{L}{T} = \frac{gT}{2\pi}$
3. Wave Length	$L = T\sqrt{gd} = CT$	$L = \frac{gT^2}{2\pi}\tanh\left(\frac{2\pi d}{L}\right)$	$L = L_o = \frac{gT^2}{2\pi} = C_oT$
4. Group Velocity	$C_g = C = \sqrt{gd}$	$C_g = nC = \frac{1}{2}\left[1 + \frac{4\pi d/L}{\sinh(4\pi d/L)}\right]C$	$C_g = \frac{1}{2}C = \frac{gT}{4\pi}$
5. Water Particle Velocity a) Horizontal	$u = \frac{H}{2}\sqrt{\frac{g}{d}}\cos\theta$	$u = \frac{H}{2}\frac{gT}{L}\frac{\cosh[2\pi(z+d)/L]}{\cosh(2\pi d/L)}\cos\theta$	$u = \frac{\pi H}{T}e^{\frac{2\pi z}{L}}\cos\theta$
b) Vertical	$w = \frac{H\pi}{T}(1+\frac{z}{d})\sin\theta$	$w = \frac{H}{2}\frac{gT}{L}\frac{\sinh[2\pi(z+d)/L]}{\cosh(2\pi d/L)}\sin\theta$	$w = \frac{\pi H}{T}e^{\frac{2\pi z}{L}}\sin\theta$
6. Water Particle Accelerations a) Horizontal	$a_x = \frac{H\pi}{T}\sqrt{\frac{g}{d}}\sin\theta$	$a_x = \frac{g\pi H}{L}\frac{\cosh[2\pi(z+d)/L]}{\cosh(2\pi d/L)}\sin\theta$	$a_x = 2H\left(\frac{\pi}{T}\right)^2 e^{\frac{2\pi z}{L}}\sin\theta$
b) Vertical	$a_z = -2H\left(\frac{\pi}{T}\right)^2(1+\frac{z}{d})\cos\theta$	$a_z = -\frac{g\pi H}{L}\frac{\sinh[2\pi(z+d)/L]}{\cosh(2\pi d/L)}\cos\theta$	$a_z = -2H\left(\frac{\pi}{T}\right)^2 e^{\frac{2\pi z}{L}}\cos\theta$
7. Water Particle Displacement a) Horizontal	$\xi = -\frac{HT}{4\pi}\sqrt{\frac{g}{d}}\sin\theta$	$\xi = -\frac{H}{2}\frac{\cosh[2\pi(z+d)/L]}{\sinh(2\pi d/L)}\sin\theta$	$\xi = -\frac{H}{2}e^{\frac{2\pi z}{L}}\sin\theta$
b) Vertical	$\zeta = \frac{H}{2}(1+\frac{z}{d})\cos\theta$	$\zeta = \frac{H}{2}\frac{\sinh[2\pi(z+d)/L]}{\sinh(2\pi d/L)}\cos\theta$	$\zeta = \frac{H}{2}e^{\frac{2\pi z}{L}}\cos\theta$
8. Subsurface Pressure	$p = \rho g(\eta - z)$	$p = \rho g\eta\frac{\cosh[2\pi(z+d)/L]}{\cosh(2\pi d/L)} - \rho gz$	$p = \rho g\eta e^{\frac{2\pi z}{L}} - \rho gz$

(AFTER SHORE PROTECTION MANUAL, 1977)

the amplitude, which is equal to H/2. Another useful parameter is the wave steepness, H/L. See Figure 1 for a definition of terms.

b. Relative Depth. Waves can be categorized as shallow-water waves, transitional-water waves, or deepwater waves, depending upon the value of the dimensionless parameter, d/L (relative depth), where d is the still water depth; still water depth is the depth in the absence of waves. Table 1 presents mathematical expressions, categorized by relative depth, for various wave parameters. Throughout the text, the subscript "o" refers to the deepwater value of a wave parameter.

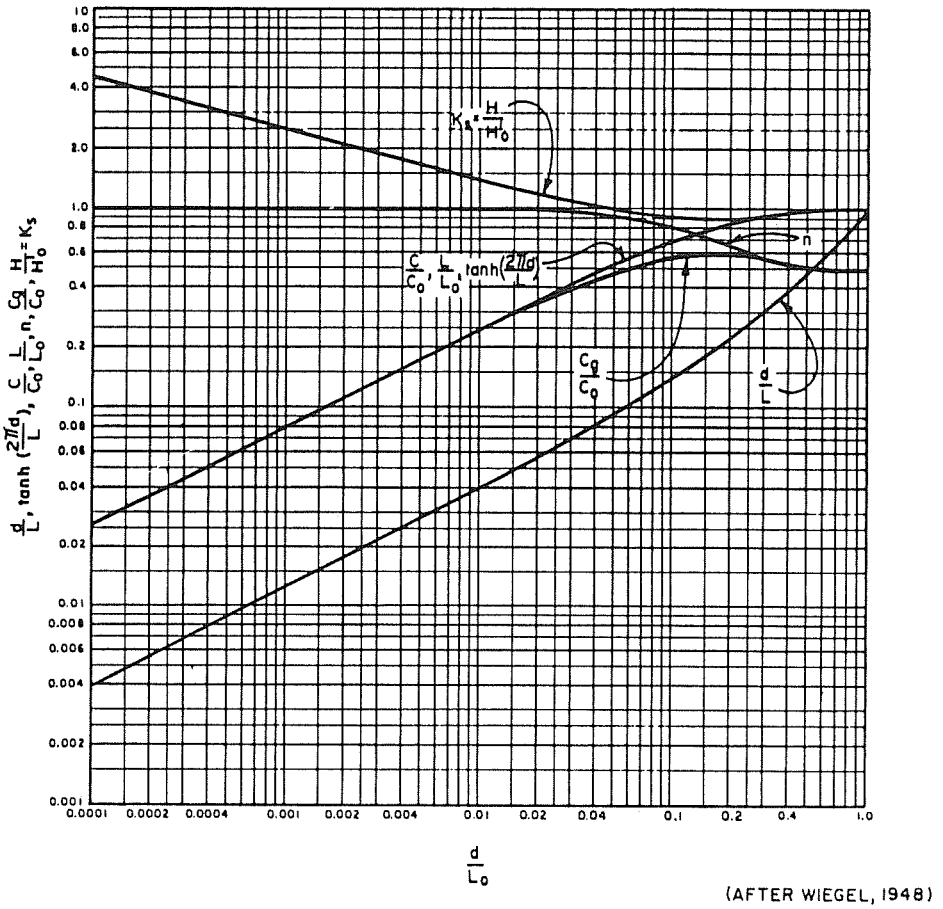

(AFTER WIEGEL, 1948)

FIGURE 2
Value of Various Wave Parameters as a Function of d/L_o for Linear Wave Thoery

EXAMPLE PROBLEM 1

Given: a. Wave height, H = 10 feet
b. Water depth, d = 20 feet
c. Wavelength, L = 100 feet

Find: Wave steepness, H/L, and relative depth, d/L.

Solution: H/L = 10/100 = 0.100

d/L = 20/100 = 0.200

c. Wavelength. The wavelength, L, for a given water depth, d, can be determined graphically by first computing the deepwater wavelength, L_o, from:

$$L_o = (g/2\pi)\, T^2 \qquad (1\text{-}1)$$

WHERE:
L_o = deepwater wavelength, in feet
g = gravitational acceleration (32.2 feet per second^2)
T = wave period, in seconds

The value thus determined for L_o is used to determine d/L. Figure 2 gives the value of d/L and other parameters as a function of d/L. The other parameters will be discussed later. (More accuracy can be obtained by the use of Table C-1 of Appendix C, Shore Protection Manual (1977) (SPM), or by the use of tables found in other wave-theory texts. However, adequate accuracy in most design situations can be obtained by the use of Figure 2.) From Figure 2, the value of d/L for the determined value of d/L may be found; from d/L, the L for the given depth, d, may be calculated. The hyperbolic functions tanh(x), sinh(x), and cosh(x), which need to be computed for many of the equations found in Table 1, may be found in Figure 3.

EXAMPLE PROBLEM 2

Given: a. Wave period, T = 10 seconds
b. Water depth, d = 20 feet

Find: Wavelength, L, for d = 20 feet

Solution: (1) Using Equation (1-1), find the deepwater wavelength:

$L_o = (g/2\pi)\, T^2 = (32.2/2\pi)(10)^2 = 512$ feet

(2) Determine d/L_o:

$d/L_o = 20/512 = 0.039$

(3) From Figure 2 for $d/L_o = 0.039$:

$d/L = 0.082$

$L = d/0.082 = 20/0.082 = 244$ feet

7. WAVE TRANSFORMATIONS. As waves propagate from deep water into intermediate (transitional) and shallow waters, their properties are transformed. The wave period is assumed to remain constant during these transformations. The wave height first decreases relative to the deepwater wave height, H_o, then increases rapidly with a decrease in water depth, d, until breaking occurs. The change in wave height as a function of water depth is termed "wave shoaling." Waves also change height and direction of propagation by refraction. Upon encountering a breakwater, waves propagate into the lee

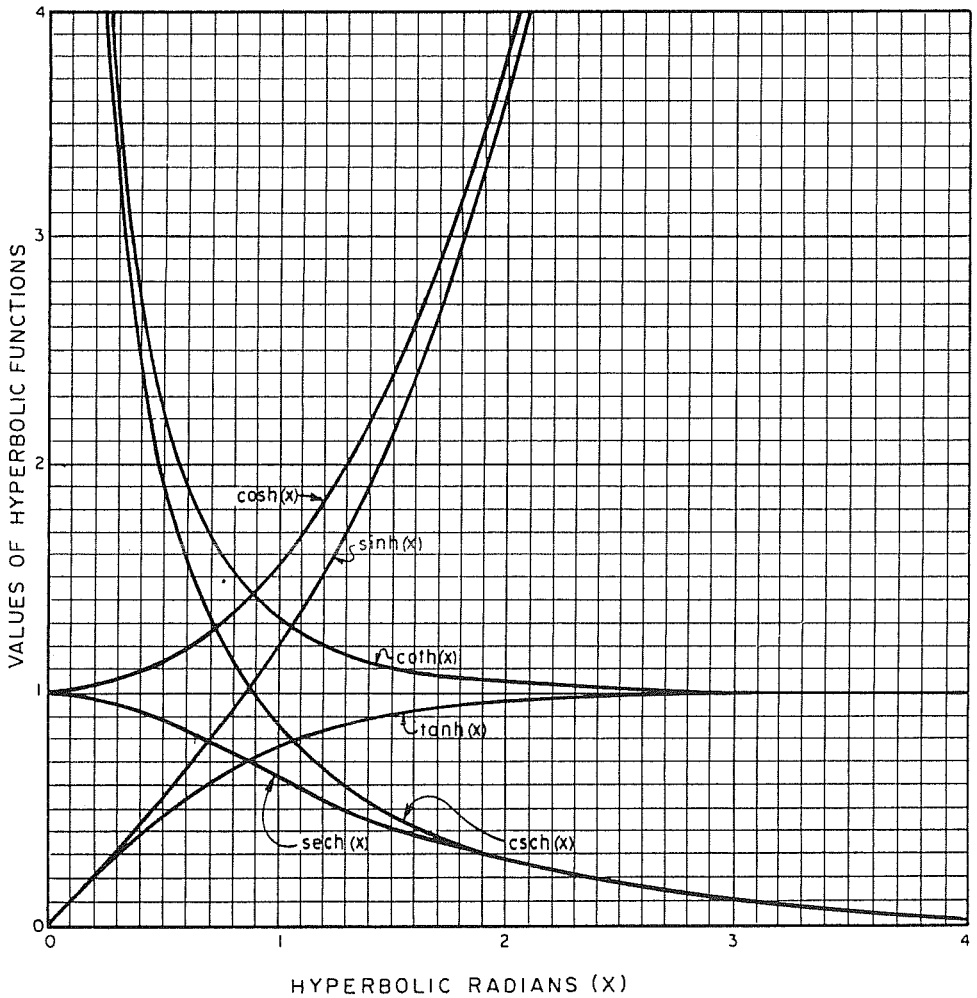

FIGURE 3
Hyperbolic Functions

of the structure by wave diffraction. Waves propagating in deep water over long distances attenuate in height by dispersion and viscous dissipation. In transitional and shallow water, waves decay due to breaking, bottom friction, and percolation. Waves break when the wave steepness, H/L, approaches about 0.14, or when the wave height relative to water depth, H/d, is from 0.70 to 1.2, depending upon bottom slope. Waves also reflect off beaches, shorelines, and structures.

The wave height, H, at a given location is the product of the shoaling, K_s, refraction, K_R, diffraction, K', and decay, K_f, coefficients, as given by the equation:

$$H = K_s K_R K' K_f H_o \qquad (1\text{-}2)$$

WHERE:
H = local wave height
K_s = shoaling coefficient
K_R = refraction coefficient
K' = diffraction coefficient
K_f = decay coefficient
H_o = deepwater wave height

Methods for determining the values for these coefficients and breaking wave heights are presented in the following subsections. The maximum value of H is limited by breaking.

a. Wave Shoaling.

(1) Linear Shoaling. The change in wave height due to a wave entering transitional or shallow water can be determined by application of the shoaling coefficient, $K_s = H/H'_o$, where H'_o represents the equivalent deepwater wave height if the wave had been unaffected by refraction ($H'_o = H_o K_R$). Figure 2 shows a plot of the first-order approximation of the linear shoaling coefficient, H/H'_o, as a function of d/L_o.

(2) Nonlinear Shoaling. As the wave approaches very shallow water several wavelengths seaward of breaking, shoaling becomes highly nonlinear, and the linear shoaling coefficient may significantly underpredict the wave height, especially for long waves in shallow water. Figure 4 gives an approximation of the nonlinear shoaling coefficient, K_{sNL}, for values of deepwater wave steepness, H'_o/L_o, versus relative depth, d/L_o. The lines of slope, m, are used to determine whether breaking has occurred for the given set of conditions. Also plotted on Figure 4 is the linear shoaling coefficient, K_s, which is given by the curve denoted m = 0. This graph should be used as a check to determine the relative importance of nonlinear properties on the shoaling of a given wave. Figure 4 plots the nonlinear shoaling coefficient, K_{sNL}, as a function of d/L_o for isolines of H'_o/L_o. To find an appropriate shoaling coefficient, enter the abscissa of Figure 4 with a given value of d/L_o. Proceed, extending a vertical line from the d/L_o value, until intersection with the given value of H'_o/L_o. If the lines do not intersect and the H'_o/L_o value lies to the left of the d/L_o value, then the nonlinear properties of the wave are not affecting wave shoaling in the given water depth; in that case, the linear shoaling coefficient, K_s, denoted by the m = 0 line, would be used. If the lines do not intersect and the H'_o/L_o value lies to the right of the given d/L_o value, then the wave

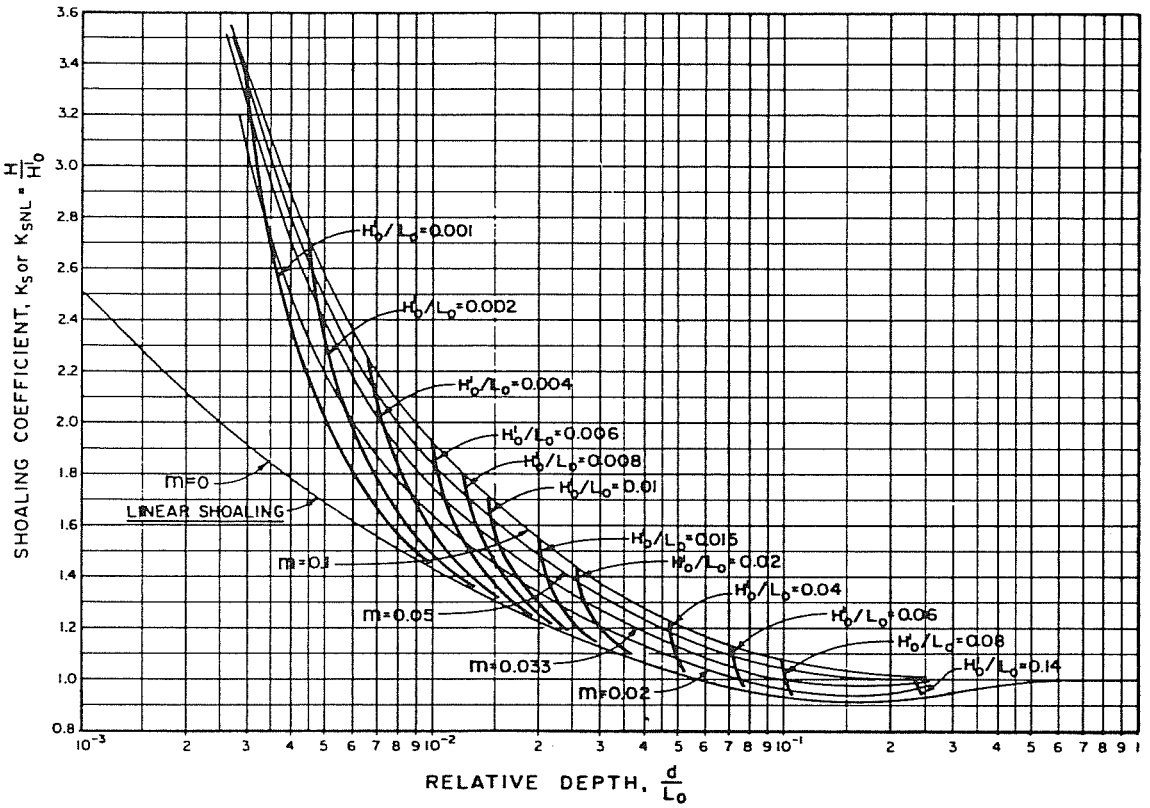

FIGURE 4
Shoaling Coefficient, K_S or K_{SNL}

has already broken in deeper water. Where the line extending from the given d/L_o and the given H'_o/L_o do intersect, a horizontal line is extended to the ordinate to obtain the value of the nonlinear shoaling coefficient, K_{SNL}. However, if the given value of m lies below the intersection of the given d/L_o and H'_o/L_o, then the wave has broken and the wave will not shoal as high as the K_{SNL} value indicates. If the given value of m lies above the intersection of given d/L_o and H'_o/L_o, then the indicated K_{SNL} should be used. The lines labeled with various values of slope (in addition to m = 0) indicate the breaking limits (indices) for a given m, d/L_o, and H'_o/L_o. The wave cannot shoal past the breaking limit for a given bottom slope, m. the wave shoals to higher breaking limits for steeper slopes. The region of validity of Figure 4 is restricted to the region just prior to breaking. Figure 4 is a semiempirical plot based on breaking indices described in Subsection 1.6.e, Wave Breaking, and on theoretical nonlinear shoaling curves. The K_{SNL} is only an approximation to account for the discrepancy between linear shoaling and empirical breaking indices. Application of Figure 4 is illustrated in Example Problem 3.

EXAMPLE PROBLEM 3

Given: a. Case I: H_o = 10 feet, T = 12 seconds, d = 11.8 feet, m = 0.033, K_R = 0.74

b. Case II: H_o = 5.75 feet, T = 15 seconds, d = 5.8 feet, m = 0.033, K_R = 0.4

c. Case III: H = 2.5 feet, T = 10 seconds, d = 5.12 feet, m = 0.033

Find: a. Case I: shallow-water wave height, H, using K_{SNL} and compare to H obtained using linear K_S.

b. Case II: shallow-water wave height, H, using K_{SNL} and compare to H obtained using linear K_S.

c. Case III: equivalent unrefracted deepwater wave height, H'_o, using K_{SNL}.

Solution: a. Case I:

(1) Using Equation (1-1), find L_o:

$L_o = (g/2\pi)\,T^2 = (32.2/2\pi)(12)^2 = 738$ feet

(2) Determine d/L_o:

$d/L_o = 11.8/738 = 0.016$

(3) Determine H'_o:

$H'_o = H_o\,K_R = (10)(0.74) = 7.4$ feet

(4) Determine deepwater steepness, H'_o/L_o:

$H'_o/L_o = 7.4/738 = 0.01$

(5) From Figure 4 for $d/L_o = 0.016$, $H'_o/L_o = 0.01$, and m = 0.033:

$K_{SNL} = 1.48$

THEREFORE: Nonlinear value of $H = K_{SNL}\,H'_o = (1.48)(7.4) = 11.0$ feet

(6) From Figure 4 for $d/L_o = 0.016$, $H'_o/L_o = 0.01$, and m = 0 (linear shoaling):

$K_S = 1.28$

THEREFORE: From linear theory, $H = K_S\,H'_o = (1.28)(7.4) = 9.5$ feet

THEREFORE: Nonlinear shoaling predicts a wave height that is 16 percent greater than that predicted by linear shoaling.

Note: If the slope had been m = 0.02 instead of 0.033, the wave would have broken at a value of $K_{SNL} = 1.39$.

b. Case II:

(1) Using Equation (1-1), find L_o:

$L_o = (g/2\pi)\,T^2 = (32.2/2\pi)(15)^2 = 1{,}153$ feet

(2) Determine d/L_o:

$d/L_o = 5.75/1{,}153 = 0.005$

(3) Determine H'_o:

$H'_o = H_o K_R = (5.75)(0.4) = 2.3$ feet

(4) Determine deepwater steepness, H'_o/L_o:

$H'_o/L_o = 2.3/1,153 = 0.002$

(5) From Figure 4 for $d/L_o = 0.005$, $H'_o/L_o = 0.002$, and $m = 0.033$:

$K_{sNL} = 2.33$

THEREFORE: Nonlinear value of $H = K_{sNL} H'_o = (2.33)(2.3) = 5.36$ feet

(6) From Figure 4 for $d/L_o = 0.05$, $H'_o/L_o = 0.002$, and $m = 0$:

$K_s = 1.69$

THEREFORE: From linear theory, $H = K_s H'_o = (1.69)(2.3) = 3.89$ feet

THEREFORE: Nonlinear shoaling predicts a wave height that is 38 percent greater than that predicted by linear shoaling.

c. Case III: to determine the value of H'_o requires an iterative process. First assume a value of H'_o/L_o; at the intersection of d/L_o line and assumed H'_o/L_o read value of K_{sNL}; compute H'_o from assumed H'_o/L_o and L_o; use K_{sNL} and H'_o to get a value of H; compare computed H to actual value of H. Repeat the process until the computed H converges with the actual H. Calculate H'_o from the assumed H'_o/L_o which yielded the actual H.

(1) Using Equation (1-1), find L_o:

$L_o = (g/2\pi) T^2 = (32.2/2\pi)(10)^2 = 512$ feet

(2) Determine d/L_o:

$d/L_o = 5.12/512 = 0.010$

(3) First, try $H'_o/L_o = 0.004$:

From Figure 4 for $d/L_o = 0.01$, $H'_o/L_o = 0.004$, and $m = 0.033$:

$K_{sNL} = 1.57$

$H'_o/L_o = 0.004$; $H'_o = 0.004\ L_o = (0.004)(512) = 2.05$ feet

$H = K_{sNL} H'_o = (1.57)(2.05)$

$H = 3.22$ feet; since $H = 2.5$ feet, $H'_o/L_o = 0.004$ is too high

(4) Secondly, try $H'_o/L_o = 0.003$:

From Figure 4 for $d/L_o = 0.01$, $H'_o/L_o = 0.003$, and $m = 0.033$:

$K_{sNL} = 1.53$

$H'_o/L_o = 0.003$; $H'_o = (0.003)(512) = 1.54$ feet

$H = K_{sNL} H'_o = (1.53)(1.54)$

$H = 2.36$ feet; since $H = 2.5$ feet, $H'_o/L_o = 0.003$ is too low

(5) Thirdly, try $H'_o/L_o = 0.0032$:

From Figure 4 for $d/L_o = 0.01$, $H'_o/L_o = 0.0032$, and $m = 0.033$:

$K_{sNL} = 1.54$

$H'_o/L_o = 0.003$; $H'_o = (0.0032)(512) = 1.64$ feet

$H = K_{sNL} H'_o = (1.54)(1.64)$

$H = 2.53$ feet $\simeq 2.5$ feet

THEREFORE: $H'_o = 1.64$ feet

b. Wave Refraction.

(1) General. Waves are considered to be in deep water for $d/L > 1/2$; however, when waves propagate into shallower water, the phase velocity, C, becomes a function of water depth. When the wave crests are at an angle relative to the bottom depth contours, the wave crests bend, tending to aline with the depth contours. Figure 5 schematically shows wave

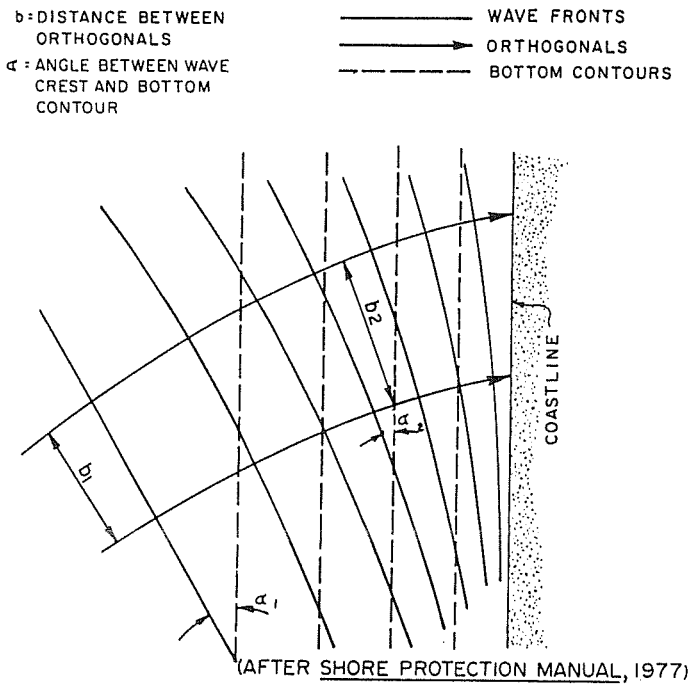

(AFTER SHORE PROTECTION MANUAL, 1977)

FIGURE 5
Schematic of Wave Refraction Over Straight and Parallel Bottom Contours

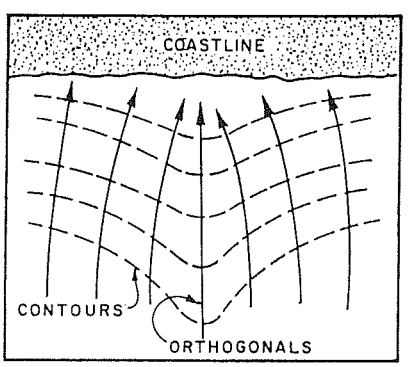

A-ORTHOGONALS CONVERGING OVER SUBMARINE RIDGE

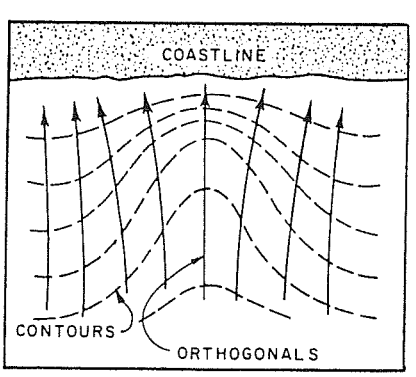

B-ORTHOGONALS DIVERGING OVER SUBMARINE CANYON

(AFTER SHORE PROTECTION MANUAL, 1977)

FIGURE 6
Converging and Diverging Wave Refraction

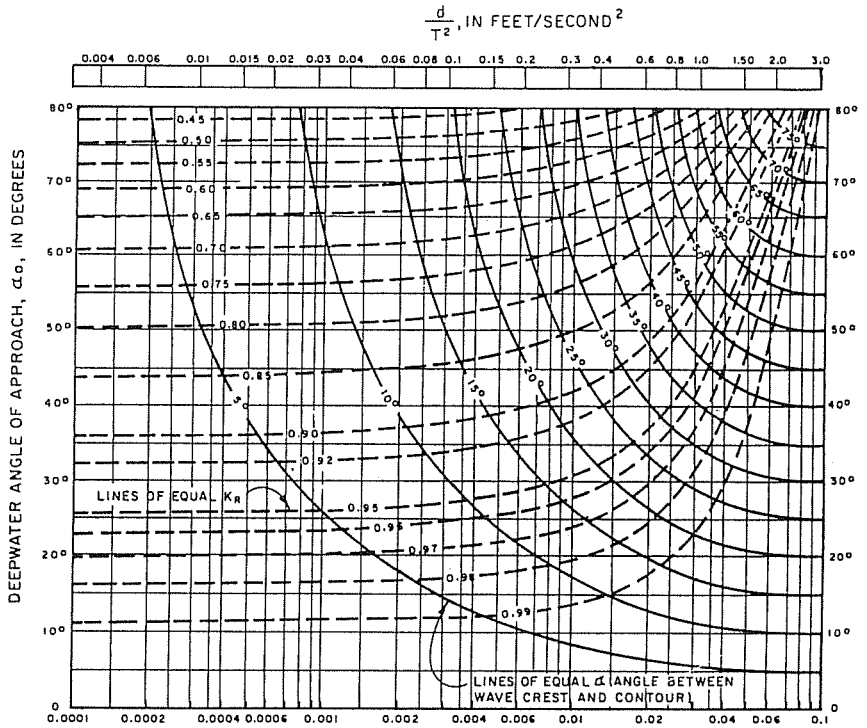

(SHORE PROTECTION MANUAL, 1977)

FIGURE 7
Wave Refraction Parameters for Straight and Parallel Contours

refraction over straight and parallel bottom contours. Wave converge over submarine ridges and diverge over submarine canyons, as shown in Figure 6. Wave orthogonals are imaginary lines drawn perpendicularly to the wave crests which indicate the direction of wave propagation. When the orthogonals converge, the wave height increases proportionally with the refraction coefficient, K_R, which is a function of the square root of the ratio of orthogonal spacing, $K_R = H_2/H_1 = (b_1/b_2)^{1/2}$. (See Figure 5). (b = distance between orthogonals.) Conversely, when the orthogonals diverge, the wave height decreases.

(2) Importance. Wave refraction and wave shoaling are important wave transformations that affect structural designs and analyses of beach systems. Refraction must be considered in design of structures to determine the angle of wave approach and the change in wave height for waves in transitional and shallow water. For example, the wave-height distribution along a shoreline can be greatly influenced by the offshore bathymetry. A harbor entrance should be located in an area of wave divergence rather than convergence. This will result in a more protected harbor. Wave refraction should be considered in determining such things as breakwater armor-unit sizes, wave-induced forces on piles and other structures, and wave runup. Wave refraction is also an important phenomenon in studying littoral transport and shoreline configurations. (See DM-26.3)

(3) Refraction Over Straight and Parallel Contours. Refraction effects over a bottom having straight and parallel depth contours can be calculated by application of Figure 7. The refraction coefficient, K_R, and the angle of wave crest relative to the depth contour, α, at a given depth, d, for a given period, T, can be determined by entering Figure 7 on the abscissa with a value of $d/g\,T^2$ and the ordinate with a deepwater angle of approach, α_o.

The local wave height is given by:

$$H = K_S\, K_R\, H_o \qquad (1\text{-}3)$$

EXAMPLE PROBLEM 4

Given: a. A beach with straight and parallel contours
b. Incident deepwater wave characteristics: H_o = 6 feet and T = 10 seconds with wave crests at a 30° angle relative to the bottom contours

Find: Wave height and direction of wave propagation at d = 30 feet.

Solution: (1) Find $d/g\,T^2$:

$d/g\,T^2 = 30/[(32.2)(10)^2] = 0.0093$

(2) From Figure 7 for $\alpha_o = 30°$ and $d/g\,T^2 = 0.0093$:

$\alpha = 17.0°$ and $K_R = 0.95$

(3) Find d/L_o:

$L_o = (g/2\pi)\,T^2 = (32.2/2\pi)(10)^2 = 512$ feet

$d/L_o = 30/512 = 0.0586$

(4) From Figure 2 for $d/L_o = 0.0586$:

$K_s = 1.0$

(5) Using Equation (1-3):

$H = K_s\, K_R\, H_o = (1.0)(0.95)(6) = 5.7$ feet

(4) Refraction Over Irregular Bathymetry. Refraction over irregular bathymetry, such as over submarine ridges and canyons, requires the use of graphical methods or computer programs. These methods are described in the Shore Protection Manual (1977).

EXAMPLE PROBLEM 5

Given: Deepwater waves, H_o = 10 feet, T = 10 seconds from the northeast entering Main Pass of Diego Garcia. The shoaling coefficient, $K_s = 1.52$.

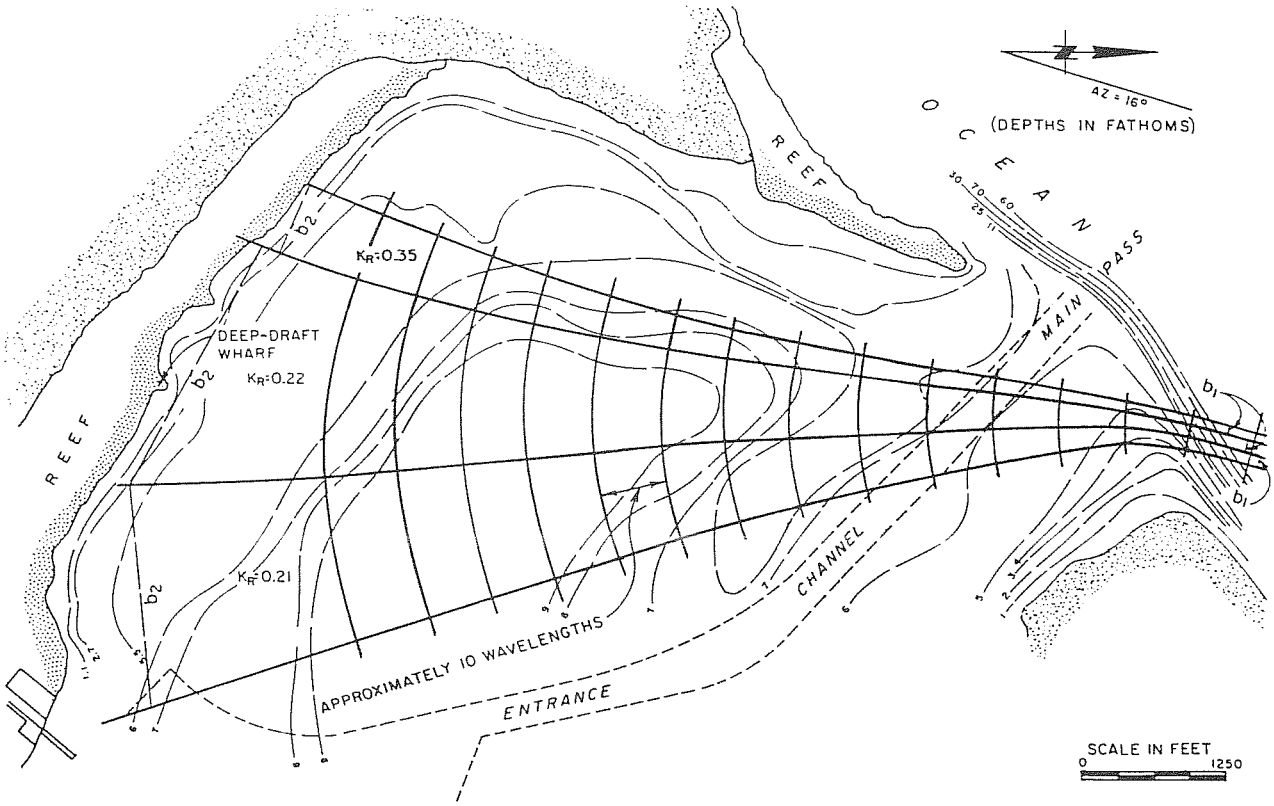

FIGURE 8
Bathymetry, Project Site, and Refraction Diagram for Example Problem 5

Find: Determine the wave height and angle of incidence at the entrance of a proposed boat harbor in 10 feet of water.

Solution: The project site is shown in Figure 8 with its bathymetry and refraction diagram. The bathymetry is very complex and the straight-and-parallel-depth-contour assumption is not appropriate. The refraction must be solved by graphical procedures described in the Shore Protection Manual (1977), or by a computer program.

The solution given in Figure 8 shows a severe refraction of incident wave energy around the sloping banks of Main Pass. At the project site, the refraction coefficient is $K_R = 0.22$ as determined by using the distance between orthogonals and the equation $K_R = (b_1/b_2)^{1/2}$, where b_1 is measured in deep water outside the entrance and b_2 is measured near the deep-draft wharf. The shoaling coefficient is $K_s = 1.52$. The wave approaches from the north. The resultant wave height is:

$$H = K_s K_R H_o = (1.52)(0.22)(10) = 3.34 \text{ feet}$$

c. **Wave Diffraction**. Diffraction of water waves occurs when a wave train is interrupted by a barrier such as the breakwater shown in Figure 9. Waves propagate into the lee of the breakwater essentially in circular arcs the geometric shadow, are less than one-half the incident wave height. A diffraction diagram describes wave-height distribution in the lee of a breakwater. The diffraction diagram shows isolines of diffraction coefficients, K', for a given local wavelength and angle of approach. The wave height in the vicinity of a breakwater is determined by:

$$H = K' H_i \qquad (1\text{-}4)$$

WHERE:
H = local wave height (diffracted wave height)
K' = diffraction coefficient
H_i = incident wave height

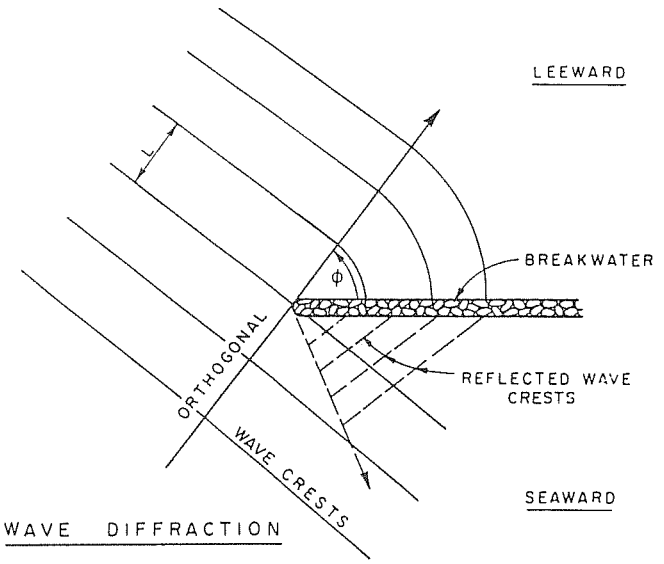

FIGURE 9
Diffraction Occurs When Wave Train is Interrupted by a Breakwater

Note: The effects of refraction and shoaling must also be included.

Waves also reflect off the obstruction, causing an interference pattern on the seaward side.

(1) Single Semi-Infinite, Rigid, Impermeable Breakwater. For a single breakwater, the diffraction coefficient, K', is a function of the angle of wave approach relative to the breakwater, ϕ, and wavelength, L, in water depth, d_s, at the toe of the breakwater head. Figures 10 through 21 give diffraction

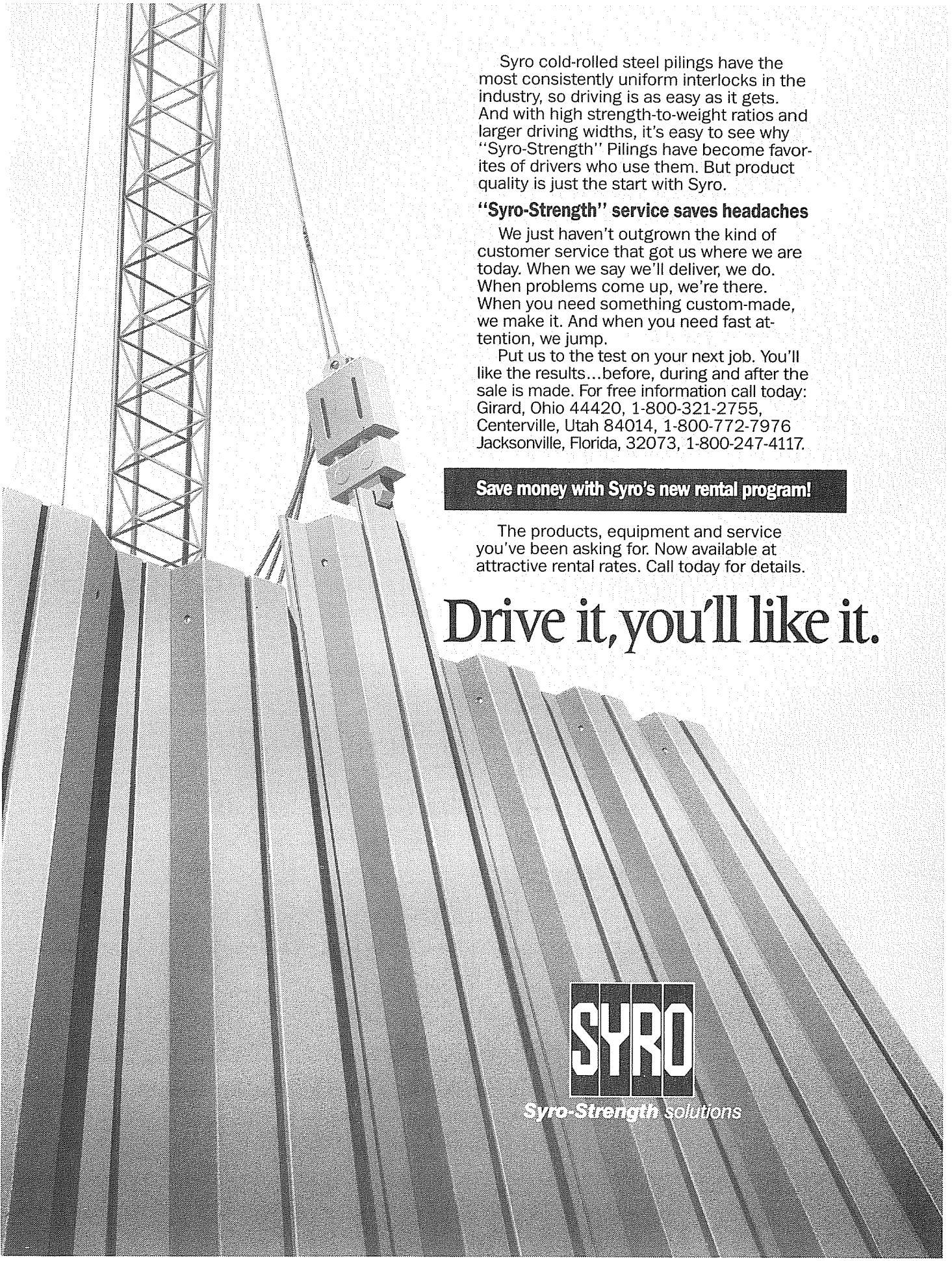

Syro cold-rolled steel pilings have the most consistently uniform interlocks in the industry, so driving is as easy as it gets. And with high strength-to-weight ratios and larger driving widths, it's easy to see why "Syro-Strength" Pilings have become favorites of drivers who use them. But product quality is just the start with Syro.

"Syro-Strength" service saves headaches

We just haven't outgrown the kind of customer service that got us where we are today. When we say we'll deliver, we do. When problems come up, we're there. When you need something custom-made, we make it. And when you need fast attention, we jump.

Put us to the test on your next job. You'll like the results...before, during and after the sale is made. For free information call today: Girard, Ohio 44420, 1-800-321-2755, Centerville, Utah 84014, 1-800-772-7976 Jacksonville, Florida, 32073, 1-800-247-4117.

Save money with Syro's new rental program!

The products, equipment and service you've been asking for. Now available at attractive rental rates. Call today for details.

Drive it, you'll like it.

SYRO

Syro-Strength solutions

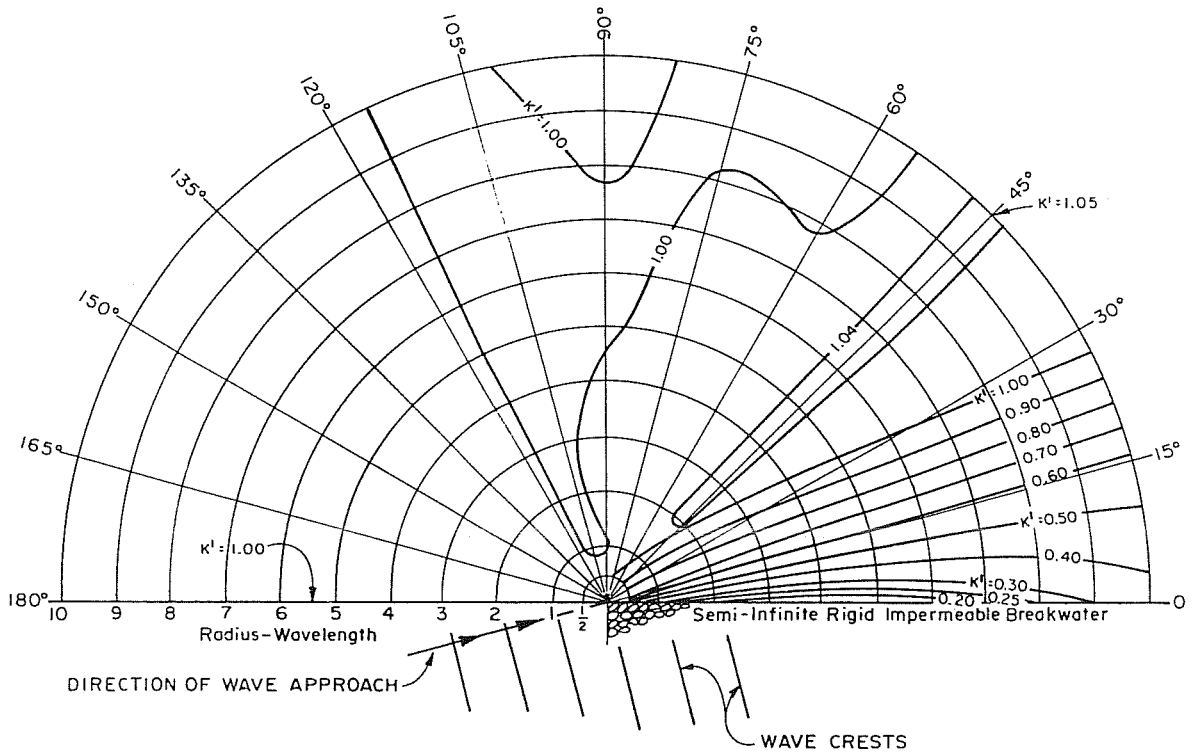

(AFTER WIEGEL, 1962)

FIGURE 10
Wave-Diffraction Diagram for 15° Angle of Wave Approach

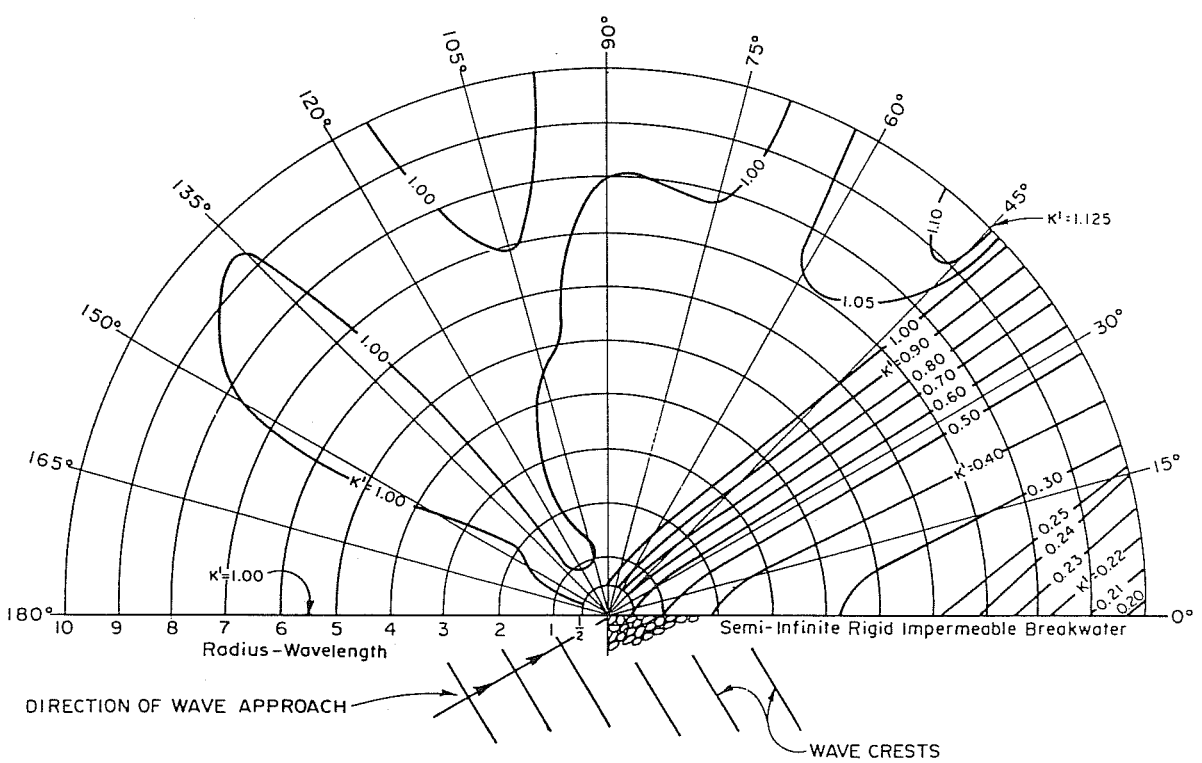

(AFTER WIEGEL, 1962)

FIGURE 11
Wave-Diffraction Diagram for 30° Angle of Wave Approach

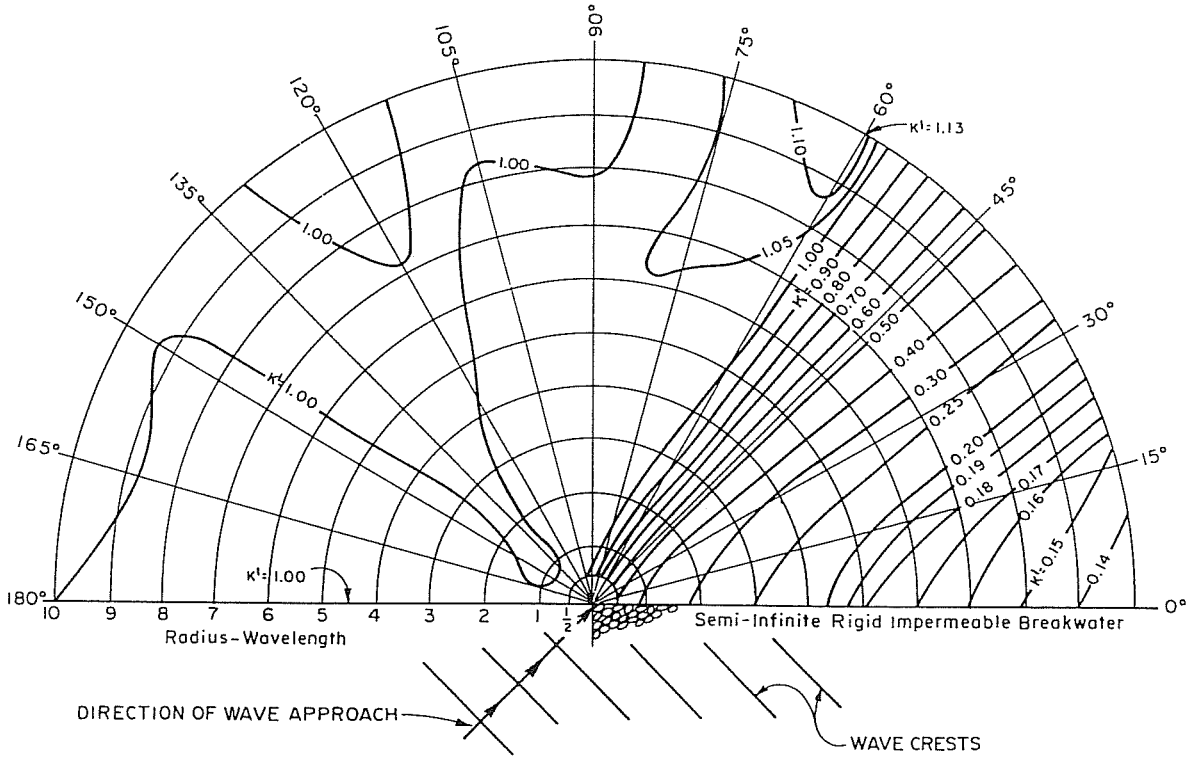

(AFTER WIEGEL, 1962)

FIGURE 12
Wave-Diffraction Diagram for 45° Angle of Wave Approach

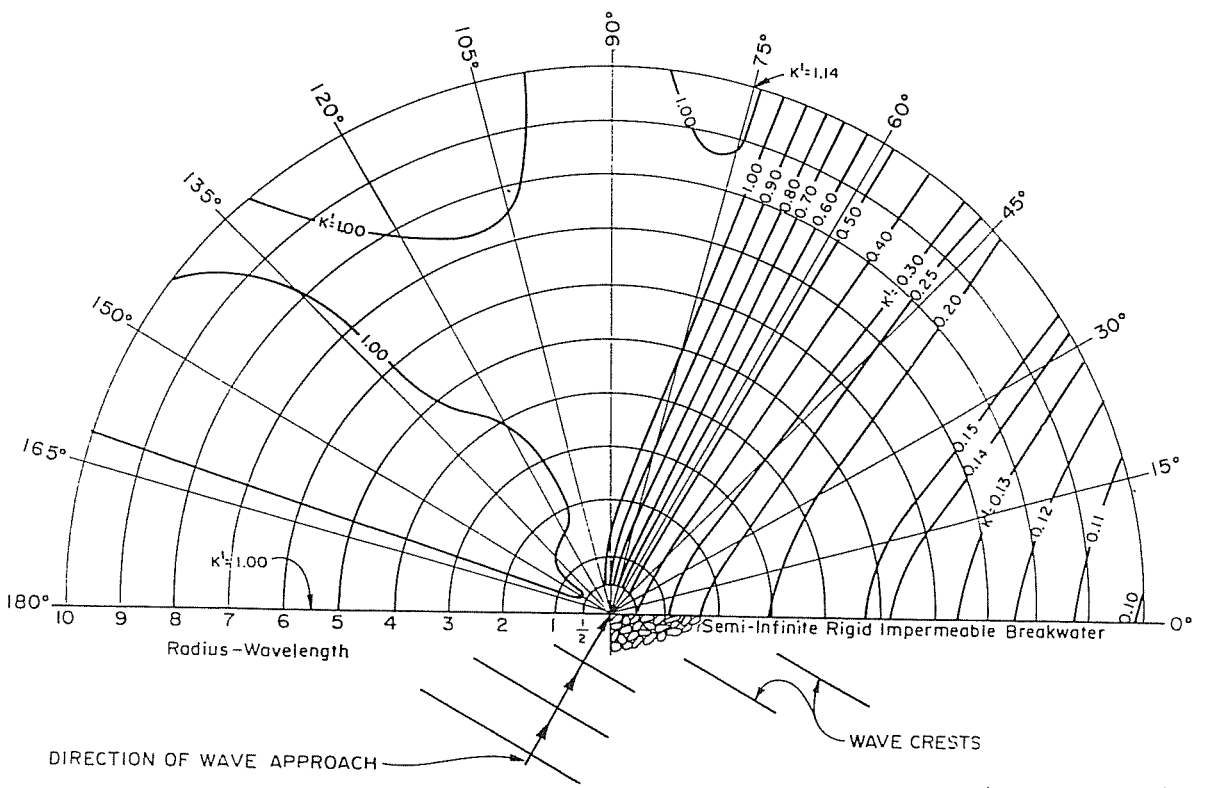

(AFTER WIEGEL, 1962)

FIGURE 13
Wave-Diffraction Diagram for 60° Angle of Wave Approach

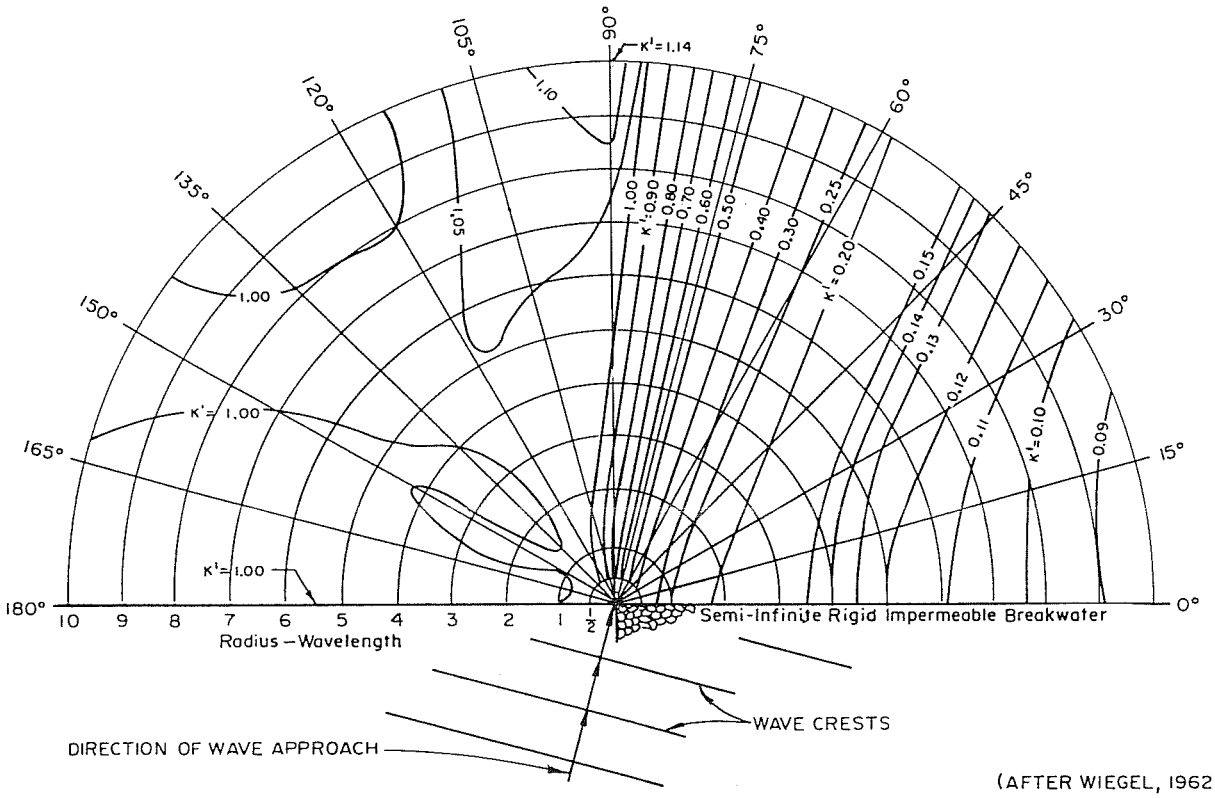

(AFTER WIEGEL, 1962)

FIGURE 14
Wave-Diffraction Diagram for 75° Angle of Wave Approach

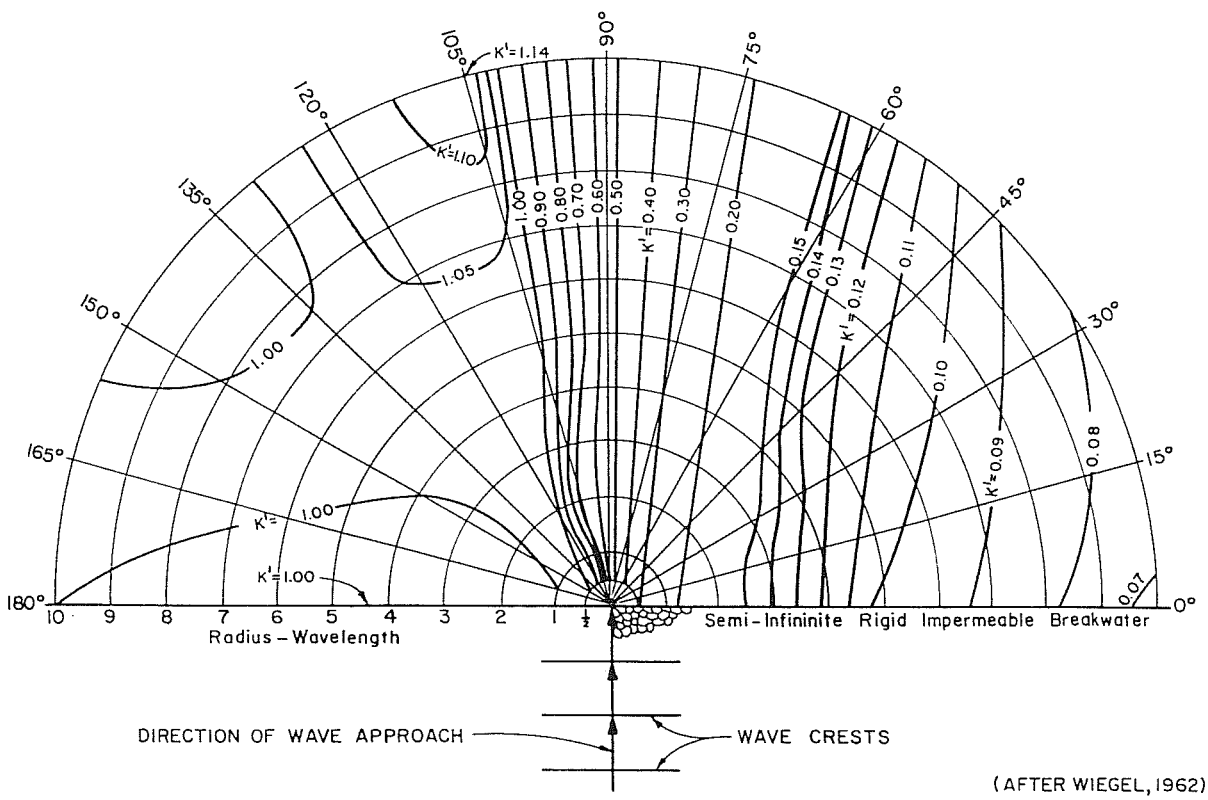

(AFTER WIEGEL, 1962)

FIGURE 15
Wave-Diffraction Diagram for 90° Angle of Wave Approach

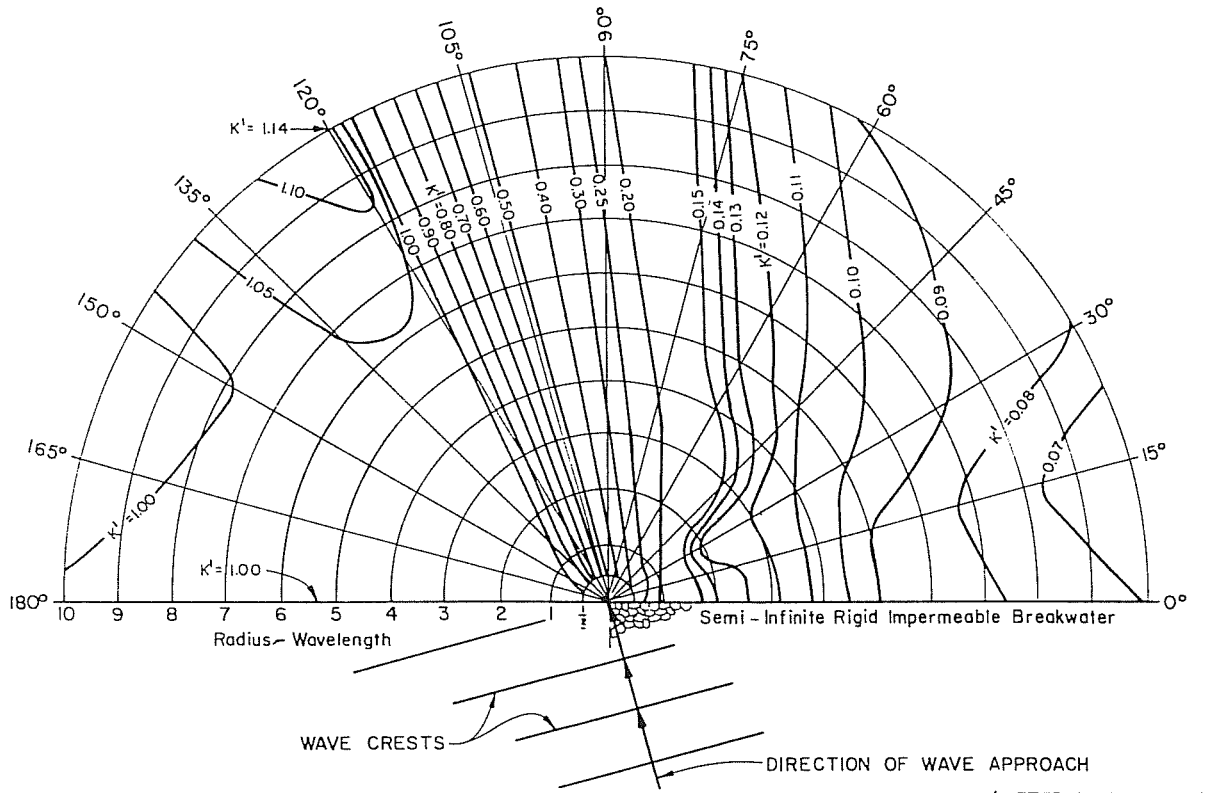

FIGURE 16
Wave-Diffraction Diagram for 105° Angle of Wave Approach

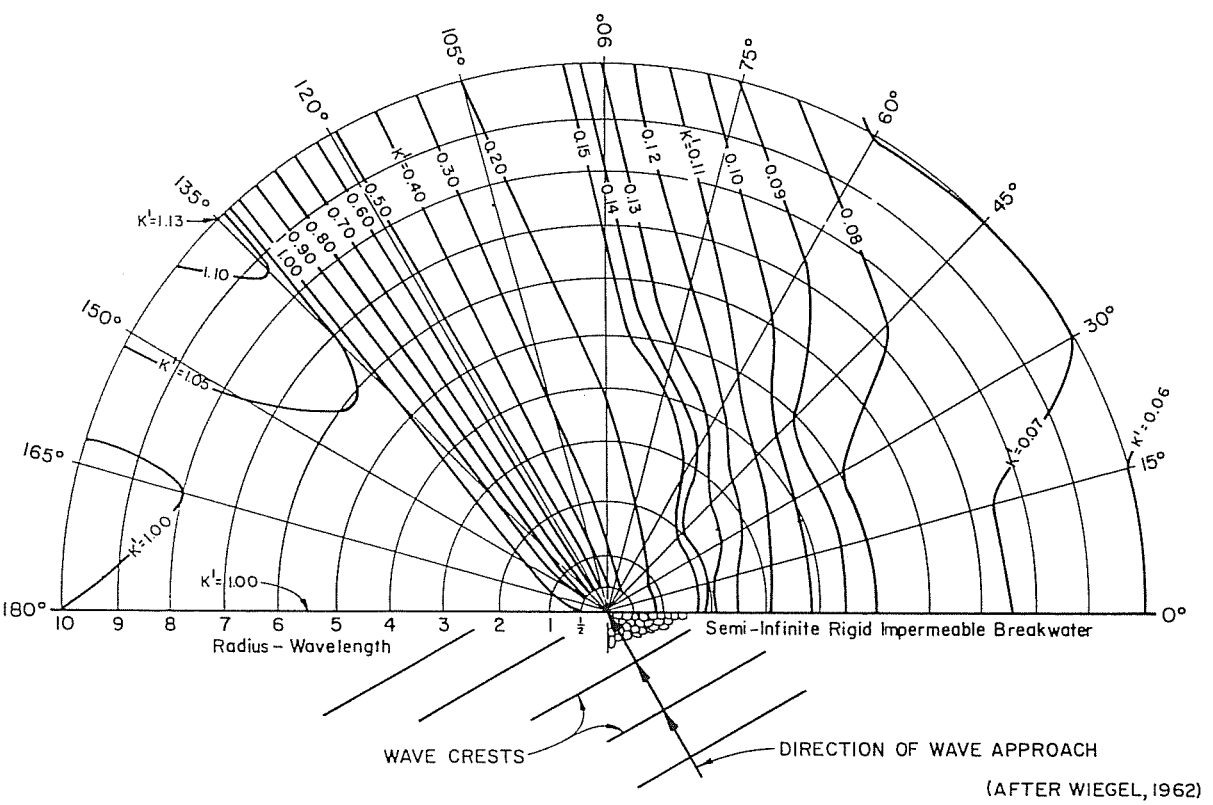

FIGURE 17
Wave-Diffraction Diagram for 120° Angle of Wave Approach

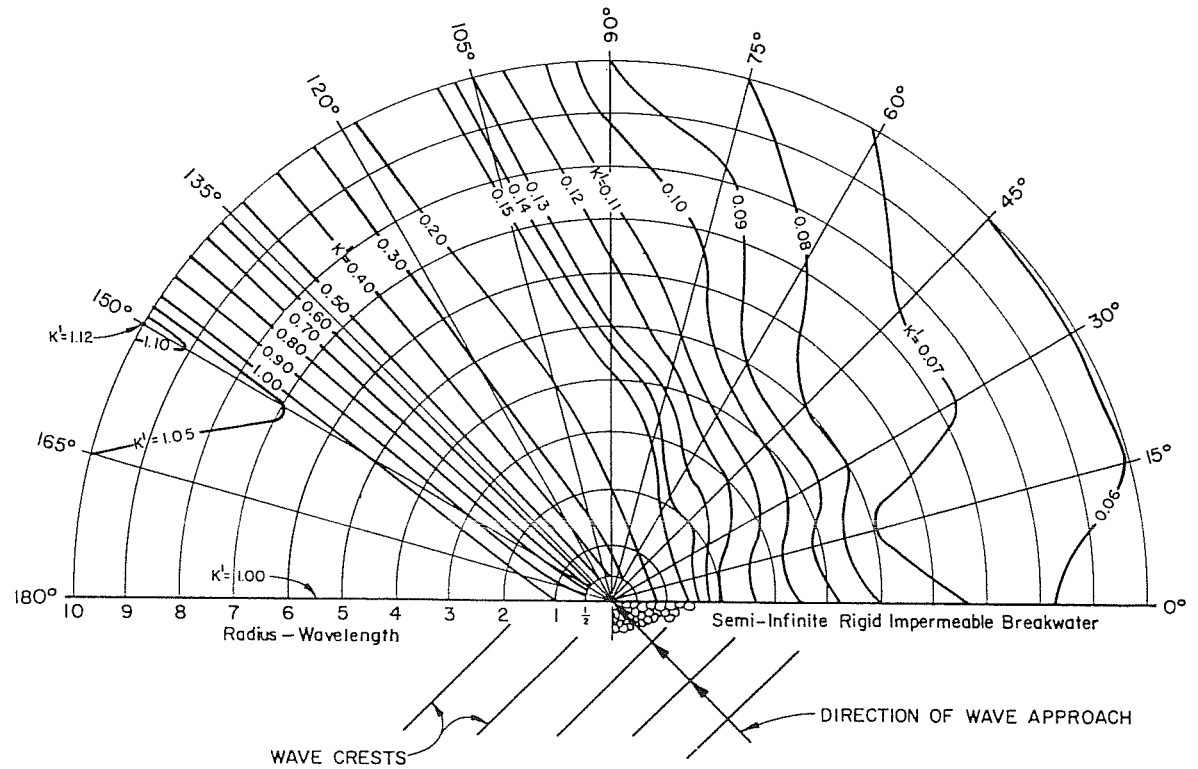

(AFTER WIEGEL, 1962)

FIGURE 18
Wave-Diffraction Diagram for 135° Angle of Wave Approach

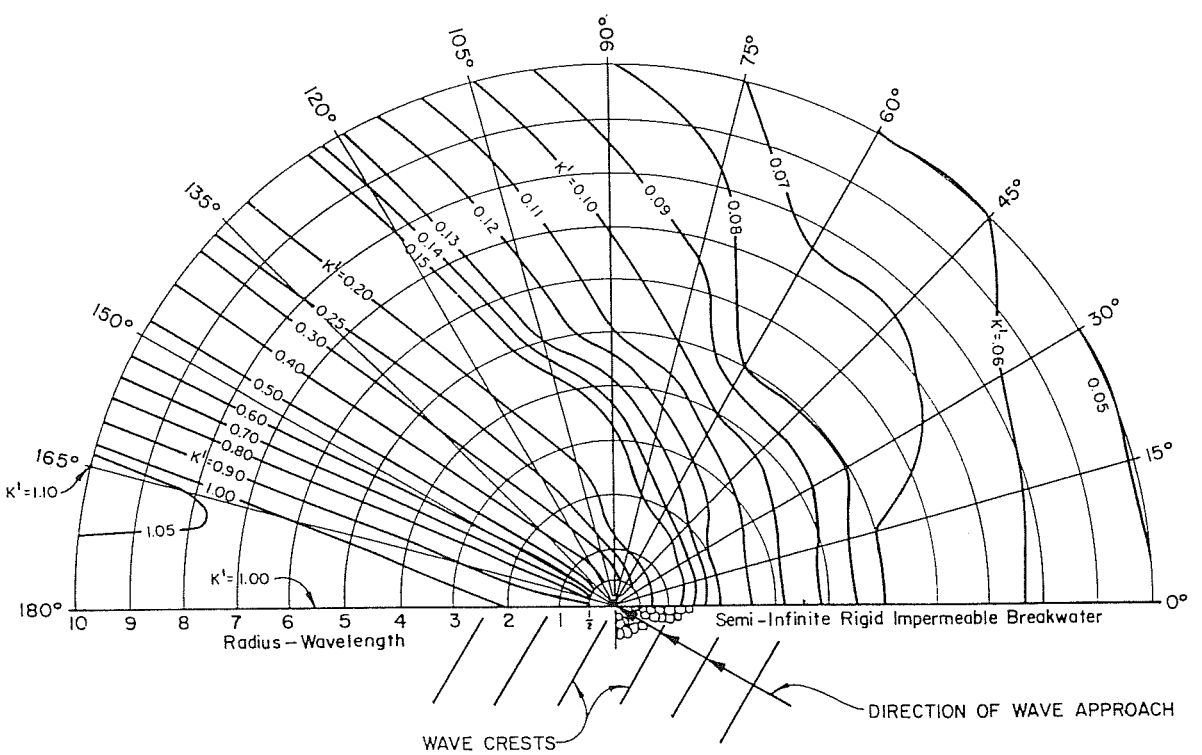

(AFTER WIEGEL, 1962)

FIGURE 19
Wave-Diffraction Diagram for 150° Angle of Wave Approach

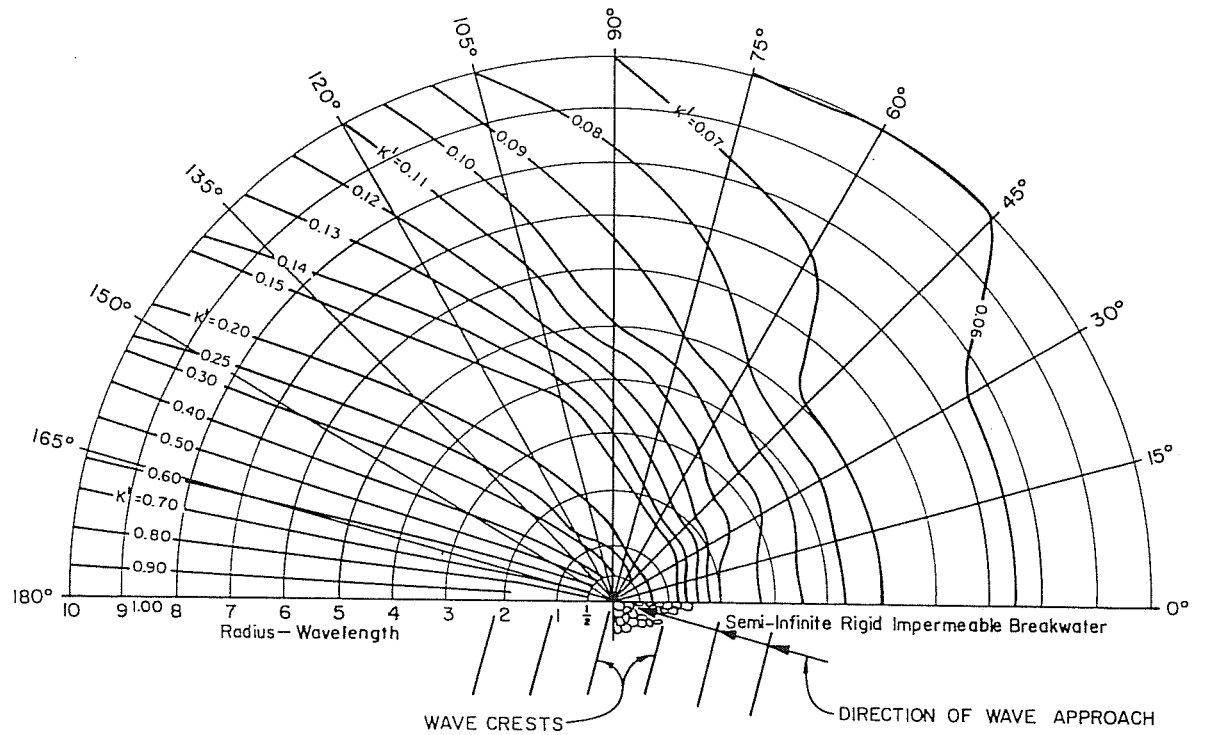

(AFTER WIEGEL, 1962)

FIGURE 20
Wave-Diffraction Diagram for 165° Angle of Wave Approach

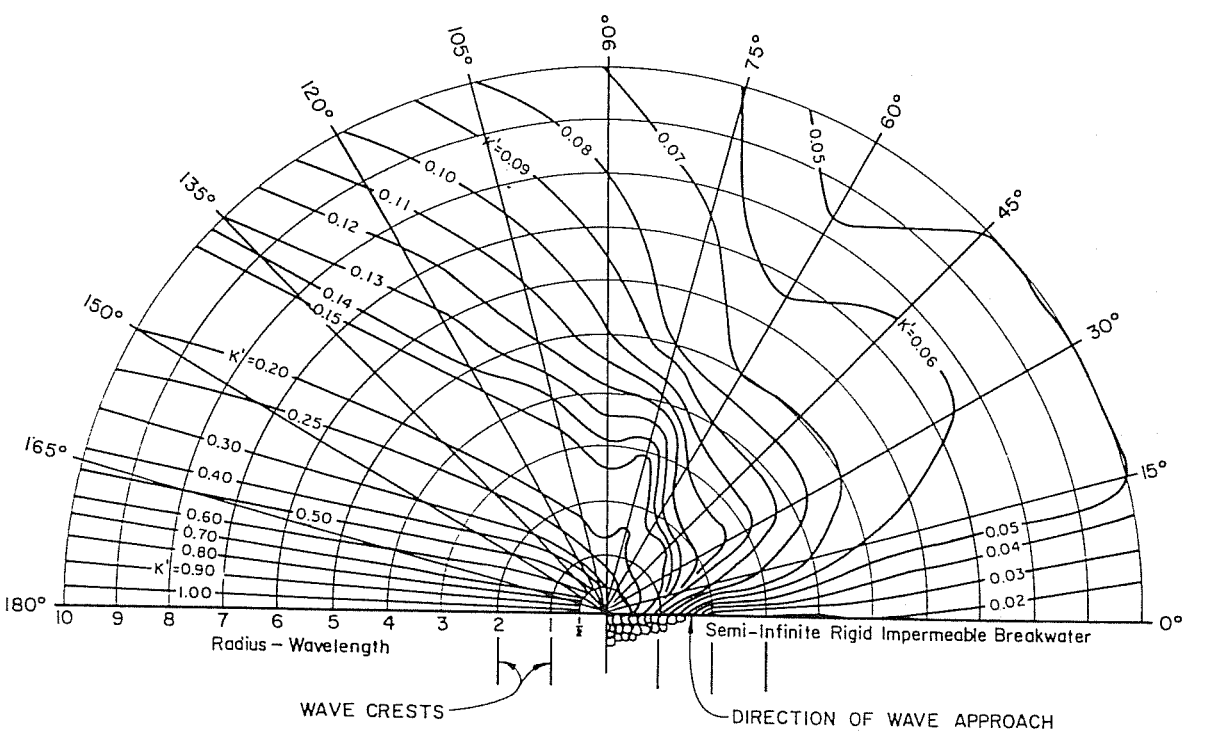

(AFTER WIEGEL, 1962)

FIGURE 21
Wave-Diffraction Diagram for 180° Angle of Wave Approach

diagrams for a thin breakwater of semi-infinite length in constant water depth for different angles of wave approach.

Diffraction diagrams are constructed polar-coordinate form and consist of arcs spaced one "radius-wavelength unit" apart, and rays, spaced 15° apart. These arcs and rays are centered at the intersection of the breakwater head with the stillwater level. The diagrams in Figures 10 through 21 show the breakwater extending to the right when looking toward the area of diffraction. (These diagrams are used for a breakwater extending to the left by simply turning over the diagrams to their opposite sides.) The angle of wave approach is measured counterclockwise from the breakwater. (This angle would be measured clockwise for a breakwater extending to the left.) To adjust a given diffraction diagram to the scale of a given working unit on the diffraction diagram is equal to one wavelength on the working drawing. A template overlay of the scaled diffraction diagram is then prepared; thus, lines of constant K' (isolines) can be easily transferred to the working drawing.

An example of the use of diffraction diagrams would be to determine the breakwater length needed to protect a boat basin. Breakwater length is measured along the breakwater on the diffraction diagram in terms of radius wavelength units, which are then converted to feet, using the map scale, to determine design breakwater length needed to achieve a given K' in a given region in the breakwater's lee. This procedure is outlined in Example Problem 6.

In the use of diffraction diagrams, wave-crest lines are required to estimate the combined effects of refraction and diffraction. Wave crests may be approximated with sufficient accuracy by circular arcs. For a single breakwater, the arcs will be centered at the intersection of the breakwater head with the still water level. That part of the wave crest extending into unprotected water beyond the K' = 0.5 line may be approximated by a straight line. Caution should be exercised because diffraction diagrams assume a constant water depth and assume that the breakwater is thin compared with the wavelength. Refraction effects should be taken into account over rapidly varying bottom depths. As a general rule, diffraction predominates over the first three wavelengths; then, if the bottom varies rapidly, refraction should be considered.

EXAMPLE PROBLEM 6

Given: a. Incident wave: H_i = 5 feet
T = 10 seconds
ϕ = 75°

b. Depth at breakwater toe, d_s = 20 feet

c. See Figure 22 for map of boat basin layout; scale on this layout is 1 inch = 600 feet.

Find: Length of breakwater required to protect a boat basin by maintaining wave heights at less than 1.5 feet in the berthing area.

Solution: (1) Find the wavelength, L, at the toe of the breakwater head, where d_s = 20 feet:

$$L_o = (g/2\pi)\,T^2 = (32.2/2\pi)(10)^2 = 512 \text{ feet}$$

$$d_s/L_o = 20/512 = 0.0391$$

From Figure 2 for $d_s/L_o = 0.0391$:

$$d_s/L = 0.0822$$

THEREFORE: $L = 20/0.0822 = 243$ feet

(2) The scale of the basin layout map is 1:600; that is, 1 inch = 600 feet. Therefore, the wavelength, L = 243 feet, is 0.4 inches on the map. This 0.4 inches represents one radius-wavelength unit.

The diffraction diagram is scaled so that one radius-wavelength unit on the diagram is equal to one wavelength (0.4 inches) on the map.

Figure 14 is the diffraction diagram used (ϕ = 75°). An overlay of the scaled Figure 14 was prepared and laid over the basin layout to produce Figure 22.

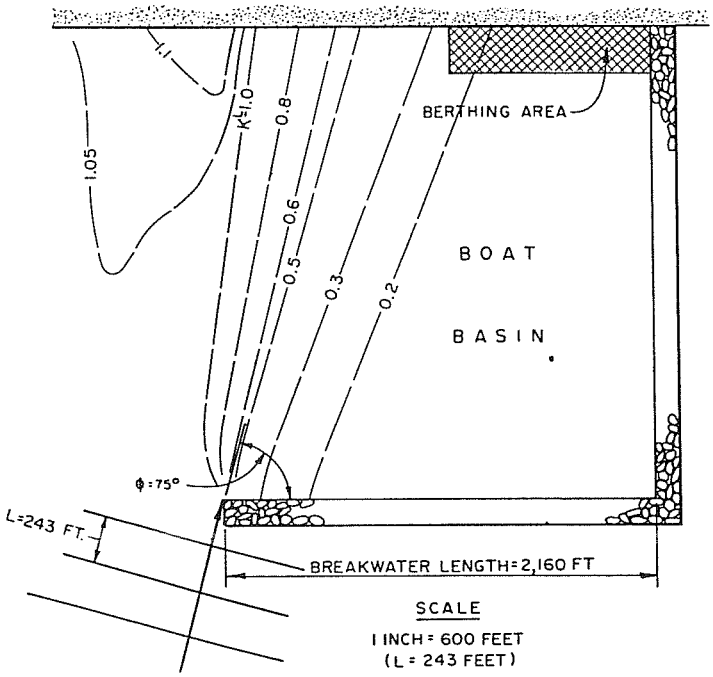

FIGURE 22
Boat Basin Layout and Diffraction Diagram for Example Problem 6

(3) Desired K' = H/H_i = 1.5/5 = 0.30. The K' = 0.30 line of the overlay should not intersect the berthing area. The length of the breakwater required to keep the K' = 0.30 line from intersecting the berthing area is thus determined to be nine radius-wavelength units.

1 radius-wavelength unit = 0.4 inches

THEREFORE: 9 radius-wavelength units = (9)(0.4) = 3.6 inches

Map scale is 1 inch = 600 feet.

THEREFORE: 3.6 inches = (3.6)(600) = 2,160 feet

Therefore, the required breakwater length is 2,160 feet.

(2) Gap Width Less Than Five Wavelengths at Normal Incidence. The determination of diffraction when the breakwater-gap width, B, is less than five wavelengths is more complex than that for a single, semi-infinite breakwater. A separate diagram for a B/L ratio of 2, shown in Figure 23, illustrates a symmetrical diagram, with the wave crests drawn on it for the purpose of illustrating its use. Figures 24 through 33 show lines of equal diffraction coefficients for B/L ratios of 0.50, 1.00, 1.41, 1.64, 1.78, 2.00, 2.50, 2.95, 3.82, and 5.00, respectively. Unlike Figure 23, only one-half of the diffraction diagram is presented on each figure of Figures 24-33; the diagrams are symmetrical about the line x/L = 0.

Wave crests to about six wavelengths may be approximated by two arcs centered on the head of each breakwater and connected by a smooth curve (approximated by a circular arc entered at the middle of the gap). Crests that are more than eight wavelengths behind the breakwater may be approximated by an arc centered at the middle of the gap.

(3) Gap Width Greater Than Five Wavelengths at Normal Incidence. Where the breakwater-gap width is greater than five wavelengths, the diffraction effects about each breakwater are nearly independent. The diagram (see Figure 15) for a single breakwater with a 90° wave approach angle may be used to define the diffraction characteristics in the lee of both breakwaters. (See Figure 34.)

(4) Gap at Oblique Incidence. When waves approach at an angle to the axis of a breakwater, the diffracted wave characteristics differ from those resulting when waves

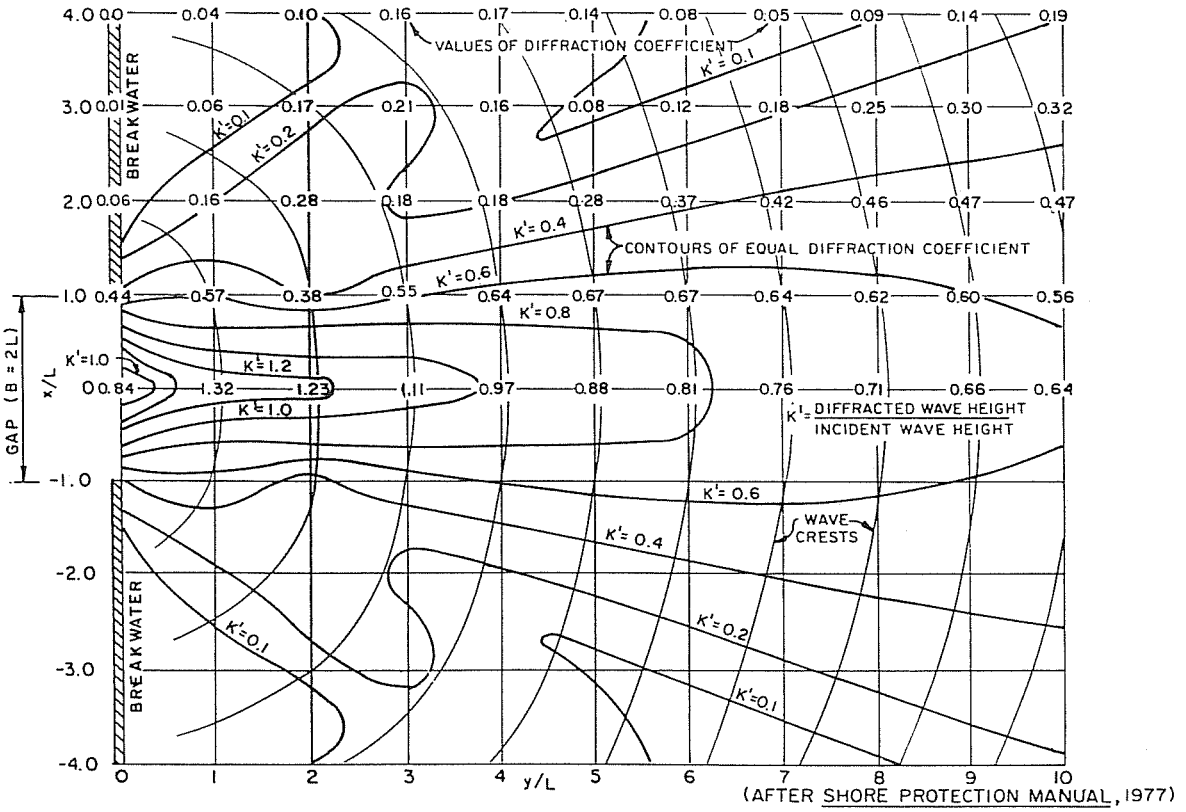

FIGURE 23
Generalized Diffraction Diagram for Two Breakwaters for B = 2L (B/L = 2)

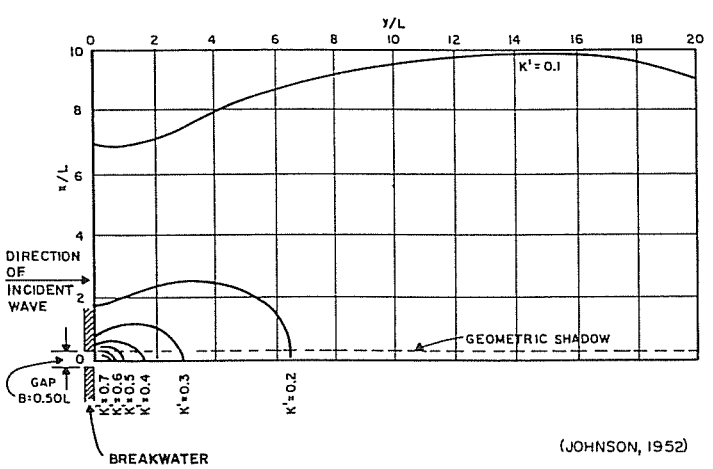

FIGURE 24
Contours of Equal Diffraction Coefficient for B = 0.5L (B/L = 0.50)

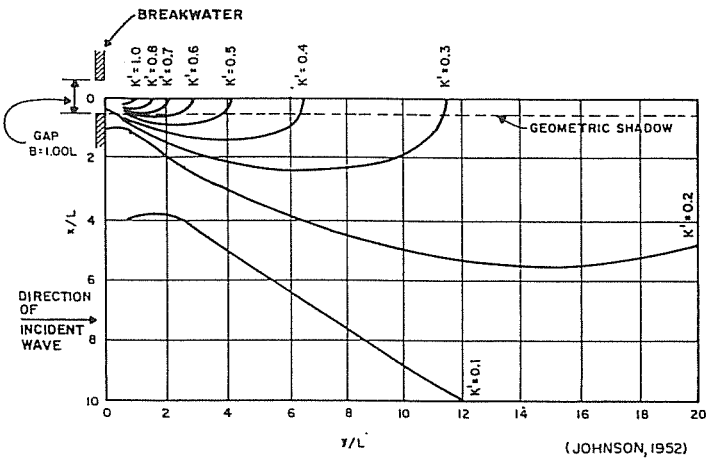

FIGURE 25
Contours of Equal Diffraction Coefficient for B = 1.00 L (B/L = 1.00)

approach normal to the axis. An approximate determination of diffracted wave characteristics may be obtained by considering the gap to be as wide as its projection in the direction of incident wave travel, B', as shown in Figure 35. Calculated diffraction diagrams for wave approach angles of 0°, 15°, 30°, 45°, 60°, and 75° are shown in Figures 36 through 41, respectively. Use of these diagrams will give more accurate results than the approximation method.

d. Wave Decay. Waves leaving their generating area radiate energy laterally through angular spreading. Waves also decay by viscous dissipation as they propagate out of their generating area. A general rule of thumb is that a wave loses one-third of its height when the distance in nautical miles it travels equals the wavelength in feet. Thus, short-period waves die out more rapidly than longer-period waves. Other factors, such as winds, currents, and other wave systems, modify waves that propagate out of their generating area. Waves propagating over shallow water decay by bottom friction and percolation. (Refer to Ippen (1966) for determination of decay due to bottom friction and percolation). Only in special cases are reductions due to bottom friction and percolation used in design practice. Neglect of these energy-reducing factors should lead to a conservative design. Bottom dissipation effects are accounted for in Subsection 3, WAVE HINDCASTING, in Section 2.

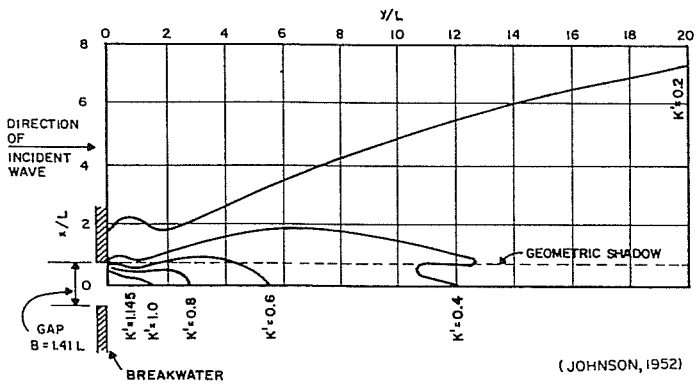

FIGURE 26
Contours of Equal Diffraction Coefficient for B = 1.41 L (B/L = 1.41)

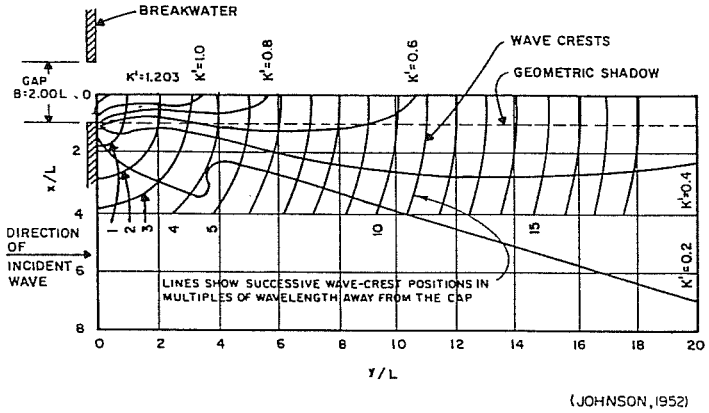

FIGURE 29
Contours of Equal Diffraction Coefficient for B = 2.00 L (B/L = 2.00)

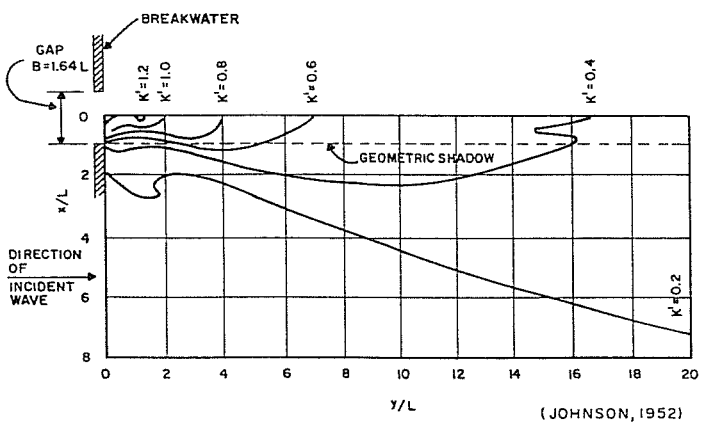

FIGURE 27
Contours of Equal Diffraction Coefficient for B = 1.64 L (B/L = 1.64)

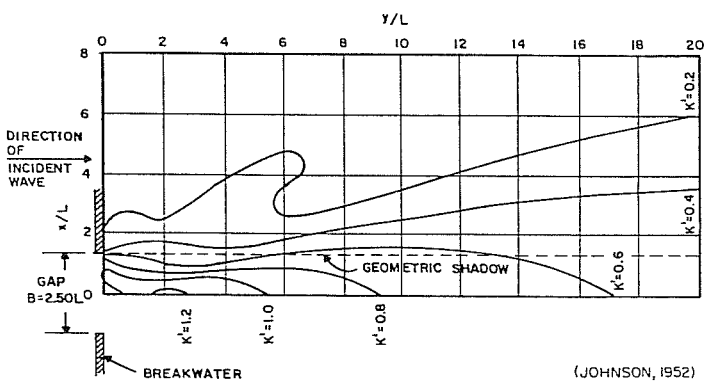

FIGURE 30
Contours of Equal Diffraction Coefficient for B = 2.50 L (B/L = 2.50)

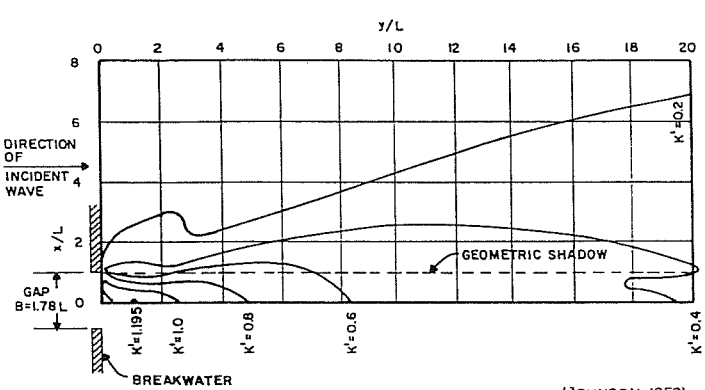

FIGURE 28
Contours of Equal Diffraction Coefficient for B = 1.78 L (B/L = 1.78)

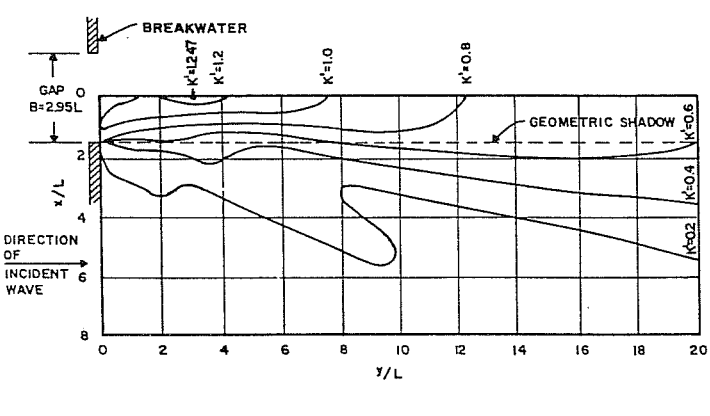

FIGURE 31
Contours of Equal Diffraction Coefficient for B = 2.95 L (B/L = 2.95)

IF IT'S STEEL AND IT GOES INTO THE CONSTRUCTION OF A MARINE STRUCTURE THEN... WE'VE GOT IT!

WALE SYSTEMS ■ CHANNEL CAPS
H-PILING ■ WIDE FLANGE BEAMS
HIGH STRENGTH SECTIONS (A-572 Gr. 50)
STEEL SHEET PILING ■ ANGLES
CORNERS ■ PLATE ■ PIPE
& MORE

New or used

We also purchase surplus inventories

The only good thing about new steel is it becomes used . . . And We Have It!

NESTOR/MERRICK
STRUCTURAL STEEL

PH) 516-546-7900
FAX) 516-546-7992

Nestor Palahnuk
1745 Merrick Avenue
Suite #7
Merrick, New York 11566

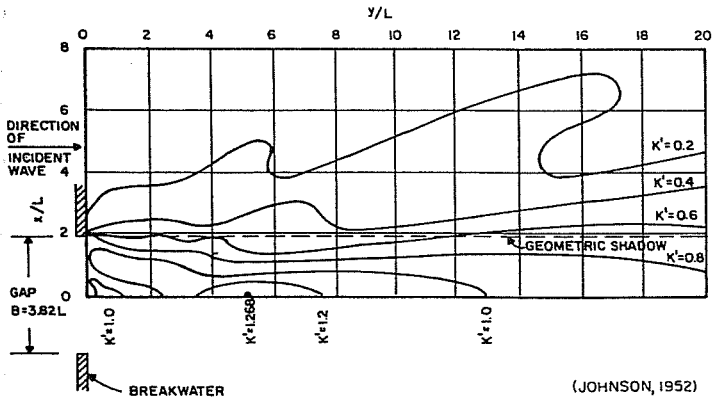

(JOHNSON, 1952)

FIGURE 32
Contours of Equal Diffraction Coefficient for B = 3.82 L (B/L = 3.82)

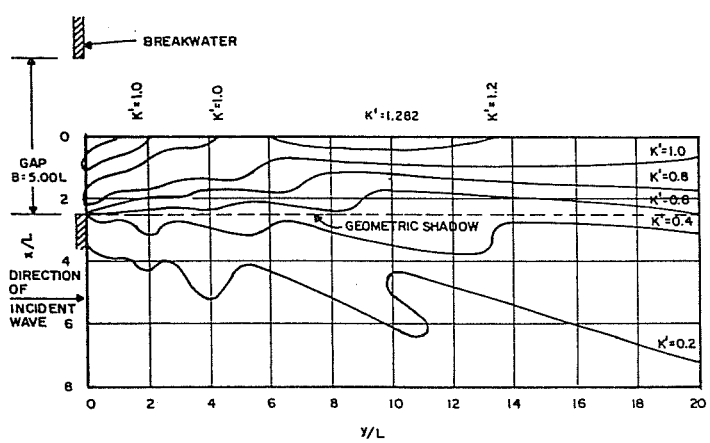

(JOHNSON, 1952)

FIGURE 33
Contours of Equal Diffraction Coefficient for B = 5.00 L (B/L = 5.00)

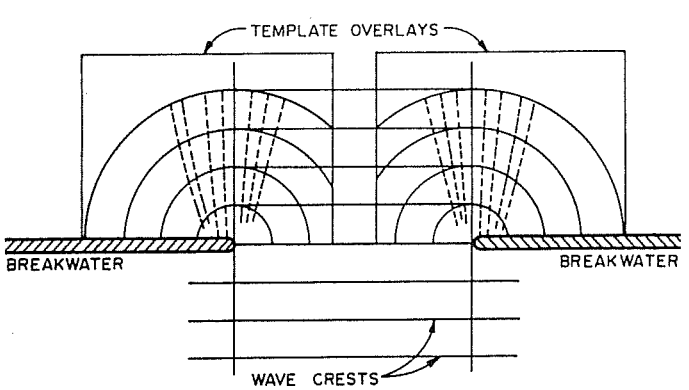

(SHORE PROTECTION MANUAL, 1977)

FIGURE 34
Diffraction Diagram for B > 5.00 L and Normal Incidence

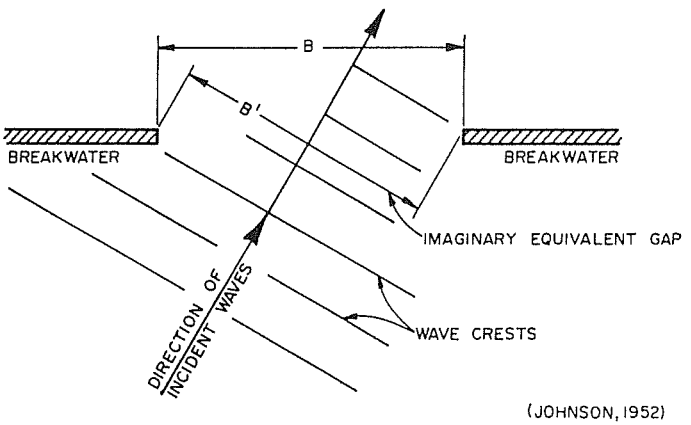

(JOHNSON, 1952)

FIGURE 35
Gap at Oblique Incidence Considered to be as Wide as Imaginary Equivalent Gap

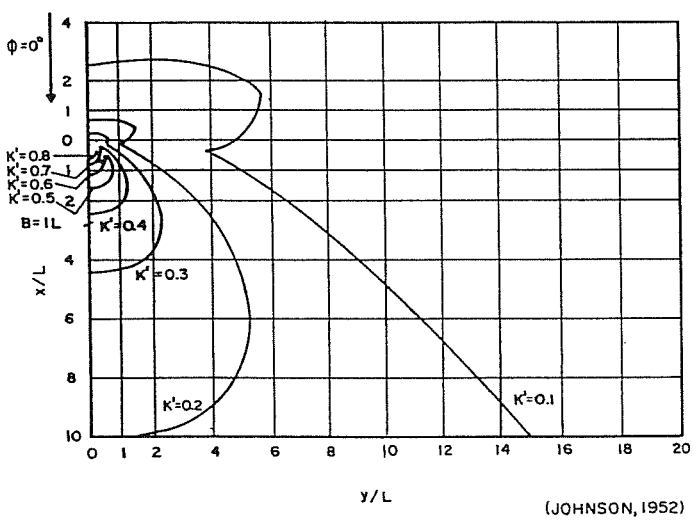

(JOHNSON, 1952)

FIGURE 36
Diffraction for a Breakwater Gap of One Wavelength Width and ϕ = 0°

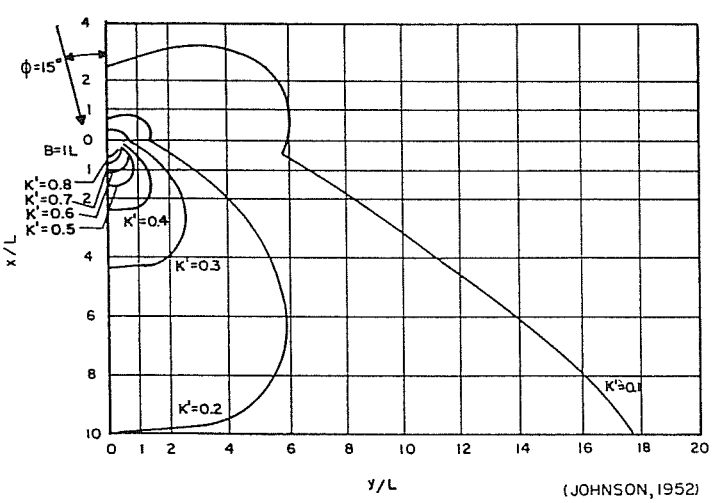

(JOHNSON, 1952)

FIGURE 37
Diffraction for a Breakwater Gap of One Wavelength Width and ϕ = 15°

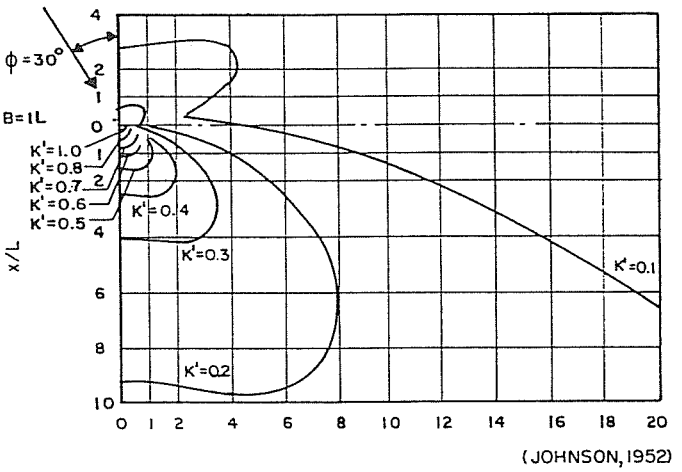

FIGURE 38
Diffraction for a Breakwater Gap of One Wavelength Width and φ = 30°

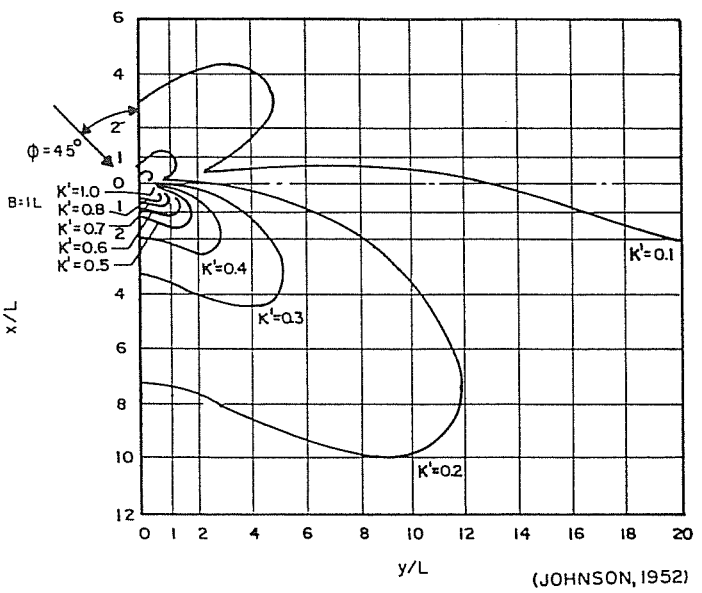

FIGURE 39
Diffraction for a Breakwater Gap of One Wavelength Width and φ = 45°

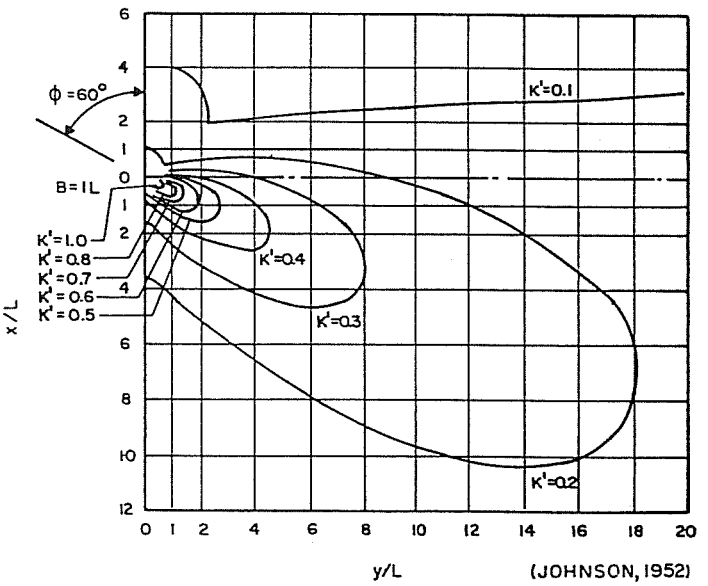

FIGURE 40
Diffraction for a Breakwater Gap of One Wavelength Width and φ = 60°

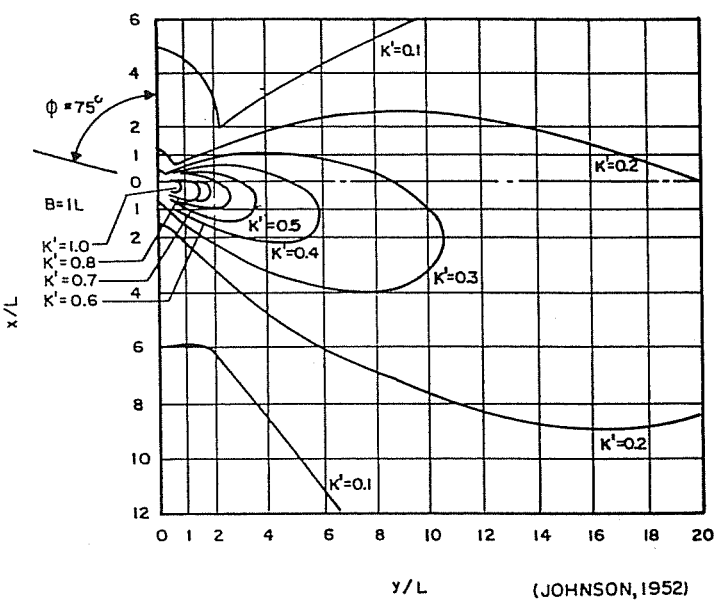

FIGURE 41
Diffraction for a Breakwater Gap of One Wavelength Width and φ = 75°

e. Wave Breaking.

(1) Limiting Factors. Waves become unstable and break when either the wave steepness, H/L, is ≥ 0.142, or the wave height relative to the water depth, H/d, is on the order of unity.

(2) Depth of Water at Breaking and Breaking-Wave Height. The depth of water at breaking, d_b, and the breaking-wave height, H_b, are functions of the bottom slope, m, and the wave steepness, H/L. The relative breaker height, H_b/H'_o, can be found from Figure 42 for the given values of $H'_o/g\ T^2$ and slope, m. (Where the bottom slope varies, choose a representative composite slope for about one wavelength seaward of the breaking point.) The relative breaker depth, d_b/H_b, can then be determined from Figure 43 for the appropriate $H_b/g\ T^2$ and slope, m. For a flat bottom, the breaking-wave height, H_b, is equal to 0.78 d_b.

EXAMPLE PROBLEM 7

Given: a. H'_o = 10 feet
b. T^o = 10 seconds
c. Bottom slope, m = 0.02

Find: The breaker height, H_b, and breaker depth, d_b.

Solution: (1) Compute $H'_o/g\ T^2 = 10/[(32.2)(10)]^2 = 0.00311$

(2) From Figure 42 for $H'_o/g\ T^2 = 0.0031$ and m = 0.02:

$H_b/H'_o = 1.2$

Then $H_b = 1.2\ H'_o = (1.2)(10) = 12$ feet

(3) Find $H_b/g\ T^2$:

$H_b/g\ T^2 = 12/[(32.2)(10)^2] = 0.00373$

(4) From Figure 43 for $H_b/g\ T^2 = 0.0037$ and m = 0.02:

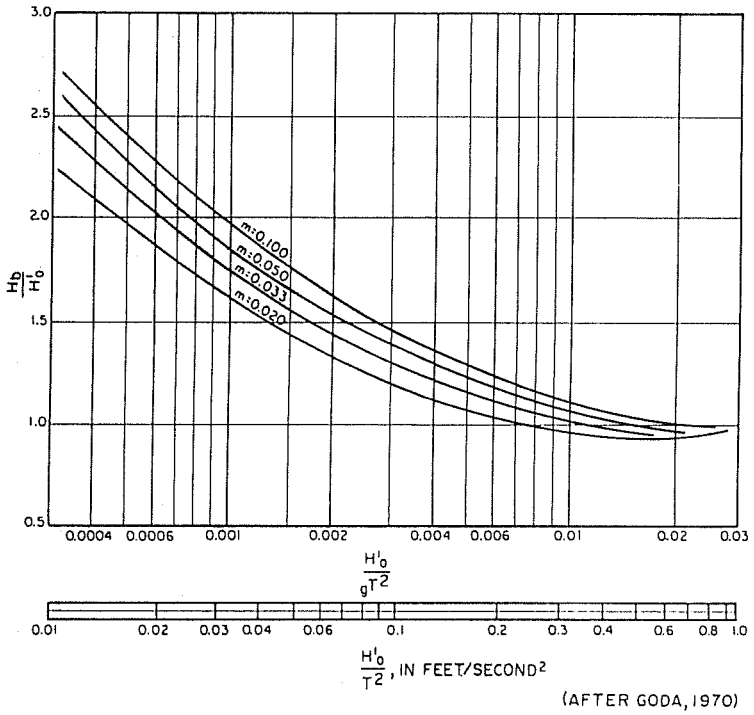

FIGURE 42
Relative Breaker Height, H_b/H'_o, Versus Deepwater Wave Steepness, $H'_o/g\,T^2$

$d_b/H_b = 1.13$

Then $d_b = 1.13\ H_b = (1.13)(12) = 13.6$ feet

Note: Experimental data were used to develop Figure 43. Breaking waves exhibit a great deal of scatter both in nature and in the model. An upper limit of relative breaker depth, d_b/H_b, is given to indicate at what depth the given wave may start breaking. In this example problem, d_b/H_b (max) = 1.5; therefore, $d_b = (1.5)(12) = 18$ feet.

(3) Design Wave Height. Waves propagating over a sloping bottom travel a distance of approximately five wave heights (5 H_b) during the breaking process. In general, larger waves can break in the deeper water seaward of a structure. Therefore, a larger wave height seaward of the toe of a structure should be used for the design wave height in limited-water depth situations. For waves approaching over a bottom with constant slope, design wave height should be determined using Figure 44, along with the wave period, T, and depth from SWL at the structure toe, d_s. For waves approaching over an irregularly sloping bottom either a model study should be conducted, or a representative wave height at a depth five wave heights seaward of the structure should be used.

EXAMPLE PROBLEM 8

Given: A breakwater is located in 10 feet of water (d_s = 10 feet = depth of water at structure toe). The breakwater is fronted by a 1:20 slope (m = 0.05). Analysis of the wave climate indicates that waves approach the site with a period, T, of 5 15 seconds.

Find: The maximum breaking-wave height, H_b, at the structure.

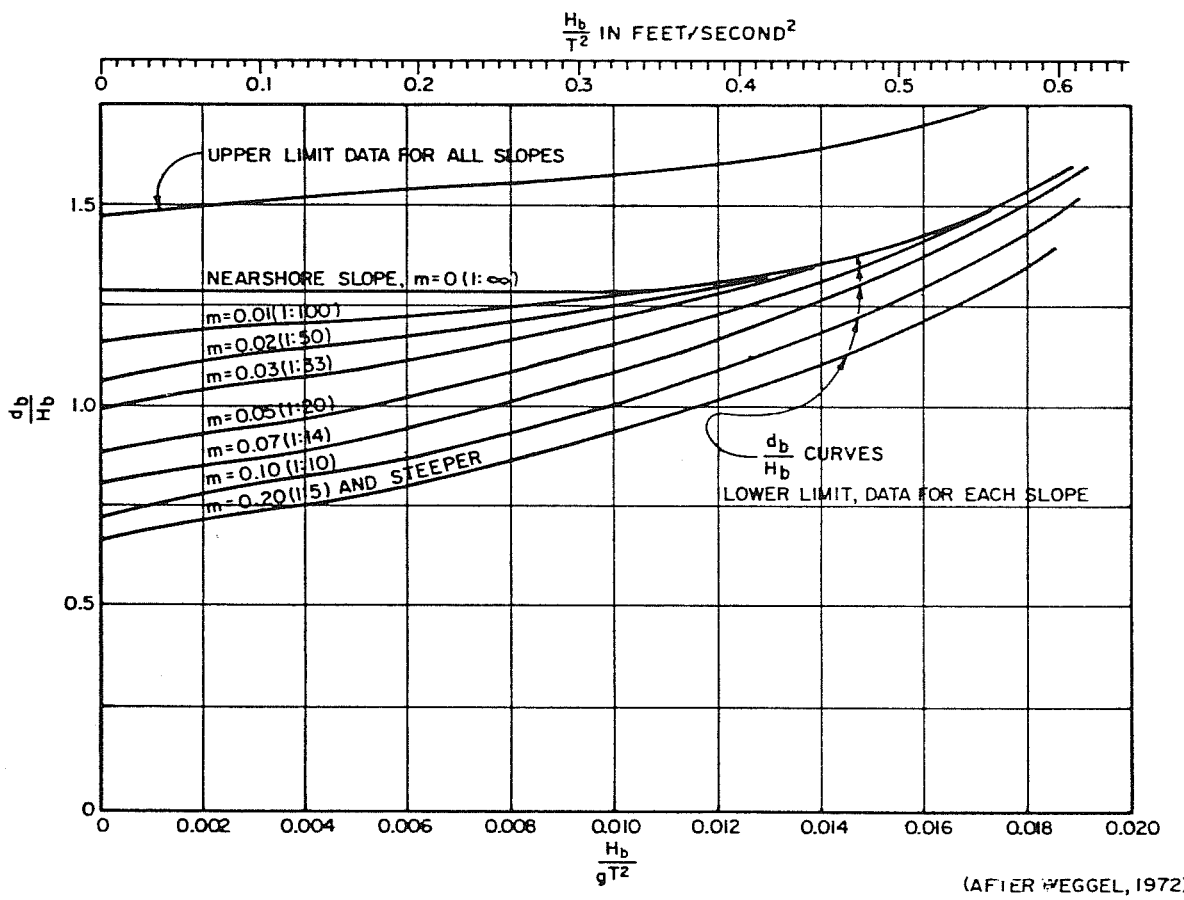

FIGURE 43
d_b/H_b Versus $H_b/g\,T^2$

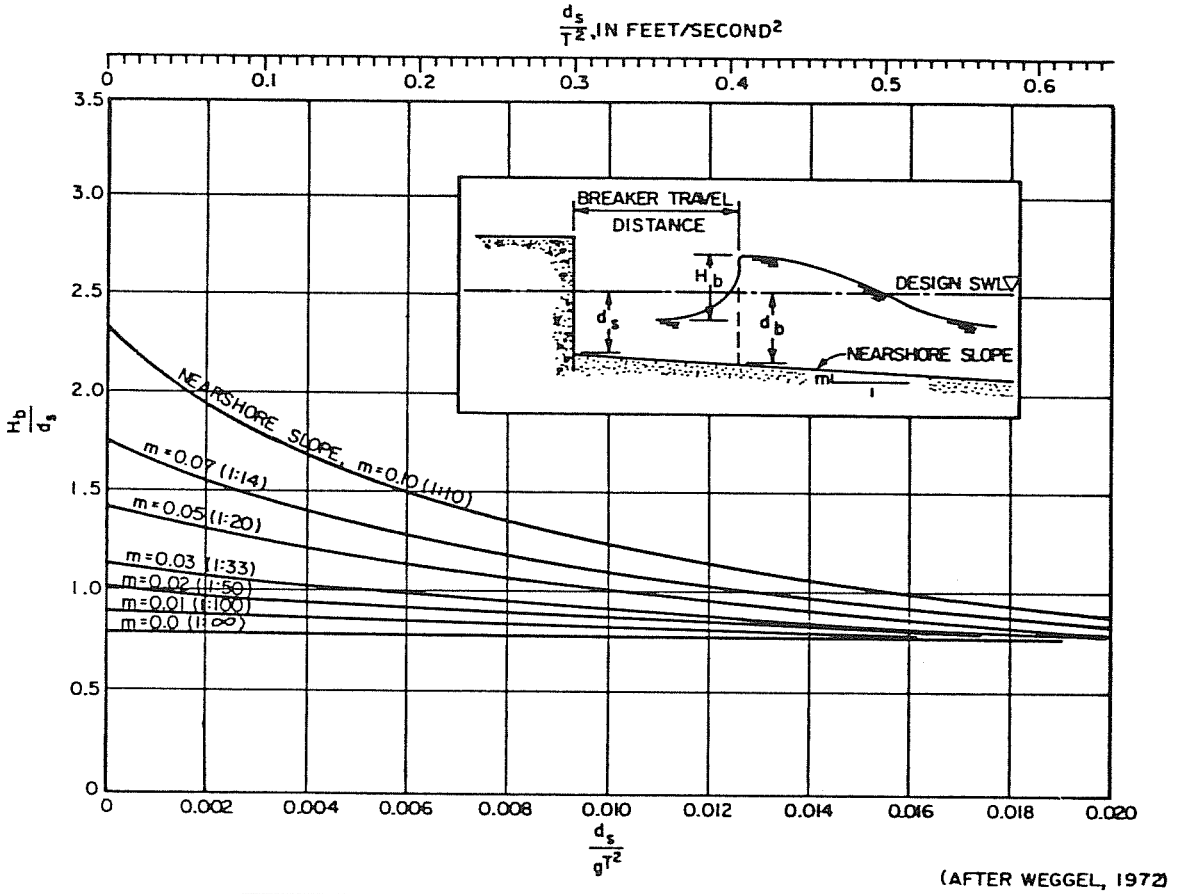

(AFTER WEGGEL, 1972)

FIGURE 44
H_b/d_s Versus $d_s/g\,T^2$

Solution: Use T = 5, 10, and 15 seconds

(1) First, calculate H_b for T = 5 seconds

Then $d_s/g\,T^2 = 10/[(32.2)(5)^2] = 0.0124$

From Figure 44 for $d_s/g\,T^2 = 0.0124$ and m = 0.05:

$H_b/d_s = 0.95$

Then $H_b = 0.95\,d_s = (0.95)(10) = 9.5$ feet

(2) Similarly, $H_b = 12.5$ feet for T = 10 seconds and

$H_b = 13.5$ feet for T = 15 seconds

THEREFORE: Maximum H_b is 13.5 feet.

(3) The maximum wave that can break on the structure has a height of 13.5 feet. However, if the wave climate is such that a 13.5-foot breaking wave could never occur, then there is no need to design for the maximum H_b. Therefore, it is necessary in this problem to see whether at least a 13.5-foot breaking wave is possible. Check wave-climate data to determine if H_o' with T = 15 seconds can form a 13.5-foot breaking wave. For example, if maximum $H_o' = 8$ feet, then:

$H_o'/g\,T^2 = 8/[(32.2)(15)]^2 = 0.00110$

From Figure 42 for $H_o'/g\,T^2 = 0.0011$ and m = 0.05:

$H_b/H_o' = 1.8$

Then $H_b = 1.8\,H_o' = (1.8)(8) = 14.4$ feet

THEREFORE: A 13.5-foot breaking wave can occur on the structure. (The 14.4-foot wave will break seaward of the structure and therefore is not the design wave.) The design wave is $H_b = 13.5$ feet.

8. METRIC EQUIVALENCE CHART. The following metric equivalents were developed in accordance with ASTM E-621. These units are listed in the sequence in which they appear in the text of Section 1. Conversions are approximate.

32.2 feet per second^2 = 9.81 meters per second^2

SECTION 2
DESIGN WAVES

1. GENERAL. A coastal structure should be designed to withstand the wave that induces the highest forces on the structure over its economic life. As a general rule of thumb for breakwaters, revetments, and seawalls, the design wave height is the maximum significant wave height that can occur once in about 20 years. Economic considerations involved in selecting the design wave for a given structure must be evaluated in detail. Waves larger than the significant wave will induce some degree of damage to a rubble-mound structure. The cost and extent of repairs to the structure, as well as potential consequences (economic and otherwise) of damage to shore facilities must be evaluated on an individual basis.

Design waves (that is, design wave height and period) can be determined by hindcasting procedures or by analysis of wave observations. When possible, both procedures should be used and the differences between results should be studied to determine which is the more reliable procedure.

2. WAVE DISTRIBUTION.

a. Significant Wave Height. A given sea will contain many waves differing height, period, and direction of propagation. A spectral approach to design will take some of these variations into account; however, this approach is not commonly used in the United States at present. The deterministic approach does involve some spectral considerations when considering wave-height variations. A representative wave height commonly used in the deterministic approach to design is the significant wave height, H_S. The significant wave height is defined below, followed by a listing of the relationships of other waves in a given sea to the significant height.

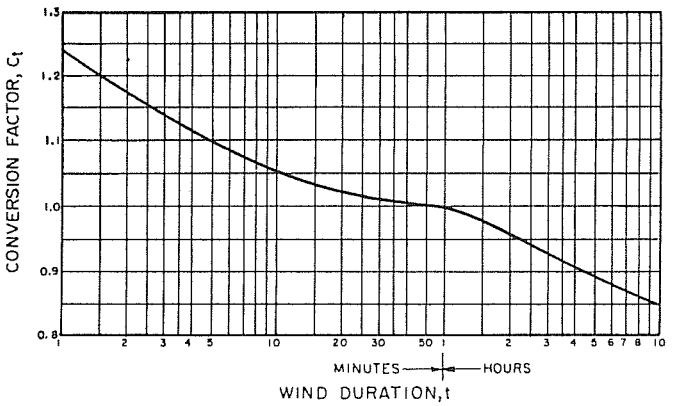

(AFTER U.S. ARMY CORPS OF ENGINEERS, 1981a)

FIGURE 45
Windspeed Conversion Factor, C_t, as a Function of Wind Duration, t

(1) $H_s = H_{1/3}$ = average of highest one-third of all waves;
(2) H = 0.626 H = average wave height;
(3) H_{10} = 1.27 H = average of highest 10 percent of all waves; and
(4) H_1 = 1.67 H_s = average of highest 1 percent of all waves.

The wave height reported by observers on ships has been shown to approximate the significant wave height.

b. Variations in Period or Direction. The wave period is normally taken as a subjective period associated with a hindcasting procedure. Wave direction can vary as much as 90° on either side of the principal wind direction. Variations in period or direction within a given sea condition are generally not taken into consideration in calculations. However, they should be considered if the design is critical to minor variations in either one.

3. WAVE HINDCASTING.

a. **Hindcast Parameters**. Wave hindcasting is the calculation of wave characteristics that probably occurred in the past based on synoptic wind data. Wave hindcasting is an art that is continuing to evolve through theoretical considerations coupled with observations. The important parameters required to estimate a wave condition for a given storm or wind condition are listed below.

(1) Fetch. Fetch, or fetch length, is the area or distance over which a wind field generates seas. The greater the distance, the larger the waves and the longer the period will be for given windspeed and wind duration. The growth of waves (that is, wave heights becoming larger and wave periods becoming longer) may be limited by fetch length.

(2) Windspeed. Windspeed is the sustained windspeed at 32.8 feet, or 10 meters, above the sea surface.

(3) Direction of Wind. Waves are assumed to propagate with the direction of the wind. However, seas may propagate up to 45° from the principal wind direction.

(4) Wind Duration. Waves increase in height and period for given windspeed and fetch, until they become fully arisen. Thereafter, a further increase in duration does not increase wave height or period.

(5) Water Depth. Bottom friction and percolation retard the growth of waves in shallow water.

(6) Decay Distance. Once the waves leave the generating area they decrease in height and the period increases.

b. Hindcasting Procedure. Hindcasts may be made by inferring wind fields from synoptic weather charts or by transforming windspeed data from wind gages. Synoptic weather charts may be obtained from the U.S. Navy Fleet Numerical Weather Central (FNWC) for a given storm. Usually, several years of storms must be analyzed. Description of the procedure for use of synoptic weather charts lies beyond the scope of this manual. (More detailed hindcasting procedures can be found in the Shore Protection Manual (1977).) Where the fetch is defined by an enclosed body of water, such as a bay or lake, and wind observations are available, the procedures outlined below should be employed.

(1) Windspeed. In order to determine the appropriate windspeed for use in hindcasting procedures, depending on the type of wind record available, the following steps should be taken. The result will be the final adjusted windspeed, U_A.

(a) Correction for elevation. If the wind is recorded at an elevation other than 10 meters, then the windspeed at 10 meters, U_{10}, is determined using the following equation:

$$U_{10} = \left(\frac{10}{z}\right)^{1/7} U_z \qquad (2\text{-}1)$$

WHERE:
U_{10} = windspeed at elevation of 10 meters
z = elevation of recorded wind, in meters (z must be < 100 meters for this method to be valid (Bretschneider, 1969)
U_z = windspeed at elevation z

(b) Correction for duration. Recorded windspeeds may vary in definition. For example, recorded windspeeds may be fastest mile, 5-minute average, or instantaneous maximum gust. For use in hindcasting, windspeed must be adjusted so that the average time is equal to or greater than the minimum duration required for the wind to fully develop the waves. This involves an iterative procedure which will be discussed in Example Problem 9. Figure 45 is used to adjust the recorded windspeed of given duration (adjusted to 10-meter elevation) to the value of windspeed, U_t, at the desired duration, where t = wind duration.

$$U_{(t_{desired})} = \left[\frac{C_{(t_{desired})}}{C_{(t_{given})}}\right]\left[U_{(t_{given})}\right] \qquad (2\text{-}2)$$

WHERE:
$U_{(t_{desired})}$ = windspeed at desired duration, adjusted for elevation and duration.
t = wind duration
$C_{(t_{desired})}$ = conversion factor (found from figure 45)
$C_{(t_{given})}$ = conversion factor (found from figure 45)
$U_{(t_{given})}$ = windspeed at given duration, adjusted for elevation

(c) Correction for overland-overwater effects. Windspeed recorded overland (U_L) must be adjusted to obtain the overwater windspeed, U_W. This can be achieved using the following procedure.

If the fetch length is less than or equal to 10 miles:

$$U_W = 1.1\ U_L \quad \text{(for fetch length} \leq 10 \text{ miles)} \qquad (2\text{-}3)$$

WHERE:
U_W = overwater windspeed
U_L = overland windspeed adjusted for elevation and duration

If the fetch length is greater than 10 miles:

$$U_W = R\ U_L \quad \text{(for fetch length} > 10 \text{ miles)} \qquad (2\text{-}4)$$

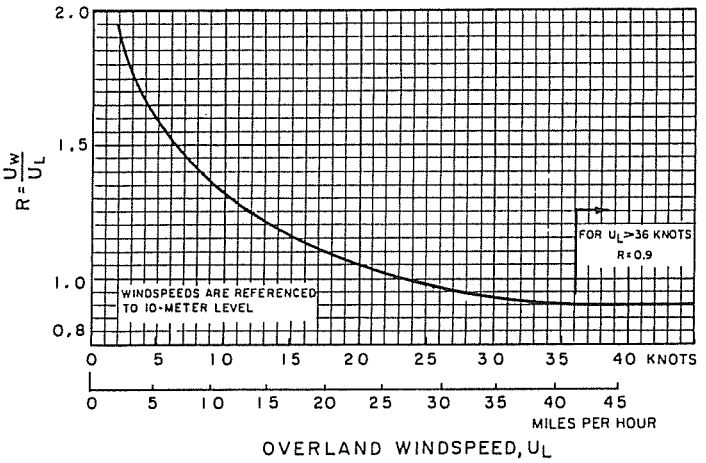

(AFTER RESIO AND VINCENT, 1976)

FIGURE 46
Ratio, R, of Overwater, U_W, to Overland, U_L, Windspeed as a Function of Overland Windspeed, U_L

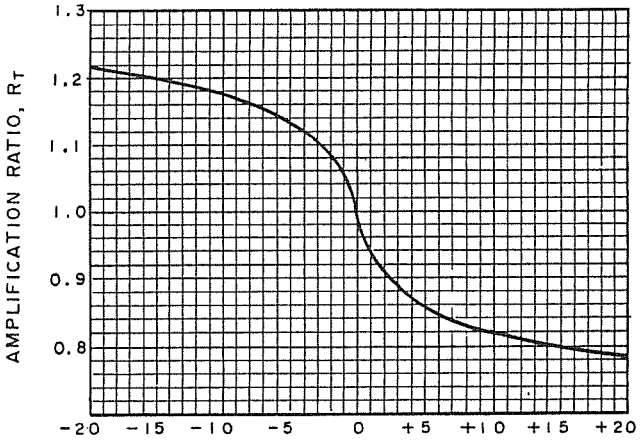

(AFTER RESIO AND VINCENT, 1976)

FIGURE 47
Amplification Ratio, R_T, as a Function of Air-Sea Temperature Difference, $T_a - T_s$

WHERE:

R = U_W/U_L = ratio of overwater windspeed to overland windspeed (found from Figure 46)

(d) Correction for nonconstant drag coefficient. Winds must be adjusted for nonconstant coefficient of drag. This can be accomplished using the following equations:

$$U'_A = 0.608\ U_W^{1.23} \quad \text{(in knots)} \qquad (2\text{-}5)$$

or

$$U'_A = 0.589\ U_W^{1.23} \quad \text{(in statute miles per hour)} \qquad (2\text{-}6)$$

WHERE:

U'_A = windspeed corrected for nonconstant drag coefficient

U_W = windspeed adjusted for elevation, duration, and overland-overwater effects

If the fetch length is less than or equal to 10 miles, then no further adjustment is necessary, and the final adjusted windspeed, U_A, is:

$$U_A = U'_A \text{ (for fetch length} \leq 10 \text{ miles)}$$

WHERE:

U_A = final adjusted windspeed used for hindcasting (for fetch length $\leq$ 10 miles)

(e) Correction for air-sea temperature difference. For fetch lengths greater than 10 miles, an adjustment resulting from the air-sea temperature difference must be made to the windspeed. If the temperature difference is specifically known in degrees centigrade, the amplification ratio, R_T, is determined from Figure 47 from known values of air temperature, T_a, minus water temperature, T_s. The resulting windspeed is:

$$U_A = R_T\ U'_A \text{ (for fetch length} > 10 \text{ miles)} \qquad (2\text{-}7)$$

WHERE:

U_A = final adjusted windspeed used for hindcasting (for fetch length > 10 miles)

R_T = amplification ratio (found from Figure 47)

U'_A = windspeed adjusted for elevation, duration, overland-overwater effects, and nonconstant drag coefficient

If the air-sea temperature difference is not known, the value of R_T may be determined by estimating the condition of the atmospheric boundary layer. If the air is warmer than the water, then the atmospheric boundary layer is assumed stable, and U_A is determined as follows:

$$U_A = 0.9\ U'_A \text{ for stable atmospheric boundary layer} \qquad (2\text{-}8)$$

If the air and water are at the same temperature, then the atmospheric boundary layer is assumed to have neutral stability. U_A for a neutrally stable atmospheric boundary layer is determined as follows:

$$U_A = 1.0\ U'_A$$

for neutrally stable atmospheric boundary layer (2-9)

If the air is cooler than the water, then the atmospheric boundary layer is assumed unstable. For an unstable atmospheric boundary layer:

$$U_A = 1.1\ U'_A$$

for unstable atmospheric boundary layer (2-10)

(2) Fetch Length. Determine the appropriate fetch length, F, by taking the straight-line distance along the axis of the wind to the opposite shore or boundary.

(3) Use of Hindcasting Charts. Values of the significant wave height, H_s, and the wave period, T_p, associated with the highest peak of the wave spectrum, can be determined for a given adjusted windspeed, U_A, fetch length, F, water depth, d, and minimum wind duration, t, using the hindcasting charts presented in Figures 48-58. For water depths greater than 50 feet, wave generation is not greatly affected by depth variations and Figure 48 is used. For water depths less than or equal to 50 feet, Figures 49 through 58 are used. These hindcasting charts plot fetch length, F, on the abscissa and adjusted windspeed, U_A, on the ordinate. Also plotted on the figures are isolines of significant wave height, H_s, peak spectral period, T_P, and minimum duration t.

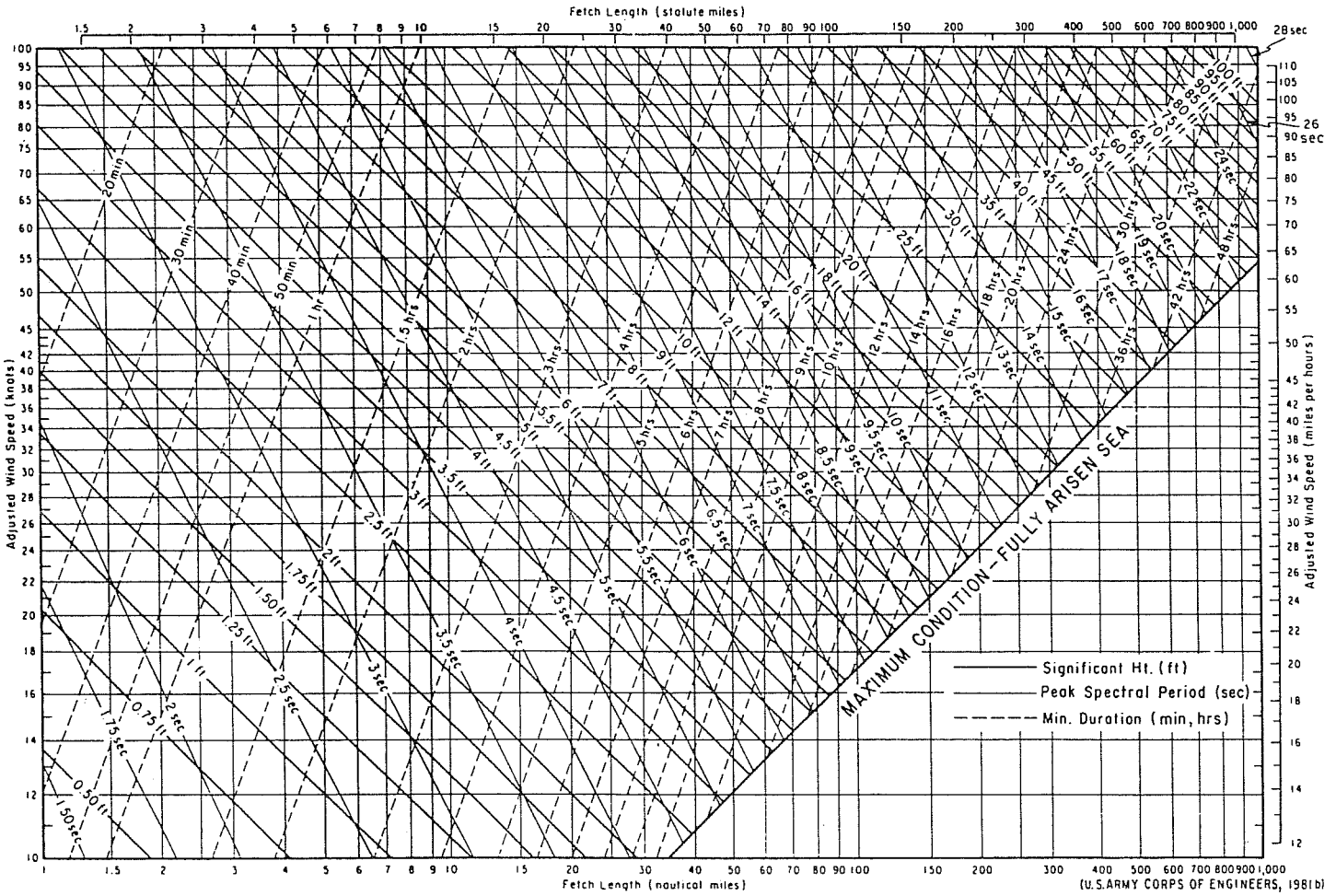

FIGURE 48
Hindcasting Chart for Deepwater Waves (Water Depth > 50 Feet)

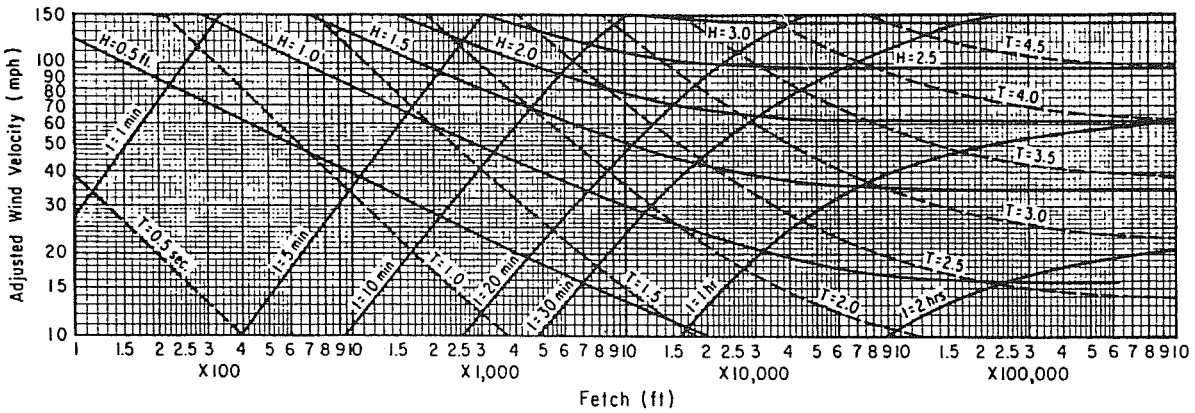

NOTE: WAVES IN A WATER DEPTH OF 5 FEET WITH WAVE PERIODS LESS THAN 1.4 SECONDS ARE CONSIDERED TO BE DEEPWATER WAVES, I.E. $d/T^2 > 2.56$

(U.S. ARMY CORPS OF ENGINEERS, 1981c)

FIGURE 49
Hindcasting Chart for Shallow-Water Waves; Constant Depth = 5 Feet

Jon Guerry Taylor, P.E., Inc.

Marina, Environmental, Permitting and General Civil Engineering Consultants

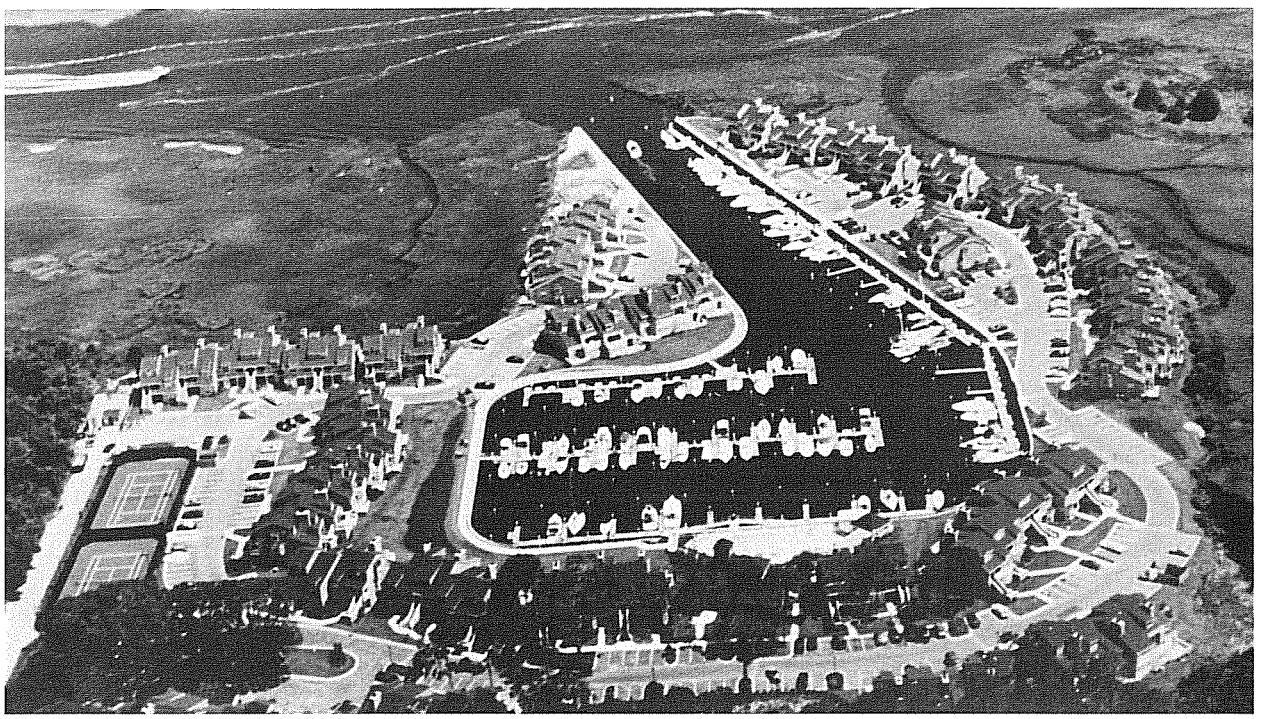

Waterfront Project Services Include:

- Marina Planning and Design
- Federal and State Agency Permitting
- Marina Industry Product Studies and Engineering
- Designs for Docks, Piers, Retaining Walls, Bulkheads, Groins and Revetments
- Dredging Studies and Design
- Marina Project Feasibility Studies
- Environmental (Wetland) Studies Including Mitigation, Remediation, and Restoration
- Marina Evaluations
- Expert Testimony and Special Technical Studies

Charleston County, P.O. Box 1082, Mt. Pleasant, South Carolina 29465
(803) 884-6415
Fax (803) 884-4026

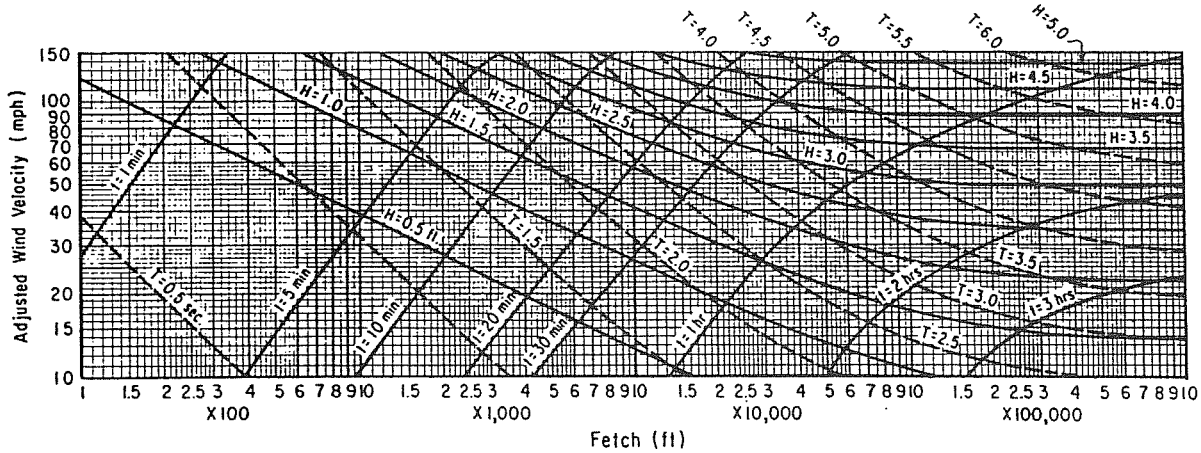

NOTE: WAVES IN A WATER DEPTH OF 10 FEET WITH WAVE PERIODS LESS THAN 2.0 SECONDS ARE CONSIDERED TO BE DEEPWATER WAVES, I.E. $d/T^2 > 2.56$

(U. S. ARMY CORPS OF ENGINEERS, 1981c)

FIGURE 50
Hindcasting Chart for Shallow-Water Waves; Constant Depth = 10 Feet

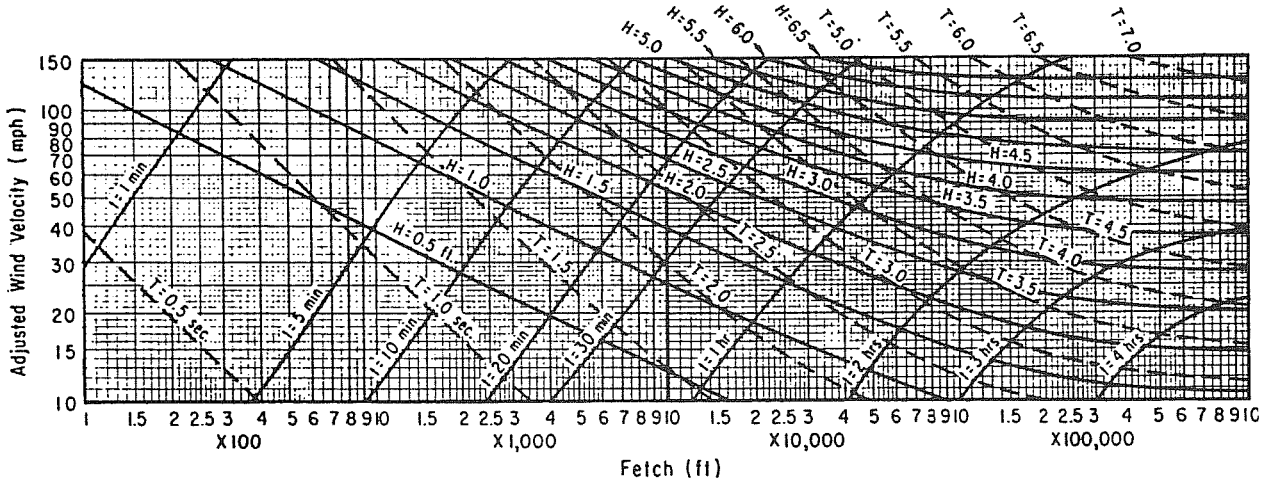

NOTE: WAVES IN A WATER DEPTH OF 15 FEET WITH WAVE PERIODS LESS THAN 2.4 SECONDS ARE CONSIDERED TO BE DEEPWATER WAVES, I.E. $d/T^2 > 2.56$

(U. S. ARMY CORPS OF ENGINEERS, 1981c)

FIGURE 51
Hindcasting Chart for Shallow-Water Waves; Constant Depth = 15 Feet

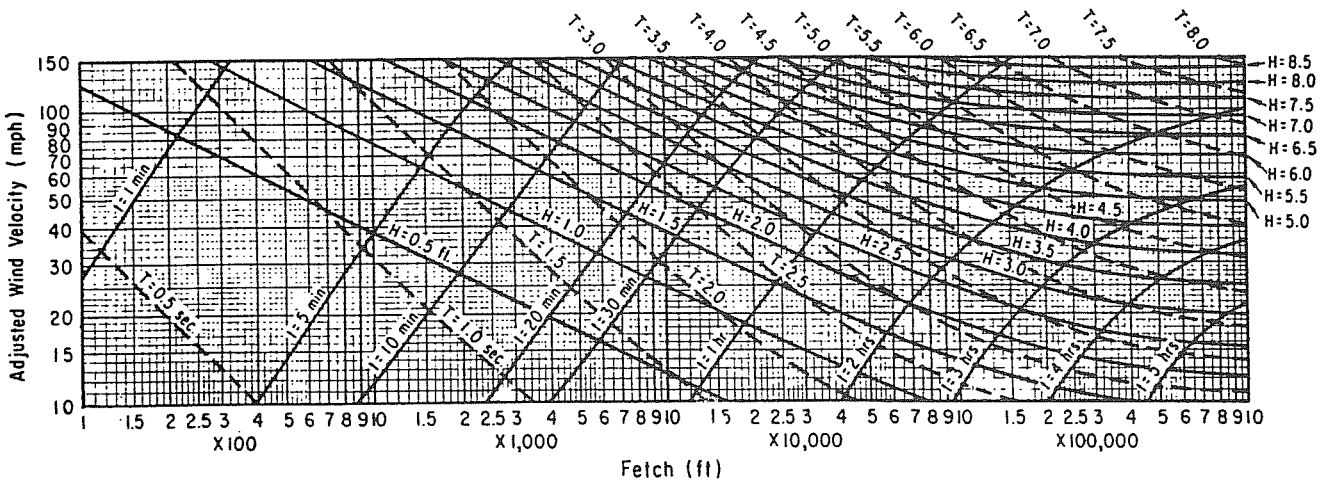

NOTE: WAVES IN A WATER DEPTH OF 20 FEET WITH WAVE PERIODS LESS THAN 2.8 SECONDS ARE CONSIDERED TO BE DEEPWATER WAVES, I.E. $d/T^2 > 2.56$

(U. S. ARMY CORPS OF ENGINEERS, 1981c)

FIGURE 52
Hindcasting Chart for Shallow-Water Waves; Constant Depth = 20 Feet

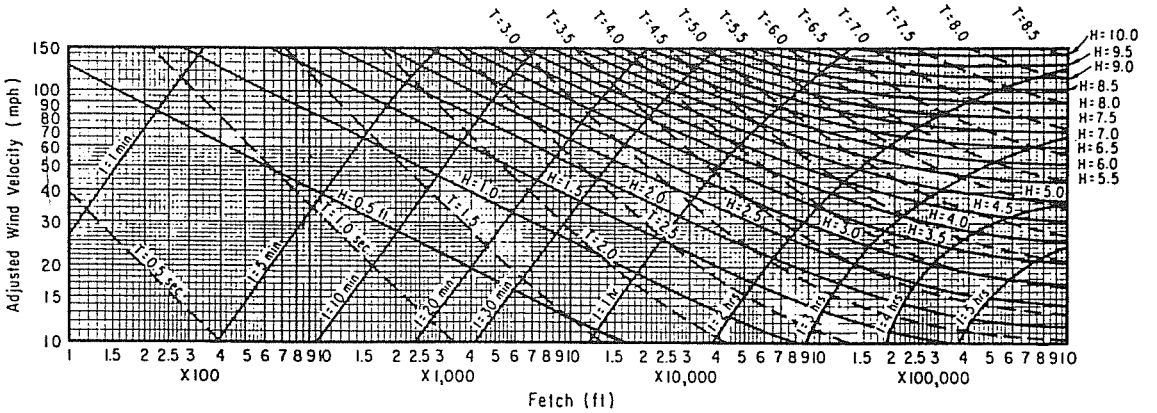

NOTE: WAVES IN A WATER DEPTH OF 25 FEET WITH WAVE PERIODS LESS THAN 3.1 SECONDS ARE CONSIDERED TO BE DEEPWATER WAVES, I.E. $d/T^2 > 2.56$

(U. S. ARMY CORPS OF ENGINEERS, 1981c)

FIGURE 53
Hindcasting Chart for Shallow-Water Waves; Constant Depth = 25 Feet

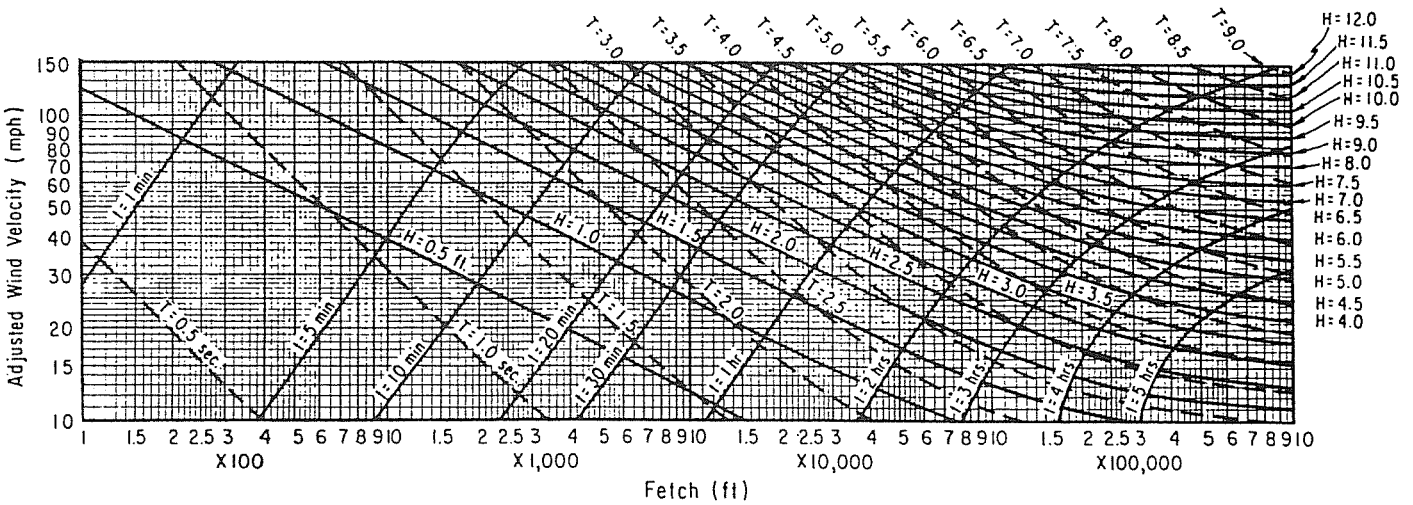

NOTE: WAVES IN A WATER DEPTH OF 30 FEET WITH WAVE PERIODS LESS THAN 3.4 SECONDS ARE CONSIDERED TO BE DEEPWATER WAVES, I.E. $d/T^2 > 2.56$

(U. S. ARMY CORPS OF ENGINEERS, 1981c)

FIGURE 54
Hindcasting Chart for Shallow-Water Waves; Constant Depth = 30 Feet

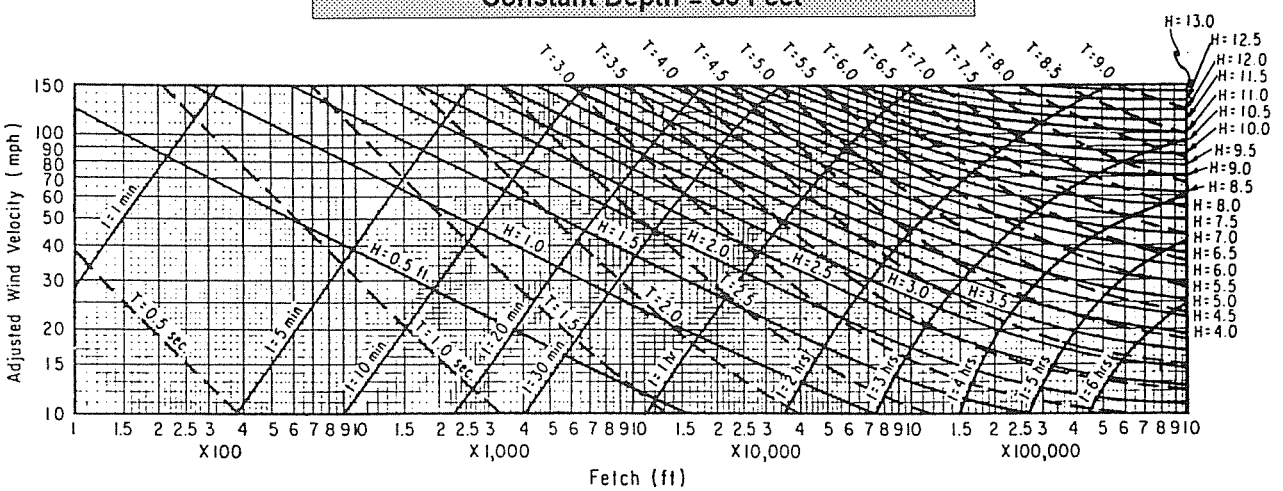

NOTE: WAVES IN A WATER DEPTH OF 35 FEET WITH WAVE PERIODS LESS THAN 3.7 SECONDS ARE CONSIDERED TO BE DEEPWATER WAVES, I.E. $d/T^2 > 2.56$

(U.S. ARMY CORPS OF ENGINEERS, 1981c)

FIGURE 55
Hindcasting Chart for shallow-Water Waves; Constant Depth = 35 Feet

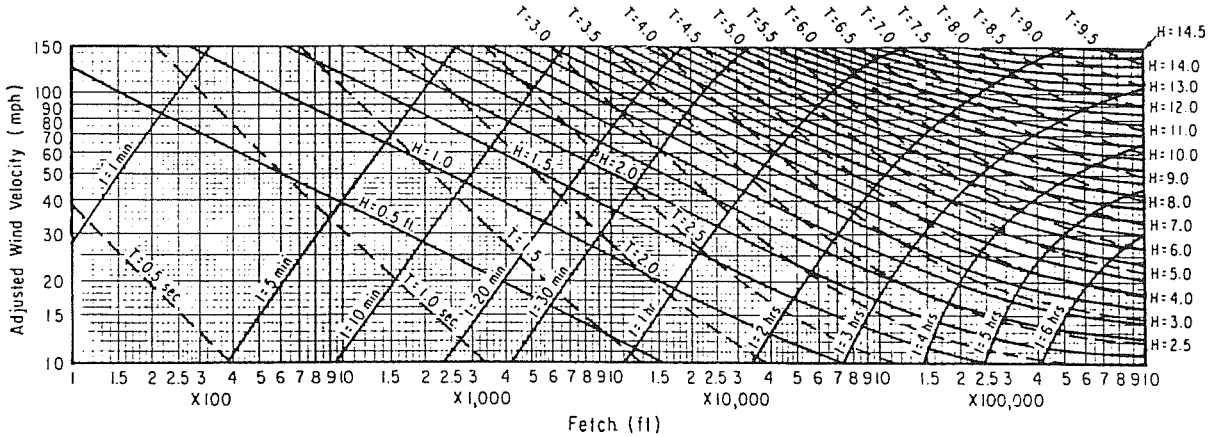

NOTE: WAVES IN A WATER DEPTH OF 40 FEET WITH WAVE PERIODS LESS THAN 4.0 SECONDS ARE CONSIDERED TO BE DEEPWATER WAVES, I.E. $d/T^2 > 2.56$

(U. S. ARMY CORPS OF ENGINEERS, 1981c)

FIGURE 56
Hindcasting Chart for Shallow-Water Waves; Constant Depth = 40 Feet

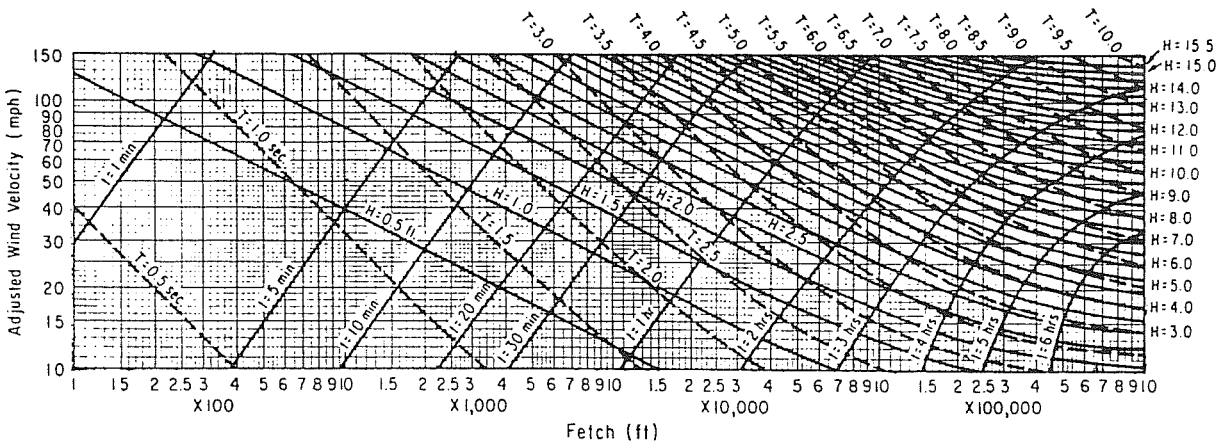

NOTE: WAVES IN A WATER DEPTH OF 45 FEET WITH WAVE PERIODS LESS THAN 4.2 SECONDS ARE CONSIDERED TO BE DEEPWATER WAVES, I.E. $d/T^2 > 2.56$

(U. S. ARMY CORPS OF ENGINEERS, 1981c)

FIGURE 57
Hindcasting Chart for Shallow-Water Waves; Constant Depth = 45 Feet

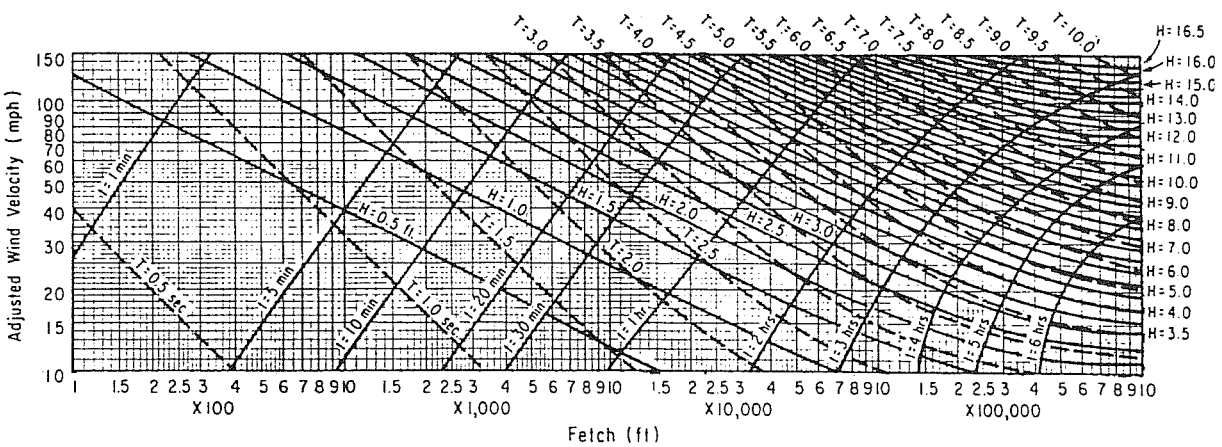

NOTE: WAVES IN A WATER DEPTH OF 50 FEET WITH WAVE PERIODS LESS THAN 4.4 SECONDS ARE CONSIDERED TO BE DEEPWATER WAVES, I.E. $d/T^2 > 2.56$

(U. S. ARMY CORPS OF ENGINEERS, 1981c)

FIGURE 58
Hindcasting Chart for Shallow-Water Waves; Constant Depth = 50 Feet

Wave conditions (or seas) can be either fetch-limited or duration-limited. For hindcasting fetch-limited seas, one enters the abscissa with the fetch length and the ordinate with the adjusted windspeed. Where these intersect, the values for H_s, T_p, and t are read from the chart. When hindcasting from wind observations recorded at an arbitrary duration, the winds should be adjusted to the duration, t. If hindcasting is carried out for a particular storm where winds are known to blow for a specific duration, the duration of the wind must equal or exceed the minimum duration, t, in order for the waves to reach H_s and T_p for a given F and U_A. If the duration of the wind is less than t, then the seas are termed duration-limited. To obtain H_s and T_p for duration-limited seas, one enters the hindcasting chart ordinate with U_A and proceeds to the intersection of the duration value equal to the duration of the storm.

Bathymetry may vary considerably over a large fetch. When the the bathymetry contains extended regions of depths less than or equal to 50 feet, the average depth, at the design water level (see DM-26.1, Section 2.7., for a discussion of design water level) may be used. A better approximation for use in hindcasting waves in variable depths ($\leq$50 feet) is to divide the fetch into discrete intervals of constant depth. Then starting with the first fetch interval, F_1, hindcast the significant wave height, H_s, for the given U_A, F_1, d_1, and t. Using the hindcasted value of H_s at the end of the first interval and the adjusted windspeed, U_A, enter the hindcasting chart for the depth of the next interval, d_2, and determine the corresponding fetch length, F'_1. This is the fetch length required to generate H_s if the water depth had been d_2 in the first interval. To this fetch length, F'_1, add the fetch length, F_2, for the second interval; use the resulting value along with U_A and d_2 for hindcasting H_s at the end of the second interval. Repeat this process for all the fetch intervals making up the total fetch length. The peak spectral period, T_p, and the minimum duration, t, are assumed to be the values obtained at the end of the last fetch interval. The hindcasting procedures are illustrated in Example Problems 9 and 10.

c. Other Considerations. The preceding procedures give estimates of wave characteristics at the end of the fetch. Refraction, shoaling, diffraction, wave-breaking, and economical analyses must be performed to determine the design wave. As the wave propagates out of the generating area, it decays. In general design calculations, wave decay is not important; however, if the wave leaves the generating area and travels great distances over shallow water, wave decay should be considered. The Shore Protection Manual (1977) gives specific guidance on this topic. Waves from tropical cyclones, known as hurricanes or typhoons, may be calculated by equations given in the Shore Protection Manual.

EXAMPLE PROBLEM 9

Given: a. Hourly average windspeed, U_z = 45 knots, measured over land at 10 feet above the ground (t = 1 hour; z = 10 feet)
b. Water temperature, T_s = 15° Centigrade and air temperature, T_a = 24.5° Centigrade
c. Fetch length, F = 35 nautical miles
d. Average water depth, d = 75 feet

Find: The adjusted windspeed, U_A, the significant wave height, H_s, and peak spectral period, T_p.

Solution: (1) Correct for elevation, using Equation (2-1):

$$U_{10} = (10/z)^{1/7} U_z$$

z = (10 feet)(0.3048 meters/foot) = 3.048 meters

$$U_{10} = (10/3.048)^{1/7}(45) = 53.3 \text{ knots}$$

(2) Correct for duration, using Equation (2-2):

The proper duration to use is the minimum duration, t, found from the hindcasting chart for the given conditions. At this point a duration must be assumed. After hindcasting, the minimum duration, t, read from the chart should be equal to the assumed duration. If not, the process should be reiterated until the values of duration are equal.

From Figure 48 for U_{10} = 53.3 knots and F = 35 nautical miles:

t = 4.4 hours = desired duration = $t_{desired}$

From Figure 45 for t = 4.4 hours (desired duration):

Conversion factor, $C_t = C_{(t_{desired})} = 0.9$, where t = 4.4 hours;

therefore, $C_{(t = 4.4 \text{ hours})} = 0.9$

From Figure 45 for t = 1 hour (given duration):

Conversion factor, $C_t = C_{(t_{given})} = 1.0$, where t = 1 hour;

therefore, $C_{(t = 1 \text{ hour})} = 1.0$

$$U_{(t = 4.4 \text{ hours})} = \left[\frac{C_{(t = 4.4 \text{ hours})}}{C_{(t = 1 \text{ hour})}}\right]\left[U_{(t = 1 \text{ hour})}\right]$$

$$U_t = \left(\frac{0.9}{1.0}\right)(53.3) = 47.97 \text{ knots}$$

(3) Correct for overland-overwater effects:

From Figure 46 for $U_t = U_L$ = 47.97 knots:

R = 0.9

Using Equation (2-4):

$$U_W = R\, U_L$$

$$U_W = (0.9)(47.97) = 43.17 \text{ knots}$$

(4) Correct for nonconstant drag coefficient:

Using Equation (2-5):

$$U'_A = 0.608\, U_W^{1.23}$$

$$U'_A = (0.608)(43.17)^{1.23} = 62.40 \text{ knots}$$

(5) Correct for air-sea temperature difference:

T_a = 24.5° C

T_s = 15° C

$T_a - T_s$ = 24.5°C − 15°C = +9.5° C

From Figure 47 for $T_a - T_s$ = + 9.5°C:

R_T = 0.82

Using Equation (2-7):

$$U_A = R_T\, U'_A$$

$$U_A = (0.82)(62.40) = 51.17 \text{ knots}$$

(6) Determine H_s, T_p, and t:

From Figure 48 for U_A = 51.17 knots and F = 35 nautical miles:

H_s = 11.4 feet

T_p = 7.4 seconds

t = 4.4 hours

THEREFORE: Assumed value of t = 4.4 hours was a good value and no further iteration is required. If the duration differed considerably then the new value of t from Figure 48 would be assumed for the duration of the wind and the process would be repeated until the answer converged.

EXAMPLE PROBLEM 10

Given: a. Fetch interval, F_1 = 90,000 feet with d_1 = 35 feet
b. Fetch interval, F_2 = 60,000 feet with d_2 = 25 feet
c. Fetch interval, F_3 = 60,000 feet with d_3 = 20 feet
d. Adjusted windspeed, U_A = 40 miles per hour

Find: The significant wave height, H_s, at the end of fetch interval, F_3.

Solution: For fetch F_1 = 90,000 feet, U_A = 40 miles per hour, and d_1 = 35 feet, use Figure 55:

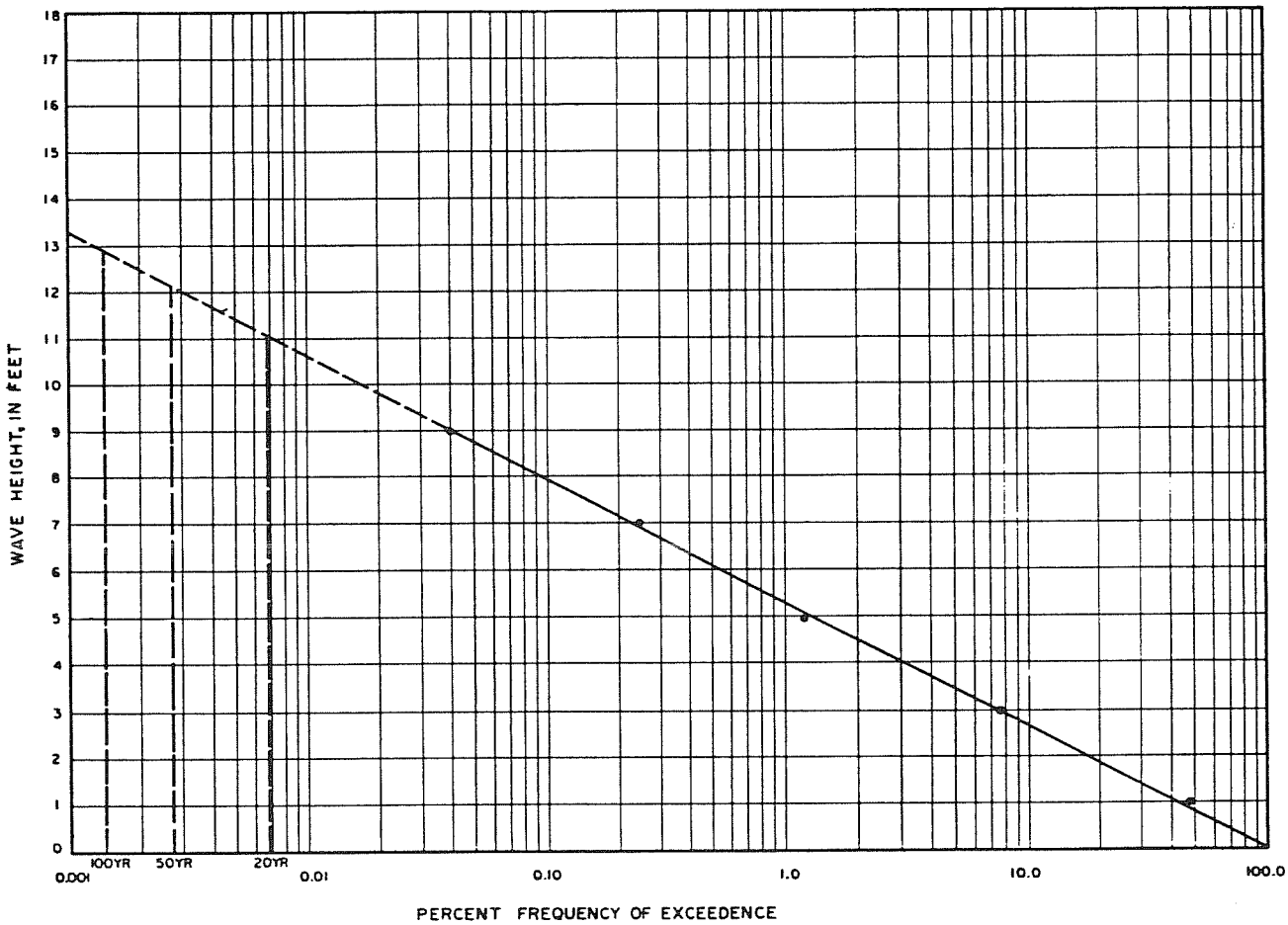

FIGURE 59
Frequency of Exceedence Curve, and 20-, 50-, and 100-Year Design Wave Heights, for Example Problem 11

H_{s_1} = 4.2 feet at the end of F_1

Entering Figure 53 (for d_2 = 25 feet) with U_A = 40 miles per hour and H_s = 4.2 feet:

F_1' = 130,000 feet

To obtain H_{s_2} at the end of F_2, enter Figure 53 (for d_2 = 25 feet) with U_A = 40 miles per hour and $F = F_1' + F_2$ = 130,000 + 60,000 = 190,000 feet:

H_{s_2} = 4.5 feet at the end of F_2

Entering Figure 52 (for d_3 = 20 feet) with U_A = 40 miles per hour and H_s = 4.5 feet:

F_2' = 420,000 feet

To obtain H_{s_3} at the end of F_3, enter Figure 52 (for d_3 = 20 feet) with U_A = 40 miles per hour and $F = F_2' + F_3$ = 420,000 + 60,000 = 480,000 feet

H_s = 4.5 feet at the end of F_3

4. SOURCES FOR WAVE OBSERVATION DATA. The U.S. Naval Weather Service Command conducts a program to publish a Summary of Synoptic Meteorological Observations (SSMO) based upon shipborne observations. The observations are given over a specified time period, usually 10 to 30 years, and within a certain geographical area. Data are presented in tables. Table 18 of the SSMO gives percent frequency of occurrence of wave height by season and direction as a function of windspeed. Table 19 of the SSMO gives percent frequency of occurrence of wave period as a function of wave height. Wave distributions can be estimated by use of these tables for large geographic areas covering grids of several degrees. The tables give observed values which are assumed to be significant heights and periods. However, caution should be exercised because ships may avoid waters with high waves and reporters often overlook a swell condition when a local wind wave obscures the swell. Data sources are as follows:

(1) In areas where heavy shipping occurs, data may be requested in specific grids of 1 degree of other larger- or smaller-degree grids at the National Climatic Center, Federal Building, Asheville, North Carolina 28801.

(2) Another source of wave data is Ocean Wave Statistics by Hogben and Lumb, London, Her Majesty's Stationery Office, 1967.

(3) The U.S. Navy Fleet Numerical Weather Central in Montery, California, may be consulted to obtain wave hindcasts for specific stations where data have been compiled.

(4) Other sources may include results of wave-gage analyses, as well as special reports and studies of hindcasts for specific locations. These must be obtained through a local source or through a search of available literature.

5. EXTREME WAVES. Selection of the design wave either requires proof that the wave height is limited by water depth or an analysis to determine the frequency of occurrence of waves in deeper water. Generally, wave-gage data sets are

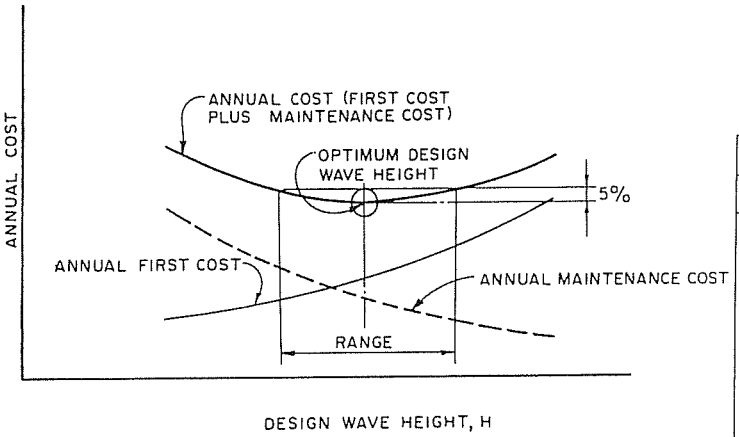

FIGURE 60
Selection of Optimum Design Wave Height

limited to 1 to 3 years of data. Shipborne observations may cover a 10- to 30-year range. Synoptic charts of extreme storm events may cover a 20- to 40-year period or more. The recurrence interval, or period of time that a given wave height should be exceeded based on statistics of past observations, is required in order to select the design wave and estimate damages if that wave height be exceeded. The normal procedure is to determine the percent frequency that the wave heights in the data set are exceeded. These data are typically plotted on, for example, lognormal, semilog, log-probability, or normal-probability graph papers. The percent frequency of exceedence must then be related to a recurrence interval in years. This is easily done if the maximum storm every year is known, or if a set of extreme storms in a given period is given. An additional assumption is required if the data are given in hours or percent occurrence per year. Normal design procedures use from 3 to 12 hours duration per year for the annual significant wave. The choice depends upon judging the factors of minimum duration that are required to develop a fully arisen sea for the design wind and fetch, the frequency of observations, and the consequences of damage if a slightly lower design wave is selected.

EXAMPLE PROBLEM 11

Given: Summary of wave statistics for all directions as shown in Table 2.

Find: Draw frequency of exceedence curve for wave height and determine design 20-, 50-, and 100-year wave heights for all directions.

Solution: Beginning with the second highest wave class (8 to 9 feet), subtract the cummulative total (99.96) of this wave class from 100. Plot this value (0.04) on semilogarithmic paper at the highest wave in that class (H = 9 feet). For the next wave class (6 to 7 feet), follow the same procedure and plot this value (0.24) at H = 7 feet. Continue for all wave classes, and then draw the best possible line through the points. This line, shown in Figure 59, is the frequency of exceedence curve.

To determine design wave heights, begin by extrapolating the frequency of exceedence curve back. The following percentages of occurrence for 20-, 50-, and 100-year storms were calculated (assuming a duration of 12 hours for a storm):

$$\text{20-year: } \left[\frac{12 \text{ hours}}{(365 \frac{\text{days}}{\text{year}})(24 \frac{\text{hours}}{\text{day}})(20 \text{ years})}\right](100) = 0.00685\%$$

$$\text{50-year: } \left[\frac{12 \text{ hours}}{(365 \frac{\text{days}}{\text{years}})(24 \frac{\text{hours}}{\text{day}})(50 \text{ years})}\right](100) = 0.00274\%$$

$$\text{100-year: } \left[\frac{12 \text{ hours}}{(365 \frac{\text{days}}{\text{year}})(24 \frac{\text{hours}}{\text{day}})(100 \text{ years})}\right](100) = 0.00137\%$$

TABLE 2
Percent Frequency of Occurrence for Example Problem 11 (10 Years of Data; 1,825 Observations)

Wave Height (feet).....	0-1	2-3	4-5	6-7	8-9	10
Direction						
N.....	2.50	1.63	0.90	0.01	0.01	0.00
NE.....	5.10	3.20	2.00	0.05	0.01	0.01
E.....	8.98	6.51	1.30	0.54	0.12	0.02
SE.....	11.22	8.10	1.30	0.03	0.03	0.01
S.....	14.61	10.81	0.10	0.02	0.02	0.00
SW.....	3.92	4.82	0.20	0.10	0.01	0.00
W.....	3.46	4.00	0.30	0.20	0.00	0.00
NW.....	2.01	1.33	0.50	0.01	0.00	0.00
Total	51.80	40.40	6.60	0.96	0.20	0.04
Cumulative Total	51.80	92.20	98.80	99.76	99.96	100.00

The 20-, 50-, and 100-year design wave heights can be found directly from the frequency of exceedence curve by reading the wave height at the respective percentage of occurrence. Thus the 20-, 50-, and 100-year design wave heights are 11.1, 12.2, and 12.9 feet, respectively. (See Figure 59.) It should be noted that in areas of typhoon or hurricane activity, more detailed studies may be required.

6. SELECTION OF DESIGN WAVES.

a. **Selection**. The selection of design waves should be related to the economics of construction, maintenance, and repairs. For small projects, a 20- to 25-year design wave, coupled with an annual extreme water level, is appropriate. In special cases, such as over a coral reef or in the breaker zone, the design water level may control the design wave height. (See DM-26.1, Section 2.7, for a discussion of design water level).

b. **Large Projects**. The selection of design conditions for larger structures requires more detailed consideration of the economics of the design. Wave analysis yields the recurrence interval of a given wave height. If, for example, the design wave height having a recurrence interval of 20 years is 10 feet, then a wave having a 30-year recurrence interval and height of 15 feet will damage the structure. The economics of increasing the first cost versus making occasional repairs must be evaluated. Furthermore, cost and extent of damages to areas that the structure is designed to protect must also be considered. The physical and economic factors, such as design wave height versus annual costs, must be optimized.

The principle of optimization is schematically shown in Figure 60, where annual cost is plotted as a function of design wave height. The plot is made by designing the structure for a range of wave heights. As the design wave height increases, first cost of the structure increases. (The first cost must be related to an annual cost. This is accomplished by amortizing the first cost by using an appropriate interest rate and time period.) The annual maintenance cost will decrease if the structure is designed for a larger wave. This curve is difficult to plot accurately because several arbitrary decisions must be made concerning how many times in the life of the structure repairs must be made and how much maintenance costs would be. By making reasonable assumptions, or at least by incorporating the principal of optimization into the design, a selection of the design wave can be made by adding the annual maintenance cost and the annual first cost to produce a third curve which represents the annual cost of the structure. The designer then can identify the wave height which represents the least annual cost. Some of the decisions involved in arriving at this optimum design wave height are arbitrary and not based on hard data regarding maintenance costs; therefore, some latitude should be permitted in the selection of the design wave height using the optimization procedure. If the cost varies 5 to 10 percent, the optimum design wave would have a range of heights. The designer should use other factors to

TABLE 3
General Factors for Wave-Height Selection

Type of Structure	Wave Height[1]	Example
Nonrigid: minor damage to armor units can be tolerated without threat to the function of the structure	H_s	Rubble-mound breakwaters and revetments; pile-supported structures
Semirigid: the structure can absorb some excessive wave force without catastrophic failure	H_{10}	Cellular sheet-pile walls
Rigid: damage may cause complete failure if the design wave is slightly exceeded	H_1	Cantilever sheet-pile walls; braced sheet-pile walls

[1]Wave heights are defined in Section 2.2.a., Significant Wave Height.

help select the proper design condition, such as environmental, operational, and maintenance considerations.

This procedure need not be strictly employed; however, the designer should consider the principles involved in selecting the optimum design. Such an analysis should prevent selection of a 1,000-year return period typhoon wave for design of a small boat harbor, or a 1-year return period sea for design of a cargo-wharf piling system.

c. Wave-Height Variability. Most wave-transformation studies calculate the significant wave height, H_S, at the project site. Wave systems have a wave-height distribution where the significant height is exceeded. The rigidity of the structure, or its ability to withstand an occasional larger wave, must be evaluated. Table 3 summarizes general guidance for selecting the appropriate wave height.

7. METRIC EQUIVALENCE CHART. The following metric equivalents were developed in accordance with ASTM E-621. These units are listed in the sequence in which they appear in the text of Section 2. Conversions are approximate.

32.8 feet = 10 meters
10 miles = 16.1 kilometers
50 feet = 15.2 meters
10 feet = 3.0 meters
15 feet = 4.6 meters

SECTION 3
BASIC PLANNING

1. GENERAL. The type of structure required for a particular design situation depends upon the protection required, such as harbor protection, beach erosion control, and stabilization of an entrance channel. Table 4 describes the primary types of coastal structures and their function. In many cases, more than one type of structure may provide a possible solution. Studies of alternative solutions, including consideration of first and annual costs, maintenance, construction methods, and environmental impacts, should be conducted to select the most appropriate one. Figures 61 through 67 give examples of typical uses and construction of each structure type. Selection of the structure type requires that the foundation condition, availability of construction materials and equipment, and probable impacts on the adjacent shores be considered.

TABLE 4
Primary Types of Coastal Structures

Structure	Function
Breakwaters.....	Primary applications of breakwaters are to provide protection against waves for shore areas, harbors, anchorages, and basins, and to enable maintenance-dredging operations. A secondary purpose is beach erosion control.
Jetties.....	Jetties are devices parallel to a navigation channel used to protect the channel from shoaling with littoral drift and to stabilize the entrance to a tidal inlet. They may also provide wave and wind protection and direct or confine the flow of river or tidal currents. Sand by-passing of jettied inlets is often necessary to preclude erosion of the downdrift coast.
Revetments, bulkheads, and seawalls.....	These structures are used to protect embankments or shore structures from eroding or from damage due to wave attack or currents and to retain or prevent sliding of land. Revetments are generally rubble construction. Seawalls and bulkheads are generally more rigid structures constructed of steel, concrete, or timber. Another design for seawalls is to use Igloos, patented by Nippon Tetrapod (see Figure 65). Igloos can be used as space-saving wave absorbers or breakwaters. Prefabricated concrete units have been used successfully as wave-dissipating walls in harbors.
Groins.....	Groins are used to protect the coast from erosion and to retard or control littoral transport to stabilize a beach. Groin fields should generally be filled with imported material to preclude erosion of the downdrift coast.
Headlands.....	Headlands are high, steep-faced border points of land extending into the ocean or other body of water. Large segments of shorelines can be stabilized by construction of artificial headlands.
Beach restoration and nourishment.....	Beaches that are eroding due to an interrupted or inadequate sand source can be stabilized by deposition of sand brought from a source on land or of dredged materials.

2. ENVIRONMENTAL CONSIDERATIONS.

a. Discussion. The Coastal Zone Management (CZM) Act of 1972, PL 92-583, establishes a national policy to preserve, protect, develop, and, where possible, restore and enhance the resources of the coastal zone of the United States. DOD Instruction 4165.59 of 29 December 1975 authorized the Navy to implement programs to achieve the objectives of PL 92-583. The Navy will cooperate and provide information on Navy programs with the coastal zone to states responsible for developing state CZM plans. Naval operations, activities, projects, or programs affecting coastal lands or waters shall insure that such undertakings, to the maximum extent practicable, comply with state-approved coastal-zone programs.

b. Guidelines and Standards.

(1) All natural resources management programs on naval installations in the coastal zone have potential effects on the coastal zone and should be reviewed for consistency with approved state Coastal Zone Management plans. The Navy shall develop, in cooperation with a designated state agency, a set of criteria and standards for judging the consistency of natural resource management programs with respect to approved state management programs. Consistency determinations shall be made in accordance with provisions of PL 92-583.

(2) Agricultural outlease of real property affecting land or water uses in the coastal zone shall provide a certification that the proposed use complies with the coastal state's approved program and that such usage will be conducted in a manner consistent with the program.

(3) Technical assistance requested by the states to assist their implementation of CZM will be provided to the extent practicable. Data collected by the NAVY on subjects such as beach erosion, hydrology, meteorology, and navigation may

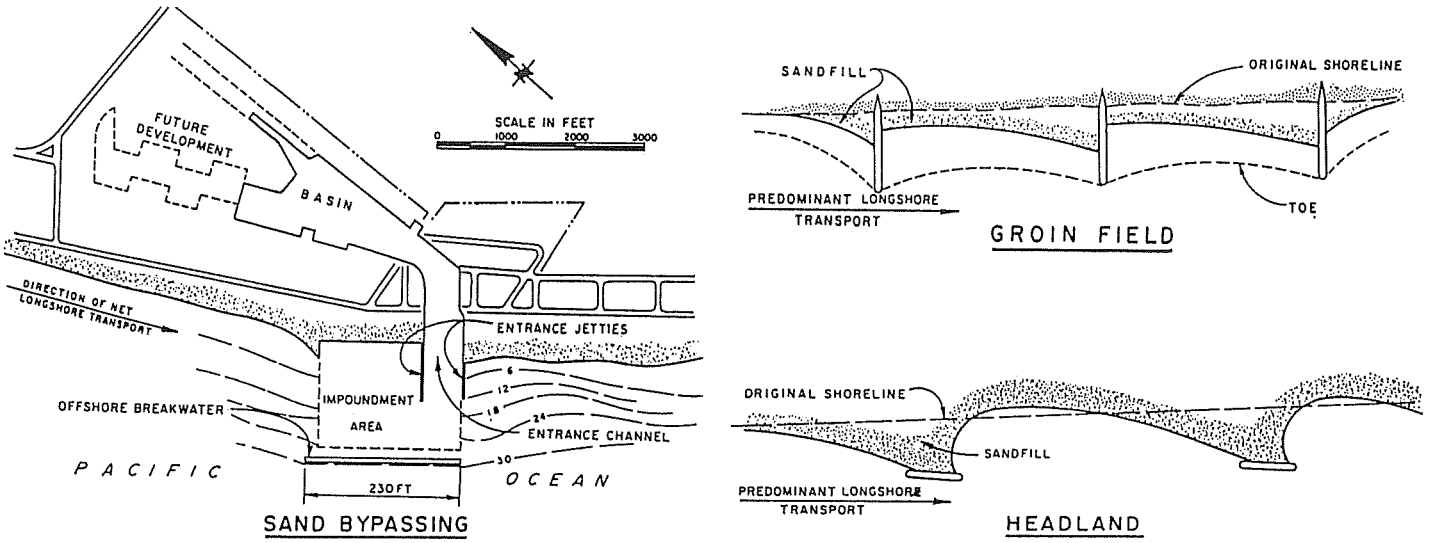

FIGURE 61
Typical Uses of Breakwaters, Jetties, Groins, and Artificial Headlands in Coastal Protection

be useful for coastal-zone planning and shall be made available.

3. FUNCTIONAL DESIGN. To be effective, a breakwater must be built to a high enough elevation and be impermeable to the extent that waves transmitted to the lee side are attenuated to acceptable levels. Wave transmission studies are required to determine appropriate crest elevations. If design criteria stipulate that a breakwater or revetment is not to be overtopped, wave-runup studies are required. Wave-runup calculations, coupled with observations at neighboring structures and beaches, are required to determine the crest elevation of a structure or the berm elevation of a protective beach. If wave overtopping can cause flooding or undesirable ponding of water, calculations of overtopping quantities are required. Methods for calculating wave runup

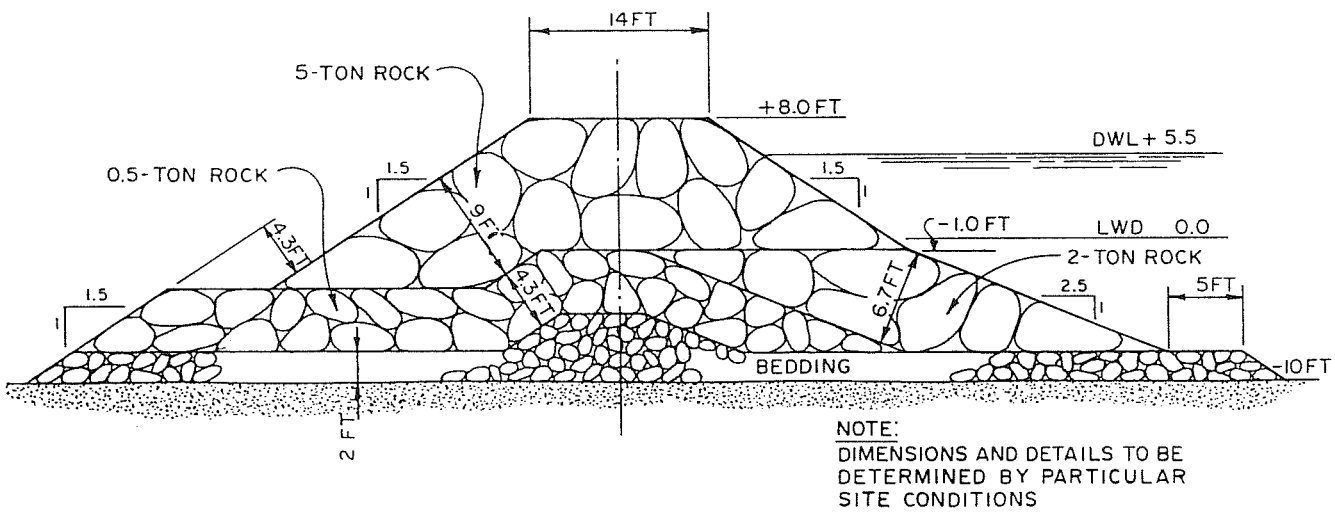

FIGURE 62
Typical Breakwater Section

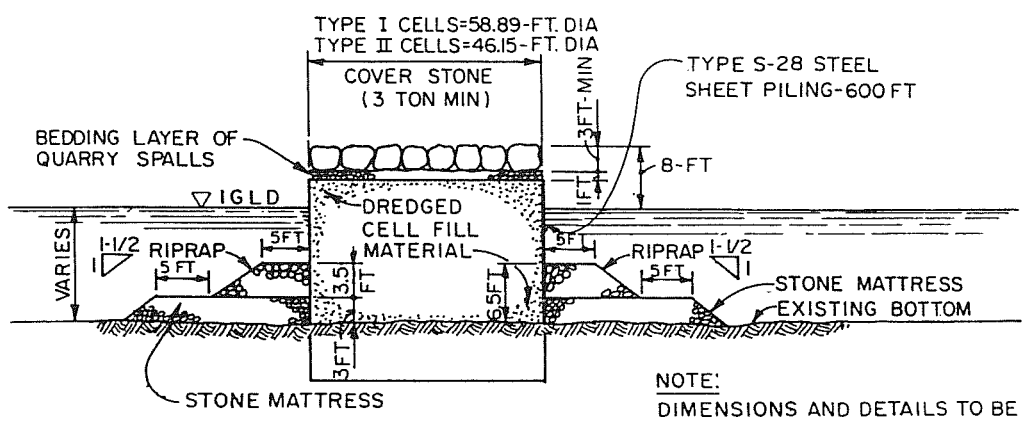

(AFTER SHORE PROTECTION MANUAL, 1977)

FIGURE 63
Typical Cellular Sheet-Pile Jetty

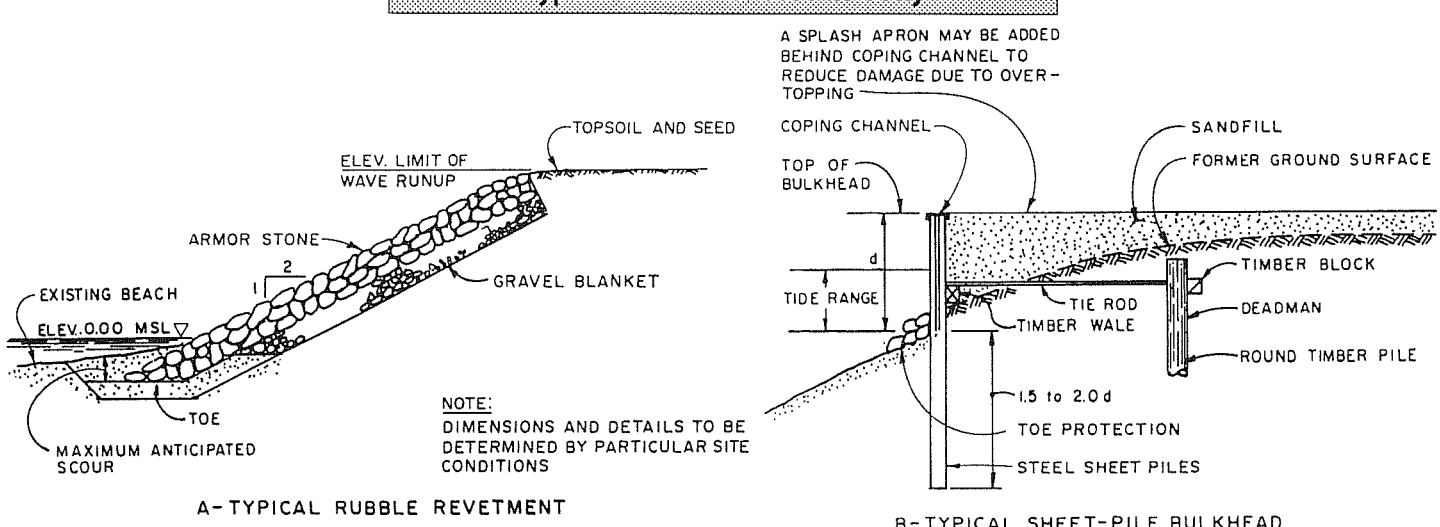

A-TYPICAL RUBBLE REVETMENT
(AFTER SHORE PROTECTION MANUAL, 1977)

B-TYPICAL SHEET-PILE BULKHEAD

FIGURE 64
Typical Rubble Revetment and Typical Sheet-Pile Bulkhead

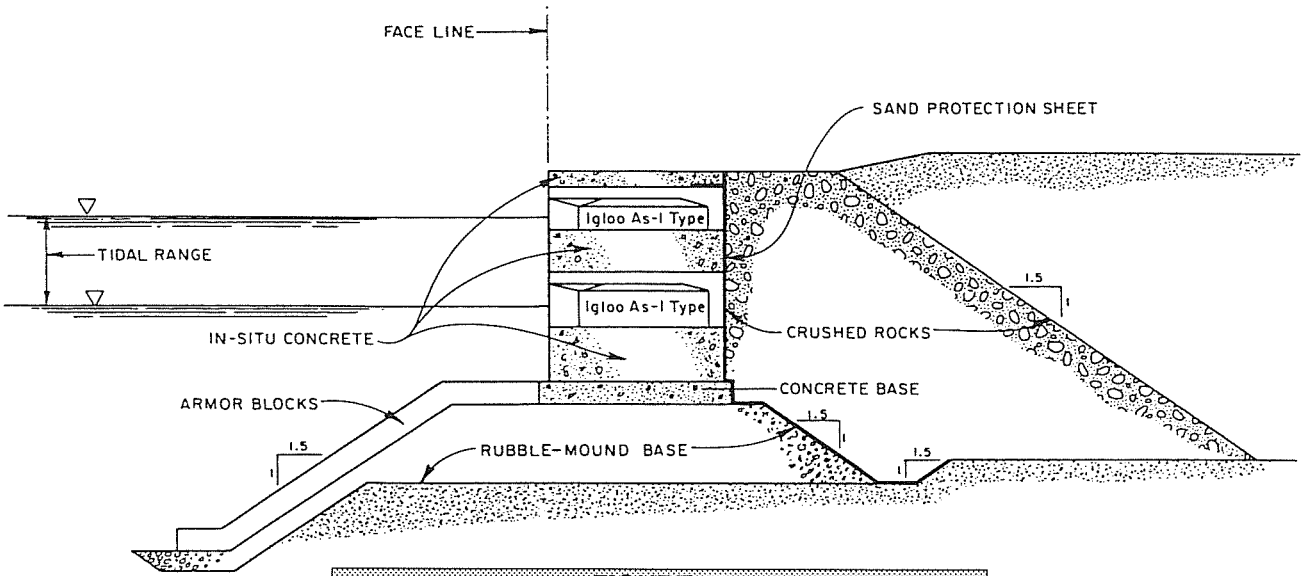

FIGURE 65
Typical Igloo Seawall

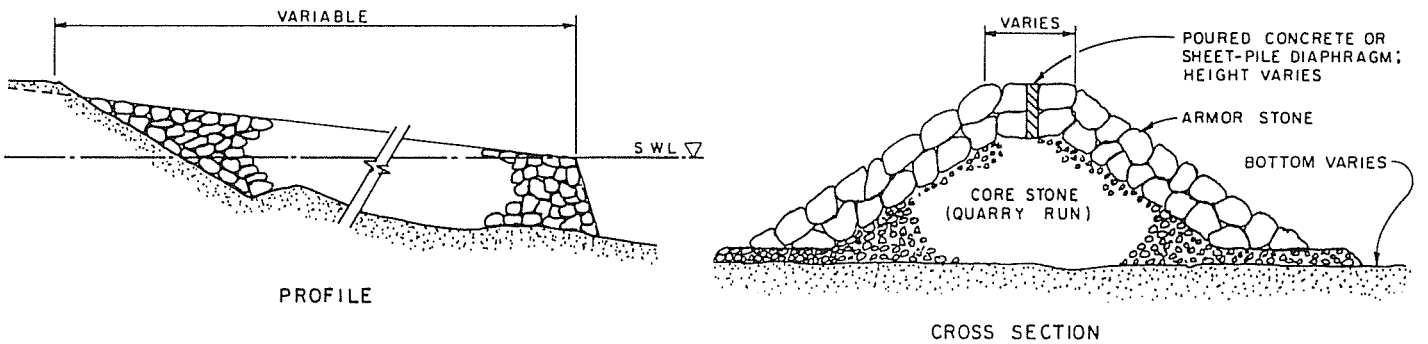

NOTE:
DIMENSIONS AND DETAILS TO BE DETERMINED BY PARTICULAR SITE CONDITIONS

(AFTER SHORE PROTECTION MANUAL, 1977)

FIGURE 66
Typical Rubble-Mound Groin

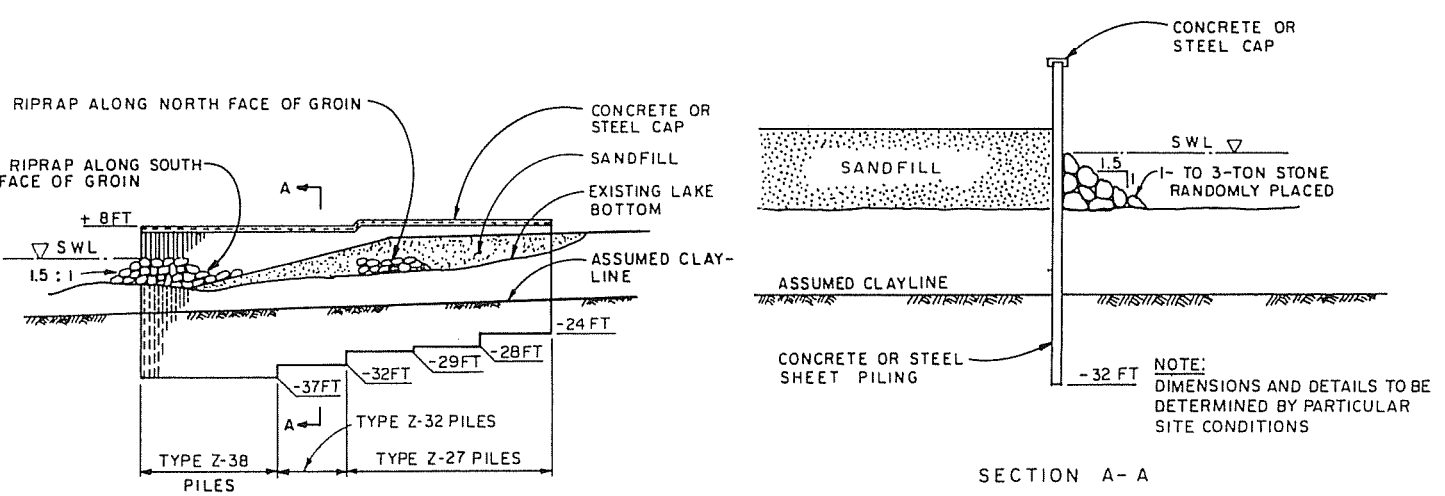

(AFTER SHORE PROTECTION MANUAL, 1977)

FIGURE 67
Typical Sheet-Pile Groin

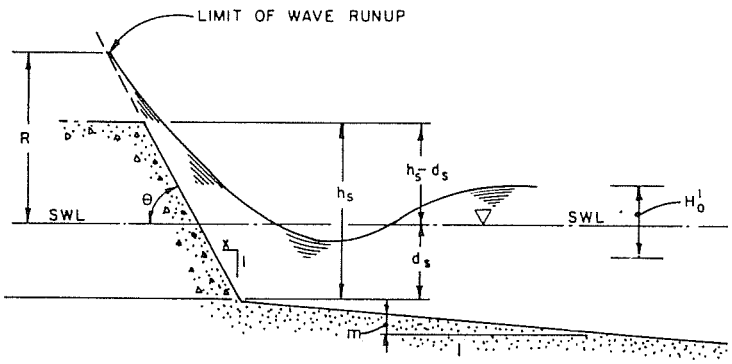

WHERE: R = RUNUP
θ = STRUCTURE-SLOPE ANGLE
h_s = HEIGHT OF STRUCTURE
d_s = WATER DEPTH AT STRUCTURE TOE
H_o' = EQUIVALENT UNREFRACTED DEEP-WATER WAVE HEIGHT
m = BOTTOM SLOPE
(AFTER SHORE PROTECTION MANUAL, 1977)

FIGURE 68
Definition of Runup and Overtopping Terms

and transmitted-wave heights are presented herein. Calculation of overtopping quantities is rarely needed; the reader is referred to the Shore Protection Manual (1977) for details on the proper procedure for such calculations.

4. WAVE RUNUP.

a. **Definition**. Wave runup, R, is the vertical height above the still water level to which water from an incident wave reaches when it encounters a structure or natural formation such as a beach. If the structure is lower in height than the runup elevation, the structure is overtopped. Figure 68 is a sketch defining runup and overtopping terms. Runup is a function of the characteristics of the wave structure and of the offshore slope. Runup on coastal structures can be calculated from small-scale model studies; however, adjustments may be necessary to account for model-to-prototype scale effects and for structure-roughness effects.

b. Calculation of Runup.

(1) General. The calculation of wave runup is based on the results of small-scale hydraulic model studies. The model studies were done for special cases of structures on horizontal bottoms, sloping bottoms, embankments or revetments, breakwaters with low, medium, or high impermeable cores, and with quarrystone or concrete armor units. Runup depends on: relative depth at the toe of the structure, wave steepness, structure slope, beach slope, roughness of the structure, and relative core heights. The equivalent unrefracted deepwater wave height, H'_o, is used in all the runup procedures given below, except for vertical walls subjected to nonbreaking or nonbroken waves. (In such a case, the incident wave height, H_i, is used.) Runup, R, is given by:

$$R = (H'_o)(R/H'_o)(r)(k) \qquad (3\text{-}1)$$

WHERE:
R = runup
H'_o = equivalent unrefracted deepwater wave height
R/H'_o = relative runup
r = rough-slope runup correction factor
k = runup scale-effect correction factor

Runup, R, is the distance above the given water level. The actual runup elevation is determined by adding the runup, R, to the water level used in the calculation.

TABLE 5
Wave-Runup Procedures

Structure Type	Armor Type	Case	Subsection
Embankment or revetment...	Quarrystone	1	3.4.b.(2)
Embankment or revetment...	Concrete	2	3.4.b.(3)
Breakwater.....	Rubble-mound		
	Low core	3	3.4.b.(4)(a)
	Medium core	4	3.4.b.(4)(b)
	High core	5	3.4.b.(4)(c)
Breakwater.....	Concrete--all co	6	3.4.b.(5)
Vertical structures.....	Solid	7	3.4.b.(6)
Beaches.....	Sand to cobble	8	3.4.b.(7)

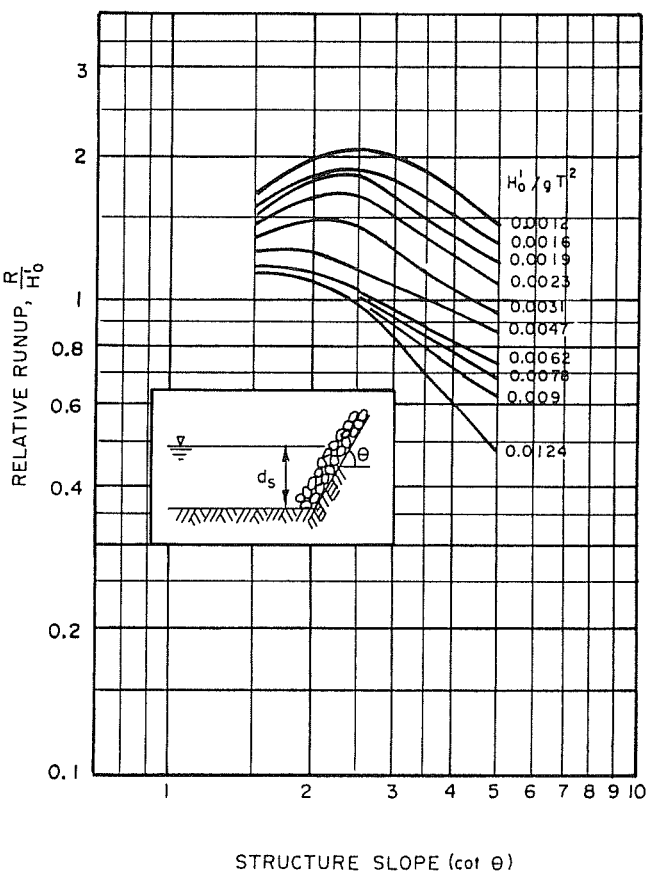

(AFTER STOA, 1979)

FIGURE 69
Relative Runup, R/H'_o, on a Rough Embankment or Revetment for Relative Depth, $d_s/H'_o = 3.0$

In the subsections which follow, procedures are described for calculating runup on different types of structures. These procedures were derived from Stoa (1979). Table 5 summarizes which procedure to follow for a given situation.

(2) Case 1: Embankment or Revetment, quarrystone Armor. Wave runup on an embankment or revetment with quarrystone armor is determined by first finding the relative runup, R/H'_o, from Figures 69-81. The figure to be used depends upon the slope fronting the structure, cot θ, and upon the value of d_s/H'_o. Figures 69-71 are "rough-slope" curves, whereas Figures 72-81 are "smooth-slope" curves. To use these "smooth-slope" curves in determining runup on the rough slope of a quarrystone embankment or revetment, the

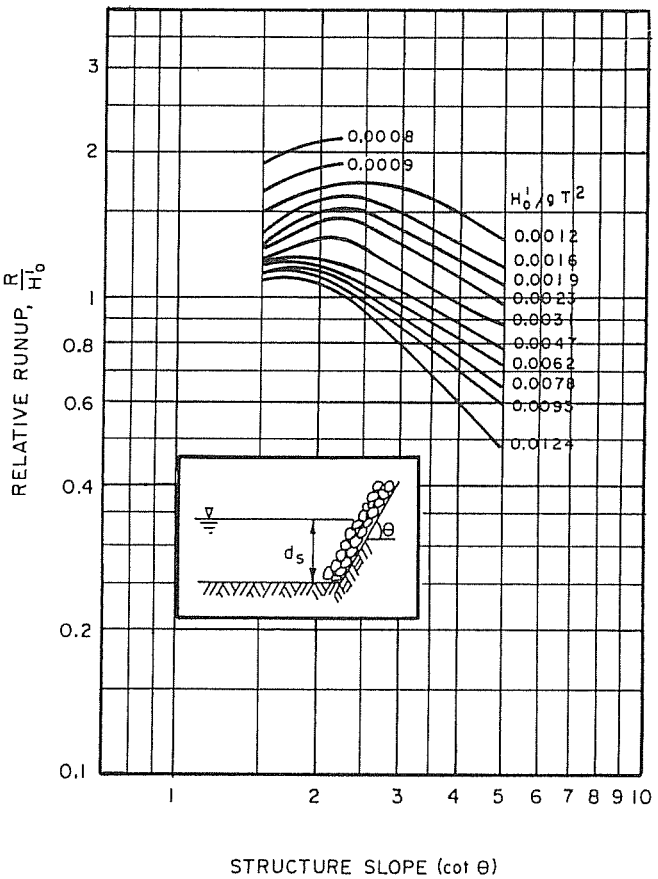

(AFTER STOA, 1979)

FIGURE 70
Relative Runup, R/H'_o, on a Rough Embankment or Revetment for Relative Depth, $d_s/H'_o = 5.0$

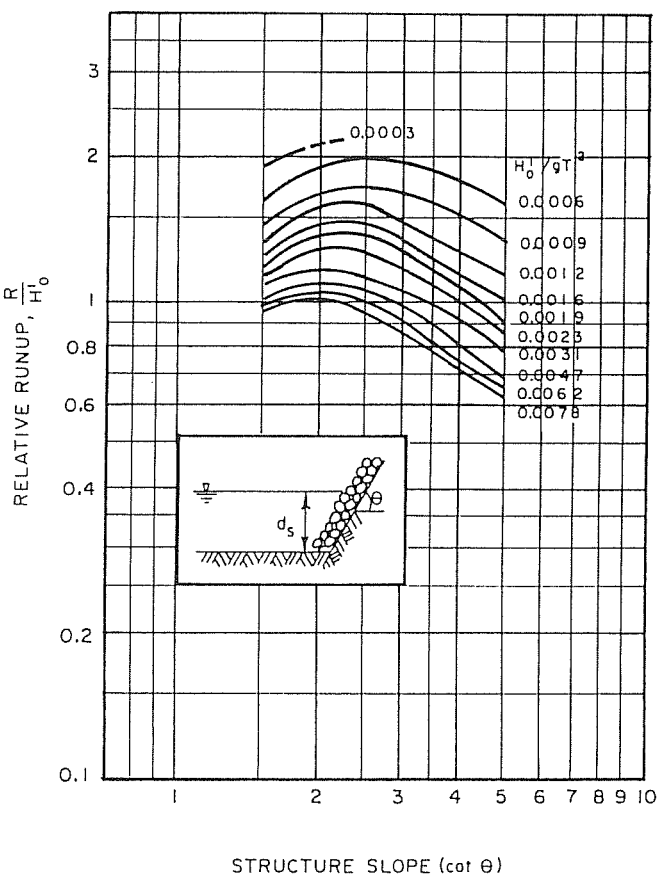

(AFTER STOA, 1979)

FIGURE 71
Relative Runup, R/H'_o, on a Rough Embankment or Revetment for Relative Depth, $d_s/H'_o \geq 8.0$

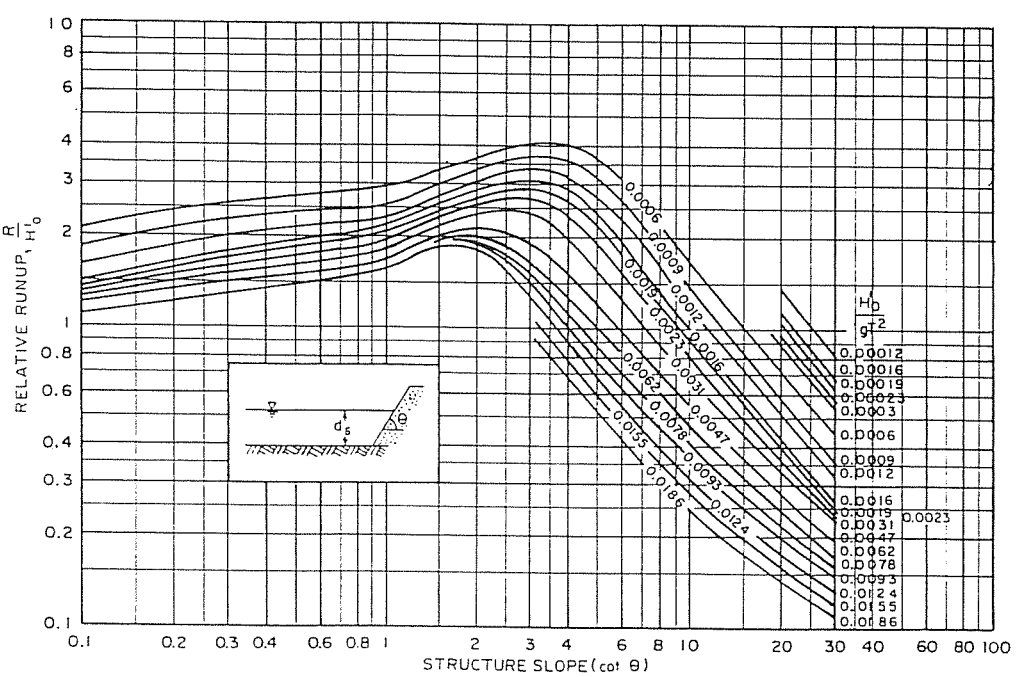

(AFTER STOA, 1978)

FIGURE 72
Relative Runup, R/H'_o, on a Smooth Embankment or Revetment for Relative Depth, $d_s/H'_o \leq 3.0$

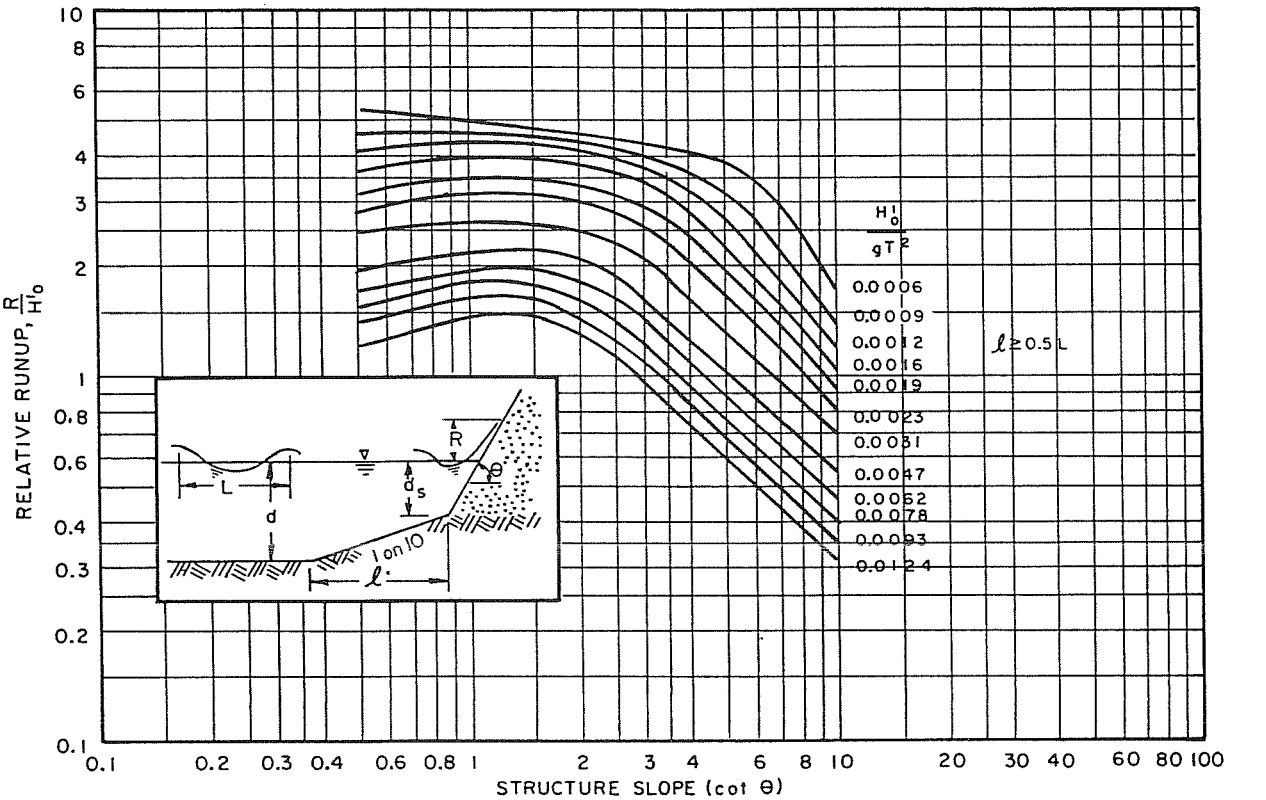

(AFTER STOA, 1978)

FIGURE 73
Relative Runup, R/H'_o, for a Smooth Embankment or Revetment Fronted by a 1-on-10 Bottom Slope for Relative Depth, $d_s/H'_o = 0.6$

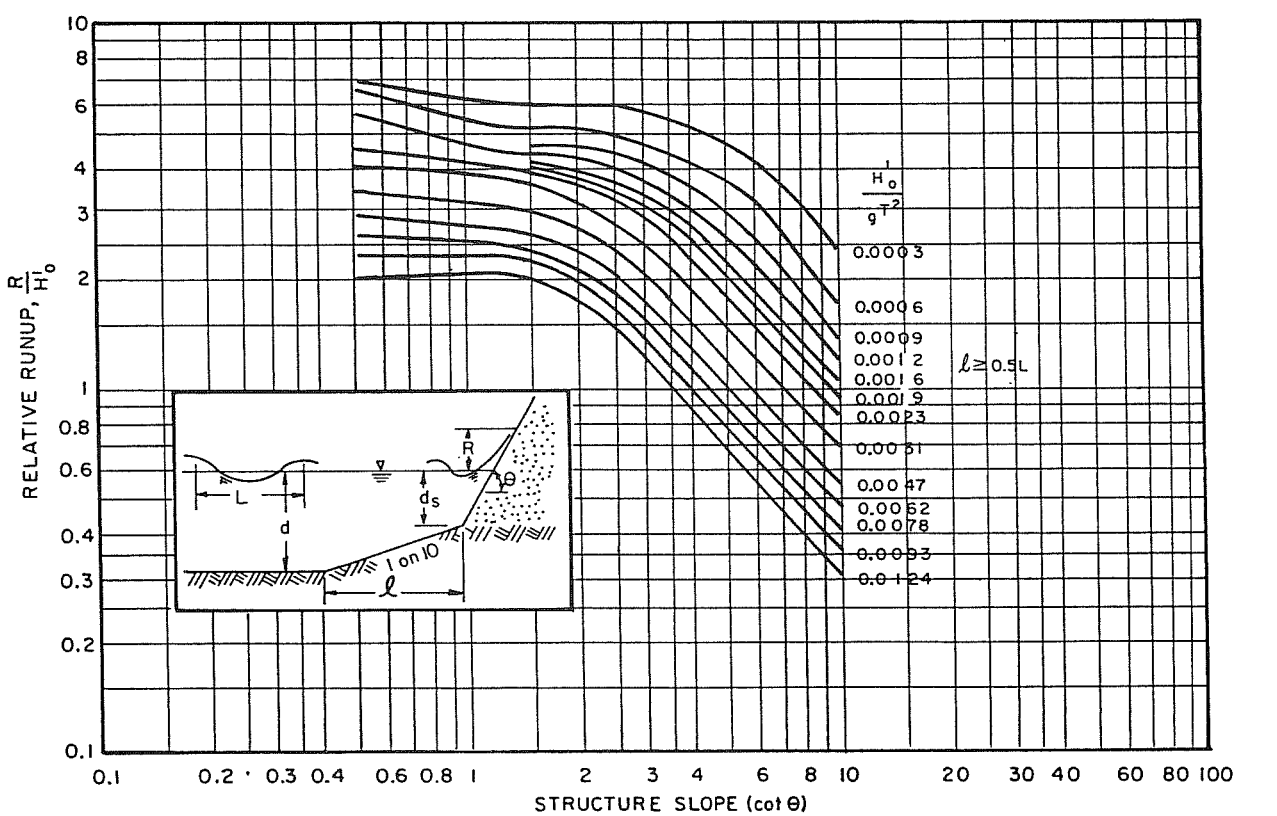

(AFTER STOA, 1978)

FIGURE 74
Relative Runup, R/H'_o, for a Smooth Embankment or Revetment Fronted by a 1-on-10 Bottom Slope for Relative Depth, $d_s/H'_o = 1.0$

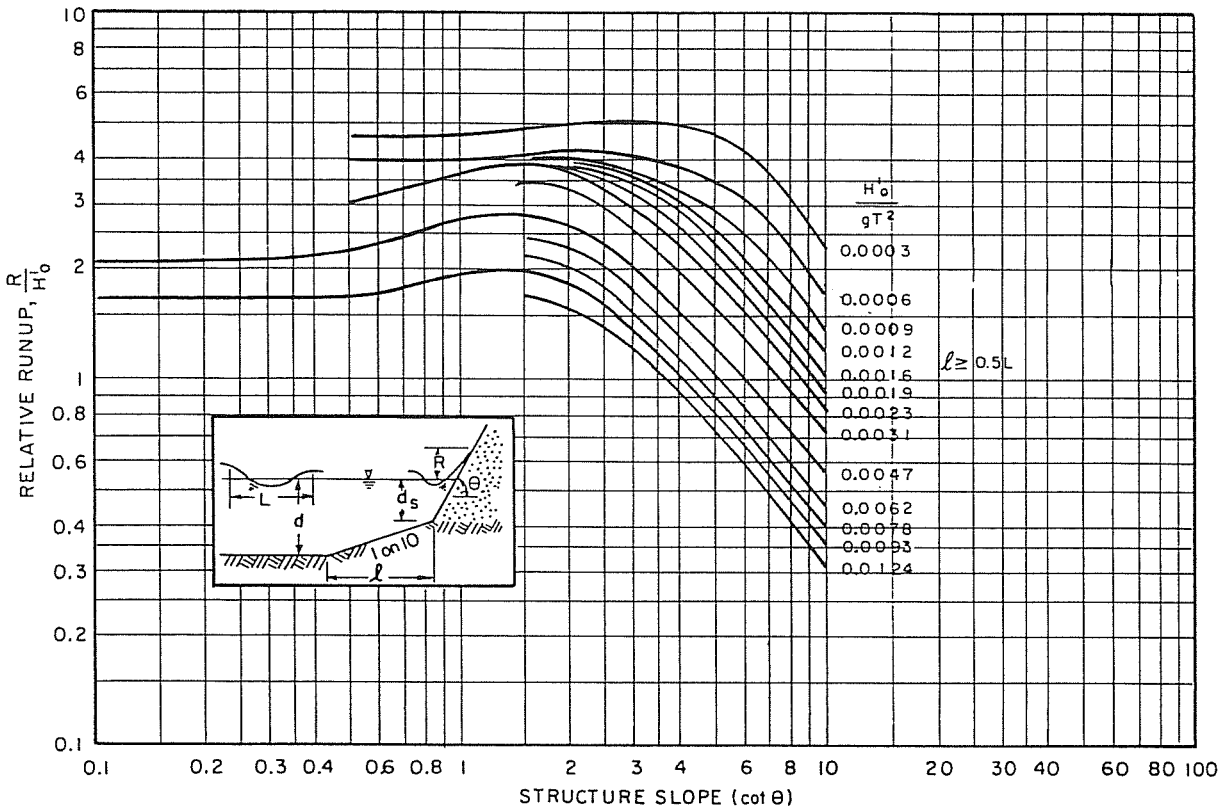

(AFTER STOA, 1978)

FIGURE 75
Relative Runup, R/H'_o, for a Smooth Embankment or Revetment Fronted by a 1-on-10 Bottom Slope for Relative Depth, $d_s/H'_o = 1.5$

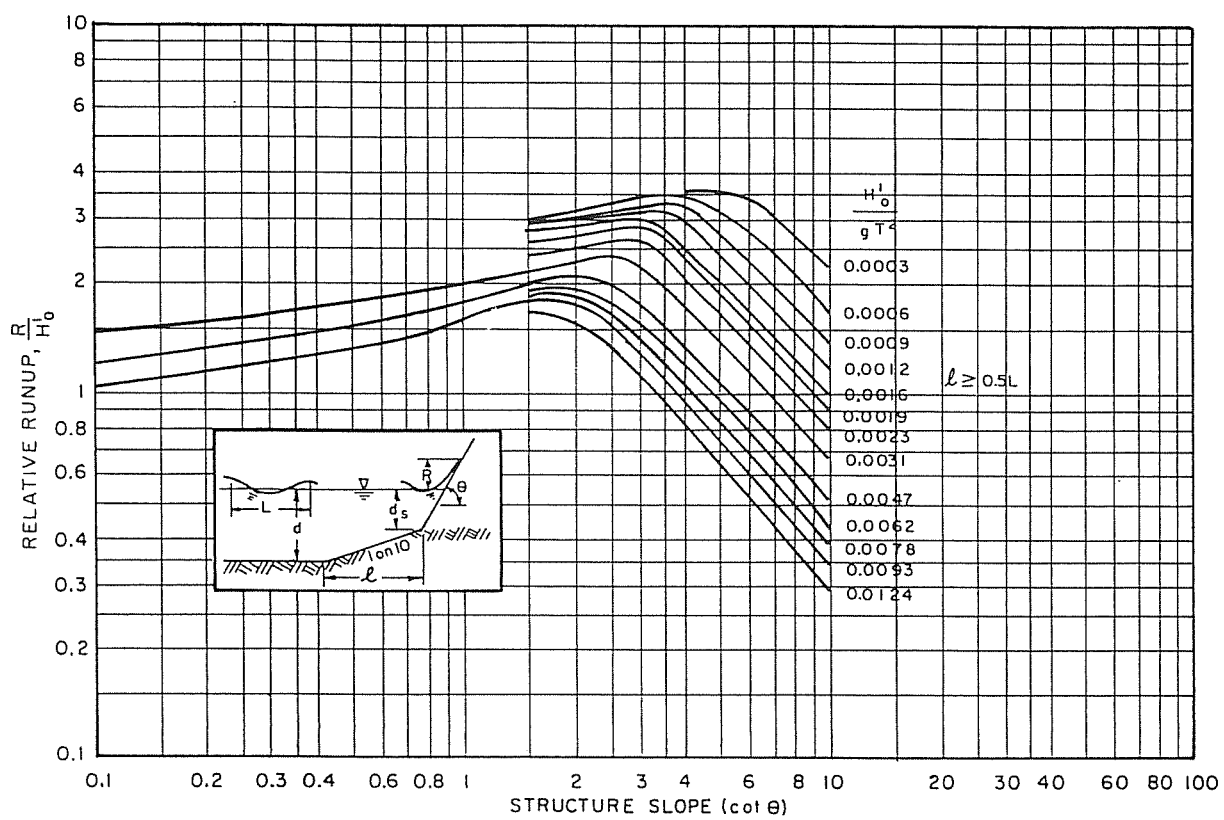

(AFTER STOA, 1978)

FIGURE 76
Relative Runup, R/H'_o, for a Smooth Embankment or Revetment Fronted by a 1-on-10 Bottom Slope for Relative Depth, $d_s/H'_o = 3.0$

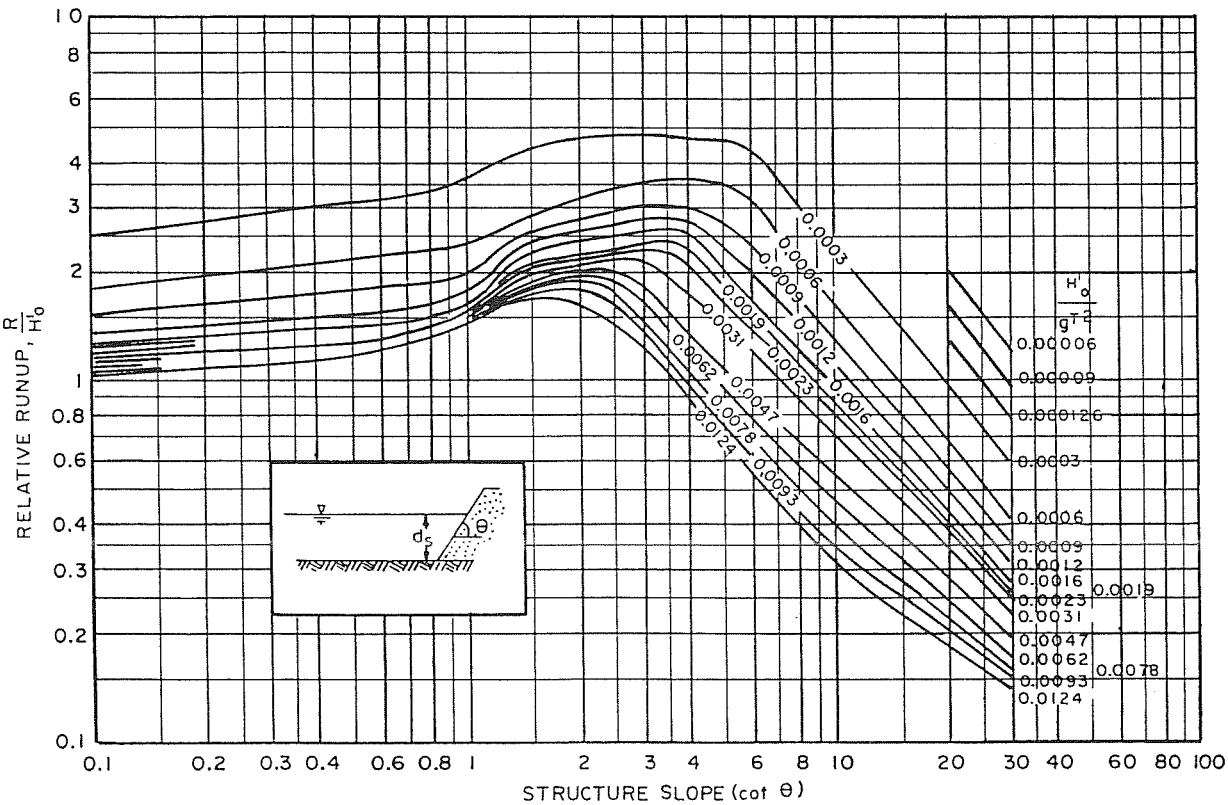

(AFTER STOA, 1978)

FIGURE 77
Relative Runup, R/H'_o, for a Smooth Embankment or Revetment for Relative Depth, $d_s/H'_o = 5.0$

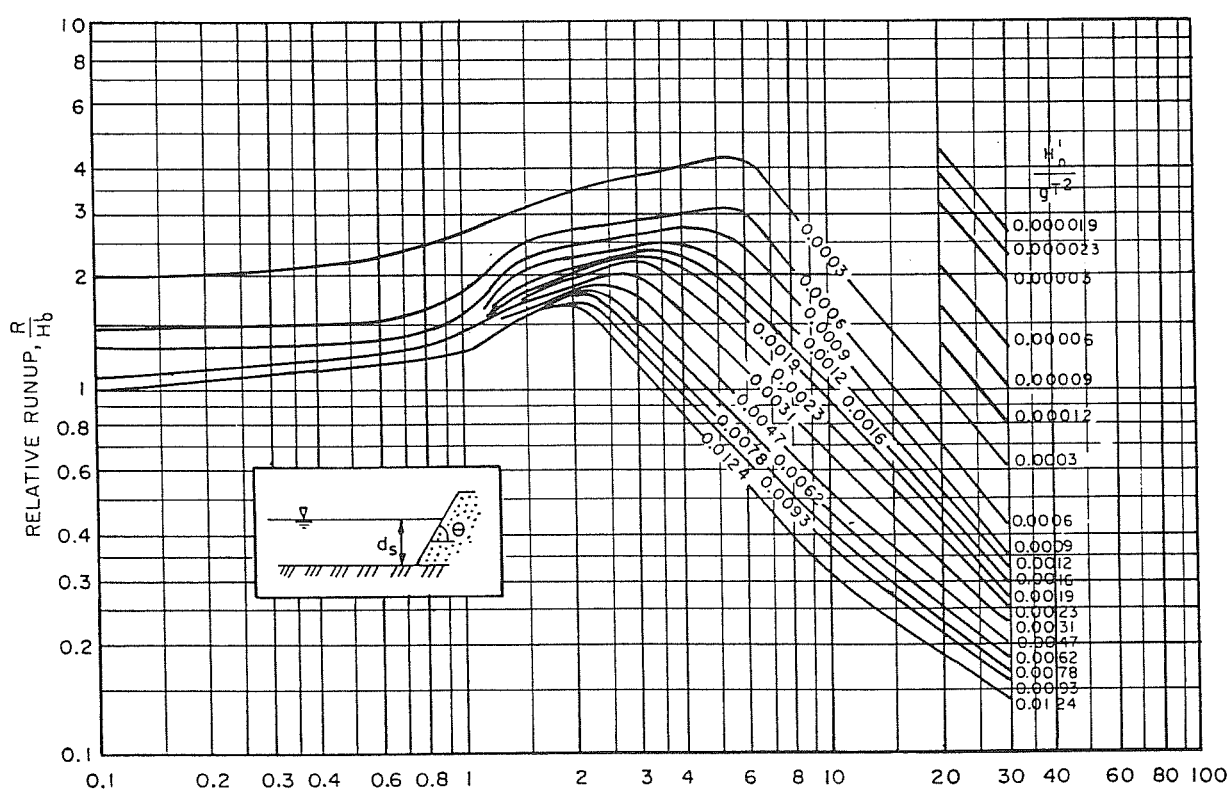

(AFTER STOA, 1978)

FIGURE 78
Relative Runup, R/H'_o, for a Smooth Embankment or Revetment for Relative Depth, $d_s/H'_o = 8.0$

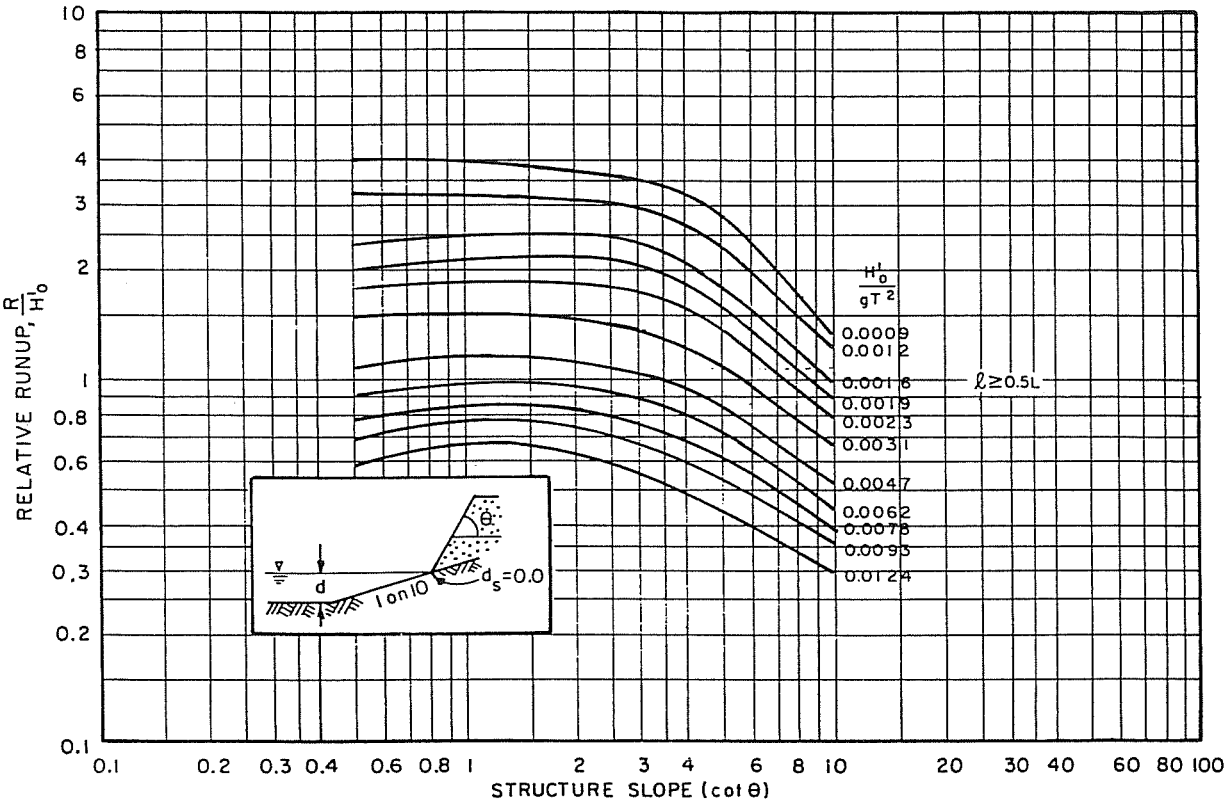

(AFTER STOA, 1978)

FIGURE 79
Relative Runup, R/H'_o, for a Smooth Embankment or Revetment With Water Depth at Toe, $d_s = 0.0$, and Relative Depth at Toe of 1-on-10 Bottom Slope, $d/H'_o = 3.0$

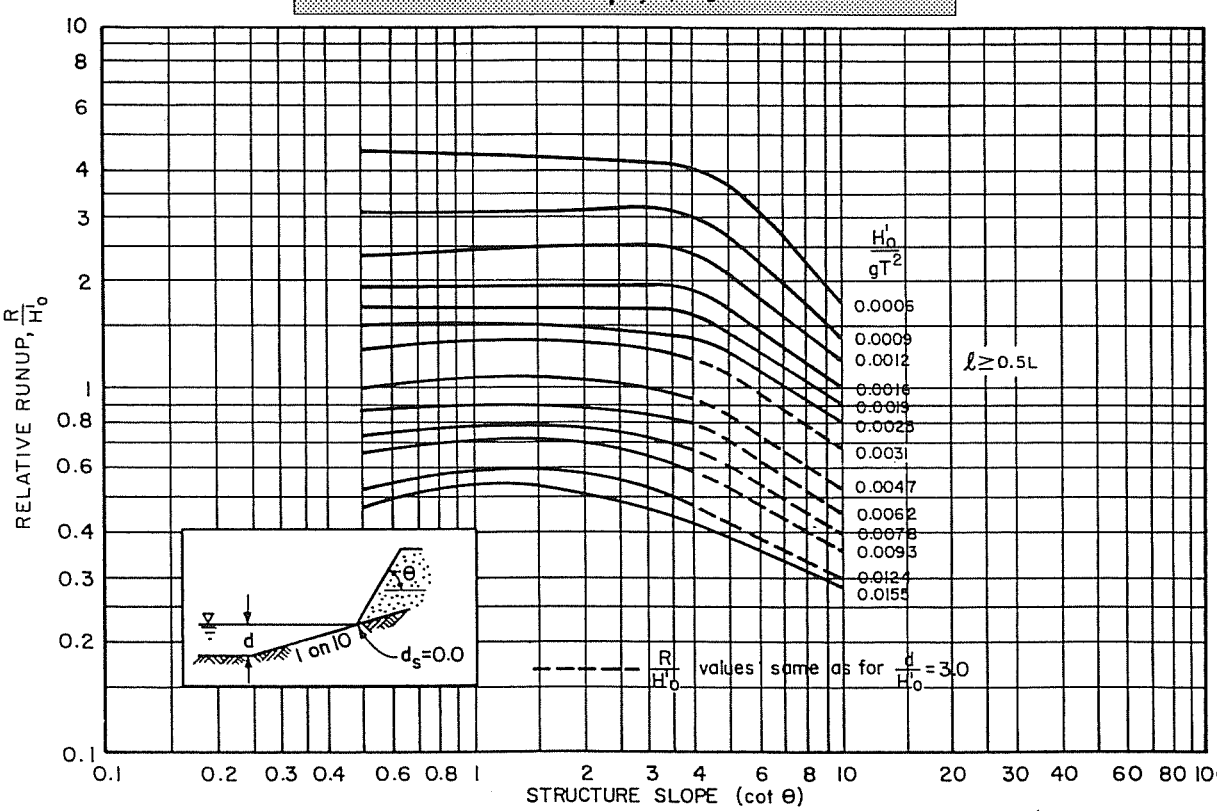

(AFTER STOA, 1978)

FIGURE 80
Relative Runup, R/H'_o, for a Smooth Embankment or Revetment With Water Depth at Toe, $d_s = 0.0$, and Relative Depth at Toe of 1-on-10 Bottom Slope, $d/H'_o = 5.0$

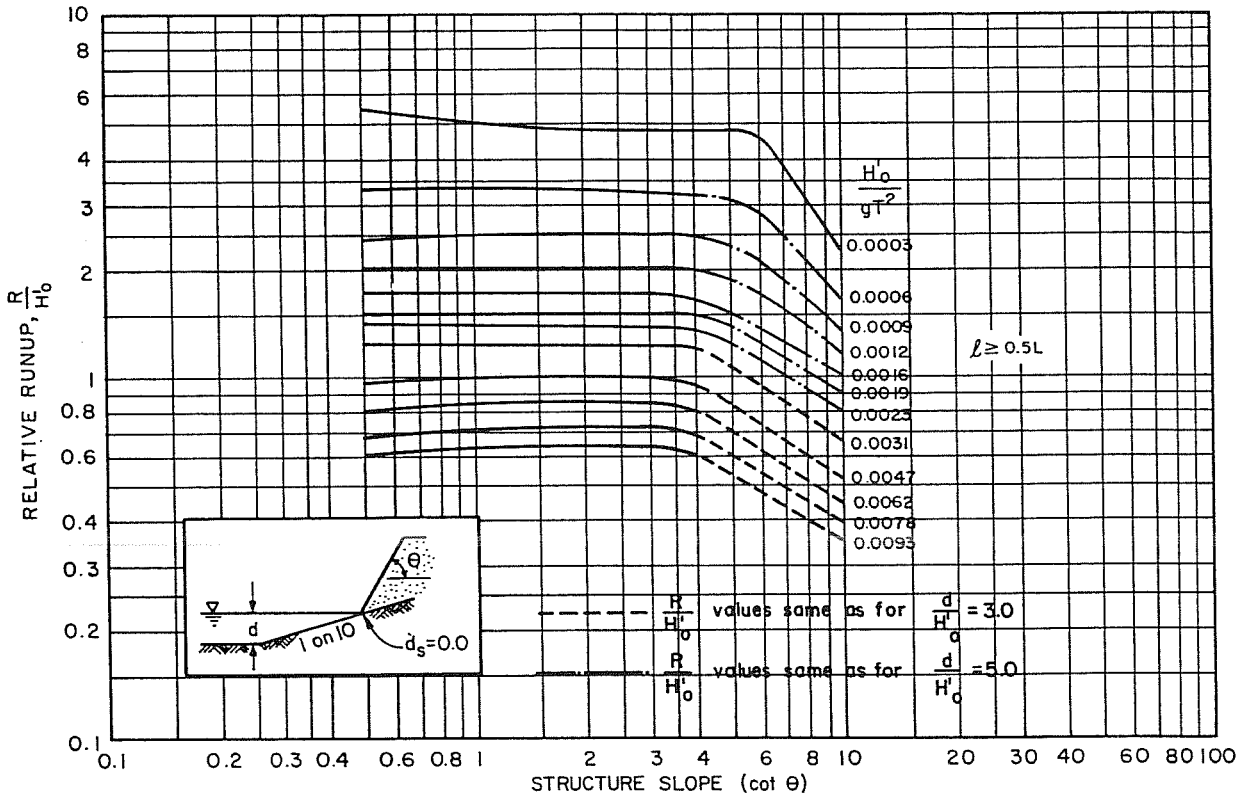

(AFTER STOA, 1978)

FIGURE 81
Relative Runup, R/H'o, for a Smooth Embankment or Revetment With Water Depth at Tie, d_s = 0.0, and Relative Depth at Toe of 1-on-10 Bottom Slope, d/H'o = 8.0

rough-slope runup correction factor, r, is applied.

(a) Structure fronted by horizontal bottom; $d_s/H'_o \geq 3$ and/or $1.5 \leq \cot\theta \leq 5$. Find the relative runup, R/H'o, as a function of the contangent of the structure slope, cot θ, and of the deepwater wave steepness, $H'_o/g\,T^2$, from Figures 69, 70, or 71, depending on relative depth, d_s/H'_o. If $d_s/H'_o = 3.0$, use Figure 69. If $d_s/H'_o = 5.0$, use Figure 70. If $d_s/H'_o \geq 8.0$, use Figure 71. The rough-slope runup correction factor, r, and the runup scale-effect correction factor, k, are both unity. Then the runup is:

$$R = (H'_o)(R/H'_o)(r)(k)$$

$$R = (H'_o)(R/H'_o) \qquad (3\text{-}2)$$

EXAMPLE PROBLEM 12

Given: a. The equivalent unrefracted deepwater wave height, H'_o = 10 feet
b. Water depth at structure toe, d_s = 30 feet
c. Wave period, T = 8 seconds
d. Structure slope, cot θ = 1.5

Find: Runup for a quarrystone revetment.

Solution: (1) Find d_s/H'_o:

$$\frac{d_s}{H'_o} = \frac{30}{10} = 3;\ \text{therefore, use Figure 69}$$

(2) Find $H'_o/g\,T^2$:

$$\frac{H'_o}{g\,T^2} = \frac{10}{(32.2)(8)^2} = 0.0049$$

(3) From Figure 69, for cot θ = 1.5 and $H'_o/g\,T^2 = 0.0049$:

$$\frac{R}{H'_o} = 1.26$$

(4) Using Equation (3-2), find R:

$$R = (H'_o)(R/H'_o)$$

$$R = (10)(1.26) = 12.6 \text{ feet}$$

$$R = 12.6 \text{ feet}$$

Note: To obtain the elevation of the structure required to prevent overtopping, add the value of runup, R, to the water level used in the calculation.

(b) Structure fronted by horizontal bottom; $d_s/H'_o < 3$ and/or $1.5 \geq \cot\theta \geq 5$. Find the relative runup, R'H'o, as a function of the cotangent of the structure slope, cot θ, and of the deepwater wave steepness, $H'_o/g\,T^2$, from Figure 72 for $d_s/H'_o \leq 3$. The rough-slope runup correction factor, r, is 0.60, and the runup scale-effect correction factor, k, is 1.00.

$$R = (H'_o)(R/H'_o)(r)(k)$$

$$R = (H'_o)(R/H'_o)(0.60) \qquad (3\text{-}3)$$

(c) Structure fronted by 1:10 slope; $d_s/H'_o \leq 3$. If the structure is fronted by a 1:10 slope with the slope length, ℓ, is equal to or greater than one-half of the wavelength, L, ($\ell \geq 0.5$ L), where L is the wavelength at the toe of the 1:10 slope, find the relative runup, R/H'o, as a function of the contangent of the structure slope, cot θ, and of the deepwater wave steepness, $H'_o/g\,T^2$, from Figures 73 through 76 for relative depths of d_s/H'_o = 0.6, 1.0, 1.5, and 3, respectively. The rough-slope runup correction factor, r, is 0.60, and the runup scale-effect correction factor, k, is 1.00; Equation (3-3) is used to calculate runup, R.

(d) Structure fronted by 1:10 slope; $d_s/H'_o > 3$. For a relative depth of $d_s/H'_o > 3$, the bottom is considered as horizontal and Figures 77 and 78 should be used. The rough-slope runup correction factor r, is 0.60, and the runup

scale-effect correction factor is 1.00; Equation (3-3) is used to calculate runup, R.

(e) Structure fronted by 1:10 slope; $d_s = 0$. If the toe of structure slope is at $d_s = 0$, then the relative runup, R/H'_o, can be found in Figures 79, 80, or 81 for d/H'_o (rather than d_s/H'_o) equal to 3.0, 5.0, and 8.0, respectively; the depth, d, is taken as the depth at the toe of the 1:10 slope. The rough-slope runup correction factor, r, is 0.60, and the runup scale-effect correction factor, k, is 1.00; Equation (3-3) is used to calculate runup, R.

EXAMPLE PROBLEM 13

Given: a. The wave height at the structure toe, H = 2.75 feet
b. Water depth at structure toe, d_s = 6 feet
c. Wave period, T = 3 seconds
d. Structure slope, cot θ = 1.5
e. The bottom slope is horizontal.

Find: Runup for a quarrystone revetment.

Solution: (1) Find H'_o:

$$L_o = (g/2\pi)T^2 = (32.2/2\pi)(3)^2 = 46.1 \text{ feet}$$

$$\frac{d_s}{L_o} = \frac{6}{46.1} = 0.130$$

From Figure 2 for $d_s/L_o = 0.13$:

$$\frac{H}{H'_o} = 0.92$$

$$H'_o = \frac{H}{0.92} = \frac{2.75}{0.92} = 2.99; \text{ use } 3.0 \text{ feet}$$

(2) Find d_s/H'_o:

$$\frac{d_s}{H'_o} = \frac{6}{3} = 2; \text{ therefore, use Figure 72 (for } d_s/H'_o \leq 3.0)$$

(3) Find $H'_o/g\,T^2$:

$$\frac{H'_o}{g\,T^2} = \frac{3}{(32.2)(3)^2} = 0.0104$$

(4) From Figure 72 for cot θ = 1.5 and $H'_o/g\,T^2 = 0.0104$:

$$\frac{R}{H'_o} = 1.80$$

(5) Using Equation (3-3), find R:

$$R = (H'_o)(R/H'_o)(0.60)$$

$$R = (3)(1.80)(0.60) = 3.24 \text{ feet}$$

$$R = 3.2 \text{ feet}$$

EXAMPLE PROBLEM 14

Given: a. The equivalent unrefracted deepwater wave height, H'_o = 6 feet
b. Water depth at structure toe, d_s = 15 feet
c. Wave period, T = 5 seconds
d. Structure slope, cot θ = 1.5
e. Slope in front of structure, m = 1:10 for slope length, ℓ = 100 feet

Find: Runup for a quarrystone revetment.

Solution: (1) Find L_o:

$$L_o = (g/2\pi)T^2 = (32.2/2\pi)(5)^2 = 128 \text{ feet}$$

(2) Determine depth at toe of 1:10 slope:

$$d = d_s + \ell m$$

$$d = 15 + (100)\left(\frac{1}{10}\right) = 25 \text{ feet}$$

(3) Find d/L_o:

$$\frac{d}{L_o} = \frac{25}{128} = 0.195$$

(4) From Figure 2 for $d/L_o = 0.195$:

$$\frac{d}{L} = 0.22$$

TABLE 6
Rough-Slope Runup Correction Factor, r, for Concrete Armor Units

Unit	Number of Layers	Placement	r	Structure Slope (cot θ)
Dolos.....	2	Random	0.45	1.3 to 3.0
Modified cube.....	2	Random	0.48	1.3 to 3.0
	1	Uniform	0.62	1.5
	1	Uniform	0.73	2.0
	1	Uniform	0.55	3.0
Quadripod.....	2	Random and uniform	0.51	1.3 to 3.0
Tetrapod.....	2	Random	0.45	1.3 to 3.0
	2	Uniform	0.51	1.3 to 3.0
Tribar.....	2	Random	0.45	1.3 to 3.0
	1	Uniform	0.50	1.3 to 3.0
Cobi blocks.....	1	Uniform	0.93	1.3 to 3.0
Stepped slopes.....	N.A.	Vertical risers	0.75	1.3 to 3.0
		Curved risers	0.86	1.3 to 3.0

(STOA, 1979)

$$L = \frac{d}{0.22} = \frac{25}{0.22} = 114 \text{ feet}$$

(5) Determine if 0.5 L:

0.5 L = 57 feet

ℓ = 100 feet

THEREFORE: $\ell \geq 0.5$ L

(6) Determine d_s/H'_o:

$$\frac{d_s}{H'_o} = \frac{15}{6} = 2.5$$

$d_s/H'_o = 2.5 < 3$ and $\ell \geq 5$ L; therefore, use Figures 73 through 76

(7) Find $H'_o/g\,T^2$:

$$\frac{H'_o}{g\,T^2} = \frac{6}{(32.2)(5)^2} = 0.0075$$

(8) Interpolate between Figures 75 and 76 to find R/H'_o for $H'_o/g\,T^2 = 0.0075$:

$$\frac{R}{H'_o} = 2.03$$

(9) Using Equation (3-3), find R:

$R = (H'_o)(R/H'_o)(0.60)$

$R = (6)(2.03)(0.60) = 7.31$ feet

R = 7.3 feet

(3) Case 2: Embankment or Revetment, Concrete Armor. Runup on revetments protected by concrete armor units is determined from the appropriate smooth-slope curves, Figures 72 through 81, for the appropriate d_s/H'_o, cot θ, and $H'_o/g\,T^2$. The rough-slope runup correction factor, r, is found in Table 6 for special concrete shapes. The runup scale-effect correction factor, k, is equal to 1.03.

$$R = (H'_o)(R/H'_o)(r)(k)$$

$$R = (H'_o)(R/H'_o)(r)(1.03) \qquad (3\text{-}4)$$

WHERE:
r is found in Table 6

EXAMPLE PROBLEM 15

Given: a. The equivalent unrefracted deepwater wave height, H'_o = 10 feet
b. Water depth at structure toe, d_s = 30 feet
c. Wave period, T = 8 seconds
d. Structure slope, cot θ = 1.5

TABLE 7
Classification of Relative Core Height, h_c/d_s

Classification	Relative Core Height	Case	Subsection
Low.....	$h_c/d_s \leq 0.75$	3	3.4.b.(4)(a)
Medium.....	$0.75 < h_c/d_s < 1.1$	4	3.4.b.(4)(b)
High.....	$h_c/d_s \geq 1.1$	5	3.4.b.(4)(c)

(AFTER STOA, 1979)

Find: Runup for a revetment armored with two layers of randomly placed tetrapods.

Solution: (1) Find d_s/H'_o:

$$\frac{d_s}{H'_o} = \frac{30}{10} = 3; \text{ therefore, use Figure 72}$$

(2) Find $H'_o/g\,T^2$:

$$\frac{H'_o}{g\,T^2} = \frac{10}{(32.2)(8)^2} = 0.0049$$

(3) From Figure 72 for cot θ = 1.5 and $H_o/g\,T^2 = 0.0049$:

$$\frac{R}{H'_o} = 1.90$$

(4) From Table 6 for tetrapod armor units, randomly placed: r = 0.45

(5) Using Equation (3-4), find R:

$R = (H'_o)(R/H'_o)(r)(1.03)$

$R = (10)(1.9)(0.45)(1.03) = 8.81$ feet

R = 8.8 feet

Compared to 12.6 feet for the quarrystone revetment in Example Problem 12, the tetrapod armor units réduce the runup by 30 percent.

(4) Cases 3, 4, and 5: Breakwater, Rubble-Mound. Wave runup on a rubble-mound breakwater is a function of the height of the impermeable core above the bottom, as well as of the parameters affecting runup on an embankment. The first step is to determine if the structure has a low, medium, or high core. The classification of core height is given in Table 7. Also to be found in Table 7 is the subsection that applies to each core height. The parameter, h_c, is the height of the core above the bottom.

(a) Case 3: low core height: $h_c/d \leq 0.75$. If $d_s/H'_o \geq 3$ and $1.25 \leq \cot\theta \leq 5$, find R/H'_o from Figure 82, 83, or 84. The rough-slope runup correction factor, r, is 1.00, and the runup scale-effect correction factor, k, is 1.06.

$$R = (H'_o)(R/H'_o)(r)(k)$$

$$R = (H'_o)(R/H'_o)(1.06) \qquad (3\text{-}5)$$

If $d_s/H'_o < 3$ and/or $1.25 > \cot\theta > 5$, find the rough-slope runup correction factor, r, from Table 8. The runup scale-effect correction factor, k, is 1.06. Then the runup is determined from the appropriate smooth-slope curve chosen from Figures 72 through 75. If $1.5 < d_s/H'_o < 3$, interpolate between Figures 75 and 76 in order to determine runup.

$$R = (H'_o)(R/H'_o)(r)(k)$$

$$R = (H'_o)(R/H'_o)(r)(1.06) \qquad (3\text{-}6)$$

WHERE:
r is found in Table 8

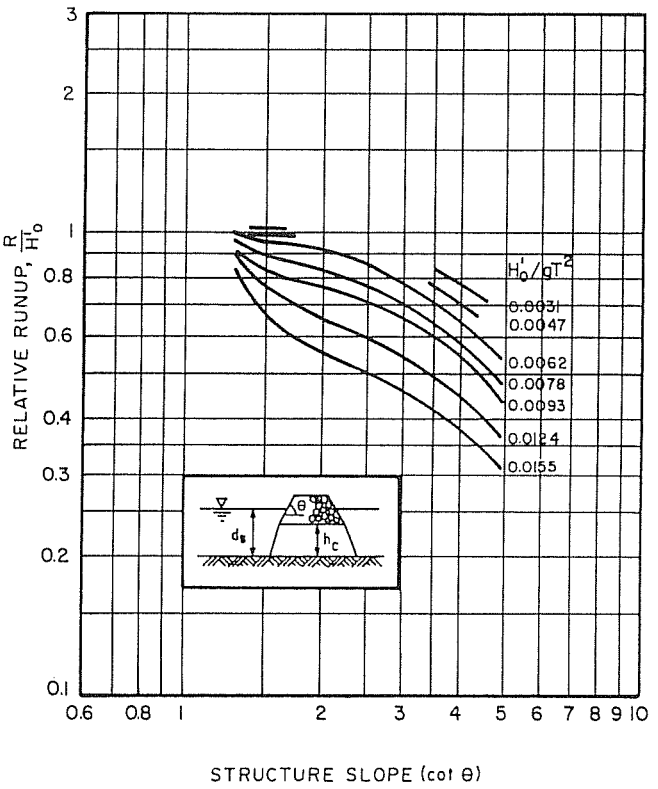

(AFTER STOA, 1979)

FIGURE 82
Relative Runup, R/H'_o, for a Rubble-Mound Breakwater for Relative Depth, $d_s/H'_o = 3.0$

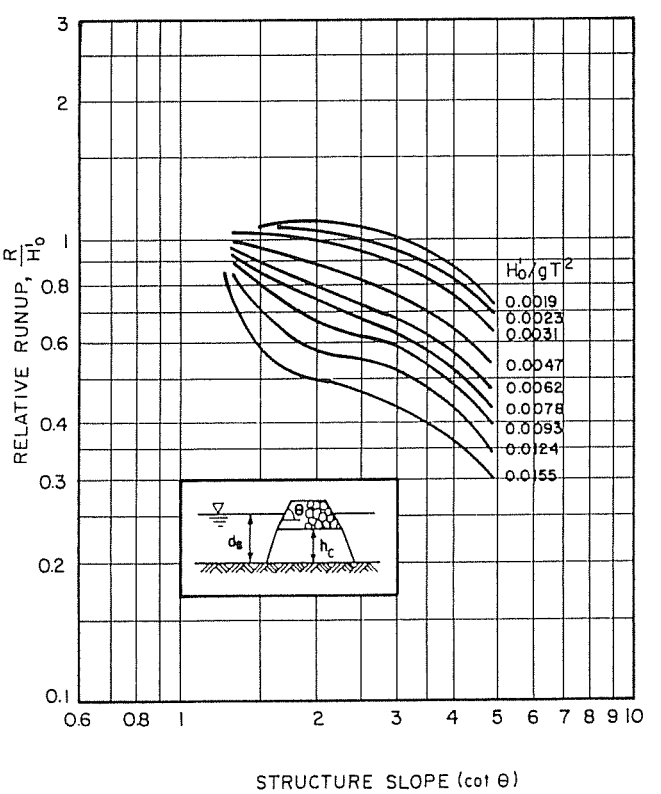

(AFTER STOA, 1979)

FIGURE 83
Relative Runup, R/H'_o, for a Rubble-Mound Breakwater for Relative Depth, $d_s/H'_o = 3.0$

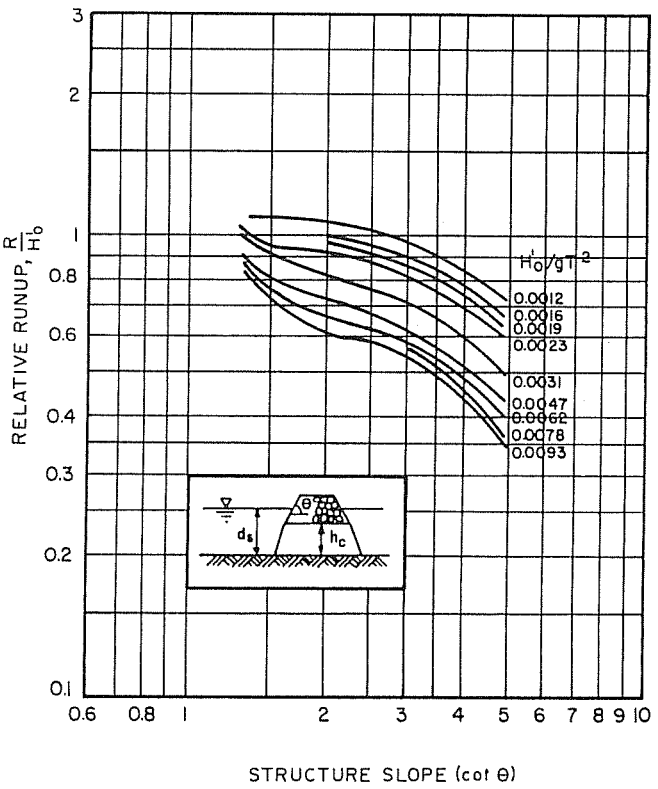

(AFTER STOA, 1979)

FIGURE 84
Relative Runup, R/H'_o, for a Rubble-Mound Breakwater for Relative Depth, $d_s/H'_o = 8.0$

TABLE 8
Rough-Slope Runup Correction Factor, r, for a Rubble-Mound Breakwater

Structure Slope (cot θ)	r
1.25	0.57
1.50	0.45
2.00	0.44
2.50	0.42
3.00	0.44
4.00	0.48
5.00	0.48

(STOA, 1979)

EXAMPLE PROBLEM 16

Given: a. The equivalent unrefracted deepwater wave height, $H'_o = 8$ feet
b. Water depth at structure toe, $d_s = 40$ feet
c. Wave period, $T = 5$ seconds
d. Structure slope, cot $\theta = 1.5$
e. Height of core, $h_c = 28$ feet

Find: Runup for a quarrystone breakwater.

Solution: (1) Determine relative core height, h_c/d_s:

$$\frac{h_c}{d_s} = \frac{28}{40} = 0.7$$

From Table 7: relative core height is low.

(2) Find d_s/H'_o:

$$\frac{d_s}{H'_o} = \frac{40}{8} = 5$$

$d_s/H_o \geq 3$ and $1.25 \leq \cot\theta \leq 5$; therefore, use Figure 82, 83, or 84

(3) Find $H_o/g\,T^2$:

$$\frac{H'_o}{g\,T^2} = \frac{8}{(32.2)(5)^2} = 0.0099$$

(4) From Figure 83 for $\cot\theta = 1.5$ and $H_o/g\,T^2 = 0.0099$:

$$\frac{R}{H'_o} = 0.78$$

(5) Using Equation (3-5), find R:

$$R = (H'_o)(R/H'_o)(1.06)$$

$$R = (8)(0.78)(1.06) = 6.61 \text{ feet}$$

$$R = 6.6 \text{ feet}$$

EXAMPLE PROBLEM 17

Given: a. Equivalent unrefracted deepwater wave height, $H'_o = 8$ feet
b. Water depth at structure toe, $d_s = 20$ feet
c. Wave period, $T = 5$ seconds
d. Structure slope, $\cot\theta = 2.0$
e. Height of core, $h_c = 15$ feet
f. Structure situated on flat bottom.

Find: Runup for a quarrystone breakwater.

Solution: (1) Determine relative core height, h_c/d_s:

$$\frac{h_c}{d_s} = \frac{15}{20} = 0.75$$

From Table 7: relative core height is low

(2) Find d_s/H'_o:

$$\frac{d_s}{H'_o} = \frac{20}{8} = 2.5$$

$d_s/H'_o < 3$ and $1.25 > \cot\theta > 5$; therefore, choose figure to use from Figures 72 through 75.

Since structure is on flat bottom, use Figure 72.

(3) Find $H'_o/g\,T^2$:

$$\frac{H'_o}{g\,T^2} = \frac{8}{(32.2)(5)^2} = 0.0099$$

(4) From Figure 72, for $\cot\theta = 2.0$ and $H_o/g\,T^2 = 0.0099$:

$$\frac{R}{H'_o} = 1.85$$

(5) From Table 8 for $\cot\theta = 2.0$: $r = 0.44$

(6) Using Equation (3-6), find R:

$$R = (H'_o)(R/H'_o)(r)(1.06)$$

$$R = (8)(1.85)(0.44)(1.06) = 6.90 \text{ feet}$$

$$R = 6.9 \text{ feet}$$

(b) Case 4: medium core height: $0.75 < h_c/d_s < 1.1$. find R/H'_o from Figures 72 through 78 for the appropriate d_s/H'_o and bottom configuration. The rough-slope runup correction factor, r, is 0.52 and the runup scale-effect correction factor, k, is 1.06.

$$R = (H'_o)(R/H'_o)(r)(k)$$

$$R = (H'_o)(R/H'_o)(0.52)(1.06) \qquad (3\text{-}7)$$

EXAMPLE PROBLEM 18

Given: a. The equivalent unrefracted deepwater wave height, $H'_o = 10$ feet
b. Water depth at structure toe, $d_s = 50$ feet
c. Wave period, $T = 8$ seconds
d. Structure slope, $\cot\theta = 2.5$
e. Height of core, $h_c = 43$ feet

Find: Runup for a quarrystone breakwater.

Solution: (1) Determine relative core height, h_c/d_s:

$$\frac{h_c}{d_s} = \frac{43}{50} = 0.86$$

From Table 7: relative core height is medium

(2) Find d_s/H'_o:

$$\frac{d_s}{H'_o} = \frac{50}{10} = 5$$

$d_s/H'_o = 5$; therefore, use Figure 77

(3) Find $H'_o/g\,T^2$:

$$\frac{H'_o}{g\,T^2} = \frac{10}{(32.2)(8)^2} = 0.0049$$

(4) From Figure 77 for $\cot\theta = 2.5$ and $H'_o/g\,T^2 = 0.0049$:

$$\frac{R}{H'_o} = 2.00$$

(5) Using Equation (3-7), find R:

$$R = (H'_o)(R/H'_o)(0.52)(1.06)$$

$$R = (10)(2.0)(0.52)(1.06) = 11.0 \text{ feet}$$

$$R = 11.0 \text{ feet}$$

(c) Case 5: high core height. Find R/H'_o from Figures 72 through 78 for the appropriate d_s/H'_o and bottom configuration. The rough-slope runup correction factor, r, is 0.60, and the runup scale-effect correction factor, k, is 1.00

$$R = (H'_o)(R/H'_o)(r)(k)$$

$$R = (H'_o)(R/H'_o)(0.60) \qquad (3\text{-}8)$$

EXAMPLE PROBLEM 19

Given: a. The equivalent unrefracted deepwater wave height, $H'_o = 20$ feet
b. Water depth at structure toe, $d_s = 60$ feet
c. Wave period, $T = 12$ seconds
d. Structure slope, $\cot\theta = 1.5$
e. Height of core, $h_c = 72$ feet

Find: Runup for a quarrystone breakwater.

Solution: (1) Determine relative core height, h_c/d_s:

$$\frac{h_c}{d_s} = \frac{72}{60} = 1.2$$

From Table 7: relative core height is high

(2) Find d_s/H'_o:

$$\frac{d_s}{H'_o} = \frac{60}{20} = 3.0$$

$d_s/H'_o = 3.0$; therefore, use Figure 72

(3) Find $H'_o/g\,T^2$:

$$\frac{H'_o}{g\,T^2} = \frac{20}{(32.2)(12)^2} = 0.0043$$

(4) From Figure 72 for $\cot\theta = 1.5$ and $H'_o/g\,T^2 = 0.0043$:

$$\frac{R}{H'_o} = 2.05$$

(5) Using Equation (3-8), find R:

$$R = (H'_o)(R/H'_o)(0.6)$$

$$R = (20)(2.05)(0.60) = 24.6 \text{ feet}$$

$$R = 24.6 \text{ feet}$$

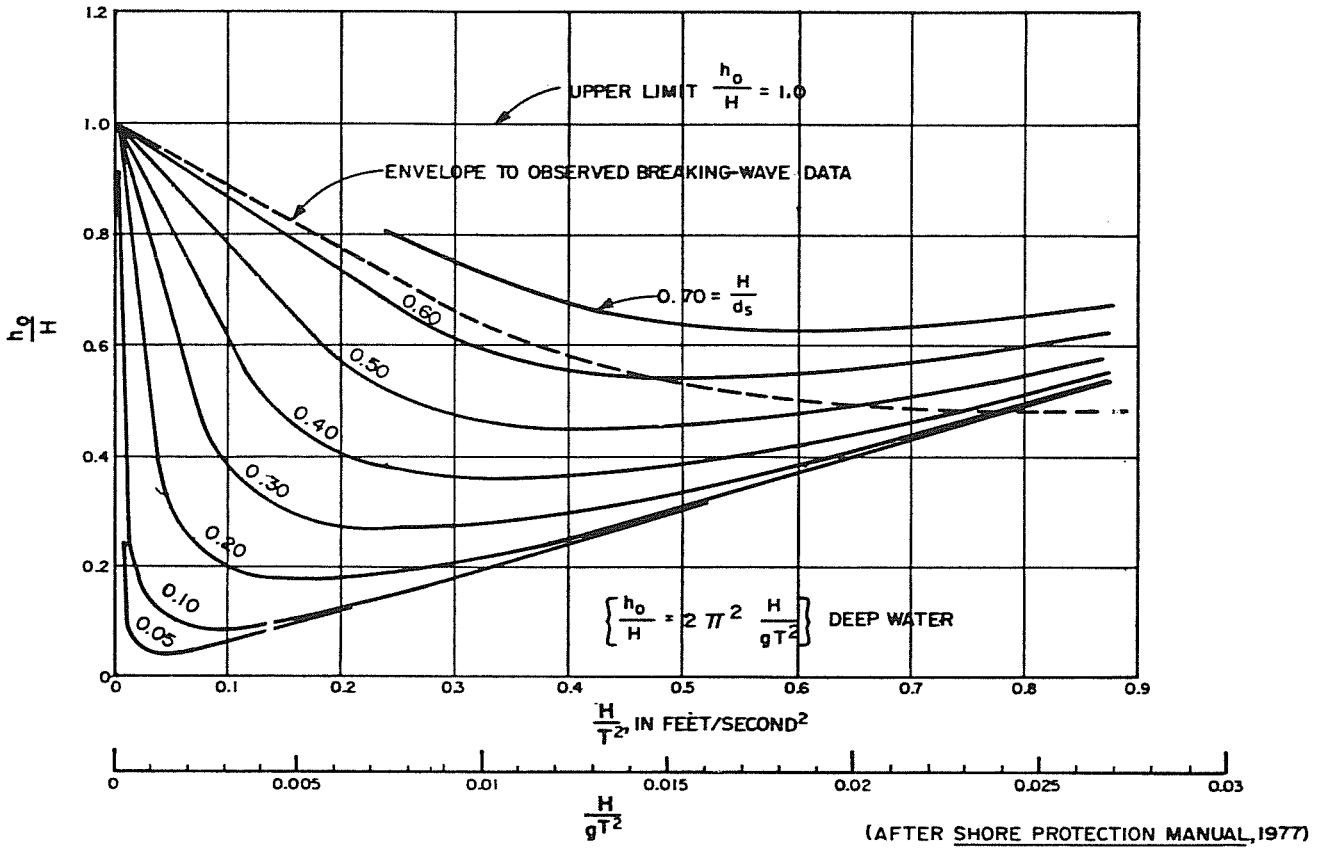

FIGURE 85
h_o/H Versus H/T^2 or $H/g\,T^2$

(5) Case 6: Breakwater, Concrete Armor. Find the relative runup, R/H'_o, on a smooth slope in Figures 72 through 78 for the appropriate d_s/H'_o and bottom configuration. Find the rough-slope runup correction factor, r, from Table 6. The runup scale-effect correction factor, k, is 1.03.

$$R = (H'_o)(R/H'_o)(r)(k)$$

$$R = (H'_o)(R/H'_o)(r)(1.03) \qquad (3\text{-}9)$$

WHERE:
r is found in Table 6

EXAMPLE PROBLEM 20

Given: a. Equivalent unrefracted deepwater wave height, H'_o = 20 feet
b. Water depth at structure toe, d_s = 60 feet
c. Wave period, T = 12 seconds
d. Structure slope, cot θ = 1.5
e. Height of core, h_c = 72 feet

Find: Runup for a breakwater armored with one layer of uniformly placed tribars.

Solution: From Example Problem 19: $R/H'_o = 2.05$

From Table 6: r = 0.50

Using Equation (3-9), find R:

$R = (H'_o)(R/H'_o)(r)(1.03)$

$R = (20)(2.05)(0.50)(1.03) = 21.1$ feet

R = 21.1 feet

Note: Runup is reduced approximately 14 percent by using tribars instead of quarrystone.

(6) Case 7: Vertical Structures. Wave runup on a smooth-faced vertical structure located on a horizontal bottom for a nonbreaking or nonbroken wave is essentially equal to the incident wave height, H_i. Waves in shoaling water have nonlinear asymmetry in that the crest height is greater than the trough depression. This, in effect, raises the height of the mean water level at the wall by an amount, h_o, above the still water level. Runup, R, is calculated from the equation:

$$R = h_o + H_i \qquad (3\text{-}10)$$

WHERE:
R = runup
h_o = amount by which the mean water level at the wall is raised above still water level
H_i = incident wave height at structure toe (as determined by the linear shoaling coefficient).

The value of h_o is determined by first finding $h_o/H = h_o/H_i$ from Figure 85. H_i is calculated from a given H'_o by first determining H_o from H_o from $H'_o = H_o K_R$ (linear shoaling) for a given K_R and then using Figure 2 to find H/H_o for the calculated value of d_s/L_o.

This procedure is not applicable if the wave has broken.

EXAMPLE PROBLEM 21

Given: a. Equivalent unrefracted deepwater wave height, H'_o = 5 feet
b. Water depth at structure toe, d_s = 15 feet
c. Wave period, T = 4 seconds
d. Refraction coefficient, K_R = 1.0

Find: The runup on a smooth-faced vertical wall.

Solution: (1) Find H_o:

$H'_o = H_o K_R$

$H_o = \frac{H'_o}{K_R} = \frac{5}{1.0}$

$H_o = 5.0$ feet

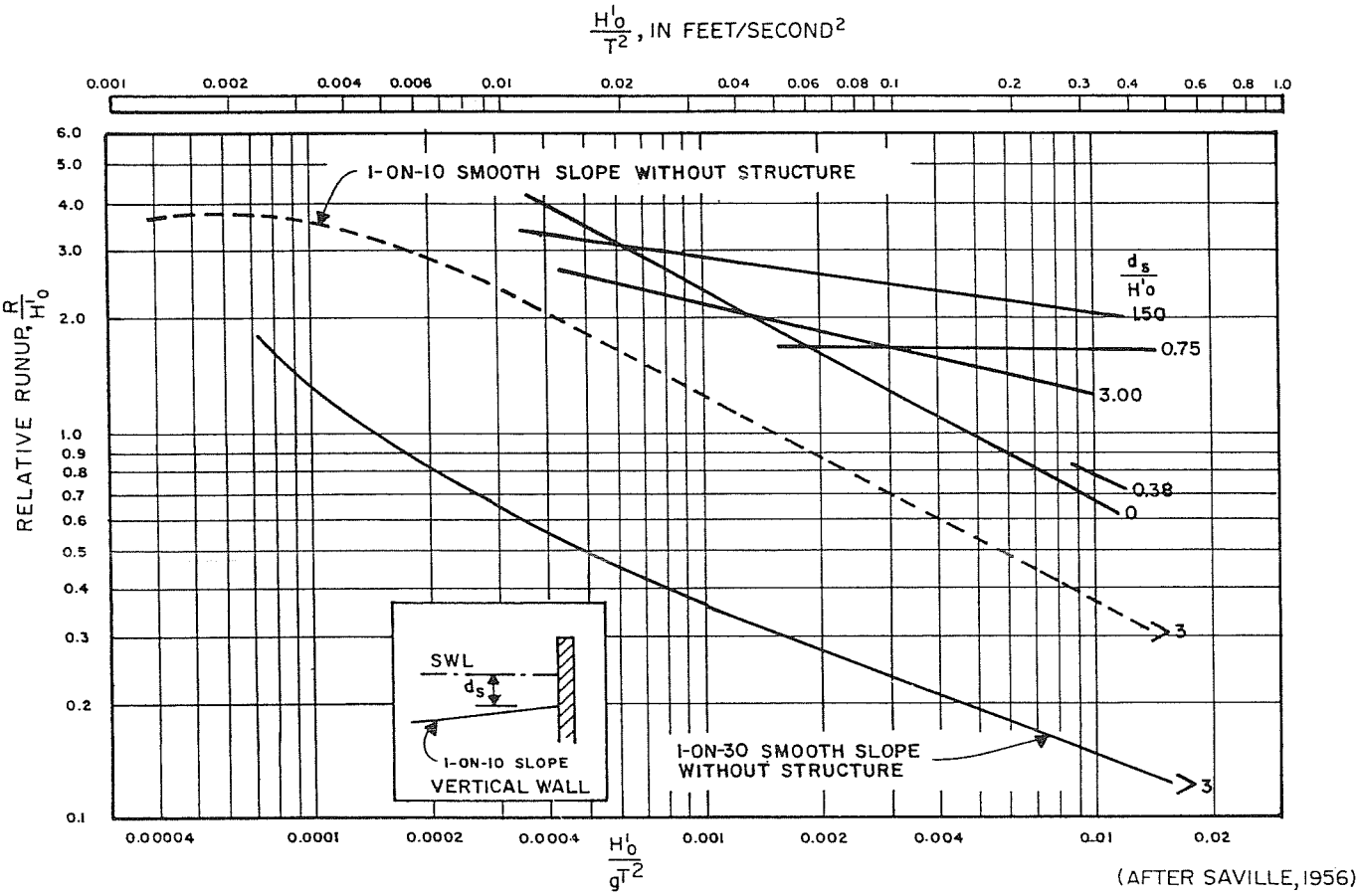

FIGURE 86
Relative Runup, R/H'o, on an Impermeable Vertical Wall

(2) Find d_s/L_o:

$L_o = (g/2\pi)\,T^2 = (32.2/2\pi)(4)^2 = 82.0$ feet

$\frac{d_s}{L_o} = \frac{15}{82.0} = 0.183$

(3) From Figure 2 for $d_s/L_o = 0.183$:

$H/H'_o = 0.92$

$H = 0.92\,H'_o$

$H = (0.92)(5)$

$H = H_i = 4.6$ feet

(4) Find H/d_s; $H = H_i$:

$\frac{H_i}{d_s} = \frac{4.6}{15} = 0.31$

(5) Find H/T^2; $H = H_i$:

$\frac{H_i}{T^2} = \frac{4.6}{(4)^2} = 0.29$

(6) From Figure 85 for $H/d_s = 0.31$ and $H/T^2 = 0.29$; $H = H_i$:

$\frac{h_o}{H_i} = 0.28$

$h_o = 0.28\,H_i$

$h_o = (0.28)(4.6) = 1.29$

$h_o = 1.3$ feet

(7) Using Equation (3-10), find R:

$R = h_o + H_i$

$R = 1.3 + 4.6 = 5.9$ feet

$R = 5.9$ feet

For shallow-water application, where the wave may break, relative wave runup, R/H'_o, for smooth-faced vertical structures and recurved seawalls fronted by nonhorizontal bottom slopes can be found in Figures 86, 87, and 88. The rough-slope runup correction factor, r, and the runup scale-effect correction factor, k, are both 1.00.

$$R = (H'_o)(R/H'_o)(r)(k)$$

$$R = (H'_o)(R/H'_o) \qquad (3\text{-}11)$$

EXAMPLE PROBLEM 22

Given: a. The equivalent unrefracted deepwater wave height, $H'_o = 3$ feet
b. Water depth at structure toe, $d_s = 4.5$ feet
c. Wave period, $T = 3$ seconds

Find: Runup on recurved Galveston-type seawall.

Solution: (1) Find d_s/H'_o:

$\frac{d_s}{H'_o} = \frac{4.5}{3} = 1.5$

(2) Find $H'_o/g\,T^2$:

$\frac{H'_o}{g\,T^2} = \frac{3}{(32.2)(3)^2} = 0.0104$

(3) From Figure 88 for $d_s/H'_o = 1.5$ and $H'_o/g\,T^2 = 0.0104$:

$\frac{R}{H'_o} = 0.54$

(4) Using Equation (3-11), find R:

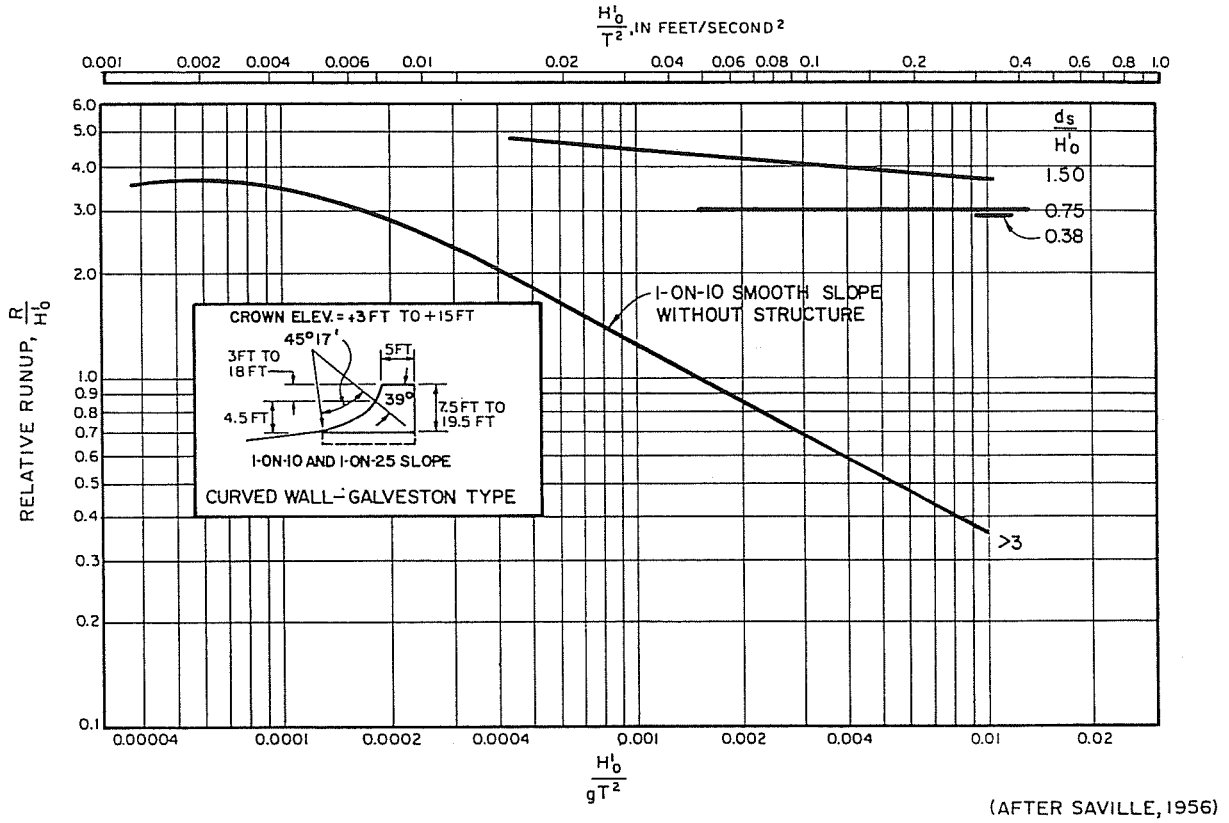

(AFTER SAVILLE, 1956)

FIGURE 87
Relative Runup, R/H'_o, on a Curved Wall -- Galveston Type

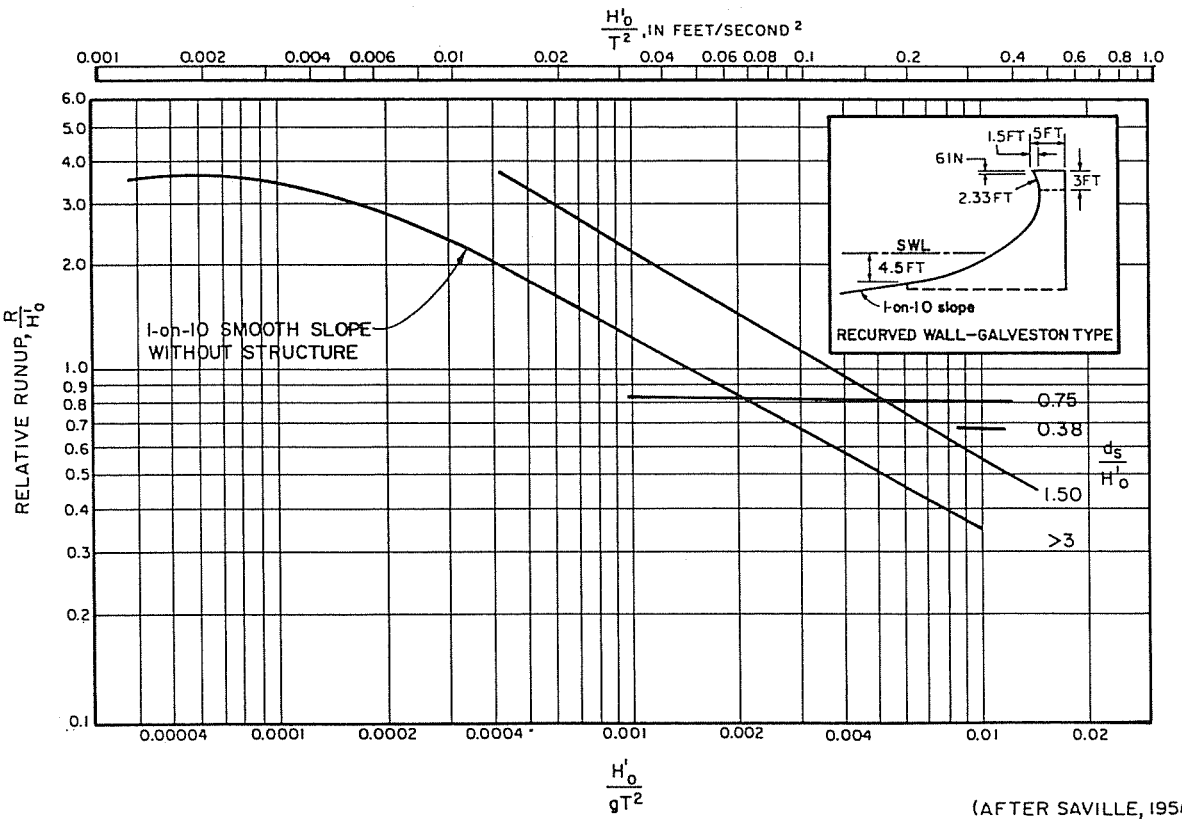

(AFTER SAVILLE, 1956)

FIGURE 88
Relative Runup, R/H'_o, on a Recurved Wall -- Galveston Type

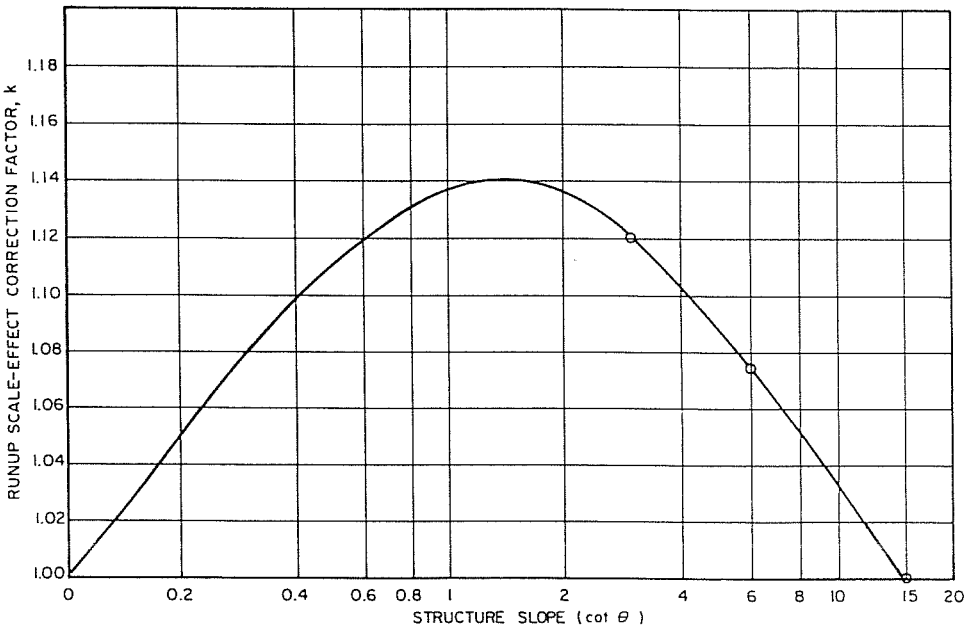

(STOA, 1979)

FIGURE 89
Runup Scale-Effect Correction Factor

$R = (H'_o)(R/H'_o)$

$R = (3)(0.54) = 1.6$ feet

$R = 1.6$ feet

$R = (H'_o)(R/H'_o)(k)$

$R = (5)(0.15)(1.00) = 0.750$ feet

$R = 0.75$ feet

(7) Case 8: Beach Slopes. Wave runup on sloping sandy beaches can be calculated by using the smooth-slope curves in Figures 72 through 81 to find R/H'_o, and by applying the appropriate runup scale-effect correction factor, k, from Figure 89. The rough-slope runup correction factor, r, is 1.00.

$$R = (H'_o)(R/H'_o)(r)(k)$$

$$R = (H'_o)(R/H'_o)(k) \qquad (3\text{-}12)$$

WHERE:
k is found from Figure 89

EXAMPLE PROBLEM 23

Given: a. Equivalent unrefracted deepwater wave height, $H'_o = 5$ feet
b. Water depth at toe of slope, $d_s = 15$ feet
c. Wave period, $T = 3$ seconds
d. Beach slope, cot $\theta = 20$

Find: Runup on beach face.

Solution: (1) Find d_s/H'_o:

$$\frac{d_s}{H'_o} = \frac{15}{5} = 3;$$ therefore, use Figure 72

(2) Find $H'_o/g\,T^2$:

$$\frac{H'_o}{g\,T^2} = \frac{5}{(32.2)(3)^2} = 0.0173$$

(3) From Figure 72 for cot $\theta = 20$ and $H'_o/g\,T^2 = 0.0173$:

$$\frac{R}{H'_o} = 0.15$$

(4) From Figure 89 for cot $\theta = 20$:

$k = 1.00$

(5) Using Equation (3-12), find R:

(8) Special Precautions. Runup calculations are usually made for the significant wave height. It should be borne in mind that larger waves can impinge on the structure if the height is not limited by water depth. The runup that 1 percent of waves exceed can be significantly more than the runup due to the significant wave. Care should be exercised when designing the structure to determine the consequences of minor and occasional overtopping. The significant wave is generally adequate for most design situations. All beach slopes and structures do not necessarily fit the design curves given above. Volume II of the Shore Protection Manual (1977) should be consulted to determine the runup over composite slopes.

5. WAVE TRANSMISSION.

a. Design Parameters. Breakwaters are designed to attenuate waves propagating into the lee of the structure. Waves incident to a breakwater can be dissipated on, transmitted through, or transmitted over the structure. The amount of wave transmission depends on the incident wave height, H_i, the wave period, T, the water depth, d_s, the breakwater type (such as vertical-wall, vertical-thin wall, composite breakwater, wave-baffle, and rubble-mound), breakwater permeability, and breakwater geometry (crest height, h_s, crest width, b, and slope, cot θ).

The ratio of the transmitted, H_t, to incident, H_i, wave height is the transmission coefficient, K_t.

$$K_t = H_t/H_i \qquad (3\text{-}13)$$

WHERE:
K_t = transmission coefficient
H_t = transmitted wave height
H_i = incident wave height

(1) Vertical-Wall, Vertical-Thin Wall, or Composite Breakwaters. These breakwaters are impermeable and

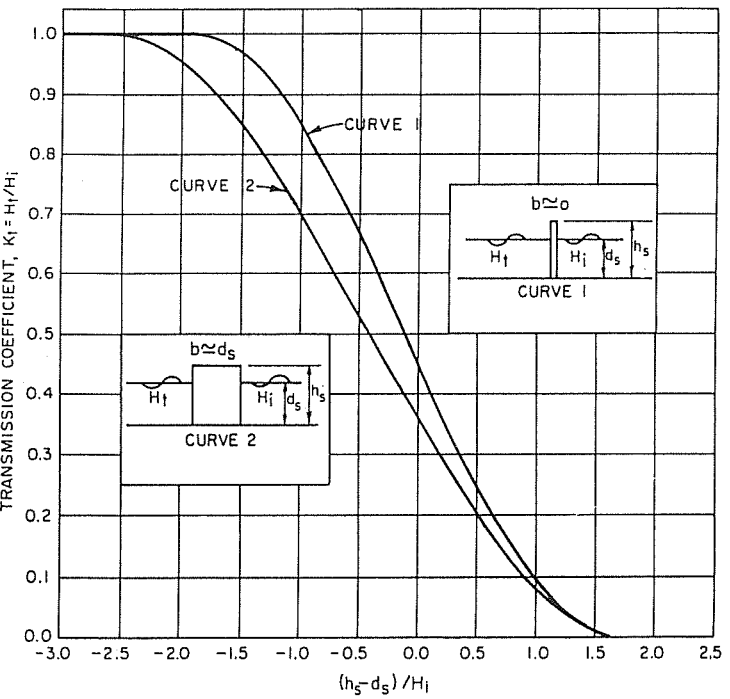

(AFTER SHORE PROTECTION MANUAL, 1977)

FIGURE 90
Transmission Coefficient, K_t, for Impermeable Structures ($0.015 \leq d_s/g\,T^2 \leq 0.0793$)

transmission occurs by overtopping, the transmission is primarily a function of the incident wave height, H_i, the water depth at the structure, d_s, the crest width, b, the slope-protection depth, d_1, and the structure height, h_s. Figures 90 and 91 are used to determine transmission coefficients for impermeable structures. These figures are applicable over the range $0.015 \leq d_s/g\,T^2 \leq 0.0793$.

EXAMPLE PROBLEM 24

Given: a. Deepwater significant wave height, $H_o = 7$ feet
b. Refraction coefficient, $K_R = 0.9$
c. Wave period, $T = 4$ seconds
d. Water depth, $d_s = 25$ feet

Find: Based on significant wave, determine the height of a thin-wall breakwater necessary to reduce the waves in its lee to 1.5 feet.

Solution: (1) Find H_o':

$$H_o' = H_o K_R = (7)(0.9) = 6.3 \text{ feet}$$

(2) Find d_s/L_o:

$$L_o = (g/2\pi)\,T^2 = (32.2/2\pi)(4)^2 = 82.0 \text{ feet}$$

$$\frac{d_s}{L_o} = \frac{25}{82.0} = 0.305$$

(3) From Figure 2 for $d_s/L_o = 0.305$:

$$H/H_o' = 0.95$$

$$H = (0.95)(6.3) = 6.0 \text{ feet}$$

$$H = H_i = 6.0 \text{ feet}$$

(4) The desired transmitted wave height, $H_t = 1.5$ feet.

$$K_t = \frac{H_t}{H_i}$$

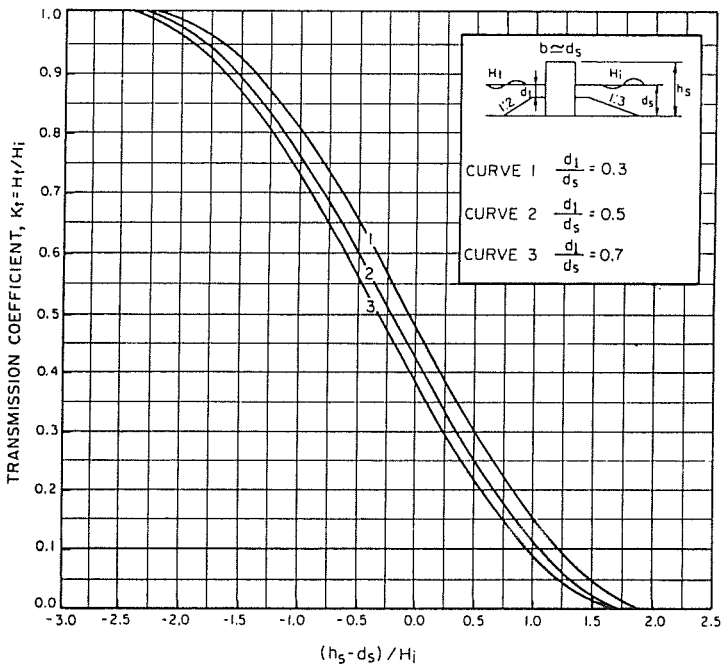

(AFTER SHORE PROTECTION MANUAL, 1977)

FIGURE 91
Transmission Coefficient, K_t, for Impermeable Structures ($0.015 \leq d_s/g\,T^2 \leq 0.0793$)

$$K_t = \frac{1.5}{6.0} = 0.25$$

(5) From Figure 90, using curve 1 and $K_t = 0.25$:

$$(h_s - d_s)/H_i = 0.5$$

$$(h_s - d_s) = 0.5\ H_i$$

$$h_s = 0.5\ H_i + d_s$$

$$h_s = (0.5)(6.0) + 25 = 28 \text{ feet}$$

h_s = 28 feet above the bottom

(2) Wave-Baffle Breakwaters. A wave-baffle breakwater consists of a pile-supported impermeable barrier extending below the surface, but not extending down the entire depth of the water column. Prediction of the wave-transmission coefficient for this structure can be made using Figure 92; this figure predicts the transmission coefficient, K_t, as a function of the depth to wavelength ratio, d_s/L, and of the depth of baffle below the surface to depth ratio, h/d_s. Figure 92 accounts for the transmission of waves under the structure. If the wave baggle is of low height, then wave overtopping may occur in addition to transmission under the structure. In this case, complex interaction between the waves and the structure precludes easy determination of wave transmission, and a physical model study would be necessary.

(3) Rubble-Mound Breakwaters. Rubble-mound breakwaters are rough and permeable, and wave energy is dissipated on the front slope, transmitted over the structure, and transmitted through the voids of the structure. The transmitted wave height is primarily a function of the incident wave steepness, $H_i/g\,T^2$, the ratio of water depth to structure height, d_s/h_s, the ratio of incident wave height to water depth, H_i/d_s, the structure permeability, and the materials making up the breakwater under consideration. Other parameters of secondary importance include type of armor unit and placement, crest width, structure slope, and relative depth, $d_s/g\,T^2$. The problem is complex and it is generally necessary to

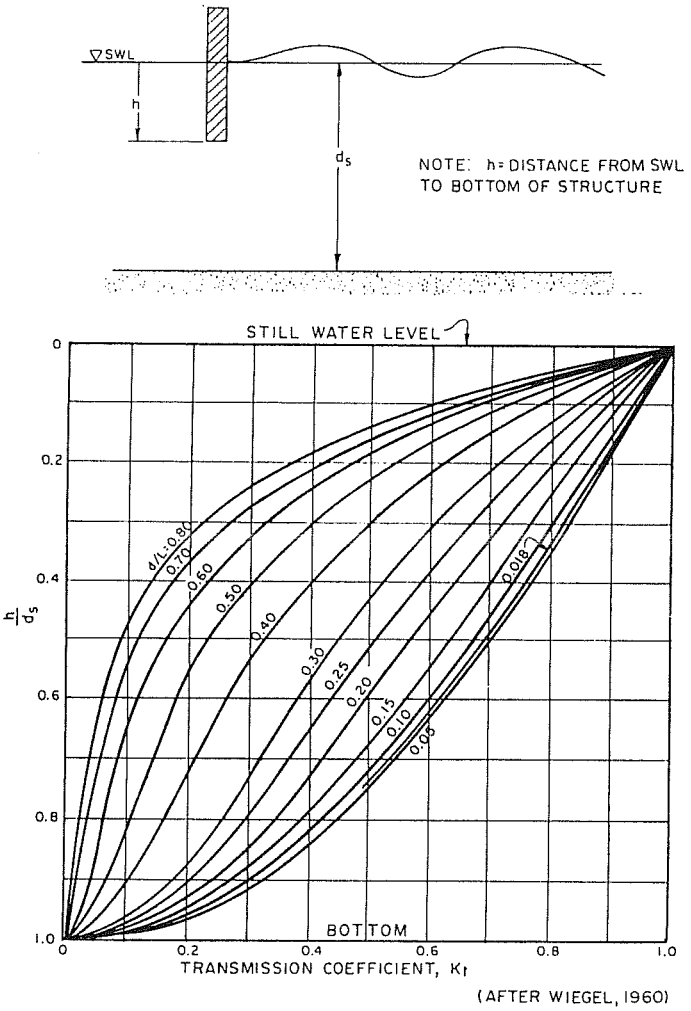

(AFTER WIEGEL, 1960)

FIGURE 92
Transmission Coefficient, K_t, for Wave-Baffle Breakwater

resort to a physical or mathematical model to determine wave-transmission characteristics if the design situation is critically dependent upon transmitted waves. The procedures described subsequently can be used as a first approximation. These procedures are based on methods given in Seelig (1980) which use a computer model for the specific breakwater cross sections shown in Figure 93; these cross sections represent typical designs for the given range of water depths and water conditions. Where breakwater construction differs significantly from that shown for each water depth, wave transmission should be determined by using procedures given in Seelig (1980) or by using a physical model. An example using the method described below is presented in Section 4, Example Problem 27.

(a) Structures in shallow water. Shallow-water breakwaters are usually relatively permeable. The core is generally low and most of the breakwater is made up of high-void armor units. Figure 94 can be used to determine the transmission coefficient, K_t, for a given $H_i/g\,T^2$, d_s/h_s, and H_i/d_s. The curves are based on analysis of the shallow-water structure shown in Figure 93 and are applicable for design water depths ranging from 5 to 10 feet.

(b) Structures in intermediate water depths. Rubble-mound structures built in intermediate design water depths (10 to 20 feet) are typically multilayered breakwaters with a relatively high core of well-graded quarry run. Transmission coefficients may be determined using figure 95. This figure is

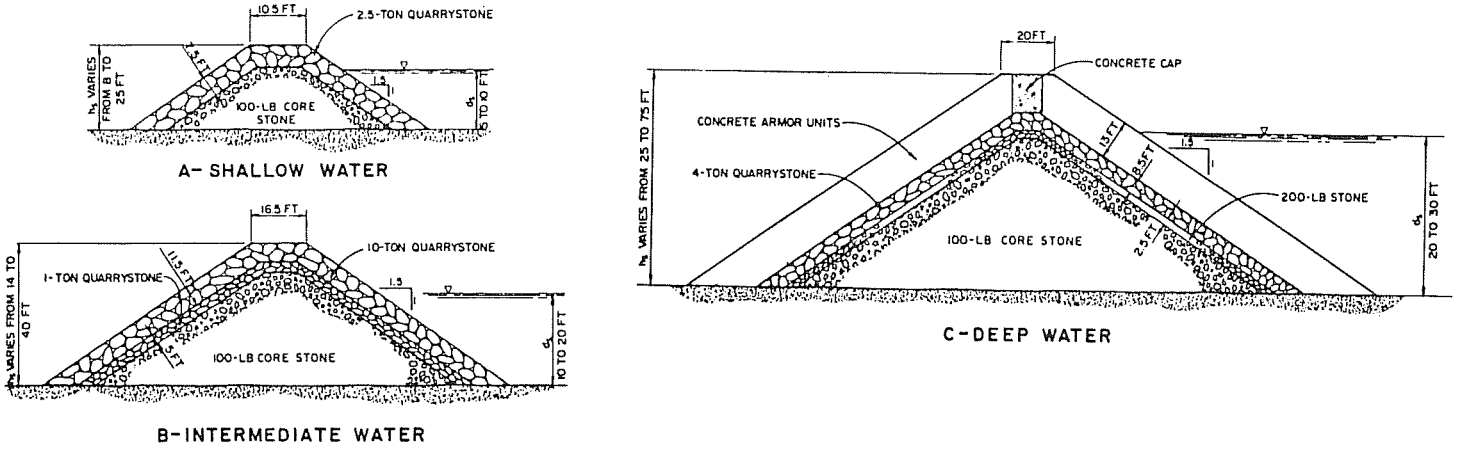

FIGURE 93
Typical Breakwater Cross Sections Used to Determine Wave Transmission

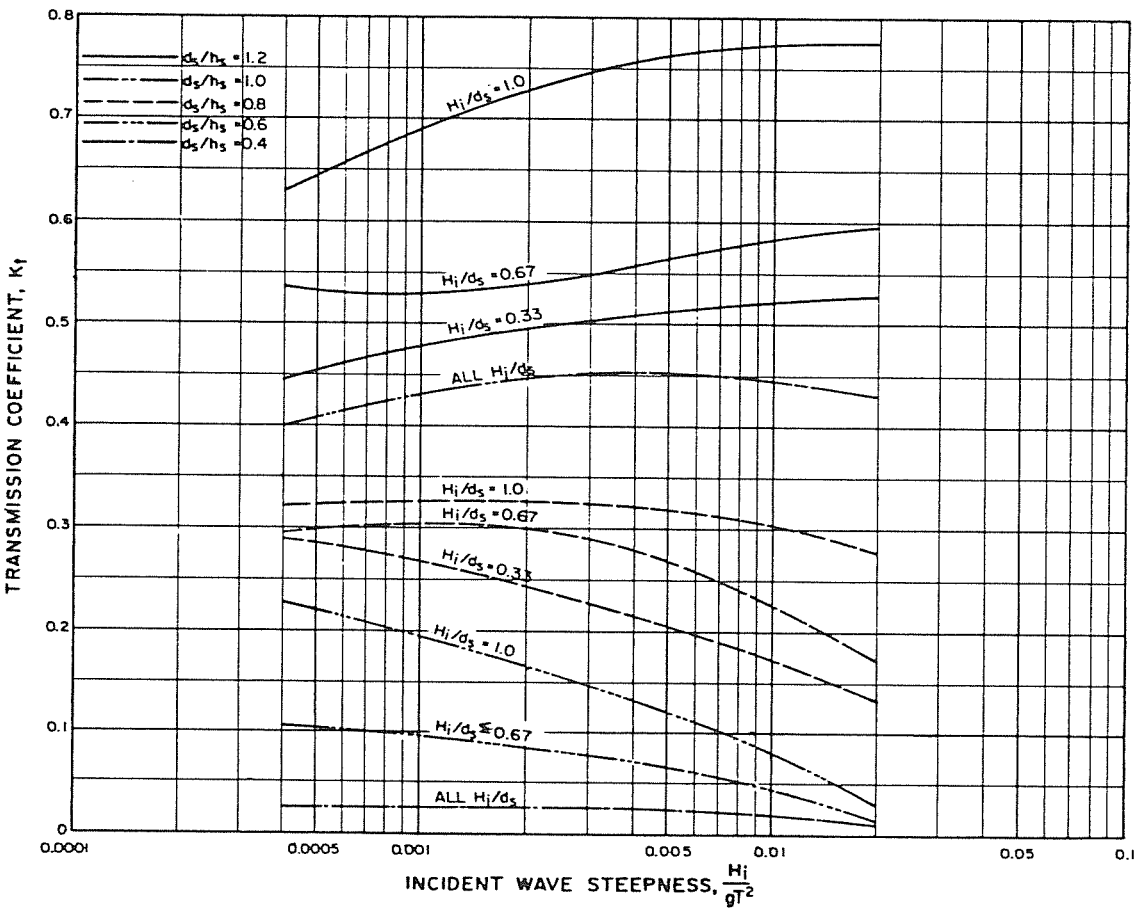

FIGURE 94
Transmission Coefficient, K_t, for a Typical Breakwater in Depths, d_s, Ranging From 5 to 10 Feet

based on analysis of the intermediate-depth-water structure shown in the Figure 93.

(c) Structures in deep water. Structures constructed in deep water (20 to 30 feet) usually have large, relatively impermeable, cores of well-graded material. The armor-layer thickness is small compared to structure height and typically is made up of concrete armor units. Figure 96 is used to determine transmission coefficients based on the deep-water structure shown in Figure 93. Breakwaters constructed in water deeper than 30 feet should be analyzed by using a physical model.

6. WAVE REFLECTION.

a. Discussion. In certain design applications, wave reflection from structures or beaches should be considered. This is true of situations where reflection will have an adverse

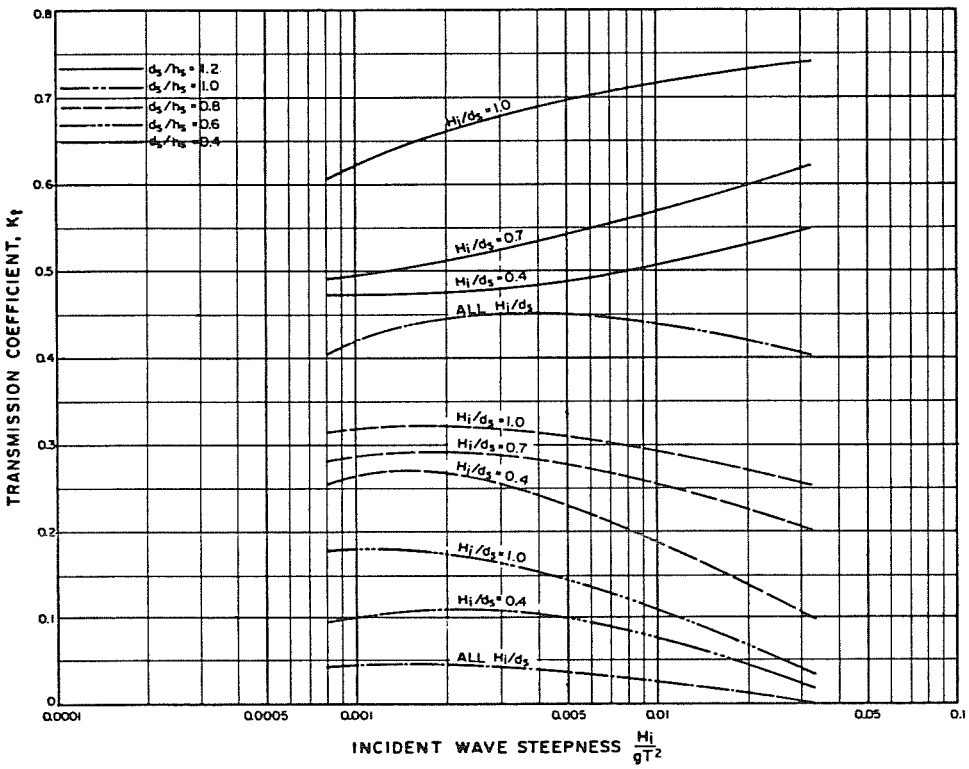

FIGURE 95
Transmission Coefficient, K_t, for a Typical Breakwater in Depths, d_s, Ranging From 10 to 20 Feet

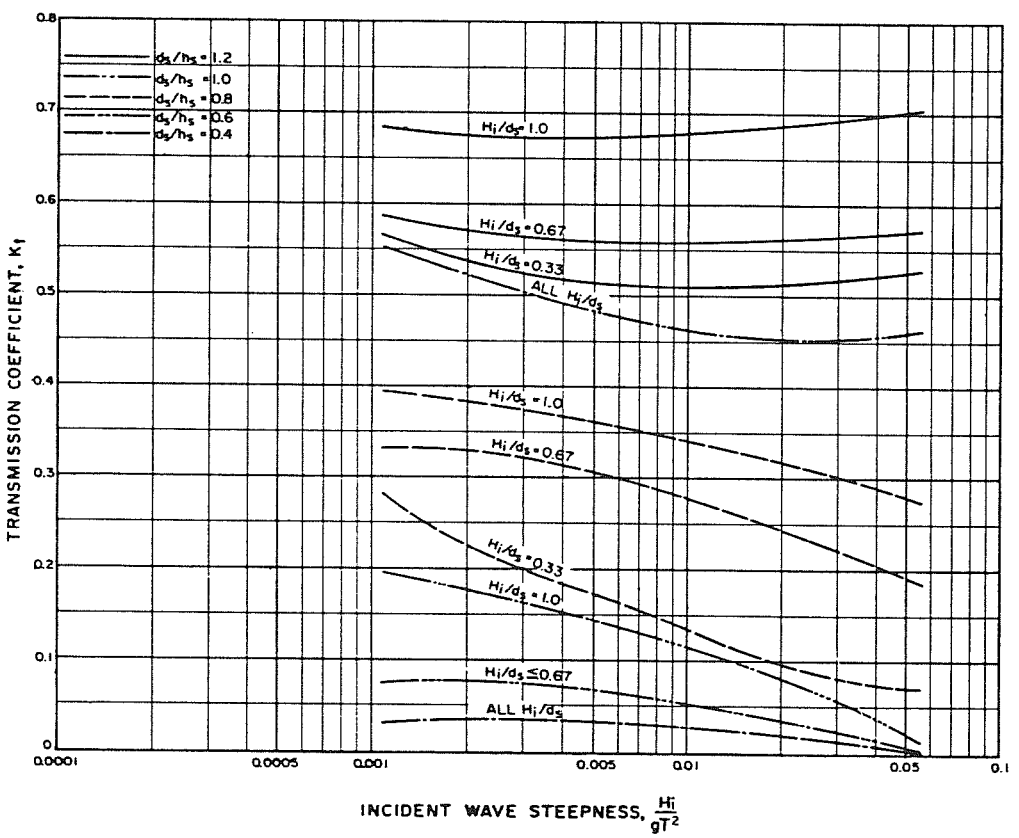

FIGURE 96
Transmission Coefficient, K_t for a Typical Breakwater in Depths, d_s, Ranging From 20 to 30 Feet

TABLE 9
Types of Wave Reflection

Reflection Type	Angle of Incidence	Reflection Pattern
Regular	$90° > \alpha > 45°$	1. $\alpha = r$
Mach	$\alpha < 20°$	1. No reflected wave 2. Mach-stem wave perpendicular to wall
	$45° > \alpha > 20°$	1. $\alpha < r$ 2. Mach-stem wave perpendicular to wall

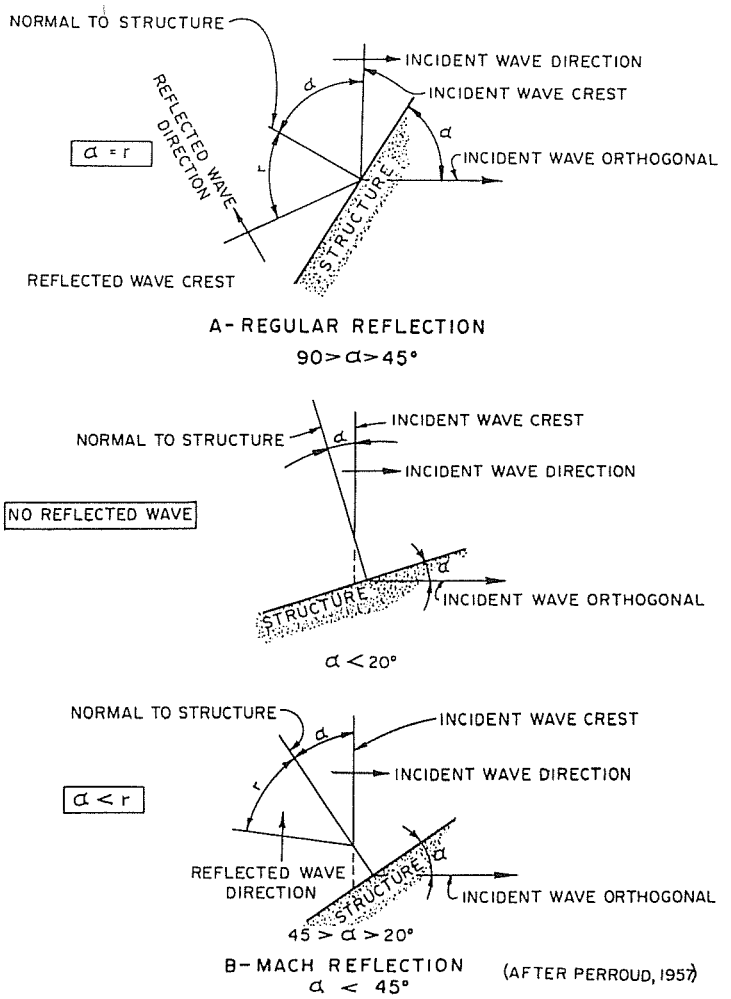

FIGURE 97
Definition of Terms Used in Reflection Calculations

effect on navigation or littoral processes. The type of reflection pattern present depends on the angle of incidence, α. The angle of reflection is denoted r.

Two basic patterns of wave reflection take place when waves approach a structure at an angle: "normal" reflection or "Mach" reflection. The critical angle of incidence separating the two patterns is 45°. For $\alpha > 45°$, the reflection pattern is "regular;" for $\alpha < 45°$, the reflection pattern is the "Mach" reflection type. The two types of wave reflection are summarized in Table 9 and diagrammed in Figure 97.

For "regular" reflection (when $\alpha > 45°$), the angle of incidence equals the angle of reflection, and the reflected wave height, H_r, is only slightly less than the incident wave height, H_i. For "Mach" reflection, there are two subcases of reflection pattern. For $\alpha < 20°$, the incident wave crest bends so that it becomes perpendicular to the structure, and no reflected wave appears. For $\alpha > 20°$ (but $< 45°$), three waves are present: the incident wave, the reflected wave, and the "Mach-stem" wave (the portion of the wave crest perpendicular to the structure). For the reflected wave, the height, H_r, is smaller than the incident wave height, H_i, and the angle of reflection is greater than the angle of incidence. The wave height of the Mach-stem wave, H_m, is greater than the incident wave height, H_i.

b. Calculation of Reflection. Wave reflection from revetments, rubble-mound breakwaters, and beaches is determined through empirical equations developed by Seelig and Ahrens (1980) for waves approaching a structure at normal incidence. Figure 98 is a sketch defining terms used in reflection calculations. The general equation for determining reflected wave height is:

$$K_r = \frac{\alpha \xi^2}{\beta + \xi^2} \qquad (3\text{-}14)$$

WHERE:

K_r = reflection coefficient, defined as the ratio of the reflected, H_r, to the incident, H_i, wave height = H_r/H_i

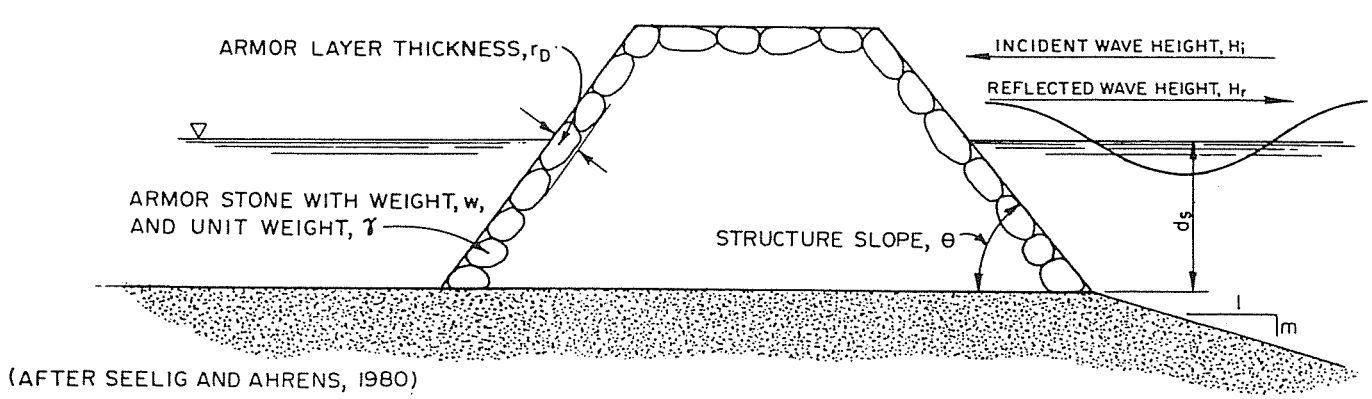

FIGURE 98
Terms Used in Reflection Calculations

α, β = empirically derived constants which depend on structure type, water depth at structure toe, roughness of slope, number of armor layers, and breaking-wave height

$\zeta = \frac{\tan\theta}{\sqrt{\frac{H_i}{L_o}}}$ = surf parameter

θ = structure-slope angle

L_o = deepwater wavelength

(1) Revetments.

(a) Smooth-face revetments, $d_s/H_i > 5$. In this situation, the interaction of the incident wave with, or modification of the incident wave by, the presence of the structure dominates the magnitude of the reflection coefficient. For values of tan $\theta \leq 0.1667$, use $\alpha = 1.0$ and $\beta = 5.5$; thus, Equation (3-14) becomes:

$$K_r = \frac{1.0\ \xi^2}{5.5 + \xi^2} \qquad (3\text{-}15)$$

(b) Smooth-face revetments, $d_s/H_i \leq 5$. In this situation, the reflection coefficient is influenced by the wave breaking at the toe or seaward of the structure. The value of α for use in Equation (3-14) is defined as:

$$\alpha = \exp\left[(-0.5)\left(\frac{H_i}{H_b}\right)^{1.3}\right] \qquad (3\text{-}16)$$

WHERE:

exp = e = base of natural logarithm = 2.178...

H_i = incident wave height

$$H_b = 0.17\ L_o \left\{1 - \exp\left[-4.712\left(\frac{d_s}{L_o}\right)(1 + 15\ m^{1.333})\right]\right\} \qquad (3\text{-}17)$$

d_s = water depth at structure toe

L_o = deepwater wavelength

m = slope in front of structure

The value for β is 5.5.

(c) Rubble-mound revetments with one layer or armor stone. In this situation, the presence of a rough surface will reduce the amount of wave reflection. The value of α for use in Equation (3-14) is defined as:

$$\alpha = \exp\left[-1.7\sqrt{\frac{r_D}{L}}\cot\theta - (0.5)\left(\frac{H_i}{H_b}\right)^{1.3}\right] \qquad (3\text{-}18)$$

WHERE:

exp = e = base of natural logarithm = 2.718...

r_D = $(w/\gamma)^{1/3}$ = representative armor-stone diameter

w = armor-stone weight

γ = unit weight of armor stone

L = wavelength at structure toe

θ = structure-slope angle

H_i = incident wave height

H_b = breaking-wave height (Equation 3-17)

The value for β is 5.5.

(d) Rubble-mound revetments with more than one layer or armor stone. As the number of armor layers increases, the reflection coefficient, K_r, decreases. In this situation, the value of α for use in Equation (3-14) is determined as follows:

$$\alpha = \alpha' \exp\left[-1.7\sqrt{\frac{r_D}{L}}\cot\theta - (0.5)\left(\frac{H_i}{H_b}\right)^{1.3}\right] \qquad (3\text{-}19)$$

TABLE 10
Reflection-Coefficient Reduction Factor, α', Due to Multiple Armor Layers

Number of Layers.....	2	3	4
r_D/H_i			
<0.75.....	0.93	0.88	0.78
0.75 to 2.0.....	0.71	0.70	0.69
>2.0.....	0.58	0.52	0.49

(SEELIG AND AHRENS, 1980)

WHERE:

α' is found in Table 10

exp = e = base of natural logarithm = 2.718...

r_D = representative armor-stone diameter

L = wavelength at structure toe

θ = structure-slope angle

The value for β is 5.5.

EXAMPLE PROBLEM 25

Given:
a. Incident wave height, H_i = 10 feet
b. Water depth at structure toe, d_s = 15 feet
c. Wave period, T = 8 seconds
d. Structure slope, tan θ = 0.667
e. Armor-stone weight, w = 3 tons
f. Unit weight of armor stone, γ = 160 pounds per cubic foot
g. Slope in front of structure, m = 1/20

Find: Height of reflected wave for structure with one layer of armor.

Solution:

(1) Find L_o:

$L_o = (g/2\pi)\ T^2 = (32.2/2\pi)(8)^2 = 327.7$ ft

(2) Using Equation (3-17), find H_b:

$H_b = 0.17\ L_o \left\{1 - \exp\left[-4.712\left(\frac{d_s}{L_o}\right)(1 + 15\ m^{1.333})\right]\right\}$

$H_b = (0.17)(327.7)\left\{1 - \exp\left\{-4.712\left(\frac{15}{327.7}\right)\left[1 + (15)\left(\frac{1}{20}\right)^{1.333}\right]\right\}\right\}$

H_b = 13.41 feet

(3) Convert armor-stone weight, in tons, to pounds:

$(3\text{ tons})\left(\frac{2{,}000\text{ pounds}}{1\text{ ton}}\right)$ = 6,000 pounds

(4) Find r_D:

$r_D = \left(\frac{w}{\gamma}\right)^{1/3} = \left(\frac{6{,}000}{160}\right)^{1/3}$ = 3.35 feet

(5) Find L:

$\frac{d_s}{L_o} = \frac{15}{328} = 0.0457$

From Figure 2 for d_s/L_o = 0.0457:

$\frac{d_s}{L} = 0.09$

$L = \frac{d_s}{0.09} = \frac{15}{0.09}$ = 166.7 feet

(6) Using Equation (3-18), find α:

$\alpha = \exp\left[-1.7\sqrt{\frac{r_D}{L}}\cot\theta - (0.5)\left(\frac{H_i}{H_b}\right)^{1.3}\right]$

$\alpha = \exp\left[-1.7\sqrt{\frac{3.35}{166.7}}(1.5) - (0.5)\left(\frac{10}{13.4}\right)^{1.3}\right]$

α = 0.49

(7) Find ξ:

$\xi = \frac{\tan\theta}{\sqrt{\frac{H_i}{L_o}}} = \frac{0.667}{\sqrt{\frac{10}{328}}} = 3.82$

(8) $\beta = 5.5$

(9) Using Equation (3-14), find K_r:

$$K_r = \frac{\alpha \xi^2}{\beta + \xi^2} = \frac{(0.49)(3.82)^2}{5.5 + (3.82)^2} = 0.36$$

(10) Find H_r:

$$K_r = \frac{H_r}{H_i}$$

THEREFORE: $H_r = K_r H_i = (0.36)(10) = 3.6$ feet

(2) Rubble-Mound Breakwaters. A conservative estimate of K_r for rubble-mound breakwaters armored with quarrystone or dolosse is determined as follows:

$$K_r = \frac{0.6 \xi^2}{6.6 + \xi^2} \qquad (3\text{-}20)$$

EXAMPLE PROBLEM 26

Given: a. Incident wave height, $H_i = 20$ feet
b. Water depth at structure toe, $d_s = 35$ feet
c. Wave period, $T = 15$ seconds
d. Structure slope, $\tan \theta = 0.5$

Find: Reflected wave height from a rubble-mound breakwater.

Solution: (1) Find L_o:

$$L_o = (g/2\pi) T^2 = (32.2/2\pi)(15)^2 = 1{,}153.1 \text{ feet}$$

(2) Find ξ:

$$\xi = \frac{\tan \theta}{\sqrt{\frac{H_i}{L_o}}} = \frac{0.5}{\sqrt{\frac{20}{1{,}153.1}}} = 3.797$$

(3) Using Equation (3-20), find K_r:

$$K_r = \frac{0.6 \xi^2}{6.6 + \xi^2}$$

$$K_r = \frac{(0.6)(3.797)^2}{6.6 + (3.797)^2} = 0.412$$

(4) Find H_r:

$$K_r = \frac{H_r}{H_i}$$

THEREFORE: $H_r = K_r H_i = (0.412)(20) = 8.24$ feet

(3) Beaches. A conservative estimate of K_r for beaches is determined as follows:

$$K_r = \frac{1.0 \xi^2}{5.5 + \xi^2} \qquad (3\text{-}21)$$

In this situation, the value of tan θ for the beach is taken at the still water line.

7. METRIC EQUIVALENCE CHART. The following metric equivalents were developed in accordance with ASTM E-621. These units are listed in the sequence in which they appear in the text in Section 3. Conversions are approximate.

5 feet = 1.5 meters
10 feet = 3.0 meters
20 feet = 6.1 meters
30 feet = 9.1 meters

SECTION 4
DESIGN OF RUBBLE-MOUND STRUCTURES

1. GENERAL. Rubble-mound structures generally have a core covered with one to several quarrystone underlayers which are protected with armor units of stone or specially shaped concrete units. Breakwaters have a core material of randomly dumped, well-graded quarry run, sand, or coral. This material is generally impermeable. Successive underlayers cover the core; the material in each successive layer is carefully increased in size to prevent loss of the smaller-sized core material. Armor units are placed on the outer surface to hold the core and the underlayers in place against wave attack. Rubble-mound revetments, groins, and jetties are similarly built in that armor units hold the underlying material in place. Rubble-mound structures are well-suited to the coastal zone because they can absorb the forces of waves with relatively minor damage even when design conditions are exceeded to a moderate degree. Table 11 summarizes principles that should be considered in the design of rubble-mound structures.

2. DESIGN.

a. **Armor Units.** Generally, quarrystone is the most cost-effective armor unit; however, the use of concrete armor units, such as tetrapods, dolosse, and tribars (see Figures 99, 100, and 101, respectively), may be advantageous when nearby quarries cannot economically produce large enough stone. The weight of an individual armor unit can be found by the equation:

$$W = (w_r H^3)/[K_D (S_r - 1)^3 \cot \theta] \qquad (4\text{-}1)$$

WHERE:

W	=	weight of individual armor unit
w_r	=	unit weight of armor material (saturated surface dry)
H	=	design wave height (use significant wave height, H_s)
K_D	=	stability coefficient (see Table 12 for appropriate value)
S_r	=	w_r/w_w = specific gravity of armor unit, based on the unit weight of water at the structure
w_w	=	unit weight of water
θ	=	angle of structure slope measured relative to the horizontal

b. Design Considerations. The following should be carefully considered:

(1) Structure slopes should not be steeper than 1:1.5 (1:2 where dolosse are used), without conducting model studies. In addition to selection of proper armor units, other considerations should be investigated in rubble-mound design, such as possible settlement of the structure and stability of the soil supporting the structure against slope failure.

(2) Armor units should be placed in at least a two-layer thickness except for uniformly fitted tribars and specially placed quarrystone. In these cases, single-layer placement is permissible if the structure is sited on a hard bottom, where foundation settlement or scour cannot occur, and if the contractor carefully keys and fits the units into place with the long axis perpendicular to the slope.

(3) Armor units for the structure head should be larger than those for the trunk and should extend along the trunk on the seaward and lee sides at least five wave heights from the end of the head. In lieu of larger armor units, the slope of the head

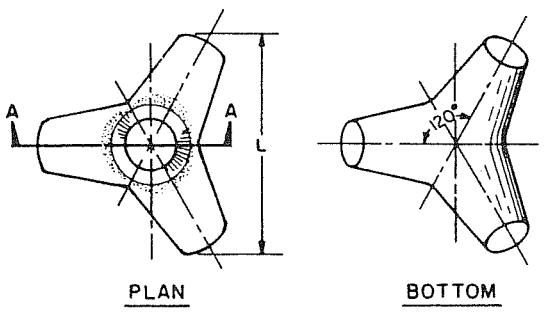

PLAN BOTTOM

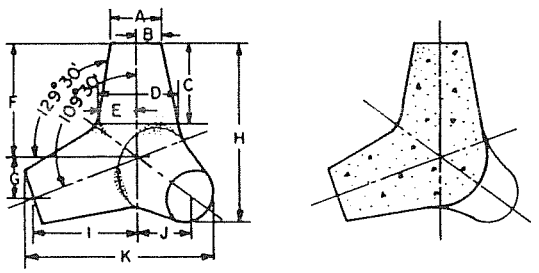

ELEVATION SECTION A-A

UNIT WEIGHT (LB/CU FT)	VOLUME OF INDIVIDUAL ARMOR UNITS (CU FT)										
	7.14	14.29	28.57	71.43	142.86	214.29	285.71	357.14	428.57	500.00	571.43
	WEIGHT OF INDIVIDUAL ARMOR UNITS (TONS)										
140.0	0.50	1.00	2.00	5.00	10.00	15.00	20.00	25.00	30.00	35.00	40.00
149.5	0.53	1.07	2.14	5.34	10.68	16.02	21.36	26.70	32.04	37.38	42.71
156.0	0.56	1.11	2.23	5.57	11.14	16.71	22.29	27.86	33.43	39.00	44.57
162.0	0.58	1.16	2.31	5.79	11.57	17.36	23.14	28.93	34.71	40.50	46.29
	AVERAGE MEASURED THICKNESS OF TWO LAYERS, RANDOMLY PLACED (FT)										
	4.01	5.05	6.36	8.63	10.87	12.45	13.70	14.76	15.68	16.51	17.26
	NUMBER OF ARMOR UNITS PER 1,000 SQUARE FEET (TWO LAYERS, RANDOMLY PLACED)										
	280.18	176.49	111.18	60.42	37.96	29.02	24.02	20.70	18.41	16.54	15.18

SYMBOL	DIMENSIONS OF ARMOR UNITS (FT)										
A	0.89	1.12	1.41	1.91	2.41	2.76	3.04	3.27	3.48	3.66	3.83
B	0.44	0.56	0.70	0.95	1.20	1.36	1.52	1.63	1.74	1.83	1.91
C	1.40	1.77	2.23	3.02	3.81	4.36	4.80	5.17	5.50	5.79	6.05
D	1.38	1.74	2.20	2.96	3.76	4.30	4.73	5.10	5.42	5.70	5.96
E	0.69	0.87	1.10	1.49	1.88	2.15	2.37	2.55	2.71	2.85	2.96
F	1.89	2.36	3.00	4.08	5.14	5.88	6.47	6.97	7.41	7.80	8.16
G	0.63	0.79	1.00	1.36	1.71	1.96	2.16	2.32	2.47	2.60	2.72
H	2.94	3.71	4.67	6.34	7.99	9.14	10.07	10.84	11.52	12.13	12.68
I	1.78	2.25	2.83	3.84	4.84	5.54	6.10	6.57	6.98	7.35	7.69
J	0.89	1.12	1.41	1.92	2.42	2.77	3.05	3.28	3.49	3.67	3.84
K	3.21	4.04	5.09	6.91	8.71	9.97	10.97	11.82	12.56	13.23	13.83
L	3.54	4.45	5.61	7.62	9.60	10.96	12.09	13.02	13.84	14.57	15.23

NOTE: DATA BASED ON TETRAPODS USED IN MODEL TESTS CONDUCTED AT THE U.S. ARMY CORPS OF ENGINEERS WATERWAYS EXPERIMENT STATION

VOLUME OF INDIVIDUAL ARMOR UNIT = $0.280\ H^3$

WHERE: H = OVERALL DIMENSION OF UNIT
A = 0.302 H
B = 0.151 H
C = 0.477 H
D = 0.470 H
E = 0.235 H
F = 0.644 H
G = 0.215 H
I = 0.606 H
J = 0.303 H
K = 1.091 H
L = 1.201 H
ARMOR-LAYER THICKNESS (2 UNITS) = 1.361 H

FIGURE 99
Tetrapod Specifications

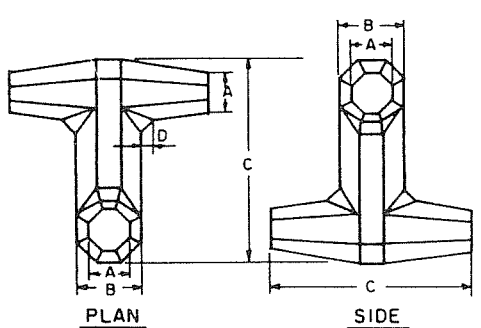

PLAN SIDE

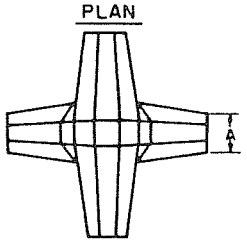

ELEVATION

UNIT WEIGHT (LB/CU FT)	VOLUME OF INDIVIDUAL ARMOR UNITS (CU FT)										
	7.14	14.29	28.57	71.43	142.86	214.29	285.71	357.14	428.57	500.00	571.43
	WEIGHT OF INDIVIDUAL ARMOR UNITS (TONS)										
140.0	0.50	1.00	2.00	5.00	10.00	15.00	20.00	25.00	30.00	35.00	40.00
149.5	0.53	1.07	2.14	5.34	10.68	16.02	21.36	26.70	32.04	37.38	42.71
156.0	0.56	1.11	2.23	5.57	11.14	16.71	22.29	27.86	32.43	39.00	44.57
162.0	0.58	1.16	2.31	5.79	11.57	17.36	23.14	28.93	34.71	40.50	46.29
	AVERAGE MEASURED THICKNESS OF TWO LAYERS, RANDOMLY PLACED (FT)										
	3.6	4.6	5.7	7.8	9.8	11.2	12.4	13.3	14.2	14.9	15.6
	NUMBER OF ARMOR UNITS PER 1,000 SQUARE FEET (TWO LAYERS, RANDOMLY PLACED)										
	223.0	104.5	88.5	48.1	30.3	23.1	19.1	16.4	14.6	13.1	12.0

SYMBOL	DIMENSIONS OF ARMOR UNITS (FT)										
A	0.71	0.89	1.13	1.53	1.93	2.20	2.43	2.61	2.78	2.92	3.06
B	1.13	1.43	1.80	2.44	3.08	3.52	3.88	4.18	4.44	4.68	4.89
C	3.55	4.47	5.63	7.64	9.63	11.02	12.13	13.08	13.89	14.62	15.29
D	0.20	0.25	0.32	0.43	0.55	0.62	0.69	0.74	0.79	0.83	0.87

NOTE: SHAPE AND DIMENSIONS OF UNIT BASED ON THOSE USED IN MODEL TESTS. AT PRESENT TIME, INVENTOR RECOMMENDS B = 0.32 C TO 0.36 C, DEPENDING ON THE WEIGHT OF THE INDIVIDUAL UNIT.

VOLUME OF INDIVIDUAL ARMOR UNIT = $0.16\ C^3$

WHERE: C = OVERALL DIMENSION OF UNIT
A = 0.20 C
B = 0.32 C
D = 0.057 C
ARMOR-LAYER THICKNESS (2 UNITS) = 1.020 C

FIGURE 100
Dolos Specifications

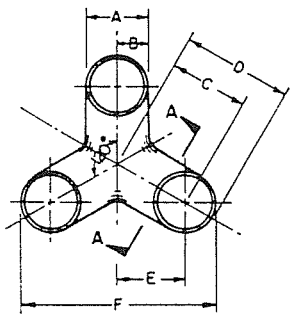

PLAN

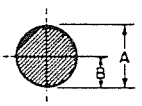

SECTION A-A

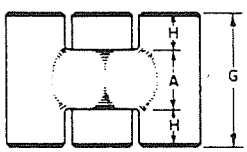

ELEVATION

UNIT WEIGHT (LB/CU FT)	VOLUME OF INDIVIDUAL ARMOR UNITS (CU FT)										
	7.14	14.29	28.57	71.43	142.86	214.29	285.71	357.14	428.57	500.00	571.43
	WEIGHT OF INDIVIDUAL ARMOR UNITS (TONS)										
140.0	0.50	1.00	2.00	5.00	10.00	15.00	20.00	25.00	30.00	35.00	40.00
149.5	0.53	1.07	2.14	5.34	10.68	16.02	21.36	26.70	32.04	37.38	42.71
156.0	0.56	1.11	2.23	5.57	11.14	16.71	22.29	27.86	33.43	39.00	44.57
162.0	0.58	1.16	2.31	5.79	11.57	17.36	23.14	28.93	34.71	40.50	46.29
	AVERAGE MEASURED THICKNESS OF ONE LAYER, UNIFORMLY PLACED (FT)										
	2.18	2.74	3.45	4.69	5.91	6.76	7.44	8.02	8.52	8.97	9.38
	AVERAGE MEASURED THICKNESS OF TWO LAYERS, PLACED PELLMELL (FT)										
	3.85	4.85	6.11	8.30	10.46	11.97	13.17	14.19	15.08	15.87	16.60
	NUMBER OF ARMOR UNITS PER 1,000 SQUARE FEET (ONE LAYER, UNIFORMLY PLACED)										
	161.34	101.63	64.02	34.80	21.86	16.71	13.83	11.92	10.60	9.52	8.74
	NUMBER OF ARMOR UNITS PER 1,000 SQUARE FEET (TWO LAYERS, PLACED PELLMELL)										
	247.85	156.12	98.35	53.45	33.58	25.67	21.25	18.31	16.28	14.63	13.43
SYMBOL	DIMENSIONS OF ARMOR UNITS (FT)										
A	1.05	1.32	1.66	2.25	2.84	3.25	3.58	3.85	4.09	4.31	4.51
B	0.52	0.66	0.83	1.13	1.42	1.62	1.79	1.93	2.05	2.15	2.25
C	1.25	1.58	1.99	2.70	3.41	3.90	4.29	4.62	4.91	5.17	5.41
D	1.78	2.24	2.82	3.83	4.82	5.52	6.08	6.55	6.96	7.33	7.66
E	1.09	1.37	1.72	2.34	2.95	3.38	3.72	4.00	4.25	4.48	4.68
F	3.22	4.06	5.11	6.93	8.74	10.00	11.01	11.86	12.60	13.26	13.87
G	2.09	2.63	3.32	4.51	5.68	6.50	7.15	7.70	8.19	8.62	9.01
H	0.52	0.66	0.83	1.13	1.42	1.62	1.79	1.93	2.05	2.15	2.25

NOTE: SHAPE AND DIMENSIONS OF UNIT BASED ON THOSE USED IN MODEL TESTS. AT PRESENT TIME, PATENTEE RECOMMENDS C = 1.25 A, AND FILLETS AT INTERSECTION OF HORIZONTAL AND VERTICAL MEMBERS WITH A RADIUS EQUAL TO A/4.

VOLUME OF INDIVIDUAL ARMOR UNIT = $6.48\ A^3$

WHERE: A = diameter of leg
B = 0.5 A
C = 1.25 A
D = 1.75 A
E = 1.08 A
F = 3.16 A
G = 2 A
H = B = 0.5 A

ARMOR-LAYER THICKNESS (2 UNITS, RANDOM) = 3.68 A

FIGURE 101
Tribar Specifications

TABLE 11
Design Principles for Rubble-Mound Structures

Feature	Function
Armor units.....	Prevent their own dislodgement by wave forces; must be dense enough and heavy enough, or have sufficient interlocking ability, to prevent dislodgement.
Crest elevation....	Sufficient crest elevation allows a structure to serve its function. In general, revetments should not be heavily overtopped. Breakwaters should provide adequate wave protection. Groins and jetties should have barriers that are impermeable to sand to a high enough elevation so that sand is prevented from leaking through or over the structure.
Underlayers.....	Prevent fines of smaller core or other underlayers from washing through voids in the structure. In the case of a revetment, the smallest underlayer prevents the in situ fines from washing through voids. (The smallest underlayer is sometimes referred to as a filter layer.)
Toe protection.....	Prevents undermining, by waves and currents, of a structure situated on unconsolidated material; allows for scour at the toe.
Core.....	Can render a breakwater or other rubble-mound structure impermeable due to the presence of the fine materials found in the relatively inexpensive quarry material used.
Flank protection...	Protects the flanks of a revetment or jetty and prevents erosion from unraveling the structure.
Concrete cap.....	Stabilizes the crest of a low-height breakwater or other rubble-mound structure and provides an access and maintenance road on the breakwater.

section may be flattened sufficiently according to Equation (4-1).

(4) If the design condition is a nonbreaking wave at high tide, a check should be made to determine if the wave breaks at a lower tide. If this is the case, the appropriate K_D for breaking waves should be selected.

(5) Armor stones should be graded such that the maximum size is 1.25 W and the minimum size is 0.75 W. Approximately 75 percent of the stones should be equal to, or larger than, W.

(6) Armor units should be hard, durable, and clean, without cracks, cleavages, or laminations. They should be chemically stable in fresh or salt water and should not weather due to freeze/thaw or wet/dry cycles.

(7) The smallest dimension of an armor unit should not be less than one-third of the largest dimension.

(8) Large concrete armor units should not be permitted to exhibit excessive movement during design conditions. A hydraulic model may be a beneficial design tool for large projects.

(9) Steel reinforcing can be used in concrete armor units to assist in handling and placing. Steel should be embedded at least 3 inches from all surfaces. The use of steel reinforcement for concrete armor units of less than 5 tons is rare. It is not mandatory to use reinforcing bars for larger units; however, reinforced units may have a longer life than nonreinforced units if they are to be subject to rocking.

(10) A graded riprap structure can be designed for waves with heights of less than about 5 feet by using the appropriate K_{RR} value in Table 12 (the value of K_{RR} is substituted for K_D in Equation (4-1). The value for the weight of the stone determined from Equation (4-1) for graded riprap is the 50-percent size in the gradation and is denoted W_{50}. The

TABLE 12
Suggested Stability Coefficient, K_D, Values for Use in Determining Armor-Unit Weight, W (No-Damage Criteria and Minor Overtopping)

Armor Units	[1] n	Placement	Slope (cot θ)	Structure Trunk K_D [2]		Structure Head K_D	
				Breaking Wave	Nonbreaking Wave	Breaking Wave	Nonbreaking Wave
Quarrystone							
Smooth, rounded...	2	Random	1.5 to 3.0	2.1	2.4	1.7	1.9
Smooth, rounded...	> 3	Random	[5] ...	2.8	3.2	2.1	2.3
Rough, angular....	1	Random [3]	[5] ...	[3] ...	2.9	[3] ...	2.3
Rough, angular....	2	Random	1.5			2.9	3.2
			2.0	3.5	4.0	2.5	2.8
			3.0			2.0	2.3
Rough, angular....	> 3	Random	[5] ...	3.9	4.5	3.7	4.2
Rough, angular....	2	Special [4]	[5] ...	4.8	5.5	3.5	4.5
Tetrapod			1.5			5.9	6.6
and	2	Random	2.0	7.2	8.3	5.5	6.1
Quadripod.....			3.0			4.0	4.4
			1.5			8.3	9.0
Tribar.....	2	Random	2.0	9.0	10.4	7.8	8.5
			3.0			7.0	7.7
Dolos.....	2	Random	[6] 2.0	22.0	25.0	15.0	16.5
			3.0			13.5	15.0
Modified Cube.....	2	Random	[5] ...	6.8	7.8	...	5.0
Hexapod.....	2	Random	[5] ...	8.2	9.5	5.0	7.0
Tribar.....	1	Uniform	[5] ...	12.0	15.0	7.5	9.5
Quarrystone (K_{RR}) [7]							
Graded, angular...	...	Random	...	2.2	2.5	...	...

[1] n is the number of units comprising the thickness of the armor layer.
[2] Applicable to slopes ranging from 1 on 1.5 to 1 on 5.
[3] The use of single layer of quarrystone armor units subject to breaking waves is not recommended, and only under special conditions for nonbreaking waves. When it is used, the stone should be carefully placed.
[4] Special placement with long axis of stone placed perpendicular to structure face.
[5] Until more information is available on the variation of K_D value with slope, the use of K_D should be limited to slopes ranging from 1 on 1.5 to 1 on 3. Some armor units tested on a structure head indicate a K_D-slope dependence.
[6] Stability of dolosse on slopes steeper than 1 on 2 should be investigated by site-specific model tests.
[7] For graded riprap, use K_{RR} instead of K_D.

(AFTER SHORE PROTECTION MANUAL, 1977)

maximum stone size is 3.6 W_{50}, the minimum is 0.22 W_{50}, and 50 percent of the material weighs W_{50} or more.

(11) Armor units must extend over the crest onto the slope on the lee side. Lee-side armor units should weigh at least as much as front-slope units if the structure-crest freeboard above the design water level (F) is less than three-fourths of the design wave height. If the structure-crest freeboard is less than one-half of the design wave height, back-slope armor units may need to weigh more than those on the front slope. If this be the case, model studies should be conducted. If the crest freeboard is greater than three-fourths of the design wave height, economy can be achieved by conducting a model study to optimize the armor-unit size for the back slope. Waves generated in the harbor may also govern back-slope armor design. (See Figure 102 for preliminary guidance on the relative weight of back-slope, W_b, to front-slope, W_f, armor units, where $F = h_s - d_s$ = freeboard.)

(12) Armor-unit stability should not depend on chinking.

(13) An allowance should be made for overbuilding the structure in the event settlement occurs.

(14) Allow at least a year for settlement prior to constructing a massive concrete cap on the breakwater.

3. CREST.

a. **Crest Height**. The height of the crest, h_s, depends upon several factors, including crest and back-slope armor-unit stability and desired transmitted-wave height. Construction techniques must also be considered. Land-based equipment requires a working road out of the normal runup zone; floating plants require sufficiently deep and quiescent waters.

b. Crest Width. The crest width, B, should be sufficient to support construction and maintenance vehicles if the breakwater is to be constructed from land. The crest should be a minimum of three stones wide for stability. The minimum width for a working platform when land-based equipment is used is 12 to 15 feet. For smaller breakwater projects, when land-based construction equipment is used, economy can be achieved by building a temporary working platform or road on the core or underlayer material. The cap stones, or armor units, can then be placed with a minimum three-stone width, which can be less than 12 feet. This is done by starting the last layer on the cap and working landward. A disadvantage of this technique is that repairs require removal of stones or working from a floating plant. The minimum crest width, B, for a moderately overtopped breakwater is:

$$B = n\, k_{\Delta} (W/w_r)^{1/3} \qquad (4\text{-}2)$$

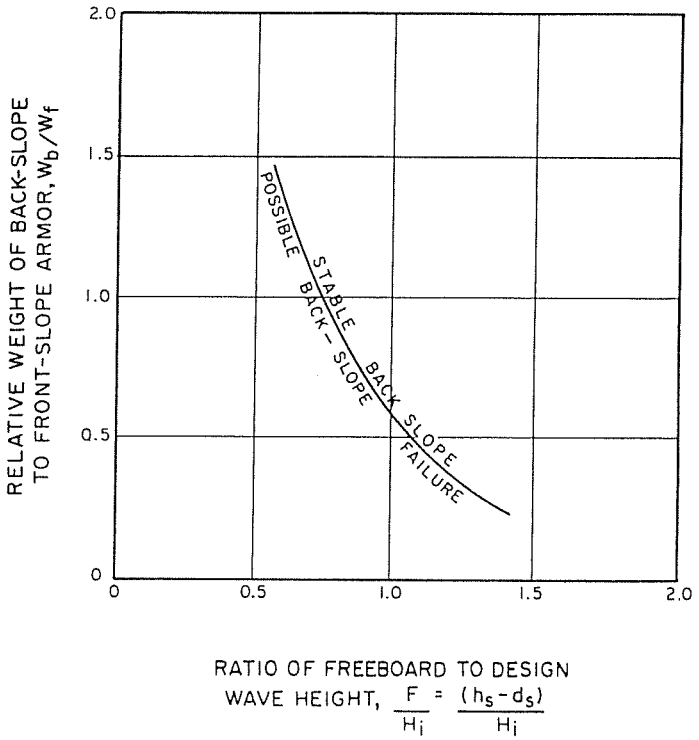

FIGURE 102
Back-Slope Stability

WHERE:

B = crest width
n = number of armor units comprising the crest width; a minimum of three
k_Δ = layer coefficient (see Table 13)[1]
W = weight of individual armor unit in primary cover layer
w_r = unit weight of armor material (saturated surface dry)

4. LAYER THICKNESS. The layer thickness, r, for armor and underlayer units, measured perpendicular to the slope, is:

$$r = n\, k_\Delta\, (W/w_r)^{1/3} \qquad (4\text{-}3)$$

WHERE:

r = layer thickness
n = number of units comprising the layer of interest; a minimum of two as a general rule (see Table 13 for exceptions)
k_Δ = layer coefficient (see Table 13)
W = weight of individual armor unit or stone in layer of interest
w_r = unit weight of armor material

[1]Table 13 presents data regarding the layer coefficient, k_Δ, and porosity, P, for various armor units placed as specified in the number of layers of thickness specified. Values of k_Δ and/or P are required for calculating layer thickness, crest width, and the number of armor units in a breakwater.

TABLE 13
Layer Coefficient and Porosity for Various Armor Units

Armor Units	Number Units Per Layer, n	Placement	Layer Coefficient, k_Δ	Porosity, P (percent)
Quarrystone (smooth)..	2	Random	1.02	38
Quarrystone (rough)...	2	Random	1.15	37
Quarrystone (rough)...	> 3	Random	1.10	40
Quarrystone.....	Graded	Random	....	37
Cube (modified).....	2	Random	1.10	47
Tetrapod.....	2	Random	1.04	50
Quadripod.....	2	Random	0.95	49
Hexapod.....	2	Random	1.15	47
Tribar.....	2	Random	1.02	54
Tribar.....	1	Uniform	1.13	47
Dolos.....	2	Random	1.00	63

(AFTER SHORE PROTECTION MANUAL, 1977)

Note: This table is used to find k_Δ for determing B and r.

TABLE 14
Guidance on Stone Size and Gradations for Breakwaters

Stone Size (weight)	Layer	Allowable Stone-Size Gradation (percent)
W.....	Primary cover layer	125 to 75
W/10 to W/15.....	Secondary cover layer and first underlayer	125 to 75
W/200 to W/4,000 or W/6,000.....	Core and bedding layer	170 to 30

Note: gradation gives the allowable stone-size variation.

(AFTER SHORE PROTECTION MANUAL, 1977)

5. NUMBER OF ARMOR UNITS. The placing density, or the number of armor or underlayer units per surface area per layer, N_r/A, is given by:

$$N_r/A = n\, k_\Delta\, [1 - (P/100)]\,(w_r/W)^{2/3} \qquad (4\text{-}4)$$

WHERE:

N_r = number of individual units in layer of interest
A = surface area
n = number of units comprising the layer of interest; a minimum of two as a general rule (see Table 13 for exceptions)
k_Δ = layer coefficient (see Table 13)
P = porosity (see Table 13)
w_r = unit weight of armor material (saturated surface dry)
W = weight of individual armor unit or stone in layer of interest

6. PRIMARY AND SECONDARY COVER LAYERS. For a breakwater subjected to nonbreaking waves, the primary armor unit should extend to a depth equal to 1.5 H below the minimum low-water level. Below this level, secondary armor units should be at least W/10 to W/15, where W is the weight of the individual armor unit in the primary cover layer. In cases where the breakwater is subject to breaking waves, the primary armor should extend to the bottom or to the bedding layer. Typical breakwater sections subjected to nonbreaking- and breaking-wave conditions are shown in Figures 103 and 104, respectively.

7. UNDERLAYERS. Underlayers provide a transition between armor units and the core. The number of underlayers depends upon the size of the armor units and the gradation of the core material. Underlayer stones should weigh W/10 to W/15, where W is the weight of the primary armor unit. A sufficient number of underlayers is required to ensure that core material is not washed through the voids of overlying stone. Table 14 gives recommended sizes and gradation of stone in a breakwater. This is for guidance only. The local quarries should be checked to ensure that stone of these gradations can be economically obtained. If not, size or gradation may have to be altered slightly or more distant quarries should be investigated. Woven plastic filter cloth may be used as an underlayer to retain fines. The filter cloth should not be overlain with stones larger than 1 ton. Sufficient folds should be allowed in the cloth to allow for settlement. Unwoven filter cloth should not be used as an underlayer.

8. BEDDING LAYER. A bedding, or filter, layer is required over sandy bottoms to prevent the large armor stone from settling into the foundation material. The bedding should have at least a 2-foot thickness of quarry waste or quarry run. A layer of bedding material arranged in filter-like fashion, with

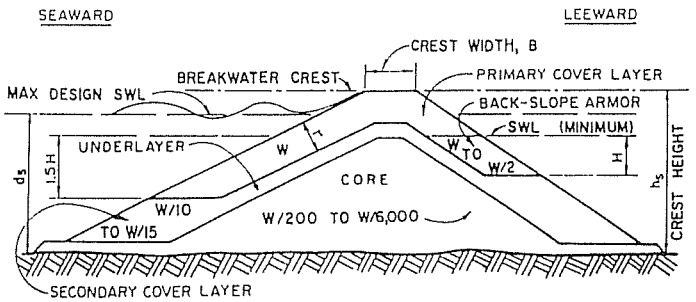

(AFTER SHORE PROTECTION MANUAL, 1977)

FIGURE 103
Typical Breakwater Section for Nonbreaking-Wave Conditions

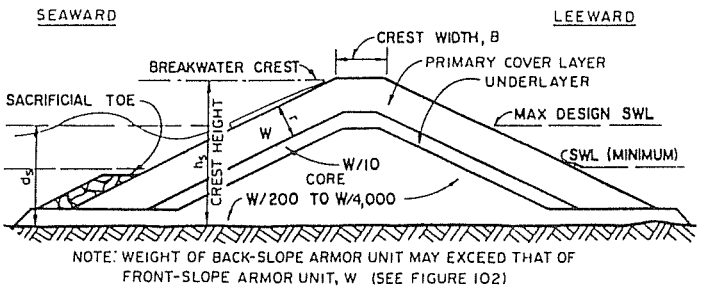

NOTE: WEIGHT OF BACK-SLOPE ARMOR UNIT MAY EXCEED THAT OF FRONT-SLOPE ARMOR UNIT, W (SEE FIGURE 102)

(AFTER SHORE PROTECTION MANUAL, 1977)

FIGURE 104
Typical Breakwater Section for Breaking-Wave Conditions

the addition of plastic filter cloth, may be required over mud and clay bottoms to reduce displacement of the structure into thick deposits of soft mud. when the structure is built over a soft mud bottom, the stability of the foundation must be investigated for sliding and settlement. Gabions or foundation mattresses with reed matting protection or plastic filter cloth can be used to prevent stone material dropped from barges from settling deeply into the mud. Woven or unwoven filter cloth may also be used as a bedding layer over silty and sandy bottom.

9. SACRIFICIAL TOES. When scour is anticipated at the toe of a structure, toe protection is required. Scour often occurs when the structure is built in the surf zone. Effects of scour can be taken into account by placing armor or secondary stones on the bedding layer at the toe to act as a sacrificial toe. The toe should contain sufficient stone to protect the structure to the depth of anticipated scour.

10. CORE. The core material should be specified within sufficiently wide gradation limits such that a local quarry product can be used at a minimal cost. Dredged material, such as sand or coral, can be used as a core, provided adequate filters are installed to retain the fines.

EXAMPLE PROBLEM 27

Given:
a. Equivalent unrefracted deepwater wave height, $H'_o = 10$ feet
b. Bottom at -15 feet MLLW
c. Design tide range = -2 to + 7 feet MLLW (therefore, d_s ranges from 13 to 22 feet)
d. Wave period, T, ranges from 5 to 12 seconds.
e. Quarrystone unit weight, $w_r = 160$ pounds per cubic foot (available for land-based construction)
f. Quarrystone is rough, angular, and randomly placed.
g. Structure slope, cot $\theta = 1.5$
h. The breakwater is fronted by a bottom slope, m = 0.033.

Find: Design a breakwater that will attenuate waves to 3.0 feet in its lee.

Solution: (1) Find design wave height at structure:

(a) Find $H'_o/g\,T^2$:

$$\frac{H'_o}{g\,T^2} = \frac{10}{(32.2)(12)^2} = 0.0022$$

(b) From Figure 42 for $H'_o/g\,T^2 = 0.0022$ and m = 0.033:

$$\frac{H_b}{H'_o} = 1.4$$

$$H_b = 1.4\,H'_o$$

$$H_b = (1.4)(10) = 14 \text{ feet}$$

(2) Check breaker depth, d_b:

(a) Find $H_b/g\,T^2$:

$$\frac{H_b}{g\,T^2} = \frac{14}{(32.2)(12)^2} = 0.003$$

(b) From Figure 43 for $H_b/g\,T^2 = 0.003$ and m = 0.033:

$$\frac{d_b}{H_b} = 1.03$$

$$d_b = 1.03\,H_b$$

$$d_b = (1.03)(14) = 14.4 \text{ feet}$$

The structure will be subject to breaking waves when water level is lower than approximately 14.4 feet.

(3) Find d_s/H'_o for the lower and upper tide levels and $H'_o/g\,T^2$ for the wave-period range:

$$\frac{d_s}{H'_o} = \frac{13}{10} = 1.3 \qquad \text{(-2 feet MLLW tide)}$$

$$\frac{d_s}{H'_o} = \frac{22}{10} = 2.2 \qquad \text{(+7 feet MLLW tide)}$$

$$\frac{H'_o}{g\,T^2} = \frac{10}{(32.2)(12)^2} = 0.0124 \qquad \text{(5-second period)}$$

$$\frac{H'_o}{g\,T^2} = \frac{10}{(32.2)(12)^2} = 0.00216 \qquad \text{(12-second period)}$$

(4) Assuming a medium core height for a first approximation, refer to Subsection 3.4.b.(4)(b), Case 4: medium core height: $0.75 < h_c/d_s < 1.1$.; for $d_s/H'_o = 1.3$ to 2.2, use Figure 72 to find R/H'_o for cot $\theta = 1.5$ and $H'_o/g\,T^2 = 0.0124$ (5-second period) or $H'_o/g\,T^2 = 0.00216$ (12-second period):

$$\frac{R}{H'_o} = 1.80 \qquad \text{(5-second period)}$$

$$\frac{R}{H'_o} = 2.40 \qquad \text{(12-second period)}$$

The maximum runup occurs for the 12-second-period wave.

(5) Using Equation (3-7), find runup, R, for a 12-second-period wave:

$$R = (H'_o)(R/H'_o)(0.52)(1.06)$$

$$R = (10)(2.40)(0.52)(1.06) = 13.2 \text{ feet}$$

The maximum elevation of runup = 13.2 + 7 = +20.2 feet MLLW; this runup elevation occurs at high tide.

(6) Find weight of armor units, W, for front of structure (assuming salt water, $w_w = 64$ pounds per cubic foot):

(a) From Table 12 for breaking waves:

$K_D = 2.9$ for head and $K_D = 3.5$ for trunk

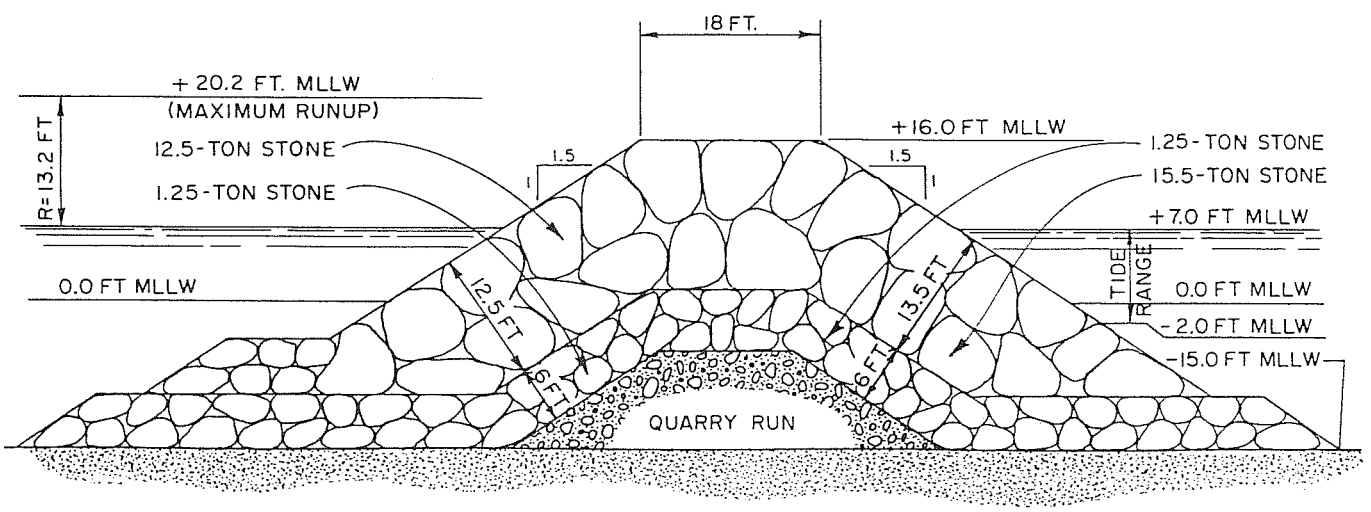

FIGURE 105
Solution to Example Problem 27

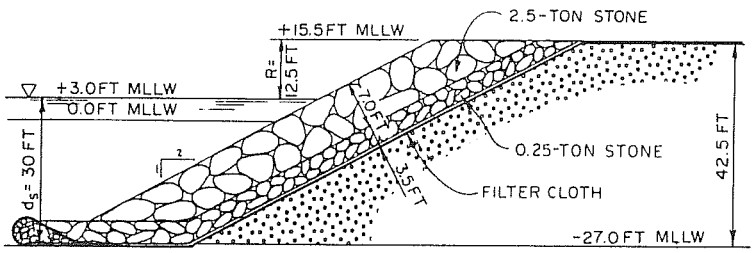

FIGURE 106
Solution to Example Problem 28

(b) Find W for armor units for structure head:

Using Equation (4-1), find W:

$$W = (w_r H^3)/[K_D (S_r - 1)^3 \cot \theta]$$

$$W = [(160)(14)^3]/[(2.9)(\frac{160}{64} - 1)^3(1.5)]$$

$$W = \frac{29{,}905 \text{ pounds}}{2{,}000 \text{ pounds per ton}}$$

W = 14.95 tons; use W = 15 tons

(c) Find W for armor units for structure trunk:

$$W = [(160)(14)^3]/[(3.5)(\frac{160}{64} - 1)^3(1.5)]$$

$$W = \frac{24{,}778 \text{ pounds}}{2{,}000 \text{ pounds per ton}}$$

W = 12.39 tons; use W = 12.5 tons

(7) Find crest height, h_s, needed to attenuate waves to 3.0 feet:

Desired transmission coefficient, $K_t = \frac{H_t}{H_i} = \frac{3.0}{14} = 0.21$

$$\frac{H_i}{g T^2} = \frac{14}{(32.2)(12)^2} = 0.00302$$

From Figure 95 for $\frac{H_i}{g T^2} = 0.003$ and $K_t = 0.21$:

$$\frac{d_s}{h_s} \simeq 0.7$$

$h_s \simeq d_s/0.7 \simeq 22/0.7 \simeq 31.4$ feet; use $h_s = 31$ feet

Elevation of structure crest would be 31 - 15 = +16 feet MLLW.

In Step (5), above, the maximum elevation of runup was determined to be +20.2 feet MLLW. Thus, with the structure crest at +16 feet MLLW, the breakwater will be overtopped by the design wave by more than 4 feet. The stability of the back-slope armor must be checked.

(8) Check back-slope armor units for back-slope stability:

$$\frac{F}{H_i} = \frac{h_s - d_s}{H_i} = \frac{31 - 22}{14} = 0.64$$

From Figure 102 for $F/H_i = 0.64$ and front- and back-slope armor units of the same weight (that is, $W_b/W_f = 1.0$), there is a possibility of back-slope failure. To achieve back-slope stability, W_b/W_f should be increased to 1.23; this is done by increasing the size of the back-slope armor on the structure trunk:

$$\frac{W_b}{W_f} = 1.23 \text{ for back-slope stability}$$

$$W_b = 1.23 W_f$$

$$W_b = (1.23)(12.5)$$

W_b = 15.375 tons; use W_b = 15.5 tons

(In a real design situation the economics of raising the structure height versus increasing the back-slope armor-unit weight should be investigated in order to minimize costs. This is normally done by conducting model tests.)

(9) Using Equation (4-2), find crest width, B:

$$B = n k_\Delta (W/w_r)^{1/3}$$

From Table 13 for rough quarrystone, randomly placed (and n = 3 from Subparagraph 3.3.b.):

k_Δ = 1.10

$$B = (3)(1.10)[\frac{(12.5)(2{,}000)}{160}]^{1/3}$$

B = 17.77 feet; use B = 18 feet

(10) Using Equation (4-3), find front- and back-slope primary-cover layer thicknesses, r, assuming the layers are two stones thick:

$$r = n k_\Delta (W/w_r)^{1/3}$$

From Table 13 for rough quarrystone, randomly placed (n = 2):

k_Δ = 1.15

(a) For the front slope:

$$r = (2)(1.15)[\frac{(12.5)(2{,}000)}{160}]^{1/3}$$

r = 12.39 feet; use r = 12.5 feet

(b) For the back slope:

$$r = (2)(1.15)\left[\frac{(15.5)(2,000)}{160}\right]^{1/3}$$

$r = 13.31$ feet; use $r = 13.5$ feet

(11) Find weight of underlayer stone:

$$\frac{W}{10} = \frac{12.5}{10} = 1.25 \text{ tons}$$

(12) Using Equation (4-3), find underlayer thickness, r, for W = 1.5 tons, assuming the layer is two stones thick:

$$r = n\, k_\Delta\, (W/w_r)^{1/3}$$

$$r = (2)(1.15)\left[\frac{(1.25)(2,000)}{160}\right]^{1/3}$$

$r = 5.75$ feet; use $r = 6$ feet

(13) Using Equation (4-4), find number of primary armor units per surface area, N_r/A, for the front slope:

$$N_r/A = n\, k_\Delta\, [1 - (P/100)](w_r/W)^{2/3}$$

From Table 13, $k_\Delta = 1.15$, $P = 37$

$$N_r/A = (2)(1.15)(1 - \frac{37}{100})\left[\frac{160}{(12.5)(2,000)}\right]^{2/3}$$

$N_r/A = 0.0499$ per square foot

This means there are roughly 50 armor units per 1,000 square feet of cover layer surface area for the front slope. A similar calculation for the back slope can be done.

For breakwater cross section, see Figure 105.

Note: Calculated stone weights should be compared with those of local quarry products. Should minor deviation in weight and gradation result in significant cost reduction, these variations may be acceptable.

11. REVETMENTS. The same general principles used for design of breakwaters are used for design of revetments. The primary difference is that a revetment protects land from erosion. The revetment must have an adequate filter material to prevent fines in the in situ soils from washing through the voids of the structure. The filter can be either layers of stones or a woven plastic filter cloth. Allowance for scour at the toe should be given in developing the design wave for the revetment. The sides of revetments should extend sufficiently landward to prevent flank erosion (see DM-26.3, Subsection 2.3.b., Harbor Entrances on Open Coasts.)

EXAMPLE PROBLEM 28

Given: a. Equivalent unrefracted deepwater wave height, $H'_o = 10$ feet
b. Bottom at -27 feet MLLW
c. Design water level at +3 feet MLLW
d. Wave period, $T = 8$ seconds
e. Quarrystone unit weight, $w_r = 160$ pounds per cubic foot
f. Quarrystone is rough, angular, and randomly placed.
g. Structure slope, $\cot \theta = 2.0$
h. The revetment is situated on a flat bottom.

Find: Design a quarrystone revetment.

Solution: (1) Find design wave height at structure:

$$L_o = (g/2\pi)\, T^2 = (32.2/2\pi)(8)^2 = 328 \text{ feet}$$

$$d/L_o = 30/328 = 0.0915$$

From Figure 2 for $d/L_o = 0.0915$:

$$\frac{H}{H'_o} = 0.94$$

$$H = 0.94\, H'_o$$

THEREFORE: $H = (0.94)(10) = 9.4$ feet

For a flat bottom, $H_b = 0.78\, d_b = (0.78)(30) = 23.4$ feet. Since $H < H_b$ $(9.4 < 23.4)$, the revetment is subject to nonbreaking waves.

(2) Find d_s/H'_o and $H'_o/g\, T^2$:

$$\frac{d_s}{H'_o} = \frac{30}{10} = 3.0$$

$$\frac{H'_o}{g\, T^2} = \frac{10}{(32.2)(8)^2} = 0.00485$$

(3) Refer to Subsection 3.4.b.(2), Case 1: Embankment or Revetment, Quarrystone Armor; for $d_s/H'_o = 3.0$, use Figure 69 to find R/H'_o for $H'_o/g\, T^2 = 0.00485$ $(\cot \theta = 2.0)$:

$$\frac{R}{H'_o} = 1.25$$

(4) Using Equation (3-2), find runup, R:

$$R = (H'_o)(R/H'_o)$$

$R = (10)(1.25) = 12.5$ feet

For no overtopping, the elevation of structure should be at 12.5 + 3 = 15.5 feet MLLW.

(5) Find weight of armor units, W (assuming salt water, $w_w = 64$ pounds per cubic foot):

(a) From Table 12 for nonbreaking waves:

$K_D = 4.0$ for trunk

(b) Using Equation (4-1), find W for structure trunk:

$$W = (w_r\, H^3)/[K_D\, (S_r - 1)^3 \cot \theta]$$

$$W = [(160)(9.4)^3]/[(4)(\frac{160}{64} - 1)^3(2.0)]$$

$$W = \frac{4,920 \text{ pounds}}{2,000 \text{ pounds per ton}}$$

$W = 2.46$ tons; use $W = 2.5$ tons

(6) Using Equation (4-3), find top layer thickness, r, assuming the layer is two stones thick:

$$r = n\, k_\Delta\, (W/w_r)^{1/3}$$

From Table 13 for rough quarrystone, randomly placed $(n = 2)$:

$k_\Delta = 1.15$

$$r = (2)(1.15)\left[\frac{(2.5)(2,000)}{160}\right]^{1/3}$$

$r = 7.24$ feet; use $r = 7.0$ feet

(7) Find weight of underlayer stone:

$$\frac{W}{10} = \frac{2.5}{10} = 0.25 \text{ ton}$$

(8) Using Equation (4-3), find underlayer thickness, r, for W = 0.25 ton, assuming the layer is two stones thick:

$$r = n\, k_\Delta\, (W/w_r)^{1/3}$$

$$r = (2)(1.15)\left[\frac{(0.25)(2,000)}{160}\right]^{1/3}$$

$r = 3.363$ feet; use $r = 3.5$ feet

For revetment cross section, see Figure 106.

12. METRIC EQUIVALENCE CHART. The following metric equivalents were developed in accordance with ASTM E-621. These units are listed in the sequence in which they appear in the text of Section 4. Conversions are approximate.

3 inches = 7.6 centimeters
5 tons = 4,536 kilograms
5 feet = 1.5 meters
12 feet = 3.7 meters
15 feet = 4.6 meters
1 ton - 907 kilograms
2 feet = 61 centimeters

SECTION 5
WALL DESIGN

1. WAVE-INDUCED FORCES ON WALLS.

a. General. Procedures for calculating wave-induced forces on vertical walls are divided into three categories: nonbreaking waves, breaking waves, and broken waves. Procedures given below assume that wave action is only on the seaward side of the wall. In cases where wave action is also on the landward or harbor side of the wall, the calculation should assume a wave crest occurs on one side of the wall simultaneously with a wave through on the opposite side of the wall. Calculations are also described for low-height walls, for walls built on a rubble base, for baffles, for wave attack at an angle other than normal to the wall, and for nonvertical walls.

b. Nonbreaking Waves. Waves impinging on a smooth, vertical-faced wall reflect most of their energy seaward. At the wall, a standing wave results for which the wave height at the wall is the sum of the incident and reflected wave heights. This standing wave is referred to as a clapotis. For perfect reflection, the resulting wave height is equal to twice the incident wave height.

Wave forces and moments for nonbreaking conditions can be estimated by the Miche-Rundgren method. It is important to realize that, when water is on both sides of the structure, the maximum force may be seaward in direction occurring when the wave trough is at the seaward side of the structure. The procedure for calculating nonbreaking wave forces is as follows (see Figure 107 for a definition of terms):

(1) Determine the wave height at the wall, H_w, by the equation:

$$H_w = 2\,H_i \qquad (5\text{-}1)$$

WHERE:
H_w = wave height at the wall
H_i = incident wave height

(2) Determine the increase in mean water level, h_o, above the still water level in Figure 85 as a function of $H_i/g\,T^2$ and H_i/d_s. If H_i/d_s is greater than 0.78, the wave is breaking or broken and procedures outlined in Subsection 5.1.c., Breaking Waves, or 5.1.d., Broken Waves, respectively, should be followed.

(3) The depth from the clapotis crest, S_c, and the depth from the clapotis trough, S_t, can be found by the following equations:

$$S_c = d_s + h_o + H_i \qquad (5\text{-}2)$$

and

$$S_t = d_s + h_o - H_i \qquad (5\text{-}3)$$

WHERE:
S_c = depth from clapotis crest (S is measured along the z-coordinate axis, a vertical axis with its origin at the bottom)
d_s = depth at structure from still water level
h_o = height of clapotis orbit center (mean water level) above SWL
H_i = incident wave height
S_t = depth from clapotis trough

(4) Wave-induced pressure distribution for nonbreaking waves is shown schematically in Figure 108. The pressure when the clapotis crest is at the wall is p_c, and the pressure when the clapotis trough is at the wall is p_t. Equations (5-4) through (5-7) give the values of p_c and p_t at different values of z. When the clapotis crest is at the wall (Figure 108A), pressure increases from zero at the free water surface (Equation (5-4)) to $w_w d_s + p_1$ at the bottom (Equation (5-5)). When the clapotis trough is at the wall (Figure 108B), pressure increases from zero at the free water surface (Equation (5-6)) to $w_w d_s - p_1$ at the bottom (Equation (5-7)).

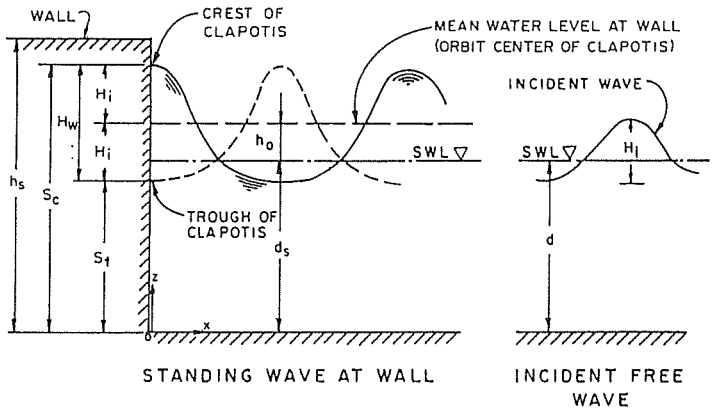

WHERE: H_w = WAVE HEIGHT AT WALL
H_i = HEIGHT OF INCIDENT FREE WAVE (IN WATER OF DEPTH d)
h_o = HEIGHT OF CLAPOTIS ORBIT CENTER (MEAN WATER LEVEL AT WALL) ABOVE THE STILL WATER LEVEL (SWL)
d_s = DEPTH OF STRUCTURE FROM STILL WATER LEVEL
S_c = DEPTH FROM CLAPOTIS CREST = $d_s + h_o + H_i$
S_t = DEPTH FROM CLAPOTIS TROUGH = $d_s + h_o - H_i$
h_s = HEIGHT OF WALL
NOTE: a) CLAPOTIS MEANS STANDING WAVE
b) EQUATIONS PRESENTED IN SECTION 1 ARE BASED ON THE z-COORDINATE AXIS WITH ITS ORIGIN AT THE STILL WATER LEVEL. EQUATIONS IN SECTIONS 5 AND 7 ARE BASED ON THE z-COORDINATE AXIS WITH ITS ORIGIN AT THE BOTTOM.

(AFTER SHORE PROTECTION MANUAL, 1977)

FIGURE 107
Definition of Terms for Wave-Induced Forces on Walls (Nonbreaking Waves)

$$p_c = 0 \qquad \text{at } z = S_c = d_s + h_o + H_i \qquad (5\text{-}4)$$

$$p_c = w_w\,d_s + p_1 \qquad \text{at } z = 0 \qquad (5\text{-}5)$$

$$p_t = 0 \qquad \text{at } z = S_t = d_s + h_o - H_i \qquad (5\text{-}6)$$

$$p_t = w_w\,d_s - p_1 \qquad \text{at } z = 0 \qquad (5\text{-}7)$$

WHERE:
p_c = pressure when clapotis crest is at wall
z = vertical distance along a coordinate axis with its origin at the bottom
S_c = depth from clapotis crest
w_w = unit weight of water
d_s = depth at structure from the still water level

$p_1 = w_w\,H_i/\cosh(2\pi\,d_s/L)$ = nonbreaking-wave pressure difference from still water hydrostatic pressure a clapotis crest (trough) passes (5-8)

H_i = incident wave height
L = wavelength
p_t = pressure when clapotis trough is at wall
S_t = depth from clapotis trough

As a first approximation, the pressure distribution can be assumed to be a straight line between p at the crest or trough and p at the bottom. (See Figure 108).

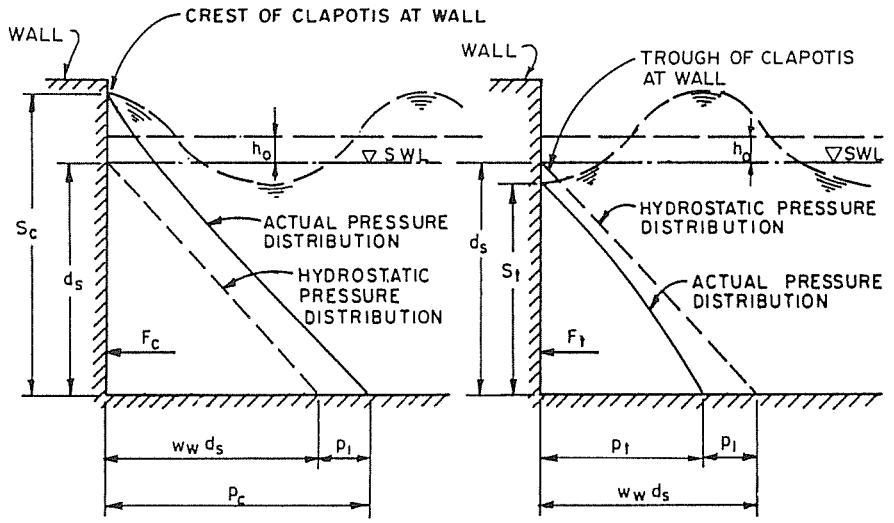

WHERE: w_w = UNIT WEIGHT OF WATER

p_l = NONBREAKING-WAVE PRESSURE DIFFERENCE FROM STILL WATER HYDROSTATIC PRESSURE AS CLAPOTIS CREST (OR TROUGH) PASSES

p_c (or p_t) = PRESSURE WHEN CREST (OR TROUGH) IS AT WALL

F_c (or F_t) = FORCE WHEN CREST (OR TROUGH) IS AT WALL

(AFTER SHORE PROTECTION MANUAL, 1977)

FIGURE 108
Wave-Induced Pressure Distribution for Nonbreaking Waves at a Wall

The wave-induced forces and moments associated with the above pressures may be determined by assuming a straight-line pressure distribution between the water surface and the bottom and then using the following equations:

$$F_c = \left(\frac{1}{2}\right)(w_w d_s + p_l)(d_s + h_o + H_i) \qquad (5\text{-}9)$$

$$M_c = \left(\frac{1}{6}\right)(w_w d_s + p_l)(d_s + h_o + H_i)^2 \qquad (5\text{-}10)$$

$$F_t = \left(\frac{1}{2}\right)(w_w d_s - p_l)(d_s + h_o - H_i) \qquad (5\text{-}11)$$

$$M_t = \left(\frac{1}{6}\right)(w_w d_s - p_l)(d_s + h_o - H_i)^2 \qquad (5\text{-}12)$$

WHERE:

F_c = Nonbreaking-wave force, per unit length of wall, when the crest of the clapotis is at the wall

M_c = Nonbreaking-wave moment, per unit length of wall, when the crest of the clapotis is at the wall

F_t = Nonbreaking-wave force, per unit length of wall, when the trough of the clapotis is at the wall

M_t = Nonbreaking-wave moment, per unit length of wall, when the trough of the clapotis is at the wall

(5) A more accurate determination of the integrated forces, F, and moments (about the mudline), M, for a nonovertopped wall subjected to nonbreaking waves can be obtained using Figures 109 and 110, respectively. On each figure, the values of $H_i/g\,T^2$ and H_i/d_s are used to determine the dimensionless force, $F/(w_w d_s^2)$, and the dimensionless moment, $M/(w_w d_s^3)$, respectively. The method for determining F and M is explained below.

On each of Figures 109 and 110, the upper family of curves is used to determine the dimensionless force or dimensionless moment, respectively, when the crest is at the wall; the lower family of curves is used to determine the force or moment when the trough is at the wall. On each of Figures 109 and 110, the horizontal line separating the two families of curves represents the dimensionless horizontal hydrostatic force, $(1/2)(w_w d_s^2)$, and moment, $(1/6)(w_w d^3)$, respectively, exerted on a wall in still water. Once $F/(w_w d_s^2)$ and $M/(w_w d_s^3)$ have been determined for the wave crest or trough from the appropriate figure, then the wave-induced horizontal force and moment acting on the wall may be determined using the following equations:

$$F_{c \text{ or } t} = \left(\frac{F}{w_w d_s^2}\right)_{c \text{ or } t} (w_w d_s^2) \qquad (5\text{-}13)$$

$$M_{c \text{ or } t} = \left(\frac{M}{w_w d_s^3}\right)_{c \text{ or } t} (w_w d_s^3) \qquad (5\text{-}14)$$

If there is water on the lee side of the wall and there is no wave action present on the lee side, then the net force, F_{net}, acting on the wall will be the difference between the wave-induced force on the seaward side of the wall (at either the crest or trough) and the hydrostatic force on the lee side of the wall. Similarly, the net moment acting on the wall will be the difference between the wave-induced moment on the seaward side on the wall and the hydrostatic moment on the lee side of the wall.

Where wave action is present on the lee side of the wall, then the maximum net force and moment are determined by assuming a wave crest occurs on one side of the wall simultaneously with a wave trough on the opposite side of the wall. This situation arises when waves are transmitted over or through the wall or when waves from another source, such as reflected waves or locally generated waves, impinge upon the wall.

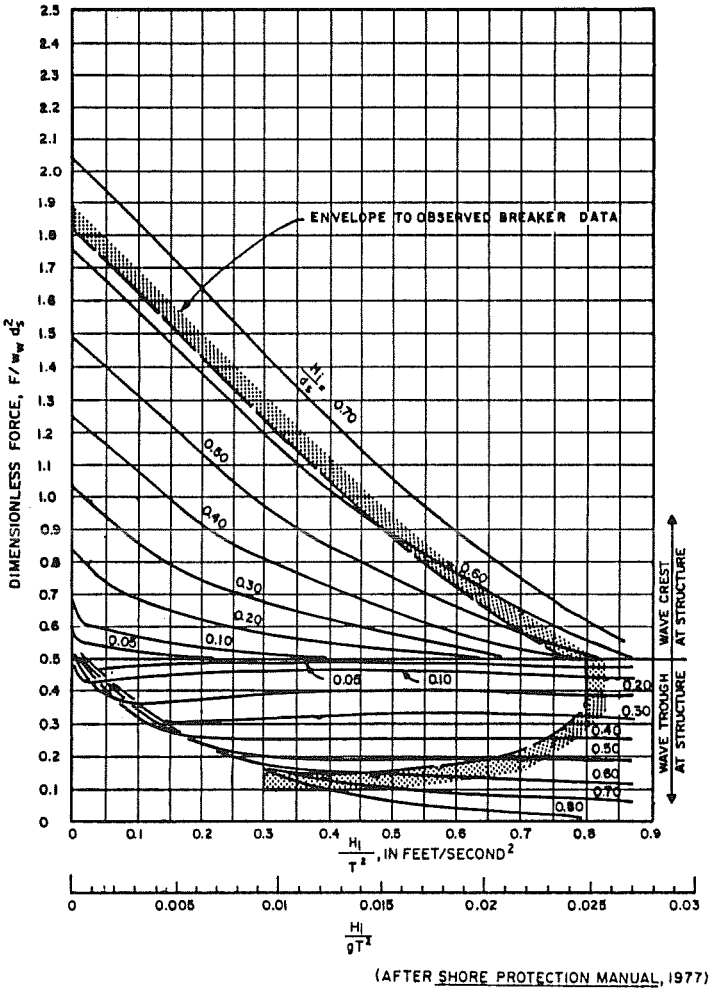

(AFTER SHORE PROTECTION MANUAL, 1977)

FIGURE 109
Nonbreaking-Wave Forces

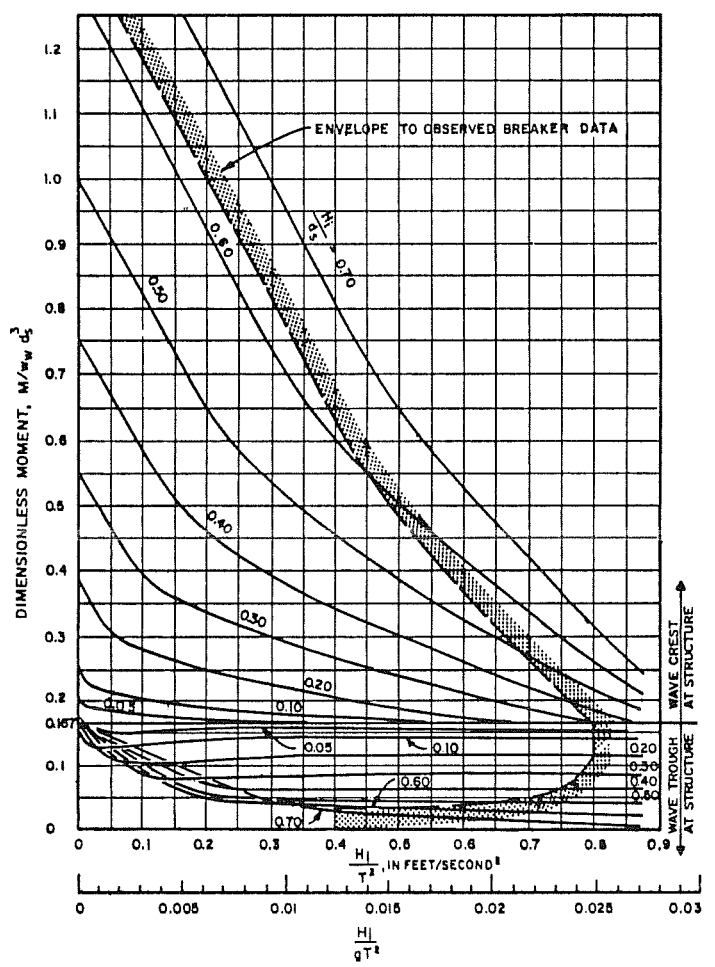

(AFTER SHORE PROTECTION MANUAL, 1977)

FIGURE 110
Nonbreaking-Wave Moment

EXAMPLE PROBLEM 29

Given: a. Incident wave height, H_i = 10 feet
b. Water depth, d_s = 20 feet
c. Wave period, T = 8 seconds
d. Sheet-pile wall as shown in Figure 111A; h_s = 40 feet

Find: The net force and moment on the sheet-pile wall.

Solution: (1) Find L at the structure depth:

$$L_o = (g/2\pi)\,T^2 = (32.2/2\pi)(8)^2 = 328 \text{ feet}$$

$$\frac{d_s}{L_o} = \frac{20}{328.0} = 0.061$$

From Figure 2 for $d/L_o = 0.061$:

$$\frac{d_s}{L} = 0.105$$

$$L = \frac{d_s}{0.105} = \frac{20}{0.105} = 190 \text{ feet}$$

(2) Determine $H_i/g\,T^2$ and H_i/d_s:

$$\frac{H_i}{g\,T^2} = \frac{10}{(32.2)(8)^2} = 0.00485$$

$$\frac{H_i}{d_s} = \frac{10}{20} = 0.5$$

(3) Find h_o:

From Figure 85 for $H_i/g\,T^2 = 0.00485$ and $H_i/d_s = 0.5$:

$$\frac{h_o}{H_i} = 0.66$$

$$h_o = 0.66\,H_i$$

$$h_o = (0.66)(10) = 6.6 \text{ feet}$$

(4) Using Equations (5-2) and (5-3), respectively, find S_c and S_t:

$$S_c = d_s + h_o + H_i = 20 + 6.6 + 10$$

$$S_c = 36.6 \text{ feet}$$

$$S_t = d_s + h_o - H_i = 20 + 6.6 - 10$$

$$S_t = 16.6 \text{ feet}$$

(5) Using Equation (5-8), find p_1:

$$p_1 = \frac{w_w H_i}{\cosh(2\pi d_s/L)}$$

Find $\cosh(2\pi d_s/L)$:

$$\frac{2\pi d_s}{L} = \frac{2\pi(20)}{190} = 0.661; \text{ use } 0.66$$

From Figure 3, cosh(0.66) = 1.23

$$p_1 = \frac{(64)(10)}{1.23} = 520.3 \text{ pounds per square foot}$$

(6) Find net force and moment when wave crest is at structure (see Figure 111B):

(a) As a first approximation, determine net force, F_{net}, and moment, M_{net}, on structure using pressure at

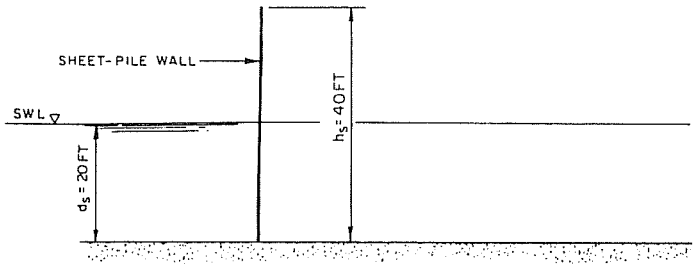

A- SHEET-PILE WALL OF EXAMPLE PROBLEM 29

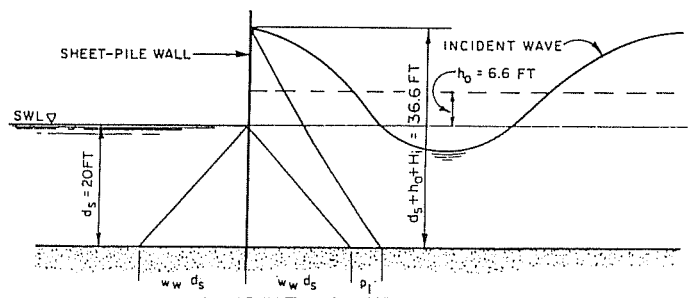

B- CREST AT STRUCTURE

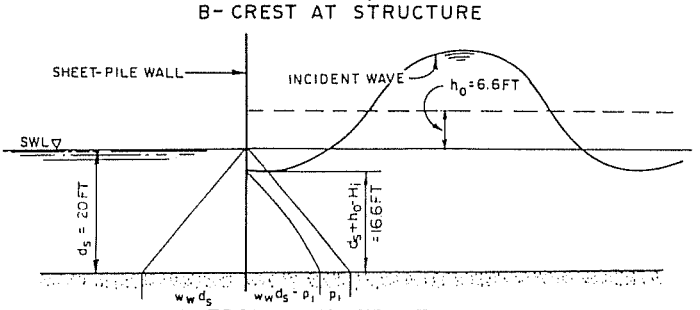

C- TROUGH AT STRUCTURE

FIGURE 111
Diagrams for Example Problem 29

bottom, p_c, and assume a straight-line pressure distribution up to the water surface, where $p_c = 0$.

Note: Water level on leeward side will be taken as 20 feet; it is assumed there is no wave transmission and no wave action present on the leeward side.

$$F_{net} = F_c - \frac{1}{2} w_w d_s^2$$

Using Equation (5-9) and the above equation:

$$F_{net} = (\tfrac{1}{2})(w_w d_s + p_1)(d_s + h_o + H_i) - \frac{1}{2} w_w d_s^2$$

(Assuming salt water, w_w = 64 pounds per cubic foot.)

$$F_{net} = (\tfrac{1}{2})[(64)(20) + 520.3](20 + 6.6 + 10) - (\tfrac{1}{2})[(64)(20)^2]$$

$$F_{net} = 32,945 - 12,800$$

F_{net} = 20,145 pounds per foot (force with crest at structure)

$$M_{net} = M_c - \frac{1}{6} w_w d_s^3$$

Using Equation (5-10) and the above equation:

$$M_{net} = (\tfrac{1}{6})(w_w d_s + p_1)(d_s + h_o + H_i)^2 - \frac{1}{6} w_w d_s^3$$

$$M_{net} = (\tfrac{1}{6})[(64)(20) + 520.3][(36.6)^2] - (\tfrac{1}{6})[(64)(20)^3]$$

$$M_{net} = 401,935 - 85,333$$

M_{net} = 316,602 foot-pounds per foot (moment with crest at structure)

(b) Now use Figures 109 and 110, respectively, to determine net wave force and moment when crest is at structure:

From Figure 109 for $H_i/g\,T^2 = 0.00485$ and $H_i/d_s = 0.5$ (wave crest at structure):

$$\frac{F_c}{w_w d_s^2} = 1.21$$

Using Equation (5-13):

$$F_c = \left(\frac{F_c}{w_w d_s^2}\right)(w_w d_s^2)$$

$$F_c = (1.21)[(64)(20)^2]$$

F_c = 30,976 pounds per foot

$$F_{net} = F_c - \frac{1}{2} w_w d_s^2$$

$$F_{net} = 30,976 - (\tfrac{1}{2})[(64)(20)^2]$$

$$F_{net} = 30,976 - 12,800$$

F_{net} = 18,176 pounds per foot (force with crest at structure)

From Figure 110 for $H_i/g\,T^2 = 0.00485$ and $H_i/d_s = 0.5$ (wave crest at structure):

$$\frac{M_c}{w_w d_s^3} = 0.72$$

Using Equation (5-14):

$$M_c = \left(\frac{M_c}{w_w d_s^3}\right)(w_w d_s^3)$$

$$M_c = (0.72)[(64)(20)^3]$$

M_c = 368,640 foot-pounds per foot

$$M_{net} = M_c - \frac{1}{6} w_w d_s^3$$

$$M_{net} = 368,640 - (\tfrac{1}{6})[(64)(20)^3]$$

$$M_{net} = 368,640 - 85,333$$

M_{net} = 283,307 foot-pounds per foot (moment with crest at structure)

Note: Values for F and M, for the wave crest at the structure, determined in step (b) (using Figures 109 and 110) are slightly lower than those calculated in step (a). This discrepancy is due to the assumption in step (a) that the pressure distribution is a straight line.

(7) Find force and moment when wave trough is at structure (see Figure 111C).

(a) As a first approximation, assume straight-line pressure distribution:

$$F_{net} = F_t - \frac{1}{2} w_w d_s^2$$

Using Equation (5-11) and the above equation:

$$F_{net} = (\tfrac{1}{2})(w_w d_s - p_1)(d_s + h_o - H_i) - \frac{1}{2} w_w d_s^2$$

$$F_{net} = (\tfrac{1}{2})[(64)(20) - 520.3](20 + 6.6 - 10) - (\tfrac{1}{2})[(64)(20)^2]$$

$$F_{net} = 6,306 - 12,800$$

F_{net} = -6,494 pounds per foot (force with trough at structure)

$$M_{net} = M_t - \frac{1}{6} w_w d_s^3$$

Using Equation (5-12) and the above equation:

$$M_{net} = (\tfrac{1}{6})(w_w d_s - p_1)(d_s + h_o - H_i)^2 - \frac{1}{6} w_w d_s^3$$

$$M_{net} = (\tfrac{1}{6})[(64)(20) - 520.3](20 + 6.6 - 10)^2 - (\tfrac{1}{6})[(64)(20)^3]$$

M_{net} = 34,890 - 85,333

M_{net} = -50,443 foot-pounds per foot (moment with trough at structure)

(b) Now use Figures 109 and 110, respectively, to determine wave force and moment (when trough is at structure):

From Figure 109 for $H_t/g\,T^2 = 0.00485$ and $H_t/d_s = 0.5$ (wave trough at structure):

$$\frac{F_t}{w_w d_s^2} = 0.28$$

Using Equation (5-13):

$$F_t = \left(\frac{F_t}{w_w d_s^2}\right)(w_w d_s^2)$$

$F_t = (0.28)[(64)(20)^2]$

F_t = 7,168 pounds per foot

$F_{net} = F_t - \frac{1}{2} w_w d_s^2$

$F_{net} = 7{,}168 - (\frac{1}{2})(64)(20)^2$

$F_{net} = 7{,}168 - 12{,}800$

F_{net} = -5,632 pounds per foot (force with trough at structure)

From Figure 110 for $H_t/g\,T^2 = 0.00485$ and $H_t/d_s = 0.5$ (wave trough at structure):

$$\frac{M_t}{w_w d_s^3} = 0.06$$

Using Equation (5-14):

$$M_t = \left(\frac{M_t}{w_w d_s^3}\right)(w_w d_s^3)$$

$M_t = (0.06)[(64)(20)^3]$

M_t = 30,720 foot-pounds per foot

$M_{net} = M_t - \frac{1}{6} w_w d_s^3$

$M_{net} = 30{,}720 - (\frac{1}{6})[(64)(20)^3]$

$M_{net} = 30{,}720 - 85{,}333$

M_{net} = -54,613 foot-pounds per foot (moment with trough at structure)

Therefore, the wave crest at the structure provides maximum net forces and moments and these should be used for structural design.

(6) Forces on segments of the wall can be estimated by calculating the area in the idealized pressure distribution suggested in item (4) under Subsection 5.b., Nonbreaking Waves.

Then the force is:

$$F = \int_{z_1}^{z_2} p\,dz \qquad (5\text{-}15)$$

and the moment is:

$$M = \int_{z_1}^{z_2} z\,p\,dz \qquad (5\text{-}16)$$

WHERE:
- F = force
- z_1 = depth from point 1
- z_2 = depth from point 2
- p = pressure
- M = moment
- z = vertical distance along a coordinate axis with its origin at the bottom

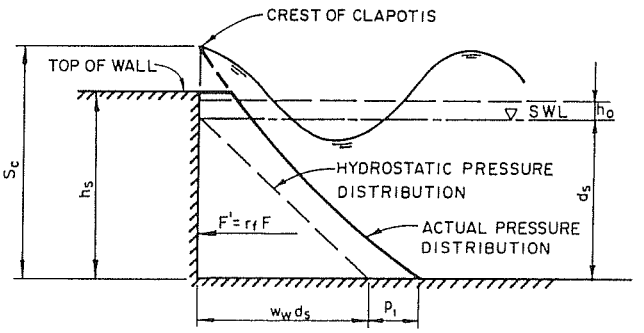

(AFTER SHORE PROTECTION MANUAL, 1977)

FIGURE 112
Pressure Distribution for Overtopped Low-Height Wall

This procedure can be used to estimate forces on walls that are overtopped and/or do not extend to the bottom.

(7) Walls of low height may be overtopped and the pressure distribution is truncated as shown in Figure 112. Forces are reduced when the wave overtops the structure; the reduced force is calculated by applying a correction factor, termed a reduction factor, to the force as calculated above. No correction is necessary for analyzing the case where the wave trough is at the structure unless the elevation of the trough is higher than the wall. Reduced forces, F', and moments (about the mudline), M', are given by:

$$F' = r_f F \qquad (5\text{-}17)$$

and

$$M' = r_m M \qquad (5\text{-}18)$$

WHERE
- F' = reduced force for overtopped wall
- r_f = reduction factor for force
- F = force determined for nonovertopped wall
- M' = reduced moment for overtopped wall
- r_m = reduction factor for moment
- M = moment determined for nonovertopped wall

Reduction factors, r_f and r_m, are determined from Equations (5-19) and (5-20), respectively:

$$r_f = (\frac{h_s}{S})(2 - \frac{h_s}{S}) \quad \text{when } \frac{h_s}{S} < 1.0 \qquad (5\text{-}19)$$

or

$$r_f = 1.0 \quad \text{when } \frac{h_s}{S} \geq 1.0$$

and

$$r_m = (\frac{h_s}{S})^2 [3 - 2(\frac{h_s}{S})] \quad \text{when } \frac{h_s}{S} < 1.0 \qquad (5\text{-}20)$$

or

$$r_m = 1.0 \quad \text{when } \frac{h_s}{S} \geq 1.0$$

WHERE:
- r_f = reduction factor for force
- h_s = height of wall
- S = depth from crest, S_c, or trough, S_t, of wave
- r_m = reduction factor for moment

EXAMPLE PROBLEM 30

Given: a. Incident wave height, H_i = 10 feet
b. Water depth, d_s = 20 feet
c. Wave period, T^s = 6 seconds
d. Sheet-pile wall as shown in Figure 113; h_s = 30 feet

Find: The net force and moment on the sheet-pile wall.

Solution: (1) Determine $H_i/g\,T^2$ and H_i/d_s:

$$\frac{H_i}{g\,T^2} = \frac{10}{(32.2)(6)^2} = 0.00863$$

$$\frac{H_i}{d_s} = \frac{10}{20} = 0.5$$

(2) Find h_o:

From Figure 85 for $H_i/g\,T^2 = 0.00863$ and $H_i/d_s = 0.5$:

$$\frac{h_o}{H_i} = 0.49$$

$$h_o = 0.49\,H_i$$

$$h_o = (0.49)(10) = 4.9 \text{ feet}$$

(3) Using Equations (5-2) and (5-3), respectively, find S_c and S_t; then determine if wall will be overtopped:

$$S_c = d_s + h_o + H_i = 20 + 4.9 + 10$$

$$S_c = 34.9 \text{ feet}$$

$$S_t = d_s + h_o - H_i = 20 + 4.9 - 10$$

$$S_t = 14.9 \text{ feet}$$

Check to see if $S_c > h_s$:

S_c = 34.9 feet and h_s = 30 feet

$S_c > h_s$; therefore, the structure will be overtopped.

(4) Use Figures 109 and 110 to determine the force and moment, respectively, acting on the seaward side of the wall, in a leeward direction ("leeward-acting") when the incident wave crest is at the seaward side of the structure (see Figure 113A):

(a) Find wave force when incident wave crest is at structure:

From Figure 109 for $H_i/g\,T^2 = 0.00863$ and $H_i/d_s = 0.5$ (wave crest at structure):

$$\frac{F_c}{w_w\,d_s^2} = 1.00$$

(Assuming salt water, w_w = 64 pounds per cubic foot.)

$$F_c = (1.00)[(64)(20)^2]$$

$$F_c = 25{,}600 \text{ pounds per foot}$$

Now apply the correction factor for a wall of low height using Equation (5-19); $S = S_c$:

$$r_f = \left(\frac{h_s}{S_c}\right)\left(2 - \frac{h_s}{S_c}\right)$$

$$r_f = \left(\frac{30}{34.9}\right)\left(2 - \frac{30}{34.9}\right)$$

$$r_f = 0.980$$

Using Equation (5-17), find F_c'; $F' = F_c'$ and $F = F_c$:

$$F_c' = r_f\,F_c$$

$$F_c' = (0.980)(25{,}600)$$

$$F_c' = 25{,}088 \text{ pounds per foot (leeward-acting force with incident crest at seaward side of structure)}$$

(b) Find moment when incident wave crest is at structure:

From Figure 110 for $H_i/g\,T^2 = 0.00863$ and $H_i/d_s = 0.5$ (wave crest at structure):

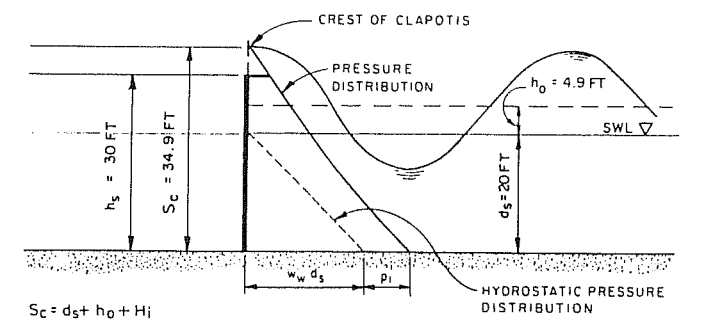

A - WAVE CREST OF CLAPOTIS AT WALL

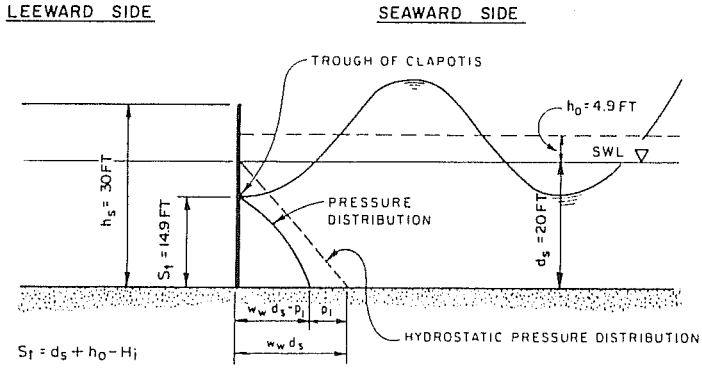

B - WAVE TROUGH OF CLAPOTIS AT WALL

FIGURE 113
Diagrams for Example Problem 30

$$\frac{M_c}{w_w d_s^3} = 0.55$$

$$M_c = (0.55)[(64)(20)^3]$$

M_c = 281,600 foot-pounds per foot

Now apply the correction factor for a wall of low height using Equation (5-20); $S = S_c$:

$$r_m = \left(\frac{h_s}{S_c}\right)^2 \left[3 - 2\left(\frac{h_s}{S_c}\right)\right]$$

$$r_m = \left(\frac{30}{34.9}\right)^2 \left[3 - 2\left(\frac{30}{34.9}\right)\right]$$

r_m = 0.946

Using Equation (5-18), find M'_c; $M' = M'_c$ and $M = M_c$:

$M'_c = r_m M_c$

$M'_c = (0.946)(281,600)$

M'_c = 266,394 foot-pounds per foot (leeward-acting moment with incident crest at structure)

(5) Determine the net force and moment when the incident wave crest is at the seaward side of the structure:

To determine the net force and moment when the crest is at the structure, the seaward-acting force and moment must be determined. The seaward-acting force and moment depend on the wave action present on the lee side of the structure. For the purposes of this example, it is assumed that the only wave action on the lee side of the wall is the transmitted wave. The methods described in Subsection 3.5.a.(1), Vertical-Wall, Vertical-Thin Wall, or Composite Breakwaters, are used to calculate H_t. For conservative design it is assumed that when a wave crest is at a structure on the seaward side, a wave trough occurs simultaneously on the leeward side, and vice versa. Furthermore, in order to ensure conservative design, it is assumed that the transmitted wave has the same wave period as the incident wave. (In nature, the wave period of the transmitted wave would probably be lower than that of the incident wave (Seelig, 1980).)

(a) Find H_t:

$$\frac{h_s - d_s}{H_i} = \frac{30 - 20}{10} = 1.0$$

From Figure 90 for $(h_s - d_s)/H_i = 1.0$:

$$K_t = \frac{H_t}{H_i} = 0.10$$

$H_t = K_t H_i = (0.10)(10) = 1.0$ foot

(b) Use Figures 109 and 110 to determine the force and moment, respectively, acting on the leeward side of the wall, in a seaward direction ("seaward-acting") when there is a transmitted trough at the leeward side of the wall:

Determine $H_t/g T^2$ and H_t/d_s:

$$\frac{H_t}{g T^2} = \frac{1.0}{(32.2)(6)^2} = 0.000863$$

$$\frac{H_t}{d_s} = \frac{1.0}{20} = 0.05$$

For consistency of symbols, H_i replaces H_t in the following calculation of transmitted-wave forces and moments.

From Figure 109 for $H_i/g T^2 = 0.000863$ and $H_i/d_s = 0.05$ (wave trough at structure):

$$\frac{F_t}{w_w d_s^2} = 0.46$$

$$F_t = (0.46)[(64)(20)^2]$$

F_t = 11,776 pounds per foot (seaward-acting force with transmitted trough at leeward side of structure)

From Figure 110 for $H_i/g T^2 = H_t/g T^2 = 0.000863$ and $H_i/d_s = H_t/d_s = 0.05$ (wave trough at structure):

$$\frac{M_t}{w_w d_s^3} = 0.15$$

$$M_t = (0.15)[(64)(20)^3]$$

M_t = 76,800 foot-pounds per foot (seaward-acting moment with transmitted trough at leeward side of structure)

(c) Find net force and moment when incident wave crest is at seaward side of structure and transmitted wave trough is at leeward side:

$$F_{net} = F'_c - F_t$$

$$F_{net} = 25,088 - 11,776$$

F_{net} = 13,312 pounds per foot (in a leeward direction: leeward-acting)

$$M_{net} = M'_c - M_t$$

$$M_{net} = 266,394 - 76,800$$

M_{net} = 189,594 foot-pounds per foot (in a leeward direction: leeward-acting)

(6) Use Figures 109 and 110 to determine the force and moment, respectively, acting on the seaward side of the wall, in a leeward direction ("leeward-acting") when the incident wave trough is at the seaward side of the structure (see Figure 113B):

(a) Find wave force when incident wave trough is at structure:

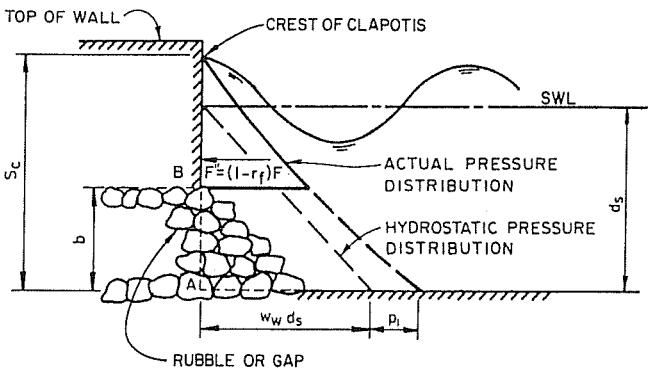

WHERE: b=HEIGHT OF RUBBLE BASE

(AFTER SHORE PROTECTION MANUAL, 1977)

FIGURE 114
Pressure Distribution for Wall Built on Rubble Base

Note: In this case, no correction for low height is necessary when the wave trough is at the structure since S_t = 14.9 feet is less than h_s = 30 feet: $S_t < h_s$.

From Figure 109 for $H_i/g\,T^2$ = 0.00863 and H_i/d_s = 0.5 (wave trough at structure):

$$\frac{F_t}{w_w d_s^2} = 0.21$$

$$F_t = (0.21)[(64)(20)^2]$$

F_t = 5,376 pounds per foot (leeward-acting force with incident trough at seaward side of structure)

(b) Find moment when incident trough is at structure:

From Figure 110 for $H_i/g\,T^2$ = 0.00863 and H_i/d_s = 0.5 (wave trough at structure):

$$\frac{M_t}{w_w d_s^3} = 0.05$$

$$M_t = (0.05)[(64)(20)^3]$$

M_t = 25,600 foot-pounds per foot (leeward-acting moment with incident trough at structure)

(7) Determine the net force and moment when the incident wave trough is at the seaward side of the structure:

(a) Use Figures 109 and 110 to determine the force and moment, respectively, acting on the leeward side of the wall, in a seaward direction ("seaward-acting") when there is a transmitted crest at the leeward side of the structure:

For consistency of symbols, H_i replaces H_t in the following calculation of transmitted-wave forces and moments.

From Figure 109 for $H_i/g\,T^2$ = 0.000863 and H_i/d_s = 0.05 (wave crest at structure):

$$\frac{F_c}{w_w d_s^2} = 0.55$$

$$F_c = (0.55)[(64)(20)^2]$$

F_c = 14,080 pounds per foot

From Figure 110 for $H_i/g\,T^2$ = 0.000863 and H_i/d_s = 0.05 (wave crest at structure):

$$\frac{M_c}{w_w d_s^3} = 0.19$$

$$M_c = (0.19)[(64)(20)^3]$$

M_c = 97,280 foot-pounds per foot

(b) Find net force and moment when incident wave trough is at seaward side of structure and transmitted wave crest is at leeward side:

$$F_{net} = F_t - F_c$$

$$F_{net} = 5,376 - 14,080$$

F_{net} = -8,704 pounds per foot (in a seaward direction: seaward-acting)

$$M_{net} = M_t - M_c$$

$$M_{net} = 25,600 - 97,280$$

M_{net} = -71,680 foot-pounds per foot (in a seaward direction: seaward-acting)

Therefore, when the wave crest is at the seaward side of the structure, the design force and moment will be at a maximum.

(8) Force, F", and moment, M", on a wall built on a rubble base (Figure 114) or on a baffle with a gap at the bottom can be calculated as follows:

$$F'' = (1 - r_f)\,F \qquad (5\text{-}21)$$

and

$$M''_A = (1 - r_m)\,M \qquad (5\text{-}22)$$

WHERE:

F" = force on wall built on rubble base or force on baffle

r_f, r_m = reduction factors determined using Equations (5-19) and (5-20) using b (the height above the bottom of the rubble base or of the gap) instead of h_s (the height of the wall) (see Figure 114)

F = force determined for "ordinary" wall

M"A = moment about the mudline (A in Figure 114) for wall built on rubble base

M = moment about the mudline determined for "ordinary" wall

The moment about the base of the wall (B in Figure 114) is determined by:

$$M''_B = M''_A - b\,F'' \qquad (5\text{-}23)$$

WHERE:

M"B = moment about the base of the wall (B in Figure 114)

b = height (above the bottom) of rubble base or of gap

EXAMPLE PROBLEM 31

Given: a. Incident wave height, H_i = 5 feet
b. Water depth, d_s = 35 feet
c. Wave period, T = 4 seconds
d. Wave-baffle structure as shown in Figure 115; distance from SWL to bottom of structure, h = 17 feet, height of gap, b = 18 feet, and height of structure, h_s = 42 feet

Find: The force and moment on the structure, when the wave crest is at the structure.

Solution: (1) Determine $H_i/g\,T^2$ and H_i/d_s:

$$\frac{H_i}{g\,T^2} = \frac{5}{(32.2)(4)^2} = 0.00970$$

$$\frac{H_i}{d_s} = \frac{5}{35} = 0.14$$

(2) Find h_o:

From Figure 85 for $H_i/g\,T^2$ = 0.00970 and H_i/d_s = 0.14:

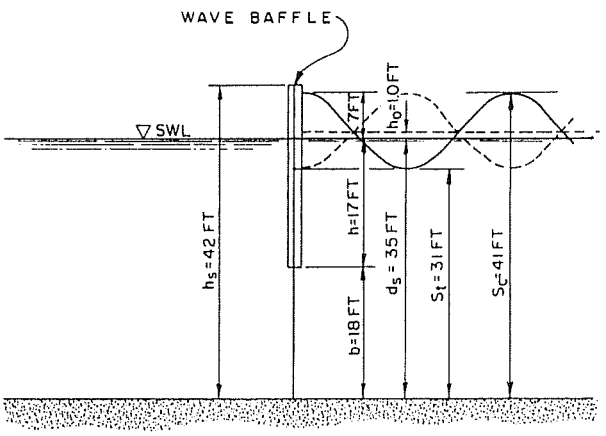

FIGURE 115
Diagram for Example Problem 31

$$\frac{h_o}{H_i} = 0.2$$

$h_o = (0.2)(5) = 1$ foot

(3) Using Equations (5-2) and (5-3), respectively, find S_c and S_t; then determine if baffle will be overtopped:

$S_c = d_s + h_o + H_i = 35 + 1 + 5$

$S_c = 41$ feet

$S_t = d_s + h_o - H_i = 35 + 1 - 5$

$S_t = 31$ feet

Check to see if $S_c > h_s$:

$S_c = 41$ feet and $h_s = 42$ feet

$S_c < h_s$; therefore, the structure will not be overtopped.

(4) Find force and moment when wave crest is at baffle (wave crest at structure):

(a) From Figure 109 for $H_i/g\,T^2 = 0.00970$ and $H_i/d_s = 0.14$:

$$\frac{F_c}{w_w d_s^2} = 0.53$$

(Assuming salt water, $w_w = 64$ pounds per cubic foot.)

$F_c = (0.53)[(64)(35)^2]$

$F_c = 41{,}552$ pounds per foot

(b) Correct for the fact that the structure does not extend to the bottom:

Using Equation (5-19), find r_f; $S = S_c$ and $h_s = b$:

$$r_f = (\frac{b}{S_c})(2 - \frac{b}{S_c})$$

$$r_f = (\frac{18}{41})(2 - \frac{18}{41})$$

$r_f = 0.69$

Using Equation (5-21), find F_c''; $F'' = F_c''$ and $F = F_c$:

$F_c'' = (1 - r_f)\,F_c$

$F_c'' = (1 - 0.69)(41{,}552) = 12{,}881$ pounds per foot

(c) Find F_c when the trough of the transmitted wave acts on the leeward side of wall:

Determine the force acting on the leeward side (seaward-acting). This is done by determining the wave transmission through the baffle using Figure 92 in Section 3, BASIC PLANNING. In order to use this figure, first determine d/L and h/d_s:

First, find d/L:

$L_o = (g/2\pi)\,T^2 = (32.2/2\pi)(4)^2 = 82.0$ feet

$$\frac{d_s}{L_o} = \frac{35}{82.0} = 0.427$$

From Figure 2 for $d_s/L_o = 0.427$:

$$\frac{d}{L} = 0.43$$

Now, find h/d_s, where h = distance from water surface (SWL) to bottom of structure; refer to Figure 115 for the given value of h:

$$\frac{h}{d_s} = \frac{17}{35} = 0.485$$

From Figure 92 for $h/d_s = 0.485$ and $d_s/L = 0.437$:

$$K_t = \frac{H_t}{H_i} = 0.3$$

$H_t = K_t\,H_i = (0.3)(5) = 1.5$ feet

Use Figure 109 to determine the force acting on the leeward side of the wall. Determine $H_t/g\,T^2$ and H_t/d_s:

$$\frac{H_t}{g\,T^2} = \frac{1.5}{(32.2)(4)^2} = 0.00291$$

$$\frac{H_t}{d_s} = \frac{1.5}{35} = 0.0429$$

For consistency of symbols, H_i replaces H_t in the following calculation of transmitted-wave forces and moments.

From Figure 109 for $H_i/g\,T^2 = 0.00291$ and $H_i/d_s = 0.0429$ (wave trough at structure):

$$\frac{F_t}{w_w d_s^2} = 0.48$$

(Assuming salt water, $w_w = 64$ pounds per cubic foot.)

$F_t = (0.48)[(64)(35)^2]$

$F_t = 37{,}632$ pounds per foot

From Figure 85 for $H_i/g\,T^2 = 0.00291$ and $H_i/d_s = 0.0429$:

$$\frac{h_o}{H_i} = 0.03$$

$h_o = (0.03)(1.5) = 0.045$ feet

Using Equation (5-3) with $H_i = H_t$, find S_t:

$S_t = d_s + h_o - H_t = 35 + 0.045 - 1.5$

$S_t = 33.55$ feet

Use Equation (5-19) for r_f with $S = S_t$ in order to correct for the fact that the structure does not extend to the bottom; $h_s = b$:

$$r_f = (\frac{b}{S_t})(2 - \frac{b}{S_t})$$

$$r_f = (\frac{18}{33.55})(2 - \frac{18}{33.55})$$

$r_f = 0.79$

Using Equation (5-21), find F_t''; $F'' = F_t''$ and $F = F_t$:

$F_t'' = (1 - r_f)\,F_t$

$F_t'' = (1 - 0.79)(37{,}632) = 7{,}903$ pounds per foot

(d) Find F_{net} when the wave crest is at the seaward side of the wall:

$F_{net}'' = F_c'' - F_t''$

$F_{net}'' = 12{,}881 - 7{,}903$

$F_{net}'' = 4{,}978$ pounds per foot

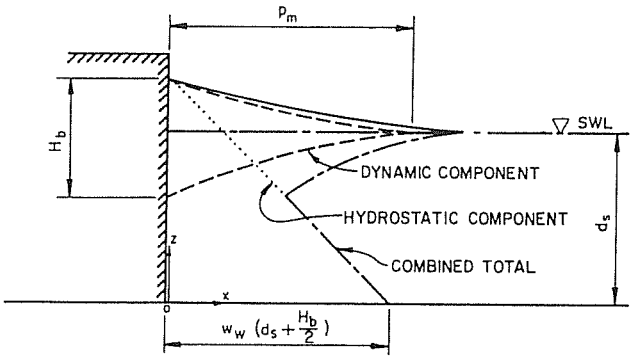

NOTE: EQUATIONS PRESENTED IN SECTION I ARE BASED ON THE z-COORDINATE AXIS WITH ITS ORIGIN AT THE STILL WATER LEVEL. EQUATIONS IN SECTIONS 5 AND 7 ARE BASED ON THE z-COORDINATE AXIS WITH ITS ORIGIN AT THE BOTTOM.

(AFTER SHORE PROTECTION MANUAL, 1977)

FIGURE 116
Pressure Distribution for Breaking Waves at a Wall (Minikin Wave-Pressure Diagram)

(e) From Figure 110 for $H_i/g\,T^2 = 0.00970$ and $H_i/d_s = 0.14$ (wave crest at structure):

$$\frac{M_c}{w_w\, d_s^3} = 0.20$$

$$M_c = (0.20)[(64)(35)^3]$$

$$M_c = 548{,}800 \text{ foot-pounds per foot}$$

(f) Correct for the fact that the structure does not extend to the bottom:

Using Equation (5-20), find r_m; $S = S_c$ and $h_s = b$:

$$r_m = \left(\frac{b}{S_c}\right)^2 \left[3 - 2\left(\frac{b}{S_c}\right)\right]$$

$$r_m = \left(\frac{18}{41}\right)^2 \left[3 - 2\left(\frac{18}{41}\right)\right]$$

$$r_m = 0.41$$

Using Equation (5-22), find M''_c; $M''_A = M''_c$ and $M = M_c$:

$$M''_c = (1 - r_m)\, M_c$$

$$M''_c = (1 - 0.41)(548{,}800)$$

$$M''_c = 323{,}792 \text{ foot-pounds per foot}$$

(g) Find net moment:

Use Figure 110 for $H_i/g\,T^2 = H_t/g\,T^2 = 0.00291$ and $H_i/d_s = H_t/d_s = 0.0429$ to determine the moment acting on the leeward side of the wall (wave trough at structure):

$$\frac{M_t}{w_w\, d_s^3} = 0.158$$

$$M_t = (0.158)[(64)(35)^3]$$

$$M_t = 433{,}552 \text{ foot-pounds per foot}$$

Using Equation (5-20), find r_m; $S = S_t$ and $h_s = b$:

$$r_m = \left(\frac{b}{S_t}\right)^2 \left[3 - 2\left(\frac{b}{S_t}\right)\right]$$

$$r_m = \left(\frac{18}{33.55}\right)^2 \left[3 - 2\left(\frac{18}{33.55}\right)\right]$$

$$r_m = 0.55$$

Using Equation (5-22), find M''_t; $M''_A = M''_t$ and $M = M_t$:

$$M''_t = (1 - r_m)\, M_t$$

$$M''_t = (1 - 0.55)(433{,}552)$$

$$M''_t = 195{,}098 \text{ foot-pounds per foot}$$

(h) Find net moment M''_{net}:

$$M''_{net} = M''_c - M''_t$$

$$M''_{net} = 323{,}792 - 195{,}098$$

$$M''_{net} = 128{,}694 \text{ foot-pounds per foot}$$

(9) In cases for nonvertical walls and for waves at angles of attack other than normal to the wall, forces are assumed to be similar to those for the case of normal wave attack.

c. Breaking Waves. Breaking waves exert hydrostatic forces and dynamic-impact forces on vertical walls. The hydrostatic forces should be used in design for preventing sliding and overturning. Dynamic-impact forces occur at the instant when the vertical front face of a breaking wave impinges on the wall, and only when a plunging wave traps a cushion of air against the wall. The dynamic-impact force occurs only on smooth-faced structures. The dynamic-impact force can be an order-or-magnitude greater than the hydrostatic force; however, it is applied on the order of 1/100 second over a small area. Because walls have a shock-absorbing capacity, they need not be designed for sliding and overturning using dynamic-impact forces. However, these forces should be considered when the wall is made of small or weak units, such as blocks. In such a case, impact forces may cause some damage to the structural components. Therefore, when designing in the region of breaking waves, the designer should calculate the hydrostatic force and determine if the dynamic-impact forces are applicable to the type of construction proposed.

When breaking waves imping on a wall, reflection is assumed to negligible and the pressures are both hydrostatic and dynamic. Figure 116 gives the pressure distribution for hydrostatic and dynamic-impact forces.

(1) Hydrostatic Force and Moment.

(a) Pressure. The hydrostatic pressure is given by:

$$p = 0 \qquad \text{at } z = S_c = d_s + \frac{H_b}{2} \qquad (5\text{-}24)$$

and

$$p = w_w\left(d_s + \frac{H_b}{2}\right) \qquad \text{at } z = 0 \qquad (5\text{-}25)$$

WHERE:

- p = pressure
- z = vertical distance along a coordinate axis with its origin at the bottom
- S_c = depth from wave crest
- H_b = breaking-wave height
- d_s = depth at structure toe from SWL
- w_w = unit weight of water

The hydrostatic pressure distribution is assumed to be linear between S_c and $z = 0$ (see Figure 116).

(b) Force and moment. The total hydrostatic force, F_s, on a nonovertopped wall is:

$$F_s = \frac{1}{2} w_w \left(d_s + \frac{H_b}{2}\right)^2 \qquad (5\text{-}26)$$

WHERE:

F_s = hydrostatic component of force for breaking wave and the hydrostatic moment, M_s, is

$$M_s = \frac{1}{6} w_w \left(d_s + \frac{H_b}{2}\right)^3 \qquad (5\text{-}27)$$

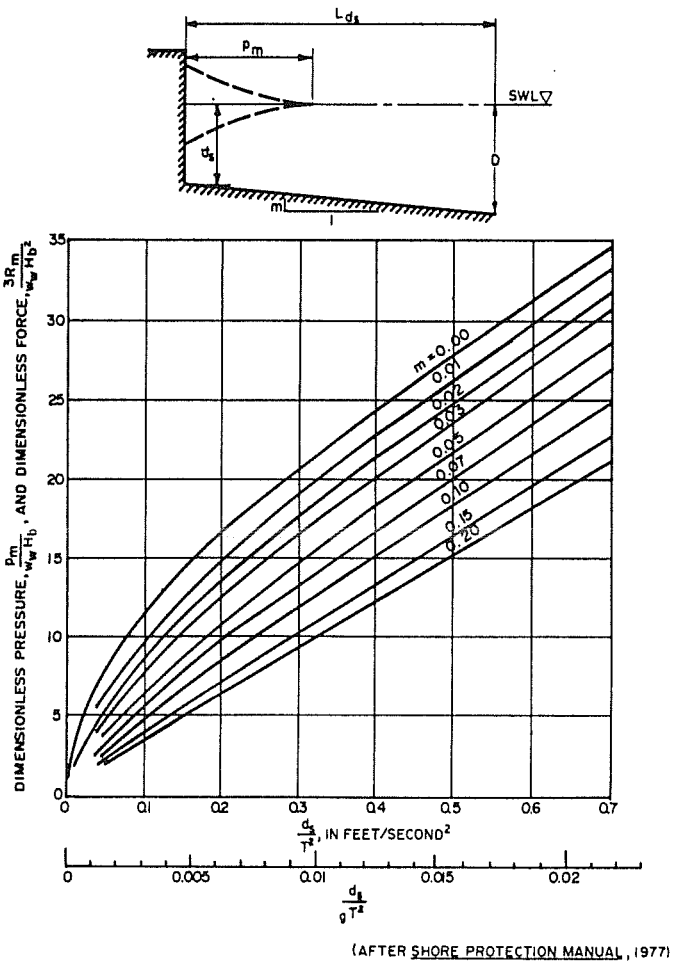

FIGURE 117
Dimensionless Wave Pressure and Force for a Wall Fronted by a Sloping Bottom

WHERE:
M_s = hydrostatic component of moment for breaking wave

(2) Dynamic Force and Moment. Equations for dynamic-impact or shock, force, F_m, and moment, M_m, due to a breaking wave acting on a smooth vertical wall are given below.

(a) Pressure. The maximum dynamic pressure, assumed to act at the still water level, is given by the Minikin equation:

$$p_m = 101\ w_w \left(\frac{H_b}{L_D}\right)\left(\frac{d_s}{D}\right)(D + d_s) \qquad (5\text{-}28)$$

WHERE:
p_m = maximum dynamic pressure
w_w = unit weight of water
H_b = breaking-wave height
L_D = wavelength at depth D
d_s = water depth at structure toe from SWL
D = water depth one wavelength seaward of the wall

The depth, D, one wavelength seaward of the wall (where the wavelength, L_d, is determined using the depth at the wall, d_s) may be determined by the following equation:

$$D = d_s + L_{d_s}\, m \qquad (5\text{-}29)$$

WHERE:
L_{d_s} = wavelength in a depth equal to d_s
m = nearshore bottom slope

The dynamic pressure distribution is shown in Figure 116. The dynamic pressure is assumed to act between $z = d_s + (H_b/2)$ and $d_s - (H_b/2)$.

(b) Force and moment. The integrated dynamic-impact force is:

$$F_m = \frac{p_m H_b}{3} \qquad (5\text{-}30)$$

WHERE:
F_m = dynamic component of force for breaking wave and the moment about the mudline is:

$$M_m = F_m d_s \qquad (5\text{-}31)$$

WHERE:
M_m = dynamic component of moment for breaking wave

(3) Total Force and Moment. The total force, F_T, is obtained by adding the hydrostatic force, F_s, to the dynamic force, F_m:

$$F_T = F_s + F_m \qquad (5\text{-}32)$$

The total moment, M_T, is obtained by adding the hydrostatic moment, M_s, to the dynamic moment, M_m:

$$M_T = M_s + M_m \qquad (5\text{-}33)$$

(4) Wall Fronted by a Sloping Bottom. Equations (5-30) and (5-31) are solved in Figure 117 as a function of $d_s/g\,T^2$ and slope, m. F_m and M_m are determined by first calculating $d_s/g\,T^2$ (or d_s/T^2) and finding the parameters $p_m/(w_w H_b)$ and $3\,F_m/(w_w H_b^2)$; then:

$$p_m = (\text{value from Figure 117})(w_w H_b) \qquad (5\text{-}34)$$

$$F_m = [(\text{value from Figure 117})(w_w H_b^2)]/3 \qquad (5\text{-}35)$$

$$M_m = F_m d_s \qquad (5\text{-}36)$$

Total forces and moments are then determined using Equations (5-32) and (5-33). (Hydrostatic forces are determined as explained previously.)

(5) Wall on a Rubble Foundation. Figure 118 solves Equations (5-30) and (5-31) for a wall built on a rubble foundation as a function of $d_s/g\,T^2$ (or d_s/T^2) and the ratio of the water depth at the wall, d_w, to water depth at the toe of the rubble foundation, d_s: d_w/d_s. Solve for p_m, F_m, and M_m by Equations (5-34), (5-35), and (5-36).

Reduced hydrostatic wave forces and moments for walls on a rubble foundation can be calculated using Equations (5-21) and (5-22), respectively. Values for r_f and r_m are obtained using Equations (5-19) and (5-20), respectively, where S equals S_c (which is $d_s + (H_b/2)$) or S_t (which is $d_s - (H_b/2)$) and $h_s = b$ = height of rubble base.

Total forces and moments are then determined using Equations (5-32) and (5-33).

(6) Wall of Low Height. For a low-height wall (when the top of the wall is lower than the height of the design breaking-wave crest), the force and moment are corrected by using a force-reduction factor, r_m. Figure 119 gives values for r_m for different values of b'/H_b. (b' is defined in Figure 119.) then:

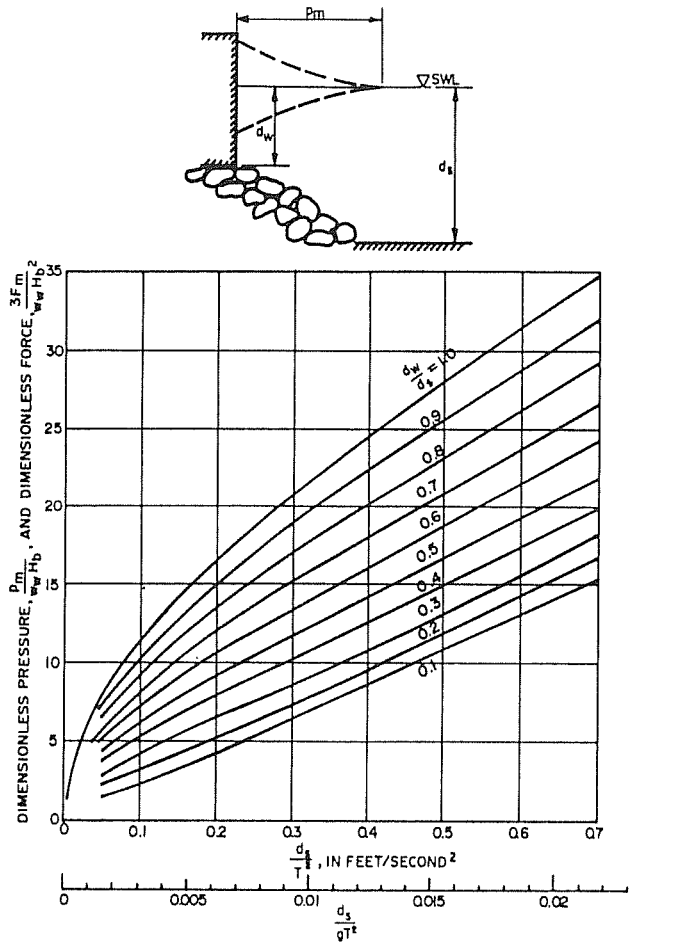

(AFTER SHORE PROTECTION MANUAL, 1977)

FIGURE 118
Dimensionless Wave Pressure and Force for a Wall on a Rubble Foundation

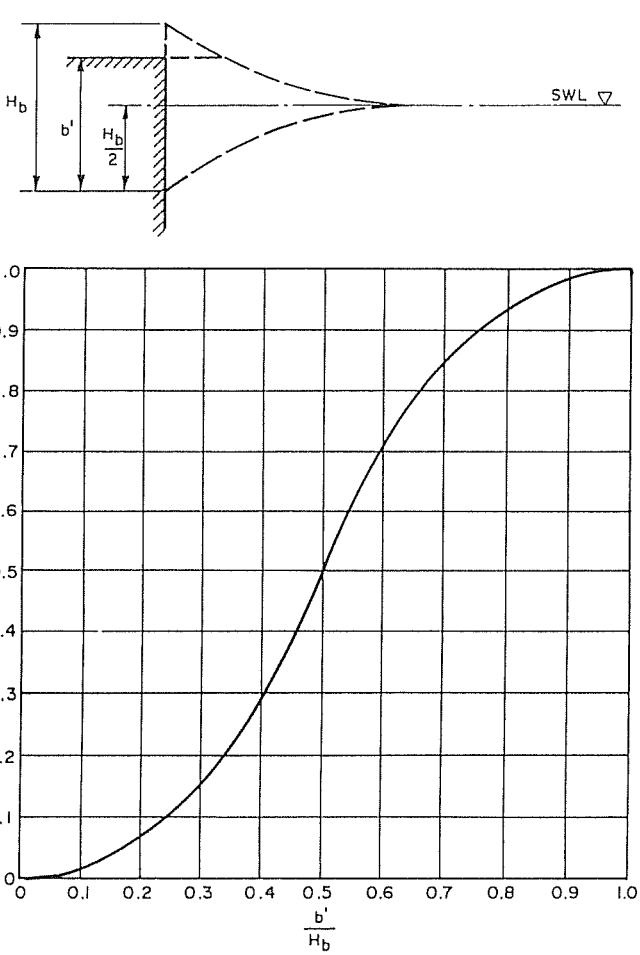

(AFTER SHORE PROTECTION MANUAL, 1977)

FIGURE 119
Force-Reduction Factor for Low-Height Wall

$$F'_m = r_m F_m \qquad (5\text{-}37)$$

WHERE:

F'_m = corrected dynamic-impact force for overtopped wall

r_m = reduction factor for dynamic-impact force (determined from Figure 119)

For the moment, M'_m, an additional reduction factor, a (from Figure 120), is required for use in the equation:

$$M'_m = d_s F_m - (d_s + a)(1 - r_m) F_m$$

which reduces to:

$$M'_m = F_m [r_m (d_s + a) - a] \qquad (5\text{-}38)$$

WHERE:

M'_m = corrected dynamic moment about the mudline for overtopping breaking wave

a = reduction factor for dynamic moment (determined from Figure 120)

Reduced hydrostatic wave forces and moments, F'_s and M'_s, respectively, for a wall of low height can be calculated using Equations (5-17) and (5-18). Values for r_f and r_m are obtained using Equations (5-19) and (5-20), respectively, with $S = S_c = d_s + H_b/2$.

EXAMPLE PROBLEM 32

Given: a. Breaking-wave height, H_b = 6.6 feet
b. Water depth at structure toe, d_s = 6.0 feet
c. Wave period, T = 5 seconds
d. Slope in front of wall, m = 0.05
e. Vertical wall as shown in Figure 121; h_s = 8 feet and b' = 5.3 feet

Find: Breaking-wave force on the vertical wall.

Solution: (1) Determine hydrostatic force and moment:

Using Equation (5-26), find F_s:

$$F_s = \frac{1}{2} w_w \left(d_s + \frac{H_b}{2}\right)^2$$

(Assuming salt water, w_w = 64 pounds per cubic foot.)

$$F_s = \left(\frac{1}{2}\right)(64)\left(6.0 + \frac{6.6}{2}\right)^2$$

F_s = 2,768 pounds per foot

Using Equation (5-19), find r_f; $S_c = d_s + H_b/2$:

$$r_f = \left(\frac{h_s}{S_c}\right)\left(2 - \frac{h_s}{S_c}\right)$$

$$S_c = d_s + \frac{H_b}{2}$$

$$S_c = 6.0 + \frac{6.6}{2} = 9.3$$

$$r_f = \left(\frac{8}{9.3}\right)\left(2 - \frac{8}{9.3}\right)$$

r_f = 0.98

Using Equation (5-17), find F'_s; $F' = F'_s$ and $F = F_s$:

$$F'_s = r_f F_s$$

$$F'_s = (0.98)(2,768)$$

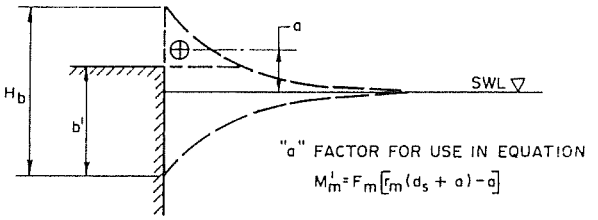

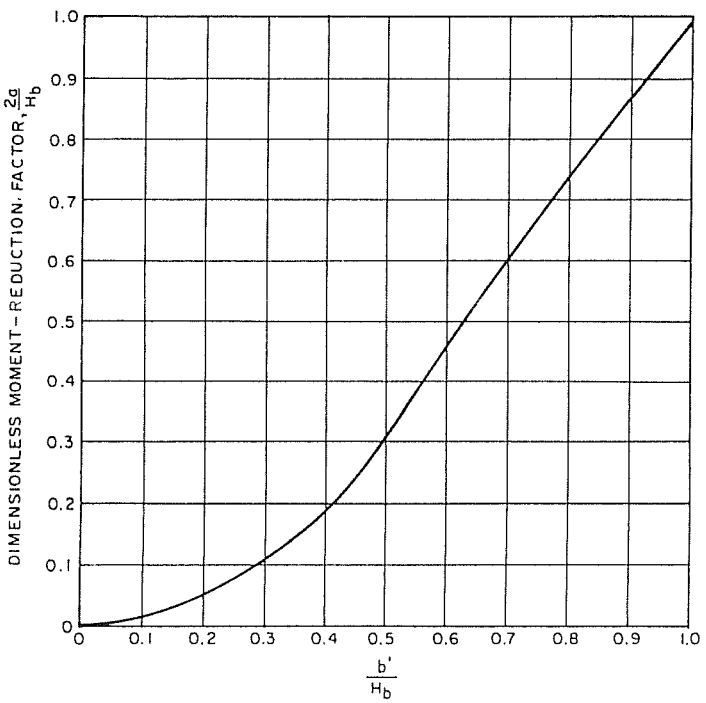

(AFTER SHORE PROTECTION MANUAL, 1977)

FIGURE 120
Moment-Reduction Factor for Low-Height Wall

F'_s = 2,713 pounds per foot

Using Equation (5-27):

$$M_s = \frac{1}{6} w_w \left(d_s + \frac{H_b}{2}\right)^3$$

$$M_s = \left(\frac{1}{6}\right)(64)(6.0 + \frac{6.6}{2})^3$$

M_s = 8,580 foot-pounds per foot

Using Equation (5-20), find r_m; $S_c = d_s + H_b/2 = 9.3$:

$$r_m = \left(\frac{h_s}{S_c}\right)^2 \left[3 - 2\left(\frac{h_s}{S_c}\right)\right]$$

$$r_m = \left(\frac{8}{9.3}\right)^2 \left[3 - 2\left(\frac{8}{9.3}\right)\right]$$

r_m = 0.95

Using Equation (5-18), find M'_s; $M' = M'_s$ and $M = M_s$:

$M'_s = r_m M_s$

M'_s = (0.95)(8,580)

M'_s = 8,151 foot-pounds per foot

(2) Determine dynamic force and moment:

$$\frac{d_s}{T^2} = \frac{6.0}{(5)^2} = 0.24$$

From Figure 117 for d_s/T^2 = 0.24 and m = 0.05:

$$\frac{3 F_m}{w_w H_b^2} = 12.5$$

Using Equation (5-35), find F_m:

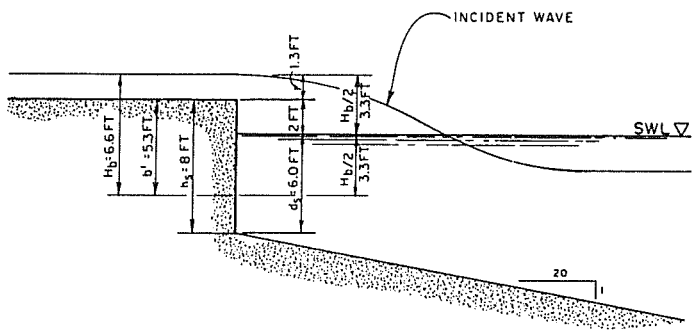

FIGURE 121
Diagram for Example Problem 32

F_m = [(value from Figure 117)($w_w H_b^2$)]/3

$$F_m = \frac{(12.5)(64)(6.6)^2}{3} = 11{,}616 \text{ pounds per foot}$$

As shown in Figure 121, the wall is overtopped; thus, the force-reduction factor, r_m, should be applied to find the force as reduced by overtopping.

From Figure 121, b' = 5.3

$$\frac{b'}{H_b} = \frac{5.3}{6.6} = 0.80$$

From Figure 119 for b'/H_b = 0.80:

r_m = 0.93

Using Equation (5-37), find F'_m:

$F'_m = r_m F_m$

F'_m = (0.93)(11,616) = 10,803 pounds per foot

The moment-reduction factor will also have to be applied:

From Figure 120 for b'/H_b = 0.80:

$$\frac{2a}{H_b} = 0.73$$

$$a = \frac{(0.73)(6.6)}{2} = 2.4$$

Using Equation (5-38), find M'_m:

$M'_m = (F_m)[r_m (d_s + a) - a]$

M'_m = (11,616)[(0.93)(6.0 + 2.4) - 2.4]

M'_m = 62,866 foot-pounds per foot

(3) Find total force and moment:

Using Equations (5-32) and (5-33), respectively, find F_T and M_T:

$F_T = F_s + F_m$, where $F_m = F'_m$

F_T = 2,714 + 10,803

F_T = 13,517 pounds per foot

$M_T = M_s + M_m$, where $M_m = M'_m$

M_T = 8,124 + 62,866

M_T = 70,990 foot-pounds per foot

d. Broken Waves. Calculation of wave pressures for structures subjected to breaking waves is done by making a series of simple assumptions which are not necessarily consistent with empirical wave-transformation data. the structure may be seaward or shoreward of the still water line.

(1) Wall Seaward of Still Water Line. (See Figure 122.)

(a) Pressure. The hydrostatic pressure is:

$$p_s = w_w (d_s + h_c) \qquad (5\text{-}39)$$

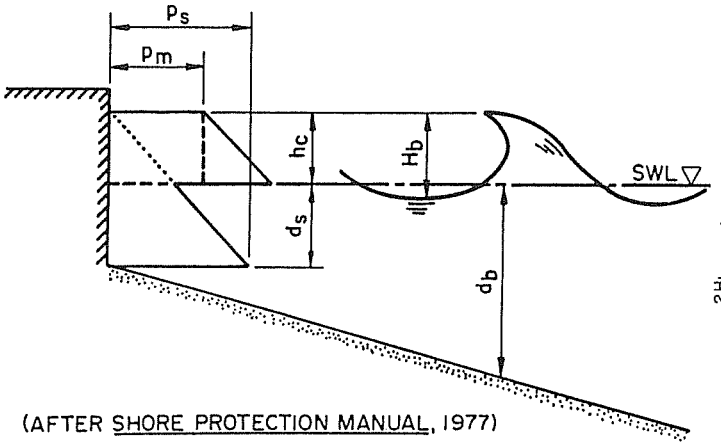

(AFTER SHORE PROTECTION MANUAL, 1977)

FIGURE 122
Wave Pressures From Broken Waves-Wall Seaward of Still Water Line

WHERE:
p_s = maximum hydrostatic pressure
w_w = unit weight of water
d_s = depth at structure toe from SWL

$$h_c = 0.78\ H_b = \text{height of broken wave above SWL} \qquad (5\text{-}40)$$

H_b = breaking-wave height (obtained from Figure 42)
and the dynamic pressure is:

$$p_m = \frac{w_w\ d_b}{2} \qquad (5\text{-}41)$$

WHERE:
p_m = maximum dynamic pressure
w_w = unit weight of water
d_b = depth of water at breaking

(b) Broken-wave forces. The hydrostatic broken-wave force is:

$$F_s = \frac{w_w\ (d_s + h_c)^2}{2} \qquad (5\text{-}42)$$

WHERE:
F_s = hydrostatic component of force for broken wave
and the dynamic breaking-wave force is:

$$F_m = p_m\ h_c \qquad (5\text{-}43)$$

WHERE:
F_m = dynamic component of force for broken wave

(c) Broken-wave moment. The hydrostatic moment is:

$$M_s = \frac{w_w\ (d_s + h_c)^3}{6} \qquad (5\text{-}44)$$

WHERE:
M_s = hydrostatic component of moment for broken wave
and the dynamic moment is:

$$M_m = F_m\ \left(d_s + \frac{h_c}{2}\right) \qquad (5\text{-}45)$$

WHERE:
M_m = dynamic component of moment for broken wave

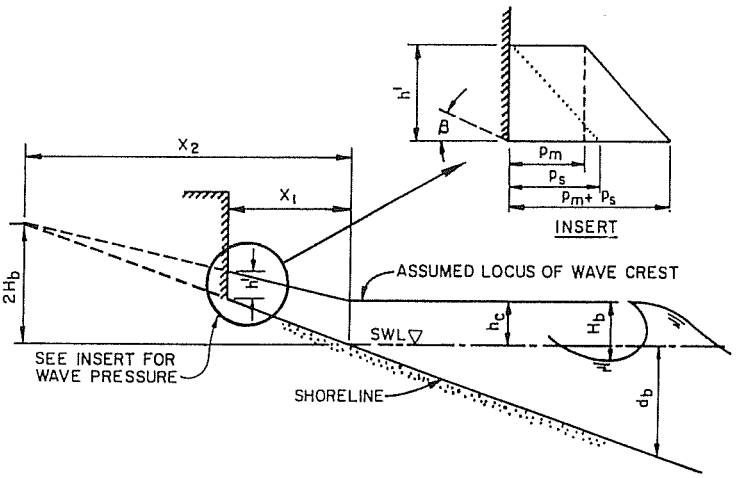

(AFTER SHORE PROTECTION MANUAL, 1977)

FIGURE 123
Wave Pressures From Broken Waves-Wall Landward of Still Water Line

(d) Total forces and moments. Total forces and moments are given by:

$$F_T = F_s + F_m \qquad (5\text{-}46)$$

and

$$M_T = M_s + M_m \qquad (5\text{-}47)$$

(2) Wall Shoreward of Still Water Line. (See Figure 123.) Structures shoreward of the still water line are subject to hydrostatic and dynamic forces due to wave runup.

(a) Wave runup. Calculate wave runup by methods outlined in Section 3.4., WAVE RUNUP, or conservatively assume:

$$R = 2\ H_b \qquad (5\text{-}48)$$

WHERE:
R = runup
H_b = breaking-wave height

(b) Wave height. Find the height of the wave on the wall, h', from:

$$h' = h_c\ \left(1 - \frac{x_1}{x_2}\right) \qquad (5\text{-}49)$$

WHERE:
x_1 = distance from the still water line to the structure
x_2 = $2\ H_b \cot \beta = 2\ H_b/m$ = distance from the still water line to the limit of wave uprush
β = angle of beach slope (see Figure 123)
m = $\tan \beta$

(c) Pressure. The maximum hydrostatic pressure is:

$$p_s = w_w\ h' \qquad (5\text{-}50)$$

The maximum dynamic pressure, assumed to act uniformly over the height, h', is:

$$p_m = \left(\frac{w_w\ d_b}{2}\right)\ \left(1 - \frac{x_1}{x_2}\right)^2 \qquad (5\text{-}51)$$

(d) Forces. The total hydrostatic force is

$$F_s = \left(\frac{w_w h_c^2}{2}\right)\left(1 - \frac{x_1}{x_2}\right)^2 \qquad (5\text{-}52)$$

WHERE:
F_s = hydrostatic component of force for broken wave and the dynamic force is:

$$F_m = \left(\frac{w_w d_b h_c}{2}\right)\left(1 - \frac{x_1}{x_2}\right)^3 \qquad (5\text{-}53)$$

WHERE:
Fm = dynamic component of force for broken wave
The total force is:

$$F_T = F_s + F_m \qquad (5\text{-}54)$$

(e) Resulting moments. The hydrostatic moment is:

$$M_s = \left(\frac{w_w h_c^3}{6}\right)\left(1 - \frac{x_1}{x_2}\right)^3 \qquad (5\text{-}55)$$

WHERE:
M_s = hydrostatic component of moment for broken wave and the dynamic moment is:

$$M_m = \left(\frac{w_w d_b^1 h_c^2}{4}\right)\left(1 - \frac{x_1}{x_2}\right)^4 \qquad (5\text{-}56)$$

WHERE:
M_m = dynamic component of moment for broken wave
The resultant moment is:

$$M_T = M_s + M_m \qquad (5\text{-}57)$$

EXAMPLE PROBLEM 33

Given: a. Breaking-wave height, H_b = 7.0 feet
b. Depth at breaking, d_b = 6.4 feet
c. Water depth at structure toe, d_s = 5.0 feet
d. Vertical, smooth-faced wall situated seaward of the still water line.

Find: The broken-wave force on the wall for a normally incident wave.

Solution: (1) Using Equation (5-40), find h_c:

$h_c = 0.78\ H_b$

$h_c = (0.78)(7.0) = 5.5$ feet

(2) Find hydrostatic force:

Using Equation (5-42), find F_s:

$$F_s = \frac{w_w (d_s + h_c)^2}{2}$$

(Assuming salt water, w_w = 64 pounds per cubic foot.)

$$F_s = \frac{(64)(5.0 + 5.5)^2}{2}$$

F_s = 3,528 pounds per foot

(3) Find dynamic force:

Using Equations (5-41) and (5-43), respectively, find p_m and F_m:

$$p_m = \frac{w_w d_b}{2}$$

$$p_m = \frac{(64)(6.4)}{2}$$

p_m = 205 pounds per square foot

$F_m = p_m h_c = (205)(5.5)$

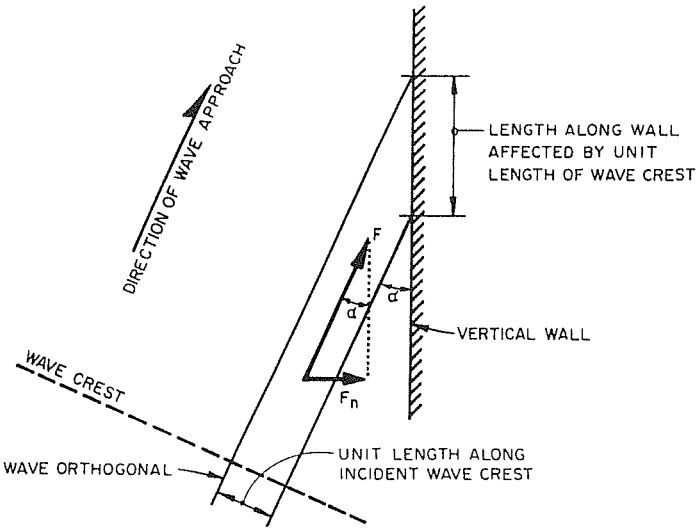

PLAN VIEW

(AFTER SHORE PROTECTION MANUAL, 1977)

FIGURE 124
Diagram Showing Effect of Angle of Wave Approach

F_m = 1,128 pounds per foot

(4) Find total force:

Using Equation (5-46), find F_T:

$F_T = F_s + F_m$

F_T = 3,528 + 1,128

F_T = 4,656 pounds per foot

e. **Effect of Angle of Wave Approach**. The dynamic forces due to breaking and broken waves can be reduced for those cases where the wave approaches at an angle relative to the wall (see Figure 124). The reduction is applied only to the dynamic force. The reduced dynamic force is:

$$F_\alpha = F \sin^2 \alpha \qquad (5\text{-}58)$$

WHERE:
F_α = reduced dynamic component of force for breaking or broken wave striking structure at oblique angle
α = angle between axis of wall and direction of wave approach
F = dynamic component of force for breaking or broken wave if wall were perpendicular to direction of wave approach

This reduction is not applicable to nonbreaking waves nor to rubble-mound structures.

f. **Nonvertical Walls**. Dynamic forces can be reduced for breaking and broken waves impinging on walls that slope landward. The resultant dynamic force is:

$$F_\theta = F_\alpha \sin^2 \theta \qquad (5\text{-}59)$$

WHERE:
F_θ = reduced horizontal dynamic component of force for breaking or broken wave striking nonvertical wall
F_α is obtained from Equation (5-58)
θ = angle between the horizontal and the structure slope

Recurved walls and stepped walls are treated as vertical walls.

2. UPLIFT FORCES.

a. General. Structures such as walls with overhanging members and piers should be designed so that the soffit of the deck is above the crest elevation of the maximum anticipated wave. If waves are expected to impinge on the deck, uplift forces may destroy the deck and its support. In the latter case, either the deck should be made strong enough to withstand the uplift forces, or vents or replaceable slabs should be installed to relieve the uplift forces. Special studies, such as those conducted by El Ghamry (1963), French (1969), and Wang (1967), should be undertaken for this complex design problem. Some uplift forces to be considered are those on wales, fenders, and overhanging decks generally associated with walls and piers. A preliminary method of estimating uplift forces on these objects, with dimensions which are much smaller than a wavelength, is given in the following subsection.

b. Forces on Wales. The vertical uplift force on a wale near a wall is assumed to be equal to or less than the hydrostatic pressure created by the elevation of the wave crest above the soffit of the wale times the projected area of the wale. Then the uplift force, F_u, is approximated by:

$$F_u = w_w (S_c - S_s) A \qquad (5\text{-}60)$$

WHERE:

F_u = uplift force

w_w = unit weight of water

S_c = depth from clapotis crest (for a standing wave); determined by methods described in Section 5.1.b., Nonbreaking Waves (Equation (5-2))

S_s = depth from soffit to bottom

A = projected area of member

It may not be feasible to design for extreme design waves using this procedure. In the event of an extreme design wave occurring, damage may take place and wales or fenders would have to be repaired.

EXAMPLE PROBLEM 34

Given:
a. Incident wave height, H_i = 10 feet
b. Wave period, T = 6 seconds
c. Water depth, d_s = 40 feet
d. Depth from soffit to bottom, S_s = 45 feet
e. The wale is placed on the front of a smooth-faced wall and its dimension measured perpendicularly to the wall is 2 feet (see Figure 125).

Find: The wave force per unit length of wale.

Solution: (1) Find S_c:

$$\frac{H_i}{g\,T^2} = \frac{10}{(32.2)(6)^2} = 0.00863$$

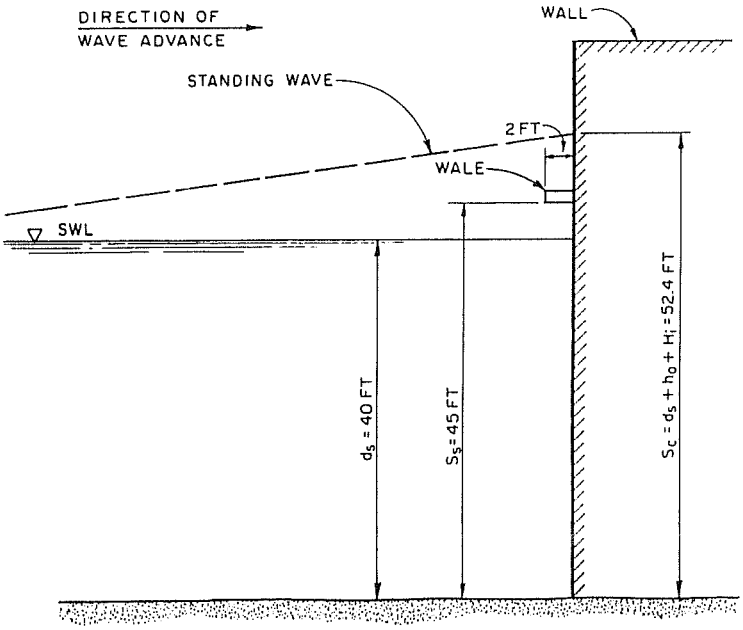

FIGURE 125
Diagram for Example Problem 34

$\frac{H_i}{d_s} = \frac{10}{40} = 0.25$

From Figure 85 for $H_i/g\,T^2 = 0.00863$ and $H_i/d_s = 0.25$:

$\frac{h_o}{H_i} = 0.24$

$h_o = (0.24)(10) = 2.4$ feet

Using Equation (5-2), find S_c:

$S_c = d_s + h_o + H_i$

$S_c = 40 + 2.4 + 10 = 52.4$ feet

(2) Using Equation (5-60), find F_u:

$F_u = w_w (S_c - S_s) A$

(Assuming salt water, $w_w = 64$ pounds per cubic foot.)

A = 2 square feet per foot of wale

$F_u = (64)(52.4 - 45)(2)$

$F_u = 947$ pounds per foot of wale

SECTION 6
FLOATING BREAKWATERS

1. DESCRIPTION. Floating breakwaters are a special classification of breakwater. A floating breakwater comprises a float, of sufficient size relative to the wavelength, held in place by mooring lines fixed to anchors or to guide piles. Figure 126 schematically shows a definition of terms. Figures 127 and 128 give schematic examples of several types of floating breakwater. Floating breakwaters can be constructed of barges, pontoons, floating docks, or rubber tires, or can be specially designed.

2. APPLICATION. Floating breakwaters are generally used or proposed for use in special cases, such as those in which: the water is deep, there is a large fluctuation of water level, the fetch is small (less than 2 to 3 miles), wind waves are less than 3 to 5 seconds). Generally, floating breakwaters are designed for temporary uses. For example, a floating breakwater may be used to provide temporary short period-wave protection during a dredging or construction project. Another possible application is to provide protection for a fleet landing or berthing area. Floating breakwaters can be easily transported compared to fixed breakwaters, and their installation is relatively insensitive to the subgrade conditions.

3. DESIGN PARAMETERS. The state-of-the-art of floating-breakwater design is in a relatively infant stage. Research has been conducted on several types of floating breakwaters, but there have been few long-term, successful installations. This section summarizes some general design principles. The transmission data can be used, with caution, for temporary installations. References are given for studies of special cases in Table 15.

a. Wave Transmission. The performance of a floating breakwater depends primarily upon the ratio of the structure beam, B, to the wavelength, L. Figure 128 plots the transmission coefficient, K_t, as a function of B/L for various moored structures; most of these structures are defined in Figures 127 and 128. The transmission coefficient, K_t, is equal to H_t/H_i, where H_t is the transmitted wave height and H_i is the incident wave height. The structure beam, B, should be on the order of half a wavelength to be assured of significant wave-height reduction. Figure 130 plots transmission coefficients versus B/L for a typical rubber-tire breakwater.

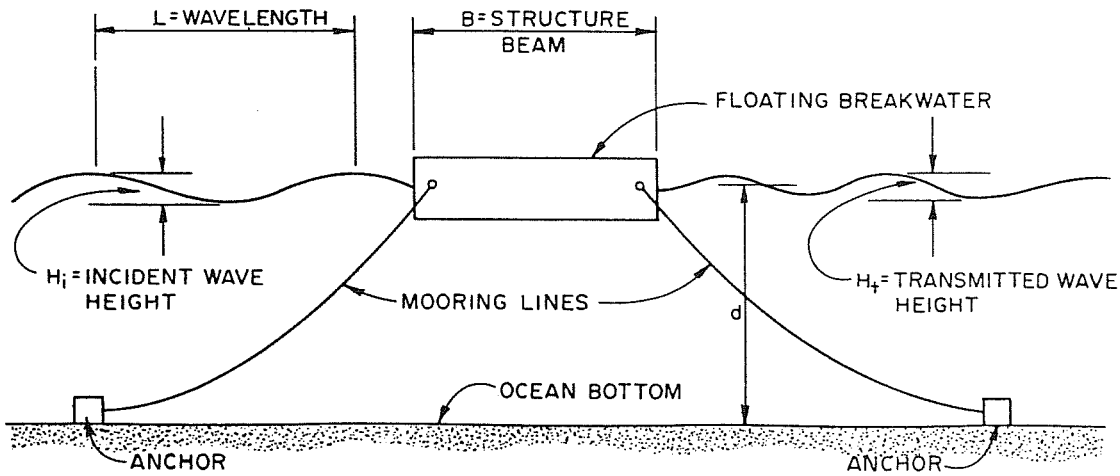

FIGURE 126
Definition of Floating-Breakwater Terms

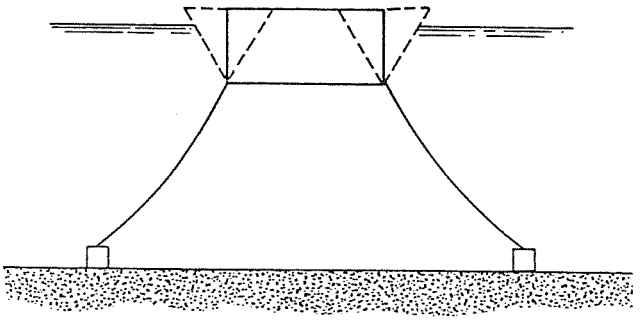

RECTANGULAR-SINGLE PRISM

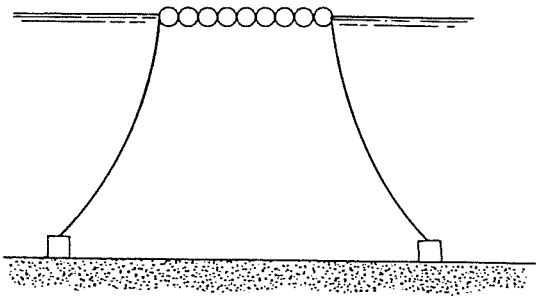

LOG-RAFT

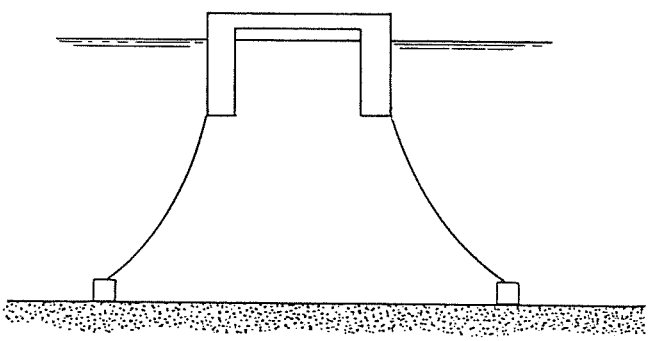

CATAMARAN

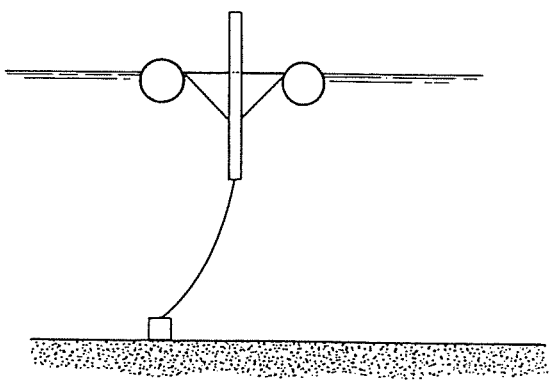

A-FRAME

FIGURE 127
Four Examples of Floating-Breakwater Types

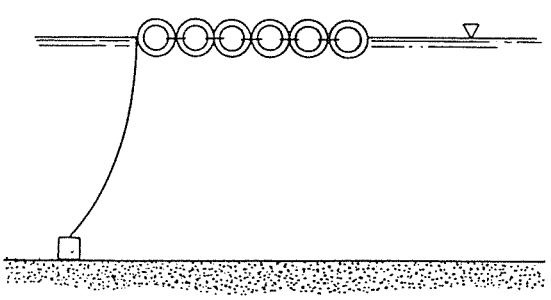

FLOATING-TIRE

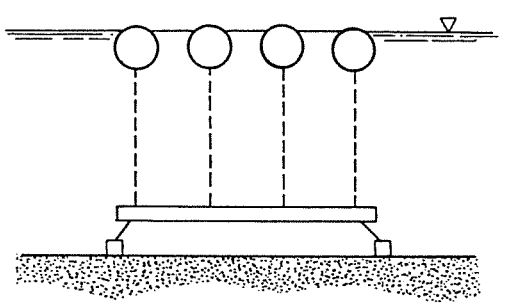

TETHERED-FLOAT

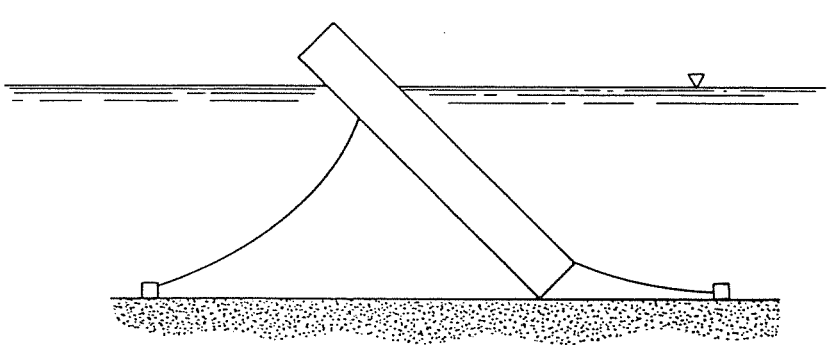

SLOPING

FIGURE 128
Three Examples of Floating-Breakwater Types

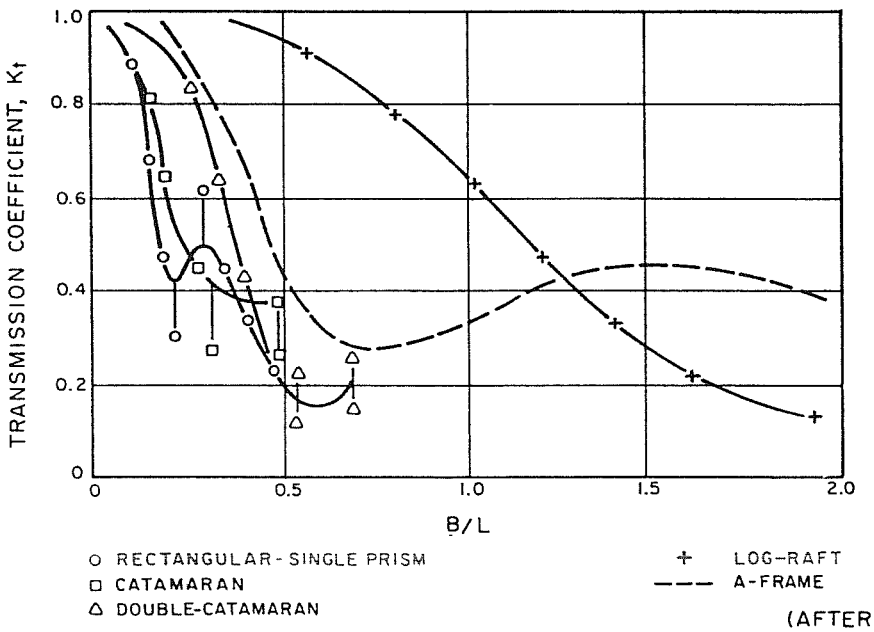

(AFTER RICHEY AND NECE, 1974)

FIGURE 129
Transmission Coefficient Versus B/L for Various Moored Structures

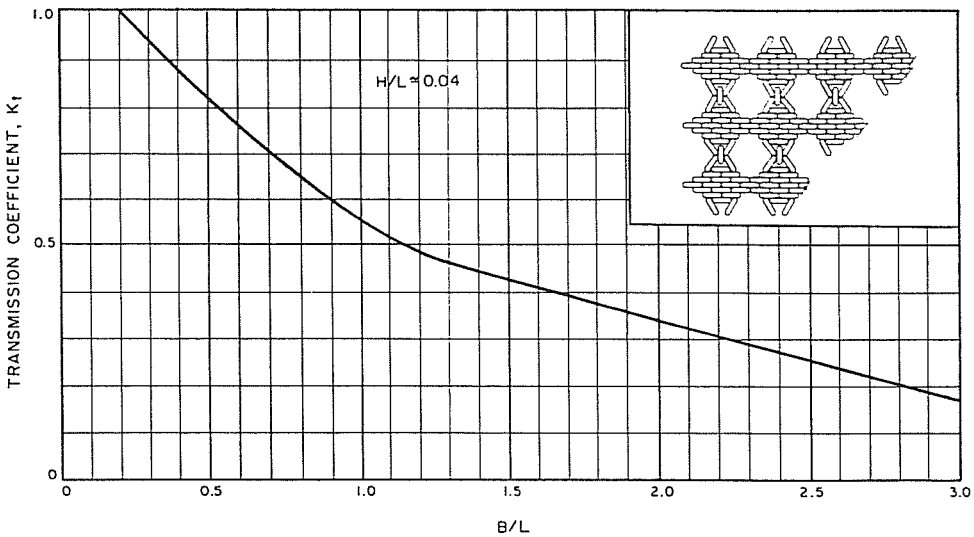

(AFTER HARMS, 1980)

FIGURE 130
Transmission Coefficient Versus B/L for a Typical Rubber-Tire Breakwater

TABLE 15
References for Floating Breakwaters

Type of Structure	Reference
Floating breakwaters, general.....	Kowalski (1974) and Hales (1980)
Floating-tire, Wave-Guard.....	Harms (1980) Harms and Bender (1978)
Tethered-float.....	Seymour and Isaacs (1974)
Inclined-plane.....	Jones (1980)
Pontoon.....	Davidson (1971)

b. Mooring Forces. Mooring forces on and hardware for floating objects are discussed in DM-26.5 and DM-26.6. While the procedures given in DM-26.5 and DM-26.6 provide approximate forces for temporary moorings, more detailed studies are required for determining forces for permanent installations. Mooring forces depend not only on wave action and the type of structure, but also on the type of mooring. A pile-moored breakwater can have an order-of-magnitude greater mooring load than that for a breakwater moored by an anchor connected to chain or to a synthetic-fiber anchor line.

EXAMPLE PROBLEM 35

Given: a. Incident wave height, H_i = 3 feet
b. Water depth, d = 20 feet
c. Wave period, T = 3 seconds

Find: The necessary width, B, of a Goodyear floating-tire breakwater such that the transmitted wave height, H_t, is 1.5 feet.

Solution: (1) Find L:

$$L_o = (g/2\pi)\,T^2 = (32.2/2\pi)(3)^2$$

$$L_o = 46.1 \text{ feet}$$

$$\frac{d}{L_o} = \frac{20}{46.1} = 0.434$$

From Figure 2 for $d/L_o = 0.434$:

$$\frac{d}{L} = 0.438$$

THEREFORE: $L = \frac{20}{0.438} = 45.7$ feet

(2) Desired $K_t = \frac{H_t}{H_i} = \frac{1.5}{3} = 0.5$

From Figure 130 for $K_t = 0.5$:

$$B/L = 1.15$$

THEREFORE: $B = 1.15\ L = (1.15)(45.7) = 52.5$ feet

4. METRIC EQUIVALENCE CHART. The following metric equivalents were developed in accordance with ASTM E-621. These units are listed in the sequence in which they appear in Section 6. Conversions are approximate.

2 miles = 3.2 kilometers
3 miles = 4.8 kilometers
3 feet = 91.4 centimeters
5 feet = 1.5 meters

SECTION 7
WAVE FORCES ON CYLINDRICAL PILES

1. INTRODUCTION. Methods for the calculation of wave forces on piles are divided into eight cases, as listed in Table 16. The cases are examined in order of complexity. The relative complexity depends upon:

(1) The shape of the pile: piles may be either uniform on nonuniform in diameter from the bottom to the surface. Nonuniformity in diameter is usually a result of marine fouling near the intertidal zone or of the use of a protective jacket around a section of the pile.
(2) The complexity of the structure: force may be calculated for a single pile or for a group of piles.
(3) The ratio of the pile diameter to the local wavelength and to the local wave height: these ratios determine the relative effects of inertial forces and wave diffraction.
(4) The accuracy needed for the project: preliminary planning studies may only require an order of magnitude estimate of the wave force.

TABLE 16
Wave Forces on Piles

Case	Description	Application	Section	Parameters
		Uniform Diameter Only		
1	Drag only.....	Preliminary design: small-diameter piles	7.5	d/L_o, H/H_b
2	Drag and inertial--maximum nonlinear theory.....	Preliminary design: intermediate-diameter piles	7.6	d/L_o, H/H_b, $(C_M D)/(C_D H)$
		Nonuniform and Uniform Diameters		
3	Drag.....	Preliminary design: small-diameter piles	7.7	d/L_o, z/d
4	Drag and inertial...	Preliminary design: intermediate-diameter piles, arbitrary wave-phase angle	7.8	d/L_o, z/d, $(C_M D)/(C_D H)$, θ
5	Nonlinear corrections.....	Final design for Case 4: arbitrary wave-phase angle	7.9	d/L_o, z/d, $(C_M D)/(C_D H)$, θ, H/H_b
		Miscellaneous		
6	Combination of piles.....	Bents	7.10	All of the above, plus phase difference between piles
7	Bracing.....	Crossmembers	7.11	
8	Forces due to breaking waves.....	Shallow water	7.12	

Case 1 assumes a uniform pile of small diameter compared to the local wavelength and wave height. Calculations of the wave force are based only on the drag force. Case 2 assumes a uniform pile of intermediate diameter compared to the local wavelength and wave height. Calculations of the wave force are based on both the inertial and drag forces. Case 3 provides a method for determining the wave forces on a pile of small, nonuniform diameter. The assumptions made are the same as for Case 1 and the estimates of wave force are based solely on drag. The method uses linear theory but provides a nonlinear correction factor. Case 4 provides an approximate method for calculating the force-time history on a single pile of nonuniform, intermediate diameter. This method incorporates both inertial and drag forces; however, it is based on linear theory and, therefore, should be used only for preliminary design. Case 5 provides nonlinear corrections which, when used in conjunction with the method outlined in Case 4, will provide wave forces for final design. Case 6 provides a method for determining wave forces on a combination of piles. Case 7 provides a method for determining the wave forces on bracing used between vertical piles. Case 8 outlines a method for determining the breaking-wave forces on a pile.

2. BASIC EQUATIONS. Figure 131 defines terms used to describe wave forces on piles. Basic equations and other definitions required for calculation of wave-induced forces on cylindrical piles are as given below.

a. Forces. The total force, F_T, on a pile subjected to nonbreaking waves is the sum of the drag force, F_D, and the inertial force, F_I:

$$F_T = F_D + F_I \qquad (7\text{-}1)$$

The drag force is given by:

$$F_D = \int_o^z f_D\, dz \qquad (7\text{-}2)$$

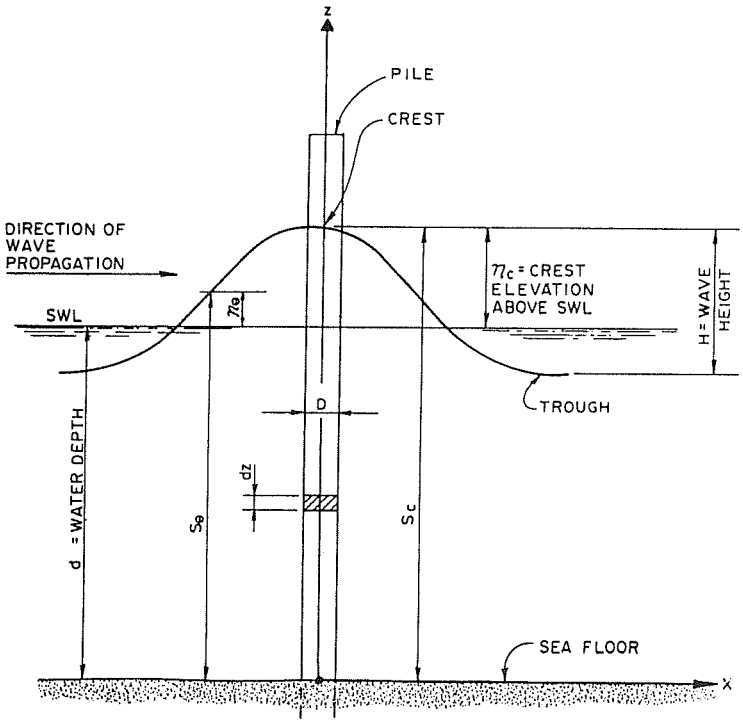

NOTE: IN SECTION 7, THE NOTATION USED FOR THE FREE SURFACE WILL BE AS FOLLOWS:

η_θ = VALUE OF FREE-SURFACE ELEVATION FROM SWL AT AN ARBITRARY WAVE-PHASE ANGLE, θ

η_c = VALUE OF FREE-SURFACE ELEVATION FROM SWL (MEASURED AT THE PILE) WHEN THE WAVE CREST IS AT THE PILE

S_θ = DISTANCE OF FREE SURFACE MEASURED FROM THE BOTTOM AT AN ARBITRARY WAVE-PHASE ANGLE, θ

S_c = DISTANCE OF FREE SURFACE FROM THE BOTTOM (MEASURED AT THE PILE) WHEN THE WAVE CREST IS AT THE PILE

FIGURE 131
Definition of Terms Used to Describe Wave Forces on Piles

WHERE:

z = depth in terms of vertical distance along a coordinate axis with its original at the bottom

$$f_D = (\tfrac{1}{2}) \rho C_D D u \left| u \right| \qquad (7\text{-}3)$$

= drag force per unit length of pile

ρ = density of water

C_D = drag coefficient (dimensionless), obtained from Table 17

D = pile diameter

u = instantaneous horizontal water-particle velocity

The inertial force, F_I, is given by:

$$F_I = \int_o^z f_I \, dz \qquad (7\text{-}4)$$

WHERE: $$f_I = \rho C_M \pi (D^2/4) (du/dt) \qquad (7\text{-}5)$$

= inertial force per unit length of pile

C_M = inertial, or added-mass, coefficient (dimensionless), obtained from Table 18

du/dt = instantaneous horizontal water-particle acceleration

TABLE 17
Drag Coefficient

C_D	Reynolds Number, R_e	Comments
0.7.....	$> 5 \times 10^5$	Used for most design applications
1.2 to 0.7.....	2×10^5 to 5×10^5	Transitional
1.2.....	$< 2 \times 10^5$	Subcritical

TABLE 18
Inertial Coefficient

C_M	Reynolds Number, R_e	Comments
2.0.....	$> 2.5 \times 10^5$	
1.5 to 2.0.....	2.5×10^5 to 5×10^5	
1.5.....	$< 5 \times 10^5$	Used for most design applications

A transverse force due to alternate eddy formation and sheeding, known as the "lift force," will also result from the wave-pile interaction. The lift force acts perpendicularly to both wave direction and pile axis. The lift force is analogous to a drag force and is maximum at the same moment as the drag force. For design of rigid structures, a lift force is automatically taken into account by adopting a conservative C_D value regardless of the force direction. For design of flexible structures, dynamic response of the structure must be analyzed (see Laird (1962)).

b. Moments. The moment, M, about the mudline is given by:

$$M = \int_o^z (f_D + f_I) \, z \, dz \qquad (7\text{-}6)$$

WHERE:

z = depth in terms of vertical distance along a coordinate axis with its origin at the bottom

f_D = drag force per unit length of pile (Equation (7-3)

f_I = inertial force per unit length of pile (Equation (7-5)

c. Drag and Inertial Coefficients. Drag and inertial coefficients for cylindrical piles subject to ocean waves are a function of Reynolds number. The Reynolds number, R_e, is given by:

$$R_e = (u_m D)/\nu \qquad (7\text{-}7)$$

WHERE:

u_m = approximate maximum horizontal water-particle velocity given by the appropriate equation and $\theta = 0°$ for u in Table 1 (Section 1) at $z = \eta_c$. Note that the value of z is referenced to SWL in Section 1 instead of to the bottom, as in Section 7. (See Table 1 for Water Particle Velocity, Horizontal.)

θ = wave-phase angle

z = depth in terms of vertical distance along a coordinate axis with its origin at the bottom

η_c = water-surface elevation at wave crest relative to SWL

H = local wave height

g = gravitational acceleration (32.2 feet per second^2)

d = water depth

D = pile diameter

ν = kinematic viscosity (approximately 1×10^{-5} feet^2 per second for salt water)

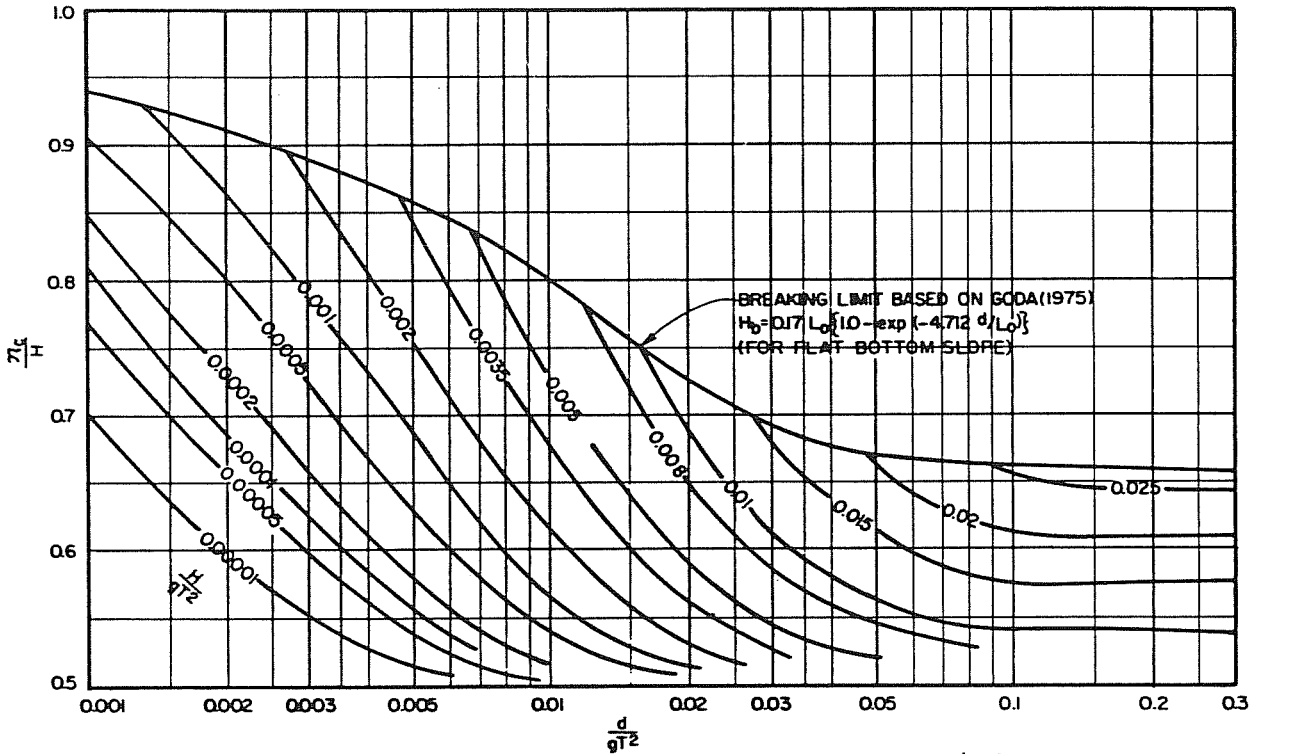

FIGURE 132
Relative Wave-Crest Elevation Above SWL, η_c/H, as a Function of $d/g\,T^2$ and $H/g\,T^2$

3. LIMITING WAVE HEIGHT. The linear and nonlinear stream-function wave theories (Dean, 1965) are used for calculation of wave forces. The forces are calculated throughout Section 7 by application of a series of figures and equations which relate the given wave height to the limiting height over a horizontal bottom. Calculation requires entering the figures with a value of H/H_b, where H_b = breaking-wave height, to find various force and moment coefficients. The local wave height, H, can be determined through use of the nonlinear shoaling curve (Figure 4) for a nonhorizontal bottom. For horizontal bottoms, the local wave height, H, is determined using the linear shoaling coefficient (Figure 2). The breaking-wave height, H_b, can be determined using Figure 42 for nonhorizontal bottoms. H_b is taken as 0.78 d for horizontal bottoms.

Stream-function theory has been developed strictly for a horizontal bottom; however, sloped bottoms occur more frequently in design situations. Consequently, while only strictly accurate for a horizontal bottom, the methods presented herein, in conjunction with the aforementioned methods for determining local wave heights over a sloped bottom, should provide conservative estimates of wave forces on piles. If H/H_b is found to be > 1, refer to Subsection 7.12, CASE 8--FORCES DUE TO BREAKING WAVES. Example Problem 36 demonstrates the determination of H/H_b.

EXAMPLE PROBLEM 36

Given: a. Equivalent unrefracted deepwater wave height, H'_o = 10 feet
b. Water depth, d = 17 feet
c. Wave period, T = 10 seconds
d. Bottom slope, m = 0.02

Find: H_b and H/H_b for wave-force calculations.

Solution: (1) Find H:

(a) Calculate L_o, d/L_o, and H'_o/L_o:

$$L_o = (g/2\pi)\,T^2 = (32.2/2\pi)(10)^2 = 512 \text{ feet}$$

$$d/L_o = 17/512 = 0.0332$$

$$H'_o/L_o = 10/512 = 0.0195$$

(b) From Figure 4 for $d/L_o = 0.0332$ and $H'_o/L_o = 0.0195$:

$$H/H'_o = 1.13$$

$$H = 1.13\,H'_o$$

$$H = (1.13)(10) = 11.3 \text{ feet}$$

(2) Find H_b:

(a) Find $H'_o/g\,T^2$:

$$\frac{H'_o}{g\,T^2} = \frac{10}{(32.2)(10)^2} = 0.00311$$

(b) From Figure 42 for $H'_o/g\,T^2 = 0.00311$ and m = 0.02:

$$\frac{H_b}{H'_o} = 1.2$$

$$H_b = 1.2\,H'_o$$

$$H_b = (1.2)(10) = 12 \text{ feet}$$

(3) Find H/H_b:

$$\frac{H}{H_b} = \frac{11.3}{12}$$

$H/H_b = 0.942$; use $H/H_b = 0.94$

4. WAVE-CREST ELEVATION. Knowledge of the wave-crest elevation above still water level, η_c, is necessary not only to calculate wave force, but also to determine the height of a pile-supported structure above sea level. The relative wave-crest elevation above the still water level, η_c/H, is greater than or equal to one-half ($\eta_c/H \geq 1/2$) and is given in

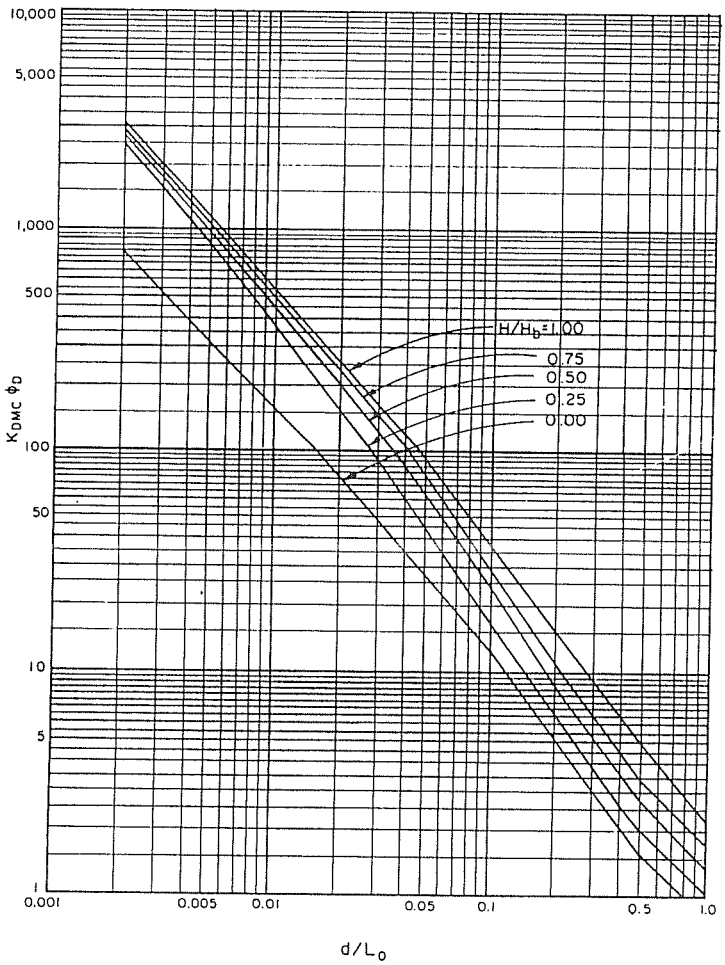

FIGURE 133
($K_{DMC}\,\phi_D$) as a Function of d/L_o and H/H_b

Figure 132 as a function of $d/g\,T^2$ and $H/g\,T^2$. Figure 132 is based on stream-function theory and was developed by Seelig and Ahrens (1981). The distance of the wave crest above the bottom when the crest is at the pile, S_c, is:

$$S_c = \eta_c + d \qquad (7\text{-}8)$$

WHERE:
S_c = distance of free surface measured from the bottom to the wave crest when the crest is at the pile
η_c = water-surface elevation at wave crest relative to SWL
d = water depth at the pile from SWL

Example Problem 37 shows the calculation of S_c.

EXAMPLE PROBLEM 37

Given: a. Equivalent unrefracted deepwater wave height, H'_o = 10 feet
b. Water depth, d = 17 feet
c. Wave period, T = 10 seconds

Find: Wave-crest elevation above the bottom, S_c.

Solution: (1) From Example Problem 36, H = 11.3 feet

(2) Find $d/g\,T^2$ and $H/g\,T^2$:

$$\frac{d}{g\,T^2} = \frac{17}{(32.2)(10)^2} = 0.00528$$

$$\frac{H}{g\,T^2} = \frac{11.3}{(32.2)(10)^2} = 0.00351$$

(3) From Figure 132 for $d/g\,T^2 = 0.00528$ and $H/g\,T^2 = 0.00351$:

$\eta_c/H = 0.83$

$\eta_c = (0.83)(11.3) = 9.38$ feet; use $\eta_c = 9.5$ feet

$S_c = \eta_c + d = 9.5 + 17 = 26.5$ feet

5. CASE 1--MAXIMUM FORCE ON SINGLE PILE OF SMALL, UNIFORM DIAMETER (PRELIMINARY DESIGN).

a. Range of Application. Case 1 is applicable to piles of small, uniform diameter and for values of D/H and d/L_o as follows:

(1) Shallow and transitional water: Case 1 is applicable in shallow and transitional water when $d/L_o < 0.1$ and $D/H < 0.6$.

(2) Deep water: Case 1 is applicable in deep water when $d/L_o > 0.5$ and $D/H < 0.15$.

(3) If the conditions in (1) and (2) are not met, refer to Case 2.

Note: See Section 1, Table 1, for a definition of shallow, transitional, and deep water.

b. Maximum Drag Force. The maximum drag force, F_{mD}, occurs under the crest and is determined by:

$$F_{mD} = \left(\frac{1}{2}\right) \rho\, C_D\, D \left(\frac{H}{T}\right)^2 d\, (K_{DMC}\,\phi_D) \qquad (7\text{-}9)$$

WHERE:
ρ = density of water
C_D = drag coefficient (obtained from Table 17)
D = pile diameter
H = local wave height
T = wave period
d = water depth

The value of ($K_{DMC}\,\phi_D$) can be obtained from Figure 133 as a function of d/L_o and H/H_b.

c. Maximum Moment. The maximum drag moment, M_{mD}, is given by:

$$M_{mD} = \left(\frac{1}{2}\right) \rho\, C_D\, D \left(\frac{H}{T}\right)^2 d^2\, (\tau_{DMC}\,\psi_D) \qquad (7\text{-}10)$$

WHERE:
ρ = density of water
C_D = drag coefficient (obtained from Table 17)
D = pile diameter
H = local wave height
T = wave period
d = water depth

The value of ($\tau_{DMC}\,\psi_D$) can be obtained from Figure 134 as a function of d/L_o and H/H_b.

d. Reaction. The lever arm, or distance of the point of application of force above the bottom, z_{mD}, is:

$$z_{mD} = \frac{M_{mD}}{F_{mD}} \qquad (7\text{-}11)$$

EXAMPLE PROBLEM 38

Given: a. Equivalent unrefracted deepwater wave height, H'_o = 10 feet
b. Water depth, d = 17 feet
c. Wave period, T = 10 seconds
d. Vertical pile with diameter, D = 1 foot
e. Bottom slope, m = 0.02

Find: The maximum force and moment about the mudline on the vertical pile; also find the lever arm above the bottom.

Solution: (1) From Example Problem 36:

$d/L_o = 0.0332$

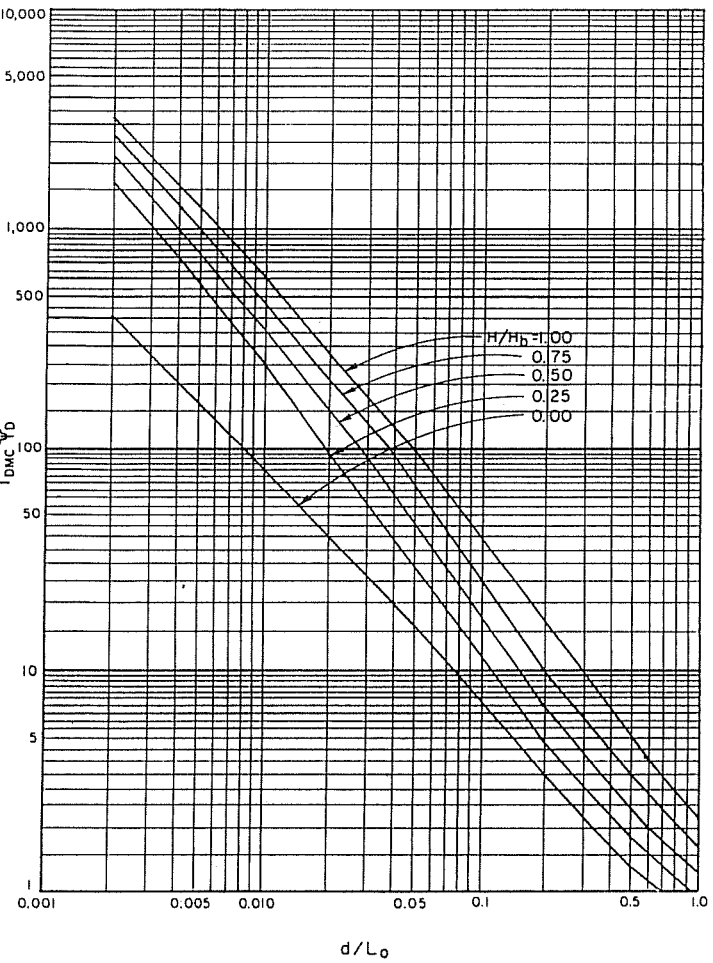

FIGURE 134
($\tau_{DMC}\ \psi_D$) as a Function of d/L_o and H/H_b

H = 11.3 feet, H_b = 12 feet, and H/H_b = 0.94

(2) From Example Problem 37:

$d/g\ T^2 = 0.00528$

$H/g\ T^2 = 0.00351$

η_c = 9.5 feet

(3) Determine if Case 1 is applicable to this problem:

(a) Determine if water depth is shallow, transitional, or deep:

From Figure 2 for d/L_o = 0.0332:

$d/L = 0.075$

$\frac{1}{25} < \frac{d}{L} < \frac{1}{2}$

The wave is in transitional water.

(b) d/L_o = 0.0332 (from Example Problem 36)

(c) Find D/H:

$\frac{D}{H} = \frac{1}{11.3} = 0.088$

$d/L_o = 0.0332 < 0.1$

and $D/H = 0.088 < 0.6$

THEREFORE: Case 1 is applicable.

(4) Determine Reynolds number, R_e:

(a) Find L:

$\frac{d}{L} = 0.075$

$L = \frac{d}{0.075}$

$L = \frac{17}{0.075} = 227$ feet

(b) Find u_m:

From Table 1 (Section 1) for transitional water; $u = u_m$:

(Note that in this equation, z is referenced to SWL.)

$$u_m = \left(\frac{H}{2}\right)\left(\frac{gT}{L}\right)\left(\frac{\cosh[2\pi(z+d)/L]}{\cosh(2\pi d/L)}\right)(\cos\theta)$$

For the maximum value of u, use $z_c = \eta_c$ = 9.5 feet and $\cos\theta = 1$

$$u_m = \left(\frac{11.3}{2}\right)\left[\frac{(32.2)(10)}{(227)}\right]\left\{\frac{\cosh[2\pi(9.5+17)/227]}{\cosh[2\pi(17/227)]}\right\}(1)$$

$$u_m = (8.01)\left[\frac{\cosh(0.733)}{\cosh(0.471)}\right]$$

From Figure 3:

$\cosh(0.733) = 1.28$

and $\cosh(0.471) = 1.11$

$u_m = (8.01)\left(\frac{1.28}{1.11}\right) = 9.2$ feet per second

(c) Using Equation (7-7), find R_e:

$R_e = (u_m D)/\nu$

$R_e = [(9.2)(1)]/(1 \times 10^{-5})$

$R_e = 9.2 \times 10^5$

(5) Find F_{mD}:

(a) Determine drag coefficient, C_D:

From Table 17 for $R_e = 9.2 \times 10^5$:

$C_D = 0.7$

(b) Determine ($K_{DMC}\ \phi_D$):

From Figure 133 for d/L_o = 0.0332 and H/H_b = 0.94:

($K_{DMC}\ \phi_D$) = 154

(c) Assuming salt water, ρ = 2 slugs per cubic foot.

(d) Using Equation (7-9), the maximum force is:

$F_{mD} = \left(\frac{1}{2}\right)\rho\ C_D\ D\ \left(\frac{H}{T}\right)^2 d\ (K_{DMC}\ \phi_D)$

$F_{mD} = \left(\frac{1}{2}\right)(2)(0.7)(1)\left(\frac{11.3}{10}\right)^2(17)(154)$

F_{mD} = 2,340 pounds

(6) Find M_{mD}:

(a) Determine ($\tau_{DMC}\ \psi_D$):

From Figure 134 for d/L_o = 0.0332 and H/H_b = 0.94:

($\tau_{DMC}\ \psi_D$) = 147

(b) Using Equation (7-10), the maximum moment is:

$M_{mD} = \left(\frac{1}{2}\right)\rho\ C_D\ D\ \left(\frac{H}{T}\right)^2 d^2(\tau_{DMC}\ \psi_D)$

$M_{mD} = \left(\frac{1}{2}\right)(2)(0.7)(1)\left(\frac{11.3}{10}\right)^2(17)^2(147)$

M_{mD} = 37,973 foot-pounds

(7) Find z_{mD}:

Using Equation (7-11), the lever arm above the bottom is:

$z_{mD} = \frac{M_{mD}}{F_{mD}} = \frac{37,973}{2,340}$

z_{mD} = 16.2 feet

6. CASE 2--PILE OF INTERMEDIATE, UNIFORM DIAMETER (PRELIMINARY DESIGN).

a. **Range of Application**. This method is applicable to most cases of H/D and d/L_o, although the pile diameter should be small compared to the wavelength (that is, D/L < 0.2). For larger values of D/L, the diffraction effects induced by the wave interacting with a pile of larger diameter cannot be neglected. Case 2 is strictly applicable to single piles where

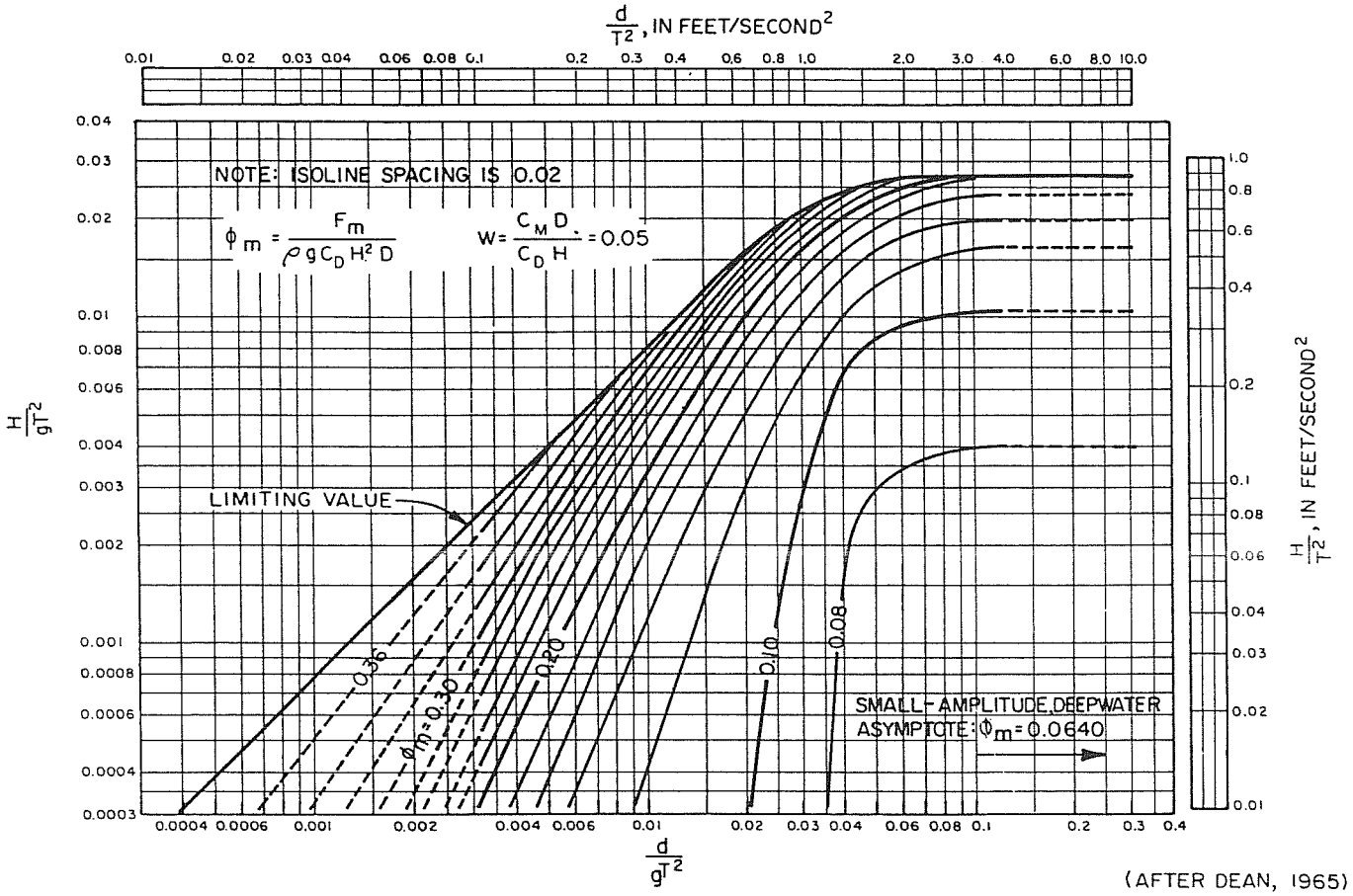

(AFTER DEAN, 1965)

FIGURE 135
Isolines of ϕ_m as a Function of d/g T² and H/g T² for W = 0.05

the spacing between piles, Δ, is greater than 10 D (Δ > 10 D). However, reasonable accuracy can be obtained using this method for closer-spaced piles to an arbitrary limit, Δ > 2 D.

b. Maximum Force. The maximum force on a single pile is the sum of drag and inertial forces. This maximum force occurs in front of the wave crest. The maximum force, F_{mDI}, is given by:

$$F_{mDI} = \rho\ g\ C_D\ H^2\ D\ \phi_m \qquad (7\text{-}12)$$

WHERE:

- ρ = density of water
- g = gravitational acceleration (32.2 feet per second²)
- C_D = drag coefficient (obtained from Table 17)
- H = local wave height
- D = pile diameter
- ϕ_m = a coefficient given in Figures 135 through 138 as a function of d/g T² and H/g T² for various values of W

$$W = \frac{C_M\ D}{C_D\ H} = \text{parameter used in pile force and moment calculations} \qquad (7\text{-}13)$$

- C_M = inertial, or added-mass, coefficient (obtained from Table 18)

c. Maximum Moment. The maximum moment about the mudline, M_{mDI}, is given by:

$$M_{mDI} = \rho\ g\ C_D\ H^2\ D\ d\ \alpha_m \qquad (7\text{-}14)$$

WHERE:

- ρ = density of water
- g = gravitational acceleration (32.2 feet per second²)
- C_D = drag coefficient (obtained from Table 17)
- H = local wave height
- D = pile diameter
- d = water depth
- α_m = a coefficient given by Figures 139 through 142 as a function of d/g T² and H/g T² for various values of W

W is defined in Equation (7-13)

d. Reaction. The lever arm, z_{mDI}, is given by Equation (7-11), substituting z_{mDI} for z_{mD}, M_{mDI} for M_{mD}, and F_{mDI} for F_{mD}.

EXAMPLE PROBLEM 39

Given: a. Equivalent unrefracted deepwater wave height, H'_o = 10 feet
b. Water depth, d = 17 feet
c. Wave period, T = 10 seconds
d. Diameter of pile, D = 1 foot
e. C_D = 0.7 and C_M = 2.0

Find: Maximum force and moment about mudline, considering both drag and inertial forces, and compare the results to those obtained in Example Problem 38; also find lever arm above the bottom.

Solution: (1) From Example Problem 37:

$$\frac{d}{g\ T^2} = 0.00528$$

$$\frac{H}{g\ T^2} = 0.00351$$

(2) Using Equation (7-13), W is:

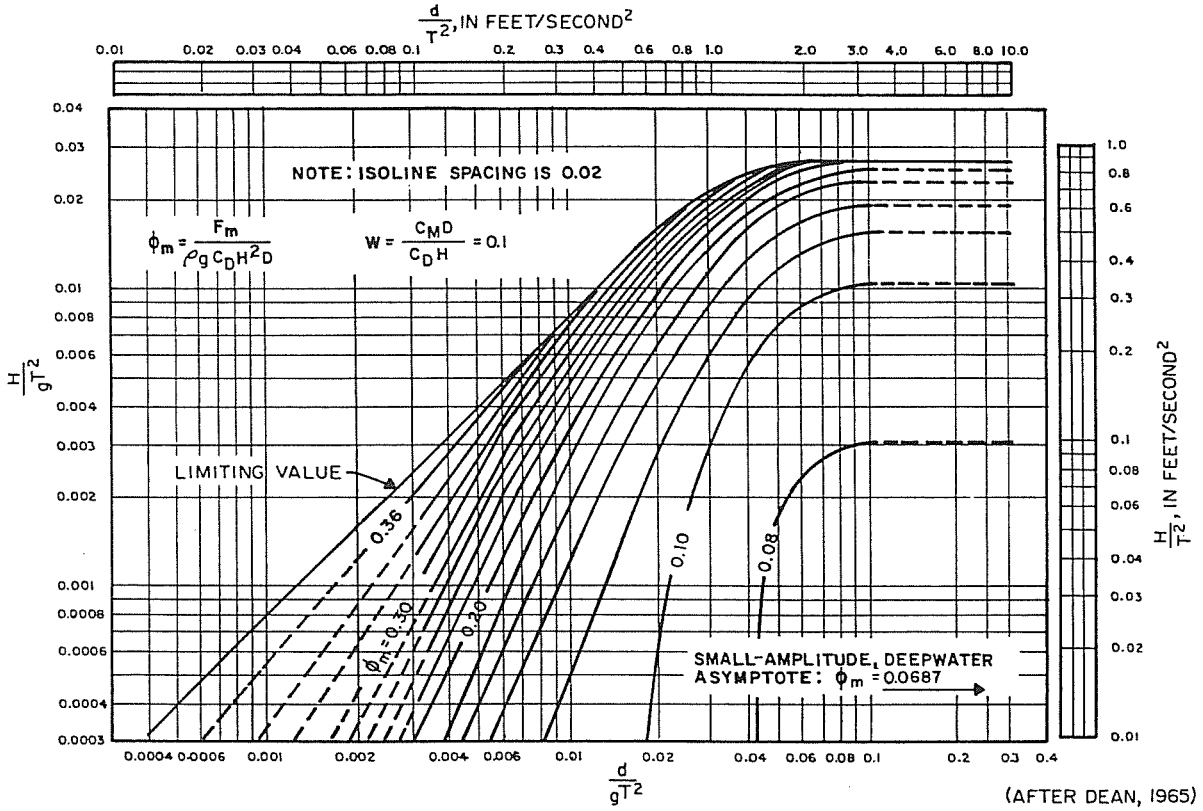

FIGURE 136
Isolines of ϕ_m as a Function of $d/g\,T^2$ and $H/g\,T^2$ for W = 0.1

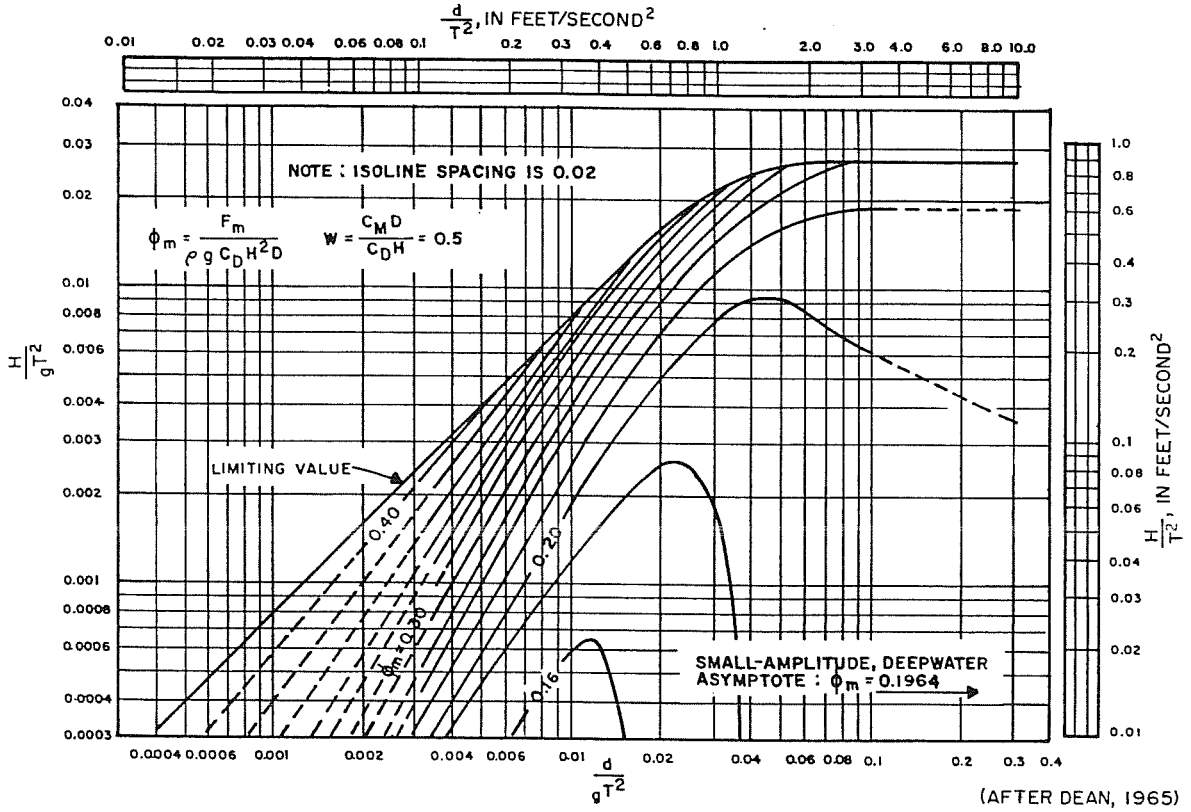

(AFTER DEAN, 1965)

FIGURE 137
Isolines of ϕ_m as a Function of d/g T^2 and H/g T^2 for W = 0.5

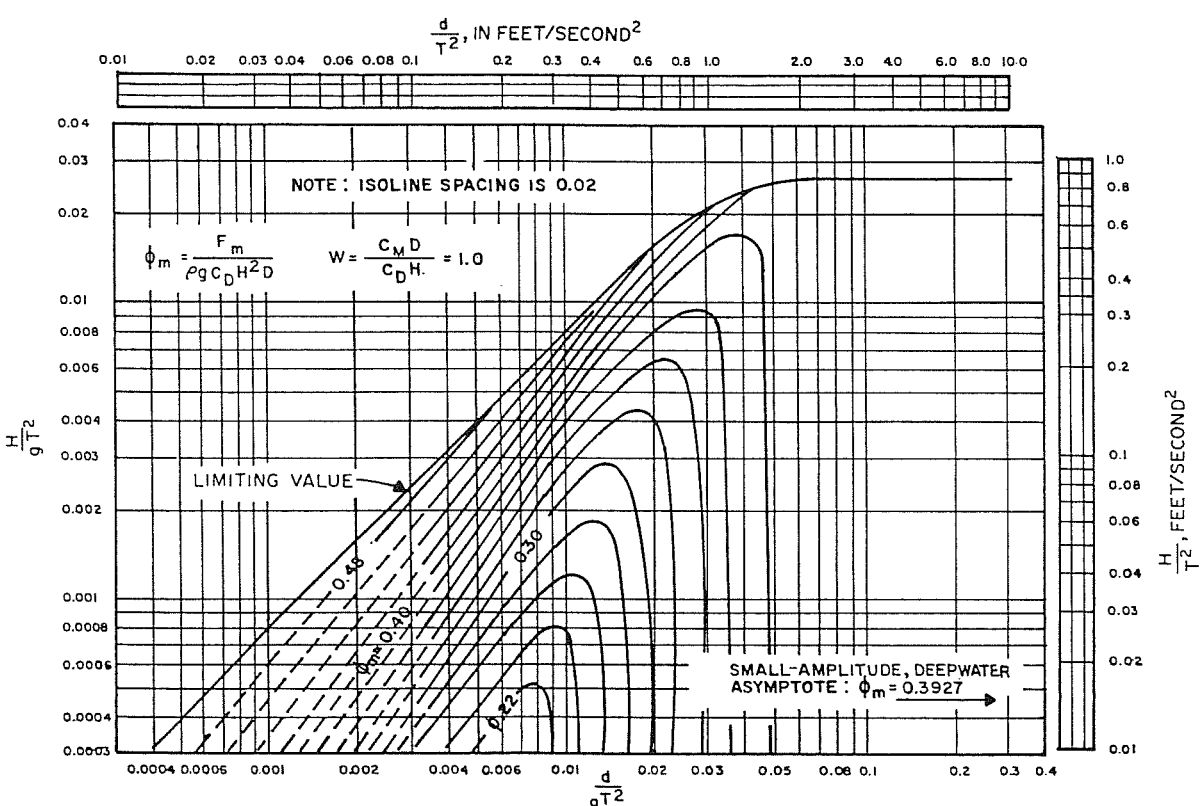

(AFTER DEAN, 1965)

FIGURE 138
Isolines of ϕ_m as a Function of d/g T^2 and H/g T^2 for W = 1.0

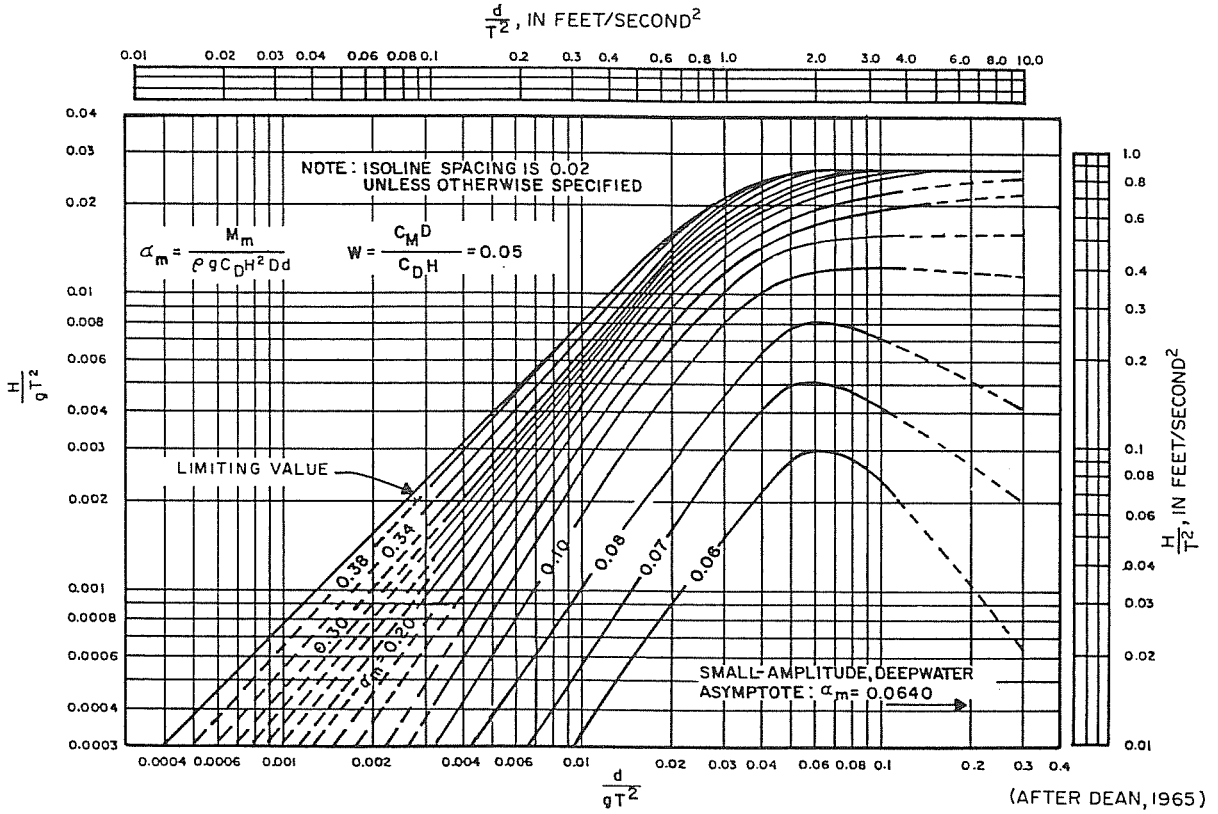

FIGURE 139
Isolines of α_m as a Function of d/g T^2 and H/g T^2 for W = 0.05

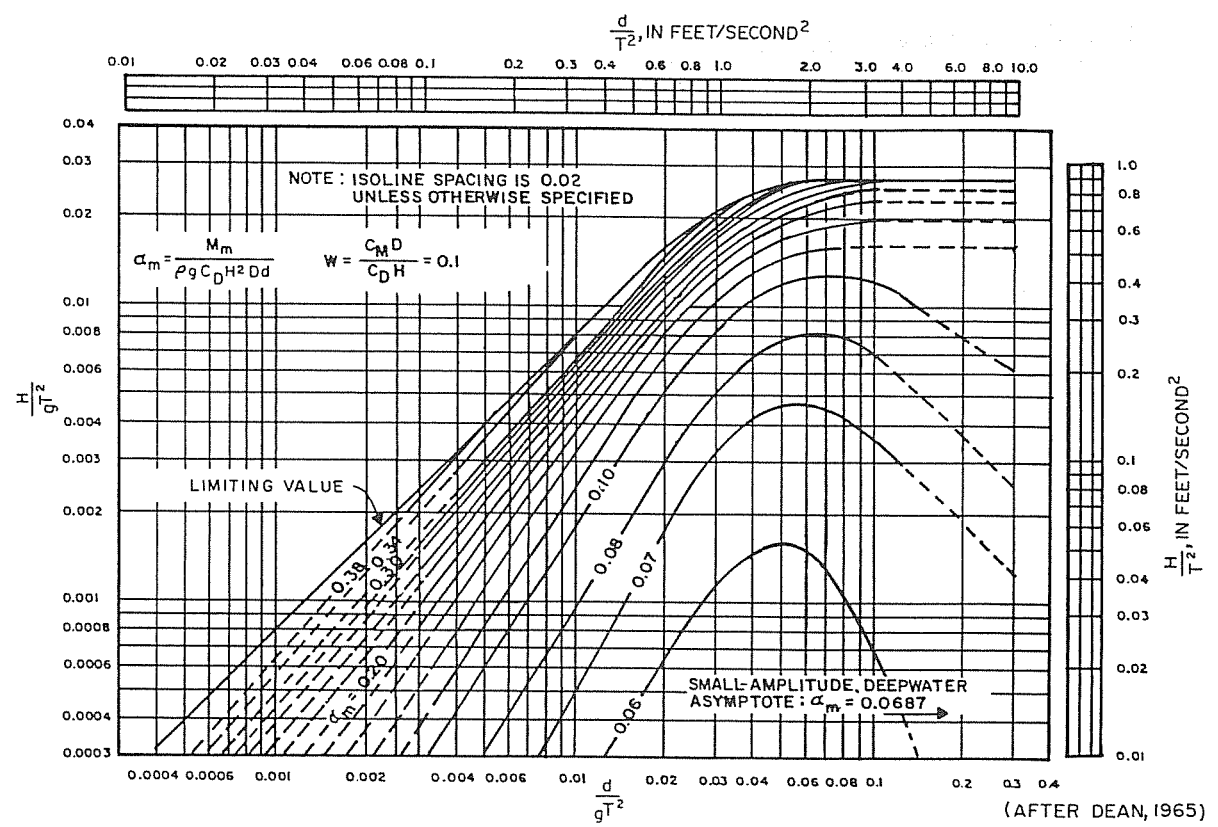

FIGURE 140
Isolines of α_m as a Function of d/g T^2 and H/g T^2 for W = 0.5

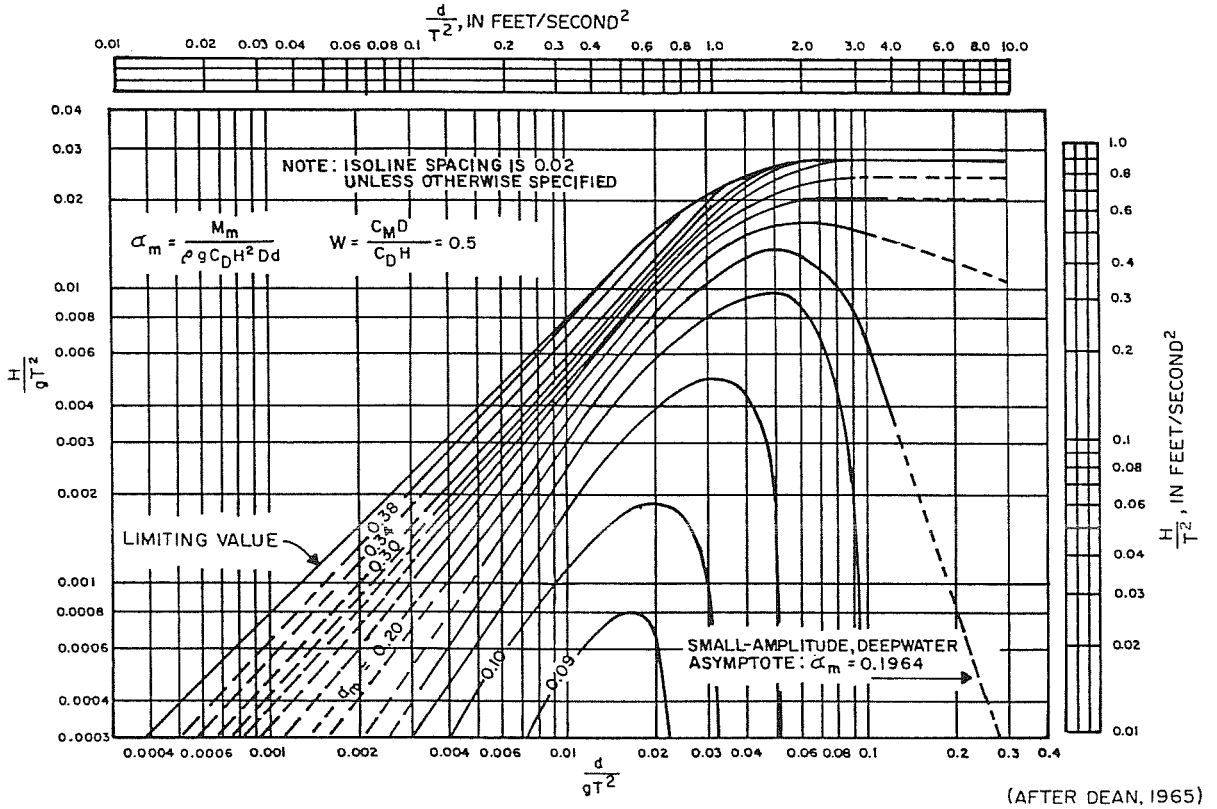

(AFTER DEAN, 1965)

FIGURE 141
Isolines of α_m as a Function of d/g T^2 and H/g T^2 for W = 0.5

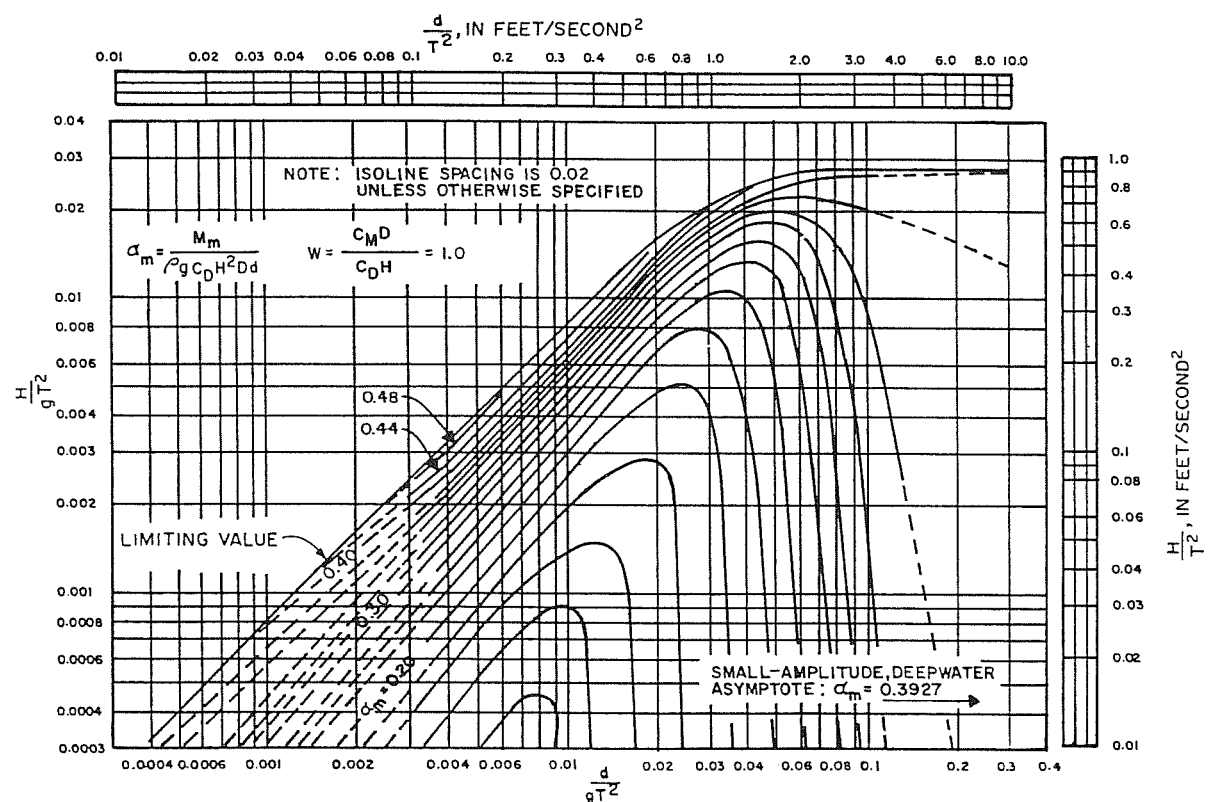

(AFTER DEAN, 1965)

FIGURE 142
Isolines of α_m as a Function of d/g T^2 and H/g T^2 for W = 1.0

$$W = \frac{C_M}{C_D}\frac{D}{H}$$

$$W = \frac{(2.0)(1)}{(0.7)(11.3)} = 0.253;\ \text{use } W = 0.25$$

(3) ϕ_m and α_m are found by interpolation of Figures 136 and 137, and 140 and 141, respectively, for $d/g\,T^2 = 0.00528$, $H/g\,T^2 = 0.00351$, and $W = 0.25$:

$$\phi_m = 0.35$$

$$\alpha_m = 0.34$$

(4) Using Equation (7-12), find F_{mDI}:

$$F_{mDI} = \rho\, g\, C_D\, H^2\, D\, \phi_m$$

(Assuming salt water, $\rho = 2$ slugs per cubic foot.)

$$F_{mDI} = (2)(32.2)(0.7)(11.3)^2(1)(0.35)$$

$$F_{mDI} = 2{,}015 \text{ pounds}$$

(5) Using Equation (7-14), find M_{mDI}:

$$M_{mDI} = \rho\, g\, C_D\, H^2\, D\, d\, \alpha_m$$

$$M_{mDI} = (2)(32.2)(0.7)(11.3)^2(1)(17)(0.34)$$

$$M_{mDI} = 33{,}271 \text{ foot-pounds}$$

Note: The values obtained for force and moment are less than, but compare reasonably well to (within the accuracy of the figures), those obtained in Example Problem 38. This indicates that the values in Case 1 provide conservative results and that effects of inertial forces are secondary.

(6) Using Equation (7-11), find z_{mDI}, the lever arm above the bottom:

$$z_{mDI} = \frac{M_{mDI}}{F_{mDI}} = \frac{33{,}271}{2{,}015} = 16.5 \text{ feet}$$

7. CASE 3--MAXIMUM FORCE ON SINGLE PILE OF SMALL, NONUNIFORM DIAMETER (PRELIMINARY DESIGN). Piles of nonuniform diameter can be designed in special cases, or the nonuniformity may also occur naturally, as on a uniform-diameter pile when marine fouling increases the diameter of the pile in the intertidal zone. Marine fouling is primarily a function of biological activity. Nutrients, water temperature, salinity, turbidity, exposure to sunlight, wave activity, tides, and currents are factors which determine the fouling. Measurement of nearby existing pile structures should be made to determine the fouling characteristics, or, as a first approximation, the pile diameter should be increased by 1 foot within the range of low water to mean high tide. Nonuniformity of diameter also occurs when wooden piles are protected with a jacket about the waterline to prevent deterioration by marine borers. The method presented for Case 3 enables the designer to determine the effect of marine fouling or of a jacket on wave-induced forces.

Figure 143 is a definition sketch of a pile of three diameters. Element 2 represents marine fouling or a jacket in the intertidal zone. The method presented for Case 3 will give maximum forces and moments according to drag force only. In this case, the maximum force occurs under the crest. If inertial forces are important, then Case 4 and Case 5 must be used.

a. Range of Application. The range of application for Case 3 is the same as that for Case 1.

b. Force Calculations. The unit drag forces, f_D, are integrated from the bottom, $z = 0$, to the crest, $z = S_c$. The results of the integration are shown graphically in Figures 144, 145, and 146. The method used herein calculates the forces on each pile element.

c. Maximum Force. The maximum drag force, F_{mD}, under the crest is given by:

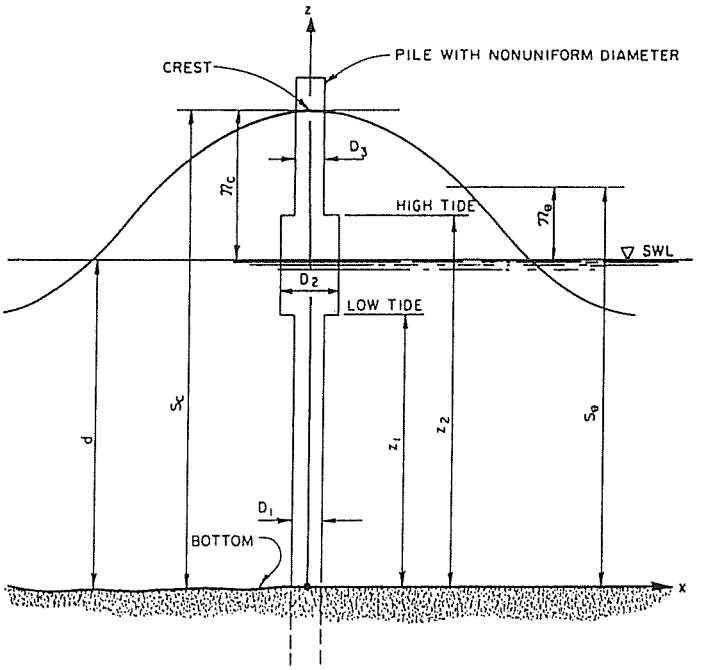

FIGURE 143
Definition of Terms for a Pile With Three Diameters

$$F_{mD} = \left(\frac{1}{2}\right) \rho\, C_D \left(\frac{H}{T}\right)^2 d\, \phi_{DM} \left[(K_{DM})_{z=z_1}(D_1 - D_2) + (K_{DM})_{z=z_2}(D_2 - D_3) + (K_{DM})_{z=S_c}(D_3)\right] \quad (7\text{-}15)$$

WHERE:

ρ = density of water
C_D = drag coefficient (obtained from Table 17)
H = local wave height
T = wave period
d = water depth
ϕ_{DM} = a nonlinear correction factor (determined from Figure 146)
$(K_{DM})_{z=z_i}$ is found in Figure 144 as a function of z/d and d/L_o
z_i = distance above bottom of point i
S_c = distance of free surface measured from the bottom to the wave crest when the crest is at the pile
D_i = respective pile diameter

d. Maximum Moment. The maximum drag moment, M_{mD}, can be determined by:

$$M_{mD} = \left(\frac{1}{2}\right) \rho\, C_D \left(\frac{H}{T}\right)^2 d^2\, \psi_{DM} \left[(\tau_{DM})_{z=z_1}(D_1 - D_2) + (\tau_{DM})_{z=z_2}(D_2 - D_3) + (\tau_{DM})_{z=S_c}(D_3)\right] \quad (7\text{-}16)$$

WHERE:

ρ = density of water
C_D = drag coefficient (obtained from Table 17)
H = local wave height
T = wave period
d = water depth
ψ_{DM} = a nonlinear correction factor (determined from Figure 146)
$(\tau_{DM})_{z=z_i}$ is found in Figure 145 as a function of z/d and d/L_o
z_i = distance above bottom of point i
S_c = distance of free surface measured from the bottom to the wave crest when the crest is at the pile

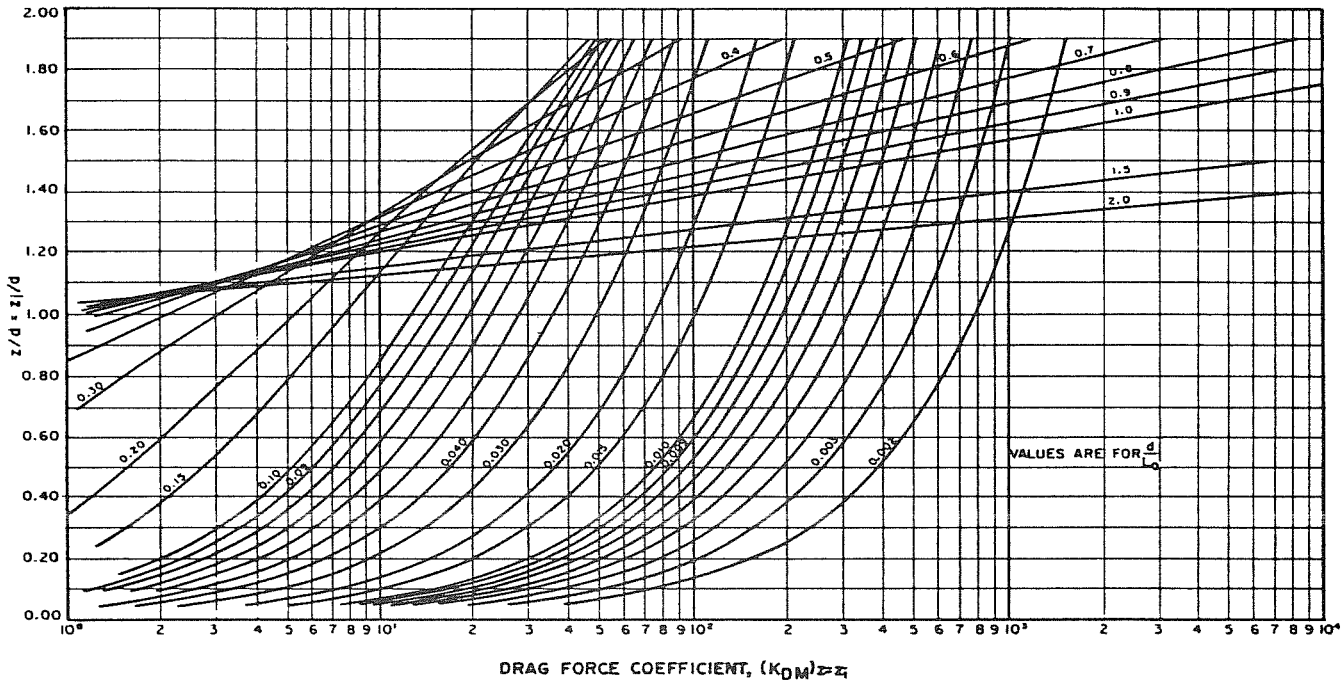

FIGURE 144
$(K_{DM})_{z=z_i}$ as a Function of z/d and d/L_o

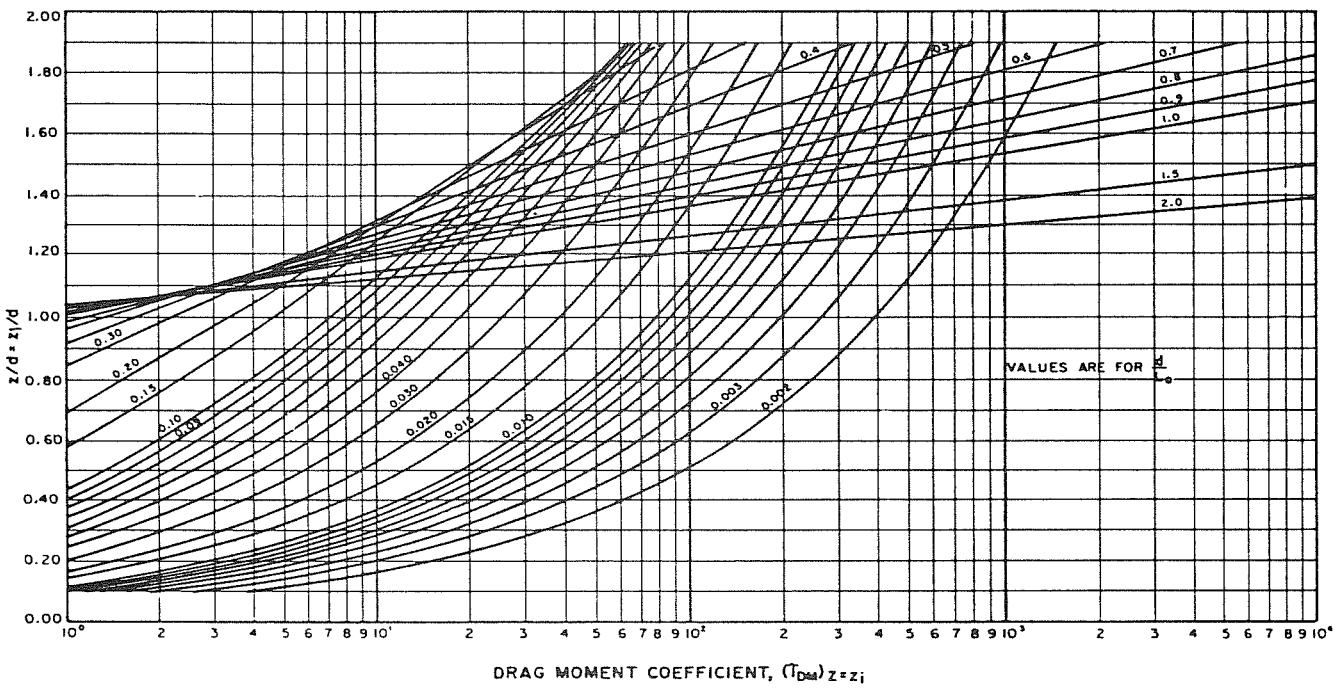

FIGURE 145
$(T_{DM})_{z=z_i}$ as a Function of z/d and D/L_o

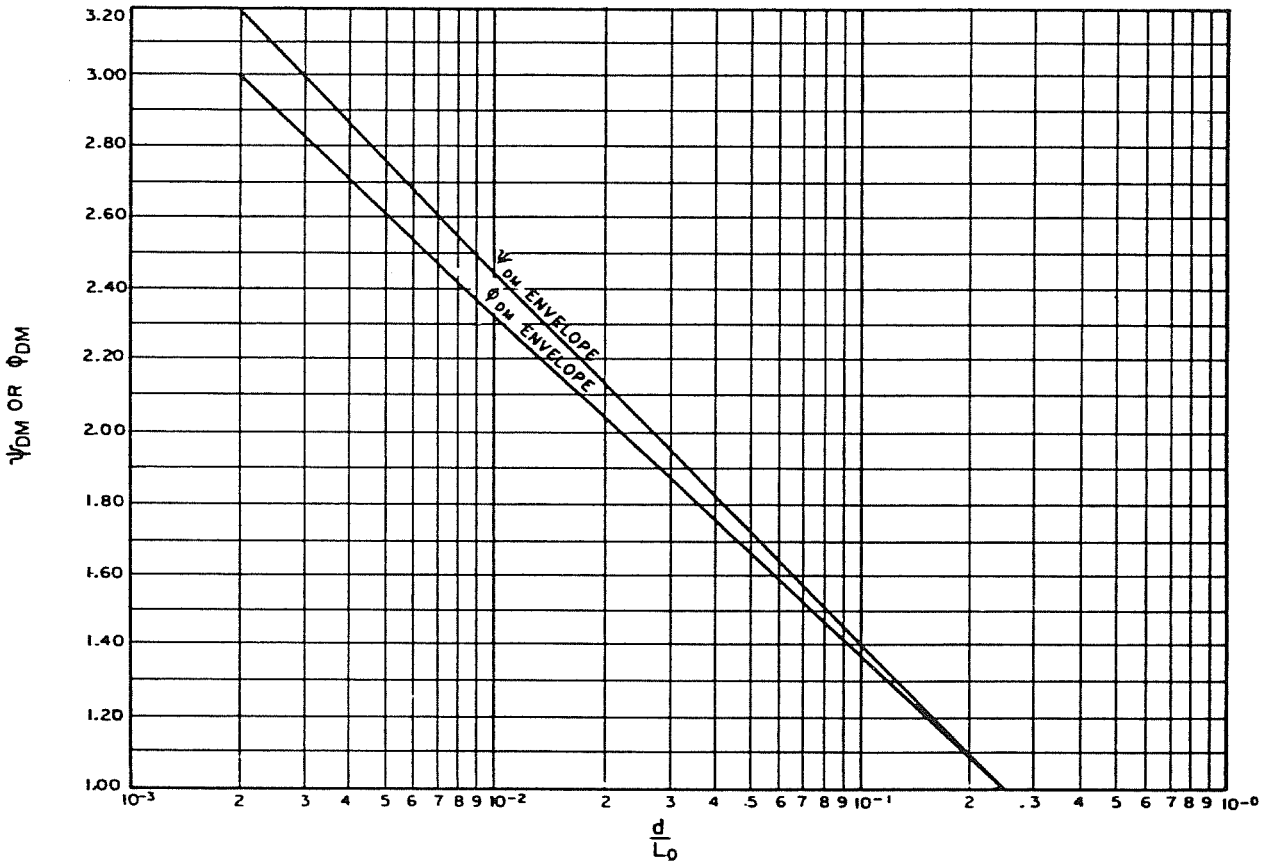

FIGURE 146
Envelopes of Nonlinear Correction Factors, ϕ_{DM} and ψ_{DM}, for Determining Maximum Drag Force and Moment, Respectively, as a Function of d/L_o

e. Reaction. The lever arm, z_{mD}, is given by Equation (7-11).

EXAMPLE PROBLEM 40

Given: a. Local wave height, H = 15 feet
b. Water depth, d = 20 feet
c. Wave period, T = 10 seconds
d. $C_D = 0.7$
e. Pile diameter is:

$D_1 = 1.5$ feet for $z_o = 0$ feet to $z_1 = 18$ feet
$D_2 = 2$ feet for $z_1 = 18$ feet to $z_2 = 24$ feet
$D_3 = 1.5$ feet for $z_2 = 24$ feet to $z_3 = S_c$

Find: The maximum drag force, maximum drag moment, and lever arm on the given pile of nonuniform diameter, and compare the results to those which would be obtained for a pile of uniform diameter, D = 1.5 feet.

Solution: (1) Calculate $d/g\,T^2$ and $H/g\,T^2$:

$$\frac{d}{g\,T^2} = \frac{20}{(32.2)(10)^2} = 0.00621$$

$$\frac{H}{g\,T^2} = \frac{15}{(32.2)(10)^2} = 0.00466$$

(2) Using Equation (7-8), find S_c:

(a) Find η_c:

From Figure 132 for $d/g\,T^2 = 0.00621$ and $\frac{H}{g\,T^2} = 0.00466$:

$$\frac{\eta_c}{H} = 0.84$$

$$\eta_c = 0.84\,H = (0.84)(15) = 12.6 \text{ feet}$$

(b) $S_c = \eta_c + d$

$S_c = 12.6 + 20 = 32.6$; use $S_c = 33$ feet

(3) Determine drag force and drag moment coefficients, $(K_{DM})_{z=z_i}$ and $(\tau_{DM})_{z=z_i}$, from Figures 144 and 145, respectively:

(a) Find d/L_o:

$$L_o = (g/2\pi)\,T^2 = (32.2/2\pi)(10)^2 = 512 \text{ feet}$$

$$d/L_o = \frac{20}{512} = 0.0391; \text{ use } d/L_o = 0.039$$

(b) The results obtained from Figures 144 and 145 for $d/L_o = 0.039$ and desired values of z_i/d are tabulated below:

z_i	z_i/d	$(K_{DM})_{z=z_i}$	$(\tau_{DM})_{z=z_i}$
$z_1 = 18$ ft	18/20 = 0.90	32	16
$z_2 = 24$ ft	24/20 = 1.20	47	30
$z_3 = S_c$	33/20 = 1.65	72	67

(4) Determine nonlinear correction factors, ϕ_{DM} and ψ_{DM}, from Figure 146 for $d/L_o = 0.039$:

$\phi_{DM} = 1.76$

$\psi_{DM} = 1.83$

(5) Using Equation (7-15), find the maximum drag force for the nonuniform-diameter pile:

$$F_{mD} = \left(\tfrac{1}{2}\right) \rho\, C_D \left(\tfrac{H}{T}\right)^2 d\, \phi_{DM} \left[(K_{DM})_{z=z_1}(D_1 - D_2) + (K_{DM})_{z=z_2}(D_2 - D_3) + (K_{DM})_{z=S_c}(D_3)\right]$$

$$F_{mD} = \left(\tfrac{1}{2}\right)(2)(0.7)\left(\tfrac{15}{10}\right)^2(20)(1.76)[(32)(1.5 - 2) + (47)(2 - 1.5) + (72)(1.5)]$$

F_{mD} = 6,403 pounds

(6) Using Equation (7-16), find the maximum drag moment for the nonuniform-diameter pile:

$$M_{mD} = (\tfrac{1}{2}) \rho C_D (\tfrac{H}{T})^2 d^2 \Psi_{DM} [(\tau_{DM})_{z=z_1} (D_1 - D_2) + (\tau_{DM})_{z=z_2} (D_2 - D_3) + (\tau_{DM})_{z=S_c} (D_3)]$$

$$M_{mD} = (\tfrac{1}{2})(2)(0.7)(\tfrac{15}{10})^2(20)^2(1.83)[(16)(1.5 - 2.0) + (30)(2.0 - 1.5) + (67)(1.5)]$$

M_{mD} = 123,937 foot-pounds

(7) Using Equation (7-11), find z_{mD}:

$$z_{mD} = \frac{M_{mD}}{F_{mD}}$$

$$z_{mD} = \frac{123,937}{6,403}$$

z_{mD} = 19.4 feet

(8) Compare the above results to those for a uniform pile of diameter, D = 1.5 feet:

(a) In order to use Figures 144 and 145, substitute S_c/d for z/d.

$z/d = S_c/d = 33/20 = 1.65$

Then $(K_{DM})_{z=S_c}$ = 72

and $(\tau_{DM})_{z=S_c}$ = 67

(b) In order to determine the maximum drag force, Equation (7-15) is used, with $z_i = S_c$:

$$F_{mD} = (\tfrac{1}{2}) \rho C_D (\tfrac{H}{T})^2 d \Phi_{DM} [(K_{DM})_{z=S_c} (D)]$$

$$F_{mD} = (\tfrac{1}{2})(2)(0.7)(\tfrac{15}{10})^2(20)(1.76)[(72)(1.5)]$$

F_{mD} = 5,988 pounds

(c) In order to determine the maximum drag moment, Equation (7-16) is used, with $z_i = S_c$:

$$M_{mD} = (\tfrac{1}{2}) \rho C_D (\tfrac{H}{T})^2 d^2 \Psi_{DM} [(\tau_{DM})_{z=S_c} (D)]$$

$$M_{mD} = (\tfrac{1}{2})(2)(0.7)(\tfrac{15}{10})^2(20)^2(1.83)[(67)(1.5)]$$

M_{mD} = 115,866

THEREFORE: The values of maximum drag force and maximum drag moment are approximately 7 percent higher for the nonuniform-diameter pile than for the uniform-diameter pile.

(9) Using Equation (7-11), find z_{mD}:

$$z_{mD} = \frac{M_{mD}}{F_{mD}} = \frac{115,866}{5,988} = 19.3 \text{ feet}$$

8. CASE 4--WAVE FORCE, AT AN ARBITRARY WAVE-PHASE ANGLE, ON SINGLE PILE OF INTERMEDIATE, NONUNIFORM DIAMETER (PRELIMINARY DESIGN). Calculation of the wave force at an arbitrary wave-phase angle is required to estimate the maximum forces on both uniform- and nonuniform-diameter piles and to estimate forces on a combination of piles.

a. Range of Application. This case includes both drag and inertial forces and therefore makes no assumption regarding D/H or d/L_o. However, it does not apply to closely spaced piles ($\Delta \leq 2$ D), nor for D greater than 20 percent at the wavelength. This case deals with linear theory to illustrate the method. Case 5 incorporates nonlinear corrections for final design.

b. Linear Forces.

(1) Drag Force. The linear drag force, F_D, on a uniform-diameter pile as a function of phase angle is given by:

$$F_D = (\tfrac{1}{2}) \rho C_D D (\tfrac{H}{T})^2 d (K_D)_z \qquad (7\text{-}17)$$

WHERE:

ρ = density of water
C_D = drag coefficient (obtained from Table 17)
D = pile diameter
H = local wave height
T = wave period
d = water depth
$(K_D)_z = (K_{DM})_z \cos\theta \,|\cos\theta|$
θ = wave-phase angle

$(K_{DM})_z$ is found in Figure 144 as a function of z/d and d/L_o.

The linear drag force, F_D, on a nonuniform-diameter pile as a function of phase angle is given by:

$$F_D = (\tfrac{1}{2}) \rho C_D (\tfrac{H}{T})^2 d [(K_{DM})_{z=z_1} (D_1 - D_2) + (K_{DM})_{z=z_2} (D_2 - D_3) + (K_{DM})_{z=S_\theta} (D_3)] \cos\theta |\cos\theta| \qquad (7\text{-}18)$$

WHERE:

D_i = respective pile diameter
S_θ = distance of free surface measured from the bottom at an arbitrary wave-phase angle, θ

(2) Inertial Force. The linear inertial force, F_I, on a uniform-diameter pile as a function of phase angle is given by:

$$F_I = \rho C_M \pi \left(\frac{D^2}{4}\right)\left(\frac{H}{T^2}\right) d (K_I)_z \qquad (7\text{-}19)$$

WHERE:

C_M = inertial, or added-mass, coefficient (obtained from Table 18)
$(K_I)_z = (K_{IM})_z \sin\theta$

$(K_{IM})_z$ is found in Figure 147 as a function of z/d and d/L_o.

The linear inertial force, F_I, on a nonuniform-diameter pile as a function of phase angle is given by:

$$F_I = \rho C_M (\tfrac{\pi}{4}) \left(\frac{H}{T^2}\right) d [(K_{IM})_{z=z_1} (D_1^2 - D_2^2) + (K_{IM})_{z=z_2} (D_2^2 - D_3^2) + (K_{IM})_{z=S_\theta} (D_3^2)] \sin\theta \qquad (7\text{-}20)$$

c. Linear Moments.

(1) Drag Moment. The linear drag moment, M_D, for a uniform-diameter pile as a function of phase angle is given by:

$$M_D = (\tfrac{1}{2}) \rho C_D D (\tfrac{H}{T})^2 d^2 (\tau_D)_z \qquad (7\text{-}21)$$

WHERE:

ρ = density of water
C_D = drag coefficient (obtained from Table 17)
D = pile diameter
H = local wave height
T = wave period
d = water depth
$(\tau_D)_z = (\tau_{DM})_z \cos\theta \,|\cos\theta|$

$(\tau_{DM})_z$ is found in Figure 145 as a function of a/d and d/L_o.

The linear drag moment, M_D, on a nonuniform-diameter pile as a function of phase angle is given by:

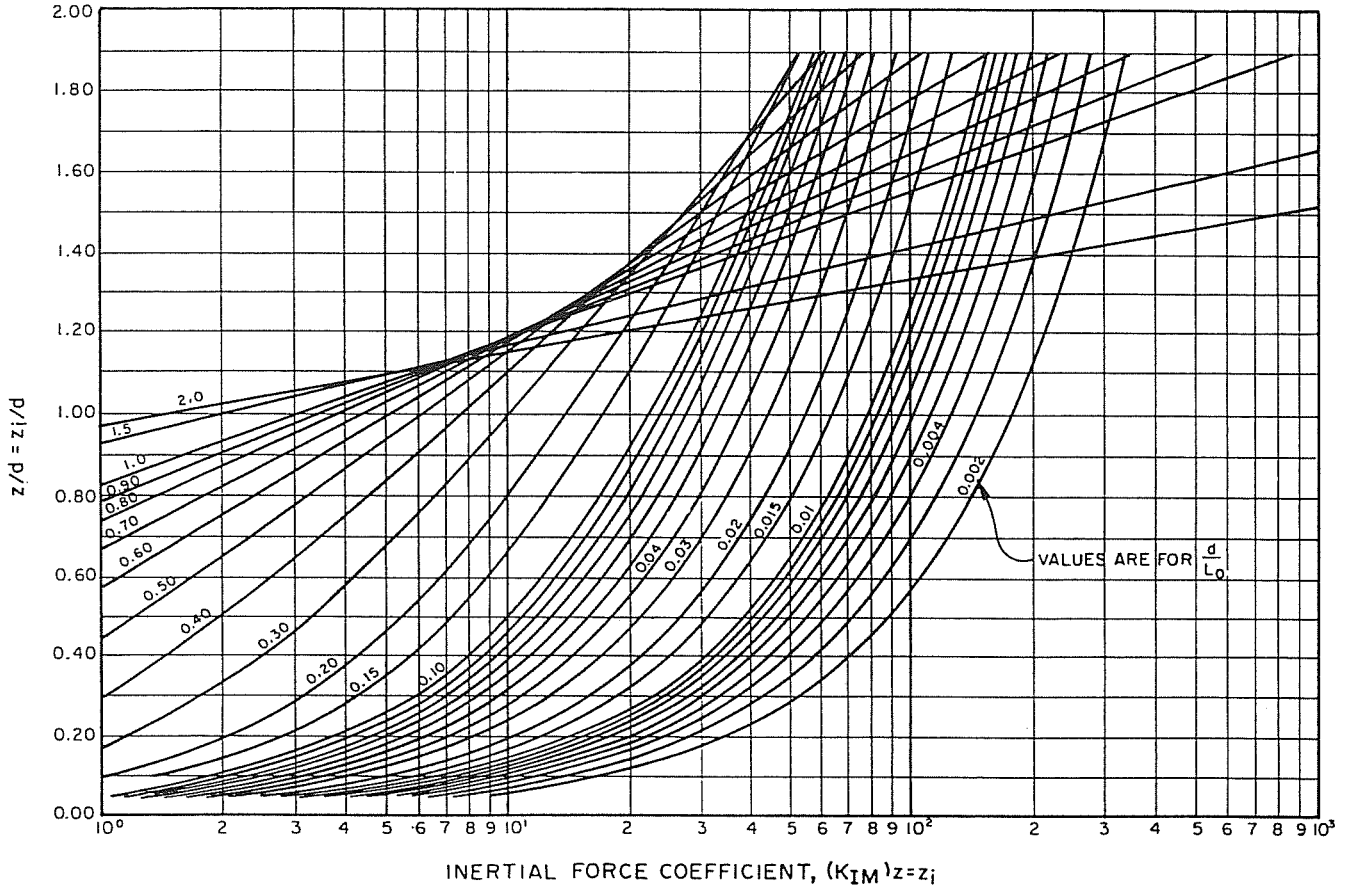

FIGURE 147
$(K_{IM})_z$ as a Function of z/d and d/L_o

$$M_D = \left(\frac{1}{2}\right) \rho C_D \left(\frac{H}{T}\right)^2 d^2 \left[\left(\tau_{DM}\right)_{z=z_1} (D_1 - D_2) + \left(\tau_{DM}\right)_{z=z_2} (D_2 - D_3) + \left(\tau_{DM}\right)_{z=S_\theta} (D_3) \right] \cos\theta |\cos\theta| \qquad (7\text{-}22)$$

WHERE:
D_i = respective pile diameter
S_θ = distance of free surface measured from the bottom at an arbitrary wave-phase angle, θ
θ = wave-phase angle

(2) Inertial Moment. The linear inertial moment, M_I, for a uniform-diameter pile as a function of phase angle is given by:

$$M_I = \rho C_M \left(\frac{\pi}{4}\right) D^2 \left(\frac{H}{T^2}\right) d^2 \left(\tau_I\right)_z \qquad (7\text{-}23)$$

WHERE:
C_M = inertial, or added-mass, coefficient (obtained from Table 18)
$(\tau_I)_z$ = $(\tau_{IM})_z \sin\theta$

$(\tau_{IM})_z$ is found in Figure 148 as a function of z/d and d/L_o.

The linear inertial moment, M_I, on a nonuniform-diameter pile as a function of phase angle is given by:

$$M_I = \rho C_M \left(\frac{\pi}{4}\right) \left(\frac{H}{T^2}\right) d^2 \left[\left(\tau_{IM}\right)_{z=z_1} (D_1^2 - D_2^2) + \left(\tau_{IM}\right)_{z=z_2} (D_2^2 - D_3^2) + \left(\tau_{IM}\right)_{z=S_\theta} (D_3^2) \right] \sin\theta \qquad (7\text{-}24)$$

d. Phases. Figure 149 plots an example of the phase relationships among the drag, inertial and total forces. The drag components are functions of $\cos\theta|\cos\theta|$; therefore, they are positive between $-90° < \theta < 90°$ and are negative otherwise. Drag components are positive when the free surface is above the still water level and they are symmetrical about the wave crest. The drag components are maximum under the wave crest. The inertial components are a function of $\sin\theta$; therefore, they are positive in front of the wave crest for θ values between 0 and 180°, and negative behind the wave crest. The total forces and total moments are obtained by adding drag and inertial components in front of the wave crest for θ values between 0° and 90°. Behind the wave crest, the inertial components are subtracted from the drag components.

(1) Total Force. The value of θ for which the total force is maximum is, according the linear theory:

$$\theta = \theta_{Fm} = \sin^{-1}\left\{ \left(\frac{\pi}{4}\right) \left(\frac{D}{H}\right) \left(\frac{C_M}{C_D}\right) \left[\left(K_{IM}\right)_{z=S_c} / \left(K_{DM}\right)_{z=S_c} \right] \right\} \qquad (7\text{-}25)$$

WHERE:
θ = wave-phase angle
θ_{Fm} = wave-phase angle for which total force is maximum
D = pile diameter
H = local wave height
C_M = inertial, or added-mass, coefficient (obtained from Table 18)
C_D = drag coefficient (obtained from Table 17)
$(K_{IM})_{z=S_c}$ is found in Figure 147 as a function of z/d and d/L_o.

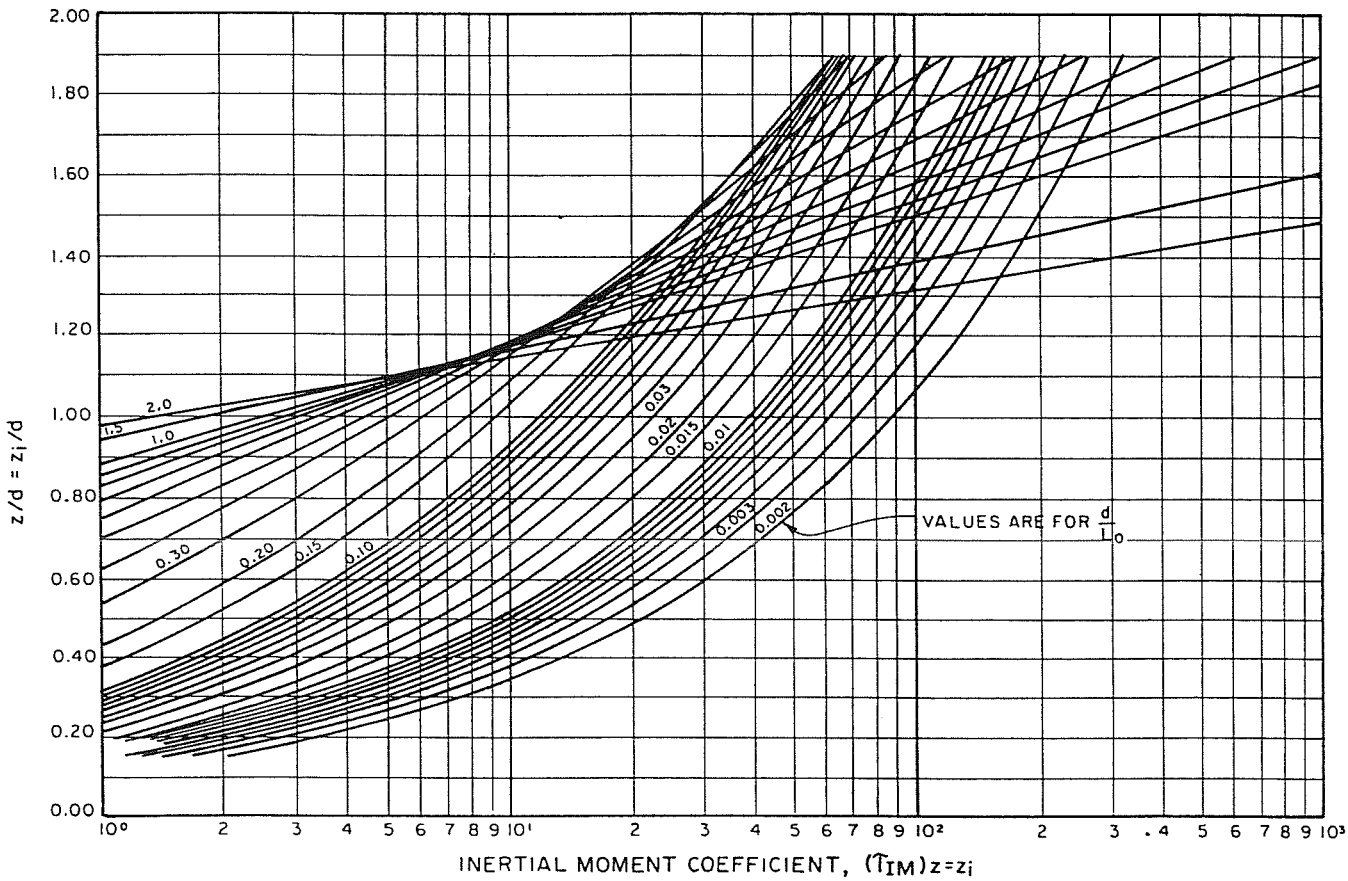

FIGURE 148
$(\tau_{IM})_z$ as a Function of z/d and D/L_o

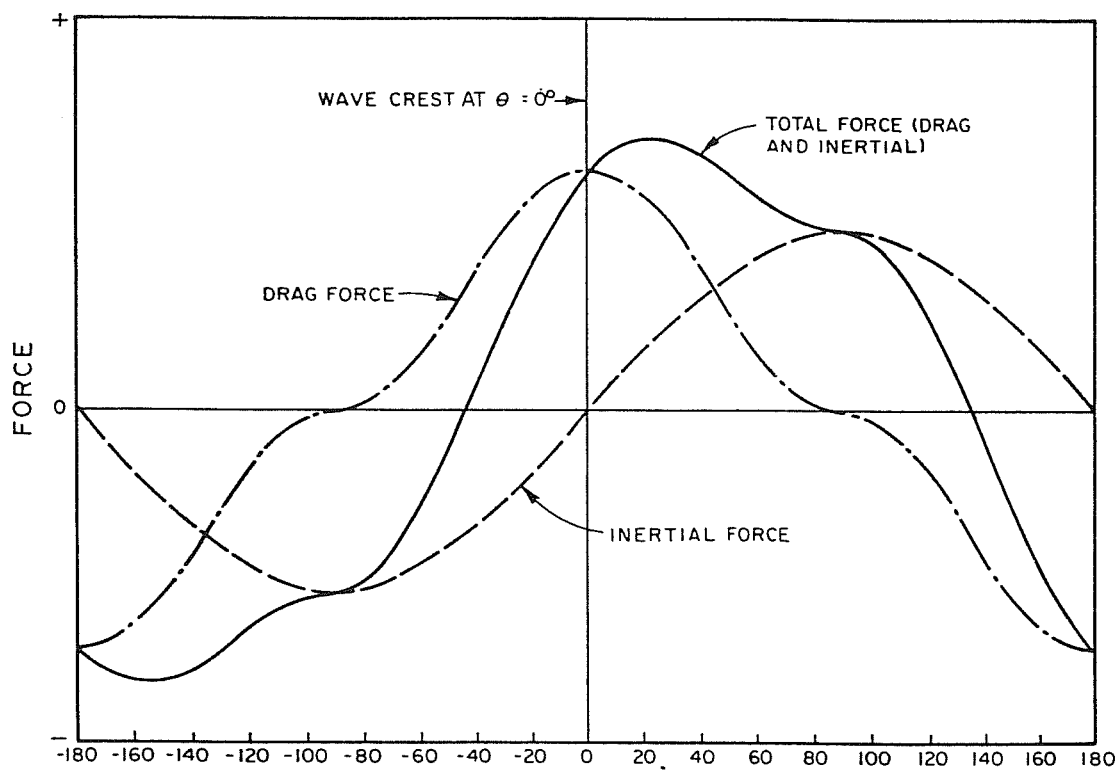

(AFTER SHORE PROTECTION MANUAL, 1977)

FIGURE 149
Phase Relationships Among Drag, Inertial, and Total Forces

$(K_{DM})_{z=S_c}$ is found in Figure 144 as a function of z/d and d/L_o.

S_c = distance of free surface measured from the bottom to the wave crest when the crest is at the pile

(2) Total Moment. The total moment is maximum when:

$$\theta = \theta_{Mm} = \sin^{-1}\left\{\left(\frac{\pi}{4}\right)\left(\frac{D}{H}\right)\left(\frac{C_M}{C_D}\right)\left[\left(\tau_{IM}\right)_{z=S_c}/\left(\tau_{DM}\right)_{z=S_c}\right]\right\} \quad (7\text{-}26)$$

WHERE:

θ_{Mm} = wave-phase angle for which total moment is maximum

$(\tau_{IM})_{z=S_c}$ is found in Figure 148 as a function of z/d and $/L_o$.

$(\tau_{DM})_{z=S_c}$ is found in Figure 145 as a function of z/d and d/L_o.

The values of θ for maximum force and moment are close to one another, but are not identical. However, both occur before the wave crests.

e. Reaction. The lever arm, z_{mDI}, is given by Equation (7-11), substituting z_{mDI} for z_{mD}, M_{mDI} for M_{mD}, and F_{mDI} for F_{mD} for $\theta = \theta_{Fm}$.

f. Example of Application. An example of the application of Case 4 is provided at the end of Subsection 7.9, CASE 5--NONLINEAR CORRECTIONS, with the nonlinear corrections shown.

9. CASE 5--NONLINEAR CORRECTIONS FOR MAXIMUM WAVE FORCES ON SINGLE PILES OF NONUNIFORM DIAMETER (FINAL DESIGN).

a. Definitions. The application of the linear theory gives a good order of magnitude of forces and moments acting on a pile or a combination of piles. However, for more accuracy and safety, nonlinear corrections may be important. These corrections apply to:

(1) the definition of the free surface;

(2) the definition of the velocity and acceleration field; and

(3) the variation of the submerged mass of the pile.

Item (3), which is of secondary importance, occurs near the breaking zone. The correction is necessary because of rapid change in the submerged mass of the pile,due to the rapid change in free surface. This correction is usually small and, for this reason, a procedure for correcting for the variation in submerged mass is not included in this manual. The case of breaking waves is treated in Subsection 7.12, CASE 8--FORCES DUE TO BREAKING WAVES.

b. Corrections Due to Nonlinear Free Surface. The first nonlinear correction is due to the fact that the free surface is not defined by a sinusoid, as it is in linear theory, but is rather defined by a complex function of the phase angle, θ, and the relative wave height, H/H_b. H_b is the limiting height of a wave over the bottom. The limiting wave height is $H_b = 0.78\ d$ for a flat bottom; H_b can be determined from Figure 42 for a sloped bottom. The relative free surface, S_θ/d, is given as a function of H/H_b, d/L_o, and θ in Figure 150.

EXAMPLE PROBLEM 41

Given: a. Equivalent unrefracted deepwater wave height, H'_o = 10 feet
b. Water depth, d = 17 feet
c. Wave period, T = 10 seconds
d. Bottom slope m = 0.02

Find: Nonlinear free surface at phase angle, $\theta = 20^\circ$.

Solution: (1) From Example Problem 36:

$d/L_o = 0.0332$

H = 11.3 feet, H_b = 12 feet, and $H/H_b = 0.94$

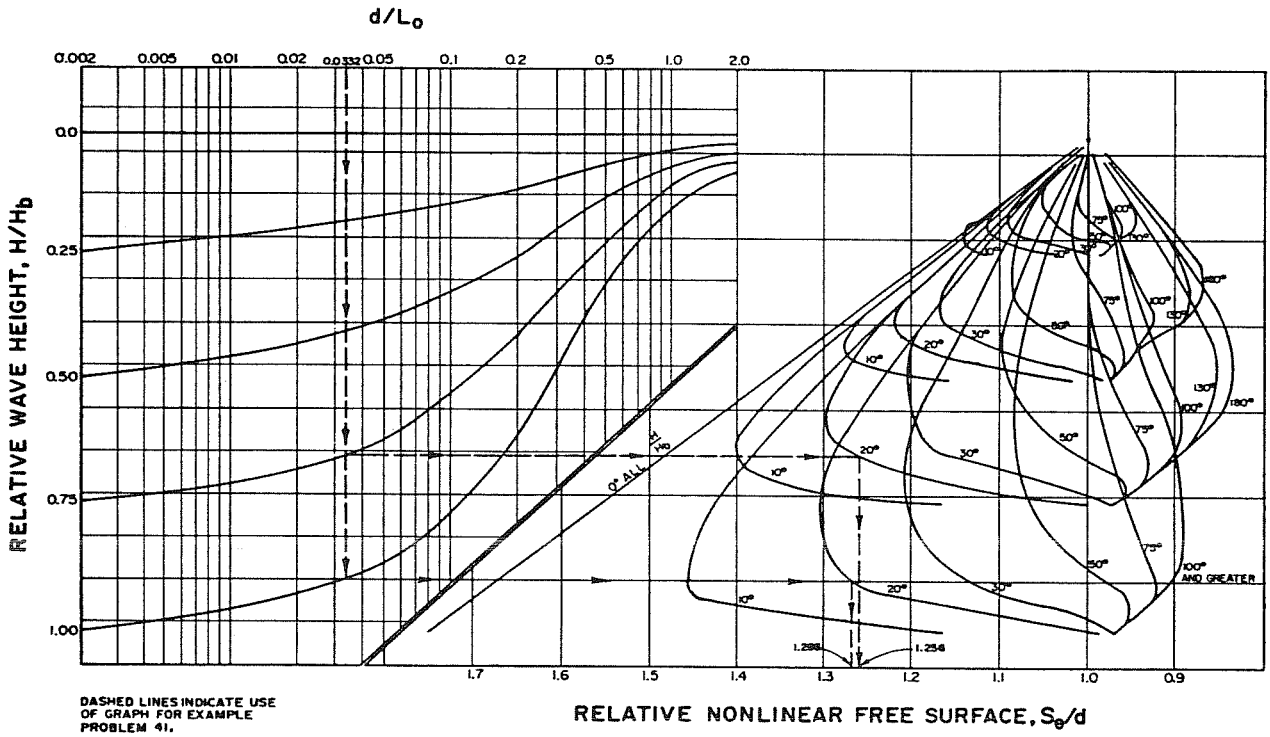

FIGURE 150
Relative Nonlinear Free Surface, S_θ/d, as a Function of H/H_b, d/L_o, and θ

(2) Using Figure 150, enter the d/L_o abscissa with $d/L_o = 0.0332$; at the point of intersection with the H/H_b curves encompassing the given value of $H/H_b = 0.94$ (in this case, $H/H_b = 1.00$ and $H/H_b = 0.75$), lines are drawn horizontally to the right until intersection with the corresponding θ curves. (Note that each H/H_b curve has its own set of θ curves.) Finally, vertical lines are drawn from the intersection points on the θ curves to give two values for S_θ/d from which the correct value of S_θ/d is found by interpolation:

(a) When $\theta = 20^\circ$ and $H/H_b = 1.00$:

$S_\theta/d = 1.266$

(b) When $\theta = 20^\circ$ and $H/H_b = 0.75$:

$S_\theta/d = 1.256$

(c) By interpolation:

When $\theta = 20^\circ$ and $H/H_b = 0.94$:

$S_\theta/d = 1.264$; use $S_\theta/d = 1.26$

(3) Find S_θ:

$S_\theta/d = 1.26$

$S_\theta = 1.26\ d$

$S_\theta = (1.26)(17) = 21.4$ feet

THEREFORE: The free-surface elevation is 21.4 feet above the bottom, or $S_\theta - \eta_\theta = 21.4 - 17 = 4.4$ feet above the still water level.

c. Correction of Forces and Moments Due to Nonlinear Velocity and Acceleration Fields. Nonlinear correction factors are applied to the forces and moments determined by linear theory in Subsection 7.8 (Case 4) using the nonlinear distance of the free surface above the bottom determined in Subsection 7.9.b., Corrections Due to Nonlinear Free Surface, above. Conservative estimates of the nonlinear correction are made by choosing its value at the free surface and neglecting any correction less than unit. Then the nonlinear forces and moments as a function of phase angle are determined as follows:

$$F_{DS_\theta} = F_D\ \phi_D \quad (7\text{-}27)$$

$$F_{IS_\theta} = F_I\ \phi_I \quad (7\text{-}28)$$

$$M_{DS_\theta} = M_D\ \psi_D \quad (7\text{-}29)$$

$$M_{IS_\theta} = M_I\ \psi_I \quad (7\text{-}30)$$

WHERE:
S_θ subscript refers to values at an arbitrary phase angle, θ.
F_{DS_θ} = drag force corrected for nonlinear effects
ϕ_D = drag-force correction factor for nonlinear velocity and acceleration fields (found in Figures 151-154 as a function of d/L_o, H/H_b, and θ)
F_{IS_θ} = inertial force corrected for nonlinear effects
ϕ_I = inertial-force correction factor for nonlinear velocity and acceleration fields (found in Figures 155-158 as a function of d/L_o, H/H_b, and θ)
M_{DS_θ} = drag moment corrected for nonlinear effects
ψ_D = drag-moment correction factor for nonlinear velocity and acceleration fields (found in Figures 159-162) as a function of d/L_o, H/H_b, and θ)
M_{IS_θ} = inertial moment corrected for nonlinear effects
ψ_I = inertial-moment correction factor for nonlinear velocity and acceleration fields (found in Figures 163-166) as a function of d/L_o, H/H_b, and θ)

d. Total Force and Moment. The total force on the pile at a given phase angle is given by:

$$F_{TS_\theta} = F_{DS_\theta} + F_{IS_\theta} \quad (7\text{-}31)$$

The total moment on the pile at a given phase angle is given by:

$$M_{TS_\theta} = M_{DS_\theta} + M_{IS_\theta} \quad (7\text{-}32)$$

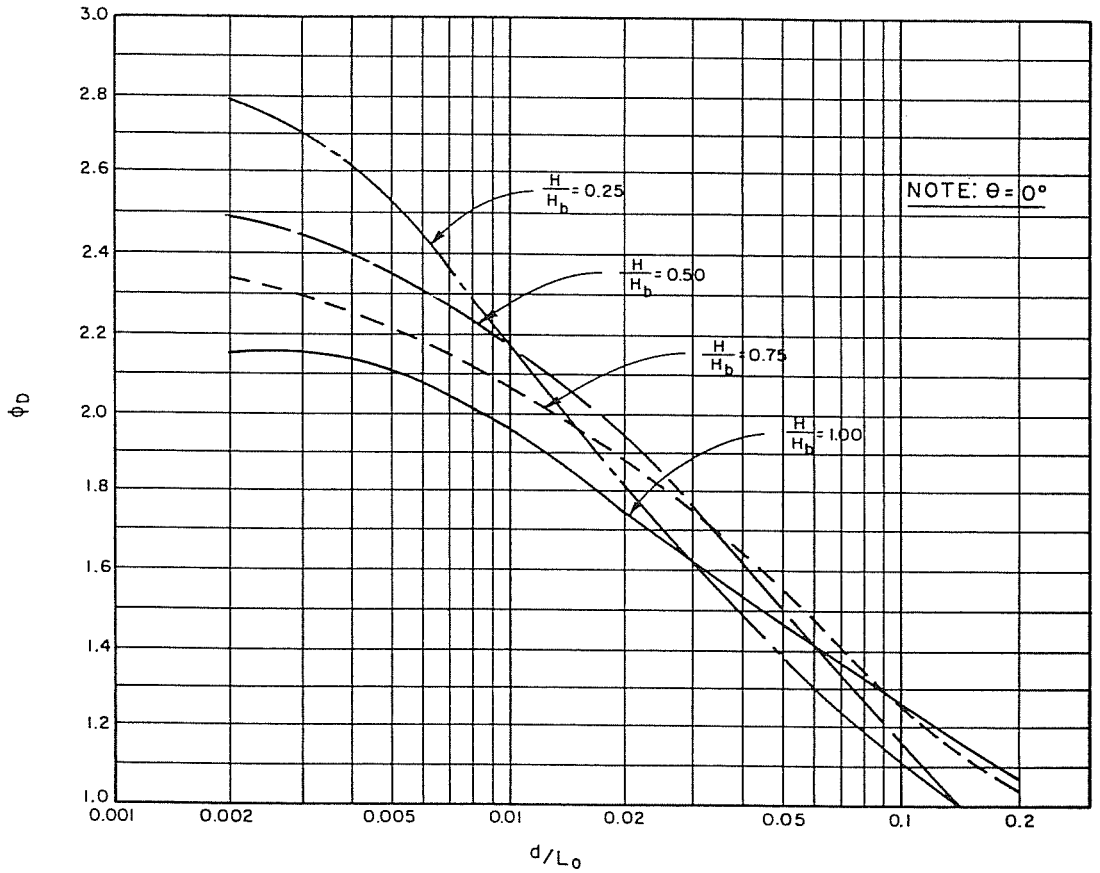

FIGURE 151
Nonlinear Drag-Force Correction Factor, ϕ_D, as a Function of d/L_o and H/H_b for $\theta = 0°$

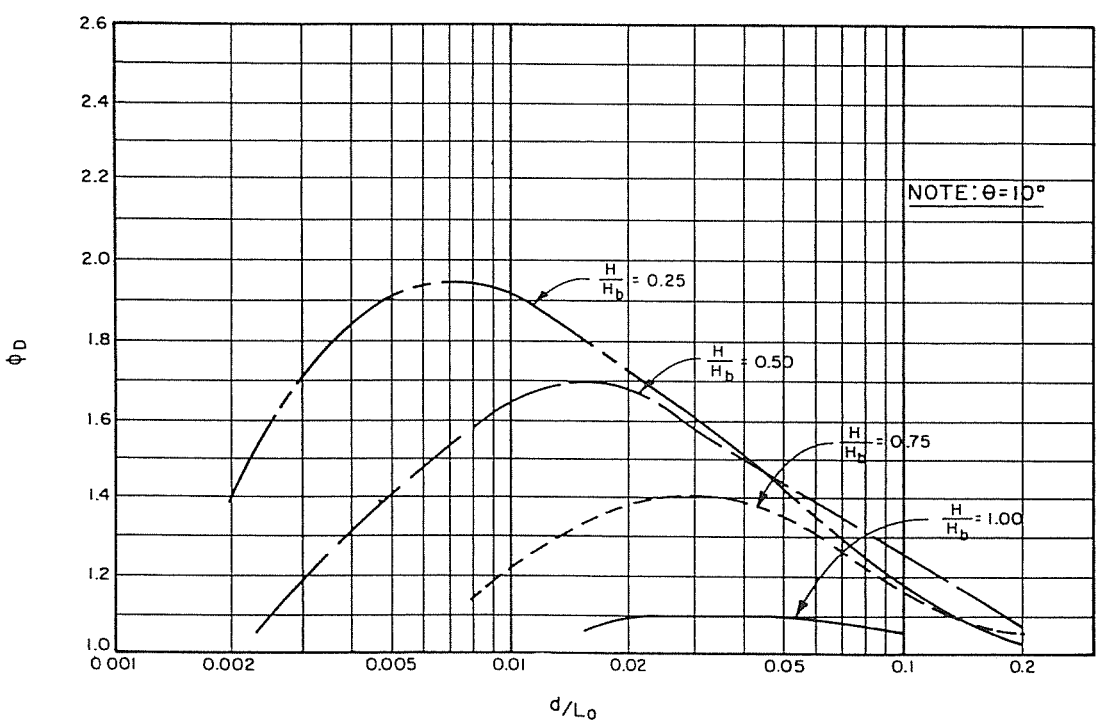

FIGURE 152
Nonlinear Drag-Force Correction Factor, ϕ_D, as a Function of d/L_o and H/H_b for $\theta = 10°$

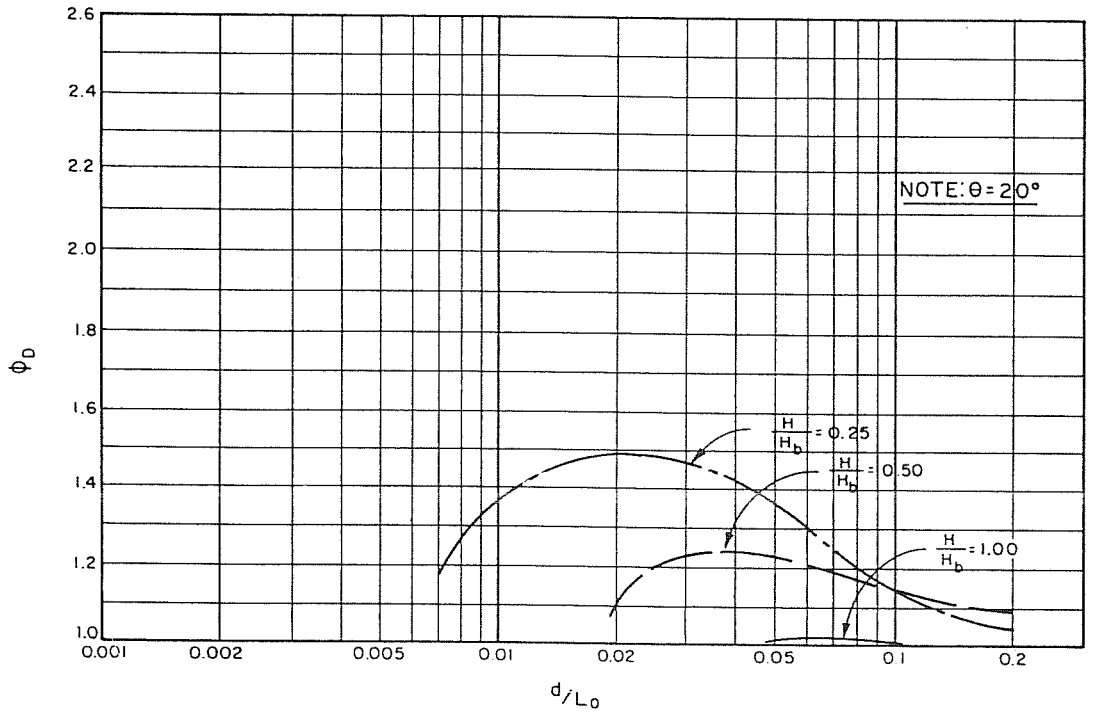

FIGURE 153
Nonlinear Drag-Force Correction Factor, ϕ_D, as a Function of d/L_o and H/H_b for $\theta = 20°$

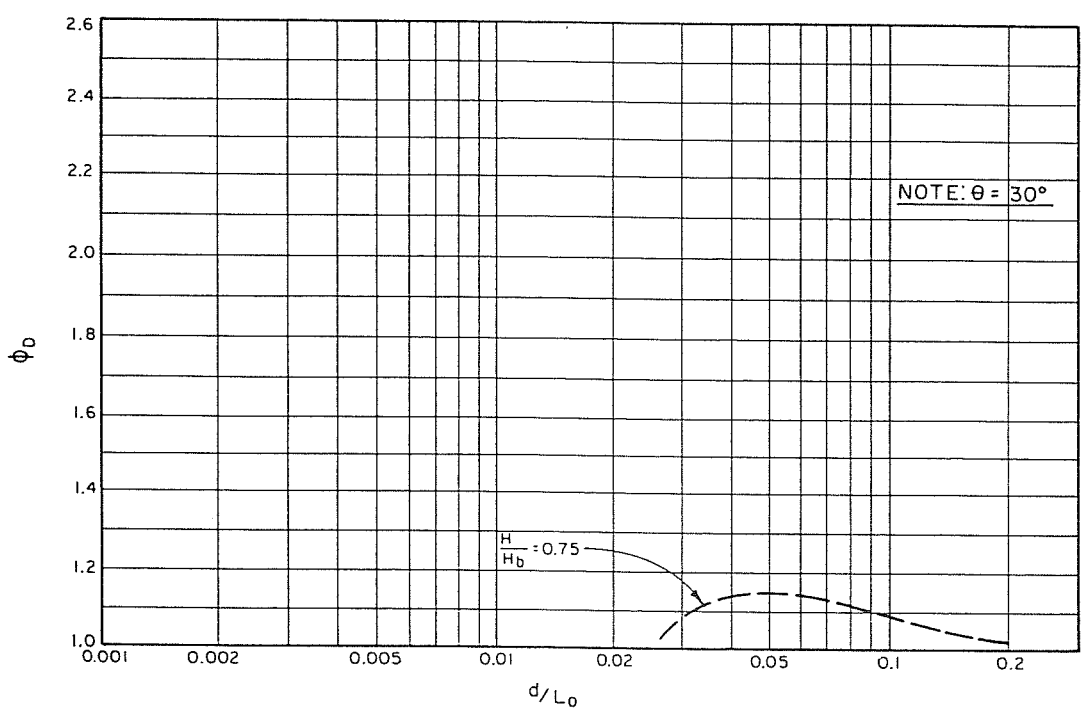

FIGURE 154
Nonlinear Drag-Force Correction Factor, ϕ_D, as a Function of d/L_o and H/H_b for $\theta = 30°$

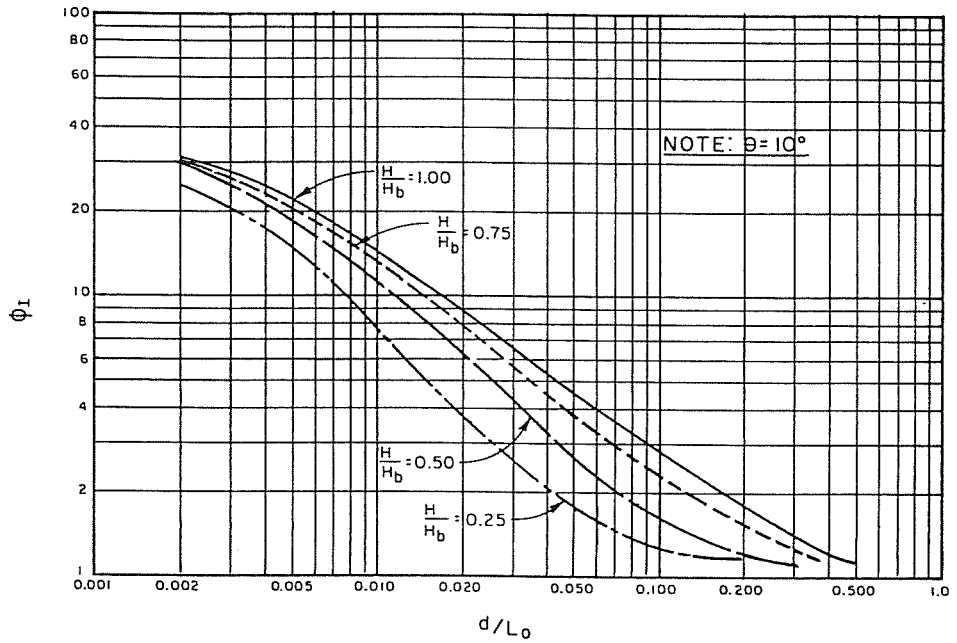

FIGURE 155
Nonlinear Inertial-Force Correction Factor, ϕ_I, as a Function of d/L_o and H/H_b for $\theta = 10°$

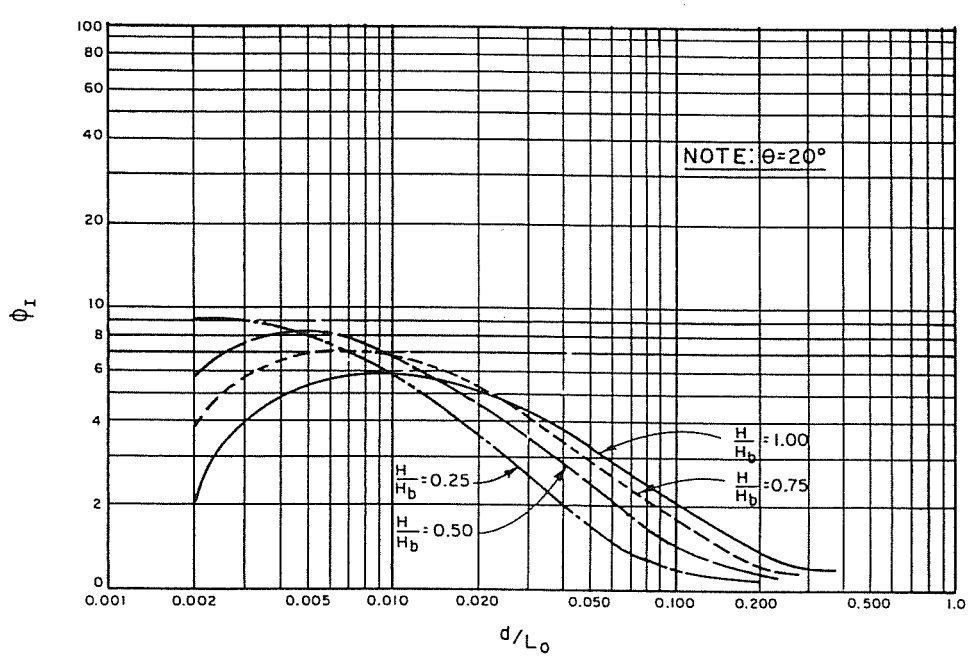

FIGURE 156
Nonlinear Inertial-Force Correction Factor, ϕ_I, as a Function of d/L and H/H_b for $\theta = 10°$

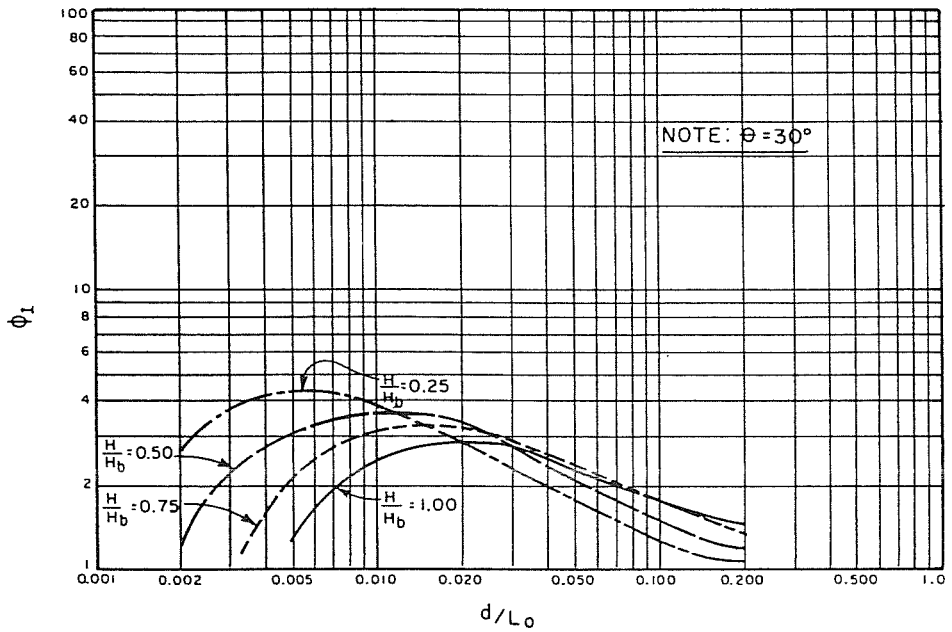

FIGURE 157
Nonlinear Inertial-Force Correction Factor, ϕ_I, as a Function of d/L_o and H/H_b for $\theta = 30°$

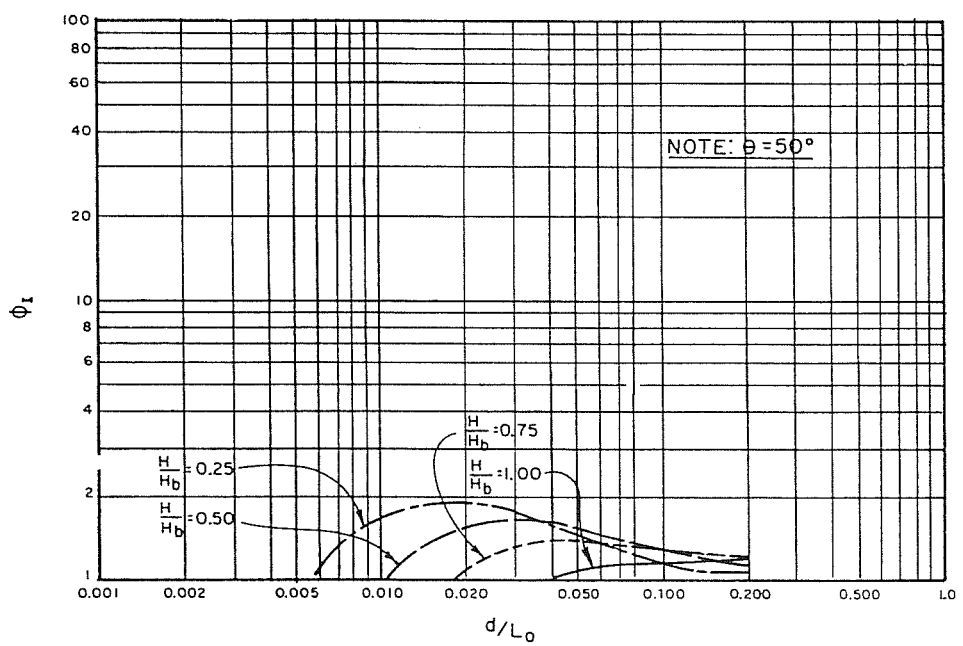

FIGURE 158
Nonlinear Inertial-Force Correction Factor, ϕ_I, as a Function of d/L_o and H/H_b for $\theta = 50°$

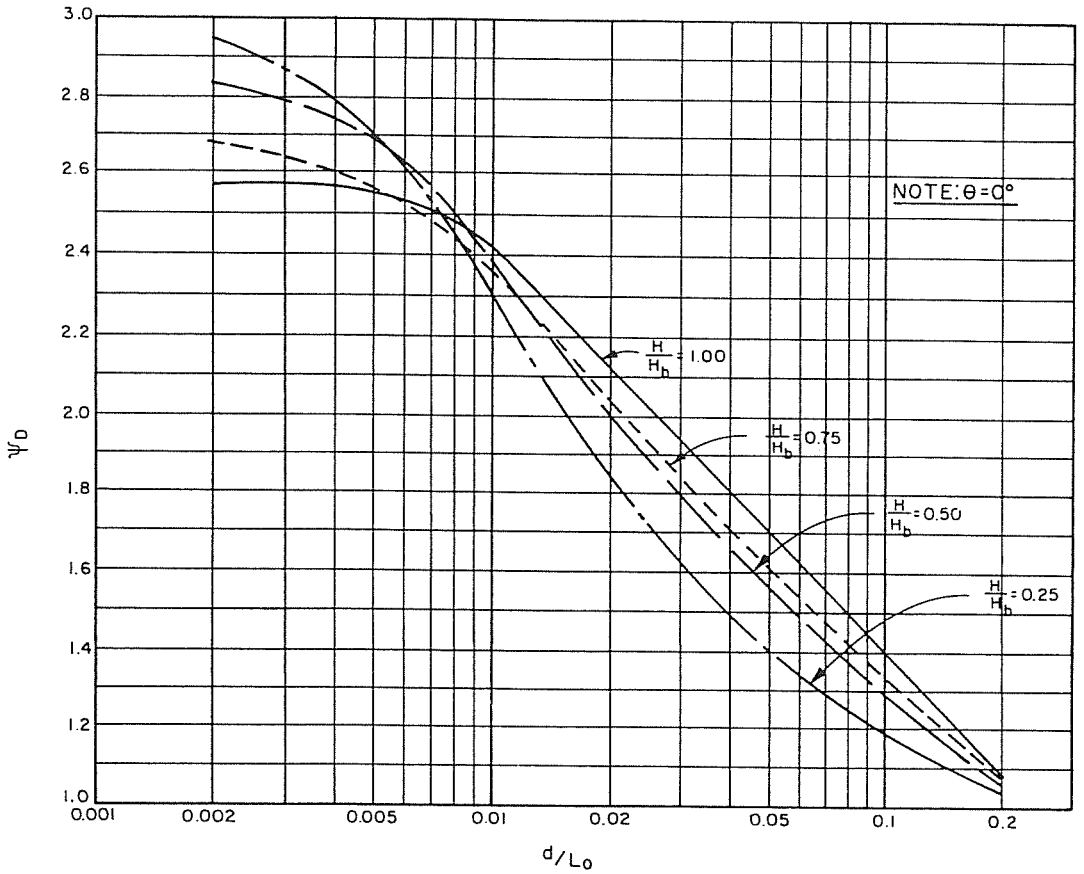

FIGURE 159
Nonlinear Drag-Moment Correction Factor, ψ_D, as a Function of d/L_o and H/H_b for $\theta = 0°$

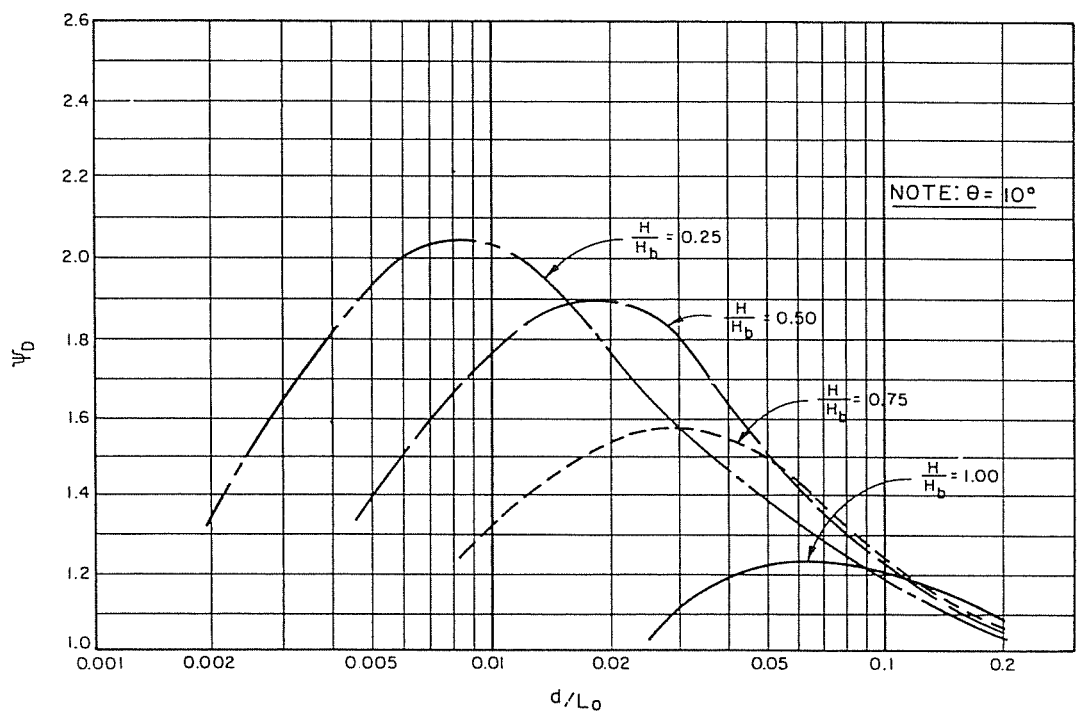

FIGURE 160
Nonlinear Drag-Moment Correction Factor, ψ_D, as a Function of d/L_o and H/H_b for $\theta = 10°$

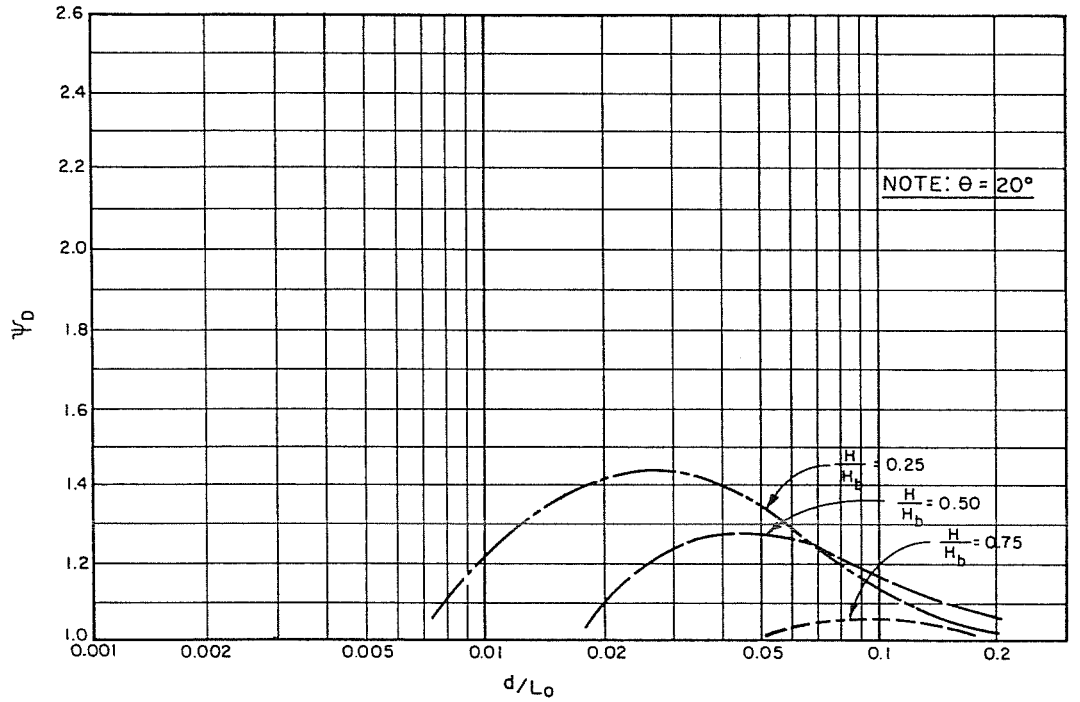

FIGURE 161
Nonlinear Drag-Moment correction Factor, ψ_D, as a Function of d/L_o and H/H_b for $\theta = 20^\circ$

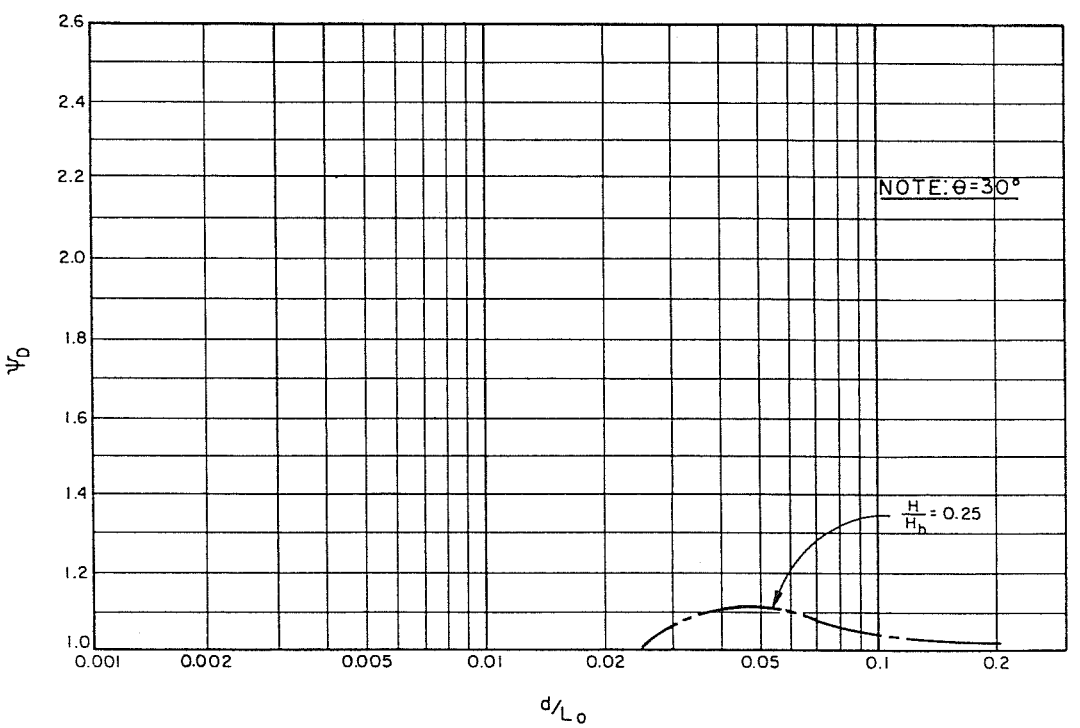

FIGURE 162
Nonlinear Drag-Moment Correction Factor, ψ_D, as a Function of d/L_o and H/H_b for $\theta = 30^\circ$

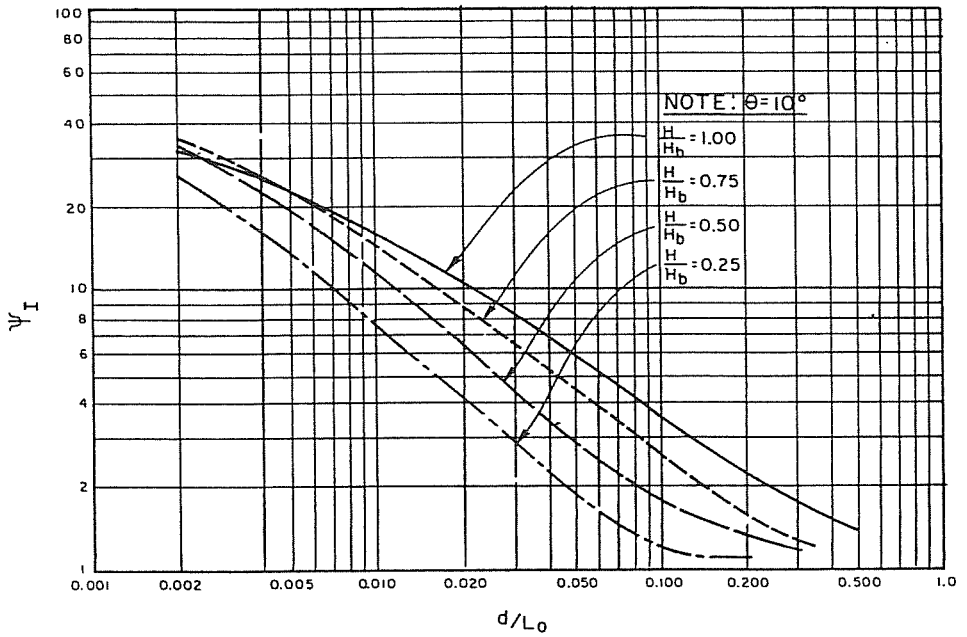

FIGURE 163
Nonlinear Inertial-Moment Correction Factor, ψ_I, as a Function of d/L_o and H/H_b for $\theta = 10°$

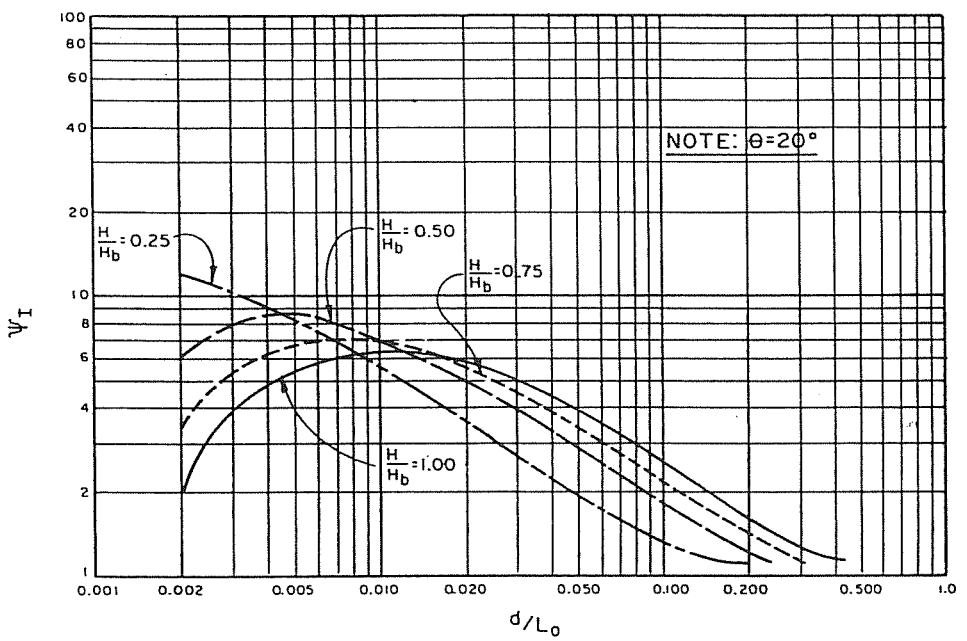

FIGURE 164
Nonlinear Inertial-Moment Correction Factor, ψ_I, as a Function of d/L_o and H/H_b for $\theta = 20°$

e. Maximum Values and Phase.

(1) Drag Force and Moment. The maximum drag force and moment, as well as the maximum nonlinear corrections, always occur under a wave crest; that is, when $\theta = 0°$. Therefore, Figures 151 and 159, for which $\theta = 0°$, yield well-defined nonlinear corrections as a function of d/L_o and H/H_b for the maximum drag force and moment, respectively. Drag components are symmetrical about $\theta = 0°$; therefore, force and moment for negative values of θ correspond to those for positive values of θ.

(2) Inertial Force and Moment. The maximum inertial force and the corresponding maximum inertial moment are complex functions of θ. These quantities are positive in front of the wave crest and negative behind it. However, the value of the wave-phase angle, θ, corresponding to the maximum inertial force and moment is unknown, a priori. Figures 167 and 168 give nonlinear correction factors, ϕ_{IM} and ψ_{IM}, corresponding to the maximum values of inertial force and moment as a function of d/L_o and H/H_b. (Note: the values are not presented as a function of θ because the values of θ corresponding to the maxima are unknown.) These nonlinear corrections are given with respect to a standard reference level, namely $z = d$, and not with respect to the free surface, S_θ, as in Figures 151 to 166. As a result these correction factors can

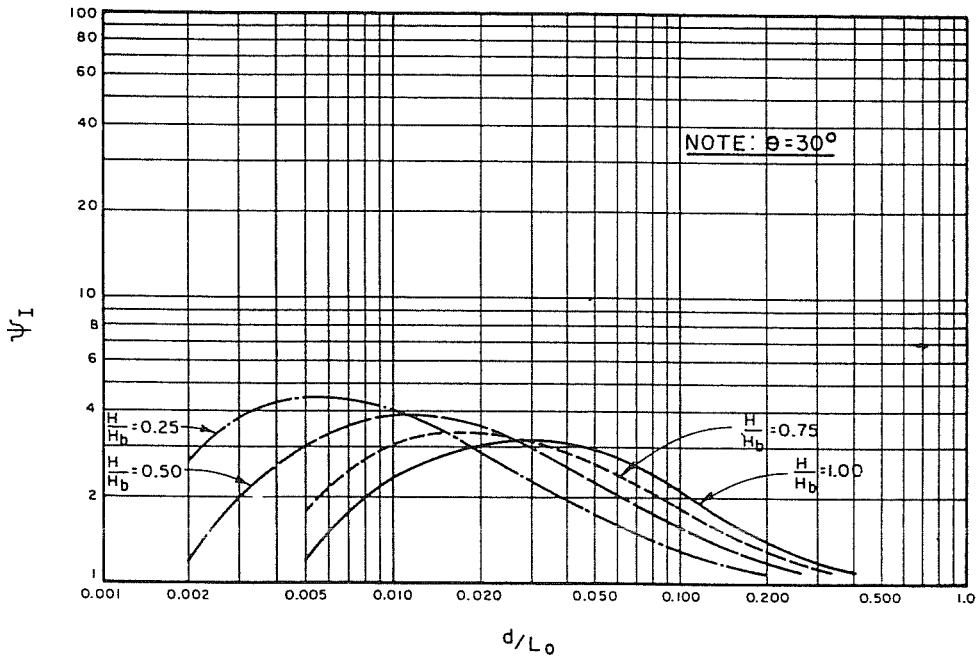

FIGURE 165
Nonlinear Inertial-Moment Correction Factor, ψ_I, as a Function of d/L_o and H/H_b for $\theta = 30°$

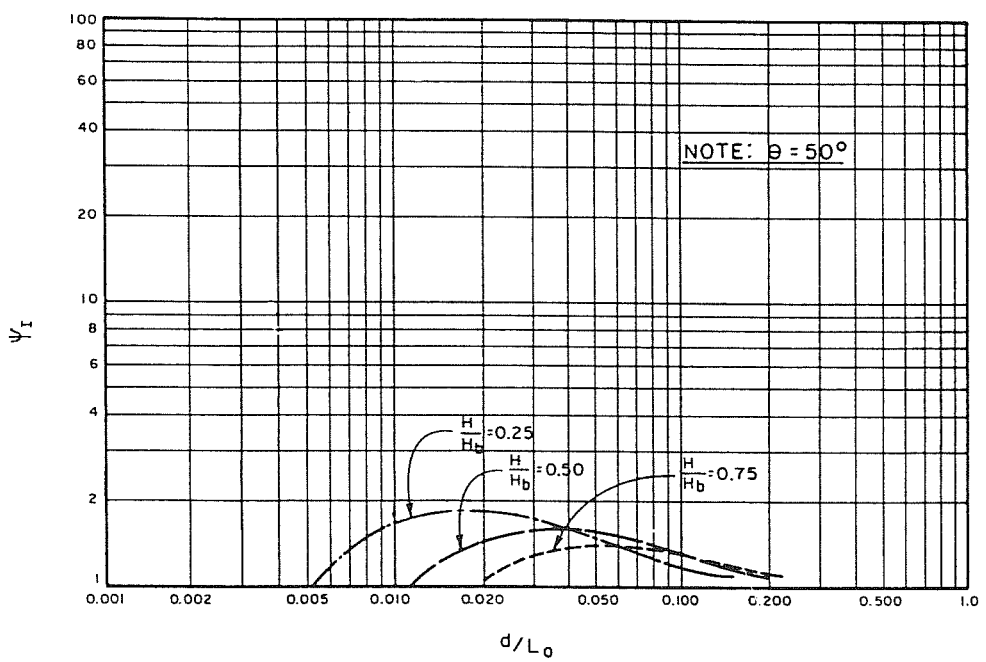

FIGURE 166
Nonlinear Inertial-Moment Correction Factor, ψ_I, as a Function of d/L_o and H/H_b for $\theta = 50°$

only be used for uniform-diameter piles. The maximum value of inertial wave force, F_{mI}, on a uniform-diameter pile is given by:

$$F_{mI} = \rho C_M \pi \left(\frac{D^2}{4}\right)\left(\frac{H}{T^2}\right) d \, (K_{IM})_{z=d} \, \phi_{IM} \qquad (7\text{-}33)$$

WHERE:
- ρ = density of water
- C_M = inertial, or added-mass, coefficient, obtained from Table 18
- D = pile diameter
- H = local wave height
- T = wave period
- d = wave depth

$(K_{IM})_{z=d}$ is found in Figure 147 as a function of z/d and d/L_o, where z/d = 1.

ϕ_{IM} is found in Figure 167 as a function of d/L_o and H/H_b.

The maximum value of inertial wave moment, M_{mI}, on a uniform-diameter pile is given by:

$$M_{mI} = \rho C_M \pi \left(\frac{D^2}{4}\right)\left(\frac{H}{T^2}\right) d^2 \, (\tau_{IM})_{z=d} \, \psi_{IM} \qquad (7\text{-}34)$$

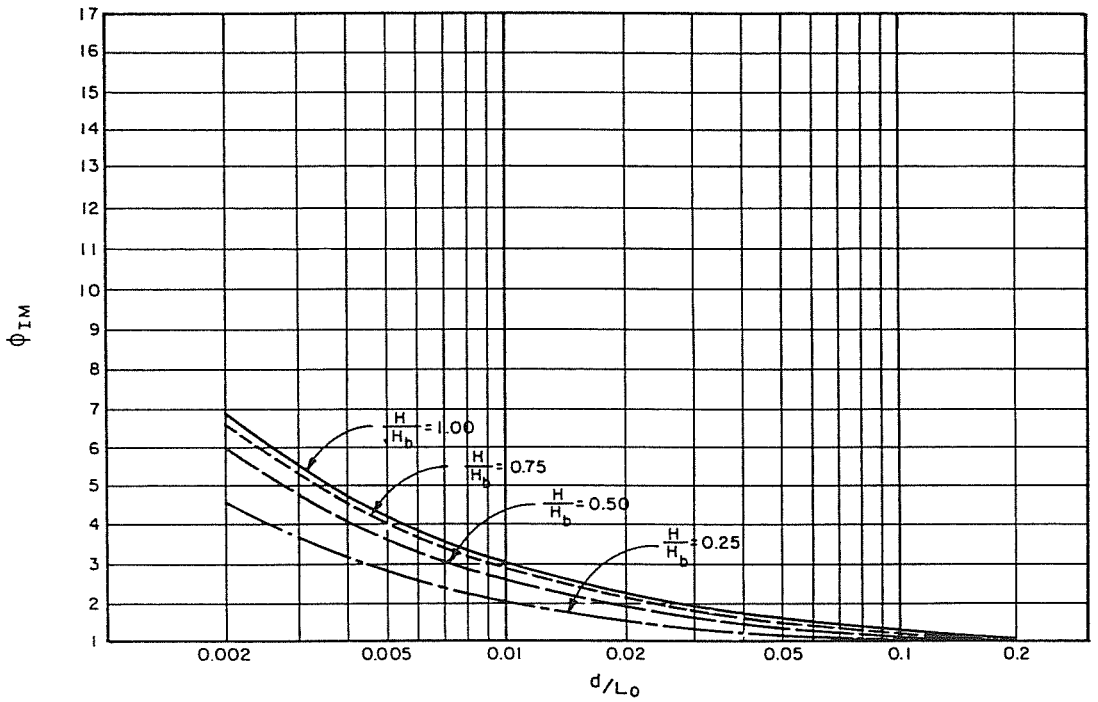

FIGURE 167
Nonlinear Correction Factor, ϕ_{IM}, for Determining Maximum Inertial Force, as a Function of d/L_o and H/H_b

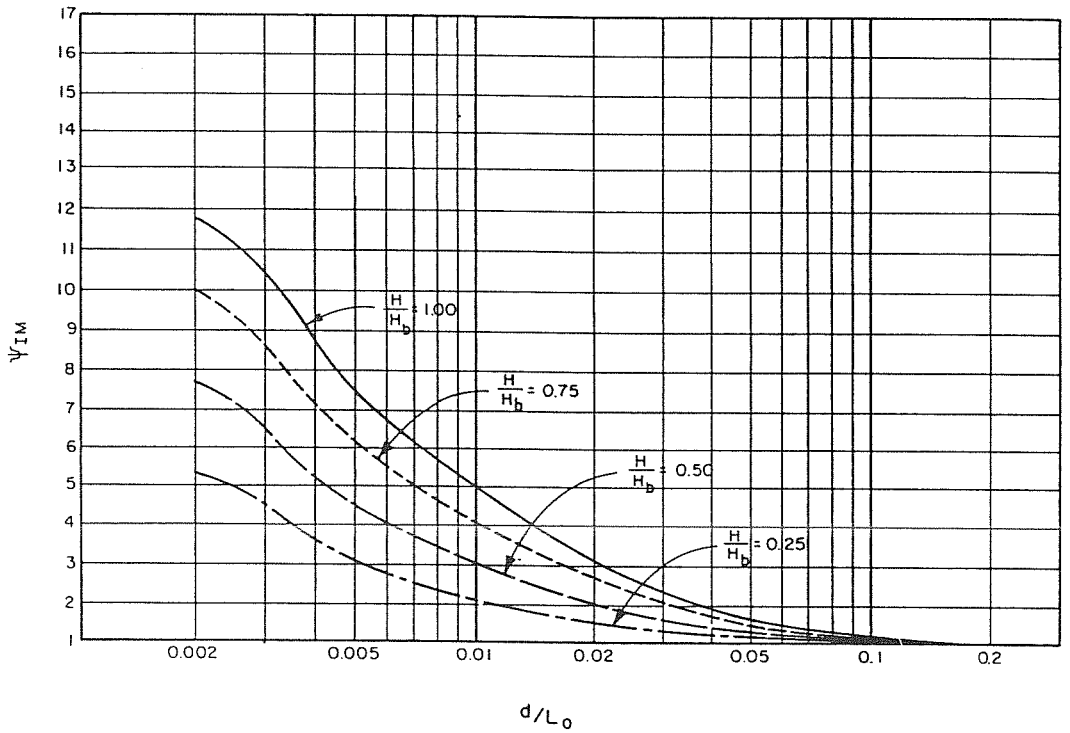

FIGURE 168
Nonlinear Correction Factor, ψ_{IM}, for Determining Maximum Inertial Moment, as a Function of d/L_o and H/H_b

WHERE:
$(\tau_{IM})_{z=d}$ is found in Figure 148 as a function of z/d and d/L_o, where z/d = 1
ψ_{IM} is found in Figure 168 as a function of d/L_o and H/H_b.

Drag and inertia add positively in front of the wave crest, and the maximum value for the total force and total moment occur in front of the wave crest. Inertia has a negative sign behind the wave crest; therefore inertial components must be subtracted from drag components behind the wave crest.

EXAMPLE PROBLEM 42

Given: a. Local wave height, H = 15 feet
b. Water depth, d = 20 feet
c. Wave period, T = 10 seconds
d. Bottom slope is flat.
e. $C_D = 0.7$ and $C_M = 1.6$
f. Pile diameter is:

$D_1 = 1.5$ feet for $z_o = 0$ foot to $z_1 = 18$ feet
$D_2 = 2.0$ feet for $z_1 = 18$ feet to $z_2 = 24$ feet
$D_3 = 1.5$ feet for $z_2 = 24$ feet to $z_3 = S_c$

Find: The force and moment acting as a function of wave-phase angle on a vertical pile.

Assume: $\rho = 2$ slugs per cubic foot

Solution: (1) Find L_o:

$L_o = (g/2\pi)\, T^2 = (32.2/2\pi)(10)^2 = 512$ feet

(2) Determine the relative depth, d/L_o:

$d/L_o = 20/512 = 0.0391$; use $d/L_o = 0.039$

(3) Determine the breaking-wave height, H_b, and find H/H_b:

For a flat bottom slope: $H_b = 0.78\, d = 15.6$ feet

$H/H_b = 15/15.6 = 0.962$; use $H/H_b = 0.96$

$H/H_b < 1$

THEREFORE: The wave is nonbreaking.

(4) Determine the relative free surface, S_θ/d, for different phase angles, θ:

The S_θ/d values defining the position of the surface can be read from Figure 150; enter the d/L_o abscissa with $d/L_o = 0.039$.

At the point of intersection with the H/H_b curves encompassing the given value of $H/H_b = 0.96$ (in this case, $H/H_b = 1.00$ and $H/H_b = 0.75$), lines are drawn horizontally to the right until intersection with the corresponding θ curves. (Note each H/H_b curve has its own set of θ curves.)

Finally, vertical lines are drawn from the intersection points on the θ curves to give two values for S/d from which the correct value of S/d is found by interpolation. For example:

(a) When $\theta = 30^o$ and $H/H_b = 1.00$:

$S_\theta/d = 1.15$

(b) When $\theta = 30^o$ and $H/H_b = 0.75$

$S_\theta/d = 1.17$

(c) By interpolation:

When $\theta = 30°$ and $H/H_b = 0.96$:

$S_\theta/d = 1.15$

Table 19 was prepared following this procedure.

TABLE 19
Tabulation of S/d Values for Example Problem 42

θ (degrees)....	0	10	20	30	50	75	100	130	180
H/H_b									
1.00.....	1.66	1.46	1.28	1.15	0.99	0.92	0.89	0.89	0.89
0.75.....	1.47	1.40	1.27	1.17	1.02	0.93	0.90	0.89	0.89
0.96.....	1.63	1.45	1.28	1.15	1.00	0.92	0.89	0.89	0.89

TABLE 20
Linear Force and Moment Coefficients for Example Problem 42 (d/L = 0.039)

± θ (degrees)[3] .... [1] .... [2]	0	10	20	30	50	75	100	130	180
z_i/d or S_θ/d	0.90	1.20	1.63	1.45	1.28	1.15	1.00	0.92	0.89	0.89	0.89
Coefficient											
	From Figure 144:										
$(K_{DM})_{z=z_i}$	33	48	71	60	50	44	37	34	33	33	33
	From Figure 147:										
$(K_{IM})_{z=z_i}$	35	48	0	59	51	46	39	36	34	34	0
	From Figure 145:										
$(\tau_{DM})_{z=z_i}$	16	30	67	48	36	28	19	17	16	16	16
	From Figure 148:										
$(\tau_{IM})_{z=z_i}$	17	30	0	45	34	28	19	18	16	16	0

[1] Values in this column are for z_i/d where i = 1.

[2] Values in this column are for z_i/d where i = 2.

[3] Values in third through ninth columns are for S_θ/d, where θ is from 0° to 180°.

(5) The z_i/d values for the changes in pile diameter are:

$$\frac{z_1}{d} = \frac{18}{20} = 0.90$$

$$\frac{z_2}{d} = \frac{24}{20} = 1.20$$

(6) Linear force and moment coefficients:

The linear forces coefficients, $(K_{DM})_{z=z_i}$ and $(K_{IM})_{z=z_i}$, and moment coefficients, $(\tau_{DM})_{z=z_i}$ and $(\tau_{IM})_{z=z_i}$, are obtained from Figures 144, 147, 145, and 148, respectively, for the values of $z_i/d = z_1/d$, z_2/d, and for all possible values of S_θ/d as a function of θ.[2] These values are presented in Table 20.

(7) Drag force on a single pile:

For each θ value, the drag force is computed using Equation (7-18):

$$F_D = \left(\tfrac{1}{2}\right) \rho C_D \left(\tfrac{H}{T}\right)^2 d \left[(K_{DM})_{z=z_1} (D_1 - D_2) + (K_{DM})_{z=z_2} (D_2 - D_3) + (K_{DM})_{z=S_\theta} (D_3)\right] \cos\theta |\cos\theta|$$

For example, for θ = 0°:

$$F_D = \left(\tfrac{1}{2}\right)(2)(0.7)\left(\tfrac{15}{10}\right)^2(20)[(33)(1.5 - 2.0) + (48)(2.0 - 1.5) + (71)(1.5)](1)(1)$$

$$F_D = 3{,}591 \text{ pounds}$$

For other θ values, the F_D is found by varying K_{DM} according to Table 20, and using this value in Equation (7-18). The value of the function cos θ| cos θ| will vary with θ. Values obtained for F_D for other values of θ are presented in Table 21.

(8) Inertial force on a single pile:

The inertial force on a single pile is computed using Equation (7-20):

$$F_I = \rho C_M \left(\tfrac{\pi}{4}\right)\left(\frac{H}{T^2}\right) d \left[(K_{IM})_{z=z_1} (D_1^2 - D_2^2) + (K_{IM})_{z=z_2} (D_2^2 - D_3^2) + (K_{IM})_{z=S_\theta} (D_3^2)\right] \sin\theta$$

$$F_I = (2)(1.6)\left(\tfrac{\pi}{4}\right)\left(\frac{15}{10^2}\right)(20)\left\{(35)[(1.5)^2 - (2.0)^2] + (48)[(2.0)^2 - (1.5)^2] + (59)(1.5)^2\right\}(0.1736)$$

$$F_I = 204 \text{ pounds}$$

The results for other values of θ are given in Table 21 for F_I.

(9) Drag moment on a single pile:

The drag moment on a single pile is computed using Equation (7-22):

$$M_D = \left(\tfrac{1}{2}\right) \rho C_D \left(\tfrac{H}{T}\right)^2 d^2 \left[(\tau_{DM})_{z=z_1} (D_1 - D_2) + (\tau_{DM})_{z=z_2} (D_2 - D_3) + (\tau_{DM})_{z=S_\theta} (D_3)\right] \cos\theta |\cos\theta|$$

For example, for θ = 0°:

$$M_D = \left(\tfrac{1}{2}\right)(2)(0.7)\left(\tfrac{15}{10}\right)^2(20)^2[(16)(1.5 - 2.0) + (30)(2.0 - 1.5) + (67)(1.5)](1)(1)$$

$$M_D = 67{,}725 \text{ foot-pounds}$$

The results for other values of θ are given in Table 21 for M_D.

(10) Inertial moment on pile:

The inertial moment is computed using Equation (7-24):

$$M_I = \rho C_M \left(\tfrac{\pi}{4}\right)\left(\frac{H}{T^2}\right) d^2 \left[(\tau_{IM})_{z=z_1} (D_1^2 - D_2^2) + (\tau_{IM})_{z=z_2} (D_2^2 - D_3^2) + (\tau_{IM})_{z=S_\theta} (D_3^2)\right] \sin\theta$$

For example, for θ = 10°:

$$M_I = \left(\tfrac{\pi}{4}\right)(2)(1.6)\left(\frac{15}{10^2}\right)(20)^2\left\{(17)[(1.5)^2 - (2.0)^2] + (30)[(2.0)^2 - (1.5)^2] + (45)(1.5)^2\right\}(0.1736)$$

$$M_I = 3{,}246 \text{ foot-pounds}$$

The results for other values of θ are found in Table 21 for M_I.

TABLE 21
Linear Values of Force and Moment for Example Problem 42

θ (degrees).....	0	10	20	30	50	75	100	130	180
Force or Moment									
F_D (pounds).....	3,591	2,979	2,295	1,736	820	123	-54	-742	-1,796
F_I (pounds).....	0	204	355	476	638	756	737	573	0
F_T (pounds).....	3,591	3,183	2,650	2,212	1,458	879	683	-169	-1,796
M_D (foot-pounds)...	67,725	48,269	33,935	23,153	9,241	1,372	-589	-8,069	-19,530
M_I (foot-pounds)...	0	3,247	5,119	6,465	7,566	9,213	8,725	6,787	0
M_T (foot-pounds)...	67,725	51,516	39,054	29,618	16,807	10,585	8,136	-1,282	-19,530

(11) Total forces and total moments are obtained using Equation (7-1) and a similar equation for moment:

$F_T = F_D + F_I$

$M_T = M_D + M_I$

for each value of θ. The corresponding results are found in Table 21 for F and M.

Recall that the values of F_D and M_D for the negative values of θ ($-180^o \leq \theta \leq 0^o$) are identical to the values of F_D and M_D for the respective positive values of θ ($0 \leq \theta \leq 180^o$); that is:

F_D for $\theta = F_D$ for $-\theta$
M_D for $\theta = M_D$ for $-\theta$

whereas the values of F_I and M_I for negative values of θ are of opposite sign from the values of F_I and M_I for the respective positive values of θ; that is:

F_I for $\theta = -F_D$ for $-\theta$

M_I for $\theta = -M_D$ for $-\theta$

Therefore, Table 21 can easily be computed for the entire cycle of θ ($-180° \leq \theta \leq +180°$).

(12) Maximum values--linear theory:

The maximum total force and maximum total moment on a single pile according to linear theory are seen from Table 21 to occur when $\theta \simeq 0^o$, which is the value of θ when the wave crest is at the structure:

$F_m = 3,591$ pounds

$M_m = 67,725$ foot-pounds

The lever arm at the maxima linear force and moment is:

$$z_{mDI} = \frac{M_{mDI}}{F_{mDI}} = \frac{67,725}{3,591} = 18.9 \text{ feet}$$

(13) Nonlinear correction due to velocity and acceleration field:

The nonlinear correction factor, ϕ_D, for the drag forces is given by Figures 151 to 154 and presented as a function of θ in Table 22.

The nonlinear correction factor, ϕ_I, for the inertial forces is given by Figures 155 to 158 and presented as a function of θ in Table 22.

The nonlinear correction factor, Ψ_D, for the drag moments is given by Figures 159 to 162 and presented as a function of θ in Table 22.

TABLE 22
Nonlinear Corrections for Example Problem 42 (d/L = 0.039)

±θ (degrees)....	0	10	20	30	50
Correction Factor					
ϕ_D.....	1.56	1.15	1	1	1
ϕ_I.....	....	5.26	3.79	2.68	1
Ψ_D.....	1.80	1.25	1	1	1
Ψ_I.....	....	6.73	4.40	3.10	1

The nonlinear correction factor, Ψ_I, for the inertial moments is given by Figures 163 to 166 and presented as a function of θ in Table 22.

The nonlinear corrections apply only for:

$0^o \leq \theta \leq 30^o$ for drag

$10^o \leq \theta \leq 50^o$ for inertial

For values of wave-phase angle outside of these values, the linear theory gives larger values of force and moment than nonlinear theory and therefore should prevail as a conservative estimate.

The nonlinear corrections are identical for θ and -θ values. However, when θ is negative, the inertial forces and moments are subtracted from the drag forces and moments. Multiplying the correction factors, ϕ_D or $_I$ and Ψ_D or I' by the corresponding forces and moments given by Table 21 (Equations (7-27)-(7-30)) yields the nonlinear values for force and moment, which exceed the linear results.

The nonlinear results (of applying the correction factors given in Table 22 to the values in Table 21) are given in Table 23.

(14) Total forces and moments for positive and negative values of θ:

Adding F_{DS_θ} and F_{IS_θ} and M_{DS_θ} and M_{IS_θ} gives the total values of the force, F, and moment, M (Equations (7-31) and (7-32)). The corresponding results for $0^o \leq \theta \leq 180°$ are shown in Table 23. For $-180° \leq \theta \leq 0°$, the inertial

TABLE 23
Forces and Moments for Phase Angles for Example Problem 42 After Nonlinear Correction

θ (degrees).....	0	10	20	30	50	75	100	130	180
Force or Moment									
F_{DS}.....	5,602	3,426	2,295	1,736	820	123	-54	-742	-1,796
F_{IS}.....	0	1,073	1,346	1,276	638	756	737	573	0
F_T.....	5,602	4,499	3,641	3,012	1,458	879	683	-169	-1,796
M_{DS}.....	121,905	60,336	33,935	23,153	9,241	1,372	-589	-8,069	-19,530
M_{IS}.....	0	21,852	22,524	20,042	7,566	9,213	8,725	6,787	0
M_T.....	121,905	82,188	56,459	43,195	16,807	10,585	8,136	-1,282	-19,530
θ (degrees).....	0	-10	-20	-30	-50	-75	-100	-130	-180
Force or Moment									
F_T.....	5,602	2,353	949	460	182	-633	-791	-1,315	-1,796
M_T.....	121,905	38,484	11,411	3,111	1,675	-7,841	-9,314	-14,856	-19,530

forces and moments are subtracted from the drag forces and moments, respectively, to obtain the total values for force and moment, respectively. The results of this calculation are also shown in Table 23. Recall that a positive value of force and moment is in the direction of wave travel and that a negative value is in the opposite direction.

Figures 169 and 170 present the final result of force and moment on the single pile of this example problem. It is seen that the maximum force occurs when $\theta = 2^o$ and is equal to $F_m = 5,650$ pounds. The maximum moment also occurs when $\theta = 2^o$ and is equal to $M_m = 123,450$ foot-pounds.

(15) The lever arm at the maxima nonlinear force and moment is:

$$z_{mDI} = \frac{M_{mDI}}{F_{mDI}} = \frac{123,450}{5,650} = 21.8 \text{ feet}$$

10. CASE 6--FORCES AND MOMENTS ON A COMBINATION OF PILES. Wave forces on a combination of piles supporting a structure are calculated by plotting the forces on a single pile as a function of phase angle. The combination of piles is then superimposed over the plot of wave forces, and the maximum force for the system is found by summing the forces, and the maximum force for the system is found by summing the forces on he individual piles for small changes in phase angle, θ. The maximum force generally occurs when the central pile is located near the wave crest. A similar procedure is used to determine the maximum moment. The procedure is illustrated by Example Problem 43. The following equation is used to determine the phase difference between piles:

$$\Delta\theta = \left(\frac{2\pi}{L}\right)(\Delta x) \qquad (7\text{-}35)$$

WHERE:
$\Delta\theta$ = phase difference between the piles
L = wavelength
Δx = spacing between the piles in the direction of wave advance (that is, along the x-coordinate axis)

EXAMPLE PROBLEM 43

Given: Five identical piles, identical also to the one given in the previous example problem, separated by a distance of $\Delta x = 16$ feet and structurally connected.

Find: The maximum force and moment on the combination of piles.

Solution: (1) Find L:

From Example Problem 42, $d/L_o = 0.039$

From Figure 2 for $d/L_o = 0.039$:

$d/L = 0.082$

$$L = \frac{d}{0.082} = \frac{20}{0.082}$$

$L = 244$ feet

(2) Find F and M:

The phase difference between piles is given by Equation (7-35):

$$\Delta\theta = \left(\frac{2\pi}{L}\right)(\Delta x) = \left(\frac{360}{243}\right)(16) = 23.7^\circ$$

Because the maximum forces generally occur when the central pile is located near the wave crest, use Pile 3 as the reference pile, at which $x = 0$ (see Table 24).

Referring to Figures 169 and 170, one shifts the location of the pile group with respect to θ by 2-degree increments. The results of this procedure are shown in Table 24, which indicates that the maximum force and moment occur when the middle pile is about 2^o ahead of the wave crest. Therefore, the maximum force on the total piling system is:

$F = 11,495$ pounds

and the sum of all moments (not to be taken as the total moment) is:

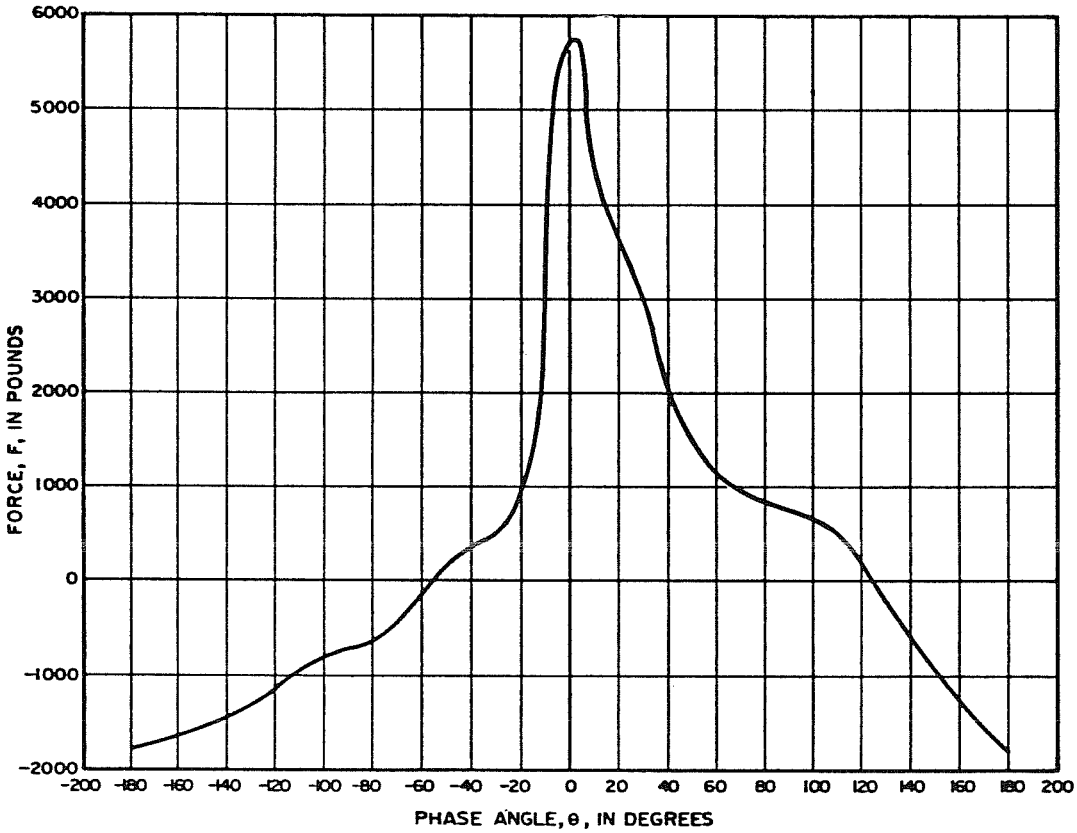

FIGURE 169
Results of Example Problem 42: Force

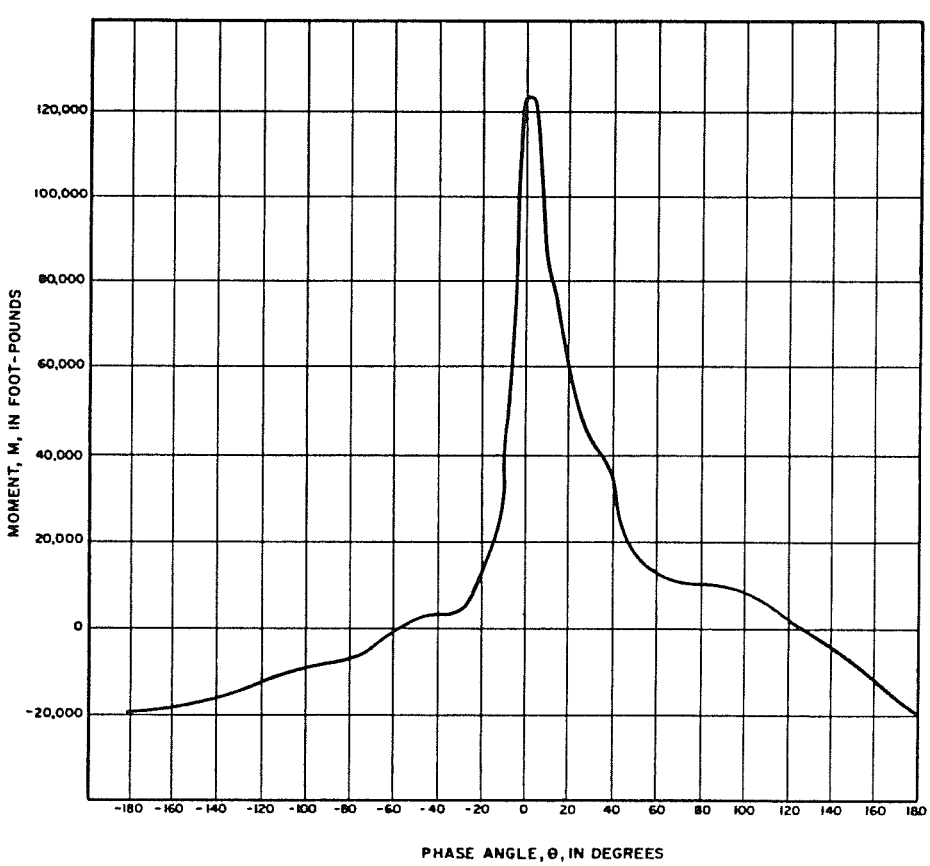

FIGURE 170
Results of Example Problem 42: Moment

TABLE 24
Forces and Moments for Example Problem 43

Pile Number.....	1	2	3	4	5	Total Acting on Pile Group
θ (degrees)...	-47.20	-23.70	0	23.70	47.40	
Force.....	208	750	5,602	3,290	1,625	11,475 lb
Moment.....	2,500	7,500	123,100	50,000	19,500	202,600 ft-lb
θ (degrees)...	-45.20	-21.70	2	25.70	49.40	
Force.....	270	825	5,650	3,208	1,542	11,595 lb
Moment.....	3,000	11,500	123,900	48,000	18,100	204,500 ft-lb
θ (degrees)...	-43.20	-19.70	4	27.70	51.40	
Force.....	290	917	5,646	3,063	1,438	11,354 lb
Moment.....	3,500	13,000	123,100	45,000	16,800	201,400 ft-lb

M = 206,750 foot-pounds

11. CASE 7--BRACING.

a. General. The wave force on a bracing beam between two vertical piles is determined by the same method as in the case of a vertical pile; that is, the wave force per unit length, Δz, is also the sum of a drag force per unit length of pile, f_D, and an inertial force per unit length of pile, f_I. However, bracings are generally beams of small diameter such that only the drag force is of importance. In addition, a horizontal beam parallel to the wave crest in and out of the water is subjected to a wave-slamming force. This subject is not presented herewith because such design is not recommended.

The local force per unit length of bracing is a function of the distance, z_B, of the beam above the bottom; if the beam is at an angle with the wave crest, this force is also a function of the wave-phase angle, θ.

b. Horizontal Bracing.

(1) Force. In order to determine the wave force on a horizontal beam of diameter, D, at relative distance above the bottom, z_B/d, first determine the wave forces at distances above the bottom of:

$$z_1/d = z_B/d - D/(2\,d) \qquad (7\text{-}36)$$

and

$$z_2/d = z_B/d + D/(2\,d) \qquad (7\text{-}37)$$

WHERE:
z_i = distance above bottom of point i
d = water depth
z_B = distance of center of beam above bottom
D = beam diameter

From Figure 144, find $(K_{DM})_{z1}$ and $(K_{DM})_{z2}$ for z_1/d and z_2/d. The force per unit length of bracing, F_B, is then determined as follows:

$$F_B \text{ per unit length of bracing} = (F)_{z_2} - (F)_{z_1} \qquad (7\text{-}38)$$

WHERE: $(F)_{z_i} = (\frac{1}{2})\,\rho\, C_D\,(\frac{H}{T})^2\, d\,(K_{DM})_{z=z_i}$ = force per unit length of bracing at an arbitrary distance above bottom, z_i (7-39)

z_i = distance above bottom of point i
ρ = density of water
C_D = drag coefficient (obtained from Table 17)
H = local wave height
T = wave period
d = water depth
$(K_{DM})_{z=}$ z_i is obtained from Figure 144 as a function of z/d and d/L_o.

(2) Moment. The corresponding moment, M_B, about the mudline is:

$$M_B = (F_B \text{ per unit length of bracing})(z_B) \qquad (7\text{-}40)$$

WHERE:
z_B = distance of center of beam above bottom

c. Angle Bracing. If the beam is at an angle with the vertical, one must initially determine the force on each pile element of unit length as a function of elevation. If the beam is at an angle with the wave direction, the phase angle, θ, becomes an additional parameter.

All these calculations are based on the linear wave theory. Therefore, appropriate safety margins are recommended to account for nonlinear effects, particularly when determining the force near the free surface.

12. CASE 8--FORCES DUE TO BREAKING WAVES.

Just prior to the inception of wave breaking, a wave traveling on a slope peaks up to a limiting value, H_b, as described in Subsection 6.3., LIMITING WAVE HEIGHT.

In shallow water, near breaking, the drag force is the primary component of wave force on piles. Both small and full-scale laboratory experiments indicate that breaking waves on rigidly supported piles induce a short-duration "slamming" force caused by the impact of the breaking wave on the pile (Hall (1958) and Ross (1959)). This slamming force (analogous to the dynamic component of force on walls subjected to breaking waves) is superimposed on a wave force similar to that for a nonbreaking wave. The slamming force is of short duration (< 0.1 second) and occurs over a small portion of the wave profile. Furthermore, prototype piles have elasticity, which may not have been properly scaled in the model tests. The elastic properties of the pile can absorb very

short-duration loads, as is evidenced by numerous prototype installations located in the surf zone which have performed adequately without taking the slamming force into account. The slamming force is usually of such magnitude that the sizing of structural members may lead to impractical designs if design criteria were to include the slamming force.

The recommended procedure for determining breaking-wave forces and moments on piles is to use the procedure outlined in Subsection 7.7, CASE 3, based solely on drag, for $H/H_b = 1$ and a drag coefficient of $C_D = 1.0$. For situations where the wave slamming force is believed to be critical to design, force and moment may be conservatively estimated by multiplying the values obtained in the above procedure by two.

13. METRIC EQUIVALENCE CHART. The following metric equivalents were developed in accordance with ASTM E-621. These units are listed in the sequence in which they appear in the text of Section 7. Conversions are approximate.

$$32.2 \text{ feet}_2 \text{ per second}^2 = 9.81 \text{ meters per second}^2$$
$$1 \times 10^{-5} \text{ feet per second} = 9.29 \times 10^{-7} \text{ meters}^2 \text{ per second}$$
$$1 \text{ foot} = 30.5 \text{ centimeters}$$

REFERENCES

Shore Protection Manual, U.S. Army Coastal Engineering Research Center, 3d ed., Vols. I, II, and III, Stock No. 008-022-00113-1, U.S. Government Printing Office, Washington, DC, 1977.

Wiegel, R.L.; "Oscillatory Waves," Bulletin, Special Issue No. 1, U.S. Army, Beach Erosion Board, July 1948.

Wiegel, R.L.; "Diffraction of Waves by a Semi-Infinite Breakwater," Journal of the Hydraulics Division, ASCE, Vol. 88, HY 1, January 1962, pp. 27-44.

Johnson, J.W.; "Generalized Wave Diffraction Diagrams," Proceedings of Second Conference on Coastal Engineering, Houston, Texas, November 1951, Council on Wave Research, The Engineering Foundation, Berkely, CA, 1952.

Ippen, Arthur T., ed.; Estuary and Coastline Hydrodynamics, McGraw-Hill Book Company, New York, 1966.

Goda, Y.; "A Synthesis of Breaker Indices," Transactions of the Japanese Society of Engineers, Vol. 2, Pt. 2, 1970.

Weggel, J.R.; "Maximum Breaker Height," Journal of the Waterways, Harbors and Coastal Engineering Division, ASCE, Vol. 98, No. WW4, Paper 9384, 1972.

ASTM E-621; "Standard Practice for the Use of Metrics (SI) Units in Building Design and Construction," Annual Book of ASTM Standards, Part 18, American Society for Testing and Materials (ASTM), Philadelphia, PA, 1979.

Bretschneider, Charles L.; "Overwater Wind and Wind Forces," Handbook of Ocean and Underwater Engineering, McGraw-Hill Book Company, New York, 1969, pp. 12-2 - 12-24. (Editors: John J. Myers, Carl H. Holm, and Raymond F. McAllister)

U.S. Army Corps of Engineers; "Method of Determining Adjusted Windspeed, U_A, for Wave Forecasting," Coastal Engineering Technical Note, CETN-I-5, Coastal Engineering Research Center, Fort Belvoir, VA, 1981a.

Resio, D.T., and Vincent, C.L.; "Estimation of Winds Over the Great Lakes," MP H-76-12, U.S. Army Engineer Waterways Experiment Station, Vicksburg, MS, June 1976 (Final Report).

U.S. Army Corps of Engineers; "Revised Method for Wave Forecasting in Deep Water," Coastal Engineering Technical Note, CETN-I-7, Coastal Engineering Research Center, Fort Belvoir, VA, 1981b.

U.S. Army Corps of Engineers; "Revised Method for Wave Forecasting in Shallow Water," Coastal Engineering Technical Note, CETN-I-6, Coastal Engineering Research Center, Fort Belvoir, VA 1981c.

Summary of Synoptic Meteorological Observations, prepared under the direction of the U.S. Naval Weather Service Command by the National Climatic Center, Asheville, NC. (Copies are obtainable from the National Technical Information Service, Springfield, VA 22161.)

Hogben, N., and Lumb, F.E.; Ocean Wave Statistics, Ministry of Technology, National Physical Laboratory, Her Majesty's Stationery Office, London, 1967.

Coastal Zone Management (CZM) Act of 1972, PL 92-583.

DOD Instruction 4165.59 of 29 December 1975.

Stoa, Philip N.; "Wave Runup on Rough Slopes," Coastal Engineering Technical Aid (CETA) No. 79-1, U.S. Army, Corps of Engineers, Coastal Engineering Research Center, Fort Belvoir, VA, July 1979.

Stoa, Philip N.; "Revised Wave Runup Curves for Smooth Slopes," Coastal Engineering Technical Aid (CETA) No. 78-2, U.S. Army, Corps of Engineers, Coastal Engineering Research Center, Fort Belvoir, VA, July 1978.

Saville, T., Jr.; "Wave Runup on Shore Structures," Journal of the Waterways and Harbors Division, ASCE, Vol. 82, No. WW2, 1956.

Seelig, William N.; "Two-Dimensional Tests of Wave Transmission and Reflection Characteristics of Laboratory Breakwaters," Technical Report No. 80-1, U.S. Army, Corps of Engineers, Coastal Engineering Research Center, Fort Belvoir, VA, June 1980.

Wiegel, Robert L.; "Transmission of Waves Past a Rigid Vertical Thin Barrier," Journal of the Waterways and Harbors Division, ASCE, Vol. 86, No. WWI, March 1960, pp. 1-12.

Perroud, Paul Henri; "The Solitary Wave Reflection Along a Straight Vertical Wall at Oblique Incident," Ph.D. Thesis, University of California; also, Inst. Eng. Res., Tech. Rept. No. 99-3, September 1957 (Unpublished).

Seelig, William N., and Ahrens, John P.; "Estimation of Wave Reflection and Energy Dissipation Coefficients for Beaches, Revetments and Breakwaters," Unpublished Draft, U.S. Army Coastal Engineering Research Center, Fort Belvoir, VA, 18 August 1980.

Walker, James R., Palmer, Robert Q., and Dunham, James W.; "Breakwater Back Slope Stability," Proceedings, Civil Engineering in the Oceans/III, 9-12 June 1975, Vol. 2, ASCE, New York, 1975, pp. 879-898.

El Ghamry, Osman A.; "Wave Forces on a Dock," Hydraulic Engineer Laboratory, Wave Research Projects, University of California, Institute of Engineering Research, Technical Report HEL-9-1, Berkeley, CA, October 1963 (Submitted under contract with the Beach Erosion Board, Corps of Engineers, U.S. Army).

French, Jonathan A.; "Wave Uplift Pressures on Horizontal Platforms," W.M. Keck Laboratory of Hydraulics and Water Resources, Division of Engineering and Applied Science, California Institute of Technology, Pasadena, CA, Report No. KH-R-19, July 1969.

Wang, Hsiang; "Estimating Wave Pressures on a Horizontal Pier," Technical Report No. R 546, Naval Civil Engineering Laboratory, Port Hueneme, CA, October 1967.

Richey, E.P., and Nece, R.E.; "Floating Breakwaters--State of the Art," Proceedings, 1974 Floating Breakwaters Conference Papers, Newport, RI, University of Rhode Island Marine Technical Report Series No. 24, Kingston, RI, April 1974, pp. 1-20.

Harms, Volker W.; "Floating Breakwater Performance Comparison, 17th International Conference on Coastal

Engineering, Abstracts-in-Depth, Sydney, Australia, 23-28 March 1980, The Institution of Engineers, Australia, Barton, A.C.T., Australia, pp. 328-329.

Kowalski, T., ed.; Proceedings, 1974 Floating Breakwaters Conference Papers, Newport, RI, University of Rhode Island Marine Technical Report Series No. 24, Kingston, RI, April 1974.

Hales, Lyndell Z.; "Floating Breakwater State-of-the-Art Literature Review," Unpublished Draft, Hydraulics Laboratory, U.S. Army Engineer Waterways Experiment Station, Vicksburg, MS, September 1980. (Prepared for U.S. Army Engineer Coastal Engineering Research Center, Fort Belvoir, VA.)

Harms, Volker W., and Bender, Thomas J.; "Preliminary Report on the Application of Floating-Tire-Breakwater Design Data," Water Resources and Environmental Engineering Research Report No. 78-1, Department of Civil Engineering, State University of New York at Buffalo, NY, April 1978.

Seymour, R.J., and Isaacs, J.D.; "Tethered Float Breakwaters, "Proceedings, 1974 Floating Breakwaters Conference Papers, Newport, RI, University of Rhode Island Marine Technical Report Series No. 24, Kingston, RI, April 1974, pp. 55-72.

Jones, D.B.; "Sloping Float Breakwaters; Interim Data Summary," Technical Note No. 1568, U.S. Navy Civil Engineering Laboratory, Port Huneme, CA, January 1980.

Davidson, D.D.; "Wave Transmission and Mooring Force Tests of Floating Breakwater, Oak Harbor, Washington," Technical Report H-71-3, U.S. Army Engineer Waterways Experiment Station, Vicksburg, MS, April 1971.

Laird, Alan D.K.; "Water Forces on Flexible Oscillating Cylinders," Journal of the Waterways and Harbors Division, ASCE, Vol. 88, No. WW3, August 1962, pp. 125-137.

Dean, R.G.; "Stream Function Representation of Nonlinear Ocean Waves," Journal of Geophysical Research, Vol. 70, No. 18, 1965.

Goda, Y.; "Irregular Wave Deformation in the Surf Zone," Coastal Engineering in Japan, Vol. 18, 1975, pp. 13-25.

Seelig, William N., and Ahrens, John P.; "The Elevation and Duration of Wave Crests," Unpublished Draft, U.S. Army Coastal Engineering Research Center, Fort Belvoir, VA, 2 January 1981.

Hall, Michael A.; "Laboratory Study of Breaking Wave Forces on Piles," Technical Memorandum No. 106, Department of the Army, Corps of Engineers, August 1958.

Ross, Culbertson W.; "Large-Scale Tests of Wave Forces on Piling (Preliminary Report)," Technical Memorandum No. 111, Beach Erosion Board, Department of the Army, Corps of Engineers, May 1959.

LIST OF SYMBOLS

Symbol	Definition
A	surface area
A	projected area of member
a	amplitude
a	breaking-wave dynamic moment reduction factor for low wall
B	gap spacing between breakwaters
B	crest width for rubble-mound structure
B	structure beam for floating breakwater
B'	imaginary equivalent breakwater gap
b	spacing between wave orthogonals
b	breakwater crest width
b	height above the bottom of rubble base (for wall built on rubble base) or of gap (for wave baffle)
b'	overtopped wall height above trough
C	wave celerity; phase velocity
C_D	drag coefficient (dimensionless)
C_M	inertial, or added mass, coefficient (dimensionless)
C_g	group velocity
C_t	windspeed conversion factor (where t = desired duration or given duration)
D	water depth one wavelength seaward (in front) of wall
D	- pile diameter - beam diameter
D_i	respective pile diameter
d	water depth from still water level (SWL)
d/H'_o	relative depth where toe of structure slope is at $d_s = 0$
d/L	relative depth (dimensionless)
d_b	depth of water at breaking
d_b/H_b	relative breaker depth
d_s	- water depth from still water level at structure toe - water depth from still water level at toe of rubble foundation for wall built on rubble foundation
d_s/H'_o	relative depth
du/dt	instantaneous horizontal water-particle acceleration
d_w	depth from still water level (SWL) at base of wall for wall built on rubble foundation
$d_{i(etc.)}$	depth for fetch interval, F_i
d_1	slope-protection depth; depth below still water level (SWL) of rubble-foundation crest
F	dynamic force per unit length of wall if wall is perpendicular to direction of wave approach
F	fetch length
F	structure freeboard
F'	reduced force on overtopped wall (nonbreaking wave)
F_B	force per unit length of bracing
F_D	linear drag force
F_{DS_θ}	drag force corrected for nonlinear effects
F_I	linear inertial force
F_{IS_θ}	inertial force corrected for nonlinear effects
F_T	- total force - total force on a pile subjected to nonbreaking waves
F_{TS_θ}	total force on a pile at a given phase angle (corrected for nonlinear effects)
F"	reduced force on wall built on rubble base or force on baffle (nonbreaking wave)
F_c	force on wall when crest is at wall
$F_c/w_w d_s^2$	dimensionless F_c
F_m	dynamic component of force for breaking or broken wave
F_{mD}	maximum drag force
F_{mDI}	maximum (drag and inertial) force
F_{mI}	maximum inertial force
F'_m	corrected dynamic-impact force for overtopped wall
F_n	component of F normal to wall
F_s	hydrostatic component of force for breaking or broken wave
F'_s	reduced hydrostatic moment for wall of low height

F_t	force on wall when trough is at wall
$F_t/w_w\ d_s^2$	dimensionless F_t
F_{net}	net force on wall for nonbreaking wave
F_u	uplift force
$(F)_{z_i}$	force per unit length of bracing at an arbitrary distance above bottom, z_i
F_α	reduced dynamic component of force for breaking or broken wave striking structure at oblique angle
F_θ	reduced horizontal dynamic component of force for breaking or broken wave striking nonvertical wall
F_i	fetch for interval i
$F'_{l(etc.)}$	fetch length required to generate significant wave height, H_s, if depth, d, had been d_2 in F_1, etc.
f_D	drag force per unit length of pile
f_I	inertial force per unit length of pile
g	gravitational acceleration (32.2 feet per second^2)
H	wave height measured between crest and trough; local wave height
H	average wave height; 0.626 H_s (not same as local wave height)
H/H_b	relative wave height
H/d	wave height relative to water depth
H/L	wave steepness
H_b	- breaking-wave height - limiting height
H_b/H'_o	- relative breaker height - breaker height index
H_i	incident wave height
$H_i/g\ T^2$	incident wave steepness
H_m	Mach-stem wave height
H_r	reflected wave height
H_s	significant wave height; $H_{1/3}$; average height of highest one-third of waves for specified time period
H_t	transmitted wave height
H_t/H_i	transmission coefficient (see K_t)
H_w	wave height at wall
H_o	deepwater wave height
H'_o	equivalent unrefracted deepwater wave height if wave unaffected by refraction and friction = $H_o\ K_R\ K_f = H/K_s$
$H'_o/g\ T^2$	deepwater wave steepness
H'_o/L_o	deepwater wave steepness
$H_{1/3}$	average of highest one-third of all waves; H_s; significant wave height
H_1	average of highest 1 percent of all waves for a given time period; 1.67 H_s
H_{10}	average of highest 10 percent of all waves for a given time period; 1.27 H_s
h	distance from SWL to bottom of structure (such as wall built on rubble base or wave baffle)
h_c	height above bottom of core (of breakwater)
h_c	height above still water level (SWL) of broken wave
h_c/d_s	relative core height
h_o	height of clapotis orbit center above still water level (SWL)
h_s	- height of structure - height of baffle structure from mudline to top of baffle
h'	broken-wave height above ground surface at structure toe shoreward of still water level SWL
K_D	armor-unit stability coefficient
$(K_D)_z$	drag-force coefficient
$(K_{DM})_{z=z_i}$	linear maximum drag-force coefficient
$(K_I)_z$	inertial-force coefficient
$(K_{IM})_{z=z_i}$	linear maximum inertial-force coefficient
$(K_{DMC}\phi_D)$	factor used in determining maximum drag force
K_R	refraction coefficient
K_f	decay coefficient
K_r	reflection coefficient
K_{RR}	stability coefficient for graded riprap
K_s	shoaling coefficient; H/H'_o
K_{sNL}	nonlinear shoaling coefficient
K'	diffraction coefficient
K_t	transmission coefficient; H_t/H_i
k	runup scale effect correction factor
k_Δ	rock layer-thickness coefficient
L	wavelength
L_D	wavelength in water depth D
L_{d_s}	wavelength in water depth d_s
L/T	phase velocity, C
L_o	deepwater wavelength
ℓ	structure slope length
M	moment about mudline
M_B	moment about mudline corresponding to force per unit length of bracing, F_B
M_D	linear drag moment
M_{DS_θ}	drag moment corrected for nonlinear effects
M_I	linear inertial moment
M_{IS_θ}	inertial moment corrected for nonlinear effects
M_{TS_θ}	total moment on a pile at a given phase angle
M_c	moment about mudline of wall for nonbreaking wave when crest is at wall
$M_c/w_w\ d_s^3$	dimensionless M_c
M_m	dynamic component of moment for breaking or broken wave
M_{mD}	maximum drag moment
M_{mI}	maximum inertial moment
M_{mDI}	maximum (drag and inertial) moment
M'_m	corrected dynamic moment about the mudline for overtopping breaking wave
M_{net}	net moment about mudline of wall for nonbreaking wave
M_s	hydrostatic component of moment for breaking or broken wave
M'_s	reduced hydrostatic force for wall of low height
M_T	total moment
M_t	moment when trough is at wall
$M_t/w_w\ d_s^3$	dimensionless M_t
M'	reduced moment about mudline for wall overtopped by nonbreaking wave
M''_A	moment about mudline for wall built on rubble base (non-breaking wave)
M''_B	moment about base of wall for wall built on rubble base (nonbreaking wave)
m	bottom slope

N_r	number of individual units in layer of interest
N_r/A	placing density
n	- number of units comprising the layer of interest - number of armor units comprising the crest width
P	porosity
P_c	pressure when clapotis crest is at wall
P_m	maximum dynamic pressure by breaking and broken waves on vertical wall
P_s	maximum hydrostatic pressure by broken wave
P_t	pressure when clapotis trough is at wall
P_1	nonbreaking-wave pressure difference from still-water hydrostatic pressure as clapotis crest (or trough) passes
R	ratio of U_W/U_L
R	wave runup
R/H'_o	relative runup
R_e	Reynolds number
R_T	amplification ratio
r	rough-slope runup correction factor
r	angle of reflection
r	layer thickness
r_D	representative armor-stone diameter
r_f	reduction factor for force on wall of height lower than clapotis crest
r_m	- reduction factor for moment on wall of height lower than clapotis crest - reduction factor for maximum dynamic component of force when breaking wave height is higher than wall height
S	distance to water free surface measured along the z-coordinate axis, a vertical axis with its origin at the bottom
S_c	- depth from wave crest - distance of free surface measured from the bottom to the wave crest when the crest is at the pile
S_r	specific gravity of armor unit based on the unit weight of water at the structure; w_r/w_w
S_s	depth from soffit to bottom
S_t	depth from wave trough
S_θ	distance of free surface measured from the bottom at an arbitrary wave-phase angle, θ
$\sim S_\theta$	subscript S_θ refers to values at an arbitrary wave-phase angle, θ
S_θ/d	relative free surface
T	wave period
T_a	air temperature
T_P	wave period associated with the highest peak of the wave spectrum ("peak spectral period")
T_s	water temperature
t	- time - wind duration
U_A	final adjusted windspeed used for hindcasting
U_L	overland windspeed, adjusted for elevation and duration
$U_{t=\text{desired duration}}$	windspeed at desired duration, adusted for elevation and duration
$U_{t=\text{given duration}}$	windspeed at given duration, adjusted for elevation
U_W	overwater windspeed, adjusted for elevation and duration
U_z	windspeed at elevation z
U_{10}	windspeed at elevation of 10 meters
U'_A	windspeed corrected for nonconstant drag coefficient
u	instantaneous horizontal water-particle velocity
u_m	approximate maximum horizontal water-particle velocity
W	weight of individual armor unit or stone in layer of interest
W	parameter used in pile force and moment calculations
W_b	weight of back-slope armor unit
W_f	weight of front-slope armor unit
W_{50}	weight of 50-percent size of armor riprap gradation (50 percent of the material weighs W_{50} or more)
w	armor-stone weight
w	unit weight
w_r	unit weight of armor material (saturated surface dry)
w_w	unit weight of water (64 pounds per cubic foot for salt water)
x	coordinate axis in direction of wave propagation relative to wave crest
x_1	distance from still water level (SWL) to structure shoreward of still water level
x_2	distance from still water level (SWL) to limit of wave uprush
z	elevation of recorded wind
z	- vertical distance along a coordinate axis with its origin at still water level (SWL) (Section 1)
	- depth in terms of vertical distance along a coordinate axis with its origin at the bottom (Sections 5 and 7)
z_B	distance of center of beam above bottom
z_i	distance above bottom of point i
z_{mD}	lever arm; distance of point of application of drag force above bottom
z_{mDI}	lever arm for drag and inertial force
z_1	depth from point 1
z_2	depth from point 2
α	angle between wave crest and bottom contour
α	angle between axis of wall and direction of wave approach
α	angle of incidence
α_m	coefficient used in determinination of maximum total moment on pile
α'	reflection-coefficient reduction factor (for multiple armor layers)
α, β	empirically derived constants which depend on structure type, water depth at structure toe, roughness of slope, number of armor layers, and breaking-wave height
β	angle of beach slope with horizontal
γ	unit weight of armor stone
Δ	spacing between adjacent piles
Δx	spacing between piles in the direction of wave advance (that is, along the x-coordinate axis)
Δz	unit length of pile
$\Delta\theta$	phase difference between piles
η	water-surface elevation at a given point relative to the still water level (SWL)
η_c	water-surface elevation at wave crest relative to still water level (SWL)
η_c/H	relative wave-crest elevation above still water level (SWL)
θ	angle of structure slope measured relative to the horizontal
θ	wave-phase angle
θ_{Fm}	wave-phase angle for which total force is maximum

θ_{Mm} wave-phase angle for which total moment is maximum

cot θ cotangent of structure-slope angle, θ

tan θ tangent of structure-slope angle, θ

ν kinematic viscosity (approximately 1 x 10^{-5} $feet^2$ per second for salt water)

ξ surf-similarity parameter

π constant = 3.14159

ρ density of water (2.0 slugs per $foot^3$ for salt water)

$(\tau_{DM})_{z=z_1}$ linear drag moment coefficient

$(\tau_{DMC}\Psi_D)$ factor used in determining drag moment

$(\tau_D)_z$ drag-moment coefficient

$(\tau_I)_z$ inertial-moment coefficient

$(\tau_{IM})_{z=z_1}$ linear inertial moment coefficient

ϕ angle of wave approach relative to breakwater

ϕ_D drag-force correction factor for nonlinear velocity and acceleration fields

ϕ_{DM} a nonlinear correction factor

ϕ_I inertial-force correction factor for nonlinear velocity and acceleration fields

ϕ_{IM} nonlinear inertial-force correction factor for maximum inertial force

Ψ_m coefficient used in determination of maximum total force on piles

Ψ_D drag-moment correction factor for nonlinear velocity and acceleration fields

Ψ_{DM} a nonlinear correction factor

Ψ_I inertial-moment correction factor for nonlinear velocity and acceleration fields

Ψ_{IM} nonlinear inertial-moment correction factor for maximum inertial moment

COASTAL SEDIMENTATION AND DREDGING

Department of the Navy
Naval Facilities Engineering Command
December 1981

EDITORS NOTE

This chapter, based on the U.S. Navy manual DM 26.3, is one of a series of Navy guide publications relating to harbors and coastal facilities which we have selected for re-printing. The material presented in this manual focuses on the littoral transport of soil, and the affect of this natural process upon existing or proposed harbors. Formulas are presented for predicting transport rates under various circumstances, and sample problems are solved.

The function of control structures such as breakwaters, jetties, and groins and their application to these problems are also well covered. Finally, the manual discusses dredging equipment and procedures for clearing channels and harbors of littorally deposited sediment.

ABSTRACT

Design and planning guidelines are presented for the layout of harbors where coastal and estuarine sedimentation are factors. Section 1 is an introduction. Section 2 includes basic principles of sedimentation, harbor siting, and shore protection. Section 3 gives planning considerations for dredging works and discusses general dredge types.

Section 1. INTRODUCTION

1. SCOPE. This manual presents general phenomena involved in and planning guidelines for the construction of harbors in regions prone to coastal and estuarine sedimentation problems. Discussed are basic principles of sedimentation, harbor siting, and shore protection, along with planning considerations for dredging works. General dredge types are also described.

2. CANCELLATION. This manual, NAVFAC DM-26.3, Coastal Sedimentation and Dredging, cancels and supersedes Chapter 3 and portions of Chapters 1 and 2 of the basic Design Manual 26, Harbor and Coastal Facilities, dated July 1968, and Change 1, dated December 1968.

3. RELATED CRITERIA. Certain criteria related to coastal sedimentation and dredging appear elsewhere in the design manual series. See the following sources:

Subject	Source
Coastal Sedimentation	
Coastal protection	DM-26.2
Harbors	DM-26.1
Pollution control	DM-5.8
Soil mechanics	DM-7
Dredging	
Dredges and dredge capabilities	DM-38
Dredging records	DM-6
Geometric requirements	DM-26.1
Hydrographic surveys	DM-5
Jurisdiction over navigable waters	DM-26.1
Subsoil exploration	DM-7

4. COLLATERAL READING.

(1) Shore Protection Manual, U.S. Army Coastal Engineering Research Center, 3d ed., Vols. I, II, and III, Stock No. 008-022-00113-1, U.S. Government Printing Office, Washington, D.C., 1977.

(2) Vanoni, V.A., Editor; Sedimentation Engineering, ASCE, Manuals and Reports on Engineering Practice, No. 54, Prepared by the ASCE Task Committee for the Preparation of the Manual on Sedimentation of the Sedimentation Committee of the Hydraulics Division, American Society of Civil Engineers, New York, NY, 1977.

(3) Wicker, C.F.; Evaluation of Present State of Knowledge of Factors Affecting Tidal Hydraulics and Related Phenomena, Report No. 3, Committee on Tidal Hydraulics, Corps of Engineers, U.S. Army, Vicksburg, MS, May 1965.

Section 2. COASTAL SEDIMENTATION AND EROSION

1. GENERAL. This section addresses general concepts of coastal sedimentation and erosion and their application to design and construction in coastal areas. Soil classification, transport potential, littoral processes, the siting of harbors on open, sandy coasts, in inlets, and in estuaries, as well as shore protection, are discussed.

2. BASIC CONSIDERATIONS. Sediment transport and deposition occur on open coasts, in tidal inlets, in estuaries, in harbors, and in rivers. The types of sedimentation problems that occur at each of these locations depend on the soil type, continuity of materials and the potential for fluid motion to transport the material. Soil classification, the principle of continuity, and an analysis of transport potential are presented in the following subsections.

a. Soil Classification. Sediments can be classified as cohesionless or cohesive. Cohesionless sediments include boulders, cobbles, gravel, sand, and some silts. They generally are found on open coasts, in tidal inlets, and in upper reaches of fluvial channels where there is high-velocity flow.

Cohesive sediments include some silts, clays, and organic materials. These sediments are generally found in estuaries, harbors, and rivers, or where lower-velocity flow is prevalent. Cohesive sediments bind together by molecular forces and deform plastically. In estuaries, suspended clay particles bind with one another to form a larger mass which eventually can settle as a group.

Table 1 gives a classification of soils according to grain size. Two methods of classification are provided: the Wentworth Scale and the Unified Soil Classification. The Wentworth Scale is based on a phi-unit (Ø) scale, where phi units are defined as:

$$\emptyset = -\log_2 d \qquad (2\text{-}1)$$

WHERE:
d = grain diameter, in millimeters

The Unified Soil Classification is based on U.S. Standard Sieve sizes. In engineering practice, it is common to classify the sediment by its median grain size. The median grain size is the size in millimeters that divides the sediment sample so that half the sample, by weight, has particles coarser than that size.

TABLE 1
Grain-Size Scales for Soil Classification

Wentworth Scale (Size Description)		Phi Units $^1\phi$	Grain Diameter d (mm)	U.S. Standard Sieve Size	Unified Soil Classification (USC)	
Boulder		-8	256		Cobble	
Cobble			76.2	3 in		
Pebble		-6	64.0		Coarse	Gravel
			19.0	3/4 in		
			4.76	No. 4	Fine	
Granule		-2	4.0		Coarse	Sand
Sand	Very Coarse	-1	2.0	No. 10		
	Coarse	0	1.0		Medium	
	Medium	1	0.5			
			0.42	No. 40		
	Fine	2	0.25		Fine	
	Very Fine	3	0.125			
			0.074	No. 200		
Silt		4	0.0625		Silt or Clay	
		8	0.00391			
Clay		12	0.00024			
Colloid						

$^1\phi = -\log_2 d$, where d = diameter, in millimeters

(SHORE PROTECTION MANUAL, 1977)

b. Continuity. The principle of continuity of sediments is based to sedimentation problems. Continuity accounts for the conservation of sediment materials throughout a region of study in a given time period. Given a control volume as shown in Figure 1, the outflux, Q_{out}, of material moving out of the control volume must equal the influx, Q_{in}, minus the amount stored, $+Q_{stored}$, or eroded, $-Q_{stored}$. If the Q_{in} equals Q_{out}, then a stability is achieved and the control volume contains a constant amount of material. This state of stability is referred to as a "dynamic equilibrium." Examples of dynamic equilibria are a beach of constant width and a channel of constant cross section. On the other hand, if material is stored, the beach accretes or the channel section decreases. If material is eroded, the beach decreases in width or the channel section increases.

A balance of material must always be accounted for in all analyses of sediments within a control volume. Sources and sinks may exist, which must be accounted for in the balance of material. A source is defined as any process that increases the quantity of sediment in a defined control volume. Examples of sources are: rivers, streams, discharge of dredged materials, discharge of human and industrial wastes, and erosion of dunes and cliffs. A sink is defined as any process that decreases the quantity of sediment in a defined control volume. Examples of sinks are: submarine canyons, inlets, offshore sand transport, and removal of dredge material. When considering sources and sinks, one must consider the potential transport of material in and out of the control volume. However, when the principle of continuity is invoked, it is the difference of transport into and out of the control volume that is important, not the absolute values..

c. Transport Potential. Transport potential is the amount of material that a flow of water can move provided there is material available to be moved. The principle of continuity must be invoked to ensure that the material for transport is available. The transport rate is the actual amount of material moved per unit time into or out of the control volume. Transport results because a flow of water over a bed of sediment produced a tractive force on the sediment which acts

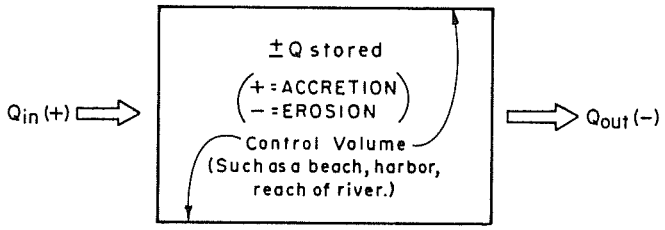

WHERE: Q = volume of sediment transported per unit time

Q_{in} = influx

Q_{out} = outflux

$+Q_{stored}$ = deposition or accretion

$-Q_{stored}$ = scouring or erosion

IF $Q_{in} > Q_{out}$, sediment will deposit or accrete in control volume

IF $Q_{in} < Q_{out}$, sediment will be scoured or eroded from control volume

IF $Q_{in} = Q_{out}$, the control volume is in a state of dynamic equilibrium

FIGURE 1
Control-Volume Approach to Sediment Continuity

to dislodge and move the sediment particles. The transport rate is a function of the material type, material availability, and power available in the flow to move the material. In general, it is the weight of cohesionless particles which resists the tractive force produced by the flowing fluid. On the other hand, sediments which contain significant fractions of cohesive soils resist the tractive force more by cohesion than by weight. Tractive forces include wind, stream flow, waves and wave-induced currents, tidal-induced currents in inlets, and estuarine flows (these include density currents, tidal currents, and currents which result from reversing flows in curved sections of the estuary and Coriolis forces induced by the earth's rotation). These mechanisms will be discussed in subsequent paragraphs.

Movement of sediment by water generally falls into two basic categories: bedload and suspended load. Bedload is moved along the bottom by rolling and bouncing motions. Suspended load is material suspended in the water column by the turbulence of the water motion. For a given flow condition, fine, cohesionless material is more likely to be carried in suspension than a coarse, cohesionless or a cohesive material

(1) Initiation of Motion of Cohesionless Sediments. The initiation of motion of cohesionless bed sediments has been related to bed shear stress or tractive force under steady, uniform-flow conditions. The bed shear stress, τ_o, is defined as follows:

$$\tau_o = \gamma_w R S \qquad (2\text{-}2)$$

WHERE:

τ_o = bed shear stress, in pounds per square foot

γ_w = unit weight of water, in pounds per cubic foot

R = hydraulic radius of channel, in feet (R is equal to channel depth, d_c, for a very wide channel)

S = channel slope

The bed shear stress, t_o, may be related to the mean channel velocity, $\overline{V}$, as follows:

$$\overline{V} = \sqrt{C_h \frac{\tau_o}{\gamma_w}} \qquad (2\text{-}3)$$

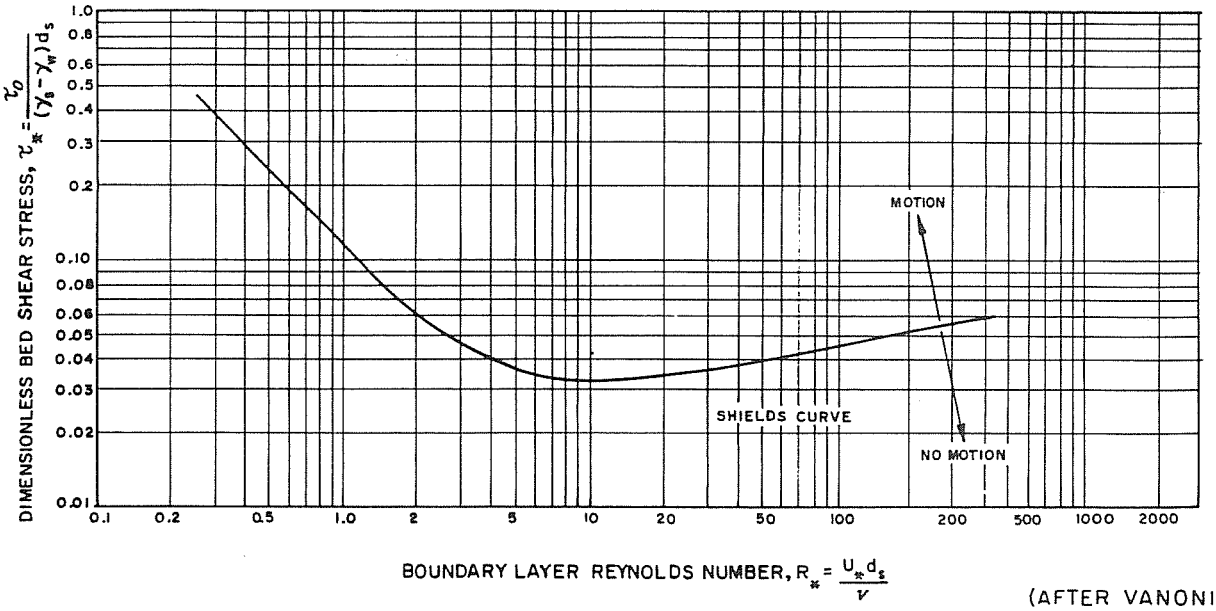

(AFTER VANONI, 1977)

FIGURE 2
Shields Diagram: Dimensionless Bed Shear Stress Versus the Boundary Layer Reynolds Number

WHERE:

$\overline{V}$ = mean channel velocity, in feet per second
C_h = Chezy coefficient
τ_o = bed shear stress, in pounds per square foot
γ_w = unit weight of water, in pounds per cubic foot

The bed shear stress on a cohesionless sediment of given size increases as the flow velocity increases. A critical point is reached at which the bed shear is sufficient to move a given bed sediment. Figure 2 is a graph of the dimensionless bed shear stress, τ_*, versus the boundary layer Reynolds number, R_*. These two parameters, τ_* and R_*, are defined as follows:

$$\tau_* = \frac{\tau_o}{(\gamma_s - \gamma_w)\, d_s} \qquad (2\text{-}4)$$

WHERE:

τ_* = dimensionless bed shear stress
τ_o = bed shear stress as defined by Equation (2-2), in pounds per square foot
γ_s = unit weight of bed sediment, in pounds per cubic foot
γ_w = unit weight of water, in pounds per cubic foot
d_s = diameter of bed sediment, in feet

$$R_* = \frac{U_*\, d_s}{\nu} \qquad (2\text{-}5)$$

WHERE:

R_* = boundary layer Reynolds number
U_* = $\sqrt{\tau_o/\rho}$ = shear velocity, in feet per second
ρ = density of water, in slugs per cubic foot
d_s = diameter of bed sediment, in feet
ν = kinematic viscosity of water, in square feet per second

Also plotted on Figure 2 is the Shields curve, which separates the regions of motion and no motion for cohesionless sediments.

The use of Figure 2 is illustrated in the example which follows.

EXAMPLE PROBLEM 1

Given:
a. A channel with hydraulic radius R = 5 feet
b. Channel slope, S = 0.00015
c. Diameter of bed sediment, d_s = 0.003 feet
d. Unit weight of water, γ_w = 62.4 pounds per cubic foot
e. Unit weight of bed sediment, γ_s = 165 pounds per cubic foot
f. Kinematic viscosity of water, ν = 1.08×10^{-5} square feet per second
g. Density of water, ρ = 1.94 slugs per cubic foot

Find: Determine whether sediment will move.

Solution: (1) Using Equation (2-2), find τ_o;

$$\tau_o = \gamma_w R S$$

$$\tau_o = (62.4)(5)(0.00015)$$

$$\tau_o = 0.0468 \text{ pounds per square foot}$$

(2) Using Equation (2-5), find R_*:

$$R_* = \frac{U_* d_s}{\nu}$$

WHERE: $U_* = \sqrt{\tau_o/\rho} = \sqrt{\frac{0.0468}{1.94}} = 0.155$ feet per second

$$R_* = \frac{(0.155)\, d_s}{\nu} = \frac{(0.155)(0.003)}{1.08 \times 10^{-5}} = 43.06$$

(3) Using Equation (2-4), find τ_*:

$$\tau_* = \frac{\tau_o}{(\gamma_s - \gamma_w)\, d_s}$$

$$\tau_* = \frac{0.0468}{(165 - 62.4)(0.003)} = 0.152$$

(4) On Figure 2, find the point of intersection of τ_* and R_*. This point is above the Shields curve for the values of τ_* and R_* determined above; therefore, the sediment will move.

Because of variations in material shape and size, grain-size distribution, and water-flow characteristics, there exist numerous empirical and theoretical relationships between unidirectional stream fluid flow and sediment transport capacity. These relationships have produced scatter in their quantitative predictions of transport; this scatter is indicative of the complexity of the phenomena involved.

(2) Initiation of Motion of Cohesive Sediments. A

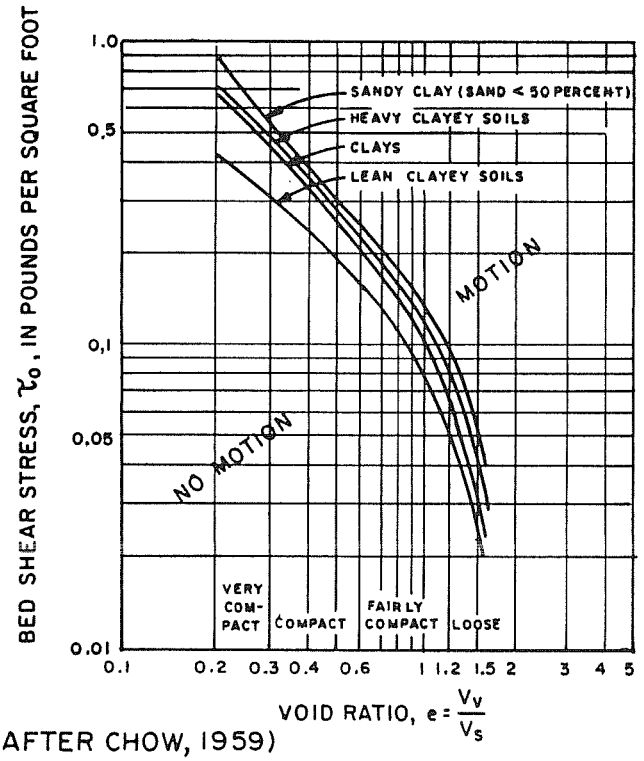

(AFTER CHOW, 1959)

FIGURE 3
Critical Bed Shear Stress Required to Initiate Scour of Cohesive Sediments in Canals

sediment will have cohesive properties when it contains significant portions of silts and clays. Cohesive sediments are more resistant to bed shear stress than cohesionless soils. The behavior of cohesive sediments under fluid flow is complex and depends no only on the flow regime but also on the electrochemical properties of the sediments. Little is known of the critical bed shear stress required to initiate scour of cohesive sediments, but a preliminary procedure is provided below. Estimates of the critical bed shear stress required to initiate scour of cohesive sediments in canals are given in Figure 3. This figure shows that the critical bed shear stress is a strong function of the void ratio of the sediment and of the sediment type.

The void ratio, e, is defined as follows:

$$e = \frac{V_v}{V_s} \qquad (2\text{-}6)$$

WHERE:

e = void ratio
V_v = volume of voids
V_s = volume of solids

The use of Figure 3 is illustrated in the example which follows.

EXAMPLE PROBLEM 2

Given: a. A channel, with clay bed sediment, with hydraulic radius R = 5 feet
b. Channel slope, S = 0.00015
c. Void ratio, e = 0.56
d. Unit weight of water, γ_w = 62.4 pounds per cubic foot

Find: Determine whether the sediment bed will erode under the flow condition.

Solution: (1) Using Equation (2-2), find τ_o:

$$\tau_o = \gamma_w R S$$

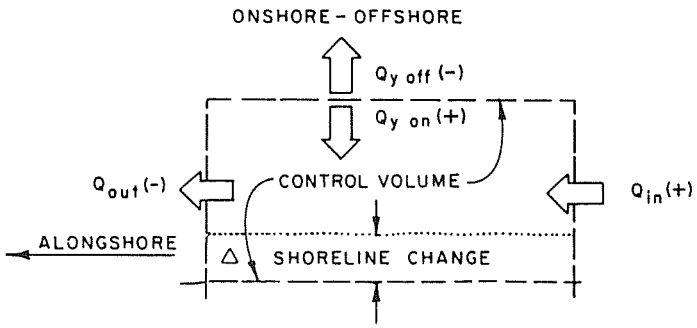

FIGURE 4
Control Volume for a Littoral Transport Budget

τ_o = (62.4)(5)(0.00015)

τ_o = 0.0468 pounds per square foot

(2) From Figure 3 for e = 0.56, it can be seen that this flow condition is not sufficient to erode the bed.

Note: The same flow condition which erodes the cohesionless sediment is not capable of eroding the cohesive sediment.

3. **HARBOR SITING.** Consideration should be given to sedimentation when siting a harbor on an open-coastal littoral system, in an inlet system, or in a river-mouth estuary system. In each of these systems, the various factors of transport capacity and sediment supply must be taken into account. A natural equilibrium may be evidence by unchanging channel depths or stable shoreline positions. Conversely, gradual and long-term sedimentation or erosion processes may be occurring.

a. Littoral Processes. Siting a harbor on the shore of any large body of water where wave action is present involves understanding and taking into account littoral processes and their possible effects on the entrance. The continuity relationship for a given length of beach is illustrated in Figure 4.

Littoral transport is the movement of littoral material, such as sand along or across a beach, due to the interaction of wind, waves, and currents with sediments. Littoral transport on a beach differs from that in a river in that, on a beach, oscillatory wave-induced motions play a significant role in initiating sediment-movement force. The turbulence of breaking waves entrains material in the water column, where it is susceptible to transport by currents. Wave action moves sediments up, down, towards, and away from the beach, tending to establish a beach and offshore profile that is in a state of quasi-equilibrium with the forces induced by water motion and gravity. As the incident wave conditions change, the beach profile and plan forms change to a new equilibrium condition. Material can move onshore, offshore, or alongshore, depending on the wave conditions relative to the beach conditions.

Longshore transport is the movement of sediments parallel to the beach. When a wave approaches the shoreline at an oblique angle, longshore currents landward of the breaker line result. These currents, generated by the longshore component of momentum of the fluid entering the surf zone, transport suspended sediments in the alongshore direction. Figure 5 shows the longshore-current velocity profile, which indicates a maximum value at some distance landward of the breaker line. Figure 5 also shows the zigzag transport of material along the beach face. This zigzag pattern results from the superposition of the flow of wave uprush on the beach face with the longshore current.

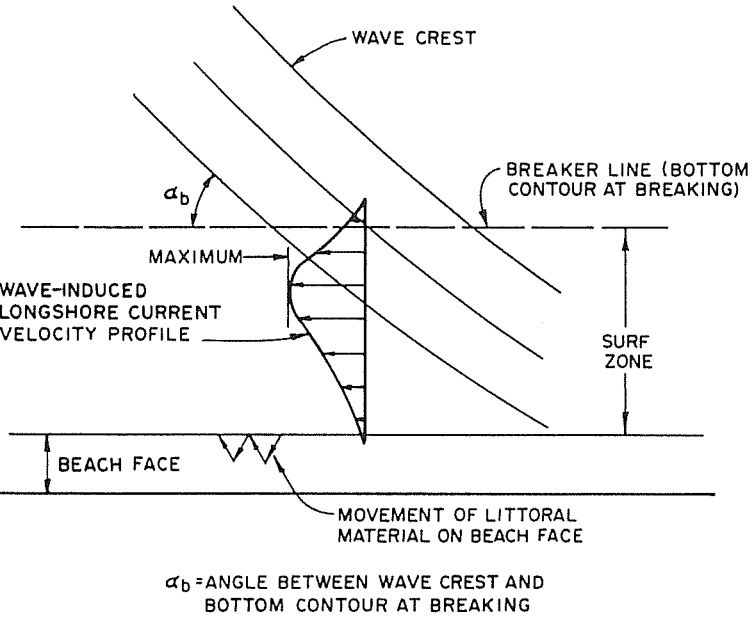

FIGURE 5
Longshore-Current Velocity Profile

Because longshore transport is a function of the breaking-wave climate and because the wave climate varies as a function of meteorological events, the longshore transport rate on a beach varies on a daily basis. Wave energy generally arrives from different meteorological sources during different seasons of the year. This seasonal variation in wave energy will change the longshore transport and offshore transport rates and may also change their directions. Hence, the rate and direction of material movement can be characterized by seasons. The term "gross transport" is the absolute value of littoral transport in all directions. The term "net transport" is the difference in littoral transport in each direction both up and down the coast. The direction of net longshore transport is called the "downdrift" direction and the direction from which material is arriving is called the "updrift" direction. Gross transport material can be trapped in a harbor entrance channel, whereas net transport can accumulate in the area on the updrift side of a jetty and erode from the area on the downdrift side.

Offshore and beach profiles adjust to the incident-wave conditions. High, steep storm waves tend to pull material off the beach and deposit it offshore in a bar. This results in what is often called a storm or winter profile. Low-height, long-period swell tends to move sediment back onto the beach. The result is often called the summer profile. Examples of winter and summer profiles are shown in Figure 6. This adjustment to the seasonal wave climate is one form of onshore and offshore movement. Quantification of this movement is difficult within the present state of knowledge. It is important to note that surveys made in shoreline studies for comparative purposes should be conducted at the same time of the year.

Another form of onshore and offshore transport is due to a winnowing process whereby material is sorted by wave action. Fine material is carried offshore, while coarse material remains on the beach. This phenomenon can occur during a beach-nourishment project as well as near a river delta which supplies sediment to the beach.

The wind can also transport material onshore, alongshore, or offshore. Fine-grained sands tend to be more susceptible to wind transport. Strong, predominant, onshore winds transport sand shoreward to form sand dunes. Sand can also be transported alongshore to shoal in channels or inlets.

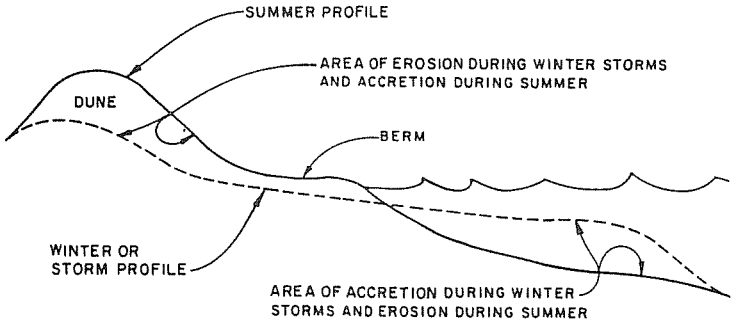

FIGURE 6
Summer and Winter Beach Profiles

(1) Prediction of Longshore Transport. The potential longshore-transport rate on an open coast has been empirically linked to the longshore component of wave-energy flux reaching any given shore segment or control volume. A widely used method of calculating the potential longshore-transport rate, Q, is the SPM formula:

$$Q = K P_{ls} \qquad (2\text{-}7)$$

WHERE:

Q = potential longshore-transport rate, in cubic yards per year

K = an empirical constant (7.5×10^3)

$$P_{ls} = \frac{\rho g}{16} H_b^2 C \sin 2\alpha_b$$

= longshore component of wave-energy flux in the surf zone, in foot-pounds per second per foot of shoreline (2-8)

ρ = density of water in slugs per cubic foot

g = gravitational acceleration (32.2 feet per second^2)

H_b = wave height at breaking, in feet

C = wave-phase velocity at breaking, in feet per second

α_b = angle between wave crest and bottom contour at breaking

The various parameters are illustrated graphically in Figure 7.

The various steps involved in the prediction of longshore transport are as follows:

(1) Obtain offshore wave data information from sources described in DM-26.2. These data must include a tabulation of incremental wave heights and periods by percent of annual occurrence for each deepwater sector approach of direction.

(2) Prepare refraction diagrams for each wave period and direction tabulated in the offshore wave data and determine refraction effects to a region near the shoreline reach. (See DM-26.2.)

(3) Compute breaking-wave height and depth for each offshore wave-height increment. (See DM-26.2).

(4) Using refraction diagrams, compute the longshore component of energy flux and wave direction at breaking for each wave-height increment.

(5) Compute the gross potential longshore transport rate using each direction, and subtract the smaller (updrift) from the larger (downdrift) value to obtain an estimate of the net potential longshore transport rate in the downdrift direction.

A simplified example of this procedure is given in Example Problem 3.

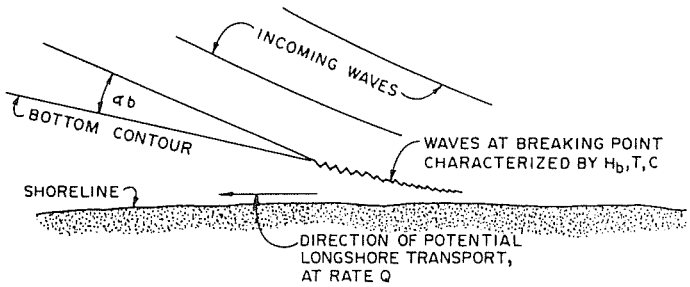

H_b = WAVE HEIGHT AT BREAKING

T = WAVE PERIOD

C = WAVE-PHASE VELOCITY AT BREAKING

α_b = ANGLE BETWEEN WAVE CREST AND BOTTOM CONTOUR AT BREAKING

FIGURE 7
Illustration of Parameters Involved in Calculating Potential Longshore-Transport Rate

EXAMPLE PROBLEM 3

Given:
a. Breaking-wave height, H_b = 10.0 feet
b. Angle between wave crest and shoreline at breaking, $\alpha_b = 45°$
c. Wave-phase velocity, C = 20.3 feet per second
d. Density of water, ρ = 2.0 slugs per cubic foot
e. Gravitational acceleration, g = 32.2 feet per second^2
f. Repeat problem for H_b = 3.0 feet and C = 11 feet per second

Find: The potential longshore-transport rate for the two given wave conditions.

Solution: (1) Using Equation (2-8), find P_{ls}:

$$P_{ls} = \frac{\rho g}{16} H_b^2 C \sin 2\alpha_b$$

$$P_{ls} = \frac{(2.0)(32.2)}{16} (10.0)^2 (20.3) \sin 2(45°)$$

P_{ls} = 8,170.8 foot-pounds per second per foot

(2) Using Equation (2-7), find Q:

$Q = K P_{ls}$

$Q = (7.5 \times 10^3)(8,170.8)$

$Q = (7.5 \times 10^3)(8,170.8)$

Q = 61,281,000 cubic yards per year

Repeat steps (1) and (2) for H_b = 3.0 ft and C = 11:

(1) Using Equation (2-8), find P_{ls}:

$$P_{ls} = \frac{(2.0)(32.2)}{16} (3.0)^2 (11) \sin 2(45°)$$

P_{ls} = 398.48 foot-pounds per second per foot

(2) Using Equation (2-7), find Q:

$Q = (7.5 \times 10^3)(398.48)$

Q = 2,988,600 cubic yards per year

Note: This value, for the 3-foot breaking-wave height, is approximately 5 percent of that for the 10-foot breaking-wave height. This difference in transport capacity indicates the potential for storm events to move large amounts of material.

(2) Littoral Transport Determined From Historical Shoreline Changes. Determination of the littoral-transport rate from historical records involves review of shoreline changes caused by a discontinuity along a reach of shoreline. Examples of shoreline discontinuities are groins, jetties, tidal inlets, and harbor entrances. Analysis of shoreline changes in the vicinity of discontinuities may be achieved through analysis of beach surveys, charts, aerial photographs, or records of dredging tidal inlets. Analysis of historical shoreline changes will give a true indication of the transport rate only until the shoreline

TABLE 2
Longshore-Transport Rates at Selected Coastal Locations

Location	Predominant Direction of Transport	Longshore Transport[1] (cu yd/yr)	Date of Record
Atlantic Coast			
Suffolk County, NY	W	200,000	1946-55
Sandy Hook, NY	N	493,000	1885-1933
Sandy Hook, NY	N	436,000	1933-51
Asbury Park, NJ	N	200,000	1922-25
Shark River, NJ	N	300,000	1947-53
Manasquan, NJ	N	360,000	1930-31
Barneget Inlet, NJ	S	250,000	1939-41
Absecon Inlet, NJ[2]	S	400,000	1935-46
Ocean City, NJ[2]	S	400,000	1935-46
Cold Spring Inlet, NJ	S	200,000	....
Ocean City, MD	S	150,000	1934-36
Atlantic Beach, NC	E	29,500	1850-1908
Hillsboro Inlet, FL	S	75,000	1850-1908
Palm Beach, FL	S	150,000-225,000	1925-30
Gulf of Mexico			
Pinellas County, FL	S	50,000	1922-50
Perdido Pass, AL	W	200,000	1934-53
Pacific Coast			
Santa Barbara, CA	E	280,000	1932-51
Oxnard Plain Shore, CA	S	1,000,000	1938-48
Port Hueneme, CA[3]	S	1,000,000	....
Santa Monica, CA	S	270,000	1936-40
El Segundo, CA	S	162,000	1936-40
Redondo Beach, CA	S	30,000	....
Anaheim Bay, CA[2]	E	150,000	1937-48
Camp Pendleton, CA	S	100,000	1950-52
Great Lakes			
Milwaukee County, WI	S	8,000	1894-1912
Racine County, WI	S	40,000	1912-49
Kenosha, WI	S	15,000	1872-1909
IL State Line to Waukegan	S	90,000	....
Waukegan to Evanston, IL	S	57,000	....
South of Evanston, IL	S	40,000	....
Hawaii			
Waikiki Beach, HI[2]	...	10,000	....

[1] Transport rates are estimated net transport rates. In some cases, these approximate the gross transport rates.

[2] Method of measurement is by accretion except for Absecon Inlet, NJ, Ocean City, NJ, and Anaheim Bay, CA, (by erosion) and Waikiki Beach, HI, (by suspended load samples).

[3] Reference for Port Hueneme, CA, is U.S. Army (1980).

(SHORE PROTECTION MANUAL, 1977)

discontinuity ceases to trap all the material that reaches it. A useful rule of thumb used in the analysis of historical shoreline changes on open coasts is that a loss or gain of 1 square foot of beach area of the berm is equivalent to the loss or gain of 1 cubic yard of beach material from that same area.

(3) Reliability of Predicted Longshore-Transport Rates. The estimates of littoral-transport rates derived by energy-flux calculation or by poorly defined measurements at littoral barriers are approximations. Although analysis of historical shoreline changes may provide a higher level of confidence, underestimation of the transport rate has not been uncommon in past practice. Where accuracy is critical to project development, construction and monitoring of a test groin to verify the estimate should be considered. However, the test groin must extend seaward far enough to trap all the littoral material.

Table 2 provides general estimates of longshore-transport rates at selected U.S. coastal locations. These rates are often modified when additional studies are conducted. The primary source for measured littoral-transport rates is the local District Office of the U.S. Army Corps of Engineers.

b. Harbor Entrances on Open Coasts.

(1) Shoreline Response. Harbors located on or near an open coast often require the construction of a jettied entrance

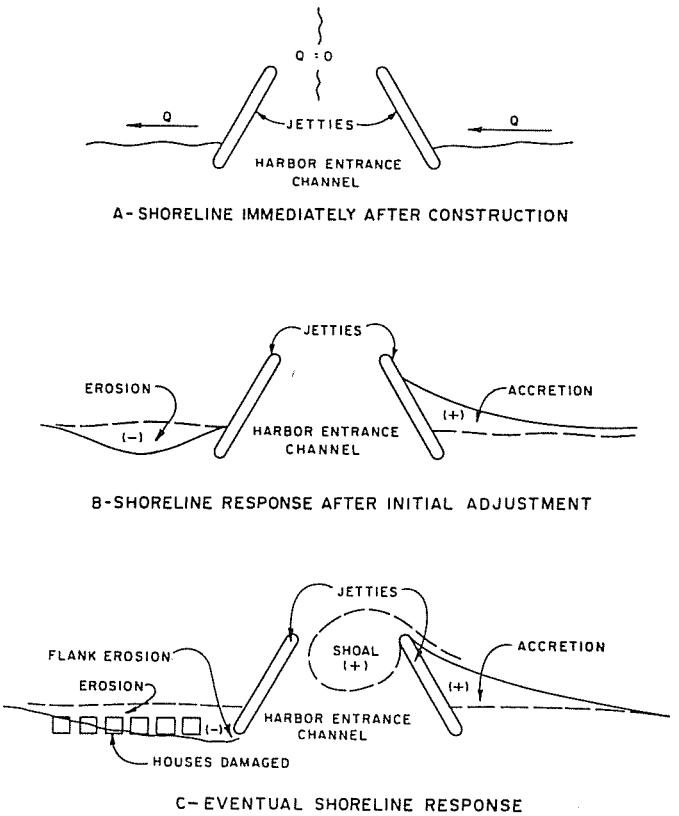

FIGURE 8
Progression of Shoreline Response After Construction of a Jettied Harbor Entrance on an Open Coast

channel. Jetties serve to stabilize the position of the entrance, keep littoral material from entering the navigation channel, modify tidal currents in the channel, and reduce wave action within the channel. The jettied entrance channel will interrupt the natural transport of littoral material alongshore. This is particularly apparent and has adverse effects when there is a predominant direction of longshore transport. Interruption of the longshore transport results in modifications of the shoreline both up- and downdrift of the entrance. Figure 8 (A through C) shows the progression of shoreline response after the construction of a jettied harbor entrance on a coast with a predominant direction of longshore transport. Immediately after construction is completed, the littoral transport across the entrance is completely blocked, as shown in Figure 8A. In time sand accretes, forming a fillet on the updrift side of the entrance. Accompanying this accretion is erosion downdrift of the entrance, resulting from the lack of material supplied from the updrift coast (see Figure 8B.) Eventually, the updrift fillet accretes past the seaward end of the jetty and material forms a shoal in the navigation channel, as shown in Figure 8C. Further erosion downdrift of the entrance may cause property damage. The downdrift erosion may also cause flank erosion, which is erosion past the landward end of the downdrift jetty. The extent and rate of updrift accretion, channel shoaling, and downdrift erosion depend on longshore-transport rate and the hydraulics of the entrance-channel system.

(2) Sand Bypassing at Harbor Entrances. The sedimentation problems associated with harbor entrances on open coasts where there is a predominant direction of

longshore transport are often mitigated by physically transferring littoral material across the entrance in a process referred to as sand bypassing. A properly managed bypassing scheme, incorporating an efficient bypassing system, will provide the needed littoral material to the downdrift beach and will prevent the eventual shoaling of the navigation channel. In general, an investigation of several sand-bypassing systems is necessary to determine the most feasible solution. the possibility of reversals in transport direction needs to be taken into consideration in the investigation. Several sand-bypassing systems are discussed below.

(a) Land-based dredge plant. This system generally consists of dredging the updrift fillet using a clamshell, and trucking the material to the downdrift side. Unlike some of the other systems, this is a mobile system and access throughout the updrift "impoundment" area is often possible. If this system can be employed, all the littoral material may be stopped from reaching the entrance channel. This method can be very effective; however, it becomes cost-prohibitive if long hauling distances are involved.

(b) Fixed hydraulic dredging plant. This method consists of a hydraulic pumping system permanently fixed on the updrift jetty in a region where littoral material is expected to accumulate. The pumping system will pump material from the updrift side and discharge it on the downdrift side. Detailed study of the longshore-transport rate (short-term extremes and average annual rates) is necessary to ensure that the pumping capacity of the system is not exceeded. If the capacity of the pump is exceeded regularly, adequate amounts of sand will not be provided to the downdrift shore. Furthermore, excess accretion on the updrift side may result in loss of material around the seaward end of the jetty. Analysis of littoral processes should also be made to determine the best position for the pumping system along the updrift beach profile and for the discharge pipe on the downdrift beach. If the pumping system is placed too far seaward, it will not pump enough material downdrift. If the pumping system is placed too far landward, sediment may be lost around the jetty. The downdrift discharge pipe must be positioned such that discharged material is not lost offshore or carried back towards the entrance.

(c) Floating Suction or pipeline dredge. This method for bypassing is efficient, but provides high production rates only as long as the dredge is protected from wave activity. With some entrance configurations, a suction dredge can use the entrance structures for wave protection.

(d) Seagoing hopper dredge. A hopper dredge can be used for a bypassing operation. The primary advantage of the hopper dredge is that it can be operated in the open ocean. In general, unless it has pump-out capability, a hopper dredge cannot be used unless it can discharge in an area where the material can be rehandled by another type of dredge.

(e) Jet eductor. An eductor, or jet-pump, system is a recent development in sand-bypassing methods. Clear, high-pressure water is pumped to a nozzle which converts it into a high-velocity, low-pressure jet stream. The suction created by the partial vacuum induced by the jet entrains sand, which is mixed with the water jet and discharged through a pipeline. The sand and water mixture is then pumped to the downdrift beach, aided by a booster pump. The basic principle of operation has been to lower an eductor into the sand and allow the eductor to excavate a crater. Wave action and currents theoretically feed the crater. While the system is promising, its effectiveness is not entirely known and it is currently still in a developmental stage.

(3) Entrance Configurations. Figure 9 shows examples of harbor entrance configurations where sand bypassing has been

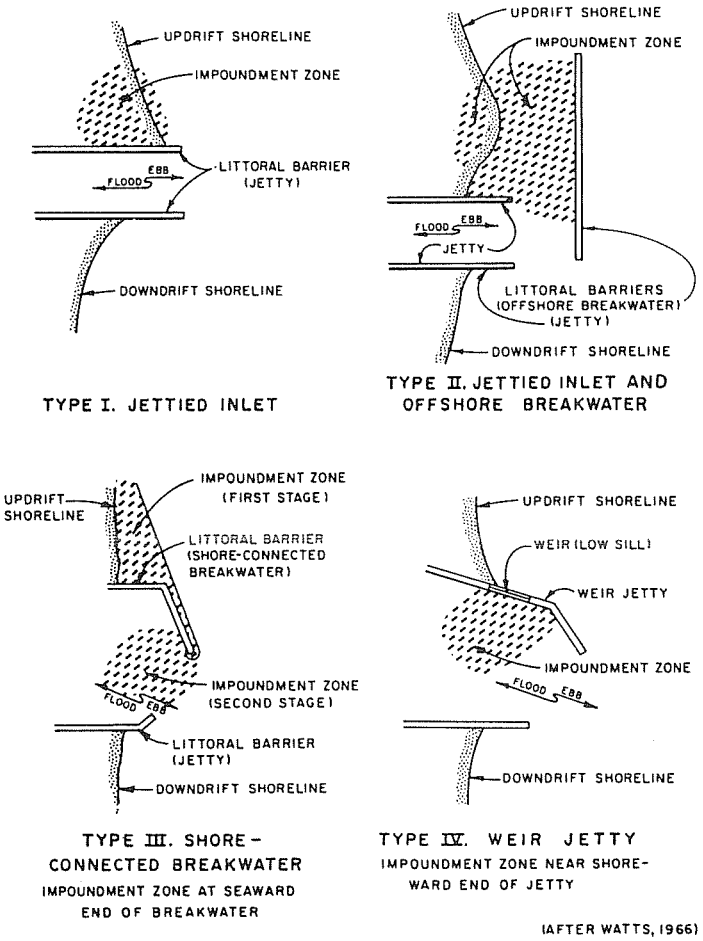

FIGURE 9
Harbor-Entrance Configurations

carried out in the past. A discussion of each entrance configuration is given below.

(a) Type I: jettied inlet. This entrance configuration consists of parallel jetties. Land-based or fixed hydraulic dredge plants have been used in conjunction with this configuration in the past. A floating suction dredge can only be used if the impoundment zone is subject to light wave action.

(b) Type II: jettied inlet and offshore breakwater. This entrance configuration consists of a channel protected by two parallel jetties with an offshore breakwater protecting the impoundment zone on the updrift side. The offshore breakwater on the updrift side provides a sheltered region for dredging activities so that a floating suction dredge may be used to transfer material to the downdrift coast in a high energy-wave environment. Furthermore, this system provides an effective means for trapping littoral material on the updrift side of the inlet, which prevents the possibility of shoaling in the entrance. However, the layout of the system is such that noen of the material trapped in the lee of the breakwater can be transported updrift during periods of longshore transport reversals. Hence, the system traps the gross longshore transport material, and frequent longshore transport reversals may lead to updrift erosion. A thorough knowledge of the littoral processes and possible longshore transport reversals is necessary for this system to be effectively utilized.

(c) Type III: shore-connected breakwater. This entrance configuration consists of a shore-connected breakwater with an impoundment zone at its seaward end. For this system to

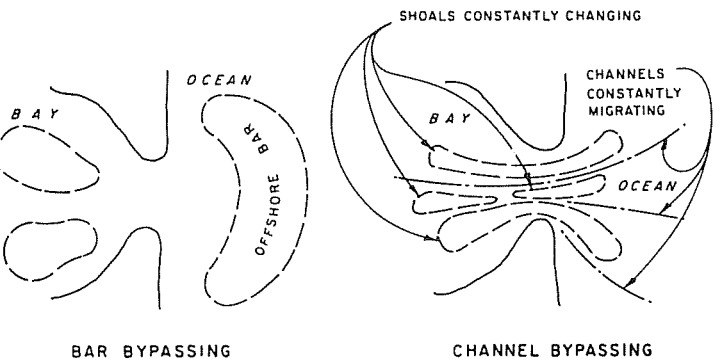

FIGURE 10
Mechanisms of Natural Inlet Bypassing

be effective, a detailed analysis of the short-term, storm-induced longshore-transport potential is necessary. In this system, sand accumulates at the seaward tip of the breakwater in an area adjacent to the entrance channel. If bypassing operations are not carried out properly and at the correct time intervals, a storm may result in significant shoaling of the entrance channel. This system, like the Type III system, provides a sheltered region in the lee of the seaward end of the breakwater where bypassing may be achieved through the use of a floating suction or hopper dredge. However, waves arriving from critical directions may force a temporary delay in dredging activities. Unlike the Type II system, this system, if properly designed, will allow the movement of littoral material in the upcoast direction during times of longshore-transport reversals.

(d) Type IV: weir jetty. This entrance configuration consists of a weir (or low sill) near the shoreward end of a jetty. This system provides a sheltered impoundment zone where a suction pipe or hopper dredge may be used to transfer littoral material to the downdrift side. A thorough knowledge of littoral processes and entrance-channel hydraulics is necessary for this system to be effectively utilized. This is particularly true if the channel entrance is a natural inlet. (This will be discussed in Subsection 2.3.c., Harbor Entrances Through Natural Inlets.) Currently, a large amount of research is being conducted on wier-jetty systems.

c. Harbor Entrances Through Natural Inlets. Natural inlets on sandy coasts often provide good entrances to sheltered harbor sites inside a bay or lagoon. Tidal currents through the inlet produce a sediment-flushing action which provides a mechanism for the natural transfer of littoral sediments from one side of the entrance to the other. This mechanism may be either of two types, or, in most cases, a combination of both. The two types, bar bypassing and channel bypassing, are shown schematically in Figure 10.

In bar bypassing, the sediment is transferred by tidal flow and wave-induced longshore transport from the bay side to offshore bars on the ocean side, until the sediment migration across the inlet is completed. The sediments will then proceed downdrift as they did before they reached the channel. With this type of transfer, the throat of the inlet remains deep and fairly stable. Meanwhile, the bars may vary in size and shape, but remain clear of the throat area. In channel bypassing, the sediment is transferred across the inlet through a series of parallel shoals and channels in the inlet throat. The inlet channels are continually migrating across the inlet mouth as part of the transfer system.

The dominant method of inlet bypassing appears related to the ratio, r, of littoral-transport rate, Q_{mean}, to inlet flushing capacity, Q_{Tmax}. Where the mean littoral-transport rate is high relative to inlet flushing, bar-bypass mechanics dominate; where the littoral-transport rate is low relative to inlet flushing, channel-bypass mechanics dominate. This ratio may be expressed as:

$$r = \frac{Q_{mean}}{Q_{T_{max}}} \qquad (2\text{-}9)$$

WHERE:
Q_{mean} = net longshore-transport rate, in cubic yards per year
Q_{Tmax} = maximum discharge through the inlet under spring-tide conditions, in cubic yards per second

IF: r > 200 to 300, bar bypassing usually prevails
IF: r < 10 to 20, channel bypassing usually prevails

In many regions throughout the world, it has been noted that the maximum average velocity, $(\bar{V}_m)_{max}$, measured in the inlet-throat cross section, is relatively constant:

$$(\bar{V}_m)_{max} \simeq 3.3 \text{ feet per second} \qquad (2\text{-}10)$$

WHERE:
$(\bar{V}_m)_{max}$ = maximum average cross-section velocity at maximum tidal flow during spring-tide conditions, is, in feet per second

The exact value of $(\bar{V}_m)_{max}$ depends on the longshore-transport rate, sediment size, inlet characteristics (width, depth, and bottom friction), and whether or not the inlet is protected by jetties.

Both the sediment-transport capacity of the inlet currents and the longshore sediment-transport rate vary with time; therefore, it is to be expected that, during any given year, the cross-sectional area of the inlet will show variations about the long-term equilibrium value. If short-term variations decrease the cross-sectional area below a certain value, the inlet can conceivably close.

An important factor in evaluating the degree of stability of an inlet (its resistance against closing) is the closure curve shown in Figure 11. The closure curve represents the relationship between the average cross-section velocity, $\bar{V}_m$, at maximum tidal flow during spring-tide conditions, and the cross-sectional area, A_c, both measured in the most restricted reach of the inlet. For relatively short and deep bays, the values of $\bar{V}_m$ may be calculated for different values of A_c from Equation (2-9) in Section 2 of DM-26.1. In order to compute K_1 for use in the equation for V_m, it will be necessary to assume a relationship between the hydraulic radius R and A_c. (See Equation (2-10) in Section 2 of DM-26.1). For relatively wide inlets, the hydraulic radius can be determined as follows:

$$R = A_c / \bar{w}_m \qquad (2\text{-}11)$$

WHERE:
R = hydraulic radius of inlet, in feet
A_c = cross-sectional area of inlet, in square feet
w_m = width of the inlet measured at mean sea level, in feet

For small values of A_c, the closure curve is difficult to determine. This is due to the fact that the depth may be small and the possibility of subcritical flow exists. However, for most practical purposes, it will be sufficient to compute the closure curve starting with values of A_c slightly smaller than the maximum value of A_c until A_{c1} is reached, and then sketch the remaining portion of the closure curve corresponding to smaller values of A_c in by hand. The horizontal line in Figure 11 corresponds to the long-term equilibrium velocity, $(\bar{V}_m)_{max}$. This curve will be referred to as the sediment curve.

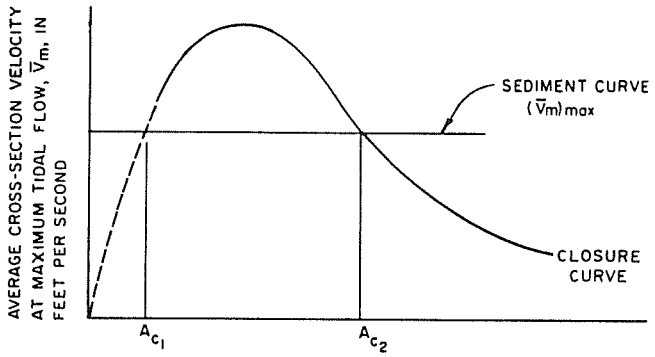

A_{c_1} = SMALLEST CROSS-SECTIONAL AREA OF INLET FOR WHICH INLET IS STABLE

A_{c_2} = EQUILIBRIUM CROSS-SECTIONAL AREA OF INLET

FIGURE 11
Inlet-Closure Curve

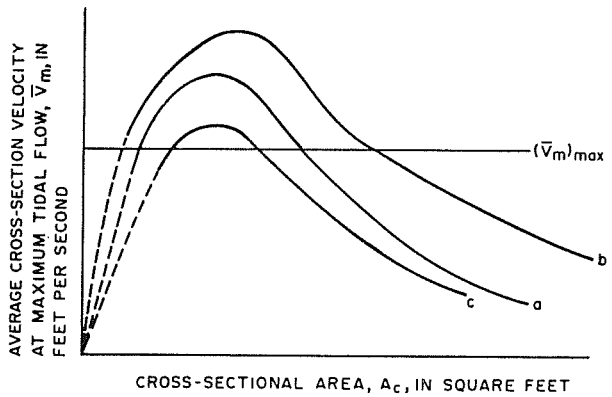

a – closure curve for existing situation

b – closure curve when increasing bay area and/or improving hydraulics of interior bay channel

c – closure curve when narrowing inlet

FIGURE 12
Changes in Closure Curve

It follows from Figure 11 that for values of the cross-sectional area smaller than A_{c1} (corresponding to the first intersection of the closure curve and the sediment curve), tidal velocities are too small to maintain the cross section, and the inlet will shoal and ultimately close. For values larger than A_{c1} and smaller than A_{c2} (corresponding to the second intersection of the closure curve and the sediment curve), the tidal velocity is larger than the velocity required to maintain the cross-sectional area and the inlet cross section will scour until it reaches the value A_{c2}. Inlets with cross sections larger than A_{c2} will shoal until the cross-section reaches the value A_{c2}. Thus A_{c2} represents the long-term equilibrium cross-sectional area. The foregoing analysis implies that a condition for the inlet to remain open is that the closure and sediment curves intersect; that is, $\bar{V}_m \geq (\bar{V}_m)_{max}$.

The following equation permits a measure of the degree of stability of an inlet (whether or not the inlet will stay open):

$$P_R = [(A_{c2} - A_{c1})/A_{c2}][100] \qquad (2\text{-}12)$$

WHERE:

P_R = percentage by which the inlet cross section can be reduced before the inlet will close.

A_{c2} = equilibrium cross-sectional area of inlet, in square feet

A_{c1} = smallest cross-sectional area of the inlet for which inlet is stable, in square feet

For inlets with considerable longshore transport, it is recommended that P_R be larger than 0.5. For inlets with little longshore sediment transport, P_R can be smaller.

From the foregoing, certain inferences can be developed regarding the use of natural inlets as harbor entrances:

(1) When dredging a new inlet connecting a landlocked bay to the ocean, the dredged channel should have a cross section larger than A_{c1}.

(2) If existing natural channel depths are adequate for navigation, it may not be necessary to adjust the cross section at all, except to perhaps stabilize the inlet position with short jetties. If this is the case, a channel-bypass inlet will require continuous monitoring, and channel marker buoys may have to be shifted frequently to respond to natural channel migrations.

(3) Moderate deepening of a channel may be necessary for navigational purposes. Deepening can be achieved by increasing the cross-sectional area of the inlet. This change can be accomplished by increasing the bay water area and/or by improving the hydraulics of interior by channels to make remote water areas contribute an additional volume of water to the inlet system. This requires a change in the closure curve, as qualitatively shown in Figure 12. These modifications will increase the cross-sectional area of the inlet and deepen the channels where the channel-bypass mechanism predominates. However, these modifications may not be effective in an inlet where the bar-bypass mechanism predominates and where the critical depth is offshore and not in the inlet throat.

(4) A tidal inlet can also be deepened by reducing its width. This technique can be quite sensitive to various aspects of the tidal hydraulics of the system. The result of decreasing the width of the inlet is to shift the closure curve to become that labeled c in Figure 12, resulting in a smaller cross-sectional area. Whether this will lead to a larger depth in the inlet depends on whether A_c decreases faster than the width. Therefore, any design for major inlet-constriction works should be well-documented and verified with a physical model.

(5) Where significant deepening of a natural inlet is proposed, jetties are usually required, and entrance sedimentation considerations become similar to those for siting a harbor on an open sandy coastline.

d. Harbors in Estuaries. Harbors can be sited in estuaries. In many cases, there are problems associated with excess shoaling of the harbor with cohesive sediments. Cohesionless sediments may also be a factor; however, in general they are not a major factor unless the harbor is located in an estuary, in contrast to one on an open coast, is generally subject to a different set of hydraulic and sedimentary conditions. The hydraulic regime is a result of complex intersections among the fresh-water discharge of the river, tidal currents, currents resulting from the difference in density between fresh water and sea water, and transverse currents resulting from two phenomena: reversing flows in curved sections of the estuary and Coriolis forces induced by the earth's rotation. Furthermore, wave action, either near the entrance to the estuary or in shallow areas of the estuary, may be an important factor. With regard to the sedimentary regime, sediment within an estuary can vary from cobbles to very fine colloidal materials in suspension. However, typical sediments reaching an estuary will consist of fine silts and clays carried in suspension.

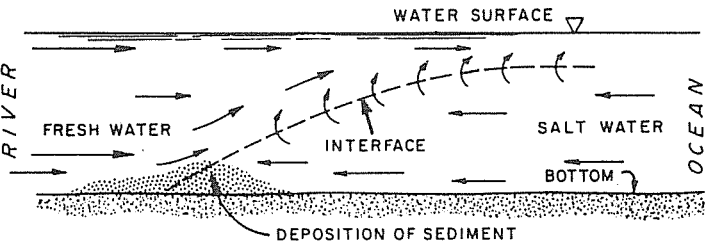

FIGURE 13
Schematic of Fresh Water-Salt Water Interface in a Highly Stratified Estuary

(1) Classification of Estuaries. An estuary system is characterized as a semienclosed body of water having a free connection with the open sea and within which sea water is measurably diluted by fresh-water discharge of a river entering the bay. Estuaries can be classified by the degree of mixing between the fresh and salt water in terms of observed vertical salinity distribution. The classifications are given below:

(1) highly stratified;
(2) moderately stratified;
(3) well-mixed vertically, but with measurable lateral gradients; and
(4) well-mixed.

In general, the type of estuary system will go from (1) to (4) with decreasing river flow, increasing tidal velocities, increasing width, and decreasing depth. The classification of an estuary is related to the relative magnitude of fresh-water flow during a tidal cycle and the total amount of water that flows into and out of an estuary with the movement of the tide (tidal prism). The ratio of fresh-water flow per tidal cycle to the tidal prism is relatively large (greater than 1) for highly stratified cases and small (smaller than 0.1) for completely mixed cases. A highly stratified estuary will exhibit a well-defined interface or discontinuity in vertical salinity distribution. On the other hand, in a well-mixed estuary, the local salinity will vary a large amount vertically compared to the mean local salinity. In many cases, fresh-water flow quantities vary seasonally and can produce highly stratified flow during flood runoff, whereas a moderately stratified or even well-mixed estuary may prevail during offpeak periods.

The hydraulics of a well-mixed estuary are generally similar to those involving a homogeneous fluid. However, the hydraulics of a highly stratified estuary are treated as though they involve a nonhomogeneous fluid. Figure 13 is a schematic of the interface between fresh water and salt water in a highly stratified estuary. This interface is referred to as an arrested salt-water wedge. The fresh-water discharge, being lighter than sea water, flows over the underlying salt-water wedge. Upstream movement of the wedge is arrested by the shear along the salt water-fresh water interface, which in turn returns a portion of the salt water downstream. This loss of salt water from the wedge is balanced by an upstream current within the salt-water body. The result is a system of strong, density-generated currents. In a constant-width channel, the fresh-water flow accelerates over the wedge, creating high surface velocities. Superposition of these density currents and tidal currents produces maximum ebb currents near the surface and maximum flood currents near the bed. The position of the interface varies with the tides, moving upstream with flood flow and downstream with ebb flow. An increase of fresh-water flow of the river will also move the interface downstream.

(2) Sedimentation in Estuaries. Sediment carried by upland discharge of a river may vary from cobbles to colloids and may be transported as suspended or bed load. However, due to the

lower velocities prevalent in most rivers as they enter estuaries, a large portion of the coarse sediment will settle out by the time the sediment reaches the toe of the salt-water wedge. Consequently, most sediment within an estuary consists of suspended silts and clays, and it is these particles which are transported back and forth with the flood and ebb currents of the tide. These sediments also create major shoaling problems in estuarine harbors. Currents in an estuary are produced by the tide, and, to a lesser degree, by the fresh-water discharge; therefore, both the currents and the fresh-water discharge are time-dependent. Consequently, the current-sediment system seldom reaches an equilibrium. Transportation of sediment from the bed, which in general consists of cohesive material, will only occur when the bed shear stress, which is related to tidal and fresh-water currents, is sufficient to entrain the material. Transportation of suspended sediments will vary according to the various states of turbulence present during a tidal cycle. Nevertheless, when considering a particular control volume, a net, or long-term, trend of erosion or deposition will occur. Deposition is the usual case.

In addition to the complex hydraulic and sediment phenomena present, the electrochemical properties of clay material add yet another complicating factor to the process. These electrochemical properties are such that, as the clay particles reach sufficient concentrations of salinity, a complex process takes place, which results in the ability of the particles to aggregate. Aggregation, also called flocculation, is the process whereby smaller particles adhere together to form larger particles, called flocs. These larger particles are more likely to settle; thus, the process of aggregation promotes shoaling of fine material in estuaries. The rate of aggregation increases as the amount of sediment in suspension increases. It also increases through turbulence, which increases the amount of interparticle collisions, to a point, after which further increase in turbulence will break up the relatively loose bond of the flocs.

If the bed shear stress is sufficiently low, as it is under low-velocity flow, these flocs, along with the fine silts, will deposit on the bottom. As they settle on the bottom, these cohesive sediments form interparticle bonds and consolidate with increasing overburden pressure. The greater the elapsed time and overburden, the more resistant the bed is to erosion. Determination of the critical bed shear stress to cause motion of these consolidated, cohesive bed forms is difficult.

When a harbor is placed in an estuary, it is often susceptible to shoaling. This results because the accompanying navigation channels, along with the supporting structures such as piers and breakwaters, often provide areas of low-velocity flow conditions where sediment may settle. Furthermore, the presence of the harbor, navigation channels, and supporting structures often modifies the flow conditions to the point where the estuary in the region of the harbor may shift to a stratified condition. This can be achieved by any measures which reduce the tidal flow or prism, any diversion of additional water into the estuary, or deepening and narrowing of the channel. Any shift towards a stratified condition will increase the amount of shoaling in the region of the harbor.

It is important to maintain adequate depths of a harbor to accommodate vessels using the harbor. (See DM-26.1.) The result is that, in many estuarine harbors, considerable maintenance dredging of shoaled material is required to ensure adequate depths in the harbor. This maintenance dredging is expensive and often may involve the dredging of quantities of up to 2,000,000 cubic yards per year. Therefore, it is desirable to design, or make modifications to, harbors such that adverse shoaling of cohesive sediments is minimized. This generally requires an investigation of the sediment characteristics, salinity distributions, and the hydraulic regime for the harbor. Krone and Einstein (1963) provide the following guidelines for procedures to minimize shoaling in estuarine harbors:

(1) Minimize the amount of suspended sediment entering a probable shoaling area. This can be achieved, to some degree, by preventing movements of tidal water containing suspended sediment from reaching a shoaling area through the use of dikes. It is also important to ensure that material dredged from shoaled areas is removed entirely from the estuary, if possible, as material dumped back into the water may return to the dredged area. This also can be achieved through the use of diked disposal sites; these are described in Section 3 of this manual.

(2) Minimize flow conditions which promote aggregation and low bed shear stress. The enlargement of channels generally reduces the bed shear stress. Unfortunately, it is usually necessary to enlarge natural channels in estuaries to provide safe navigation for vessels to be accommodated by a harbor. Maintenance of bed shear stress greater than the critical value required to initiate scour for most of the tidal cycle can be facilitated with the use of dikes. However, the economic feasibility of using these structures must be thoroughly investigated. This usually requires the use of physical-model studies. Flow conditions conducive to aggregation often occur in areas near piling and sudden enlargements of a channel. Where possible, smooth channel boundaries and gradual channel transitions, particularly those of the channel bottom, should be used. Parallel docking, with covered dock faces, may be used, where feasible, to provide minimum disturbance to flow. Where a salt-water wedge and clay sediment are present, shoaling is inevitable. The toe of the salt-water wedge may be moved by combining flows or by narrowing channels. In these ways, the location of shoaling may be moved to an area where maintenance dredging is more easily accomplished. A detailed investigation, including physical-model studies, is necessary to ensure the proper design of these types of modification.

(3) Minimize the amount of water containing suspended sediment that enters detached, off-channel harbor basins. This can be achieved by the use of a single, narrow opening. Such openings provide a minimum movement of water into and out of the basin during a tidal cycle. This method, however, may reduce water quality in the basin, which is generally not desirable.

Harbors sited in estuaries are generally susceptible to large amounts of shoaled material. Detailed investigations are recommended to adequately minimize the adverse effects of this shoaling.

4. SHORE PROTECTION.

a. General. Where sediment-transport capacity exceeds sediment supply, shoreline erosion occurs. Shore-protection measures usually comprise either armoring the shoreline against further erosion or artificially preserving the beach. Fundamental to an understanding of littoral transport is the concept of the littoral cell, schematically illustrated in Figure 14. Sand is supplied from cliff erosion or from upland sources through river discharges. Most of this material is transported laterally along the beach and offshore by waves, where it is ultimately lost offshore in deep water. In addition, some material is lost inland by wind transport. Little of the material passes the downdrift headland. On other coastlines, this downdrift boundary could be an underwater canyon instead of a headland. Beach-preservation techniques may be implemented in the vicinity of the updrift side of the downdrift headland without inducing erosion of the beach downdrift of the headland. On the other hand if protective measures are implemented elsewhere in the cell, the possibility of downdrift erosion should be investigated.

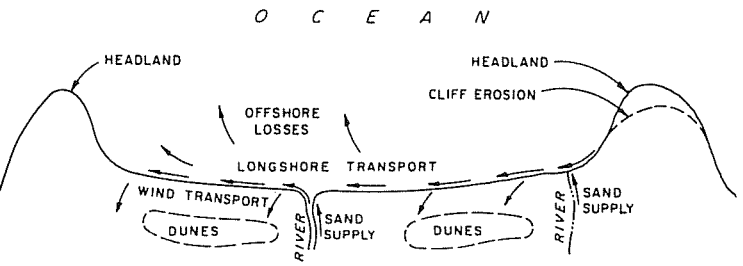

FIGURE 14
Littoral Cell (Closed Littoral System)

b. Shoreline Armoring. This method of shore protection involves the construction of seawalls or revetments. The structural design of these structures is discussed in DM-26.2. Because these structures are normally built in the surf zone, design wave heights are normally based on depth-limited breaking-wave conditions at storm-water levels or at extreme high tide. A major consideration in seawall design is the anticipated scour depth at the structure toe. The estimation of scour depth requires judgment. A steep foreshore slope fronting the structure requires little material removal to produce significant toe scour. A flat foreshore slope fronting the structure requires a significant quantity of material removal to produce toe scour. Vertical seawalls induce more toe scour than sloping revetments because of reflected wave energy. As mentioned in Subparagraph 3a (Littoral Processes), the beach face is usually eroded by steep winter waves, and the sandline is lowered. If a seawall is designed on the basis of a summer survey, this phenomenon must be taken into account. The customary provision for toe scour generally ranges from 2 to 4 feet below the winter sandline, depending on the type of structure, the relative coarseness of the beach material, and the foreshore slope. Long-term erosion effects must also be considered in the design of seawalls.

The designer needs to also consider failure modes (see DM-7) and repair possibilities in selecting design scour depths. A flexible rubble-mound revetment normally undergoes progressive failure, while a rigid seawall may fail suddenly when undermined. Where the wall is subject to periodic overtopping, care should be taken to provide adequate relief of pore pressure by providing weepholes through solid structures and an adequate filter material under porous revetments.

c. Beach Preservation. Where an eroding shoreline contains a beach or remnants thereof, it may be stabilized by preservation techniques. This can be accomplished either by increasing the material supply or by reducing beach losses. Reduction of losses can be achieved by creating downdrift barriers to arrest sand movement or by reducing the capacity of the mechanism that transports the sand through the reach. Beach-preservation techniques are presented below.

(1) Beach Nourishment. This method consists of direct placement of sand on the eroding beach from some outside source of sediment. This method supplements the natural supply of material to the reach of shoreline. The nourishment is usually carried out on a periodic basis. Where practical, it is desirable to place nourishment sand of equal or coarser grain size than that of the existing beach sand. Parameters controlling material loss to deep water due to winnowing (removal of fines) and offshore transport have been suggested by Krumbein and James (1965), James (1975), and Dean (1974); the relative winnowing-loss rate can be estimated through comparison of the grain-size distribution curves for both the borrow and the existing beach material. The material is generally distributed uniformly, in a width of approximately 50 feet, along the depleted shoreline beginning at the updrift end. Artificial beach nourishment has the advantage of

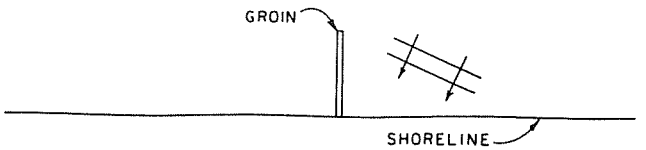

FIGURE 15
Groin Constructed Normal to Shoreline, Forming a Littoral Barrier

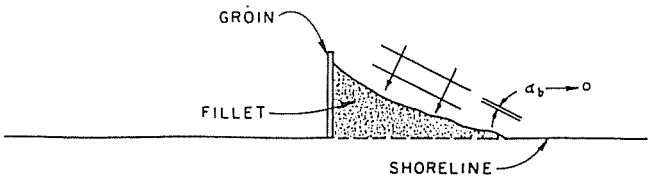

FIGURE 16
Updrift Fillet Face Alined With Breaker Angle Reduces Littoral Transport

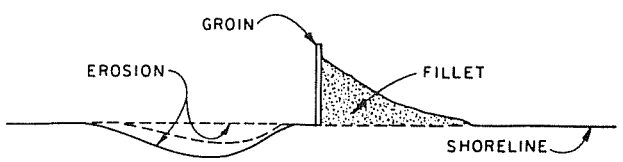

FIGURE 17
Unnourished Downdrift Beach Subject to Erosion

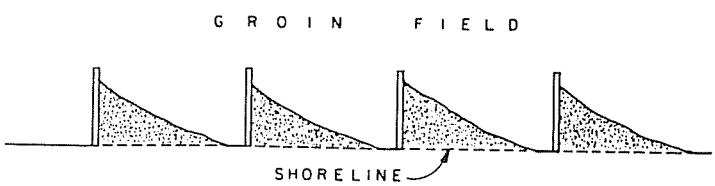

FIGURE 18
Groin Field

supplying material to shorelines downcoast of the placement zone. This method is most effective where the transport rates are relatively low in comparison to the periodic renourishment quantity. Under these conditions, a single placement may sustain a beach for 5 or more years. The disadvantages of beach nourishment are few, but the possibility of filling up drainage pipes in the nearshore area exists.

(2) Beach-Loss Reduction Measures. As previously discussed, in Subparagraph 3a (Littoral Processes), the longshore-transport capacity is a function of the alongshore component of wave-energy flux; the main variables are wave height and breaker angle. The adjustment, or reduction, of these variable factors can result in the reduction of material loss, or may even induce accretion of material, along the affected coastline reach.

(a) Groins. Groins are commonly used as a means of beach preservation. The groin is a littoral barrier which reduces the amount of longshore transport by reducing the breaker angle. This is illustrated in Figures 15 through 18. In Figure 15, the shoreline configuration immediately after groin construction is shown. In time, material carried by longshore transport will be trapped against the groin in a fillet, as shown in Figure 16. The orientation of the fillet shoreline will be such that the angle between the breaking-wave crest and the fillet shoreline will be zero. However, because the groin is a littoral barrier, the

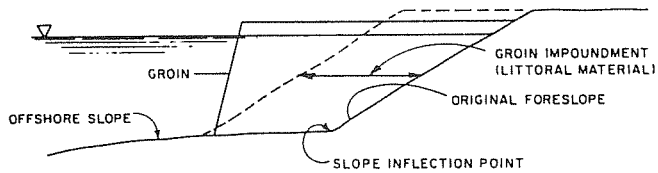

FIGURE 19
Groin Profile With Gently Sloping Offshore Bottom

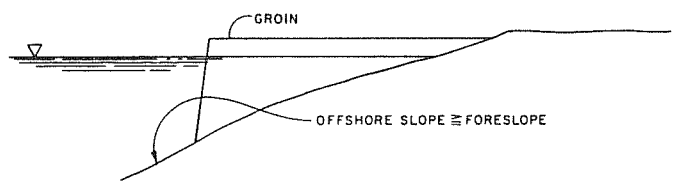

FIGURE 20
Groin Profile With Steepening Offshore Slope

downdrift side of the groin will be subject to erosion, as shown in figure 17. In most cases, the downdrift erosion is alleviated through the placement of a groin field. If the groin field is properly constructed, the result will be a series of sand fillets on the updrift sides of the groins; with proper groin spacing, these fillets will achieve an equilibrium configuration that prevents erosion on the downdrift sides of the groins. (See Figure 18.)

Several factors must be taken into account to make a groin field effective. It must first be determined whether a dominant longshore component of wave-energy flux exists. If a dominant component does not exist, a groin field will not be effective. If it does exist, the dominant breaker angle must be determined. Groin length and groin spacing then become a function of this breaker angle and the beach profile.

In forming a littoral barrier, the shoreline of each fillet face moves seaward in an accretion profile until sand begins to move around the groin tips at the prevailing rate of longshore transport along the reach. If the groin head is in rather deep water, much of this material may be carried seaward by waves and lost offshore in deep water, thus aggravating downcoast erosion. Conversely, if the head is extended only into relatively shallow water, the littoral barrier is not effective in trapping material.

Groins appear to be most successful on a shoreline with a fairly steep foreshore slope that toes out on a flat or gently sloping offshore bottom, as illustrated in Figure 19. The profile of the foreshore accretion generally parallels the profile of the original foreshore, with the fillets accreting along the updrift side of the groin for an offshore distance approximately equal to the groin-tip extension beyond the slope inflection point. Where the inflection point occurs in relatively shallow water (to a depth less than twice the dominant breaker height), significant quantities of littoral material can pass the groin head, remaining in the longshore-transport zone to continue along to the downcoast beach. Conversely, where the underwater slope steepens with distance offshore, as shown in Figure 20, groins may move the sand off into deep water without creating an effective barrier.

Groin spacing is based on refraction analysis. (See DM-26.2.) By using refraction analysis, the designer should make sure that groin spacing will allow the shoreline configuration of the fillet to remain normal to the breaker direction as the fillet accretes on the updrift side of the groin. Where there exists one dominant wave direction, the refraction analysis will provide reliable results. Where there are several dominant wave directions, investigations should be made to ensure that the groins provide adequate littoral barriers when

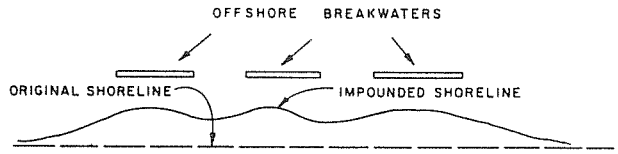

FIGURE 21
Beach Impoundment by Offshore Breakwaters

the direction of longshore transport changes.

Design of a groin field must include an investigation of the possibility of erosion downdrift of the field. If severe erosion downdrift will result, then it may be necessary to either extend the groin field downdrift or to use another means of shore protection. During construction, it is often desirable to fill the fillets with imported sand as part of the beach-preservation project.

(b) Offshore Breakwaters. Another method of beach preservation involves the placement of a detached breakwater system offshore in order to stabilize a reach of shoreline in its lee. The transport of sediment is diminished principally through the reduction of wave heights by the breakwaters and the realinement of wave-energy propagation. Figure 21 illustrates this method.

5. METRIC EQUIVALENCE CHART. The following metric equivalents were developed in accordance with ASTM E-621. These units are listed in the sequence in which they appear in the text of Section 2. Conversions are approximate.

32.2 feet per second^2	= 9.81 meters per second^2
1 square foot	= 0.09 square meter
1 cubic yard	= 0.76 cubic meter
3.3 feet per second	= 1 meter per second
2,000,000 cubic yards per year	= 1,530,000 cubic meters per year
2 feet	= 61.0 centimeters
4 feet	= 1.2 meters
50 feet	= 15.2 meters

Section 3. DREDGING

1. GENERAL. This section sets forth general criteria and procedural guidelines to use in dredging projects for harbors, turning basins, anchorage areas, and channels.

2. ACCOMPLISHMENT OF WORK.

a. Navy-Owned Equipment. Navy-owned dredges should be used to the maximum extent consistent with economy.

b. Corps of Engineers Equipment. When Navy-owned equipment suitable for the project is not available, the work may be accomplished by agreement with the Corps of Engineers, U.S. Army. (See NAVFAC P-68).

c. Contracts with Private Firms. When the only suitable dredging equipment is in private ownership, or when the workload exceeds the capability of available government dredging facilities, dredging may be accomplished by private contractors.

3. CURRENT DREDGING PRACTICE. The dredging of naval harbors may involve the dredging of clay and silt from estuarine harbors or the dredging of sand from harbors on open coasts. By 1980, 87 percent of the Navy's total annual maintenance-dredging volume consisted of cohesive sediments, while 13 percent consisted of sand. Table 3 provides a list of harbors within the continental United States whose annual maintenance-dredging volumes exceed 100,000

TABLE 3
Listing of 12 Naval Harbors With Annual Maintenance-Dredging Averages and Sediment Types

Harbor	Average Annual Maintenance Dredging (million cubic yards)	Sediment Type
Mare Island Naval Shipyard	0.5	Mud
Alameda Naval Air Station	0.9	Mud
Molate Point Naval Fuel Depot	0.12	Mud
Port Hueneme Harbor	0.19	Sand
New London Naval Submarine Base	0.1	Mud
Naval Weapons Station Earle	0.2	Mud
Philadelphia Naval Shipyard	0.2	Mud
Norfolk Naval Station	0.38	Mud
Charleston Naval Base and Weapons Station	1.7	Mud
King's Bay Trident Base	2.0-2.2	70% Mud 30% Sand
Mayport Naval Station Basin	0.6	Mud
Port Canaveral	0.15	Sand

cubic yards per year. A large part of the total dredging in naval harbors consists of removing shoaled material from under berthing piers. Other dredging activities include dredging of navigation channels and turning basins, as well as channel-entrance bypassing.

4. ECONOMIC FACTORS. The economic factors affecting the dredging of naval harbors are the following (Malloy, 1980):

a. Amount of Material to be Dredged. The mobilization and demobilization costs will constitute a significant portion of the total project cost for small-volume dredging projects. For large-volume dredging projects, the mobilization and demobilization costs will only increase the cost per cubic yard by a relatively small amount.

b. Distance From the Dredging Site to the Disposal Site. This distance depends on the availability of disposal sites, the volume, and the environmental quality of the dredged material. If the sediment is contaminated, regulatory agencies may require dumping at a "contained" land disposal site. In many areas these sites are limited. Ocean disposal sites are attractive alternatives because of their unlimited capacity and general proximity to Navy harbors. In either case additional costs and time delays may be incurred because the dredged material must be proven environmentally clean prior to issuance of a dredging permit. Regardless of where the material is dumped, cost is a function of distance to the disposal site and mode of transport.

c. Environmental Considerations. Some form of environmental documentation is required for every dredging project and can add substantial costs. The minimum requirement is a Preliminary Environmental Assessment. Additional chemical or biological testing may be required to supplement this document. If ocean disposal is proposed, bioassays will probably be required at an additional cost. Most costly of all are environmental surveys of the dredge site and the disposal site which may be required in environmental sensitive areas or cases of critical contamination.

d. New Work Versus Maintenance Dredging. Where an area has not been dredged before, the bottom sediments may be consolidated and difficult to dredge. The added time required to dredge new material may incur additional costs.

e. Other Factors. Other factors include the cost of fuel, competition between private and public dredgers, and the configuration and use of the naval harbor to be dredged.

5. PLANNING.

a. Jurisdiction and Permits.

(1) Jurisdiction. The U.S. Army Corps of Engineers has jurisdiction over construction and dredging in the navigable waters of the United States and of its territories and possessions. The U.S. Environmental Protection Agency (EPA) has jurisdiction over water quality relating to dredging, disposal of dredged material, and fill activities. Dredging activities and equipment must comply with U.S. Coast Guard regulations. Consultation with the district office of the U.S. Coast Guard is recommended before dredging projects are started.

(2) Permits.

(a) Federal permits. A Corps of Engineers permit is required to locate a structure, excavate, or discharge dredged or fill material in waters of the United States. A corps of Engineers permit is also necessary for transport of dredged materials into ocean waters for the purpose of dumping. Application for Federal permits can be made through the local district office of the Corps of Engineers, U.S. Army. Applications must be accompanied by drawings of the dredge and disposal areas and a description of the proposed work. Although there are general guidelines established for the permit process, each district is somewhat autonomous and has the authority to amend the requirements for each particular project. These requirements include explanatory documentation of existing data, supplementary chemical and biological testing, and additional environmental surveys. The extent of each requirement is dependent upon the quantity and quality of the dredged material, the proposed form of disposal,

and the environmental sensitivity of the area. To expedite permit application processing, cognizant regulatory agencies (Corps of Engineers/Environmental Protection Agency) should be contacted early in project planning. If environmental impact is assessed early, subsequent plans and alternatives can be guided by environmental considerations. In extreme cases, early notification can expedite processing emergency dredging permits by the Corps of Engineers.

(b) State permits. Federal law assures the right of any state or interstate agency to control the discharge of dredged or fill material in any portion of the navigable waters of any state jurisdiction. Typically, a water-quality certificate, a hydraulic-fill permit, or both, are required at the state level.

(c) Local permits. In certain areas, a local permit may be required.

b. Dredging-Site Investigations.

(1) Hydrographic Surveys. Proper planning cannot be accomplished without accurate hydrographic data. Factors affecting hydrographic surveys are given below.

(a) Horizontal control and adequate working charts. These must be available to provide accurate horizontal positioning for surveys and execution of work.

(b) Depth soundings. These can be accomplished by fathometer, leadline, or pole. The soundings should be reduced to the appropriate local low water datum.

(c) Tidal datum. Mean Low Water (MLW) and Mean Lower Low Water (MLLW) shall be used for soundings or depth measurements in all tidal waters as appropriate. Existing Corps of Engineers projects in rivers already have a specified datum. In areas outside the continental United States, the datum shall be that established for official use in the particular area involved.

(2) Sediment analysis. Sediment samples from the dredge area should be obtained and analyzed.

(a) Grab samples. Samples for maintenance dredging are often not necessary as review of historical records reveals sediment characteristics. If samples are necessary for maintenance projects they are usually grab samples taken from the bed surface.

(b) Subsurface Investigation. New-work dredging requires subsurface investigation. Recoverable cores are recommended where consolidated sediments may be encountered.

(c) Probing or sonar profiling. If rock pinnacles or debris are detected by grab or core samples, extensive probing or sonar profiling of the dredging area should be accomplished to locate and quantify rock and debris.

(d) Sediment testing. To evaluate dredging-plant requirements and disposal procedure, cohesionless samples should undergo mechanical sieve analysis. A chemical analysis is necessary for cohesive sediments. Bioassays may be necessary for cohesive sediments, depending on results of chemical analysis and proposed disposal action. If the project involves dredging of new sediments, a principal element of interest may be the density (or consistency) of material and, for cohesive sediments, the shear strength. (Refer to DM-38 for test data).

(3) Test Dredging. For very large new-work projects, consider test dredging in representative areas. This procedure is expensive due to mobilization and demobilization costs. As a result, this approach is seldom used.

(4) Environmental Analysis. Some form of environmental documentation is required as part of the permit process for all dredging projects. The extent of the documentation is determined by the quantity and quality of the sediment to be dredged and the proposed disposal methods. Chemical and biological testing may also be required, and in extreme cases, environmental surveys may be necessary. The material to be dredged must always be classified as unpolluted material.

(a) Dredging effects. If disposal effects are not an environmental concern, the effects of dredging can usually be evaluated with only a written document, particularly if there are some data available on the site and if the site is relatively uncontaminated. A significant amount of supplementary chemical and biological testing may be required, however, if the sediments are highly polluted. Field surveys of the dredge site may be necessary in cases of extreme environmental sensitivity of critical contamination.

(b) Disposal effects. Even if the potential impact of dredging can be evaluated with existing data and documentation, additional chemical and biological testing or field surveys may be required to evaluate the environmental impact of disposal. These evaluations can be even more extensive than those required for dredging effects. For example, if ocean dumping is proposed and there is a possibility that the sediment is contaminated, bioassays must be conducted according to rigid guidelines established in the Corps of Engineers/Environmental Protection Agency Implementation Manual. As with dredging, in cases of extreme environmental sensitivity or critical contamination, field surveys of the disposal site may be necessary in order to provide a complete evaluation of disposal effects.

c. Dredging Quantities. Dredging quantities are usually determined by the average-area method, using depths and locations on the hydrographic surveys. Accurate control of dredging is not possible. In some situations, it is less expensive to overdredge an area by 1 or 2 feet than to pay for the careful manipulation of dredging equipment and for the extra time involved in dredging to the exact depth required. Overdredging also allows for some additional shoaling before dredging is required again. Overdredging should be investigated for each specific site as it cannot be used in every situation.

d. Disposal Areas. Disposal locations are described as upland or inland water sites. The locations can be open or diked. Selection of an upland site requires consideration of return of effluent water to the water. Unnecessary entrapment of water that may cause flooding must be avoided. It must be assured that effluent water does not pick up additional turbidity or toxic chemicals as it returns to the waterway.

(1) Upland Open Site. This disposal location is generally used for placement of coarse, cohesionless sediments. Material placement is controlled with small berms constructed by a bulldozer or similar land-construction equipment.

(2) Upland Diked Site. This type of disposal location is generally used for the confined placement of fine-grained sediments. Dikes constructed prior to sediment placement typically have overflow weirs to minimize turbidity in receiving waters. Dikes may be constructed of existing soil or may be built up with hydraulically placed fill. Soil embankments should have a maximum slope of 1 vertical to 2 horizontal on the exterior face and 1 vertical to 3 horizontal on the interior face. Hydraulic fill must be placed at the natural angle of repose. Care should be taken to provide a cross-sectional area sufficient to withstand the water depths in the fill. A minimum freeboard of 2 feet is typical. Placement of dredged material at an upland diked site may cause ground-water contamination; investigations should be made to determine if this possibility exists. Certain situations require that the diked site be lined with filter cloth or a layer of clay to prevent penetration of pollutants into the ground-water system.

(3) Open-Water Site. With this type of disposal location, materials are generally limited to coarse sediments due to environmental considerations. EPA regulations and designated disposal areas should be investigated.

(4) Contained-Water Site. For this type of disposal

location, earthen dikes are usually constructed prior to dredging. The use of silt curtains instead of earthen dikes is possible under certain combinations of sediment, tides, currents, and environmental considerations.

e. Use of Dredge Materials. Disposal of dredged material generally presents problems, particularly when there is a lack of candidate disposal sites. The beneficial use of dredged materials should be investigated. Common beneficial uses of dredge materials include the following:

(1) Landfill. Dredged sediments may be used as a landfill for commercial, industrial, and recreational purposes.

(2) Construction Materials. Coarse sediments are often suitable for use as construction aggregate. These sediments may be stockpiled for present and future use.

(3) Marshland Wetland Habitat. After Intertidal- and submerged-fill operations are completed, shellfish larvae, wetland vegetation, or other organisms indigenous to the locale may be placed in the area to create a productive marshland.

(4) Upland Wildlife Habitat. During and after completion of above-water fills, seeding and contouring of sediments can provide a habitat indigenous to wildlife; this procedure may also prevent erosion.

(5) Beach Nourishment. Placement of suitable fill in water or on beaches can help to replenish losses of material caused by seasonal storms, washouts, currents, and other natural phenomena.

6. DREDGING EQUIPMENT.

a. **Mechanical Dredges.**

(1) Description. Mechanical dredges dislodge and raise sediment by mechanical means. mechanical-dredging methods are generally used in protected waters, but because the equipment is relatively mobile, some mechanical dredging may be accomplished in open water during short-term, calm-water conditions. Mechanically dredged sediments may be disposed alongside the dredge at a dumpsite or may be transferred to scows which transport the sediments to a dump site. The production rate by means of mechanical dredging is relatively low.

(2) Types.

(a) Clamshell, grab, or bucket dredge. This system consists of a crane, or derrick, mounted on a floating barge, with a clamshell, orangepeel, or dragline bucket used to pick up sediment and transfer it to an adjacent scow or barge. This dredge may be a specially built machine or may consist of land equipment on a suitable floating platform. this form of dredging can remove loose, unconsolidated sediments ranging in size from silts and clays to blasted rock. The dredge can be used in moderate-swell conditions. The system is not exceedingly efficient but has the advantage of high mobility. This mobility enables dredging at the base of bulkheads, piers, and fender piles without damaging these structures or the dredge equipment.

(b) Ladder, or bucket-ladder, dredge. This dredge consists of a floating dredge that has a continuous chain of buckets on a frame which is called a ladder. Each of the buckets possesses a cutting edge for digging into the sediment. The ladder is lowered to the bed so that the buckets can reach and cut sediments to be dredged. The buckets dump the dredged sediment by gravity at the opposite end of the ladder onto a conveyor system or an adjacent open barge. The barge may then transport the material to the disposal site. This dredging system is effective in hardpan and cemented sediments, but is ineffective in firm rock. The system cannot be used in swell conditions. This system is not often used in the United States.

(c) Dipper-barge dredge. This dredge consists of a backhoe mounted on a barge equipped with a trapdoor shovel. Sediment is removed from the bed and deposited alongside the dredge, in another barge, in the water or onshore. Where the sediment is deposited depends on the length of backhoe reach. Spuds, which penetrate the bottom, are usually used to keep the barge from moving during a dredging activity. This dredging method is effective for hardpan and cemented sediments, as well as for firm rock that has been blasted. The effectiveness of this type of dredging system is limited in moderate-swell conditions.

b. Hydraulic Dredges.

(1) Description. Hydraulic dredges lift sediment from the bottom and transport it by means of a centrifugal pump. Hydraulic dredges can be used in either open or protected waters, depending on the type of dredge. The dredged material is transported in a slurry and is generally discharged by a pipeline in the hull of the dredge; the slurry is discharged alongside the dredge, or it may be pumped ashore. The rate of production depends on sediment type, depth of cut, and dredge size and power; it generally exceeds that of mechanical dredges.

(2) Types.

(a) Pipeline, or suction, dredge. This dredge consists of a barge-mounted centrifugal pump. A suction line, or pipe, extends from the pump beyond the bow and is lowered to the bed by means of an "A" frame and ladder. At the end of this ladder, the pipe moves along the bottom dislodging the material. The material is then pumped in a slurry to a discharge line extending beyond the stern of the dredge. The material may then be pumped to the disposal site through a discharge line. The distance through which the material may be pumped can be extended by using booster pumps. Sweeping the suction pipe over an area at constant depth will result in the excavation of the channel bottom. Pipeline dredges are not self-propelled, but move by forward-mounted swing wires and aft-mounted walking spuds or wires. this type of dredged can be operated safely only in the absence of moderate to high swell; it can excavate material ranging from clays and silts to blasted rocks. The dredge is generally capable of dredging large volumes of material. Pipeline dredges are usually limited to excavation depths of approximately 60 feet. The rate of production will decrease with increased length of discharge line, increased lift, and increased bed-sediment compaction.

(b) cutterhead dredge. This dredge consists of a pipeline dredge equipped with a rotary cutter at the end of the ladder. The head is equipped with water jets which are used to dislodge bed sediments.

(c) Dustpan dredge. This dredge consists of a pipeline dredge with a dustpan-shaped head at the end of the ladder. The head is equipped with water jets which are used to dislodge bed sediments.

(d) Bucket-wheel excavator. this dredge consists of a pipeline dredge with a bucket wheel rotating (on a horizontal axis) at the end of the ladder.

(e) Trailing suction dredge. This dredge consists of a self-propelled or tug-assisted vessel. The hull of the vessel contains a hopper and the dredge is equipped with one or two suction pipes (normally fitted with drag heads) extending below the hull to the bed. This dredge usually operates while underway, drawing slurry by centrifugal pumps to the hopper, where excess water is overflowed back to the waterway. Sediment is discharged at the disposal site by opening doors located on the hopper bottom or by pumping out the hopper. This dredge is a self-contained unit and is capable of operating in higher swell conditions. Because the dredge is self-propelled, it is capable of dredging material from sites which are large distances from the point of disposal.

(f) Hopper dredge. This dredge consists of a trailing suction dredge with a ship-shaped hull, a bridge, an engine room, and crew quarters.

This dredge is typically used for the dredging of estuary and river-mouth bars that are prone to ocean-swell conditions.

c. Special Equipment.

(1) High Solids-Content Dredge. This dredge consists of a floating system capable of pumping high concentrations of solids through the use of compressed air. It is primarily used for removal of industrial wastes from rivers and harbors. The production rates are generally low and the distance over which the material may be pumped is limited. This type of dredge is not generally available.

(2) Elevated-Platform Dredge. This system consists of a pipeline dredge that incorporates a "jack-up" barge to elevate the equipment above the surface swells. The system incorporates a submerged discharge pipeline. Availability of this type of dredged is very limited.

d. Selection of Dredging Equipment. Principal considerations upon which equipment selection is made include:

(1) exposure of dredging site;
(2) volume and distribution of materials to be dredged;
(3) type of material to be dredged;
(4) location of disposal area;
(5) distance to disposal area;
(6) time available for work;
(7) vessel traffic; and
(8) availability of equipment.

7. METRIC EQUIVALENCE CHART. The following metric equivalents were developed in accordance with ASTM E-621. These units are listed in the sequence in which they appear in the text of Section 3. Conversions are approximate.

100,000 cubic yards	= 76,500 cubic meters
1 foot	= 30.5 centimeters
2 feet	= 61.0 centimeters
60 feet	= 18.3 meters

REFERENCES

Shore Protection Manual, U.S. Army Coastal Engineering Research Center, 3d ed., Vols. I, II, and III, Stock No. 008-022-00113-1, U.S. Government Printing Office, Washington, D.C., 1977.

Vanoni, V.A., Editor; Sedimentation Engineering, ASCE, Manuals and Reports on Engineering Practice, No. 54, Prepared by the ASCE Task Committee for the Preparation of the Manual on Sedimentation of the Sedimentation Committee of the Hydraulics Division, American Society of Civil Engineers, New York, NY, 1977.

Wicker, C.F.; Evaluation of Present State of Knowledge of Factors Affecting Tidal Hydraulics and Related Phenomena, Report No. 3, Committee on Tidal Hydraulics, Corps of Engineers, U.S. Army, Vicksburg, MS, May 1965.

Chow, Ven Te; Open Channel Hydraulics, McGraw-Hill Book Company, Inc., New York, NY, 1959.

Watts, George M.; "Trends in Sand Transfer Systems," Coastal Engineering, Santa Barbara Specialty Conference, October 1965, American Society of Civil Engineers, New York, NY, 1966, pp. 799-804.

Krone, R.B., and Einstein, H.A.; "Modes of Sediment Behavior and Selection of Harbor Design and Maintenance Techniques for Minimum Shoaling in Estuaries," Proceedings of Eighth Conference on Coastal Engineering, Mexico City, Mexico, November 1962, Council on Wave Research, The Engineering Foundation, 1963, pp. 331-338.

Krumbein, W.C., and James, W.R.; A Lognormal Size Distribution Model for Estimating Stability of Beach Fill Material, Technical Memorandum No. 16, U.S. Army Coastal Engineering Research Center, Washington, D.C., November 1965.

James, W.R.; Techniques in Evaluating Suitability of Borrow Material for Beach Nourishment, Technical Memorandum No. 60, U.S. Army, Corps of Engineers, Coastal Engineering Research Center, Fort Belvoir, VA, December 1975.

Dean, R.G.; "Compatibility of Borrow Material for Beach Fills," Proceedings of the Fourteenth Coastal Engineering Conference, Copenhagen, Denmark, June 1974, Vol. II, American Society of Civil Engineers, 1974, pp. 1319-1333.

ASTM E-621: "Standard Practice for the Use of Metric (SI) Units in Building Design and Construction," Annual Book of ASTM Standards, Part 18, American Society for Testing and Materials (ASTM), Philadelphia, PA, 1979.

NAVFAC P-68: Contracting Manual.

Malloy, R.J.; U.S. Navy Harbor Maintenance Dredging Atlas, TN-1597, Civil Engineering Laboratory, Port Hueneme, CA December 1980.

NAVFAC Documents are available at U.S. Naval Publications and Forms Center, 5801 Tabor Avenue, Philadelphia, PA 19120. TWX: 710-670-1685, TELEX: 834295, AUTOVON telephone number: 422-3321. The stock number is necessary for ordering these documents and should be requested from the NAVFAC division in your area. For non-Government organizations, Design Manuals may be obtained only from the Superintendent of Documents, U.S. Government Printing Office, Washington, D.C. 20402.

DM-5	Civil Engineering
DM-5.8	Pollution Control Systems
DM-6	Drawings and Specifications
DM-7	Soil Mechanics, Foundations, and Earth Structures
DM-26.1	Harbors
DM-26.2	Coastal Protection
DM-38	Weight Handling Equipment and Service Craft

TIDAL HYDRAULICS

Dept. of the Army
U.S. Army Corps of Engineers
March 1991

EDITORS NOTE

Tidal Hydraulics is the subject of a U.S. Army Corps of Engineers manual EM 1110-2-1607, issued in 1991. Pile Buck selected this for inclusion with the coastal protection volume because of the keen interest today in environmental problems associated with tidal estuaries. This text discusses such questions as water quality, sedimentation, salinity, flood control, shore protection, development and other related items. The planning of control structures including breakwaters, weirs, check dams, tidal barriers and others are well presented. Finally, a number of case histories involving hydraulic problems and the solutions utilized are offered by way of sharing the Corps experience with this subject.

CHAPTER 1
INTRODUCTION

1-1. Purpose. This manual provides design guidance for the development or improvement of navigation and flood control projects in estuaries. Factors are presented that should be considered in providing safe and efficient navigation facilities with lease construction and maintenance costs and/or providing protection from design floods. Considerations for preventing damage to the environmental quality of the estuary are also presented. The design engineer is expected to adopt the general guidance presented in this manual to specific projects. Deviations from this guidance are acceptable if adequately substantiated. It should be noted that coastal structures and approach channels are not included in this manual.

1-2. Appendices. Appendix A is the alphabetical listing of references cited in this manual. Appendix B discussed field data collection considerations along with an example. Appendix C presents an example numerical model investigation. Appendix D presents greater details of sedimentation analysis than provided in Chapter 4. Appendix E is a summary of generic or overall lessons learned from various Corps navigation projects, and appendix F is a listing of tidal model investigations conducted at the US Army Engineer Waterways Experiment Station (WES). Appendices B through F have been included to provide general guidance and examples.

1-3. Training. The US Army Engineer Division, Huntsville, offers a short-term (1-week) training course entitled "Hydraulic Design for Tidal Waterways" (formerly called "Tidal Hydraulics") within the Proponent Sponsored Engineer Corps Training Program (PROSPECT). The course the latest engineering and design considerations for the development and improvement of Corps projects in tidal waters as contained in this manual. Other related courses on the TABS numerical modeling system, referenced in several of the chapters and appendices, are also listed in the PROSPECT Purple Book. Several other PROSPECT courses also are available on various topics directly related to tidal hydraulics. Interested Corps employees should check with their supervisor or Training Officer and the Purple Book for required qualifications and prerequisites for the particular training course. If qualified, the employee should follow the standard training application procedure for his or her District or Division.

1-4. Available Assistance. The USACE Committee on Tidal Hydraulics (CTH) provides expert consultation on problems related to tidal hydraulics. Address inquiries to the Chairman, CTH, WES, ATTN: CEWES-HV-Z, 3909 Halls Ferry Road, Vicksburg, MS 39180-6199.

1-5. References. Required references are listed as follows. Related references are listed in Appendix A.

a. EM 1110-2-1202 (Environmental Engineering for Deep-Draft Navigation Projects).
b. EM 1110-2-1412 (Storm Surge Analysis and Design Water Level Determination).
c. EM 1110-2-1611 (Layout and Design of Shallow Draft Waterways).
d. EM 1110-2-1613 (Hydraulic Design of Deep-Draft Navigation Projects).
e. EM 1110-2-5025 (Dredging and Dredged Material Disposal).
f. ER 1105-2-50 (Environmental Resources).
g. ER 1110-2-1404 (Deep-Draft Navigation Project Design).
h. ER 1110-2-1457 (Hydraulic Design of Small Boat Navigation).
i. ER 1110-2-1458 (Hydraulic Design of Shallow Draft Navigation Projects).

CHAPTER 2
DEFINITION AND FORCING FUNCTIONS OF ESTUARIES

Section I. Definition

2-1. Definition. An estuary is an area of interaction between salt and fresh water. The most common definition used is that of Cameron and Pritchard (1963) that states, "An estuary is a semi-enclosed coastal body of water which has a free connection with the open sea and within which sea water is measureably diluted with fresh water derived from land drainage." Hopkinson and Hoffman (1983) argue that the estuarine influence may extend to the nearshore coastal waters where seawater is diluted by land drainage but beyond the confines of emergent land masses. Using the Cameron-Pritchard definition, the brackish waters of the Amazon and Mississippi Rivers seaward of the river mouths are not estuarine; using the Hopkinson-Hoffman definition, they are. Hopkinson and Hoffman support, from a functional point of view, the extension of the estuarine boundary to include the interface system that couples continent to ocean.

Section II. Classification of Estuaries

2-2. General. To more fully understand what an estuary is, some sort of classification system must be established. Pritchard's definition is one for a positive estuary (Pritchard 1952a), an estuary where freshwater input (river flow and precipitation) exceeds losses due to evaporation. thus the surface salinities in a positive estuary are lower than in the open ocean. A situation in which freshwater input is less than in the

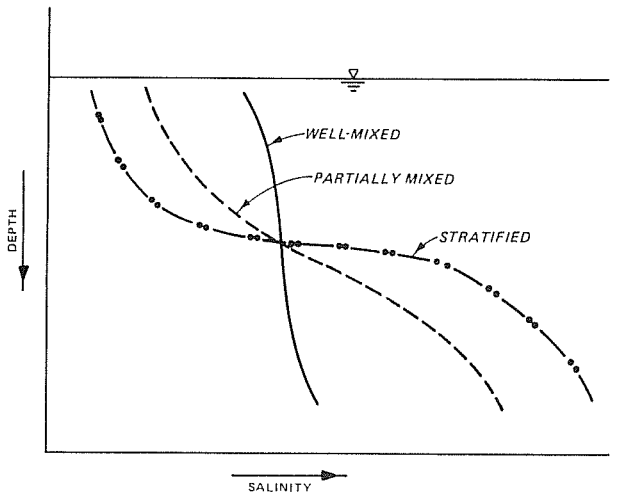

FIGURE 2-1
Vertical salinity structure. Classification depends on salinity difference between surface and bottom values.

open ocean. A situation in which freshwater input is less than losses due to evaporation results in a negative estuary, such as Laguna Madre in Texas. Most estuaries are positive; however, a negative situation can occur, resulting in different circulation patterns caused by hypersaline conditions.

2-3. Classification. Estuaries are also classified by topography and salinity structure. Ratio parameters of flow, stratification, and stratification-circulation can be used to identify the salinity structure class.

2-4. Topographic Classification. Pritchard (1952b) has suggested a topographic classification of three groups: coastal plain estuaries, fjords, and bar-built estuaries.

a. Coastal Plain Estuaries. Coastal plain estuaries, or drowned river valleys, were formed as the melting waters from the last ice age flooded the existing river valleys. River flow is normally small compared to tidal prism (the volume of water between high and low tides) and sedimentation has not kept pace with inundation. The resulting estuary has maintained the topography of the former river valley but is relatively shallow (rarely deeper than 100 feet (30 metres)). There are extensive mud flats with a sinuous, deeper central channel. Coastal plain estuaries are generally found in temperate latitudes. Examples are the Chesapeake Bay estuary system in the United States and the Thames and Mersey systems in England.

b. Fjords. Fjords, estuaries that have been formed by glacial erosion, generally occur at higher latitudes, are relatively long and deep, and possess a shallow sill at the fjord mouth and fjord intersections. These shallow sills can restrict the free exchange of ocean and estuary waters, in some cases producing a small tidal prism with respect to river flow. Examples of fjords are Puget Sound (United States), Alberni Inlet (British Columbia, Canada), Sogne Fjord (Norway), and Milford Sound (New Zealand).

c. Bar-built Structures. Bar-built estuaries are formed by the same processes as the drowned river valleys, the difference being that sedimentation has kept pace with inundation, with a characteristic bar forming at the mouth. Associated with depositional areas, bar-built estuaries are shallow with extensive lagoons and waterways inside the mouth. Entrance velocities can be quite high but quickly diminish as the estuary widens. This type of high sediment volume estuary is most often found in tropical or active coastal

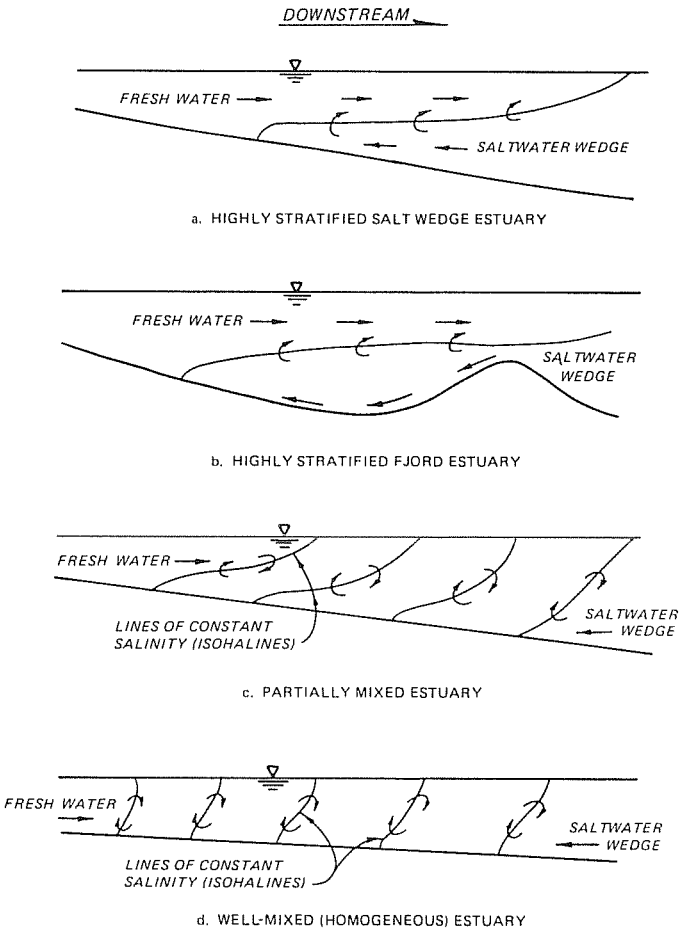

FIGURE 2-2
Estuary classification by salinity structure

deposition areas. Examples of bar-built estuaries are the Roanoke River (United States) and the Vellar Estuary (India).

d. Other. A fourth group of estuaries would be those not belonging to the previously mentioned three. This group would include estuaries formed by volcanic eruptions, faulting, landslides, or other processes.

2-5. Classification by Salinity Structures. Most estuary systems are coastal plain estuaries with individually unique salinity and flow characteristics. To understand the circulation of these estuaries, Pritchard (1955) and Cameron and Pritchard (1963) have classified estuaries using stratification and salinity distribution as the governing criteria. The major classifications are highly stratified, partially mixed, and well-mixed (homogeneous) (Figure 2-1).

a. Highly Stratified. A highly stratified, salt wedge type estuary is one in which the outgoing lighter fresh water overrides a dense incoming salt layer. The dense salt wedge will advance along the bottom until the freshwater flow forces can no longer be overcome. At this point, the tip of the salt wedge will be blunt during rising ride and tapered during falling tide. Mixing occurs at the saltwater/freshwater interface by entrainment, a process caused by shear forces between the two moving layers. As small amounts of dense water are mixed in the upper layers, more fluid enters the estuary near the bottom to compensate for the loss, and more fluid leaves the estuary in the upper layers to attain equilibrium of forces (Figure 2-2a). In these river-dominated, poorly mixed estuaries, such as Southwest Pass on the Mississippi River, upstream flow occurs in the salt wedge regardless of tidal phase, with downstream flow on the surface. In the

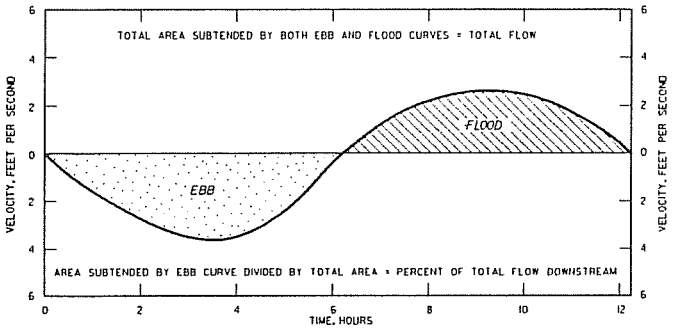

FIGURE 2-3
Definition sketch: flow predominance

shallower South Pass, also on the Mississippi River, upstream flow occurs in the wedge during flood tide simultaneously with surface downstream flow, while during ebb tide, flow at all depths is in the seaward direction (Wright 1971). Examples are the Mississippi River (United States) and Vellar Estuary (India). Another form of a type, in a fjord the lower, almost isohaline, layer is very deep. The freshwater surface layer is almost homogenous, and only during low-flow periods does the maximum salinity gradient ever reach the surface. Circulation over the still may be very different from the rest of the fjord estuary because of large tidal velocities and weaker stratification at the sill. The inflow over the sill is usually a mixture of coastal and outflow water. As the water passes the sill and the tidal action decreases, the denser water settles and frequently results in a layered structure resulting from successive saltwater intrusions (Figure 2-2b). If water renewal is infrequent, anoxic conditions can develop on the bottom. Silver Bay (Alaska, United States) and Alberni Inlet (British Columbia, Canada) are examples.

b. Partially Mixed. A partially mixed estuary is one in which tidal energy is dissipated by bottom friction produced turbulence. these turbulent eddies mix salt water upward and fresh water downward with a net upward flow of saline water. As the salinity of the surface water is increased, the out-going surface flow is correspondingly increased to maintain riverflow plus the additional upward-mixed saline water. This causes a compensating incoming flow along the bottom. This well-defined, two-layer flow is typical of partially mixed estuaries. The salinity structure is very different from a highly stratified estuary because of the efficient mixing of salt and fresh water. The surface salinity increases steadily down the estuary with undiluted fresh water now occurring only near the head of the estuary. There is also a longitudinal salinity gradient along the bottom (Figure 2-2c). In a partially mixed estuary, riverflow is low compared to tidal prism. Examples are James River (United States) and Mersey and Southampton Water Estuaries (England).

c. Well-mixed or Homogeneous. In estuaries where tidal flow is much larger than riverflow and bottom friction large enough to mix the entire water column, a vertically homogeneous (well-mixed) estuary results (Figure 2-2d). If the estuary is wide, Coriolis force may form a horizontal flow separation; and in the northern hemisphere, the seaward flow would occur on the right side (looking downstream), while the compensating landward flow would be on the left. This vertically homogeneous, laterally nonhomogeneous condition can be found in the lower reaches of the Delaware and Raritan Estuaries in the United States. A vertically and laterally homogeneous (sectionally homogeneous) condition occurs in narrow estuaries in which salinity increases evenly toward the mouth.

2-6. Stratification Numbers. It is clear that the different types of estuaries are not well defined but are stages on a continuum, which is controlled by the ratio of river and tidal flow. As the estuary progresses from river to ocean, it may pass through several stages of estuary types. At the head of the estuary where tidal range is reduced and riverflow is large, a highly stratified salt wedge condition may result. Farther downstream as tidal amplitudes increase, turbulent mixing occurs, and a partially mixed estuary is created. As tidal flow becomes larger than riverflow, a vertically homogeneous situation may develop. Since these stages depend on riverflow, a seasonal flow changes will influence the estuary and its varying stages.

a. Simmons Ratio. Simmons (1955) related flow ratio (the ratio of riverflow per tidal cycle to the tidal prism) to estuary type. When the ratio is 1.0 or greater, the estuary is highly stratified. When the flow ratio is 0.2 to 0.5, the esutary is partially mixed, and when less than 0.1, a well-mixed condition exists. Pritchard (1955) considers estuary depth and width to be factors controlling the flow ratio. As the geometry of an estuary changes, the flow ratio is affected, and the estuary type will also vary. Constrictions cause increased current velocities and produce well-mixed sections, while wider areas tend to be more quiescent and more stratified.

b. Ippen Number. Using the tidal properties of amplitude and phase, Ippen and Harleman (1961) developed a relationship between energy and estuary mixing. This stratification number is a measure of the amount of energy lost by the tidal wave relative to that used in mixing the water column. Increasing values of the stratification number indicate increasingly well-mixed conditions, and low numbers indicate highly stratified conditions. Changes in riverflow, width, and depth will influence the tidal properties, and accurate tidal measurements are necessary to use this method.

c. Hansen Parameter. Hansen and Rattry (1966) chose the parameters of salinity and velocity to develop a means of estuary classification and comparison. Two dimensionless parameters, stratification (ratio of the surface to bottom salinity difference divided by the mean cross-section salinity) and circulation (ratio of the net surface current to the mean cross-sectional velocity) are used to construct a diagram. The location on the diagram will identify the estuary stage on the continuous spectrum of estuary type. Type 1 is well-mixed (homogeneous) with net seaward flow at all depths. Type 2 experiences flow reversal and is a partially mixed estuary. Types 3 and 4 are stratified estuaries, type 3 the deep fjord type, and type 4 the intensely stratified salt wedge.

2-7. Flow Predominance. The concept of flow predominance is useful in understanding the effects of density-induced currents on velocities. In a conventional 12-hour plot of velocity versus time, velocity values will be positive (flood flow into the estuary) and negative (ebb flow out of the estuary) (Figure 2-3). To determine flow predominance, the area under the ebb portion of the curve (all negative values) is divided by the total area under the curve (ebb portion plus flood portion). The resultant, ebb predominance, is the percent of the total flow per tidal cycle that is moving in the ebb direction at a given velocity sampling depth. In a highly stratified estuary, the freshwater surface flow will always be ebb dominant, while the bottom salt wedge layer will be strongly flood dominant. Near the entrance of a well-mixed estuary, the bottom flow will be slightly flood dominant, while the surface will be strongly ebb dominant. Further upstream the flow will be ebb dominant throughout the entire depth. In a partially mixed estuary, the bottom flow will be mainly flood dominant within the salinity wedge, and the surface flow predominantly in the ebb direction. Examples of

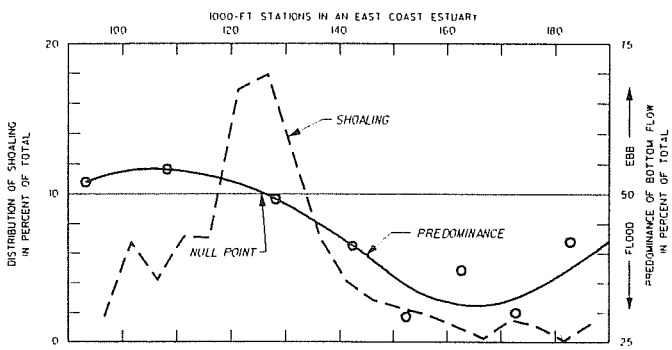

FIGURE 2-4
Relationship of shoaling and predominance of bottom flow

flow predominance in Savannah Harbor, Charleston Harbor, and the Hudson River are presented in "Field Experiences in Estuaries" by H. B. Simmons (Ippen 1966).

2-8. Null Point. Along with the concept of flow predominance is the realization that at some point the net flow may be balanced (no net flow in either direction). This point is called the null point.

2-9. Salinity Effects on Shoaling. Saltwater intrusion is important to estuary sedimentation because saline water enhances flocculation of suspended clay particles, and density currents tend to move sediments upstream along the bottom. Thus sediments entering the estuary may become trapped instead of moving out to sea. Frequently, shoaling occurs between the high-water and low-water positions of the upstream limit of salinity intrusion. The region most likely to experience heavy shoaling is the reach bracketing the 50 percent value (or null point) of the bottom flow predominance (Schultz and Simmons 1957) (Figure 2-4).

2-10. Summary. The classification of estuaries uses variables of topography, riverflow, and tidal action as factors influencing saltwater and freshwater mixing. Ultimately the salinity characteristics of an estuary determine the unique features of the system. No two estuaries are alike, but one can hope to find general principles rather than unique details to use when studying and comparing similar systems. Dyer (1973) describes in detail several estuaries with different topographies, tidal ranges, and riverflows, while Cameron and Pritchard (1963), Lauff (1967), and Ippen (1966) have tried to identify the relevant general principles governing estuarine behavior.

Section III. Tides and Other Long Waves

2-11. Tide-Generating Forces. To understand the effect of tides on an estuarine system, a brief comment should be made on the tidal-generating forces and rhythms.

a. Newton's laws of gravitation state that the force of attraction between two bodies is proportional to the product of their masses and inversely proportional to the square of the distance between their centers.

Tidal forces, acting on the surface of the earth, are less than gravitational forces and vary inversely with the cube of the distance between bodies. In our sun-moon-earth system, the sun is the largest body, but because its distance is so great from the earth, its influence on tides is only 46 percent of the moon's.

b. all forces in the sun-moon-earth system are in equilibrium; however, individual particles on the earth's surface are not. In this system of varying distances from each

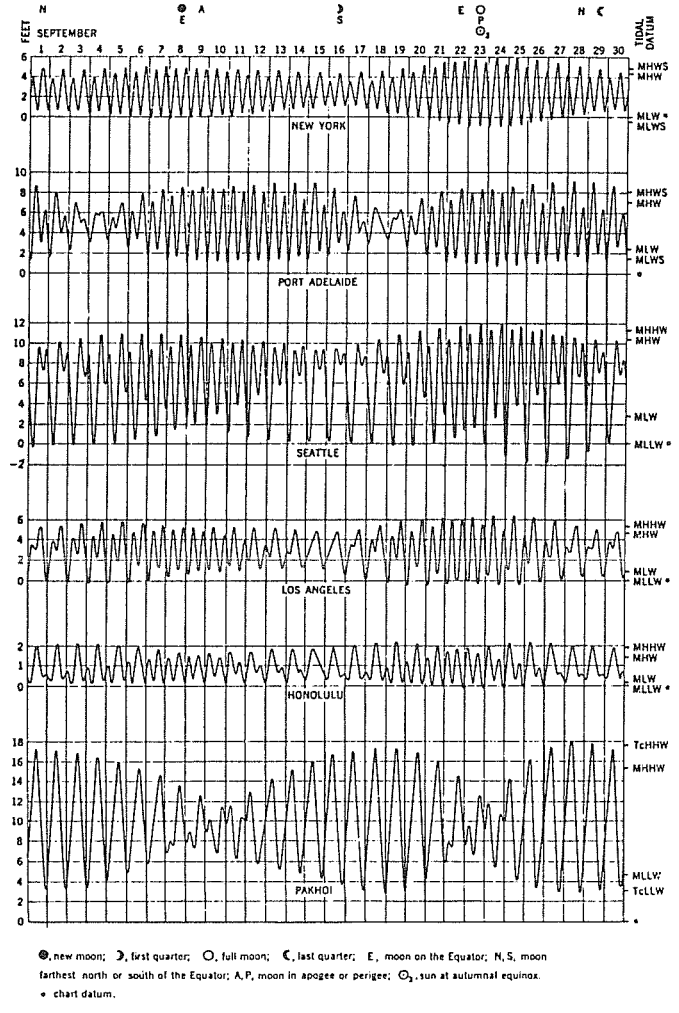

●, new moon; ☽, first quarter; ○, full moon; ☾, last quarter; E, moon on the Equator; N, S, moon farthest north or south of the Equator; A, P, moon in apogee or perigee; ♈, sun at autumnal equinox.
• chart datum.

FIGURE 2-5
Variations in tides by locations

other and different rotation rhythms (the earth once every 24 hours and the moon around the earth once every 24 hours and 50 minutes), these tide-generating forces are never constant. These forces act on land, water, and air. However, the land mass is not as elastic as liquids, and air, although elastic, has such a low density that the effects of the tidal forces, although measurable, are small. The media most free to respond in an observable manner are the earth's water masses, the oceans. Tide-generating forces are the residual forces between attraction (earth/moon and earth/sun) and centrifugal force (due to the rotation of two bodies about a common axis). A detailed description of tidal theories can be found in Darwin (1962) and Defant (1958), and in a more readable form in Wylie (1979) and Marmer (1926)

2-12. Tide Terms. Several basic terms are used to describe tides. High water is the water-surface level at is highest extent during one cycle and is also used to denote the time at which it occurs. Low water is used in the same way for the lowest water level. Where there are two unequal high waters and two unequal low waters in one day, they are distinguished by naming them higher high water, lower high water, lower low water, and higher low water. A tidal current that is flowing landward is termed a flood current, while on flowing seaward is called an ebb current.

2-13. Types of Basic Tides. The basic tide is the cyclic rise and fall of the water surface as the result of the

tide-generating forces. There are three types of tides--diurnal, semidiurnal, and mixed--which are a result of tide-generating forces and location on the earth.

a. Diurnal. A diurnal tide is one high and one low water level in lunar day (24.84 hours). Diurnal tides predominate in the Gulf of Mexico, some parts of the Pacific Ocean, e.g., the Philippines, and certain places in Alaska.

b. Semidiurnal. Semidiurnal tides produce a tidal cycle (high and low water) in one-half the lunar day (12.42 hours) or two nearly equal tidal cycles in one lunar day. Semidiurnal tides occur along the east coast of the United States.

c. Mixed. Mixed tides are a combination of diurnal and semidiurnal characteristics and are found on the west coast of the United States. There is a marked inequality in the heights of the succeeding tides, especially low waters, and there is also an equality in time. There are usually two high and two low waters each day. Typically, there is a high tide, then a low tide, followed by a scanty high tide and a moderate low tide.

2-14. Spring and Neap Tides. Due to the unequal rotational rhythms of the members of the sun-moon-earth system, their forces are preiodically in and out of phase. Every 14.3 days (twice a month) the earth, moon, and sun are aligned in phase. At this time the gravitational forces reinforce each other to form higher than average tides called "spring tides." Also twice a month the moon and sun are at right angles to the earth and the forces are subtracted from each other to form lower than normal tides called "neap tides."

2-15. Influence of Moon and Sun. Another factor influencing the tide is the declination of the moon and sun--their angular distance north or south of the equator. The relationship of the earth's axis to the plane of its orbit around the sun results in an apparent yearly north-south movement of the sun. The plane of the moon's orbit is tilted also, and the apparent north-south migration across the equator occurs every 27-1/3 days. This monthly migration results in observable tidal changes. figure 2-5 illustrates the differences in tides at various places for a month. During this month, spring tides (new and full moon) happen to occur when the moon is crossing the equator. Neap tides occur at the quarter moon, and apogee (moon furthest from the earth) and perigee (moon closest to the earth) effects are noted. The spring tide occurring at perigee is larger because of the increase in tidal forces. The tides at New York are semidiurnal with a strong spring and neap influence. Tides at Port Adelaide, Australia, go from mixed to semidiurnal when the moon is over the equator, while tides at Seattle, Washington, are mixed at all times. Tides at Los Angeles, California, and Honolulu, Hawaii, are diurnal during neap tide when the moon is south of the equator, semidiurnal during spring tide, and mixed at other times of the month. Tides at Pakhoi, China, are strongly diurnal except when the moon is over the equator.

2-16. Tide Prediction Tables. The National Oceanic and Atmospheric Administration (NOAA) annually publishes "Tide Tables, High and Low Water Predictions" (NOAA, year of interest). The four volumes include the entire maritime world and contain daily tide predictions for 198 reference ports and tidal differences and other constraints for about 6,000 subordinate stations. Each volume, which covers a different section of the world, contains tables for obtaining the approximate height of the tide at any time; local mean time of sunrise and sunset for every fifth day of the year for different latitudes; the reduction of local mean time to standard time; moonrise and moonset for a number of locations; the

Greenwich mean time of the moon's phase, apogee, perigee, greatest north and south zero declination, and the time of the solar equinoxes and solstices; and a glossary of terms.

2-17. Tidal Constituents. The tide-producing forces exerted by the moon, sun, and other astronomical bodies are represented by mathematical expressions. There are over 128 tidal constituents used to represent the various wavelengths and frequencies found in nature (Schureman 1940).

2-18. Nonastronomical Forces. Nonastronomical forces can also produce waves. A tsunami, or seismic sea wave, is a very long wave originating from a disturbance in the seafloor. The wave train generated from such an event (earthquake, mud slide, volcanic explosion) contains huge amounts of energy and moves at high speeds. When it reaches shallow water and the shoreline, it can be extremely destructive. Other nonastronomical waves are produced by boat wakes, explosions, landslides, and any force that can disturb the surface of the water.

2-19. Waveforms. The tide may enter the estuary as a progressive wave manifested by the forward movement of the waveform. The current velocity and water-surface elevations in this waveform are in phase. As the wave progresses up the estuary, the waveform changes shape, the face steepening and the rear slope becoming more gradual. Areas of constriction increase the wave amplitude, and boundary friction is a means of energy dissipation. At some point in time, as the wave reaches the end of the estuary, it may be reflected and the interaction of the forward-advancing progressive wave and the returning reflected wave may produce a standing wave. In a standing or stationary wave, the current velocity and water-surface elevation are out of phase by 90 degrees. Most estuaries are intermediate, displaying characteristics somewhere between progressive and standing wave features.

Section IV. Winds and Wind-Generated Waves

2-20. General. Meteorological factors such as changes in barometric pressure and the uneven heating and cooling of the earth produce pressure differences that result in winds. Winds blowing across the surface of bodies of water transmit energy to the water, and waves are formed. The size of these wind-generated waves depends on the wind velocity, the length of time the wind is blowing, and the extent of open water over which it blows (fetch).

2-21. Wind Effects. The water surface absorbs energy from the wind and from smaller waves to form higher, longer waves. At any point in time, the resultant waves are the summation of all the waves passing through a given location. The concept of wavelength and period no longer applies in such an unsteady environment. Instead, a method of describing waves by means of their energy spectra is used. Tables have been developed relating wind description and its observed effects on the water surface to a classification system such as the Beaufort Scale and the International Code for state of the sea. Examples of these and information on other topics in this section can be found in many publications such as Bascom (1980).

2-22. Setup and Setdown. In addition to the creation of wind waves, wind can also cause a condition known as "setup" or "setdown." Wind stress on the water surface can result in a pushing or piling up of water in the downwind direction and a lowering of the water surface in the upwind direction. When the wind blows landward, water will set up against the land. This setup, superimposed on the normal tidal elevation, causes apparent higher than normal tides. This frequently produces flooding during storm events. A seaward wind will push water toward the sea and away from land, causing a lower than normal water level. When the wind stops, the setup or setdown water surface will return to normal levels. In enclosed waters, this return may occur as successive oscillations that are diminished by friction.

2-23. Seiche. If the surface of an enclosed body of water such as a harbor or bay is disturbed, long waves may be generated that will rhythmically slosh back and forth as they reflect off the opposite ends of the basin. These waves, called seiches, will travel back and forth until the energy is lost to frictional forces. The period of a seiche is dependent upon the size and depth of the basin in which it occurs. If an arriving wave train has a period similar to the natural frequency of a harbor, each arriving wave will increase the intensity of the seiche, producing rougher waters inside the harbor than on the surrounding sea.

2-24. Storm Surge. During a storm, there may be a substantial rise in the sea level along the coast called a "storm tide" or surge caused by wind setup, wave setup, and air pressure drop. The difference in pressure between an atmospheric low-pressure area and the surrounding high-pressure area causes the sea surface to "hump" under the influence of lower atmospheric pressure. The wind-generated storm waves superimposed on the normal tides and storm surge can have disastrous effects on shore structures and produce flooding of the coastal and inland areas.

Section V. Freshwater Inflow

2-25. Freshwater Sources. So far the topographic classification of estuaries, the astronomical tide-generating factors, and the meteorological and seismic wave-generating factors have been discussed. The final critical forcing function of an estuary is the amount of fresh water delivered to the system. This fresh water can be flow from the drainage basin of the river, ground water, discharge from dams and reservoirs, and rain falling on the water surface. The US Geological Survey (USGS), Water Resources Division, in cooperation with state and local governments, collects and disseminates hydrologic data of stream discharge or stage, reservoir and lake storage, ground-water levels, and the quality of surface and ground water. All data are stored in the USGS National Water Storage and Retrieval System (WATSTORE) and are available upon request to the USGS regional office or the USGS in Reston, Virginia.

2-26. Episodic Events. Episodic events that produce extreme quantities of water in a drainage basin can have a significant effect on the freshwater/salinity balance of an estuary. The seaward displacement of the salinity zone by sediment-laden fresh water will result in drastically different salinity and shoaling patterns.

Section VI. Changes in Sea Level

2-27. Sea Level Rise. Sea level rise refers to the rise in sea level or the apparent rise in the ocean surface when compared to a stable landmark. This, however, is a very general description for a more complicated event. The actual rise in the ocean is not one that is readily noticeable, especially when the average value varies 0 to +1 centimetre per year. The geologic record indicates that shifts in climate and the associated changes in sea level are attributed to the global

freeze and thaw cycles. These trends are most noted in the Pleistocene epoch, or ice age, when the ocean level was much lower due to the fact that much of the available water was frozen in the glaciers. Other events and factors can affect the rate of change:

a. The Greenhouse Effect. Overall global warming (postulated by the greenhouse effect) will cause thermal expansion of the seas and melting of snow and ice at increased rates and thus increase ocean levels. The greenhouse effect is not a part of the cyclic warming or cooling periods of natural weather patterns, but is related to man- influenced changes in the atmosphere and ozone layer. Future rates of change caused by warming are unknown.

b. Subsidence. Along coasts consisting of deposited materials, subsidence may occur due in part to consolidation of recent sediments. Subsidence may also occur due to man's activities, such as withdrawal of oil, natural gas, and water, or by the additional weight of structures.

c. Tectonic Activity. Such events as earthquakes and crustal movements may in fact raise or lower coastal areas somewhat and as a result negate or magnify the rising sea level.

d. Geomorphology of the Area. Some coastlines are termed as sinking (such as the US east coast) whereas some are considered rising (US west coast). Few, if any, reliable measurements are available.

2-28. Apparent Sea Level Rise. Because of these and other factors, it would be more accurate to use the term apparent sea level rise since there is the possibility that the particular area in question may actually be subsiding. Additional reading on this topic can be found in most books dealing with oceanography, geology, and geomorphology.

Section VII. Summary

2-29. Classifying an Estuary. The classic definition of an estuary includes these three characteristics: semienclosed, free connection with the open sea, and fresh water derived from land drainage. These three characteristics govern the concentration of seawater; therefore, salinity is the key to estuarine classification. The mixing of fresh water and seawater produces density gradients that drive distinction estuarine (gravitational) circulation patterns. These circulation and shoaling patterns differ with each estuary system according to the depth, tidal amplitude and phase at the mouth, and the amount of fresh water flowing into the basin. The tide that approaches the mouth of the estuary is the result of all the astronomical, meteorological, seismic, and man-made factors affecting amplitude and frequency of the wave. As the tide enters the estuary, it is greatly influenced by the river depth, width, and discharge. Tides exhibit wave behavior, usually as a combination of progressive and standing waves, with maximum flood velocity occurring 1-3 hours after high water. Superimposed on this tidal action is the freshwater/saltwater interaction. Salt water will advance up a system until the tidal flow can no longer overcome the riverflow. Depending on the relationship between tidal flow and riverflow, the estuary can be classified by its salinity structure and resulting circulation patterns.

CHAPTER 3
HYDRODYNAMIC ANALYSIS OF ESTUARIES

Section I. Factors Influencing Hydrodynamics

3-1. Introduction. A hydrodynamic analysis of a complex estuarine system requires a reasonable knowledge of those factors influencing estuarine circulation. Circulation in estuaries is quite complex and mainly dependent on the relative magnitudes of tidal variations in water levels and currents, freshwater inflow, gravitational forces caused by density differences between the ocean and fresh water, and to a lesser extent, the Coriolis acceleration. Wind and waves also become important for some estuaries and for short durations in most estuaries. The mixing regime and resultant salinity distribution depend on the relative magnitudes of these forces.

3-2. Tides. See Paragraphs 2-11 through 2-19.

3-3. Freshwater Inflow. See Paragraphs 2-25 and 2-26.

3-4. Salinity. See Paragraphs 2-5 through 2-9.

3-5. Coriolis Force. In large estuaries the earth's rotation deflects flowing water to the right in the northern hemisphere and to the left in the southern hemisphere. In the northern hemisphere, flood tide currents are deflected towards the left (looking seaward) and ebb current to the right, resulting in a net counterclockwise circulation. This circulation is referred to as Coriolis circulation. Therefore, water-surface elevations are higher on the left (looking seaward) during flood tide and higher on the right during ebb tide. Coriolis force explains why in Chesapeake Bay the salinity is, on the average, higher on the eastern shore (on the left looking seaward) than on the western shore. A detailed discussion on Coriolis is given by Officer (1976).

3-6. Geometric Influences. The amplitude of a tidal wave progressing up an estuary is influenced by the geometry of the estuary in several ways:

a. If the estuary is convergent, the amplitude tends to increase.

b. Since the length of the estuary is generally less than the tidal wavelength, wave reflection from the sidewalls may be expected due to rapid convergence. This continuous reflection of energy tends to reduce the incident wave amplitude.

c. Energy dissipation by boundary friction tends to reduce the amplitude of the incident wave. If the estuary has a small bottom slope and is very long and without physical obstructions, the latter two effects may dominate and the tidal amplitude may gradually diminish to zero. The motion in such an estuary is therefore characterized by a single progressive wave. In such case the incident wave at the ocean entrance is equal to that which would be observed by a tide gage at that point.

3-7. Seiching. Seiches are standing waves of relative long periods that occur in basins. Seiches in basins within estuaries can be generated by local changes in atmospheric pressure and wind and by oscillations transmitted into an estuary from the open sea. Standing waves of large amplitude are likely to be generated if the force that sets the water basin in motion is periodic in character, especially if the period of the force is the same as, or is in resonance with, the natural free oscillating period of the basin. Equations that can be used to evaluate basins with regard to seiching problems have been developed (Abbot 1979 and Silvester 1974).

3-8. Temperature. The density of seawater depends on both the salinity and temperature, but in estuaries the salinity range is large and the temperature range is generally small. Consequently, temperature has a relatively small influence on the density. Little information has been published on temperature fluctuations in estuaries. One can visualize

estuaries, however, where temperature could be a dominant factor at times. Many tropical estuaries have little riverflow entering them during the hot season. Surface heating could then provide sufficient density difference between the estuary and the sea to maintain a gravitational circulation; however, these effects would be transitory. In many fjords there is no river discharge in winter and surface waters can then become more dense than those at depth and will tend to sink. This vertical circulation phenomenon is known as thermocline convection.

Section II. Solution Methods

3-9. General. Solutions to estuarine hydrodynamic problems are obtained principally by use of the four primary methods--field observations, analytical solutions, numerical models, and physical models. Any of these four, or a combination thereof, may be the best approach for solving a particular problem. Choosing between them requires knowledge of the phenomena that are important to the problem and an understanding of the strengths and weaknesses of the solution methods (McAnally et al. 1983).

3-10. Field Observations. Field (prototype) data collection and analysis serve both as an important aspect of the other solution methods and as an independent method. Alone, field data demonstrate the estuary's behavior under the specific set of conditions that existed during the time of measurement. By skillful scheduling of data collection, careful analysis, and luck, one can obtain estimates of the separate effects of tides, river discharge, wind, and other variables. Field data can reveal problem areas, define the magnitude of problems, and can, to a limited extent, be used to estimate the estuary's repsonse to different conditions of tide and river discharge. They can also be used in an attempt to identify changes caused by a modification to the estuary. Field data are also an indispensable element in verification of numerical and physical models; they are used by the modeler to adjust the model and show that model results are reliable. Obtaining sufficient temporal and spatial data coverage in the field is a formidable and expensive talk; available field data are often too sparse to describe an estuary in any but the most general terms. Those not intimately familiar with data collection and analysis often overestimate the accuracy and reliability of the data. Information on the design of a field survey along with an example is given in Appendix B.

3-11. Analytical Solution Methods. Analytical solutions are recognized as a separate solution method, but they must be carefully defined to distinguish them from numerical models. Analytical solutions are those in which answers are obtained by use of mathematical expressions. These expressions or equations describe physical phenomena in mathematical terms and thus may be considered to be mathematical models of physical reality. For example, Manning's equation is a simple analytical model of the complex process of energy losses in open-channel flows. A more rigorous and complete analytical model of the losses is included in the turbulent version of the Navier-Stokes equations, known as the Reynolds equations.

a. Analytical models usually combine complex, poorly understood phenomena into coefficients that are determined empirically. Manning's roughness coefficient, for instance, combines the various effects of energy dissipation into a single parameter. The degree of simplification of the analytical model dictates how it is solved. For example, Manning's equation can be solved directly, whereas the Reynolds equations must be simplified and solved by numerical methods.

b. In an analytical model can be solved by substituting values of the independent variables into the equation (a closed form solution), then the solution method is also analytical. The calculation may be performed by hand or by a computer, but the solution is still an analytical one.

c. The analytical solution method has advantages of speed and simplicity but it cannot provide many details. In estuaries, analytical solutions can be used for gross representations of tidal propagation and average cross-sectional velocities in simple geometries. Details of flow cannot be predicted. The usefulness of analytical solutions declines with increasing complexity of geometry or increasing detail of results desired.

d. As an example, an analytical solution technique for the prediction of salinity intrusion in an estuary is given in Appendix C.

3-12. Numerical Modeling. Numerical modeling employs special computational methods, such as iteration and approximation, to solve mathematical expressions that do not have closed form solutions. A numerical model thus applies numerical (computational) analysis to solve mathematical expressions that describe the physical phenomena. The distinction between analytical solutions obtained by computer calculations and numerical modeling solutions may become this EM, the computer programs used to solve the governing equations are referred to as generalized computer programs or codes. When the codes are combined with a geometric mesh (grid) and specified parameters representing a particular estuary, the combination is called a model.

a. Numerical models used in coastal hydraulic problems are of two principal types--finite difference and fine element. The finite difference method (FDM) approximates derivatives by differences in the value of variables over finite intervals of space and time. This requires discretization of space and time into regular grids of computation points. Finite difference methods have been in widespread use for unsteady flow problems since 1970, whereas the finite element method (FEM) has been widely applied to open-channel flow problems only since 1975. The latter method employs piecewise approximations of mathematical expressions over a number of discrete elements. The assemblage of piecewise approximations is solved as a set of simultaneous equations to provide answers at points in space (nodes) and time.

b. Numerical models are classified by the number of spatial dimensions over which variables are permitted to change. thus in a one-dimensional flow model, currents are averaged over two dimensions (usually width and depth) and vary only in one direction (usually longitudinally). Two-dimensional models average variables over one spatial dimension, either over depth (a horizontal model) or width (a vertical model). Three-dimensional models solve equations accounting for variation of the variables in all three spatial dimensions.

c. Numerical modeling provides much more detailed results than analytical methods and may be substantially more accurate, but it does so at the expense of time and money. Models of sufficient detail may require very large computers to solve the large systems of equations and store results. Once a numerical model has been formulated and verified for a given area, it can quickly provide results for different conditions. Numerical models are capable of simulating some processes that cannot be handled in any other way. However, they are limited by the modeler's ability to provide and accurately solve mathematical expressions that truly represent the physical processes being modeled. For example, existing three-dimensional models are presently considered to be the most effective method for predicting wind-induced currents in complex geometry, but physical models are considered superior for salinity-induced density current prediction in complex geometries. Because of their newness, much less is

known about the ability of numerical three-dimensional models to reproduce estuarine flows. An example two-dimensional numerical model investigation is given in Appendix C.

3-13. Physical Models. Physical scale models have been used for the past century to solve estuarine hydraulic problems. Careful observance of appropriate scaling requirements permits the physical modeler to obtain reliable solutions to problems that often can be solved no other way. Physical hydraulic models of estuaries can reproduce tides and other long waves, some aspects of short-period wind waves, longshore currents, freshwater flows, pollutant discharges, some aspects of sedimentation, and three-dimensional variations in currents, salinity, density, and pollutant concentration. Applicability of model laws and choice of model scales are dependent on which of these phenomena are of interest. Present practice does not include simulation of water-surface setup and currents due to wind. Conflicts in similitude requirements for the various phenomena usually force the modeler to neglect similitude of some phenomena to reproduce more accurately the dominant processes of the situation. For example, correct modeling of tides and currents often requires that a model have different scales for vertical and horizontal lengths. This geometric distortion permits accurate reproduction of estuarine flows and is a common and acceptable practice, but it does not permit optimum modeling of short-period waves, which requires an undistorted-scale model for simultaneous reproduction of refraction and diffraction.

3-14. Hybrid Method. The preceding paragraphs have described the four principal solution methods and some of their advantages and disadvantages. In practice, two or more methods are used jointly, with each method being applied to that portion of the problem for which it is best suited. For example, field data are usually used to define the most important processes and verify a model that predicts hydrodynamic conditions in an estuary. Combining two or more methods in simple ways has been common practice for many years. Combining physical modeling and numerical modeling to provide results not obtainable any other way is termed a hybrid solution method; combining them in a tainable any other way is termed a hybrid solution method; combining them in a closely coupled fashion that permits feedback between the models is termed an integrated hybrid solution. Judicious selection of solution methods in a hybrid approach can greatly improve accuracy and detail of the results. By devising means to combine results from several methods, the modeler can include effects of many phenomena that previously were neglected or poorly modeled. Examples of processes that are good candiditates for hybrid modeling are sediment transport and flow hydrodynamics or tidal flows and short-period waves. In the first case, hydrodynamics drives the sediment transport process, and if the study is carefully designed, the feedback from bed change to hydrodynamics is minimal. In the second case, the interaction of the two processes is often dominated by one or the other such that they can be analyzed as independent events and the results combined. Processes that have a strong feedback loop, such as the hydrodynamics of freshwater/saltwater interaction, are not suitable for the hybrid approach and consequently should be analyzed together.

CHAPTER 4
SEDIMENTATION ANALYSIS OF ESTUARIES

4-1. Introduction. This chapter will provide an overview of the various concepts of sedimentation in estuaries, the processes and transport, and the analysis and modeling methods currently in use. For those readers of this manual who are concerned directly with problems of estuarine sedimentation, a more complete treatment of this subject, including notation, is presented in Appendix D.

4-2. Sedimentation Sources. Identification of the sources of sediment can be a key factor in problem solving.

a. Upland. The predominant source usually is erosion of lands bordering the water body, but erosion of banks by currents and waves within the estuary itself, as well as aeolian transport, introduces smaller amounts of sediment more directly. Municipal, agricultural, and industrial wastes may also be a significant source of sediments.

b. Biogenic. In biologically active areas, production within marshes and the main esturial water body itself can significantly enhance suspended sediment load (Kranck 1979).

c. Coastal. Close to the esturial mouth, the sediment is often of marine origin. In areas where the open seacoasts are sandy, such as along much of coastal Florida, it is common to find the bed in the mouth or entrance channel to consist predominantly of sand. Landward of the entrance the grain size decreases and the fraction of fine-grained material or marshy origin tends to increase with distance upstream (Mehta and Jones 1977). In some estuaries, e.g., the Mississippi or the Amazon, where sediment supply from upstream sources has been relatively high on a geologic time scale, the offshore ebb delta is laden with deep layers of fine-grained material (Gibbs 1977; Wells 1983). Salinity- and tide-driven flows can transport some of the ebb deltaic deposits (resuspended during flood flows coupled, oftentimes, with offshore wave activity) upstream through the channel. The material is then redeposited in reaches where the currents are too weak to transport the material further (Partheniades 1966).

4-3. Sediment Classification. For engineering purposes, sediments are customarily classified primarily according to particle size. Sediment of size greater than about 0.074 mm (No. 200 sieve size) is considered to be coarse, and less than this size, fine-grained. The boundary between cohesive and coheisonless sediment is, unfortunately, not clearly defined and generally varies with the type of material. It is, however, appropriate to state that cohesion increases with decreasing particle size. Clays (particle size < 0.005 mm) are much more cohesive than silts (0.005 to 0.074 mm), and, in fact, cohesion in natural muds is due primarily to the presence of clay-sized sediment.

a. Muds. Esturial muds are typically composed of a wide range of materials including clay and nonclay minerals in the clay- and silt-size ranges, organic matter, and sometimes small quantities, e.g., ~5-10 percent by weight, of very fine sand.

b. Size. The particle size distribution of cohesionless materials is easily determined by sieve analysis, and reported in terms of either diameter d or in ϕ units (i.e., as $-\log_2$ x diameter, mm) (Vanoni 1975).

c. Settling Velocity. The key transport-related parameter of sediments is the settling velocity, which, unfortunately, does not bear a unique relationship to particle size. Laboratory settling columns can be used to measure settling velocity distribution, which may be considered as a very useful property for sediment classification (Channon 1971; Vanoni 1975).

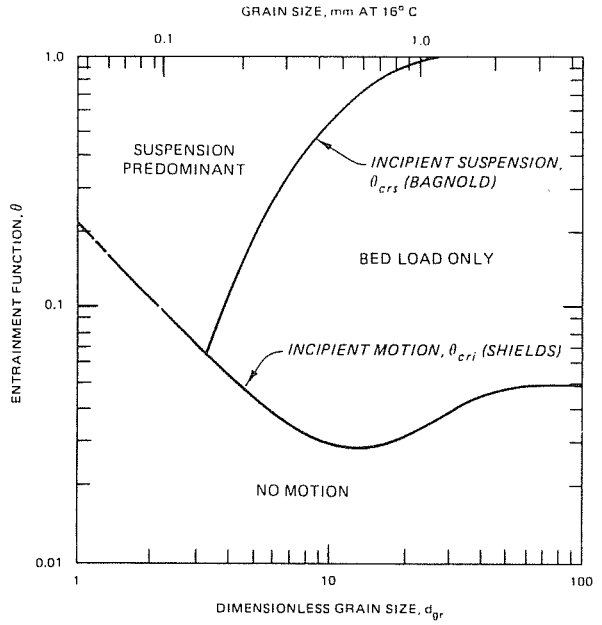

FIGURE 4-1
Relationship between entrainment function θ and dimensionless grain size d_{gr} (after Ackers 1972)

d. Cohesive Treatment. Standard hydrometer or pipette methods are used to determine the dispersed particle size distribution (American Society for Testing and Materials (ASTM) 1964). The original sample should not be dried before determining the size distribution, inasmuch as prior drying prevents the material from dispersing adequately (Krone 1962).

e. Deflocculation. Cohesive sediment size distribution obtained without dispersion will be that of the flocculated material.

f. Settling Tests. A convenient laboratory procedure for obtaining the settling velocity of flocculated sediment consists of settling tests in a column from which suspended sediment can be withdrawn at various elevations and different times after test initiation (Owen 1976; Vanoni 1975).

4-4. Coarse Sediment Transport. Coarse-grained sediment includes material with particle sizes larger than about 0.074 mm (74 μm), the most common sediment being sand, although some estuarial beds are laden wholly with coarser material including shells and gravel (Kirby 1968).

a. Tidal Entrance. With reference to sand transport, the estuarial mouth or tidal entrance can be conveniently treated as a geomorphologic unit separate from the remainder of the estuary.

b. Formula Application. The application of sediment transport formulas developed for unidirectional flows is usually suitable to tide-dominated oscillatory flows because the tidal frequency is low, and tidal currents may be considered to be "piecewise" steady. Differences tend to arise due mainly to three causes:

(1) The complexity of flow distribution resulting from salinity effects.

(2) The condition of slack water and flow reversal following slack.

(3) The dependence of bed forms and associated bed resistance on the stage of tide and the direction of flow (Ippen 1966).

c. Rate of Transport. The total rate of sediment transport is the sum of contributions from bed load and suspended load. A dependence of bed-load rate on flow velocity cubed is consistent with the concept of relating sediment transport to unit stream power (Yang 1972; Vanoni 1975).

d. Total Load. Bed material load is that portion of the total load represented in the bed. The remainder is wash load. As is evident, this material is typically fine-grained and, unlike bed material load, it is believed to be independent (uncorrelated) of flow condition (Partheniades 1977).

e. Sediment Behavior. Whether a sediment under a given flow condition behaves as bed load or as suspended load depends on the relationship between the entrainment function and the dimensionless grain size as illustrated in Figure 4-1 (Ackers 1972).

f. Contribution by Load. The contribution of suspended load relative to bed load (in total load) depends on the grain size, the flow regime, and the estuarial morphology.

g. Sediment Supply. The rate of supply of "new" sediment from the river varies widely from one estuary to another, and, in a given estuary, there is usually a strong seasonal dependence as well (Krone 1979). Normally, however, the oscillatory, "to and fro," tide-controlled transport is orders of magnitude higher than the net (incoming minus outgoing) input of sediment. In the long term, such factors as changes in the upstream discharge hydrograph and sediment supply rates, morphologic changes within the estuary, sea level change, and eustatic effects will alter the sediment transport regime (Dyer 1973; McDowell and O'Connor 1977).

h. Closure. Closure or tidal choking is a potential problem at sandy entrances in which the strength of flow is insufficient to scour the bed, with the result that littoral drift is deposited in the mouth, the depths become shallow, and the entrance closes eventually (Brunn 1978). Training walls or jetties and dredging between the jetties coupled, sometimes, with a system for bypassing sand from the updrift beach to the downdrift beach can be used to keep entrances open (Brunn 1978).

4-5. Cohesive Sediment Transport. Cohesion results from interparticle electrochemical forces, which become increasingly important relative to the gravitational force with decreasing particle size below ~0.04 mm. Clays, which have sizes less than 0.005 mm, are particularly cohesive (van Olphen 1963). In addition to the negative charge on its surface, the clay particle, like all material surfaces, possesses London-van der Waals electrochemical forces of atomic origin. If sufficient salt is present, the double layer is considerably compressed and the London-van der Waals forces "stick out" beyond the double layer. In this event, the micelles will attract each other and coagulation will occur.

a. Particle Cohesion. Particle cohesion requires interparticle collision. There are three basic mechanisms for collision: Brownian motion, flow shear due to turbulence, and settling of particles at different speeds, or differential settling (Hunt 1980). Out of these, shearing in the fluid column, which is prevalent throughout the tidal cycle except at slack water, produces the strongest interparticle bonds (Krone 1972).

b. Salinity Effects. When salt concentration in water exceeds 2 to 3 ppt, coagulation of major clay types, i.e., kaolinite, illite, and montmorillonite, is complete (Hayter 1983).

c. Settling Velocity. Under continued collision, aggregates tend to build up into units of different densities, shear strengths, and sizes, and these consequently have different settling velocities. Each sediment-fluid mixture has its own characteristic settling velocity-concentration relationship (Kron 1962; Burt and Stevenson 1983).

d. Concentration Effects. At very low concentrations, e.g., ~100 mg/ℓ or less, interparticle collision frequency is restricted and the settling velocity shows no significant

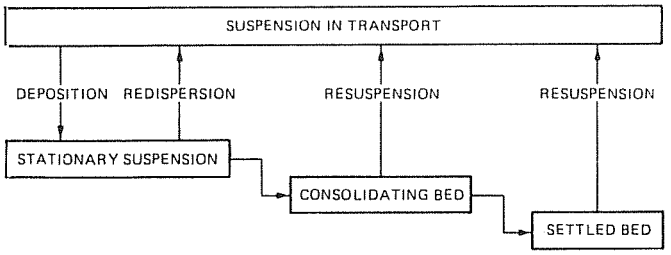

FIGURE 4-2
Schematic representation of the physical states of cohesive sediment in estuarial waters (from Mehta et al. 1982)

dependence on concentration. At higher concentrations, up to ~3,000-5,000 mg/ℓ, aggregation is enhanced with increasing concentration. At even high concentrations the settling velocity begins to decrease with increasing concentration. This is referred to as hindered or zone settling. The term fluid mud is often used to describe a high concentration (> 10,000 mg/ℓ) suspension that characteristically exhibits the hindered settling behavior (Krone 1962).

e. Exceptions. Aggregates of sediment in the clay- and silt-size range typically behave as bed material load (however, not as bed load), while every fine material, e.g., derived from biogenic sources, often behaves as wash load, not being represented in the bed.

f. Particle Size. Inasmuch as cohesive aggregate properties (e.g., size, density, and shear strength) depend on the type of sediment-fluid mixture as well as on the flow condition itself, particle size has a different meaning here than in the case of cohesionless sediment, since aggregate size is not an easily characterized quantity. Critical shear stress for erosion depends on the mode of formation and degree of consolidation of the bed (Mehta et al. 1982). It becomes essential to conduct laboratory erosion tests to evaluate the bed shear strength for a given mud-fluid mixture (Mehta et al. 1982; Parchure 1984).

g. Deposition. The processes of cohesive sediment deposition and erosion are interlinked through bed consolidation. Rates of deposition and erosion in turn determine the rate of horizontal transport in suspension. In a tidal estuary, these processes are characteristically cyclic in nature; their interrelationship is schematized in Figure 4-2 (Mehta et al. 1982). As observed, suspension in horizontal transport interacts with the bed through tide-controlled, time-dependent, deposition-consolidation-erosion process. During consolidation (and gelling), upward escape of the pore water occurs, the bed density increases, and physiochemical changes occur within the bed as the deposited aggregates are crushed slowly under overburden. A settled, or fully consolidated, bed eventually results. Relatively thin deposits, on the order of a few centimetres thickness, practically consolidate in a week or two, but thick deposits may remain underconsolidated for months or even years.

h. Erosion. Immediately following slack water, a stationary suspension begins to erode or resuspend rapidly as the flow speed picks up. This is often referred to as mass erosion or redispersion (Park and Kirby 1982). A fully consolidated or a settled bed erodes by a slightly different process. At relatively low bed shear stresses (or velocities), aggregates from the bed surface are entrained. At high shear stresses, or under rapidly accelerating flows, erosion is much more rapid, and relatively large chunks of sediment are entrained.

i. Depth Effects. In deep estuaries, there can be a significant lag between nearbed suspension response to deposition/erosion and the corresponding response at the surface. This type of hysteresis effect is set up as a result of the time it takes for sediment to diffuse upward and the corresponding sediment settling time.

4-6. Impact of Tidal Flow and Geometry. Sedimentary boundary conditions are critically important in governing estuarial sediment transport. At the mouth, tidal forcing is determined by the open coast tide characteristics as well as the geometry of the mouth itself. At the upstream end, beyond the influence of tides, the river discharge hydrograph and sediment inflow are key factors. In addition, runoff, direct precipitation, and bank erosion by currents and waves can be significant factors that contribute to the overall sedimentary regime.

a. Deposition. Deposition-dominated environment includes flood and ebb deltas near the mouth, shoal areas within the estuary including natural and dredged navigation channels, and basins including ports and marinas.

b. Erosion. Sites where erosion is predominant tend to be localized in comparison with sites of deposition, although sometimes large previously deposited shoals disintegrate in the absence of sediment supply.

c. Mixed Environment. In a mixed deposition/erosion environment in which net scour or shoaling is small, e.g., as would occur if the regime were in a state of "live bed" equilibrium, the rates of deposition and erosion can be high individually, and these would cause significant "to and fro" transport of sediment during a tidal cycle or over a spring-neap cycle.

d. Waves. Shallow- and intermediate-depth water waves provide a critically important mechanism for incipient motion and resuspension of bottom sediment. The sediment is then advected by the tidal currents. Waves breaking at the banks can also cause a measurable increase in sediment transport rates in some cases.

e. Wind. Aeolian transport is usually ignored in typical estuarial transport calculations. However, in certain well-defined areas such as small basins, windblown material can form a significant fraction of the total deposit, particularly where sediment transport rates in the water body are not high.

f. Sea Level Rise. The rise of sea level relative to land should be considered when comparing bathymetric surveys taken at different times, for the purpose of determining long-term rates of shoaling or scour (Krone 1979).

g. Geometry. The impact of estuarial geometry on sediment transport is associated with the effect of geometry on flows that transport sediment. For example, it is quite common to find relatively well-defined flood- and ebb- dominated channels with consequent implications for the direction of sediment transport. Furthermore, deep, dredged channels often are natural sites for sedimentation as are basins constructed along estuarial banks. Natural flood-plains are historic sites for deposition of alluvial material, which provides fertile soil necessary for agriculture. Diversion of tributary flows for agricultural or urban uses can have deleterious effects, on both sedimentation as well as water quality (McDowell and O'Connor 1977).

4-7. Sediment Characterization. Characterization tests for the sediment depend on the nature of sediment, i.e., coarse or fine-grained. It may be necessary to separate the coarse and fine fractions and analyze them separately.

a. Coarse Sediment. For coarse sediment it is typically useful to evaluate particle size distribution or, preferably, settling velocity distribution; material density and bed porosity; and, sometimes, the angle of repose.

b. Analysis. Size distribution is customarily obtained through sieve analysis in terms of selected sieve sizes. It is preferable to characterize sediment by its settling velocity, which is a more fundamental property than size as far as

sediment transport is concerned. Details on particle size and settling velocity measurements as well as material density and bed porosity are found in Vanoni (1975). The angle of repose is a basic property associated with bank stability as well as with incipient grain movement (Lane 1955; Mehta and Christensen 1983).

c. Cohesive Sediment. For cohesive sediment, the problem of characterization is more complex than that for coarse-grained material, because sediment aggregate properties depend on the type of sediment, the fluid, and the flow condition itself.

d. Characterizing Sediment. For characterizing the sediment, it is recommended that the following be specified through various laboratory measurement procedures:

(1) Grain size distribution of dispersed sediment using, for example, the standard hydrometer test (ASTM 1964).

(2) The relationship between the median (by weight) settling velocity and the suspension concentration of the flocculated sediment, noted in Owen (1976).

(3) Clay and nonclay mineralogical composition through X-ray diffraction analysis (Grim 1968).

(4) Organic content (Jackson 1958).

(5) The cation exchange capacity, which is a measure of the degree of cohesion of the clay (Grim 1968).

e. Characterizing Fluid. For characterizing the fluid, it is recommended that the following be specified.

(1) Concentrations of important cations (e.g., sodium (Na+), calcium (Ca++), and magnesium (mg++) and anions (e.g., chlorine (Cl-) and sulfate (So_4--)).

(2) Total salt concentration.

(3) pH.

(4) Fluid temperature during measurements as well as in laboratory experiments for determining the rates of erosion and deposition.

Items 1, 2, and 3 can be determined through standardized chemical analysis procedures.

f. Sodium Adsorption Ratio. Recognizing that sodium, calcium, and magnesium are three comparatively more abundant and influential cations, the sodium adsorption ratio (SAR) is found to be a convenient parameter for characterizing the influence of fluid chemistry on cohesive sediment transport behavior. SAR, total salt concentration, pH, and fluid temperature have been shown to control and critical shear stress for erosion of soils with uniform bed properties (Ariathurai and Arulanandan 1978).

g. Core Samples. Inasmuch as consolidation increases bed density, it is important to obtain representative in situ bottom cores for determining the depth distribution of the density (bulk and dry) of the bed. This information enables a conversion between deposition and erosion of sediment mass per unit time and the corresponding changes in the suspension concentration (mass per unit volume).

h. Rheological Properties. In studies in which dissipation of fluid energy within the bed plays an important role, e.g., wave-mud interaction, it is essential to evaluate the rheological properties, the most important one being the viscosity, which has been found to be related to sediment concentration in an approximate manner (Krone 1963). Most commonly this includes the Bingham yield stress, for a comparatively simplified rheological description.

i. Usage of Collected Data. The characterization of sediment is necessary to aid in the identification of transport and deposition processes. Preplanning for specific project data collection programs is essential so that the proper type, quantity, and data analysis can be conducted. The preceding and following paragraphs describe various field tests and sediment analysis, which may or may not be required. The amount and type of data and required procedures and tests should be determined during the project planning stage. Too much or too little data could be costly and detrimental to the project. These chapters and appendices provide general guidance; specific guidance can be found in Appendix A through the Hydraulics Laboratory, WES.

4-8. Transport Parameters. The movement of sediment is sensitive to flow speed and direction, and it is particularly important to characterize the flow regime including the influences of salinity, wind, and related factors for a comprehensive evaluation of the overall sediment transport regime.

a. Settling Velocity. Particle settling velocity is both an important sediment-characterizing parameter as well as a deposition-related parameter. The critical shear stress is the important erosion-related parameter. Field and laboratory procedures for evaluating these and associated parameters, where cohesionless sediment transport is concerned, are well documented in literature (Vanoni 1975). Use of sediment transport formulas without adequate calibration of the formula may lead to major errors in transport rate prediction.

b. Processes. Cohesive sediment transport processes that require parameter characterization include settling and deposition, consolidation, and erosion.

c. Procedures. Settling is principally characterized by the relationship between the settling velocity and suspension concentration. There are basically four procedures for evaluating this relationship, each under a specific set of conditions and therefore yielding results peculiar to those conditions:

(1) Tests in a laboratory settling column (ASTM 1964; Krone 1962; Hunt 1980).

(2) Tests in a laboratory flume (Krone 1962; Mehta and Partheniades 1975).

(3) Use of in situ settling tube. This tube, designed originally by Owen (1971), allows for on site measurements. By performing the settling test almost immediately following sample withdarwal from the water body, the aggregates are presumed to remain unaltered in composition.

(4) Comparison of measured suspended sediment concentration profiles (depth-concentration variation) with analytic prediction (O'Connor and Tuxford 1980; Mehta et al. 1982; Vanoni 1975).

d. Field Measurement. For prototype application, the in situ tube is preferred for measurement of settling velocity. Extensive measurements of this nature have, for instance, been obtained in the Thames Estuary in England (Burt and Stevenson 1983). Laboratory flume tests should be used for supplementary and/or confirmatory evidence. The same holds for settling columns. Different approaches will yield different results, in general.

e. Shear Stress. The rate of deposition depends on the rate at which the fraction of the settling sediment deposits, the remainder consisting of aggregates that break up near the bed under the action of bed shear stress and are reentrained. The critical shear stress for erosion τ_s can be evaluated from laboratory flume experiments (Krone 1962). For a uniform sediment (narrow primary particle size distribution), single values of settling velocity W_s and critical shear stress for deposition τ_{cd} will suffice. For a graded sediment (e.g., a typical mud with a relatively wide range of sizes from coarse silt to fine clay), W_s and τ_{cd} wil have corresponding wide ranges.

f. Gelling. Freshly deposited mud undergoes increases in both density and physiochemical changes associated with interparticle bonds, known as gelling. Following bed formation, gelling is complete in about a day (Krone 1983).

g. Bed Thickness. From the perspective of estuarial sediment transport, density increase and physiochemical changes are important because these in turn control corresponding changes in the bed shear strength with respect to erosion (Mehta et al. 1982). For relatively thin beds, e.g., on the order of a few centimetres in thickness, consolidation is practically complete in a period on the order of 1 or 2 weeks, and the rate of bed deformation becomes small in comparison with its value immediately following bed formation. Density and erosional shear strength become nearly invariant with further passage of time.

h. Bed Shear Strength. Investigators have found an approximate powerlaw relationship between the bed shear strength and density, specific to the type of sediment and fluid used (Migniot 1968; Owen 1970; Thorn and Parsons 1980).

4-9. Causes of Sediment Deposition. The rate of sediment mass deposition increases with increasing settling velocity W_s and with suspension concentration C and decreases with increasing bed shear stress τ_b, given τ_{cd}. It follows that the mass of sediment deposited depends on the availability of entrained sediment, its settling velocity, and flow condition as reflected primarily in the bed shear stress. This type of reasoning is generally applicable to cohesive as well as cohesionless sediment.

a. Definition. A deposition-dominated environment is characterized by a region of relatively low bed shear stress in which the rate of supply of sediment to the bed well exceeds the rate of depletion by erosion (Ippen 1966; Mehta et al. 1982).

b. Long-Term Monitoring. Estuaries tend to be in a state of quasi-equilibrium as far as the hydrodynamic and sedimentary processes are concerned. Superimposed on these processes of annual cycle of variation of tides, freshwater flows, salinity intrusion, and sediment transport, longer period variations in the physical regime also occur. Slow filling up of the existing deep channel or thalweg, coupled with scouring of a new channel elsewhere, may occur over a 10-20 year period (Calcutta Port Commissioners 1973; McDowell and O'Connor 1977). It is therefore critically important to understand the long-term estuarial behavior through an adequate monitoring program, particularly one involving extensive bathymetric surveys.

4-10. Consolidation. Consolidation is the volume change is deposited material with time. Fine or cohesive sediment deposits consolidate. Hindered settling can result in the formation of fluid mud. As sediments consolidate toward fully settled states, a self-weight component may be important to further consolidation.

a. Fluid Mud. The formation of fluid muds can alter the transport mode of fine-grained sediments and is therefore important to sediment dispersal analyses. Fine-grained material with high moisture or low bulk density has relatively low shear strength and can flow under the effects of gravity or the overlying flow. Fluid mud layers often collect in navigation channels.

b. Consolidation Tests. The amount of consolidation that disposed dredged material will undergo can be predicted by settling tube or accelerated consolidation tests and models (Montgomery 1978; Cargill 1983 and 1985). Similar zone or column settling tests can be performed on fine-grained sediments to determine settling characteristics over a range of high suspension concentrations. If self-weight consolidation modeling is to be carried out, special controlled-strain consolidation testing is required. Controlled-strain consolidation testing is performed at the WES Geotechnical Laboratory.

4-11. Physical Models. Physical hydraulic models are scaled representations of prototype estuaries. Physical hydraulic models can be important tools in sedimentation analysis of estuaries, and should be considered as one component of a program to study sedimentation if three-dimensional flow effects are known or suspected to be important. Most physical modeling of estuaries is performed at the WES Hydraulics Laboratory.

a. Scale. Sediments and sediment transport rates must be scaled in the models. Scale ratios for coarse sediments transported by quasi-steady hydraulic shear stresses are an acceptable compromise permitting useful predictions. Shoaling indices are employed. Scale ratios for fine sediments are more difficult to establish, and qualitative methods are used for hydraulic model prediction.

b. Processes. Physical hydraulic models have been successfully used to predict tidal currents, circulation, riverflows, salinity distributions, and dispersion processes. Many or all of these processes influence sedimentation. Physical hydraulic models have been successfully incorporated into hybrid model studies as will be discussed in a later section. Because they are real, physical representations, physical hydraulic models display system dynamics in a manner that can be readily assimilated by both modeler and lay persons. Physical hydraulic models can simulate long periods of time, spring-to-neap cycles, or hydrographs.

c. Test Procedures. During model verification hydraulic and salinity adjustments are made first. Sedimentation is verified to shoaling volumes computed from a series of prototype hydrographic surveys. Methods are developed during model verification to introduce, distribute, and collect model sediments.

4-12. Analytical Models. Analytical models are considerable simplifications of estuarine sedimentation processes but are useful for such tasks as screening, checking the reasonableness of other methods, and identifying important processes. The following are some examples of analytical models.

a. Prototype Data Treatment. Analytical models are a method of treating prototype data. Time series velocities and concentrations can be integrated using assumed critical shear stresses to estimate depositional flux or net deposition. Several equations can be used for this purpose and form the basis for a closed-form mathematical solution.

b. Flux Analysis. An alternate or supplemental analysis to that of the last section is horizontal suspended flux analysis using prototype data. Horizontal flux analysis makes no assumption about deposition characteristics of sediments. Deposition or erosion is inferred from longitudinal gradients of sediment flux in this method. Measurements of currents, salinities, and suspended sediment concentration over depth and over a tidal cycle can be used to calculate the total fluxes at a station.

c. Depositional Models. Zero-dimensional (in the spatial domain) models can be applied to basins or to channels with relatively steady and uniform flows. A slightly more complex model incorporating tidal prism input could be applied to an estuary as a whole or to tidal basins (Appendix D).

4-13. Numerical Models. A number of estuaries have been numerically modeled at the WES Hydraulics Laboratory. A two-dimensional (in the horizontal plane) numerical sedimentation model is included in the Corps' TABS modeling system. TABS is available to qualified users Corps-wide. Training on the TABS system is available at WES.

a. Model Processes. Numerical sediment models are transport models with nonconservative bed interaction terms.

Sediments are numerically transported by advective currents and by diffusion; therefore, sediment models require that currents be supplied by a hydrodynamic (usually numerical) model. Interactions between suspended sediments and the bed are governed by process equations in sediment transport models. Coarse sediment-bed interaction terms usually depend on the gradient of the transport potential of the material.

Fine sediment-bed interactions terms consist of process description for erosion and deposition. Bed structure or layering is usually modeled in some way to account for changes in density and shear strength with depth in fine sediments. Numerical sediment models are classified by their dimensions, sediment type, and the equations that are solved.

b. Model Applications. Numerical models are the most advanced modeling method available for simulating sedimentation. Numerical modeling, like other modeling methods, remains an art-science, and successful application to real problems depends heavily on the skill and intuition of the model user.

4-14. Hybrid Models. Combining two or more models in a solution method is a hybrid model. Hybrid models attempt to use the best modeling methods available for each "part" of sedimentation problems: current structure and sediment transport. The following are the most frequently used hybrid techniques, starting with the most rigorous.

a. Physical-Numerical. The physical-numerical hybrid modeling apporach uses a physical model to predict currents and a numerical model to predict sediment transport. This approach has been successfully applied to a number of estuarine sediment problems at the WES Hydraulics Laboratory (McAnally et al. 1983). The physical model can be used to generate boundary conditions for the detailed numerical mesh or grid of the sediment model.

b. Physical-Analytical. The physical-analytical hybrid modeling approach uses a physical model for currents and an analytical model to predict sedimentation. Velocities and bed shear stress histories can be collected at various points in the physical model. Physical model results can then be extended using some appropriate analytical expression(s).

c. Numerical-Analytical. A numerical-analytical hybrid model uses a numerical model to predict sedimentation. The numerical-analytical hybrid technique avoids the costs associated with numerical sediment modeling, but at the expense of considerable rigorousness. The results from a hydrodynamic model can be used to address limited questions on sedimentation with analytical models. The shear stress at various points can be evaluated to predict an indication of deposition or erosion (Hauck 1989).

4-15. Field Data Requirements. All analyses depend on field data. Field data acquisition may be the most costly part of a sedimentation study. Required data can be grouped into system definitin and behavior and boundary data. The following discussion is limited to sediment data requirements.

a. A good way to determine system behavior is to conduct a boat survey in which currents, salinities, and suspended sediment concentrations are collected at short time intervals (half hour) with depth at several stations across several cross sections over a tidal cycle. Tides at several locations and supporting measurements or observations of winds and other conditions are also required.

b. Bed sediment properties are required for system definition. Methods for sediment characterization were described in earlier sections. Fine-grained sediments require settling velocity evaluation, since settling is not related directly to individual particle size. Vertical profiles of suspended sediment concentration can be used to deduce settling velocities. Settling velocities can be estimated in the field using settling tube samplers. Settling experiments in the field are preferred to laboratory tests, although conditions may require the latter. It is usually not practical to carry out enough settling tests in the field to obtain sufficient spatial and temporal coverage. Therefore it is necessary to supplement field settling data with analysis of many vertical suspended sediment profiles or high-resolution particle size analysis (such as Coulter Counter analysis). Water column measurements of sediment concentration should be supplemented by some measurements near or at the sediment bed-water interface. Specifically, the presence of fluid mud should be checked using acoustic soundings, densimetric profiling, or low-disturbance coring devices. Shallow coring is also a good method of determining bed structures such as armoring, density differences, or layering.

c. Classification by the methods described in earlier sections may be useful in estimating sediment properties from existing data. Settling velocities, critical shear stresses for erosion and deposition, and the densities of fine-grained deposited material are properties that might require supplemental laboratory study.

CHAPTER 5
DESIGN CONSIDERATIONS

Section I. Control Works

5-1. Purpose. Control works are constructed in estuaries to confine channels to definite alignments, reduce or relocate shoaling, reduce wave action in harbor areas, improve navigation conditions, prevent or reduce salinity intrusion, or prevent or reduce flooding.

5-2. Types. The principal types of control works in estuaries are as follows:

a. Breakwaters. These structures are partial barriers at the entrance to embayments, coves, or channels in water subject to severe wave action for the purpose of providing shelter from waves. Examples are shown in Figure 5-1.

b. Training Dikes. Training dikes may be longitudinal structures extending along the course of the waterway in the critical reach, or alternatively a series of structures extending our from the shore generally perpendicular to the currents to guide or direct the currents, reduce channel shoaling, or prevent bank erosion. Examples are shown in Figure 5-2.

c. Salinity Barriers. One type is a dam that extends completely across the waterway to exclude saline waters from upstream areas. This type necessarily includes spillways to discharge flows from the upland, and often one or more sets of locks to permit vessels to navigate beyond the barrier. An example of this type of salinity barrier is shown in Figure 5-3. Another type of salinity barrier is the submerged sill. This type is intended to reduce salinity intrusion by disrupting the bottom salinity wedge as it intrudes upstream or to induce vertical mixing of the salt and fresh waters. The sill can be permanent, constructed of stone or other permanent material, or temporary, constructed of sand. A sketch of this type of barrier is shown in Figure 5-4.

d. Hurricane Barriers. Hurricane barriers are structures that extend completely across the waterway, except for gaps at navigation channels. The purpose of hurricane barriers is to reduce the magnitude of hurricane surges upstream of the barrier. An example is shown in Figure 5-5.

e. Revetments. Revetments are constructed along the banks of the waterway to prevent erosion by currents and waves. An example is shown in Figure 5-6.

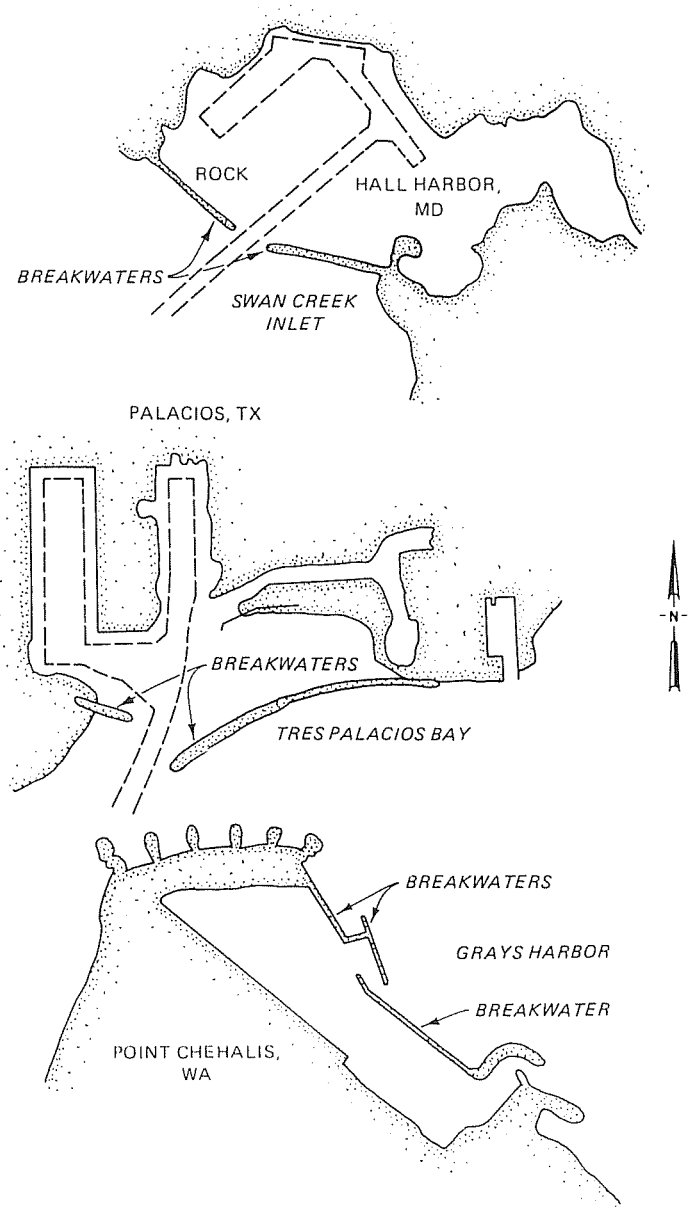

FIGURE 5-1
Estuarine breakwaters

f. Diversion Works. These works intercept freshwater discharges from upland areas and cause them to be discharged to sea using an adjacent waterway. An example is shown in Figure 5-7.

g. Sediment Traps. These traps (or sediment basins) are areas in the waterway that are excavated to depths and widths equal to or greater than those of the adjacent navigation channel. They generally extend across the navigation channel although sometimes they are located in a side channel that is connected with the navigation channel. Their purpose is to reduce maintenance dredging costs by accumulating sediments within the trap rather than in scattered deposits along the channel in areas sometimes difficult to dredge or remote from disposal sites. Examples of estuarine sediment traps are given in Figure 5-8.

Section II. Design Factors

5-3. General. In control works projects, there are usually six factors that must be addressed by hydraulic engineers during the design of the project. The impact of the project of

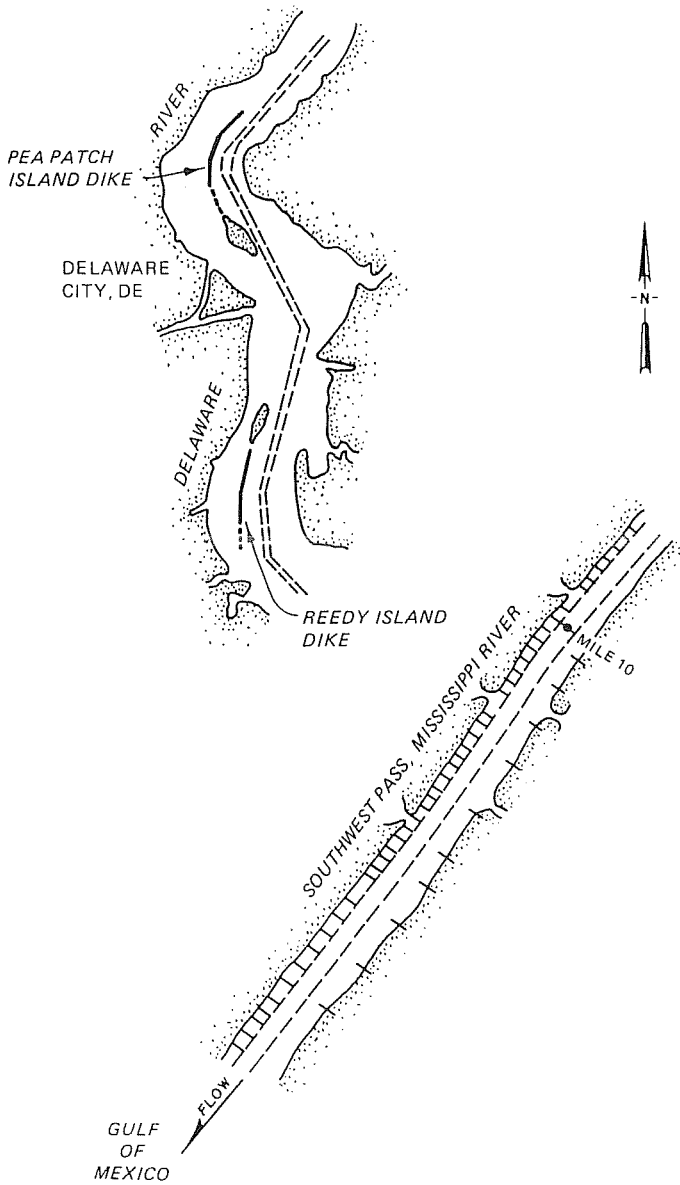

FIGURE 5-2
Training dikes

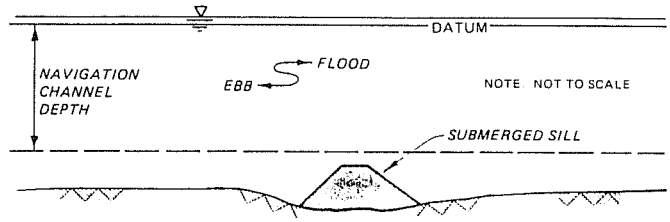

FIGURE 5-4
Submerged sill salinity barrier

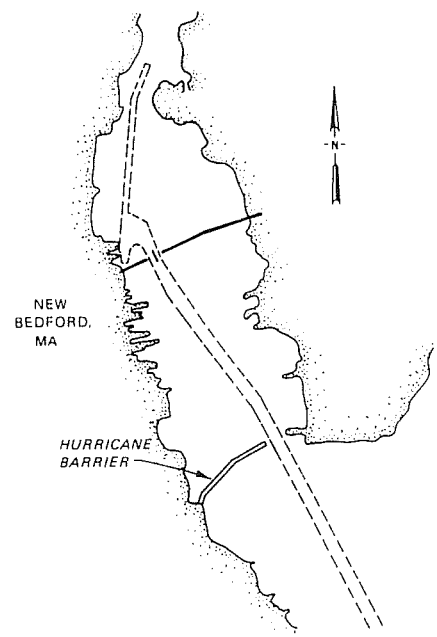

FIGURE 5-5
Hurricane barrier

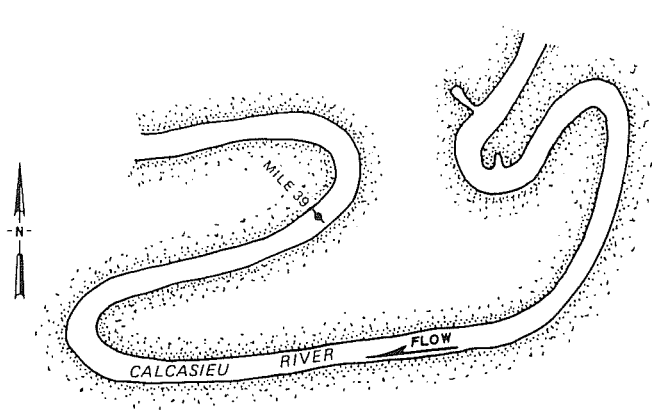

a. MEANDER PRIOR TO CONSTRUCTION

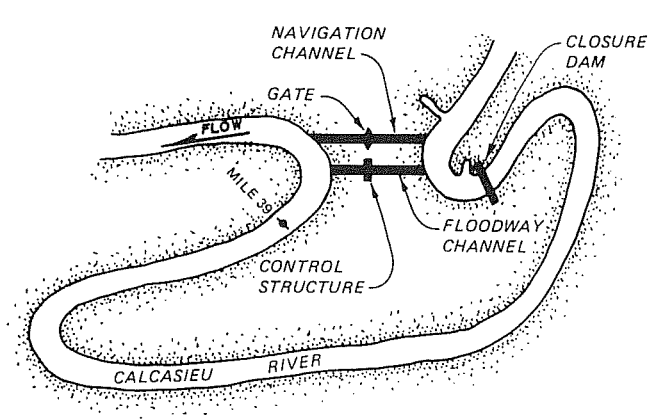

b. MEANDER WITH SALINITY BARRIER IN PLACE

FIGURE 5-3
Salinity barrier structure

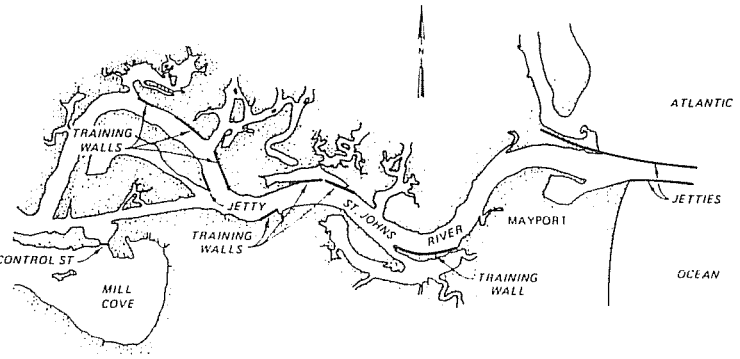

FIGURE 5-6
Revetments

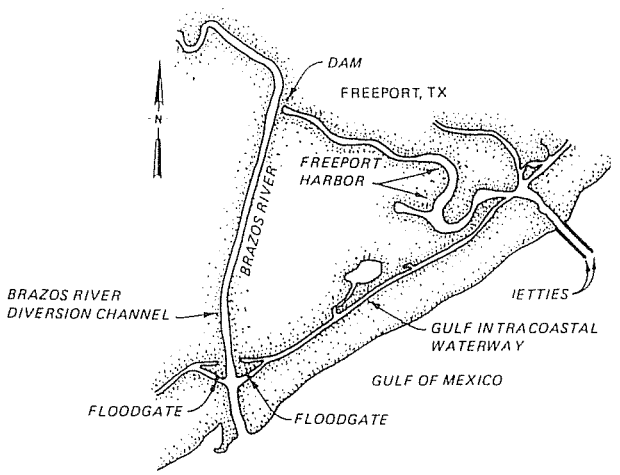

FIGURE 5-7
Flow diversion

any of these factors can control the design of the project. These factors are navigation safety, salinity, water quality, navigation channel sedimentation, general sedimentation, and flooding.

5-4. Navigation Safety. In control works projects where structures hazardous to navigation are planned adjacent to or near navigation channels, navigation safety may be a controlling factor in project design. Navigation safety may also be a controlling factor in control works projects that cause changes in currents along navigation channels, since altered current patterns can adversely impact vessel navigability. The recent development of the numerical ship/tow simulator has greatly enhanced the capability to solve existing navigation safety problems and to evaluate proposed designs to eliminate problems before construction. For detailed information on the ship/tow simulator and navigation safety, see Hewlett, Daggett, and Heltzel (1987); Huval, Comes, and Garner (1985); and Huval (1985) as well as EM 1110-2-1613.

5-5. Salinity. Freshwater supplies often are derived from the freshwater zones in the upper portions of many estuaries. The fresh water is typically used in the upper portions of many estuaries. The fresh water is typically used for municipal, agricultural, or industrial purposes. The development of any control works project within an estuary that might cause increased intrusion of salt into the estuary can be a threat to existing freshwater supplies. In such cases increased salinity intrusion can be a controlling factor in designing the control works project. Estuarine ecological features such as oyster beds or fish and shrimp nurseries can be significantly harmed

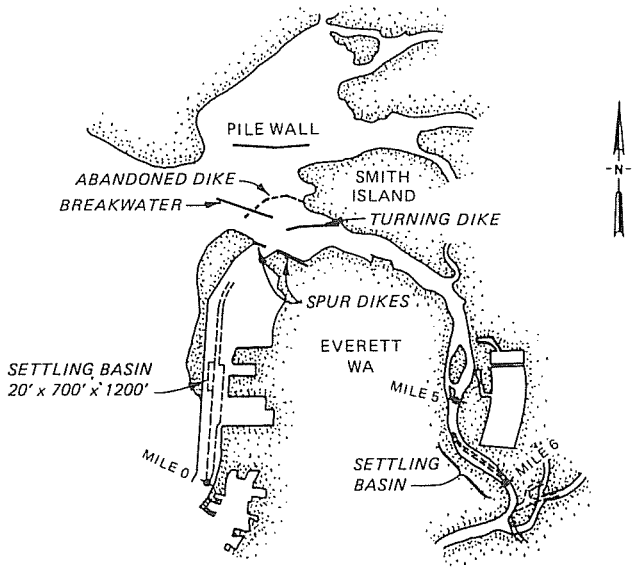

FIGURE 5-8
Sediment trap

by changes in the local salinity regime. Thus salinity can be a design factor in control works projects that alter the salinity regime in portions of an estuary.

5-6. Water Quality. Many control works projects within estuaries have the potential of changing circulation patterns and flushing rates. Flushing rates can be a controlling design factor if reduced flushing results in concentrations of dissolved or suspended materials being outside acceptable or safe limits in portions of an estuary.

5-7. Channel Sedimentation. Changes in channel sedimentation can be a controlling factor in project design if sedimentation is significantly increased or redistributed from low-cost to high-cost maintenance dredging areas.

5-8. General Sedimentation. Changes in general estuary sedimentation patterns can be a design factor in control works projects if the ecology of the estuary is threatened. For example, a benthic community could be threatened by a control works project that causes increased sedimentation or erosion in its bottom area of the estuary.

Section III. Siting of Control Works

5-9. Flooding. Control works projects within estuaries also have the potential of acting as a flood-control measure or increasing local flooding. During the project planning stage, it should be considered that the control works may function as barriers during peak hydrograph and actually create or increase localized flooding.

5-10. Estuarine Breakwaters and Jetties. The principal criteria to be observed in the layout of an estuarine breakwater are adequate depths in the area to be protected from waves; adequate depths in the approaches to the harbor entrance; and an entrance that will minimize wave action within the harbor while providing adequate clearances for navigation.

a. Design Considerations. The orientation of the entrance should be such that entrance approaches and departures can follow a course generally in the direction of the more severe waves. Safe navigation will generally require an entrance channel much wider than that of the interior channel, since

control under severe wave conditions will tend to be difficult for both large and small vessels. Bar channels and entrances partly protected by jetties and training structures will require special studies of tidal currents, waves, littoral transport, and shoaling tendencies to determine the optimum relations with regard to channel width, cross section, alignment, and degree of exposure. Channel widths in entrances will have to be judiciously selected based on the analysis of conditions at each project. For detailed guidance see EM 1110-2-1613.

b. Waves. The design of the entrance for the purpose of excluding or minimizing the propagation of waves into the harbor may be accomplished by procedures described in the Shore Protection Manual (US Army Engineer Waterways Experiment Station 1984).

5-11. Salinity Barriers.

a. Dam Type. The dam type of salinity barrier should be located as far upstream as is practicable without defeating the purpose of the structure in order to interfere with navigation as little as possible. Where feasible, it should be located in a reach where vessels can approach the locks on a straight course for at least a mile before entering the guide structure. The approach reach should be free of large waves and crosscurrents, which might throw the vessel off course and make the approach to the locks difficult, see EM 1110-2-1611 and 1110-2-1613 for details of navigation channel design.

(1) Lockages will admit salt water to the upstream pool. If there are many lockages per day, it is likely that the pool will become contaminated by salt water, possibly to a greater extent than would have been the case without the barrier. There are several methods that have been employed successfully to prevent or minimize this contamination. Among these are the following: separate emptying and filling systems; a "scavenger" pool with a discharge pipeline extending through the barrier; a hinged-leaf barrier in the lock; and a pneumatic barrier. Details of these devices are given in Abraham and Burgh (1964), Wicker (1965), and Ables (1978).

(2) The barrier will impound upland discharges. During floods, the impoundment may be high enough to cause damage to shoreline installations unless the spillway is adequate to pass such discharges with a minimum of backwater effect, or unless levees are constructed along the shoreline for a sufficient distance upstream of the barrier to extend beyond the limits of such backwater effects. The normal elevation of the pool with the barrier in place may cause damages to shoreline property.

(3) The barrier should be high enough to be secure against overtopping by hurricane surges and superimposed storm waves, if it is in a locality subject to hurricanes, or it may be economical to provide lower crest elevations, depending on the uses made of the impounded water and the efficiency of the scavenger pool that may be provided to remove the salt water.

(4) The barrier will cause important modifications of the regimen of the waterway both downstream and upstream. Downstream, the tide will rise higher and fall lower than before, the effect being greatest at the barrier and diminishing downstream. Shoreline properties will be inundated to an extent, and navigation depths decreased. Shoaling may become more serious. Upstream from the dam, the tide will be eliminated as will any existing saltwater penetration. Also, the waterway above the barrier could be transformed from free flowing to an impounded pool. Typically riverflow will be maintained by operation of a control structure. An approximation of the order of magnitude of the changes may be computed by methods described in Wicker (1965), Dronkers-Schoenfeld (1955), Ippen and Harleman (1961), and McDowell and O'Connor (1977).

(5) The changes in the regimen of the waterway may be so great and of such significance that consideration should be given to conducting a numerical or physical hydraulic model study. The investigation should include consideration of the changes in the regimen downstream, the potential effects on shoaling both upstream and downstream of the barrier, the effects on pollutant accumulations upstream, the design of the scavenger pool and appurtenances to prevent intrusions, and the elevations of the pool upstream at normal and at various flood discharges.

b. Submerged Sill.

(1) A second type of salinity barrier, the submerged sill, is designed to retard salinity intrusion upstream of the sill. Because the sill crest must be below the elevation of the authorized navigation channel bottom, it must be placed in a location naturally deeper than the authorized navigation channel depth. The vertical salinity structure at the sill location should be at least partially stratified, since the disruption of the bottom density current along with increased vertical mixing are the factors that make the sill effective in reducing upstream salinity intrusion. the greater the height of the sill, the greater the potential for reduced salinity intrusion upstream. The sill may be designed to be permanent or temporary. Examples of the design of both types are given in US Army Engineer District (USAED), San Francisco (1979), and Johnson, Boyd, and Keulegan (1987). The only reliable predictive techniques to investigate the effectiveness of submerged sills are physical and numerical hydraulic models.

(2) A submerged sill of the temporary type was successfully used in the Lower Mississippi River during the 1988 drought to limit saltwater intrusion. The sill, constructed of locally dredged river sands nad located near river mile 63, limited the salt water approaching the freshwater intake for the city of New Orleans. The US Army Engineer District, New Orleans, designed the sill to erode away at high river discharges.

5-12. Hurricane Barriers. Hurricane barriers should be located as far downstream as is practicable, as they not only protect a larger area, but their effects on the heights of hurricane surges and on the normal regimen downstream of the barrier will be felt over lesser distances. (The fact that such structures may have important effects downstream as well as upstream should not be overlooked.) They should be located where the approaches to the gap for navigation will permit a straight sailing course for at least a mile, and where such a course will not be subject to crosscurrents and frequent severe wave action.

a. To reduce surge transmission as much as possible, the gap for ungated barriers should be as narrow and shallow as the needs of navigation will permit. The sill should be deep enough to provide adequate clearance for the vessels of the foreseeable future that will be employed in the commerce of the waterway. It should be remembered in this connection that the current velocities through the gap will undoubtedly be greater than the normal currents along the course of the waterway, ahd that there will be adverse effects for some distance both upstream and downstream of the gap. The width of the gap must be determined with these considerations in mind.

b. The barrier will have effects on the regimen of the waterway both upstream and downstream. Shoaling may be accelerated; the tides may rise higher and fall lower on the downstream side; the tide range may be decreased upstream; and the elevation of mean river level may be increased.

c. A satisfactory design of the navigation gap usually cannot be accomplished without benefit of a numerical or physical hydraulic model study and a ship simulator study. From these studies, the best arrangement and location for the barrier as well as for the navigation gap can be determined. These studies will also provide reliable information on the

effects of the barrier, with gaps of various dimensions installed, on the regiment of the waterway upstream and downstream, as well as on the navigability of the gaps tested. Tests including a range of upland discharges should be run in the hydraulic model to determine the backwater effects of the barrier.

d. The barrier should be high enough to protect against the design hurrican surge. Surge heights may be computed according to the procedures described in EM 1110-2-1412.

5-13. Training Dikes. In reaches of the waterway where it is necessary to locate the navigation channel elsewhere than in the natural thalweg, the currents will be at an angle to the channel rather than parallel with it, and shoaling is likely to be heavy. It may be possible to force the currents into a course that parallels the navigation channel rather than the thalweg (which then will shoal and the navigation channel will become the new location of the thalweg) by constructing dikes. These may be either parallel with the navigation channel, or consist of a system of spur dikes extending our from the shore into the current that is to be diverted. The effects of longitudinal dikes on the regimen of the waterway are generally local. As spur dikes necessarily cause a constriction, they may have important effects both downtream and upstream possibly for considerable distances. Longitudinal dikes also cause a constriction if they are connected to shore at one or both ends.

a. The location, layout, and orientation of training dikes, as well as scour problems around the structure, can be determined best by use of a physical or numerical hydraulic model. Without the use of a model, there will be little assurance that a satisfactory design has been obtained until the structures have been built and their action observed. These structures are expensive, and it is necessary to have the best obtainable assurance that they will have the desired effects on the regimen of the waterway.

b. The clearance between the edge of the channel and the ends of spur dikes or a longitudinal dike must be adequate to assure safe navigation. Vessels get off course, particularly during low visibility, and they may suffer damage if they strike the dike. It is desirable to avoid locating dikes adjacent to curves or turns in the channel, as vessels are more likely to stray from the channel in negotiating the turn. It is important to keep in mind that the existing navigation channel may not be the ultimate configuration or depth; therefore, consideration should be given to so locating the dike to permit an improved channel to be excavated with the dike still at an adequate distance from its edge. Adequacy of clearance between the edge of the channel and training works varies from waterway to waterway and reach to reach. Channel design procedures for navigation safety are discussed in ER 1110-2-1404 and EM 1110-2-1613.

5-14. Revetments. Revetment of the banks of tidal waterways is usually necessary where the width is only slightly greater than the width of the navigation channel, and where wave wash due to passing vessels will cause erosion. If a bank needs protection from erosion by revetment, it is essential that the bank be reveted to as low a level as possible and that undercutting be prevented. Revetments are usually expensive to construct and require periodic maintenance. Design considerations for revetments are given in US Army Engineer Waterways Experiment Station (1984), McDowell and O'Connor (1977), Peterson (1986), and EM 1110-2-1601.

5-15. Diversion Works. Upland discharges of sediment-laden fresh water into the tidal waterway often results in heavy shoaling. Under favorable circumstances, it may be possible to divert the principal upland discharge from ane stuary having important navigation channels that are subject to heavy shoaling into a nearby waterway where shoaling is inconsequential.

a. The water in the estuary from which the freshwater discharges are to be diverted will become more saline depending upon the fraction of fresh water removed. If the waters of the estuary are used for domestic, agricultural, or industrial purposes, the diversion will have serious effects on the local economy. It may be necessary to provide a substitute source of supply as part of the diversion scheme. As diversion may either improve or worsen water quality conditions in the waterway, the effect on water quality should be intensely studied. Similarly, the diversion will cause the waterway receiving the diversion to be less saline than before; it will accelerate the currents, possibly causing scour of the bed and banks; and it may cause shoaling in downstream reaches. The decrease in salinity may be detrimental to a seafood industry, the sediment may damage nearby beaches, and the shoaling may be harmful to the existing navigation in the waterway receiving the diverted waters. Erosion of the banks in the receiving waterway may cause significant property damages.

b. The diversion works consist of a dam to close the estuary from normal and most flood discharges, and a canal to convey the diverted waters to a neighboring stream or to the sea. If the canal is of considerable length, it may be found to be infeasible to provide a cross section adequate to discharge floods greater than some magnitude to be defined by economic analyses. The factors in such economic analyses are the costs of diversion works required for flows of the several magnitudes being considered and the adverse effects of permitting flows larger than each of these to be discharged to sea through the estuary. Sediment transport capacity should also be considered in the design of the diversion channel.

5-16. Sediment Traps. The purpose of a sediment trap is to manage sedimentation processes so that sediment can be dredged in the most cost-effective manner. Properly designed traps allow for the removal of sediment at locations that result in the least overall maintenance dredging costs. The critical factor for trap effectiveness is that the material trapped would have otherwise deposited somewhere within the project boundaries. If a large percent of material trapped would otherwise be transported through the estuary or be deposited in areas outside the project limits, the trap is ineffective and should not be maintained as a sediment trap.

a. If a physical hydraulic model of the estuary is available, much of the trial and error involved in developing an effective trap can be done in the model in a few weeks rather than in the field over a period of years. In the past, WES has conducted sediment trap tests in physical models, such as those described in Dronkers-Schoenfeld (1955), Ippen and Harleman (1961), Johnson, Boyd, and Keulegan (1987), McDowell and O'Connor (1977), Peterson (1986), Trawle and Boland (1979), and USAED, San Francisco (1979).

b. Sediment traps can now be investigated with numerical sediment transport models, a modeling tool that has only recently become available. In a numerical modeling effort, the investigation of sediment traps can be part of an overall evaluation of shoaling under proposed conditions. An example of this type of investigation is given in Granat (1987).

c. The investigation of sediment traps in an estuary using either a physical model or a numerical sediment transport model is not inexpensive. However, these are the principal tools available to address the problem in a complex system such as a tidal estuary with a reasonable degree of confidence. The investment in models can be repaid by correction of costly design deficiencies or identification of more workable solutions.

Section IV. Maintenance Dredging

5-17. Dredging Plant. The selection of dredging plant and the operational procedures to be employed are based on the in situ characteristics of the materials to be removed, traffic conditions in the waterway, the distances to disposal areas, the exposure to waves that may disrupt operations or damage equipment, availability of dredging plant, and environmental considerations. Where there are alternatives, the selection should be determined on the basis of the least cost of producing the desired channel (not the lowest unit cost of dredging) with a method that is environmentally acceptable. The cost of proper disposal of the dredged material, to the end that the material once dredged cannot return to the shoal, should be considered. On the other hand, it is conceivable that some other method is competent to remove very large volumes of material at very low costs, and even if a large portion of the material returns to the shoal, the depths provided are obtained at lower annual cost than would be experienced if the dredged material were meticulously removed from the waterway. The choice should always be for the method that produces a satisfactory channel at the least annual cost and environmental damage; the cost per cubic yard dredged is not in itself always a complete basis for selection of plant and methods for dredging.

a. When the work is to be done by contract rather than by Government plant and labor, it is rarely possible to specify the kind of plant to be employed, but the specifications will provide for the end results desired, require that plant move aside for traffic, and specify rehandling and disposal requirements. In situations where careful disposal of the dredged material is necessary to obtain a satisfactory channel at the least cost, this will be required in the specifications regardless of whether the plant of some prospective bidders will have more difficulty complying with the specifications. Environmental requirements may restrict the use of certain dredging equipment at a specific project. The conditions at the disposal area may also restrict certain equipment, i.e., if settling rates are not adequate, disposal may be limited to mechanical methods.

b. If unconsolidated or weakly consolidated deposits are to be dredged, dipper, bucket, pipeline, hopper, or sidecasting dredges may be used. Where the deposits include boulders, it may be necessary to use dipper or bucket dredges unless the boulders can be buried by overdigging with the suction head or cutterhead close to the boulder and causing it to topple into the hole. For new-work dredging, as contrasted with maintenance dredging, consolidated sand or silt or clayey materials may be encountered. For dredging such materials, the pipeline dredge with cutterhead rather than a suction head type of dredge will generally remove the material more economically. In rock or other strongly consolidated materials, it may be necessary to employ dipper or bucket dredges, and drilling and blasting may be required. Where the material is such that any of the conventional dredges can remove it effectively, the choice between them will be based on traffic density, distance to disposal areas, depth of cut, and exposure to wave action. If traffic density is so great that operations will be interrupted to an extent that results in costs being increased beyond those of plants subject to less intereference, the latter will be selected. Similar considerations will govern selection of plant in locations where significant wave action is likely. Distance to acceptable disposal areas is a factor in the cost of operations for all types of dredges, but it is likely to be most significant for pipeline dredges. When the length of pipeline to reach a given disposal area results in costs that make dipper, bucket, or hopper dredges in conjunction with remaining operations more economic, the pipeline dredge no longer is the best tool for the operation. Where the depth of cut is small in relation to the plant capability, it is usually found that the controlling factor in the cost of dipper, bucket, or pipeline dredges is the time involved in advancing the dredge into the deposit rather than the effort to remove the material. Hopper and sidecasting dredges can more effectively cope with thin cuts, and may be the most economic dredge type in these instances. For further information, EM 1110-2-5025 as well as Herbich (1975) and Huston (1970) should be consulted.

5-18. Advance Maintenance Dredging. A typical dredged channel with no provision for advance maintenance dredging is shown in Figure 5-9. The basic specifications for the dredged dimensions are the authorized or project depth, the authorized or project width, the side slopes, and the overdepth for providing channel dimensions until the next dredging cycle. The authorized depths and widths are those channel dimensions authorized by Congress. If, for some reason, it becomes unnecessary to maintain a channel at authorized dimensions, the channel is maintained only to the economic dimensions, which are less than authorized.

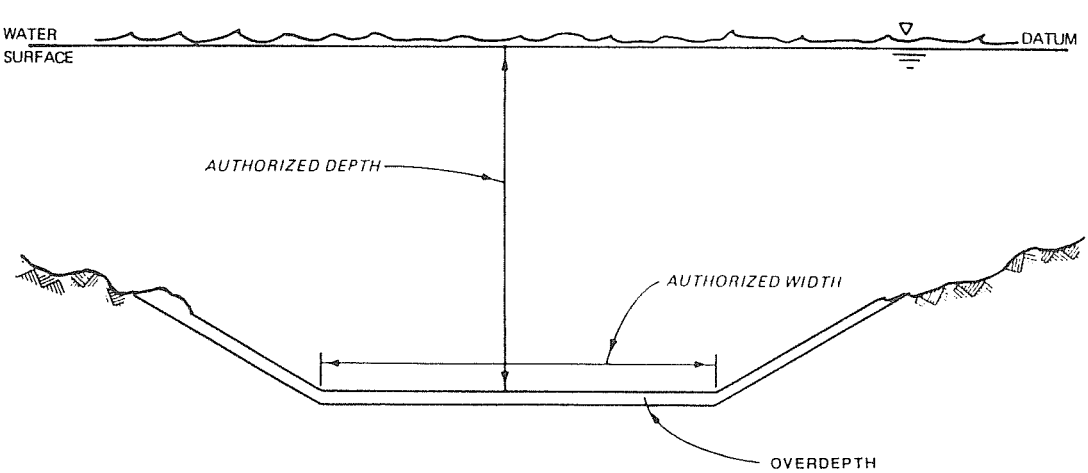

FIGURE 5-9
Typical dredged channel cross section without advance maintenance

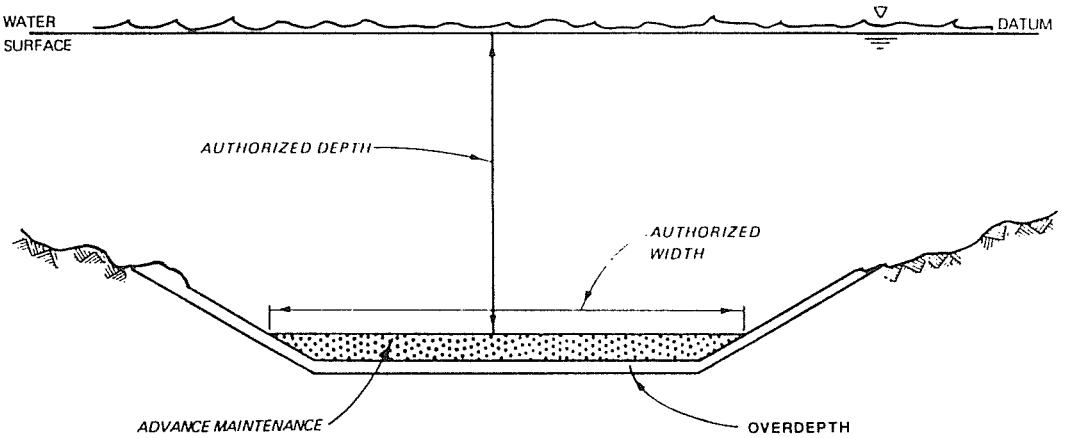

FIGURE 5-10
Typical channel cross sections with overdepth form of advance maintenance included

a. A typical project with advance maintenance dredging included in shown in Figure 5-10. Typical amounts of advance maintenance vary from 1 to 10 feet. A listing of Corps projects using advance maintenance along with specifications is provided in Trawle and Boyd (1978). The primary objective of advance maintenance dredging is to reduce the required dredging frequency, which can result in reduced overall maintenance dredging costs. A second objective can be to increase the percentage of time that a project is at project dimensions.

b. Advance maintenance dredging should not be confused with allowable dredging overdepth. The allowable dredging overdepth, usually 1 or 2 feet, is simply a margin for error that allows the dredging contractor to be paid for material dredged within a specified depth (usually 1 or 2 feet) below the required depth.

c. The key factor in advance maintenance effectiveness is the relation between depth and sedimentation rates. If increased depth causes no increase or only a slight increase in sedimentation rates, then advance maintenance can be very effective, since the required dredging frequency can be significantly reduced with little or no increase in overall maintenance dredging volumes. If, however, increased depth causes dramatic increases in the sedimentation rates, advance maintenance is probably not an effective technique, since the required dredging frequency will not be reduced significantly and overall maintenance dredging volumes can increase greatly. For more information on advance maintenance design considerations, see Trawle (1981), Berger and Boyd (1985), and Gelbert and Kean (1987).

5-19. Agitation Dredging. Agitation dredging is the removal of bottom material from a selected area by using equipment to suspend it temporarily in the water column and allowing currents to carry it away. This definition means that agitation of the bottom material is accomplished by some type of equipment and that the main purpose of the dredging equipment is to raise bottom material into the water column. Currents are used to move the material in the water column. Natural tidal currents are usually the mechanism for transport, although they may be augmented by currents generated by the agitation equipment. Since currents are a necessary part of the agitation dredging process, a good understanding of local hydrodynamics is essential for a successful operation. If the material is suspended but shortly redeposits in the same area, only agitation (not agitation dredging) has occurred. By definition, agitation dredging includes transport of material away from the problem area. However, care should be taken to assure that the agitated material does not redeposit in nearby navigational facilities. Agitation dredging can be accomplished using a wide variety of equipment. Some of the equipment that has been applied in the field to perform agitation dredging will now be discussed.

a. Hopper Dredges. Hopper dredge agitation is produced by hopper overflow. The success of this type of agitation dredging hinges on two factors:

(1) The sediments should be of such character so that the hopper dredge can easily raise bottom materials to the surface.

(2) Currents should be sufficient to remove agitated material from the navigation channel. Detailed discussions on hopper dredge agitation dredging are given in Richardson (1984), USAED, Philadelphia (1969), and USAED, New Orleans (1973).

b. Propwash. Successful agitation dredging operations by propwash tend to have the following characteristics:

(1) The propwash vessel is fitted with an adjustable deflector device and convenient anchoring system.

(2) Shoaling is localized and well-defined in moderate water depths.

(3) Shoal material is fine, easily erodible, and uncompacted.

(4) Natural currents augment the agitation and transport process.

(5) Wave action is not severe enough to cause a hazard to the dredging plant or rend the operation ineffective.

Detailed discussions on propwash agitation dredging are given in Richardson (1984), Slotta et al. (1974), Bechly (1975), and Burke and Wyall (1980).

5-20. Vertical Mixers and Air Bubblers. Vertical mixers such as the Helixor and Ventra Vac units and air bubblers are grouped together because they claim the same basic operating principle: by releasing compressed air near the bottom, the devices induce currents in the water column rising from the bottom to the surface. These currents are supposed to carry with them sediment from the bottom and near-bottom, at least part of which is to be resuspended by horizontal currents feeding the rising vertical currents.

a. In theory, such devices should work by maintaining sediment in suspension until natural currents can flush it away. In practice, however, no successful field results have been reported to date. There appear to be some fundamental problems with how the operating principle of such devices relates to the objective in agitation dredging.

b. There is no question that such devices as the Helixor,

Ventra Vac, and air bubblers can induce significant rising vertical currents extending to the water surface. In agitation dredging with these devices, however, the horizontal flow patterns and velocities are also important, since horizontal flow is what brings sediment to the vertical plume. Investigators have shown that horizontal currents into line source air bubblers are relatively weak, the zone of influence of such currents is limited, and exponential power increases are required to increase horizontal flow into the bubble plume. A detailed discussion on the use of these devices in agitation dredging is Richardson (1984) and DeNekker and Knol (1968).

5-21. Rakes and Drag Beams. Rakes, drag beams, and similar devices work by being pulled over the bottom, mechanically loosening the bottom material and raising it slightly in the water column. Although crude, they can be effective in areas with cemented, cohesive, or consolidated sediments; and they require no special equipment other than a vessel to pull them. In shallower water and with a large enough vessel, propwash may help in the agitation process as well. The draghead of a trailing suction hopper dredge acts as a rake to some degree as it is pulled along the bottom, since not all of the material it loosens is drawn into the suction tube. Since rakes and drag beams produce no currents of their own and since they do not resuspend material as much as lossen it, they must be used in conjunction with natural currents strong enough to transport the loosened material away from the shoaling site. Drag beams have been used to displace material above required depth and move it into areas that have been overdredged. One possible way for helping the dragging process is by the use of air bubblers. Another way would be to deflect the propwash of the towing vessel downward toward the dragging device. A combination of the three--dragging, air bubbler, and propwash--might prove the most effective of all, especially when the towing vessel moves into a current so maximum use is made of the propwash. A detailed discussion of agitation dredging using rakes and drag beams is given in Richardson (1984).

5-22. Water Jets. Water jets for agitation dredging operate on the same fundamental principle as propwash agitation with the following main differences:

a. Water jets can be grouped in any arrangement desired.

b. Streams issuing from the jets usually originate close to or on the bottom rather than the surface.

c. Water jets are usually used in fixed locations.

d. Water jets are usually intended for frequent operation to provide large shoaling accumulations, whereas propwash is a remedial measure to remove shoal deposits. Because of the last point mentioned, water jet installations lend themselves to automatic operation. They may also have difficulty removing larger amounts of shoaling that might accumulate during periods of non-operation. Detailed discussions on the use of water jets in agitation dredging are given in Richardson (1984), Ali and Halliwell (1980), and Barland (1980).

Section V. Case Histories

5-23. Description. A case history that describes the hydraulic processes that occur in an estuary as well as provides the history of development of that estuary is an important item when modifications to any estuary are being considered. The case history should be developed early on as a guide for scoping future design studies. Such a document should include the discussion of any changes in hydraulic behavior observed as the result of past modifications by either man or nature. This document will provide valuable information that should be summarized in subsequent design documents.

5-24. Contents. Case histories should include the following information:

a. History of project authorization and development.

b. Description of existing projects.

c. Project-related problems.

d. Facts and data bearing on the problem.

e. Description of modeling (physical or numerical) studies.

f. Analysis of problems.

g. Lessons learned.

5-25. Lessons Learned. A discussion of lessons learned from Corps navigation projects, developed by the Committee on Tidal Hydraulics (CTH), is given in Appendix E.

5-26. Physical Model Studies. A list of the various tidal hydraulic model investigations that have been constructed and operated by WES is given in Appendix F.

CHAPTER 6
ENVIRONMENTAL CONSIDERATIONS

6-1. General.

a. Environmental Impacts. Estuarine modifications are usually intended to improve navigation conditions or provide for flood control. However, these modifications may have short- and long-term impacts on the environment at the site of the control work and both upstream and downstream of the control work. New-work dredging provides access to navigational facilities, and maintenance dredging sustains that access. Impacts of dredging on both water quality and shoaling should be considered. Some modifications are described as follows:

(1) Dredging. Deepening channels often causes increased salinity intrusion, and sedimentation rates and patterns may be changed. Biota in the channel area may be destroyed. Both new-work and maintenance dredging material must be disposed in an environmentally acceptable manner.

(2) Diversion works. Diversion works may cause the salinity in the estuary from which the fresh water is diverted to become essentially as saline as the ocean at the mouth. Also, the salinity in the waterway receiving the diverted flow will decrease. The currents will be accelerated, possibly causing scour of the bed and banks, and shoaling may become a problem in the downstream reaches of the water body receiving the diverted flow.

(3) Hurricane barriers. Hurricane barriers may accelerate shoaling both upstream and downstream and cause tides to rise higher and fall lower on the downstream side. While the tide range may be decreased upstream, the elevation of the mean water level may be increased.

(4) Salinity barriers. These barriers may cause tides to rise higher and fall lower downstream of the barrier, cause shoreline properties to be inundated to an extent, and decrease navigation depths at low tide. Shoaling may become more serious both upstream and downstream of the salinity barrier.

b. Reporting Requirements. Because of the possible environmental impacts, both new projects and operation and maintenance activities must be consistent with national environmental policies. In general, these policies require creation and maintenance of conditions under which human activities and natural environments can exist in productive harmony including preservation of historic and archeological resources. Corps project development is documented by a series of studies, each more specific than the previous one. The series of reports produced for a given type of project often evolves due to changing regulations. However, in general, the

environmental impacts of the project must be included in all reports prepared prior to Congressional project authorization. (Refer to EM 1110-2-1202 for a description of this process).

c. Statutes and Regulations. Compliance with Federal statutes, Executive guidelines, and Corps regulations often requires studies of existing environmental conditions and those likely to occur in the future with and without various activities. EM 1110-2-1202 lists the major environmental statutes and regulations that are currently applicable to Corps waterway projects. Four statutes that have a major impact on the planning and operation of projects in estuaries are the Estuary Protection Act, the National Environmental Policy Act, the Clean Water Act, and the Marine Protection, Research and Sanctuaries Act. There are also State and local regulations that must be satisfied.

(1) Estuary Protection Act. With this act Congress declared that many estuaries in the United States are rich in a variety of natural, commercial, and other resources, and it is declared to be the policy of Congress to recognize, preserve, and protect the responsibilities of the States in protecting, conserving, and restoring the estuaries in the United States.

(2) Naitonal Environmental Policy Act (NEPA). NEPA is the Federal statute that established national policy for the protection of the environment and set goals to be achieved along with the means to carry out these goals. This act requires preparation of an Environmental Impact Statement (EIS) for certain Federal actions affecting the environment in accordance with US Environmental Protection Agency (EPA) implementing regulations for NEPA. Environmental assessments (EA) are prepared for all other Corps actions that may not have a significant impact on the environment except for certain minor actions that are categorically excluded from NEPA review. Emergency activities do not require the preparation of an EIS.

(3) Clean Water Act. Section 404 of the Clean Water Act governs the discharge of dredged or fill material into waters of the United States. The evaluation of the effects of discharge of dredged or fill material should include consideration of the guidelines developed by EPA.

(4) Marine Protection, Research and Sanctuaries Act (MPRSA). The MPRSA governs the transport of dredged material for the purpose of ocean disposal. Title I of the MPRSA, which is the Act's primary regulatory section, authorizes the Secretary of the Army acting through the Corps (Section 103) to establish ocean disposal permit programs for dredged materials. In addition, Section 103(e) requires that Federal projects involving ocean disposal of dredged material shall meet the same requirements as developed for permits.

d. Environmental Study Management. At each stage of a project, efforts should be made to identify key environmental concerns and corresponding future information needs. Adequate forecasting of data needs is necessary to schedule adequate time for such activities as field data collection and physical or numerical modeling. Scheduling for work by others should allow for administrative procedures such as contractor selection, review procedures, and potential delays.

(1) Critical issues. Time and money constraints preclude detailed investigations and data collection for every area of interest; therefore, the most critical issues should be identified. It is essential that the number of factors assessed be adequate to fully account for all significant effects. The addition of other factors to be considered will increase the time, funds, and expertise required for the study. Therefore, a proper balance between adequate analysis and study resources must be achieved. Criteria for determining the importance of an issue include, but are not limited to, statutory requirements, Excecutive orders, agency policies and goals, and public interest. Federal regulations must be followed when determining the scope of an EIS.

(2) Environmental data. Environmental data collection is discussed in Paragraph 6-5. Well-defined, detailed objectives must be established prior to data collection. The design for the investigation should include a rationale for variable selection, sampling locations and frequencies, data storage and analysis, and hypotheses to be tested.

(a) Environmental studies during the preliminary stages of project development should emphasize identification of resources, development of an evaluation framework, and collection of readily available information for all potential alternatives. Resources likely to be impacted are evaluated, and further information needs are identified.

(b) Detailed analysis normally occurs after two or three specific alternatives have been selected for further study. The major emphasis of environmental studies in the detailed assessment stage should be directed toward identifying, describing, and appraising individual effects and evaluating the net effects of each alternative. Both positive and negative environmental effects should be characterized in adequate detail so they can be used along with the economic and technical analyses to compare alternatives.

6-2. Water Quality Considerations.

a. General. The impacts of estuarine control works on water quality can be categorized as follows:

(1) Impacts from dredging and disposal during construction and maintenance.

(2) Altered circulation caused by changes in geometry.

(3) Increased pollutant loadings due to facility construction and accidental vessel discharges or spills.

(4) Salinity changes.

Industrial and municipal effluents and agricultural runoff with attendant problems of low dissolved oxygen (DO), eutrophication, or toxic contamination are not primary Corps concerns unless Corps activities have the potential to mitigate or itensify already existing water quality problems. However, these conditions and the potential for water quality problems should be identified and documented in the early project stages.

b. Dredging and Disposal. The major water quality considerations of dredging and dredged material disposal are directly related to the amount of contaminants present and the mobility of the contaminant into environmental pathways by biological or hydrodynamic processes. The chemistry of contaminants in sediments is controlled primarily by the physiochemical conditions under which the sediment exists. Fine-grained sediments are typically anoxic, chemically reduced, and nearly neutral in pH. The effect of disposal environments on these chemical characteristics is an important consideration in the selection of disposal options. If sediment is disposed in an aquatic environment, sediment chemistry may not change. However, transfer of the sediment to a dryer environment, such as an upland disposal site, may change the chemistry to an anoxic and lower pH condition more favorable to the release of contaminants. Biological and physical processes may also affect the release of contaminants at a disposal site. Different contaminants and sediments with different properties do not always respond to an altered biological or physiochemical condition. This would mean that contaminant release would be a site-specific process and would be difficult to predict. Procedures are available for evaluating the environmental impacts of three major disposal alternatives: open water, intertidal, and upland methods (see Paragraph 6-4). Water quality considerations for dredging and disposal operations are summarized in the Dredged Material Research Program Synthesis of Research Results report series.

An index of these reports is given in Herner and Company (1980). For detailed information on water quality considerations during dredging, refer to EM 1110-2-5025.

c. Altered Circulation.

(1) Circulation may be altered as a result of modifications to an estuary, its tributaries, or its sea connection. Changes in circulation may result in changes in the spatial distribution of water quality constituents, in the flushing rates of contaminants, and in the pattern of scour and deposition of sediments.

(2) Environmental assessment of the effects of changes in circulation should initially emphasize the physical parameters such as salinity, temperature, and velocity and their impacts on plant and animal communities. These initial analyses should consider changes in vertical stratification when deepening of a channel is proposed. Increased density stratification inhibits vertical mixing, which may result in depletion of DO in bottom waters. If minimal changes occur in these parameters, then it can be generally assumed that the chemical characteristics of the system will not change significantly. This approach is based on a methodology that permits assessment without requiring extensive data and knowledge of the processes affecting the water quality constituent of direct interest. However, this approach is invalid if preliminary water quality surveys indicate the existence of toxic constituents at concentrations potentially damaging to biotic populations. Prediction of change in circulation and its effect on the physical parameters can be achieved through comparison with existing projects, physical model studies, and numerical simulation.

d. Pollutant Loadings. Increased pollutant loadings may result from facility construction, vessel discharges, and accidental spills. Increased navigational traffic as a result of estuarine modifications may also increase contaminant release through either accidental spillage of toxic cargoes, vessel discharges, or short-term alterations in ambient estuarine hydraulic conditions (propagation of waves, generation of currents, drawdown, and pressure and velocity changes) that may resuspend bottom sediments. Resuspended bottom sediments temporarily increase turbidity and total suspended solids concentrations. Generally, photosynthesis does not decrease and may even increase because of the release of nutrients from suspended fine sediments. Resuspension of fine sediments may decrease DO by increasing oxygen demand. The additive effect of increased navigation traffic may be to maintain high levels of solids and turbidity, which could have a permanent effect on the estuarine water quality. Also modifications may result in increased industrial development, which may result in industrial effluents, spills, and contaminated surface runoff entering the estuary. All of these factors should be considered when determining the possible increase in pollutant loadings and the impact it may have on the estuarine water quality.

e. Salinity Changes. Changes in salinity may result from the construction of estuarine control works or channel deepening. Construction and operation of locks may cause salinity intrusion in upstream portions of estuaries normally used for freshwater supplies. Also, diversion works may cause normally freshwater portions of an estuary to become saline or vice versa. If these freshwater supplies are used for municipal, agricultural, or industrial purposes, then the prevention of salinity intrusion can be a controlling factor in designing the estuarine control work project. Estuarine ecological features may also be influenced by a reduction in salinity as a result of barriers or diversion structures. The decrease in salinity may be detrimental to a seafood industry, affecting such estuarine ecological features as oyster beds or fish and shrimp nurseries. Consideration should be given to both short- and long-term changes in salinity during all seasons of the year, as these changes can have a drastic effect on sensitive ecological features.

6-3. Biological Considerations.

a. General. The effects of estuarine modifications on plants and animals may result from the physical changes in habitat due to the enlargement of channels, disposal of dredged material, and the construction of various control works. Other effects may result from changes in contaminant levels, turbidity, suspended sediments, salinity, circulation, and erosion. Preliminary research suggests that navigation traffic itself affects certain species. Weather and large storm events, such as hurricanes on the Gulf Coast, can devastate an estuary in a short period of time. These effects on habitat in the estuary may be short- and long-term physical changes.

b. Reference. This and other considerations have already been addressed in EM 1110-2-1202. It should also be noted that the EM contains a glossary of the scientific terms, some of which are used in this EM.

6-4. Dredging Effects Considerations.

a. General. Dredging is a major activity in the development or improvement of navigation and flood-control projects in estuaries. During the design phase of such projects, the environmental effects associated with dredging and dredged material disposal must be considered. The primary short-term objective of a dredging project is to provide authorized project dimensions. This should be accomplished using the most technically satisfactory, environmentally compatible, and economically feasible dredging and dredged material disposal procedures. Long-term dredging objectives concern the efficient management and operation of dredging and disposal activities during continued operation and maintenance of the project. The environmental considerations required to support the design of new-work or maintenance dredging projects are outlined in the following paragraph.

b. Basic Considerations. In order to consider the environmental aspects of dredging and dredged material disposal in the design phase of a project, the activities listed in Table 6-1 are required. Although dredging and related matters have traditionally been considered an operations and maintenance function, a well-coordinated approach in the planning and design stages can minimize problems in the operatins and maintenance of the project. This is especially true regarding long-range planning for disposal of both new-work and maintenance dredged material. For a more complete discussion, along with disposal alternatives, habitat development, and associated uses (such as recreation and aesthetics, etc.) refer to EM 1110-2-1202 and EM 1110-2-5026.

6-5. Environmental Data Collection and Analysis. In the process of planning and designing estuarine navigation projects, potential environmental impacts must be assessed. This is done through very detailed and site-specific data collection efforts. However, some basic requirements are common to all data collection programs.

6-6. Mitigation Decision Analysis.

a. Policy. Care must be taken to preserve and protect environmental resources, including unique and important ecological, aesthetic, and cultural values. The Fish and Wildlife Coordination Act of 1958 (PL 85-264, 16 U.S.C. 61 et seq.) requires fish and wildlife mitigation measures when justified. Specific mitigation policy for significant fish and wildlife and historic and archeological resources is included in ER 1105-2-50, Chapters 2 and 3. Damage from Federal navigation work along the shorelines of the United States must be prevented or mitigated.

TABLE 6-1
Basic Considerations

Step	Information Source
Analyze dredging location and quantities to be dredged	Hydrographic surveys, project maps
Determine the physical and chemical characteristics of the sediments	WES TR DS-78-10 (Section 6-8) (Palermo, Montgomery, and Poindexter 1978)
Determine whether or not there will be dredging of contaminated sediments	WES TR DS-78-6 (Brannon 1978)
Evaluate disposal alternatives	EM 1110-2-5025
Select the proper dredge plant for a given project	EM 1110-2-5025
Determine the levels of suspended solids from dredging and disposal operations	WES TR DS-78-13 (Barnard 1978)
Control the dredging operation to ensure environmental protection	WES TR DS-78-13 (Barnard 1978)
Identify pertinent social, environmental, and institutional factors	Paragraph 6-1
Evaluate dredging and disposal impacts	WES TR DS-78-1 (Wright 1978); WES TR DS-78-5 (Hirsch, Di Salvo, and Peddicord 1978)

b. Types of Mitigation. Based on the Council on Environmental Quality (CEQ) definition, mitigation includes:

(1) Avoiding the impact altogether by not taking a certain action or parts of an action.

(2) Minimizing impacts by limiting the degree of magnitude of the action and its implementation.

(3) Rectifying the impact by repairing, rehabilitating, or restoring the affected environment.

b. Types of Mitigation. Based on the Council on Environmental Quality (CEQ) definition, mitigation includes:

(1) Avoiding the impact altogether by not taking a certain action or parts of an action.

(2) Minimizing impacts by limiting the degree of magnitude of the action and its implementation.

(3) Rectifying the impact by repairing, rehabilitating, or restoring the affected environment.

(4) Reducing or eliminating the impact over time by preservation and maintenance operations during the life of the action.

(5) Compensating for the impact by replacing or providing substitute resources or environments.

c. Justification for Mitigation. Justification of mitigation measures shall be based on the significance of the resource losses due to a plan, compared to the costs necessary to carry out the mitigation (ER 1105-2-50, 2-4C.1). Extent of mitigation justified will ultimately be determined through negotiation with the US Fish and Wildlife Service and the concerned state. Endangered and threatened species and critical habitats will be given special consideration.

d. Resources Impacted. Impacts from dredged material disposal and hydraulic changes affect primarily shorelines, wetlands, vegetated shallows, and riparian zones. These areas will usually be composed of or considered to be significant resources. Appendix C of ER 1105-2-50 (Subparts C-F) describes potential impacts on these resources.

e. Key Concepts for Mitigation.

(1) Early Participation. To determine significant resource losses that will occur because of a project, environmental personnel must be involved in the project from the beginning. Once such potential losses are identified, the project can be modified to reduce or eliminate them. If modification is inadequate or infeasible, measures to offset the losses should be developed. Through early participation, the definition of mitigation can serve as a sequence of steps to follow.

(2) Long-term planning. Hershman and Ruotsala (1978) suggest building mitigation into a long-term estuary management plan, such that development and environmental protection proceed simultaneously. This approach allows cumulative impacts to be mitigated, decreases time and cost per project, and spreads the mitigation burden more equitably.

(3) Mitigation planning goals. Four options for mitigation efforts are summarized as follows:

(a) In-kind: resources physically, biologically, and functionally similar to those being altered.

(b) Out-of-kind: resources as above, dissimilar.

(c) Onsite: occurring on, adjacent to, or in the immediate proximity of the project site.

(d) Offsite: occurring at a point away from the project site.

A guide to selecting any combination of (a) or (b) and (c) or (d) as a mitigation option is found in US Fish and Wildlife Service (1980) in which resource categories, attendant mitigation goals, and mitigation measures are suggested.

6-7. Checklist of Environmental Studies.

a. The following checklist consists of some of the environmental factors that should be considered for estuarine navigation projects. This checklist is cumulative, and not all studies are appropriate for all projects.

(1) Characterization of existing conditions at project site.

(2) Estimation of construction activities by others likely to be associated with Federal project.

(3) Evaluation of project effects of circulation patterns and stage variations.

(4) Evaluation of project effects on water quality.

(5) Characterization and testing of sediments to be dredged (Section 404 or 103 evaluation as appropriate).

(6) Analysis of dredging alternatives (dredge plant, timing, etc.).

(7) Analysis of disposal alternatives.

(8) Evaluation of project effects on sedimentation rates and shoaling locations.

(9) Analysis of effects of winter navigation if ice coverage will occur.

(10) Evaluation of aesthetic, cultural, and recreational aspects.

(11) Coordination with other agencies, the public, and private groups.

(12) Planning and design of monitoring programs.

b. For a more complete discussion of this checklist, refer to EM 1110-2-1202.

APPENDIX A
BIBLIOGRAPHY

Abbot, M. B. 1979. Computational Hydraulics, Theory of Free Surface Flows, Fearon-Pitman Publishers, Inc., Belmont, CA.

Ables, J. H. 1978. "Filling and Emptying System, New Ship Lock, Mississippi River-Gulf Outlet, Louisiana; Hydraulic Model Investigation," Technical Report H-78-16, US Army Engineer Waterways Experiment Station, Vicksburg, MS.

Abraham, G., and Burgh, P. V. D. 1964 (Jan). "Pneumatic Reduction of Salt Intrusion Through Locks," Journal of the Hydraulics Division, ASCE. Vol 90, HY-1, pp 83-119.

Ackers, P. 1972. "Sediment Transport in Channels, An Alternative Approach," HRS Int. Report 102, Hydraulics Research Station, Wallingord, England.

Ali, K. H. M., and Halliwell, A. R. 1980. "The Use of Water-Jets for Scouring and Dredging," Proceedings, Third

International Symposium on Dredging Technology, BHRA, pp 239-265.

American Society for Testing and Materials. 1964 (Dec). Procedures for Testing Soils, ASTM Committee D-18 on Soils and Rocks for Engineering Purposes, 4th ed., Philadelphia, PA.

Ariathurai, R., and Krone, R. B. 1976. "Mathematical Modeling of Sediment Transport in Estuaries," Estuarine Processes, Vol II, M. Wiley, ed., Academic Press, New York, pp 98-106.

Ariathurai, R., and Arulanandan, K. 1978 (Feb). "Erosion Rates of Cohesive Soils," Journal of the Hydraulics Division, ASCE. Vol 104, No. HY2, pp 279-283.

Bagnold, R. A. 1966. "An Approach to the Sediment Transport Problem from General Physics," Professional Paper No. 422-J, US Geological Survey.

Barland, J. A. 1980. "A Design Procedure for Scour Jet Arrays," Proceedings, Dredging and Sedimentation Control, 1980, Naval Facilities Engineering Command and Office of Naval Research, Washington, DC.

Barnard, W. D. 1978 (Aug). "Prediction and Control of Dredged Material Dispersion Around Dredging and Open-Water Pipeline Disposal Operations," Technical Report DS-78-13, US Army Engineer Waterways Experiment Station, Vicksburg, MS.

Bascom, W. 1980. Waves and Beaches, The Dynamics of the Ocean Surface (Revised and Updated), Anchor Press-Doubleday, Garden City, NY.

Bechly, J. 1975 (Sep). "Sandwick Gives Nature a Boost on Shoal Removal," World Dredging and Marine Construction, Vol II, No. 10, pp 37-41.

Berger, R. C., and Boyd, J. A. 1985 (Apr). "Effects of Depth on Dredging and Frequency; Report 3, Evaluation of Selection Projects," Technical Report H-78-5, US Army Engineer Waterways Experiment Station, Vicksburg, MS.

Brannon, J. M. 1978 (Aug). "Evaluation of Dredged Material Pollution Potential," Technical Report DS-78-6, US Army Engineer Waterways Experiment Station, Vicksburg, MS.

Bruun, P. 1978. Stability of Tidal Inlets, Theory and Engineering, Elsevier, Amsterdam.

Burke, T. D., and Wyall, C. E. 1980. "Using Propwash for Channel Maintenance Dredging," Proceedings, World Dredging Conference, WODCON IX, pp G09-G20.

Burt, T. N., and Stevenson, J. R. 1983 (Aug). "Field Settling Velocity of Thames Mud," Report IT 251, Hydraulic Research, Wallingford, England.

Calcutta Port Commissioners. 1973. "The Study of the Hooghly Estuary and the Project for Training Measures below Diamond Harbour," Report, Hydraulic Study Department, Calcutta, India.

Cameron, W. M., and Pritchard, D. W. 1963. "Estuaries," The Sea, M. N. Hill, ed., Vol 2, Wiley, NY, pp 306-324.

Cargill, Kenneth W. 1983. "Procedures for Prediction of Consolidation in Soft Fine-Grained Dredged Material," Technical Report D-83-1, US Army Engineer Waterways Experiment Station, Vicksburg, MS.

Cargill, Kenneth W. 1985 (Jul). "Mathematical Model of the Consolidation/Desiccation Processes in Dredged Material," Technical Report D-85-4, US Army Engineer Waterways Experiment Station, Vicksburg, MS.

Channon, R. D. 1971 (Sep). "The Bristol Fall Column for Coarse Sediment Grading," Journal of Sedimentary Petrology, pp 167-870.

Committee on Tidal Hydraulics, Corps of Engineers, US Army. 1963. "Salt Water Intrusion, Lake Washington Ship Canal, Seattle, Washington," US Army Engineer Waterways Experiment Station, Vicksburg, MS.

Darwin, G. H. 1962. The Tides and Kindred Phenomena in the Solar System. W. H. Freeman and Company, San Francisco, CA.

Defant, A. 1958. Ebb and Flow, The Tides of Earth, Air, Water. University of Michigan Press, Ann Arbor, MI.

DeNekker, J., and Knol, J. 1968. "Results of Experiments with an Air-Bubble Screen Against Siltation in the Rotterdam Harbour," Proceedings, 5th International Harbor Congress, Section 2, Paper DEN-KN.

Dronkers-Schoenfeld. 1955. "Tidal Computations in Shallow Water," Proceedings, ASCE. Vol 81, Separate 714.

Dyer, K. R. 1973. Estuaries, A Physical Introduction, Wiley, London.

Fischer, H. B., et al, 1979. Mixing in Inland and Coastal Waters, Academic Press, NY.

Gelbert, J. A., and Kean, T. L. 1987 (May). "Advance Maintenance Dredging Study for the Chesapeake and Delaware Canal and Approaches," Proceedings, Coastal Sediments '87 Symposium, ASCE, New York.

Gibbs, R. J. 1977 (Mar). "Clay Mineral Segregation in the Marine Environment," Journal of Sedimentary Petrology, Vol 47, No. 1, pp 237-243.

Granat, M. A. 1987. "Application of the TABS-2 Numerical Modeling System for the Evaluation of Advance Maintenance Dredging," Proceedings, San Francisco District Navigation Workshop, 18-21 May 87, pp 238-267. US Army Engineer District, San Francisco, San Francisco, CA.

Grim, R. E. 1968. Clay Mineralogy, McGraw-Hill, New York.

Hansen, D. V., and Rattray, M. Jr. 1966. "New Dimensions in Estuary Classification," Liminol Oceanog., 11, pp 319-326.

Hauck, L. M. 1989 (Nov). "Sedimentation Analysis of the Proposed San Rafael Canal Tidal Barrier, San Rafael, California," Technical Report HL-89-24, US Army Engineer Waterways Experiment Station, Vicksburg, Miss.

Hayter, E. J. 1983. "Prediction of Cohesive Sediment Transport in Estuarial Waters," Ph.D. Dissertation, University of Florida, Gainesville, FL.

Hayter, E. J., and Mehta, A. J. 1984 (Sep). "Modeling Estuarial Cohesive Sediment Transport," Proceedings, of the 19th Coastal Engineering Conference. ASCE, Vol III, Houston, TX, pp 2985-3000.

Herbich, J. B. 1975. Coastal and Deep Ocean Dredging, Gulf Publishing, Houston, TX.

Herner and Company. 1980 (Apr). "Publication Index and Retrieval System" Technical Report DS-78-23, US Army Engineer Waterways Experiment Station, Vicksburg, Miss.; prepared for Office, Chief of Engineers, US Army, Washington, DC, under Contract No. DACW39-77-C-0081.

Hershman, M. J., and Ruotsala, A. A. 1978 (Mar). "Implementing Environmental Mitigation Policies," Coastal Zone '78. San Francisco, CA, Vol II, pp 1333-1345, American Society of Civil Engineers, New York.

Hewlett, J. C., Daggett, L. L., and Heltzel, S. B. 1987 (Apr). "Ship Navigation Simulator Study; Savannah Harbor Widening Project, Savannah, Georgia," Technical Report HL-87-5, US Army Engineer Waterways Experiment Station, Vicksburg, MS.

Hirsch, N. D., DiSalvo, L. H., and Peddicord, Richard. 1978 (Aug). "Effects of Dredging and Disposal on Aquatic Organisms," Technical Report DS-78-5, US Army Engineer Waterways Experiment Station, Vicksburg, MS.

Hopkinson, C. S., Jr., and Hoffman, F. A. 1983. "The Estuary Extended - A Recipient-System Study of Estuarine Outwelling in Georgia," The Estuary as a Filter, V. S. Kennedy, ed., Academic Press, Orlando, Fl., pp 313-327.

Hunt, J. R. 1980. "Prediction of Oceanic Particle Size Distribution from Coagulation and Sedimentation

Mechanisms," Advances in Chemistry Series No. 189 - Particle in Water, M. D. Kavanaugh and J. T. Kekie, ed., American Chemical Society, pp 243-257.

Hunt, S. D. 1981. "A Comparative Review of Laboratory Data on Erosion of Cohesive Sediment Beds," UFL/COEL/MP - 81/7, Coastal and Oceanographic Engineering Dept, University of Florida, Gainesville, FL.

Huston, J. 1970. Hydraulic Dredging, Cornell Maritime Press, Cambridge, MD.

Huval, C., Comes, B., and Garner, R. T., III. 1985 (Jun). "Ship Simulation Study of John F. Baldwin (Phase II) Navigation Channel, San Francisco Bay, California," Technical Report HL-85-4, US Army Engineer Waterways Experiment Station, Vicksburg, Miss.

Huval, C. 1985 (Oct). "Ship Navigation Simulator Study, Upper Mobile Bay Channel," Miscellaneous Report HL-85-7, US Army Engineer Waterways Experiment Station, Vicksburg, Miss.

Inglis, C. C., and Allen, F. H. 1957. "The Regimen of the Thames Estuary as Affected by Currents, Salinities, and River Flow," Proceedings, Institution of Civil Engineering, pp 827-878.

Ippen, A. T., ed. 1966. Estuary and Coastline Hydrodynamics, McGraw-Hill, New York.

Ippen, A. T., and Harleman, D. R. F. 1961 (Jun). "One-Dimensional Analysis of Salinity Intrusion in Estuaries," "Technical Bulletin No. 5, Committee on Tidal Hydraulics, Corps of Engineers, US Army; prepared by US Army Engineer Waterways Experiment Station, Vicksburg, MS.

Jackson, M. L. 1958. Soil Chemical Analysis. Prentic-Hall, Englewood Cliffs, NJ.

Johnson, B. H., Boyd, M. B., and Keulegan, G. 1987 (Apr). "A Mathematical Study of the Impact on Salinity Intrusion of Deepening the Lower Mississippi River Navigation Channel," Technical Report TR-87-1, US Army Engineer Waterways Experiment Station, Vicksburg, MS.

Johnson, B. H., Trawle, M. J., and Kee, P. J. 1989 (Dec). "A Numerical Model Study of the Effect of Channel Deepening on Shoaling and Salinity Intrusion in the Savannah Estuary," Technical Report HL-89-26, US Army Engineer Waterways Experiment Station, Vicksburg, MS.

Kirby, R. 1969. "Sedimentary Environments, Sedimentary Processes and River History in the Lower Medway Estuary, Kent," Ph.D. Dissertation, University of London, United Kingdom.

Kranck, K. 1979. "Dynamics and Distribution of Suspended Patriculate Matter in the St. Lawrence Estuary," Naturaliste Can., Vol 106, pp 163-173.

Krone, R. B. 1962. "Flume Studies of the Transport of Sediment in Estuarial Shoaling Processes," Final Report, Hydraulic Engineering Laboratory and Sanitary Engineering Research Laboratory, Berkeley, CA; prepared for US Army Engineer District, San Francisco, San Francisco, CA, under US Army Contract No. DA-04-203 CIVENG-59-2.

Krone, R. B. 1963 (Sep). "A Study of Rheological Properties of Estuarial Sediments," Technical Bulletin No. 7, Committee on Tidal Hydraulics, Corps of Engineers, US Army; prepared by US Army Engineer Waterways Experiment Station, Vicksburg, MS.

Krone, R. B. 1972 (Jun). "A Field Study of Flocculation as a Factor in Estuarial Shoaling Processes," Technical Bulletin No. 19, Committee on Tidal Hydraulics, Corps of Engineers, US Army; prepared by US Army Engineer Waterways Experiment Station, Vicksburg, MS.

Krone, R. B. 1979. "Sedimentation in the San Francisco Bay System," San Francisco Bay: The Urbanized Estuary, American Association for the Advancement of Science, Pacific Division, California Academy of Sciences, San Francisco, CA.

Krone, R. B. 1983 (Aug). "Cohesive Sediment Properties and Transport Parameters," Proceedings of the Conference on Frontiers in Hydraulic Engineering, ASCE, Cambridge, MA., pp 66-78.

Lane, E. W. 1955. "Design of Stable Channels," Transactions, ASCE, Vol 120, Paper No. 2776, pp 1234-1279.

Lauff, G. H. 1967. Estuaries, Publication 83, American Association for the Advancement of Science, California Academy of Sciences, San Francisco, CA.

Lunz, J. D., Clarke, D. G., and Fredette, T. J. 1984. "Seasonal Restrictions on Bucket Dredging Operations, A Critical Analysis with Recommendations," Proceedings of Dredging '84, ASCE Specialty conference on Dredging and Dredged Material Disposal, Clearwater, FL.

Marmer, H. A. 1926. The Tide, D. Appleton and Co., N.Y.

McAnally, W. H., Jr., Brogdon, N. J., Jr., Letter, J. V., Jr., Stewart, J. P., and Thomas, W. A. 1983 (Sep). "Columbia River Estuary Hybrid Model Studies; Report 1, Verification of Hybrid Modeling of the Columbia River Mouth," Technical Report HL-83-16, US Army Engineer Waterways Experiment Station, Vicksburg, MS.

McDowell, D. M., and O'Connor, B. A. 1977. "The Study of Tidal Systems: Hydraulic Measurements," Hydraulic Behaviour of Estuaries, Wiley, N.Y., Chapter 5, pp 124-145.

Mehta, A. J., and Christensen, B. A. 1983. "Initiation of Sand Transport over Coarse Beds in Tidal Entrances," Coastal Engineering, Vol 7, pp 61-75.

Mehta, A. J., and Jones, C. P. 1977 (May). "Matanzas Inlet; Glossary of Inlets Report No. 5," Florida Sea Grant Program Report No. 21, Gainesville, FL.

Mehta, A. J., and Joshi, P. B. 1984 (Dec). "Review of Tidal Inlet Hydraulics," UFL/COEL-TR/054, Coastal and Oceanographic Engineering Department, University of Florida, Gainesville, FL.

Mehta, A. J., and Partheniades, E. 1975. "An Investigation of the Depositional Properties of Flocculated Fine Sediments," Journal of Hydraulic Research, Vol 13, No. 4, pp 361-381.

Mehta, A. J., Parchure, T. M., Dixit, J. G., and Auiathurai, R. 1982. "Resuspension Potential of Deposited Cohesive Sediment Beds," Estuarine Comparisone, V. S. Kennedy, ed., Academic Press, New York, pp 591-609.

Migniot, C. 1968. "A Study of the Physical Properties of Different Very Fine Sediments and Their Behavior under Hydrodynamic Action," La Houille Blanche, No. 7 pp 591-620 (in French with English abstract).

Montgomery, R. L. 1978 (Dec). "Methodology for Design of Fine-Grained Dredged Material Containment Areas for Solids Retention," Technical Report D-78-56, US Army Engineer Waterways Experiment Station, Vicksburg, MS.

O'Brien, M. P. 1969 (Feb). "Equilibrium Flow Areas of Inlets on Sandy Coasts," Journal of the Waterways and Harbors Division, ASCE, Vol 95, No. WW1, pp 43-52.

O'Connor, B. A., and Tuxford, C. 1980. "Modelling Siltation at Dock Entrances," Proceedings of the Third International Symposium on Dredging Technology, BHRA, Paper - F2, pp 359-371, Bordeaux, France.

Officer, C. B. 1976. Physical Oceanography of Estuaries (and Associated Coastal Waters), Wiley, New York.

Owen, M. W. 1970 (Sep). "A Detailed Study of the Settling Velocities of an Estuary Mud," Report No. INT 78, Hydraulics Research Station, Wallingford, England.

Owen, M. W. 1971 (Aug). "The Effect of Turbulence on the Settling Velocities of Silt Flocs," Proceedings of the 14th Congress of I.A.H.R., Vol 4, Paris, pp 27-32.

Owen, M. W. 1973 (Dec). "Determination of the Settling Velocities of Cohesive Muds," Report No. IT 161, Hydraulics

Research Station, Wallingford, England.

Palermo, M. R., Montgomery, R. L., and Poindexter, M. E. 1978 (Dec). "Guidelines for Designing, Operating, and Managing Dredged Material Containment Areas," Technical Report DS-78-10, US Army Engineer Waterways Experiment Station, Vicksburg MS.

Parchure, T. M. 1984. "Erosional Behavior of Deposited Cohesive Sediments," Ph.D. Dissertation, University of Florida, Gainesville, FL.

Parker, W. R., and Kirby, R. 1982. "Time Dependent Properties of Cohesive Sediment in Relevant to Sedimentation Management, A European Experience," Estuarine Comparisons, V. S. Kennedy, ed., Academic Press, New York, pp 573-590.

Partheniades, E. 1966. "Field Investigations to Determine Sediment Sources and Salinity Intrusion in the Maracaibo Estuary, Venezuela," Report No. 94, MIT, Hydrodynamics Lab, Cambridge, MA.

Partheniades, E. 1977 (Sep). "Unified View of Wash Load and Bed material Load and Bed Material Load," Journal of the Hydraulics Division, ASCE, Vol 103, No. HY9, pp 1037-1057.

Peterson, M. S. 1986. River Engineering, Prentice-Hall, Englewood, NJ.

Pritchard, D. W. 1952a. "Estuaries Hydrography," Advances in Geophysics, Vol 1, pp 243-280.

Pritchard, D. W. 1952b. "Salinity Distribution and Circulation in the Chesapeake Bay Estuaries System," Journal, Marine Research, Vol 11, pp 106-123.

Pritchard, D. W. 1955. "Estuaries Circulation Patterns," Proceedings, American Society of Civil Engineers, Vol 81, No. 717.

Richardson, T. W. 1984 (Jul). "Agitation Dredging: Lessons and Guidelines from Past Projects," Technical Report HL-84-6, US Army Engineer Waterways Experiment Station, Vicksburg, MS.

Schultz, E. A., and H. B. Simmons. 1957 (Apr). "Fresh Water-Salt Density Currents, A Major Cause of Siltation in Estuaries," Technical Bulletin, No. 2, Committee on Tidal Hydraulics, Corps of Engineers, US Army; prepared by US Army Engineer Waterways Experiment Station, Vicksburg, MS.

Schureman, P. 1940. Manual of Harmonic Analysis and Prediction of Tides, Special Publication No. 98 (Revised 1940; reprinted 1958 with corrections) US Coast and Geodetic Survey, US Government Printing Office, Washington, DC.

Shields, A. 1936. "Application of Similarity Principles and Turbulence Research to Bed Load Movement," Mitteil, Preuss, Versuchsanstalt fur Wasserbau und Schiffbau, Berlin.

Silvester, R. 1974. Coastal Engineering, 2: Sedimentation, Estuaries, Tides, Effluents, and Modelling, Elsevier, New York.

Simmons, H. B. 1955. "Some Effects of Upland Discharges on Estuarine Hydraulics," Proceedings, American Society of Civil Engineers., Vol 81, No. 792.

Slotta, L. S., et al. 1974. "Effects of Shoal Removal by Propeller Wash, December 1973, Tillamook Bay Oregon," Contract No. 57-74-C-0087, Oregon State University, Corvallis, OR.

Terzaghi, K., and Peck, R. B. 1966. Soil Mechanics in Engineering Practice, 2nd ed., Wiley, New York.

Teeter, A. M. 1987 (May). "Alcatraz Disposal Site Investigaiton; Report 3, San Francisco Bay-Alcatraz Disposal Site Erodibility," Miscellaneous Paper HL-86-1, US Army Engineer Waterways Experiment Station, Vicksburg, Miss.

Teeter, A. M. 1988 (Dec). "New Bedford Harbor Superfund Project, Acushnet River Estuary Engineering Feasibility Study of Dredging and Dredged Material Disposal Alternatives; Report 2, Sediment and Contaminant Hydraulic Transport Investigations," Technical Report EL-88-15, US Army Engineer Waterways Experiment Station, Vicksburg, Miss.

Teeter, A. M. 1989 (Feb). "Effects of Cooper River Rediversion Flows on Shoaling Conditions at Charleston Harbor, Charleston, South Carolina," Technical Report HL-89-3, US Army Engineer Waterways Experiment Station, Vicksburg, Miss.

Teeter, A. M., and Pankow, W. 1989a (Sept). "The Atchafalaya River Delta; Report 2, Field Data, Section 2: Settling Characteristics of Bay Sediments," Technical Report HL-82-15, US Army Engineer Waterways Experiment Station, Vicksburg, Miss.

Teeter, A. M., and Pankow, W. 1989c (Sept). "Schematic Numerical Modeling of Harbor Deepening Effects on Sedimentation, Charleston, South Carolina," Miscellaneous Paper HL-89-7, US Army Engineer Waterways Experiment Station, Vicksburg, Miss.

Teeter, A., Hodges, S., and Coleman, C. 1987 (Sept). "Fine-Grained Sediments, An Annotated Bibliography on Their Dynamic Behavior in Aquatic Systems," Technical Report HL-87-6, US Army Engineer Waterways Experiment Station, Vicksburg, Miss.

Thomas, W. A., and McAnally, W. H. 1985 (Aug). "User's Manual for the Generalized Computer Program System: Open-channel Flow and Sedimentation, TABS-2, Main Text and Appendices A Through O," Instruction Report HL-85-1, US Army Engineer Waterways Experiment Station, Vicksburg, MS.

Thorn, M. F. C., and Parson, J. G. 1980 (Mar). "Erosion of Cohesive Sediments in Estuaries: An Engineering Guide," Proceedings of the Third International Symposium on Dredging Technology, BHRA, Paper F1, Bordeaux, France, pp 349-358.

Trawle, M. J. 1981 (Jul). "Effects of Depth on Dredging Frequency; Report 2, Methods of Estuaries Shoaling Analysis," Technical Report H-78-5, US Army Engineer Waterways Experiment Station, Vicksburg, MS.

Trawle, M. J., and Boland, R. A. 1979. "Georgetown Harbor, South Carolina; Report 2, Effects of Various Channel Schemes on Tides, Currents, and Shoaling," Miscellaneous Paper H-78-6, US Army Engineer Waterways Experiment Station, Vicksburg, MS.

Trawle, M. J., and Boyd, J. A. 1978 (May). "Effects of Depth on Dredging Frequency, Report 1, Survey of District Offices," Technical Report H-78-5, US Army Engineer Waterways Experiment Station, Vicksburg, MS.

US Army Engineer District, New Orleans, 1973. "Final Environmental Statement, Mississippi River, Baton Rouge to the Gulf of Mexico, Louisiana," New Orelans, LA.

US Army Engineer District, Philadelphia, 1969. "Long-Range Spoil Disposal Study; Part IV, Substudy 3: Development of New Dredging Equipment and Techniques," Philadelphia, PA.

US Army Engineer District, San Francisco. 1979. "Engineering Feasibility Study of a Submerged Salinity Barrier for the John F. Baldwin Ship Channel," San Francisco, CA.

US Army Engineer Waterways Experiment Station. 1984. Shore Protection Manual, 4th ed., Vicksburg, MS.

US Department of Commerce, National Oceanic and Atmospheric Administration. "Tide Tables, High and Low Water Predictions" (issued yearly for various coastlines), National Ocean Survey, US Department of Commerce, Rockville, MD.

US Fish and Wildlife Service. 1980. "US Fish and Wildlife Service Mitigation Policy," Federal Register, Vol 46, No. 15 (23 Jan 1982), pp 7644-7663.

van Olphen, H. 1963. An Introduction to Clay Colloid Chemistry, Wiley-Interscience, New York.

Vanoni, V. A., ed. 1975. "Sedimentation Engineering," ASCE Manuals and Reports on Engineering Practice No. 54, American Society of Civil Engineers, New York.

Wells, J. T. 1983. "Fluid-Mud Dynamics in Low', Moderate-, and High-Tide-Range Environments," Canadian Journal, Fish, Aquatic Sci., Vol 40, Supplement 1, pp 130-142.

Wicker, C. F., ed. 1965 (May). "Evaluation of Present State of Knowledge of Factors Affecting Tidal Hydraulics and Related Phenomena," Report 3, Committee on Tidal Hydraulics, Corps of Engineers, US Army; prepared by US Army Engineer Waterways Experiment Station, Vicksburg, MS.

Wright, L. D. 1971. "Hydrography of South pass, Mississippi River," Proceedings, American Society of Civil Engineers, Vol 97, No. WW3, p 491-504.

Wright, T. D. 1978 (Aug). "Aquatic Dredged Material Disposal Impacts," Technical Report DS-78-1, US Army Engineer Waterways Experiment Station, Vicksburg, MS.

Wylie, F. E. 1979. Tides and the Pull of the Moon, Stephen Green Press, Brattleboro, VT.

Yang, C. T. 1972 (Oct). "Unit Stream Power and Sediment Transport," Journal of the Hydraulics Division, ASCE, Vol 98, No. HY10, pp 1805-1826.

APPENDIX B
FIELD DATA CONSIDERATIONS

B-1. General. The collection of field data in an estuary is complicated by three factors: the dynamic nature and the size of estuaries and the importance of episodic events. Because of these factors, the importance of properly designing and executing a data collection program cannot be overstressed. Before actually designing a data collection program, the investigator should conduct the following tasks:

a. Clearly define the overall scope of the project and list each basic task.

b. Acquire as much information on the entire system as possible through the review of available data and literature.

c. Clearly define the objectives or goals of the field data collection program.

Only after these above tasks have been addressed should the actual design of a field data collection program be undertaken. The size of an estuary usually requires that a large number of data collection locations to be established, and its dynamic nature requires that the data by synoptic; i.e., collected simultaneously. Together, these two requirements suggest that a meaningful data collection program in an estuary is no small task.

B-2. Types of Prototype Measurements Needed. Typical prototype measurements in estuaries, along with the expected accuracy, purpose, and problems associated with each are summarized in Table B-1. As can be seen, there are nine main categories of data collection to address water resources activities.

B-3. Field Measurements. There are six basic parameters that are typically field measured as part of a field investigation: tide heights and currents, suspended solids, salinity, and bed stresses and elevation. These measurements can be made on a short-term and a long-term basis, and short term usually referring to a period of 13 or 25 hours (one tidal cycle) and the long term from months to many years. Short-term surveys of 13 hours (semidiurnal tide) and 25 hours are sometimes referred to as intensive surveys. Typically, at least two short-term surveys are planned to support a model study (for two different river discharges or two different tidal conditions). Long-term surveys are usually required to conduct rigorous time series analysis of data. Because of the expense of long-term data collection, time series analysis is often limited to tide heights, although such analysis for other parameters is certainly advantageous.

TABLE B-1
Prototype Measurements in Estuaries

Type/ Expected Accuracy	Purpose	Problems
1. Water level ±0.05 feet	Tide ranges, datum references, tide propagation, constituents, extreme levels	Usually relative levels are adequately measured, but absolute levels often inadequate, expense of establishing gage zeroes.
2. Currents ±0.15 feet per second	Three-dimensional profile of current, speed, and direction (at least 2-dimensional in horizontal plane), net transport, maximum values, circulation	Low speeds, inadequate spatial coverage, near-bed measurements, wave interference, and survivability of instruments.
3. Bed stresses ±0.1 Newton/ square metre	Shear, pressure fluctuations	Shear must be inferred from velocities/slopes. Placement of pressure sensors is sometimes tricky.
4. Suspended sediments ±5 parts per million	Concentrations, settling velocities, transport rates	Difficult to obtain representative samples plus comments on currents apply.
5. Dissolved materials ±0.1 parts per thousand	Salinity, total dissolved solids	Comments on currents apply.
6. Bed elevation ±1.0 feet	Water depth, erosion/ deposition	Accuracy is very poor, collection is complicated (density dredging, etc.).
7. Bed sediments	Rheology, density, erosional/ depositional behavior, grain sizes, etc.	Sediment characteristics mainly inferred from mineralogy, etc., or obtained from lab experiments. Undisturbed measurement techniques are needed.
8. Freshwater Inflows 5 percent of flow	Analysis of salinity and freshwater supply.	Defining the boundary conditions and hydrodynamics
9. Meteorologic Information National Weather Service standards	Effects of atmospheric pressure, wind, and surface waves.	Availability of reliable information which is site specific.

B-4. Other. Factors that will influence the quality of the collected data include

a. The expertise of personnel designing the program and collecting the data.

b. Manpower and fiscal constraints, i.e., the number of collection sites versus the number of personnel involved in the collection process (fatigue must be considered when a small number of personnel collect data from numerous sites over a large area for an extended period of time).

c. Collection platform: above-water (fixed) structure, boat, or moored (in situ) instrumentation.

d. Meteorologic conditions during the survey.

e. Freshwater inflow variability.

f. Type and condition of sample equipment and instrumentation.

g. Type and condition of laboratory sample processing equipment.

h. Timeliness of sample processing.

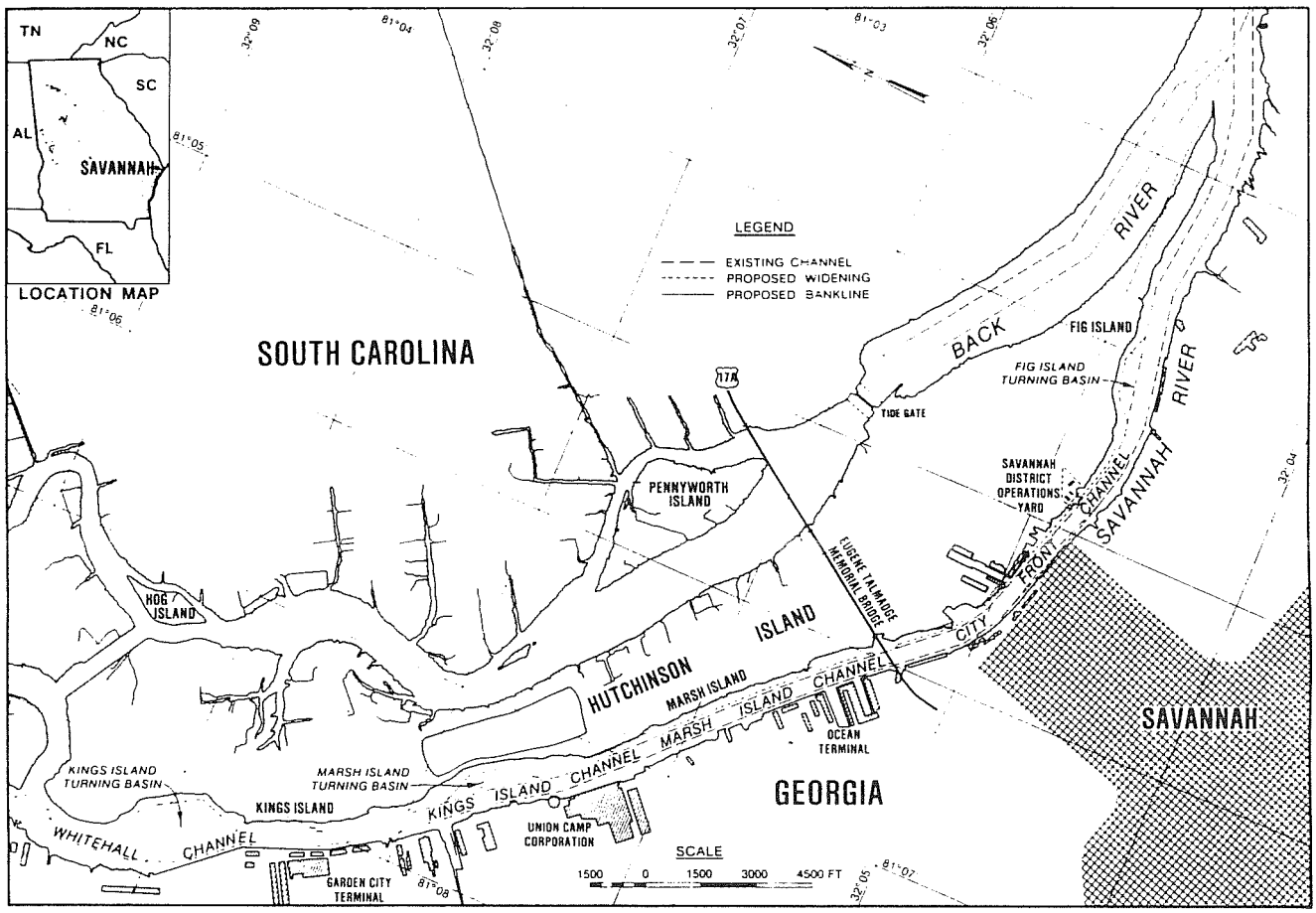

FIGURE B-1
Location map

i. Loss of or damage to moored equipment due to accident, foul weather, or vandalism.

j. Local cooperation.

B-5. Precaution Planning. Another area of consideration is that of precaution planning. In general, it is beneficial to have spare parts, extra instrumentation, and alternate plans should one or more of the factors adversely impact the data collection program. The loss of a meter or the mechanical failure of an outboard motor could mean the loss of critical data or perhaps no data at several stations. Attempting to gather this information at a later date would be costly and the additional data may not be consistent with the previous data. Equipment should be inspected regularly during a survey and maintained as needed.

B-6. Personnel Training and Experience. Substantial specialized experience and tidal hydraulics knowledge are required to collect estuarine field data successfully. Experience in inland water data collection is useful, but often insufficient to properly cope with the unique problems of highly unsteady, nonuniform flow and numerous important forcing functions in the estuarine environment. If the data are to be used to verify a model, it is also necessary for an experienced modeler to participate in planning and executing the field data collection so that the specific needs of the model are met. These factors plus the expense of estuarine data collection mandata that appropriately trained and experienced personnel plan and conduct these field programs.

B-7. Example Data Collection Program. The following example describes a short-term (13-hours) data collection effort conducted in the vicinity of Savannah Harbor, Savannah, Georgia (Johnson, Trawle, and Kee 1989). The prototype data were gathered in April 1985 by the US Army Engineer Waterways Experiment Station and the US Army Engineer District, Savannah, and were required to support a numerical model study of Savannah Harbor and vicinity. The objective of the numerical model investigation was to predict the impact of proposed channel deepening on maintenance dredging requirements and salinity intrusion.

B-8. The Savannah Estuary. The Savannah River estuary extends from the Atlantic Ocean to the northwest dividing the states of Georgia and South Carolina. It consists of a series of channels and loops, all interconnected, with the main navigation channel being North Channel and along Front River (Figure B-1). Located on Little Back River is the Savannah National Wildlife Refuge. A tide gate and a sediment trap are located on Back River (Figure B-1). During flood tide, the sediment-laden water flows upstream through the sediment trap with the tide gate open. During ebb, the gate is closed and higher ebb velocities in Front River and a decrease in shoaling along the Front River Channel. Tidal influence extends from the mouth upstream approximately 45 miles to Ebeneezer Landing.

B-9. Short-Term Survey Plan. During April 1985, an intensive 13-hour survey was conducted along the Savannah River from Fort Pulaski (river mile 0.0) upstream to Ebeneezer

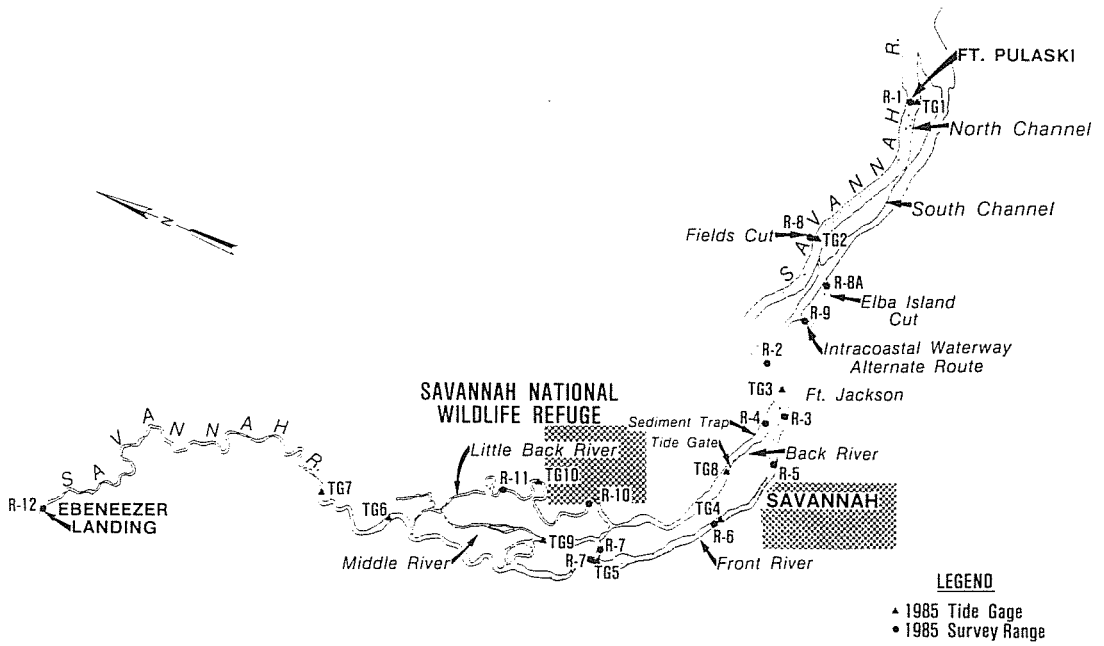

SAVANNAH HARBOR MODEL STUDY
Map Of Study Area

SCALE
1 0 1 2 3 MI

FIGURE B-2
Study location

Landing. The survey consisted of 12 ranges (Figure B-2), each with two or three stations located across the channel. Range 1 was located at Fort Pulaski. Ranges 2 and 3 and Ranges 5 through 7 were established along Front River. Range 4 was located in the sediment trap. Ranges 8, 8A, and 9 were located at Fields Cut, Elba Island Cut, and the Intracoastal Waterway Alternate Route, respectively. Ranges 10 and 11 were established along Little Back River and Range 12 established at Ebeneezer Landing. The locations were chosen to provide a range of data for sediment movement and changes in salinity. This range of data will allow a realistic model simulation of area conditions and changes as opposed to localized changes at the tide gate itself.

B-10. Actual Survey. The 13-hour survey was conducted on 4-5 April 1985 from 0600 to 1900 hour. During the survey, current velocity measurements were taken at 1-hour intervals along the left and right channel prism and along the center line of Ranges 1-6. Range 7 consisted of two transects, one along Front River near river mile 19.7 and another at the junction of Back and Front Rivers where measurements were taken at a single midchannel station. Velocity data are taken at several different depths at each station to determine sediment carrying capacity, distance carried, and also time and direction phasing. This is especially important in the near-bed region where various shear and frictional forces exist at the interface. Current velocity measurements were measured at five depths for each station at Range 1: surface, two-thirds above the bottom, middepth, one-third above the bottom, and 2 feet above the bottom. For Ranges 2 through 7 and Range 12, velocity data were collected at four depths: surface, middepth, 4 feet above the bottom, and bottom. At Ranges 8 through 11, velocity data were collected at three depths: surface, middepth, and bottom. Current velocity measurements were obtained with the use of a magnetic compass indicator and a Price-type current meter. A sample tube was attached to the meter and weight assembly, and water samples were collected to be analyzed later for salinity and suspended sediment concentration.

B-11. In addition to these intensive survey measurements, a number of bed samples were collected by grab sampler at various locations within the estuary to characterize the bed. Settling velocities of suspended sediments were also estimated during the intensive survey using a Niskin tube sampler.

B-12. Tide gages were installed at twelve locations within the estuary 1 month prior to the intensive survey and were in operation during the intensive survey as well as for 30 days preceding the survey.

B-13. Long-Term Survey. This example field survey obtained only 30 days of tide records for long-term data. Depending on the requirements of the study, availability of other data, and resource constraints, it may be necessary to collect other long-term data as part of the survey. For example, proper definition of tidal characteristics may require a minimum of 6 months record. (Twenty-nine years is commonly used for a rigorous determination of tidal constituents.) Long-term (30 days to 1 year) velocity, temperature, conductivity, turbidity, wave, and/or meteorological measurements are often obtained to fully define seasonal and episodic event responses of the estuary. These data are collected by recording meters installed for weeks to months and left untended for extended (days to weeks) periods.

B-14. Other Collection Programs. The preceding discussion of the Savannah Harbor data collection program was just one example to indicate the level of complexity. The WES HL has conducted numerous data collection programs with cooperation of several Districts for other problem areas such as location of dredge disposal sites, fate of dredged materials, salinity intrusion, hydraulic transport of contaminated sediment, and other parameters of estuarine hydrodynamics. The locations of the field collection programs have included the east, Gulf, and west coasts, and their descriptions are given in various WES technical reports. Please refer to Appendix F or contact HL for specific information.

APPENDIX C NUMERICAL MODEL INVESTIGATION OF THE SAVANNAH RIVER ESTUARY

C-1. Introduction.

a. A description of the Savannah River estuary (Figure C-1) is given in Appendix B, Paragraph B-8, of this EM and will not be repeated here.

b. The objectives of the numerical modeling effort were threefold: to predict the impact of channel deepening and widening on salinity intrusion, on channel shoaling (maintenance dredging requirements), and on navigation safety along Front River.

c. To address the first two objectives, a laterally averaged finite difference model named LAEMSED was applied. To address the third objective a ship simulator study was conducted (Hewlett, Daggett, and Heltzel 1987). To provide the channel currents required to conduct the ship simulator study, a depth-averaged, finite element model called RMA-2V was used.

C-2. Salinity Intrusion and Shoaling Study--LAEMSED.

a. Numerical Grid. The modeled area extends along Front River from river mile 0.0 (10 miles downstream from Fort Pulaski) approximately 45 miles upstream to Ebeneezer Landing (river mile 44.7). Grid generation consisted of segmenting the Savannah River system into 16 distinct branches as listed in Table C-1 and shown in Figure C-2. The vertical grid spacing on each branch was 3.0 feet. A computational time step of 60 seconds was employed. The schematization of each branch is listed in Table C-2.

b. Boundary Conditions. Daily averaged freshwater inflows at Ebeneezer Landing and tides at Fort Pulaski were recorded for several days before and after the initiation of the 13-hour detailed field survey. Ten tidal cycles were used as a "start-up" period. Tidal data at Fort Pulaski were translated to the ocean boundaries of branches A and F which extended 10 miles into the ocean. A constant salinity of 33 parts per thousand was prescribed at these boundaries. In this application the sediment computations were turned off and thus no sediment boundary conditions were required.

c. Model Verification. To match observed tides, velocities, and salinities at interior locations, the Chezy roughness coefficient and off-channel storage were adjusted. Initial estimates of storage in particular reaches were determined from National Oceanic and Atmospheric Administration/National Ocean Survey (NOAA/NOS) nautical charts showing the limits of flooding. Values of the Chezy coefficient ranged from 60 metres per second in the navigation channel to 30 metres per second in Back and Middle Rivers.

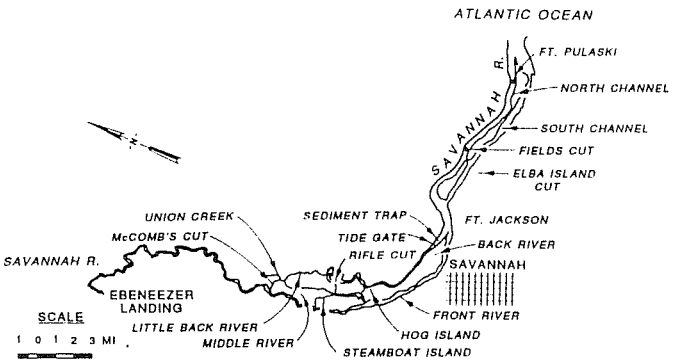

FIGURE C-1
Savannah River estuary

TABLE C-1
Branches of Savannah River

Branch	Location
1	Ebeneezer Landing through McComb's Cut along Little Back River to Front River
2	From McComb's Cut down Front River to 10 miles seaward of Fort Pulaski
3	Connection from Front River to Hog Island on Back River
4	Middle River
5	Steamboat Island Channel
6	South Channel from Front River to Ocean
7	Elba Island Cut
8	Marsh channel on Back River
9	Marsh channel on Back River
10	Marsh channel on Front River
11	Marsh channel on Little Back River
12	Marsh channel on Little Back River
13	Marsh channel on Front River
14	Rifle Cut
15	Marsh channel on Middle River
16	Union Creek

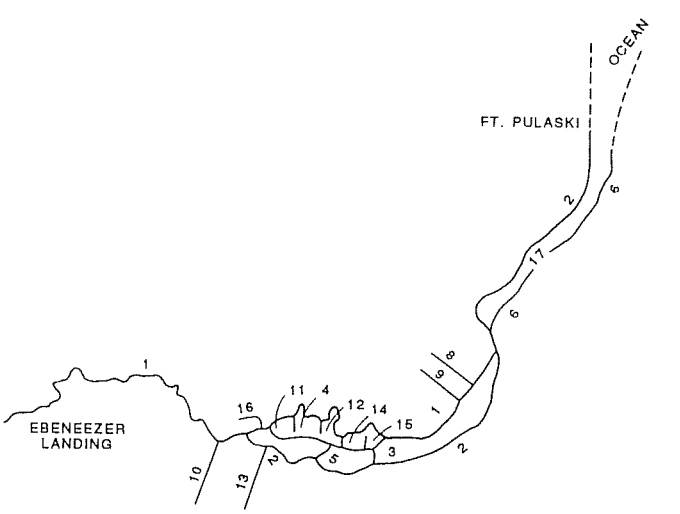

FIGURE C-2
LAEMSED branch locations

d. Tide Gate Operation. The tide gate is a gravity-operated structure. Therefore, when the water level on the riverside exceeds that on the ocean side, LAEMSED initiates the closing of the gate. This is accomplished by decreasing the Dhezy coefficient in the reach containing the gate by a factor of 10 over the next 10 time-steps (a period of 10 minutes). At the end of the tenth time-step, flow through the gate is completely stopped. This procedure reduces the initial shock to the computations caused by the closing of the gate. When the water level on the ocean side is greater than

TABLE C-2
Schematization

Branch	Δx, m	No. of Δx's
1	1,074	55
2	1,610	36
3	1,000	4
4	1,006	8
5	386	6
6	1,610	19
7	468	3
8	4,000	4
9	4,000	4
10	2,500	4
11	4,000	4
12	4,000	4
13	4,000	4
14	200	4
15	4,000	4
16	1,000	4

Note: Δx = distance between nodes (computational points)

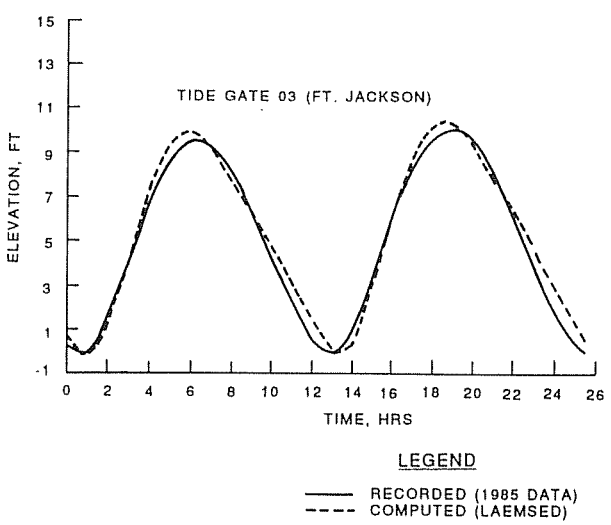

FIGURE C-3
Computed versus recorded 1985 tides at Fort Jackson

the riverside level, water is allowed to pass through the reach containing the gate in a normal fashion.

e. Results. Figures C-3 through C-5 show typical comparisons of computed and recorded tides, velocities, and salinities at Fort Jackson. As can be seen, excellent agreement of tidal ranges and phases as well as vertical distributions of velocities and salinities has been achieved.

f. Sediment Verification. Adjustment of the model's critical shear stresses and erosion rate constants to reproduce shoaling rates was accomplished by running the model for the complete 28-day cycle of tides recorded at Fort Pulaski during the 1985 survey. Computed shoaling rates along Front River and in the sediment trap were when compared with estimates based upon dredging records from 1977 to 1980.

g. Boundary Conditions. The tidal record at Fort Pulaski was prescribed at the ocean boundaries with either a low (5,200

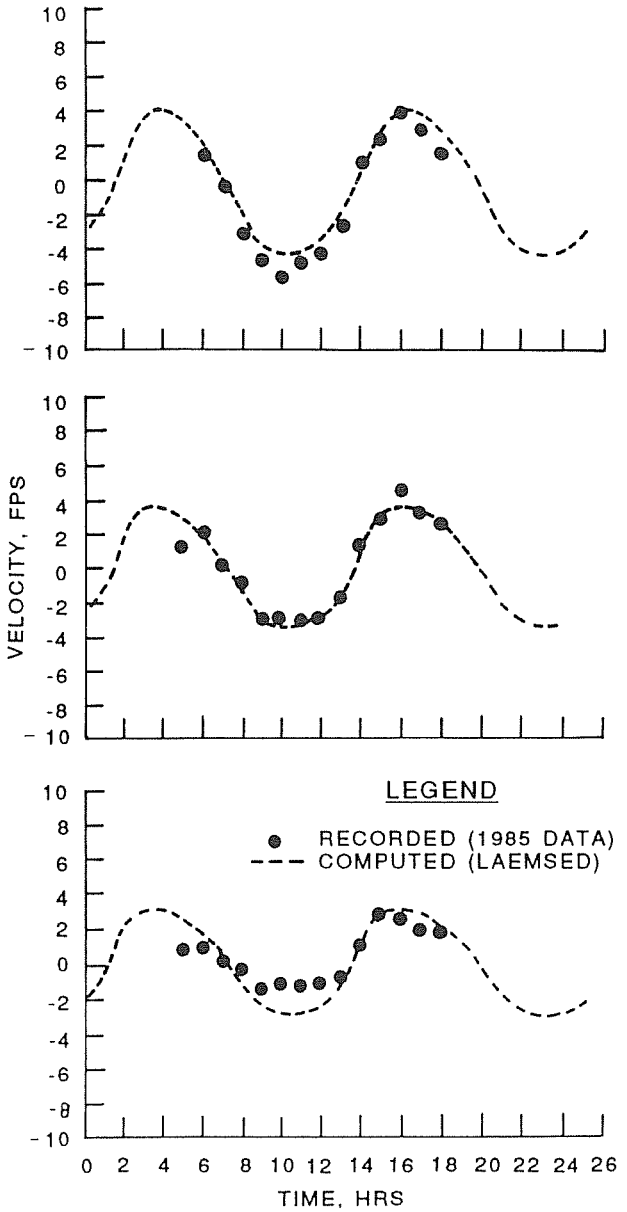

FIGURE C-4
Computed versus recorded 1985 velocities at Fort Jackson

cubic feet per second), normal (8,400 cubic feet per second) or high (16,000 cubic feet per second) constant freshwater inflow prescribed at Ebeneezer Landing. Based on 1985 survey measurements, constant suspended sediment concentrations of 30 and 300 parts per million were specified as boundary conditions at Ebeneezer Landing and the ocean boundaries, respectively. The boundary condition on salinity was as previously discussed. The 30-part-per-million concentration was applied uniformly from surface to bottom at Ebeneezer Landing, and the 300 parts per million uniformly from surface to bottom at the ocean boundary.

h. Bed Model. Shoaling problems in the Savannah Estuary result primarily from the deposition of fine-grained material. Thus the sediment was considered to be a clay. Initially, the channel bed was set to project depth in the navigation channels and to NOS chart depths elsewhere, with a spatially uniform concentration of suspended sediment of 30 parts per million in the water column. Only two layers were allowed in the bed model. The critical shear stress for erosion was set to be 0.6 Newton per square metre in the top layer and 1.0 Newton per square metre in the second layer. The

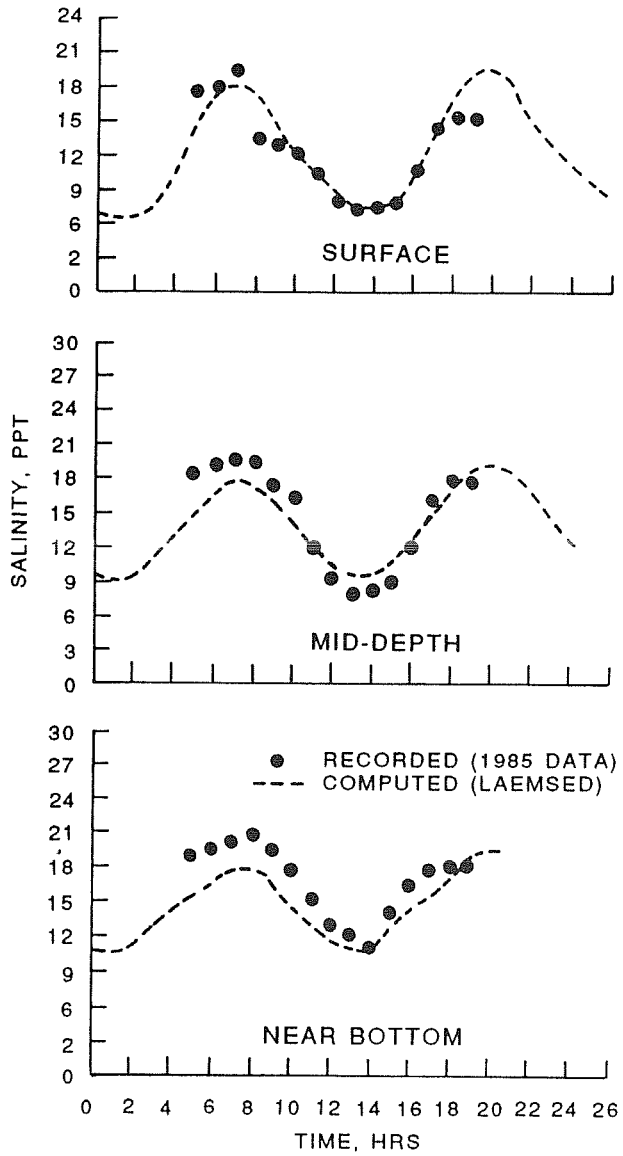

FIGURE C-5
Computed versus recorded 1985 salinities at Fort Jackson

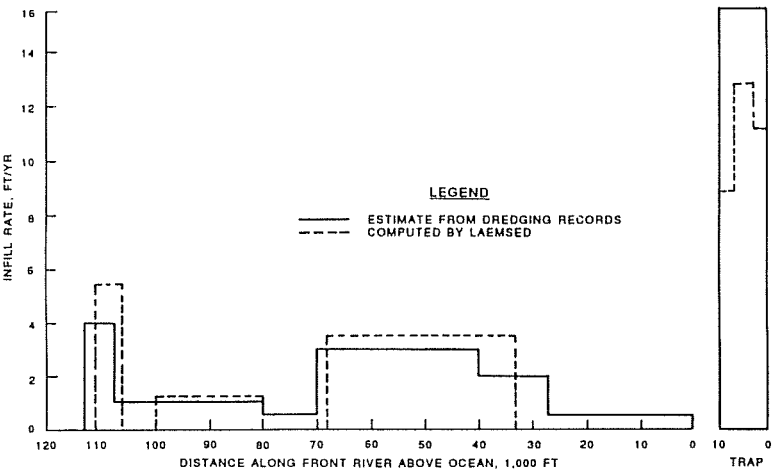

FIGURE C-6
Shoaling distribution in navigation channel

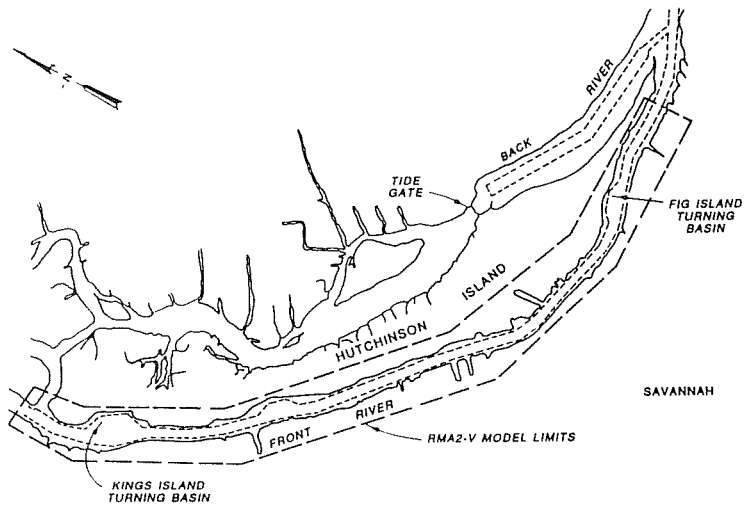

FIGURE C-7
Savannah Harbor

thickness of the upper layer was set to be constant at 0.01 metre, whereas the bottom layer thickness was variable. The concentration of material in both layers was taken as 400 kilograms per cubic metre, yielding a bulk density of the bed of 1.25 grams per cubic centimetre.

i. Results. Figure C-6 compares computed infill rates determined from 1977-1980 dredging records. The computed values were determined first as an average over the 28-day cycle of tides and then extrapolated to provide yearly averages. Little difference in shoaling rates was computed for the different freshwater inflows. Those shown in Figure C-6 are for a normal freshwater inflow.

C-3. Tidal Currents for Navigation Study--RMA-2V.

a. Of all the data required to develop a detailed scenario for a navigation channel design study, obtaining the currents in the waterway for both the existing and proposed channels is extremely important yet difficult to obtain. Currents are typically the primary source of difficulty in maneuvering a ship in a restricted waterway. To obtain these values, a finite element model of the area of a portion of the Savannah River as shown in Figure C-7 was developed. This procedure is discussed in Thomas and McAnally (1985). The finite element mesh (Figure C-8) was refined to provide adequate detail across and along the river. The model bottom definition was derived from the latest available hydrographic survey (Hewlett, Daggett, and Heltzel 1987), which was modified to reflect dredging for the proposed planned channel.

b. For the model verification boundary conditions, the US Army Engineer Waterways Experiment Station conducted a field study in the Savannah estuary in April 1985 (see Appendix B for details). Tides, velocities, salinities, and suspended sediment concentrations were recorded at several locations along the estuary from the mouth to the upstream end of tidal intrusion. The tidal and velocity measurements in the vicinity of the numerical model mesh provided the data necessary to develop boundary conditions and to ensure that the model was reproducing tidal velocity conditions within the mesh in a reasonable manner necessary to run the numerical model for a complete tidal cycle.

c. Prototype data and model results were compared at two different cross sections in the existing channel model. One of these cross sections was immediately downstream of the US Army Engineer District, Savannah, operations yard, and the other was upstream of the Talmadge Bridge at the location of the Diamond Construction Company's dock on the north bank,

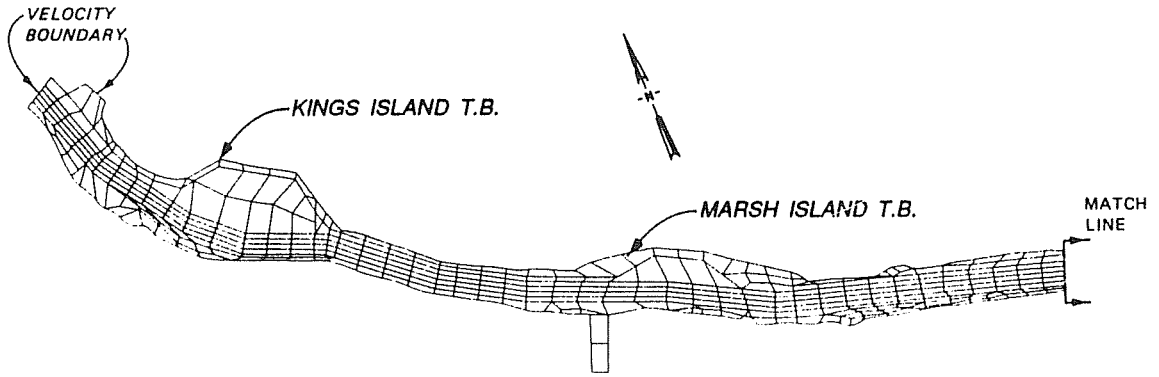

a. Upper river section

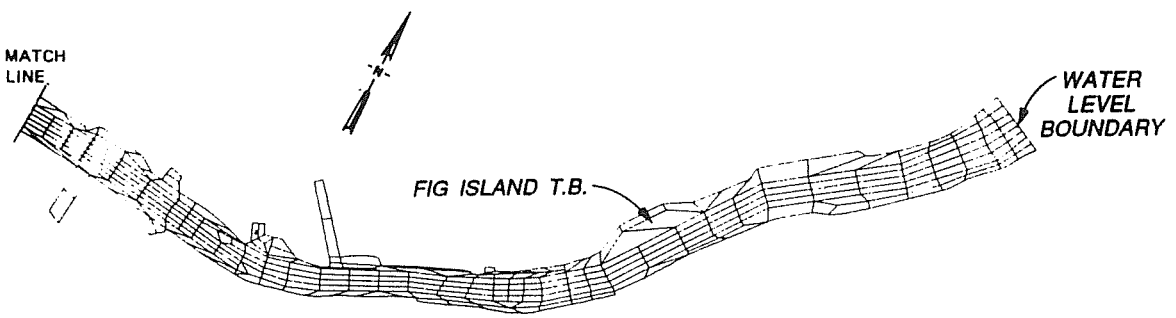

b. Lower river section

FIGURE C-8
Existing channel and tidal basin RMA-2V grid

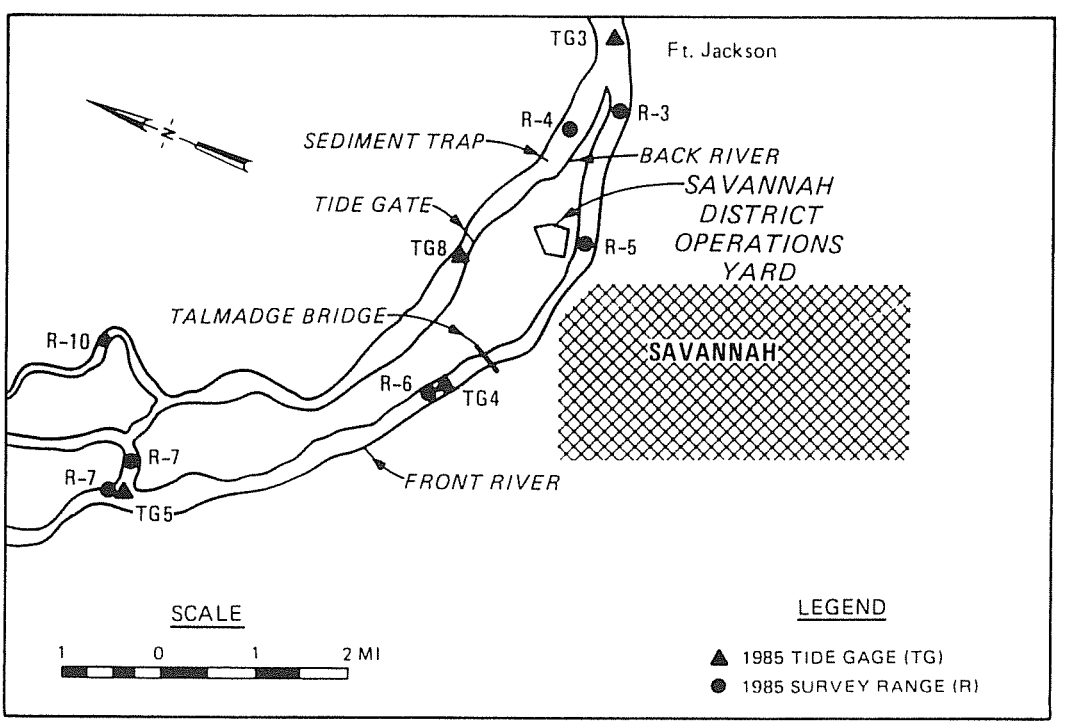

FIGURE C-9
Prototype measurement locations for Savannah Harbor ship simulation study

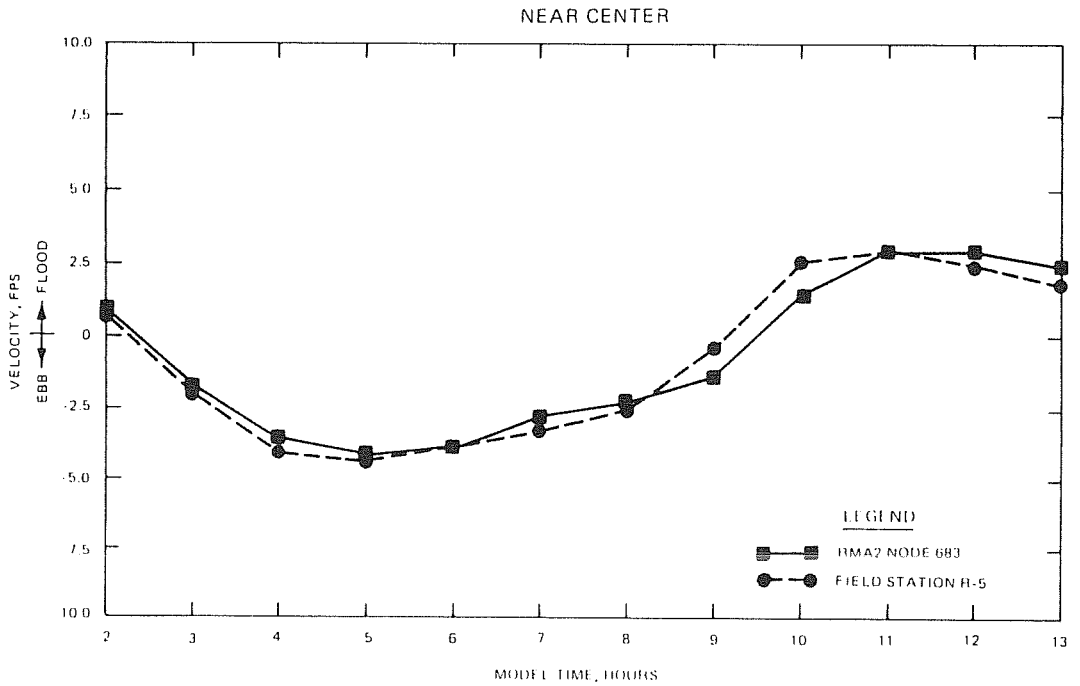

FIGURE C-10
Model-field velocity comparison at station R-5

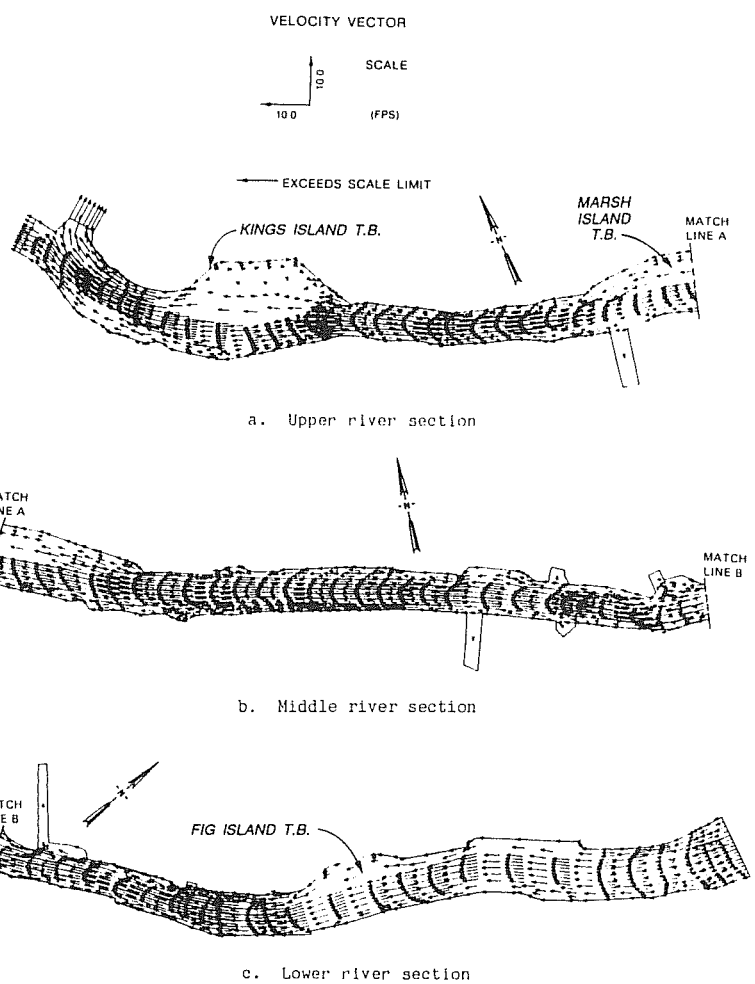

FIGURE C-11
Maximum flood velocities, existing channel, 10.5-foot tidal range

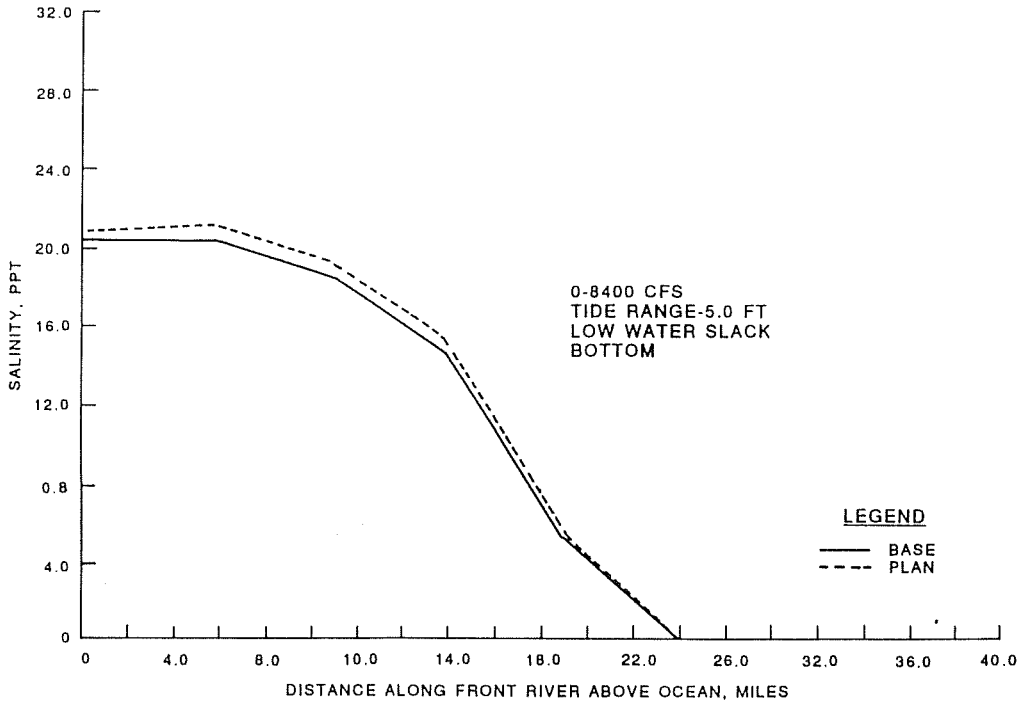

FIGURE C-12
Salinity change predicted by LAEMSED model

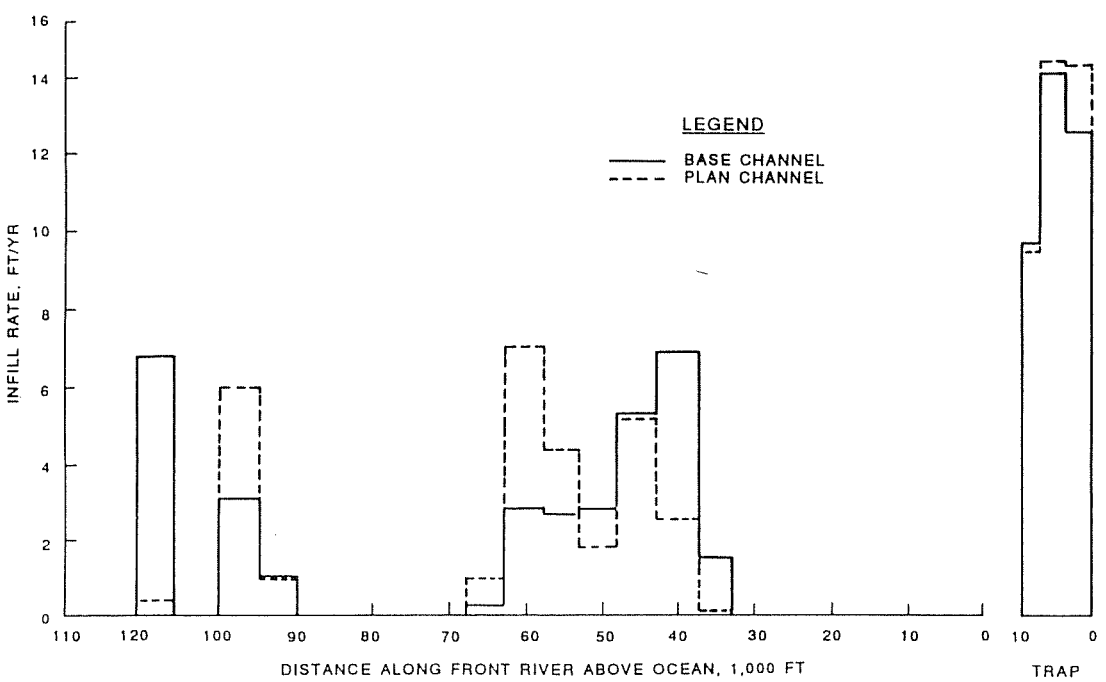

FIGURE C-13
Comparison of base and plan shoaling

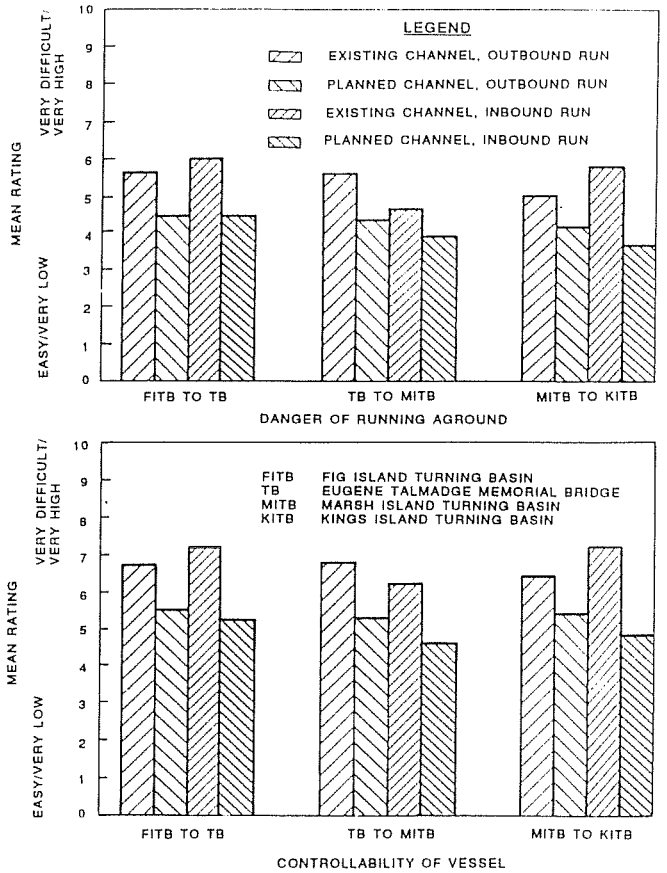

FIGURE C-14
Typical results from the ship simulator study

stations R-5 and R-6 in Figure C-9. Figure C-10 shows an example of the comparison of the field data and the numerical model results. As can be seen, agreement is close. An example plot of the current vectors from the finite element model is shown in FigureC-11.

C-4. Typical Results from Deepening Study.

a. Typical study results regarding the impact of channel enlargement on salinity intrusion predicted from the LAEMSED model are shown in Figure C-12. Typical sedimentation results, again predicted from the LAEMSED model, are given in Figure C-13.

b. Typical results from the ship simulator study, which used the currents from the RMA-2V hydrodynamic model, are shown in Figure C-14.

APPENDIX D
ESTUARINE SEDIMENTATION ANALYSIS

D-1. Sediment Sources. Identification of the sources of sediment can be a key factor in problem solving. Original sources are upland, internal, and coastal. Section D-11, subparagraphs c-e, describe the evaluation of transport routes that comprise immediate (local) sources.

a. Upland. The predominant source usually is from surface erosion of lands draining into the water body, but sediments eroded from riverbanks also contribute. In some cases, flows from the upland may carry significant quantities of organic material.

b. Internal. Currents and waves resuspend sediments from bed and banks within the estuary, and aeolian transport introduces sediment in a more direct manner. In biologically active areas, organic production within marshes and the main estuarial water body itself can significantly enhance total suspended solids and shoal volumes (Kranck 1979). Wastes can add considerably to organic loading.

c. Coastal. Close to the estuarial mouth, the sediment is often of marine origin. In areas where the open seacoasts are sandy, it is common to find the bed in the mouth or entrance channel to consist predominantly of sand. Landward of the entrance the grain size decreases and the fraction of fine-grained material tends to increase (Mehta and Jones 1977). In some estuaries, such as the Mississippi or the Amazon Rivers, where sediment supply from upstream sources has been relatively high on a geologic time scale, the offshore ebb delta is laden with deep layers of fine-grained material (Gibbs 1977; Wells 1983). Thus density- and tide-driven flows can transport some of the fine-grained ebb deltaic deposits (resuspended during flood flows coupled, oftentimes, with offshore wave activity) upstream through the channel. The material is then redeposited in reaches where the currents are too weak to transport the material further or at the nodal point for bottom flow predominance (Partheniades 1966).

D-2. Sediment Classification. For engineering purposes, sediments are customarily classified primarily according to particle size. Sediment of size greater than about 0.074 mm (No 200 sieve size) is considered to be coarse sediments, and less than this size to be fine-grained sediments. The terms "coarse" and "fine" are relative to fine-grained sedimentation and not the American Society for Testing and Material (ASTM) class. The boundary between cohesive and cohesionless sediment is not clearly defined and generally varies with the type of material. Cohesion generally increases with decreasing particle size. Thus clays (particle size <0.005 mm) are much more cohesive than silts (0.005 to 0.074 mm), and, in fact, cohesion in natural muds is due primarily to the presence of clay-sized sediment. Silt-sized material (particularly of size larger than ~0.02 mm) is only weakly cohesive, but when in combination with a sizeable fraction (by weight) of clayey sediment, constitutes a sediment which, in the flocculated state, exhibits a behavior characteristic of cohesive sediments.

a. Muds. Estuarial muds are typically composed of a wide range of materials including clay and nonclay minerals in the clay- and silt-size ranges, organic matter, and sometimes small quantities of very fine sand. Muds often occur in the presence of coarse sand, shell, and other macrosized detritus.

b. Size. The particle size distribution of coarse materials is easily determined by sieve analysis, and reported either in terms of diameter d or in ϕ units (i.e., as $-\log_2 d$). It is most common to characterize the size distribution by the median (by weight) size and the corresponding variance, standard deviation, uniformity coefficient, or sorting coefficient (Terzaghi and Peck 1966; Vanoni 1975; and US Army Engineer Waterways Experiment Station 1984). Skewness and kurtosis, particularly the latter, are less commonly used mainly because the degree of acceptable accuracy in typical sediment transport calculations does not warrant the use of these size-distribution characterizing parameters. However, they can be useful indicators of sediment sorting in studies meant to examine spatial sorting trends, e.g., of the bottom sediment with distance along the estuary.

c. Settling Velocity. The customary practice of reporting grain-size distribution has arisen out of the simplicity of sieve analysis as a measuring technique. It must, however, be noted that the key transport-related parameter is the settling velocity,

which, unfortunately, does not bear a unique relationship with particle size. laboratory settling columns can be used to measure settling velocity distribution, which may be considered as a very useful property for sediment classification (Channon 1971; Vanoni 1975).

d. Cohesive Treatment. Cohesive sediments are deflocculated, or dispersed, by removing salts from the fluid through repeated washing with saltfree water and adding a dispersing agent such as sodium-hexametaphosphate prior to particle size determination. Standard hydrometer or pipette methods are used to determine the dispersed particle size distribution (ASTM 1964). The original sample should not be dried before determining the size distribution, inasmuch as prior drying prevents the material from dispersing adequately (Krone 1962).

e. Deflocculation. Cohesive sediment size distribution obtained without dispersion will be that of the flocculated material, which bears no unique relationship to that of the dispersed material. The floc size distribution yields a qualitative indication of sediment behavior in the prototype.

f. Settling Tests. A convenient laboratory procedure for obtaining the settling velocity of flocculated sediment consists of settling tests in a column. Sediment samples are withdrawn at various elevations and different times after test initiation (Owen 1976; Vanoni 1975; Teeter and Pankow 1989a). This procedure yields an empirical relationship between the median settling velocity and suspended sediment concentration, which is unique to the type of sediment-fluid mixture used (see also section D-6 and D-7). It is preferable to the use the actual estuarial fluid in these tests. If conditions permit, field tests are recommended (Owen 1971; Teeter and Pankow 1989a).

D-3. Coarse Sediment Transport. Coarse-grained sediment includes material larger than about 0.074 mm (74 μm), the most common sediment being sand, although some estuarial beds are laden wholly with coarser material including shells and gravel (Kirby 1969).

a. With reference to sand transport, the estuarial mouth or tidal entrance can be in many cases conveniently treated as a geomorpholigic unit separately from the remainder of the estuary. Sediment transport is influenced strongly by the hydrodynamics of flood and ebb flows within the entrance channel and over the flood and ebb shoals adjacent to the channel (Mehta and Joshi 1984). In the ebb shoal area in the sea, tidal flows interact with crosscurrent generated typically by wave-driven alongshore flows. Penetration of waves from the sea into the entrance channel, particularly during flood, can have a marked effect on the rate of sediment transport and the distribution of bottom sediment (Brunn 1978; O'Brien 1969).

b. The application of sediment transport formula developed for unidirectional flows is usually suitable to tide-dominated oscillatory flows because the tidal frequency is low, and tidal currents may be considered to be "piecewise" steady. Differences tend to arise due mainly to three causes:

(1) The complexity of flow distribution resulting from salinity effects.

(2) The condition of slack water and flow reversal following slack.

(3) The dependence of bed forms and associated bed resistance on the stage of tide and the direction of flow.

c. The total rate of sediment transport is the sum of contributions from bed load and suspended load. Bed load rate varies with n^{th} power of the excess shear stress. Values of the exponent n have been found to vary from less than 1.5 to as high as 3 (Vanoni 1975; Yang 1972). Generally, for the coarse beds the exponent is nearer 1.5; for fine material the exponent is nearer 3.

d. Bed material load is a term which is sometimes confused

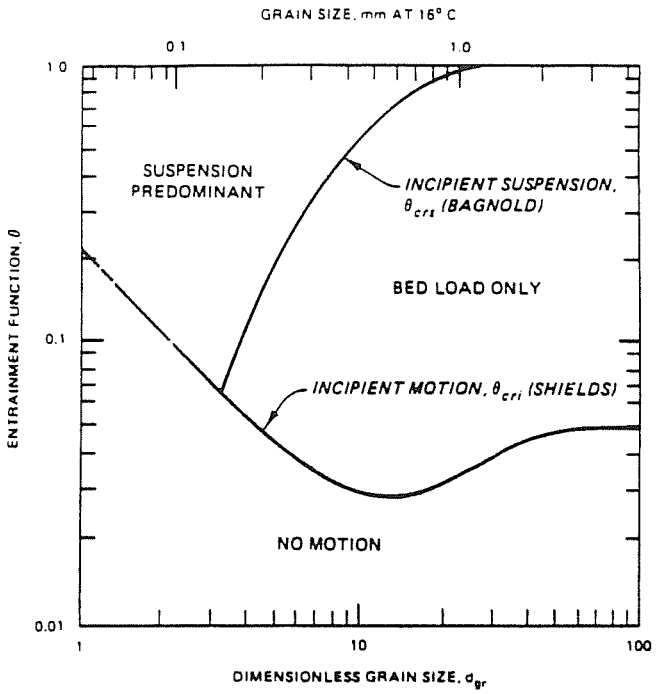

FIGURE D-1
Relationship between entrainment function, θ, and dimensionless grain size, d_{gr} (after Ackers 1972)

with bed load. Bed material load means that portion of the total load represented in the bed and includes bed load and suspended bed material. The remainder is wash load, typically fine-grained and, unlike bed material load, it is believed to the independent (uncorrelated) of flow condition. Bed load is that material moving on or near the bed. The stochastic nature of nearbed turbulence and associated sediment transport indicates that a given material can behave either as wash load or as bed material load, depending upon the properties of the material and the flow condition (Partheniades 1966).

e. Whether a sediment under a given flow condition behaves as bed load or as suspended bed material load depends on the relationship between the entrainment function θ, and the dimensionless grain size, d_{gr}, as illustrated in Figure D-1 (Ackers 1972). Here

$$\theta = \frac{\tau_b}{(\gamma_s - \gamma)d} \qquad \text{(D-1)}$$

$$d_{gr} = d\left\{ g\left[\frac{(\gamma_s - \gamma)}{\gamma\nu^2}\right]\right\}^{1/3} \qquad \text{(D-2)}$$

where

τ_b = bed shear stress
γ_s = unit weight of the sediment
γ = unit weight of water
d = grain size
g = acceleration due to gravity
ν = kinematic viscosity of the fluid

In figure D-1, the lower curve corresponds to Shields' relationship which defines a critical value θ_{cri} of entrainment function whose magnitude depends on the roughness Bagnold's number, u_*d/ν (where u_* is the friction velocity) (Shields 1936). At values below θ_{cri} there is negligible motion of bed material. The upper curve corresponds to Bagnold's (1966) relationship which defines another critical value, θ_{crs}. Above this value of θ the sediment is transported predominantly in suspension. Between the two curves is the

domain in which bed-load transport occurs. By virtue of the nature of these two curves, which intersect at a point corresponding to $d_{gr} \simeq 3.2$, for particle sizes that correspond to d_{gr} smaller than this value, transport is predominantly in suspension. Indeed for particles of sizes less than about 0.04-0.06 mm, bed-load transport does not occur (Mehta and Partheniades 1975).

f. The contribution of suspended load relative to bed load (in total load) depends on the grain size, the flow regime, and the estuarial morphology. In most estuaries, bed load is a small fraction of the total sediment load.

g. The rate of supply of "new" sediment from the river varies widely from one estuary to another, and, in a given estuary, there is usually a strong seasonal dependence as well (Krone 1979). Normally, however, the oscillatory, "to and fro," tide-controlled transport is orders of magnitude higher than the net (incoming minus outgoing) input of sediment. By the same token, the residence time of incoming sediment is usually very long and, in some cases the material is "permanently" deposited in the estuarial bed. In the long term, such factors as changes in the upstream discharge hydrograph and sediment supply rates, morphologic changes within the estuary, sea level change, and eustatic effects will alter the sediment transport regime (Dyer 1973; McDowell and O'Connor 1977). Generally estuaries import sediment and are filling with sediment.

h. Closure or tidal choking is a potential problem at sandy entrances where the strength of flow is insufficient to scour the bed, with the result that littoral drift is deposited in the mouth, the depths become shallow, and the entrance eventually closes (Brunn 1978). As a result of runoff, however, closure will be restricted to times of very low freshwater outflows, since at other times a hydrostatic head will build up sufficiently to cause an eventual breakthrough at the site of sand deposition in the mouth. When the mouth is closed, the estuary changes into a lagoon or lake of brackish water. There is no access to the sea, and water quality degradation often occurs. Training walls or jetties and dredging between the jetties coupled, sometimes, with a system for bypassing sand from the updrift beach to the downdrift beach can be used to keep entrances open (Brunn 1978).

i. Sand in transport can form waves. Sand waves occur where flows are strong and sediment supply sufficiently large. Sand waves are described as either dunes (migrate downstream) or as antidunes (migrate upstream). Dunes are by far the most common sand waves observed in rivers and estuaries. In estuaries they can grow to heights of 10 to 20 feet with wavelengths of hundreds of feet, and can impede navigation.

D-4. Cohesive Sediment Transport. Cohesion greatly influences the behavior of sediment materials and their transport processes. Cohesion results from interparticle electrochemical forces, which become increasingly important relative to the gravitational force with decreasing particle size below 0.04 mm. Clays, which have sizes less than 0.005 mm, are particularly cohesive.

a. At moderate suspended solids concentrations, depositing cohesive aggregates stick to the bed, and as they accumulate, buried aggregates are consolidated by the weight of the overburden. The strength of a deposit therefore increases with depth below its surface. The shear strength of a deposit must be overcome by the hydraulic shear stress before erosion begins. At shear stresses immediately above the critical stress for breaking of individual particle bonds, "surface" or "particle" erosion occurs. When the applied hydraulic stress is increased to the level where turbulent eddies impinge on and break small elements from the bed, "significant" erosion occurs. Significant erosion rates are much higher than particle erosion rates. When the applied hydraulic stress is increased to the level where it exceeds the bulk shear strength of a deposit, "mass" or "bulk" erosion occurs. This latter type of erosion instantaneously suspends bed material to the depth where the deposit strength equals the applied stress.

b. Particle cohesion requires interparticle collision. There are three basic mechanisms for collision: Brownian motion, flow shear due to turbulence, and settling of particles at different speeds, or differential settling (Hunt 1980). Out of these, shearing in the fluid column, which is prevalent throughout the tidal cycle except at slack water, produces the strongest interparticles bonds. Brownian motion is important in high-density suspensions, whereas at times of slack water as well as during the period immediately preceding slack water when rapid settling is occurring, differential settling plays an important role (Krone 1972).

c. At very low concentrations, e.g. ~100 mg/ℓ or less, interparticle collision frequency is restricted by the dearth of particles in suspension. Particles settle more or less independently, and the settling velocity shows no significant dependence on concentration. At higher concentrations, up to ~3,000-5,000 mg/ℓ, aggregation is enhanced with increasing concentration, and the settling velocity varies with m^{th} power of concentration, with m ranging from ~0.8 to 2, with a typical value of 1.3. At even higher concentrations, particularly in excess of ~10,000 mg/ℓ, the settling velocity begins to decrease with increasing concentration as aggregates form a continuous network through which pore water must escape upward for settling to occur. This is referred to as hindered or zone settling. The term fluid mud is often used to describe a high-concentration (>10,000 mg/ℓ) suspension that characteristically exhibits the hindered settling behavior (Krone 1962).

d. Aggregates of sediment in the clay- and silt-size range typically behave as bed material load (however not as bed load), while very fine material, e.g., derived from biogenic sources, often behaves as wash load, not being represented in the bed.

e. Inasmuch as cohesive aggregate properties (e.g., size, density, and shear strength) depend on the type of sediment-fluid mixture as well as the flow condition itself, particle size has a different meaning here than in the case of cohesionless sediment, since aggregate size is not an easily characterized quantity. The critical shear stress for erosion, or more accurately, the cohesive bed shear strength with respect to erosion, depends on the mode of formation and degree of consolidation of the bed (Mehta et al. 1982). Consequently, Shields' (1936) relationship between the critical value of the entrainment function θ_{cri} and the roughness Reynolds number, is not applicable to particles of sizes less than ~40 μm (see also Figure D-1 and Paragraph D-3). It becomes essential to conduct laboratory erosion tests to evaluate the bed shear strength for a given mud-fluid mixture (Mehta et al. 1982; Parchure 1984).

f. The process of cohesive sediment deposition and erosion are interlinked through bed consolidation. Rates of deposition and erosion in turn determine the rate of horizontal transport in suspension. In a tidal estuary, these processes are characteristically cyclic in nature; their interrelationship is schematized in Figure D-2 (Mehta et al. 1982). Suspension transport interacts with the bed through tide-controlled, time-dependent, deposition-consolidation-erosion process. The thickness and density of the deposit respond to rates of deposition and erosion, and the deposit is continually undergoing consolidation. The "bed" level changes throughout the tidal cycle; and in most cases, precise prediction of bed level changes in an environment where both deposition

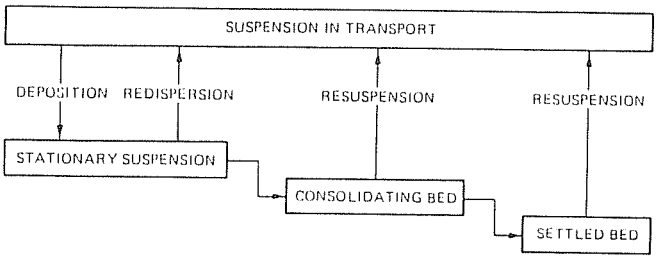

FIGURE D-2
Schematic representation of the physical states of cohesive sediment in estuarial waters (from Mehta et al. 1982)

and erosion occur over a tidal cycle requires numerical modeling of the governing equations of continuity, momentum, and mass transport (Ariathurai and Krone 1976; Hayter and Mehta 1984). In Figure D-2 it is indicated that settling of sediment (during times of decelerating flows and at slack water) results in a stationary suspension at the bottom. In this type of high-concentration suspension, hindered settling occurs; and there is, by definition, no horizontal transport (Parker and Kirby 1982). The deposit then forms a bed through settling and consolidation. During consolidation (and gelling), upward escape of the pore water occurs, the bed density increases, and physiochemical changes occur within the bed as the deposited aggregates are crushed slowly under overburden. A settled or fully consolidated bed eventually results. In such a bed, bed properties do not alter with time. Relatively thin deposits, on the order of a few centimetres thickness, consolidate in a week or two, but thick deposits may remain underconsolidated for months or even years.

D-5. Impact of Flow and Geometry. Flow and sedimentary boundary conditions are critically important in governing estuarial sediment transport. At the mouth, tidal forcing is determined by the open coast tide characteristics as well as the geometry of the mouth itself. Thus, for instance, the type of sediment in the mouth area is contingent upon the properties of the sediment discharged through the river as well as the nature of open beach deposits. At the upstream end, beyond the influence of tides, the river discharge hydrograph and sediment inflow are key factors. Within the estuarial reach, runoff, direct precipitation, and bank erosion by currents and waves can be significant factors that contribute to the overall sedimentary regime.

a. Currents broadly divide the estuarial sedimentary environment into three categories: predominantly erosional, predominantly depositional, and mixed. Deposition-dominated environments include flood and ebb deltas near the mouth, shoal areas within the estuary including natural and dredged navigation channels, and basins including ports and marinas.

b. Sites where erosion is predominant tend to be localized in comparison with sites of deposition, although sometimes large previously deposited shoals disintegrate in the absence of sediment supply.

c. In a mixed deposition/erosion environment in which net scour or shoaling is small, as would occur if the regime were in a state of "live bed" equilibrium, the rates of deposition and erosion can be high individually, and these would cause significant "to and fro" trnasport of sediment during a tidal cycle. On the other hand, in mild to moderate tidal environments, the rates of sediment transport under "normal" conditions may be small, but can be enhanced by as much as two to three orders of magnitude during episodic events including storms. In such an environment, sediment transport is not wholly tide-controlled, and it becomes essential to obtain long-term measurements of the rates of sediment transport in order to characterize seasonal and episodic influences on the physical regime.

d. The role of waves superimposed on tidal currents can be quite important. Shallow- and intermediate-depth water waves provide a critically important mechanism for incipient motion, resuspension of bottom sediment, and the formation of fluid mud layers. The sediment is then advected by the tidal currents. The often observed measureable rise in sediment transport rates during storms is quite often due mainly to bottom erosion by wave-induced oscillatory velocities since tidal velocities do not always increase significantly during storms unless a storm-induced surge occurs. Wave breaking at the banks can also cause a measurable increase in sediment concentrations and subsequent transport rates.

e. Aeolian transport is usually ignored in typical estuarial transport calculations. In certain areas, such as small basins, wind-blown material and form a significant fraction of the total deposit, particularly where sediment transport rates in the water body are not high. The degree of susceptibility of the surrounding terrain to wind-induced erosion will be a contributing factor independent of tides. However, exposure of terrain is somewhat dependent on tides; e.g., for large-amplitude tides, a greater length of beach is exposed to wind effects during low water.

f. The rise of sea level relative to land has contributed to measurable bank erosion in some estuaries and should be considered when comparing bathymetric surveys taken at widely different times (Krone 1979).

g. The impact of estuarial geometry on sediment transport is associated with the effect of geometry on flows that transport sediment. For example, it is quite common to find relatively well-defined flood- and ebbdominated channels with consequent implications for the direction of sediment transport. Furthermore, deep, dredged channels often are natural sites for sedimentation as are basins constructed along estuarial banks. Until recent times, structural means to train or control estuarial flows or shoaling/scour were often employed as and when necessary, sometimes without regard to its implications on overall estuarial stability. In some estuaries, e.g., the Mersey in England, this has resulted in severe problems for navigation and berthing (Brunn 1978). Diversion of tributary flows for agricultural or urban uses can also have deleterious effects, both with respect to sedimentation as well as water quality (McDowell and O'Connor 1977).

h. The null zone is often the area of highest concentrations of suspended particulates and rapid sediment accumulation (shoaling) (Inglis and Allen 1957). Several processes account for this. Sediments that settle into the lower part of the water column are transported upstream by tidal-residual circulation to the null zone. Sediments scoured from the bottom and transported on the flood tide and then deposited on the ebb tide phase are tidally pumped toward the null zone. At the limit of salinity intrusion (usually a relatively short distance upstream from the null zone), scour can occur on the ebb tide phase, encouraged by freshwater deflocculation of consolidated muds.

i. A constriction within a tidal flow will cause a near-bottom tidal-residual convergence zone that can trap sediments. Constrictions have been associated with shoal areas, as an example, inner and outer shoals associated with arrowhead jetties.

D-6. Sediment Characterization and Analysis. Characterization provides the basic information for identifying transport processes. Characterization tests for coarse- or fine-grained sediment depend on the nature of sediment. It is

common to find sediment from a site to consist of a range of materials from coarse size to clay size. In such a case it usually becomes necessary to separate the coarse and fine fractions and analyze them separately.

a. For coarse sediment it is typically useful to evaluate particle size distribution or, preferably, settling velocity distribution; material density and bed porosity; and, sometimes, the angle of repose.

b. Size distribution for coarse sediments is customarily obtained through sieve analysis in terms of selected sieve sizes. It is preferable to characterize sediment by its settling velocity, which is more basic to sediment transport. Since the drag coefficient of a particle in the fluid varies, in general, with particle size, shape, and density, there is no unique relationship between size and settling velocity; and it is somewhat speculative to relate particle size to settling velocity through plots or nomograms in which the particle shape must typically be assumed. Details on particle size and settling velocity measurements as well as material density and bed porosity are found elsewhere (Vanoni 1975). The angle of repose is a basic property associated with bank stability as well as incipient grain movement (Lane 1955; Mehta and Christensen 1983).

c. For cohesive sediment, the problem of characterization is more complex than that for coarse-grained material, because sediment aggregate properties depend on the type of sediment, the fluid, and the flow condition itself.

d. For characterizing the fine-grained sediment, it is recommended that the following be specified:

(1) Grain size distribution of dispersed sediment using, for example, the standard hydrometer test (ASTM 1964).

(2) The relationship between the median settling velocity and the suspension concentration of the flocculated sediment (Owen 1976).

(3) Clay and nonclay mineralogical composition through X-ray diffraction analysis (Grim 1968).

(4) Organic content (Jackson 1958).

(5) The cation exchange capacity, which is a measure of the degree of cohesion of the clay (Grim 1968).

e. For characterizing fluid in regard to fine-grained sediment, it is recommended that the following conditions be specified:

(1) Concentrations of important cations (e.g., sodium (Na+), calcium (Ca++), and magnesium (mg++)) and anions (e.g., chlorine (Cl-) and sulfate (SO_4--)).

(2) Total salt concentration.

(3) pH.

(4) Fluid temperature during measurements as well as in laboratory experiments for determining the rates of erosion and deposition.

Items (1), (2), and (3) can be determined through standardized chemical analysis procedures.

f. Recognizing that sodium, calcium, and magnesium are three comparatively more abundant and influential cations, the sodium adsorption ratio (SAR) is found to be a convenient parameter for characterizing the influence or fluid chemistry on cohesive sediment transport behavior. This parameter is defined as

$$SAR = \frac{[Na^+]}{\left\{\frac{[Ca^{++}] + [Mg^{++}]}{2}\right\}^{1/2}} \qquad \text{(D-3)}$$

where [ ] indicates ionic concentration in milliequivalents per liter. SAR is essentially a measure of the degree of abundance of sodium relative to calcium and magnesium.

g. Inasmuch as consolidation increases bed density, it is important to obtain representative in situ cores for determining the depth-distribution of the density (bulk and dry) of the bed. This information enables a conversion between deposition and erosion of sediment mass per unit time and the corresponding changes in the suspension concentration (mass per unit volume), and gages the hydraulic shear strength of the sediments.

h. In studies in which dissipation of fluid energy within the bed plays an important role, e.g., wave-mud interaction, it is essential to evaluate the rheological properties, the most important one being the viscosity, which has been found to be related to sediment concentration in an approximate manner (Krone 1963). Muds typically exhibit a non-Newtonian rehology. Thus it becomes necessary to specify parameters in addition to viscosity. Most commonly this includes the Bingham yield stress, for a comparatively simplified rheological description. The dynamic behavior of muds under wave-induced loading suggest a visco-elastic response.

i. The characterization of sediment is necessary to aid in the identification of transport and deposition processes. Preplanning for specific project data collection programs is essential so that the proper type, quantity, and data analysis can be conducted. The preceding and following paragraphs describe various field tests and sediment analyses, which may or may not be required. The amount and type of data and required procedures and tests should be determined during the project planning stage. Too much or too little data could be costly and detrimental to the project. These chapters and appendices provide general guidance; specific guidance can be found in Appendix A or through the Hydraulics Laboratory, WES.

D-7. Transport Parameters. The movement of sediment is sensitive to flow speed and direction, and it is particularly important to characterize the flow regime including the influences of salinity, geometry, and wind and related factors for a comprehensive evaluation of the overall sediment transport regime. Errors in correctly specifying the flow field will result in corresponding discrepancies in the prediction of the rate and direction of sediment transport. In a water body with large longitudinal and lateral dimensions, inadequate specification, for instance, of the flow direction, can lead to significant errors in the prediction of sites of sedimentation, particularly if the sediment is fine-grained, as a result of the relatively long distances over which the sediment is advected over each flood and ebb.

a. Particle settling velocity is both an important sediment characterizing parameter as well as deposition-related parameter. The critical shear stress is the important erosion-related parameter. Field and laboratory procedures for evaluating these and associated parameters, where cohesionless sediment transport is concerned, are well-documented in literal (Owen 1970; Vanoni 1975). It must be recognized that, as a result of estuarial variability, it is essential to obtain adequate prototype measurements for the rates of sediment transport in each site-specific investigation. Use of sediment transport formulas without adequate calibration of the formulas may lead to major errors in transport rate prediction.

b. Cohesive sediment transport processes that require parametric characterization include settling and deposition, consolidation, and erosion (Teeter, Hodges, and Coleman 1987). This information, coupled with formulations for the diffusion coefficients for sediment in suspension, forms the basis for predictive mathematical modeling for evaluating the temporal and spatial description of the suspended sediment concentration, given the flow field and boundary conditions (Hayter and Mehta 1984).

c. Settling is principally characterized by the relationship between the median settling velocity and suspension concentration.

$$W_s = f(C) \qquad (D\text{-}4)$$

where W_s is the median (by weight) settling velocity and C is the suspension concentration (dry mass of sediment per unit volume of suspension). There are basically four procedures for evaluating this relationship, each under a specific set of conditions and, therefore, yielding results which are peculiar to those conditions. These procedures are as follows:

(1) Tests in a laboratory settling column. This involves starting with an initial, flocculated suspension of known concentration in a well-shaken column, allowing the material to settle subsequently under quiescent conditions, and sampling the suspension at selected elevations and time (ASTM 1964; Hunt 1980; Krone 1962).

(2) Highly specialized tests in an appropriate laboratory flume. Sediment is initially suspended at a high flow velocity and then allowed to deposit at reduced velocity. Suspension concentration is sampled at selected times after deposition begins. The rate of aggregation is high, particularly in the beginning, provided the suspension concentration is greater than 1,000 mg/ℓ (Krone 1962; Mehta and Partheniades 1975; Teeter and Pankow 1989b).

(3) Use of in situ settling tube. This tube, designed originally be Owen (1971), allows for onsite measurements. The "Owen tube" is lowered from a boat for collecting the suspension sample. In water it is held in a horizontal horizontal attitude. When drawn out of water, it pivots vertically, and the sediment within the suspension begins to settle. Subsamples of the suspension are withdrawn at selected times from the tube, and the settling velocity determined in a manner similar to that using a laboratory settling column. By performing the settling test almost immediately following sample withdrawal from the water body, the aggregates are presumed to remain unaltered in composition. Measurements obtained through this procedure are sometimes found to yield settling velocities as much as an order of magnitude larger when compared with corresponding measurements in laboratory settling columns. Relationships obtained between settling velocity and concentration determined from field tests also include variability in sediment characteristics caused by variations in such variables as flow and inflow conditions and water chemistry (Teeter and Pankow 1989a).

(4) Comparison of measured suspended sediment concentration profiles (depth-concentration variation) with analytic prediction. The unknown in the latter is the settling velocity, which can be evaluated by matching the measured and theoretical prfiles. In some relatively "well-behaved" situations, this procedure results in acceptable values of the settling velocity (Metha et al. 1982; O'Connor and Tuxford 1980).

d. For prototype application, the use of the in situ tube is the preferred method of measurement of settling velocity. Extensive measurements of this nature have, for instance, been obtained in the Thames Estuary in England (Burt and Stevenson 1983). Comparison between measured and theoretical concentration profiles, where feasible, can yield realistic values of the settling velocity (Mehta et al. 1982). Laboratory flume or settling column tests should be used for supplementary and/or confirmatory evidence. A major difference between flume and settling column test results is that, while deposition occurs under continued aggregation in the flume under flow, settling in a column occurs in the absence of shearing rates and aggregation proceeds very slowly.

e. The rate of deposition depends on the rate at which the fraction of the settling sediment deposits, the remainder consisting of aggregates that break up near the bed under the action of bed shear stress and/or are reentrained. The reentrained pieces may reaggregate and settle again, some of those will deposit, and so on. Deposition is expressed as

$$\frac{dm}{dt} = -W_s \bar{C} \left(1 - \frac{\tau_b}{\tau_{cd}}\right); \quad \tau_b < \tau_{cd} \qquad (D\text{-}5)$$

where

m = mass of suspended sediment per unit bed area over the depth of flow
t = time
C = depth-averaged suspension concentration
τ_b = bed shear stress
τ_{cd} = critical shear stress below which all initially suspended sediment deposits eventually

For a particular sediment, τ_{cd} can be evaluated from laboratory flume experiments (Krone 1962). For a uniform (narrow primary particle size distribution) sediment, single values of W_s and τ_{cd} will suffice. For a graded sediment (e.g., a typical mud with a relatively wide range of sizes from coarse silt to fine clay), W_s and τ_{cd} will have corresponding wide ranges. These can be determined by fractionating the sediment into two or three parts in terms of size, and evaluating W_s and τ_{cd} for each fraction through flume deposition tests. On the other hand, the unfractionated sediment will exhibit a composite behavior whereby above a certain characteristic value of the bed shear stress (Teeter and Pankow 1989b), a fraction of the total initially suspended sediment will not deposit, even in the long run (Mehta and Partheniades 1975), as a consequence of the occurrence of ranges of W_s and τ_{cd}, instead of single values of these two parameters.

f. Consolidation of freshly deposited mud is accompanied by release of excess pore pressure, decrease in total bed thickness, corresponding increase in bed density and physiochemical changes associated with interparticle bonds, including gelling. Following bed formation, gelling is complete in about a day (Krone 1983).

g. From the perspective of estuarial sediment transport, the decrease in bed depth accompanying consolidation is not always of critical importance. Of much greater importance are density increase and physiochemical changes, because these in turn control corresponding changes in the bed shear strength with respect to erosion (Mehta et al. 1982). For relatively thin beds, on the order of a few centimetres in thickness, consolidation, in the absence of additional deposition, is practically complete in a period on the order of one or two weeks, and the rate of bed deformation becomes small in comparison with the rate immediately following bed formation. Bed properties including density and erosional shear strength become nearly invariant with further passage of time and a stabilized, or settled, bed (Figure D-2) results.

h. Investigators have found an approximate relationship between the bed resistance to erosion and bed density, specific to the type of sediment and fluid used (Migniot 1968; Owen 1971; Thorn and Parsons 1980; Teeter 1987). Given τ_x the critical shear stress for erosion and ρ, the dry density, the relationship is of the form

$$\tau_s = \alpha \rho^{\beta} \qquad (D\text{-}6)$$

where α and β must be determined experimentally.

i. The rate of surface erosion is obtained from

$$\frac{dm}{dt} = M \left(\frac{\tau_b - \tau_s}{\tau_s}\right); \quad \tau_b > \tau_s \qquad (D\text{-}7)$$

where M is an empirical erosion rate constant (Ariathurai and Arulanandan 1978; Mehta et al. 1982). Note that excess shear stress, $\tau_b - \tau_s$, is an important rate-determining parameter. In general, M and τ_s must be evaluated through erosion experiments in flumes. It should be noted that τ_s changes with depth of erosion into the bed. Mass erosion to the depth of the bed where shear strength equals the applied stress occurs with increasing stress.

D-8. Causes of Sediment Deposition. As evident from Equation D-5, the rate of sediment mass deposition dm/dt increases with increasing settling velocity W_s and with suspension concentration C, and decreases with increasing bed shear stress τ_b, given τ_{cd}. Likewise, Equation D-7 indicates that the rate of sediment erosion increases with increasing τ_b for given magnitudes of τ_s and M. This means the instantaneous value of the concentration C (obtained by integrating the rate of erosion over the duration of erosion) increases with τ_b as well. It follows from Equation D-5 that the mass of sediment deposited depends on the availability of entrained sediment, its settling velocity, and flow condition as reflected primarily in the bed shear stress. This type of reasoning is generally applicable to cohesive as well as cohesionless sediment.

a. A deposition-dominated environment is characterized by a region of relatively low bed shear stress in which the rate of supply of sediment to the bed well exceeds the rate of removal by erosion. Typical sites for deposition include flood and ebb deltas near the mouth, navigation channels, the region of maximum turbidity, harbors, and small basins (Ippen 1966; Mehta et al. 1982).

b. In the absence of significant and rapid natural or man-made changes, estuaries tend to be in a state of quasi-equilibrium as far as the hydrodynamic and sedimentary processes are concerned. This means that, superimposed on the annual cycle of variation of tides, freshwater flows, salinity intrusion, and sediment transport, longer period variations in the physical regime occur. Slow filling up of the existing deep channel or thalweg, coupled with scouring of a new channel elsewhere, may occur over a 10- to 20-year period, as, for example, occurs near the mouth of the Hooghly Estuary in India (Calcutta Port Commissioners 1973; McDowell and O'Connor 1977). Many estuaries are slowly filling with sediments. It is therefore critically important to understand the long-term estuarial behavior through an adequate monitoring program, particularly one involving extensive bathymetric surveys.

D-9. Consolidation. Consolidaiton is the volume change in sediment material with time. The fully consolidated volumes of fine sediments are often only a fraction of their initial deposited volumes. Coarse sediments do not consolidate under estuarine conditions; the discussion that follows deals with fine or cohesive sediments. Consolidation should be considered under the following circumstances: when evaluating sediment dispersal resulting from dredging or originating from a disposal site; when sizing confined or unconfined disposal areas for dredged materials; or when calculating dredging volumes or masses.

a. The formation of fluid muds can altar the transport mode of fine-grained sediments and therefore can be important to sediment transport and shoaling analyses. Fine-grained material with high moisture or low bulk density has relatively low shear strength, and can flow under the effects of gravity or the overlying flow. Observations of fluid mud flow have been made using radiotracers. The consolidation processes of stationary fluid mud are important to bed hydraulic shear strength and to net deposition in tidal flows. Where the thickness of fluid mud layers becomes substantial (say a foot or more), it is often referred to as "fluff." Such fluid mud layers often collect in navigation channels and can achieve thicknesses of several feet, as in the Savannah Estuary (Krone 1972). Fluid mud layers have acoustic properties resembling consolidated sediments even though they do not impede navigation. It is likely that large sums of money have been expanded to "remove" fluid mud layers. Better rapid bottom characterization techniques are needed and are currently being investigated in the Dredging Research Program at WES. Consolidation affects the ultimate volume and rate of volume change in fine-grained dredged material.

b. The amount of consolidation that disposed dredged material will undergo can be predicted by settling tube or accelerated consolidation tests and models. Reference should be made to Montgomery (1978) or to Cargill (1983 and 1985). Dredged material can be observed in large laboratory columns for a month or more to determine its final settled condition, as one method of testing. Similar zone- or column-settling tests can be performed on finegrained sediments to determine settling characteristics over a range of high suspension concentrations. Tests are performed by making serial dilutions of sediments with native water and observing settling behavior in smaller clear jars or columns. Once the relationship between concentration and settling rate is determined, further analyses can be made. By plotting settling rate versus concentration on log-log paper, the concentration at which sediments begin to behave as a deposit and how quickly concentration and strength increases can be identified. If self-weight consolidation modeling is to be carried out, special controlled-strain consolidation testing is required. Controlled-strain consolidation testing is performed at the WES Geotechnical Laboratory.

D-10. Physical Models. Physical hydraulic models are scaled representations of the prototype. They are adjusted to reproduce the important characteristics of estuarine flow. Physical hydraulic models can be important tools in sedimentation analysis of estuaries, including sedimentation patterns. Physical hydraulic modeling should be considered as one component of a program to study sedimentation if three-dimensional flow effects are known or suspected to be important. Chapter 3 described their use in hydrodynamic evaluations. Much of the physical modeling of estuaries in the United States is performed at the WES Hydraulics Laboratory and a compilation is provded in Appendix F. This section will briefly describe the use of physical hydraulic models in sedimentation studies.

a. Scales. Scale modeling of sediment transport is difficult because of scale effects and conflicting scaling requirements for the various important processes. For noncohesive sediments, compromises in scaling requirements can usually be devised by setting the time scale empirically, but considerable modeling skill is required to conduct and interpret the tests. For cohesive sediments, scale modeling is made even more difficult by the inability to scale down sediment aggregation and settling velocity. The most common practice has been to use noncohesive model sediments as tracers and apply considerable intuition and judgment to the results before drawing conclusions.

b. Processes. Physical hydraulic models are three-dimensional representations of the prototype system and have been successfully used to predict tidal currents, circulation, riverflows, salinity distributions, and dispersion processes. Many or all of these processes influence sedimentation. The ability of physical models to represent the flows in complex geometry makes them useful tools. Physical hydraulic models have been successfully incorporated into

hybrid model studies as discussed in Paragraph D-13. Because they are real, physical representations, physical hydraulic models display system dynamics in a manner that can be readily assimilated by both modeler and lay persons. The initial cost for a physical hydraulic model is somewhat higher than for other methods, but they can be operated and maintained for years and serve many studies over their lifetime. Physical hydraulic models can simulate long periods of time, spring-to-neap cycles, or hydrographs.

c. Test Procedures. During model verification, hydraulic and salinity adjustments are made first. Sedimentation is adjusted to shoaling volumes computed from a series of prototype hydrographic surveys. Methods are developed during model adjustment to introduce, distribute, and collect model sediments. Sedimentation rates are often scaled against maximum or total values. A base test is sometimes performed, but often the verification tests serve this purpose. Plan tests are then run to assess the impacts of the test modifications on sedimentation. Model sediment tracers are commonly used in fixed-bed physical models to trace the paths that eroded material will follow and to develop shoaling distribution changes caused by estuarine modifications.

D-11. Analytical Models. Analytical models are closed-form mathematical solutions for sediment transport rate of deposition. Data required to "drive" analytical models come from field surveys, another model, or assumed conditions. Analytical models are considerable simplifications of estuarine sedimentation processes but are useful for such tasks as screening, checking the reasonableness of other methods, and identifying important processes. The following are some examples of analytical models.

a. Treatment of Data. Analytical models are a method of treating prototype data. Time series velocities and concentrations can be integrated using assumed critical shear stresses to estimate depositional flux or net deposition. Equations such as D-4 or D-7 can be used for this purpose and form the basis for a closed-form mathematical solution.

b. Interpretation of Field Data. First, currents are used to calculate bed shear stress τ_b using Manning's or some other expression. Note that only an approximate estimate of shear stress can be expected from such a procedure. Using a critical shear stress for deposition ($\tau_{cd} \sim 0$ to 0.15 Newtons per square metre), deposition probabilities P are calculated over the portion of the data when $\tau_b < \tau_{cd}$ where

$$P = 1 - \frac{\tau_b}{\tau_{cd}} \; ; \; \tau_b < \tau_{cd} \qquad \text{(D-8)}$$

as described in Equation D-5. The product PW_sC_b is integrated over that portion of the tide curve, where C_b is the near-bed concentration. Erosion is estimated by integrating $M[(\tau_b/\tau_s) - 1]$ over that portion of the tide curves when bed shear stress is greater than the threshold value for bed erosion τ_s as in Equation D-7. The rate constant M has been reported to be from 0.0002 to 0.0020 kilograms per square metre per second (Hutn 1981). Deposition and erosion can then be summed to a net bed change value.

c. Flux Analysis. An alternate or supplemental analysis to that of the last section is horizontal suspended flux analysis using prototype data. Flux is the movement of material and has the units of mass per time. Horizontal flux analysis makes no assumption about deposition characteristics of sediments. Deposition or erosion can be inferred from longitudinal gradients of sediment flux using this method. Inglis and Allen (1957) presented examples and methods for computation. Measurements of currents, salinities, and suspended sediment concentration over depth and over a tidal cycle can be used to calculate the total fluxes at a station by integration over time and space (Teeter 1988). More information can be obtained from the data by decomposing sediment and salinity fluxes to identify dominant transport processes, as described in D-11e.

d. Suspended Concentration Analysis. A useful approach to the analysis of data collected over a tidal cycle, and at several depths and stations, is to reduce the data to a small number of parameters that represent important transport information (Teeter 1989). Sediment concentration, as well as velocity and salinity, data can be so reduced by a series of spatial and temporal averagings into a combination of tidal-mean and fluctuating depthmean components, as well as vertical deviations from the depth-means. For example, at some time t and station depth z, an individual datum of suspended sediment concentration C can be decomposed into components thus:

$$C(z,t) = Co + Cov(z) + Ci'(t) + Civ'(z,t) \qquad \text{(D-9)}$$

where $\overline{C}o$ is the depth-averaged tidal-mean concentration, Cov(z) is the vertical deviation of the tidal mean from the depth mean, Ci'(t) is the depth mean instantaneous concentration component, and Civ'(z,t) is the vertical deviation of the instantaneous component from the depth mean. Then by root-mean-square averaging in the remaining dimensions four components are formed. They include the depth-averaged time-mean concentration, Co, the vertical deviation from the depth mean, Cov, the depth-averaged fluctuating component, Ci, and the depth deviation in the fluctuating component, Civ. A similar approach can be used to examine lateral variations in transport.

e. Sediment Flux Components. More information on the processes responsible for estuarine suspended sediment transport can be obtained by decomposing fluxes into components. Multiplying suspended sediment concentrations by velocities and decomposing the resulting fluxes into components, as described earlier for sediment concentration, identify the relative magnitude of important processes or mechanisms including transport by net flow, vertical circulation, and tidal pumping. Net flows result from freshwater flows, from long-period (subtidal) oscillations, and from tidal asymmetry. Transport by vertical circulation (vertical shear in the mean flow) is often associated with density effects in estuaries. Vertical circulation is usually at least partially responsible for the maintenance of turbidity maximums and for high--shoaling rates in estuarine mixing zones. Tidal pumping is an advective transport process that operates in the direction of reduced concentrations. For instance, if overall suspended sediment concentrations are higher on the flood than on the ebb tide, transport by depth mean tidal pumping in the upstream direction is indicated. Further, if near-bed suspended sediment concentrations are higher on the flood than on the ebb tide (typical), and/or if the near-bed velocities are higher on the flood than on the ebb tide (also typical), transport by tidal pumping at depth is indicated. Decompose tidal-cycle suspended sediment fluxes into components or correlations thus:

$$\text{Flux of } C = A(\bar{U}o\bar{C}o + \overline{UiCi} + \overline{UovCov} + \overline{UivCiv}) \qquad \text{(D-10)}$$

where A is cross-sectional area at the sampling point. $\bar{U}o\bar{C}o$ is the product of depth and time mean values of velocity and concentration and represents sediment transport by depth-mean residual flows. $\overline{UiCi}$ is the correlation between depth-mean velocity and sediment concentration fluctuation $\overline{UovCov}$ is the transport associated with steady vertical shear and concentration deviations. $\overline{UivCiv}$ represents transports by correlations between fluctuations in velocity and concentration deviations. $\overline{UiCi}$ and $\overline{UivCiv}$ comprise tidal pumping. The first two terms on the right-hand side of Equation D-10 are

depth mean, and the last two arise from vertical effects and circulation. Similar analyses can be carried out for the lateral direction.

f. Depositional Models. Zero-dimensional (in the spatial domain) models can be applied to basins or to channels with relatively steady and uniform flows. A slightly more complex model incorporating tidal prism input could be applied to an estuary as a whole or to tidal basins. A starting point for one such model is the depth- and tidal-averaged deposition equation for fine sediments:

$$H \frac{dC}{dt} = \gamma \frac{dH}{dt} = - \Sigma_i P_i W_{si} C_{bi} \qquad \text{(D-11)}$$

where H is depth and γ is the unit weight of the bed sediments. The subscript i indicates a settling class of sediments. The solution for this equation for a single component or class after substitution of an expression relating near-bottom to depth-mean concentration is

$$\frac{C}{C_o} = \exp \left\{ -tPW_s \left[\frac{1}{H} + \frac{W_s}{K_z(1.25 + 4.75P^{5/2})} \right] \right\} \qquad \text{(D-12)}$$

where C and C_o are the depth mean and initial or inflow depth mean concentrations, respecitvely, and K_z is the depth-averaged vertical diffusivity. The last term in this expression vanishes as the suspension becomes more vertically well-mixed.

D-12. Numerical Models. Most numerical modeling of estuaries and estuarine sedimentation within the US Army Corps of Engineers is done at the WES Hydraulics Laboratory. A variety of one-, two-, and three-dimensional models have been applied. Multidimensional unsteady numerical models for sediment transport began to be developed in the mid-1970's. A two-dimensional (in the horizontal plane) numerical sedimentation model is included in the Corps' TABS-2 modeling systems (Thomas and McAnally 1985). TABS-2 is available to qualified users Corps-wide. Training on the TABS system is available at WES. An example numerical modeling investigation including sediment transport (using the two-dimensional, laterally averaged model LAEMSED) is given in Appendix C.

a. Model Processes. Numerical sediment models are transport models with nonconservative bed interaction terms. Sediments are numerically transported by advective currents and by diffusion. Sediment models require that currents be supplied by a hydrodynamic (usually numerical) model. Interactions between suspended sediments and the bed are governed by process equations in sediment transport models. Coarse sediment-bed interaction terms usually depend on the difference between sediment in transport and the competency of the flow to transport material. Fine sediment-bed interaction terms consist of process description for erosion and deposition similar to Equations D-4 and D-7. Bed structure or layering is usually modeled in some way to account for changes in density and shear strength with depth in fine sediments (Teeter and Pankow 1989c). Numerical sediment models are classified by their dimensions, by sediment type, and the equations that are solved.

b. Model Applications. Numerical models are the most advanced modeling method available for simulating sedimentation. Numerical models in general are limited to two dimensions, although three-dimensional models are currently (1989) under development and testing. Even so, numerical models contain vastly less geometric information than, say, a physical model. Also, the equations solved by numerical hydrodynamic and sediment models are simplifications or abstractions of actual behavior. Analyses suggested earlier to analyze sediment flux can also be used as a guide to select model dimensions, especially the need to include the vertical dimension. Numerical modeling, like other modeling methods, remains an art-science and successful application to real problems depends heavily on the skill, experience, and intuition of the model user.

D-13. Hybrid Models. Combining two or more models in a solution method is hybrid modeling. Hybrid models attempt to use the best modeling methods available for each "part" of sedimentation problems: current structure and sediment transport. Hybrid sediment models or analyses use one modeling method for hydrodynamics and another method for the sediment predictions. The following are the most frequently used hybrid techniques, starting with the most rigorous.

a. Physical-Numerical. The physical-numerical hybrid modeling approach uses a physical model to predict currents and a numerical model to predict sediment transport. This approach has been successfully applied to a number of estuarine sediment problems at the WES Hydraulics Laboratory. Since current velocities are needed at a great many points for the numerical sediment model, a numerical hydrodynamic model is employed as an "interpolator" of the physical model results. The physical model can be used to generate boundary conditions for the detailed numerical mesh or grid of the sediment model.

b. Physical-Analytical. The physical-analytical hybrid modeling approach uses a physical model for currents and an analytical model to predict sedimentation. Velocities can be collected at various points in the physical model and converted to bed shear stress histories. Dye study results can also give indications of circulation and residence times between various areas. Physical model results can then be extended using appropriate analytical expressions such as Equations D-4 and D-7. Only limited spatial coverage can be obtained with this technique, and simplifying assumptions must be made about the behavior of the sediments. This technique is useful when sedimentation is caused by some feature of the flow or of the residual circulation.

c. Numerical-Analytical. A numerical-analytical hybrid model uses a numerical model to predict hydrodynamics. Numerical hydrodynamic models are more costly to operate than numerical sediment models, but numerical sediment models can be significantly more costly to adjust and verify. The numerical-analytical hybrid technique avoids the costs associated with numerical sediment modeling, but at the expense of considerable rigorousness. The results from a hydrodynamic model can be used to address limited questions on sedimentation using analytical models. The shear stress at various points can be evaluated to predict deposition or erosion. Circulation and sources of sediments cannot be addressed. The analytical method can be applied only to a relatively small number of locations.

D-14. Field Data Requirements. All analyses depend on field data. Field data acquisition may be the most costly part of a sedimentation study. Required data can be grouped into system definition and behavior and boundary data. System definition includes the topography, sediment characteristics, and water level statistics. System behavior includes both synoptic tidal propagation, current structure, suspended sediment concentrations, and salinities and/or long-term records of water levels, currents, suspended sediment concentrations, salinities, and shoaling volumes. An evaluation should be made of the importance of meteorologic or hydrologic events, requiring records or samplings over an

appropriate span of time. Boundary data includes freshwater inflows to the system, tidal information, and all other modeled state variables (salinity, sediment concentration, etc.) at the boundaries of the system (see Chapter 3). The following discussion is limited to sediment data requirements.

a. A good way to determine system behavior is to conduct a boat survey in which currents, salinities, and suspended sediment concentrations are collected at short time intervals (half hour) at several stations across several cross sections over at least one tidal cycle. Normally about two to five samples in the vertical are sufficient in depths of 50 feet or less. A greater number may be required in deeper water. Onsite determinations of settling velocity should be made at strengths of flow and possibly slack waters. If suspension concentrations are high (>~1,000 mg/ℓ), vertical sampling resolution should be increased to ~2 metres or supplemented by continuous turbidity or light transmittance profiles. Tides at several locations and supporting measurements or observations of winds or other factors are also required. If an intensive boat survey is not possible, fewer points can be sampled over longer (weeks) time periods, perhaps using automated equipment. Sampling at the boundaries of the area to be modeled is particularly important.

b. Bed sediment properties are required for system definition. Methods for sediment characterization were described in Paragraph D-6. Settling experiments in the field are preferred to laboratory tests, although conditions may require the latter. It is usually not practical to carry out enough settling tests in the field to obtain sufficient spatial and temporal coverage. Supplemental information on settling can be obtained by the analysis of many vertical suspended sediment profiles and/or high-resolution non-dispersed particle size analysis (such as Coulter Counter analysis). Water column measurements of sediment concentration should include some measurements near or at the sediment bed-water interface. The presence of fluid mud should be checked using acoustic soundings, densimetric profiling, or low-disturbance coring devices. Shallow coring is also a good method of determining bed structures such as armoring, density differences, or layering.

c. It is very difficult to collect field data on all the important sediment properties. Classification by the methods described in earlier paragraphs may be useful in estimating sediment properties from existing data. Settling velocities, critical shear stresses for erosion and deposition, and the densities of fine-grained deposited material are properties that might require supplemental laboratory study. A series of laboratory settling tests on bed sediments should be run over a range of concentrations typical of the prototype to characterize this relationship. Further discussion on field data requirements for sediment transport modeling is given in Appendix B.

D-15. Notation. For the reader's convenience, notation used in Chapter 4 and Appendix D is listed here. Typical units have been included and are dependent upon the equation in which used.

- A = Cross-sectional area at the sampling point, m^2
- C = Suspension concentration, mg/ℓ or gm/m^3
- C_b = Near-bed concentration, mg/ℓ
- $Ci'(t)$ = Depth mean instantaneous concentration component
- $Civ'(z,t)$ = Vertical deviation of the instantaneous component from the depth mean
- C_o = Initial or inflow depth mean concentration, mg/ℓ
- $C_{ov(z)}$ = Vertical deviation of the tidal mean from the depth mean
- $\overline{C}$ = Depth-averaged suspension concentration, mg/ℓ
- $\overline{C}_o$ = Depth-averaged initial tidal mean concentration, mg/ℓ
- d = Grain size, m, mm, or μm
- d_{gr} = Dimensionless grain size
- g = Acceleration due to gravity, m/sec^2
- H = Depth, m
- K_Z = Depth-averaged vertical diffusivity, m^2/sec
- m = Mass of suspended sediment per unit bed area over the depth of flow, $(Kg - m^2)/m$
- M = Empirical erosion rate constant, $kg/m^2/sec$
- P = Deposition probability, nondimensional
- SAR = Sodium absorption ratio
- t = Time, sec or min
- $u*$ = Friction velocity, mm/sec
- $\overline{UiCi}$ = Correlation between depth mean velocity and sediment concentration fluctuations
- $\overline{UivCiv}$ = Transport by correlations between fluctuations in velocity and concentration deviations
- $\overline{U}\overline{o}\overline{C}o$ = Product of depth and time mean values of velocity and concentration and represents sediment transport by depth-mean residual flows
- $\overline{UovCov}$ = Transport associated with steady vertical shear and concentration deviations
- W_s = Settling velocity, cm/sec or m/sec
- z = Station depth, m
- γ = Unit weight of water, g/ℓ or kg/m^3
- γ_s = Unit weight of sediment, g/ℓ or kg/m^3
- θ = Entrainment function
- θ_{cri} = Critical value of the entrainment function
- θ_{crs} = Critical value for sediment suspension
- ν = Kinematic viscosity of fluid, m^2/sec
- ρ = Dry density, g/ℓ or kg/m^3
- τ_b = Bed shear stress, N/m^2
- τ_{cd} = Critical shear stress for deposition, N/m2
- τ_s = Critical shear stress for erosion, N/m^2

APPENDIX E
EXCERPTS FROM "LESSONS LEARNED"

E-1. Introduction. The following list of lessons learned was compiled by the Committee on Tidal Hydraulics. The Committee selected 24 US Army Corps of Engineer navigation projects to develop case histories of a variety of projects and problems that have been investigated previously.

E-2. Background. There are several hundred Corps-constructed and -maintained navigation projects. These projects include deep-draft ship channels, small boat harbors, and intracoastal waterways. A number of these projects experience higher shoaling rates and therefore burdensome maintenance dredging requirements. One of the missions of the CTH is to provide consulting services to District offices on request to review problems and to make recommendations concerning possible causes and reduction/elimination of the problem.

E-3. Lessons Learned. The following list is a compilation of generic lessons learned from the estuarine projects reviewed by the CTH.

a. Dredged channels or harbor facilities in naturally shallow water usually will require frequent maintenance dredging.

b. Where possible, docks should be located in naturally deep water.

c. An increase in channel depth usually will allow greater penetration of the saltwater wedge, which will move the shoaling location upstream.

d. Either a decrease or an increase in freshwater inflow (due

to upstream dam regulation or flow diversion) can alter the salinity characteristics of an estuary (increased intrusion length or increased stratification), which in turn can alter the location and rate of channel shoaling.

e. Increased river discharge (by diversion) can increase sediment load available for shoaling in the estuary.

f. Access channels and harbor areas off the main navigation channel should be streamlined to reduce eddies and deadwater areas where shoaling can occur.

g. Unconfined disposal of clean material usually has no adverse longterm effects on the biological population. The dredged channel and submerged disposal will be recolonized in 1 or 2 years.

h. Confined disposal will prevent the return of dredged material to the channel and reduce future channel shoaling.

i. Adjustment (sloughing) of dredged channel slopes can increase maintenance dredging for several years following construction, especially in sandtype bottom materials.

j. Isolation of the channel from sediment inflow by such training structures as dikes can reduce maintenance dredging.

k. Abandoning or relocation of projects should be considered when rapid shoaling prevents effective maintenance.

l. Change in bottom flow predominance can change volume and location of shoaling.

m. Piers on piling create eddies that increase shoaling rates of cohesive sediments.

n. Dredged disposal mounds should have relatively flat side slopes to reduce erosion. This will reduce return of material to active sediment system.

o. Suspended clay sediments can flocculate and cause shoaling with proper combination of salinity, water temperature, and flow conditions (e.g., low current velocities and slack-water periods). Flocculation is greatly accelerated by increases in the suspended sediment concentration.

p. Tide gates in secondary channels to divert ebb flow back to the main channel can aid flushing and reduce shoaling.

q. Controlled dredging and disposal practice can reduce the volume of sediment placed back in suspension. This will reduce the channel shoaling rate.

r. Expansions of harbor cross sections will reduce velocities, which can cause rapid shoaling.

s. Side channels, basins, and pier slips in estuaries are effective sediment traps.

t. Physical and/or numerical models can be very effective in studying a variety of problems, such as channel shoaling, tidal characteristics, salinity intrusion, flushing characteristics, channel alignment, training works, and flow diversions. (Various examples are cited in the preceding chapters and other appendices of this EM.)

u. Salinity behavior in many well- or partly mixed estuaries can result in a condition known as a turbudity maximum. This condition is caused by salinity-induced circulation patterns, resulting in a near-bottom flow predominance null point (no net flow in either direction). The zone of a turbidity maximum will often be subject to rather heavy shoaling; thus, this zone should be avoided when siting harbor facilities.

v. Since the inside of channel bends is usually an area of heavy shoaling, harbor facilities should be sited in the outside portion of bends.

w. Although ship simulators represent a new technology that was not available during any of the studies reported in these case histories, they are very useful in studies of channel alignment (e.g., effects of crosscurrents), dimensions (e.g., depth and width required for navigation safety), and bridge crossings (e.g., location and width of navigation openings).

x. Open-water disposal should be in a dispersive site (scour hole) where movement is out to sea, unless the site is intended to be retentive.

y. Channel alignment changes to minimize maintenance dredging should also consider alignment for safe navigation and avoid channel migration, which could undermine control structures.

z. Trench-placed riprap constructed in the dry before channel excavation is a cost-effective way to stabilize the final channel side slopes.

aa. Agitation dredging and in-channel disposal can be effective where strong ebb flow dominance exists.

bb. Some jetty systems may take years to reach equilibrium (100 or more years).

cc. Upstream bottom flow predominance can increase channel shoaling.

E-4. Summary. The preceding list of generic lessons learned was compiled by the CTH based on the review of 24 specific Corps navigation projects. The lessons learned should assist in problem avoidance before undertaking a project design or modification.

APPENDIX F
A SELECTED COMPILATION OF TIDAL HYDRAULIC MODEL INVESTIGATIONS

F-1. Introduction. This Appendix contains a selected compilation of tidal hydraulic model investigations that were conducted by the WES Hydraulics Laboratory (HL) and Coastal Engineering Research Center (CERC), for additional information and reference. The studies were selected from a much larger bibliography prepared by the USAE Committee on Tiday Hydraulics. The entries have been limited to those that are focused within and at the entrance of estuaries. Coastal design procedures and model investigations are included in other publications, such as: "Shore Protection Manual, 1084", in 2 volumes, by CERC, EM 1110-2-1614, "Design of Coastal Revetments, Seawalls, and Bulkheads" with Change 1, and EM 1110-2-1904, "Design of Breakwaters and Jetties."

F-2. The entries in this Appendix are separated into two main subdivisions:

I. Hydraulic (or physical) Model Studies, and
II. Numerical Model and Analytical Studies

The subdivisions were further organized by specific topics for ease of identification. The following prefixes are WES designations to describe the type of report:

a. GITI = General Investigation of Tidal Inlets
b. MP = Miscellaneous Paper
c. SR = Special Report
d. TM = Technical Memorandum
e. TR = Technical Report

The following outline will also serve as an index to this Appendix.

F-3. Appendix F Outline.

I. Hydraulic (or physical) Model Studies
- A. Navigation Improvements
  1. Inlets and Jetties
  2. Estuaries, Bays and Rivers
  3. Harbors
  4. Dredging and Dredged Material Disposal
- B. Hurricane Studies
  1. Storm Surge Barriers
- C. Hydrodynamic Research
  1. Salt Water Intrusion
  2. Sedimentation
  3. Currents, Tides, Dispersion and Flushing

II. Numerical Model and Analytical Studies

A. Navigation Improvements
   1. Hybrid Models
   2. Mathematical Model Studies
   3. Ship Simulation Studies

B. Hurricane Studies
   1. Storm Surge Height

C. Hydrodynamic Simulations
   1. Salt Water Intrusion
   2. Sedimentation Simulation
   3. Currents, Tides, Dispersion and Flushing

D. Dredging Related Studies
   1. Dredged Material Disposal

F-4. Availability. Corps Personnel: Most of the reports are available in either USAE District or Division libraries. If the library does not have a particular report, the librarian should contact the WES Technical Library for availability as an inter-library load. Many of these reports are available through the National Technical Information Service (or NTIS), and the librarian can contact them at 5285 Port Royal Road, Springfield, Va 22161, or via electronic mail if available. Non-Corps and non-government individuals seeking any of these references should contact their local or public library for possible inter-library loan, or write ot the NTIS at the above address.

Hydraulic Model Studies
I. A. 1. Inlets and Jetties

Number	Date	Title
TM 2-417	Nov 1955	Plans for the Improvement of Grays Harbor and Point Chehalis, Washington; Hydraulic Model Investigation
TR 2-690	Aug 1965	Plans for Reducing Shoaling, Southwest Pass, Mississippi River; Hydraulic Investigation, by H. B. Simmons and H. J. Rhodes
TR 2-735		Model Studies of Navigation Improvements, Columbia River Estuary:
	Dec 1968	Report 1 Hydraulic and Salinity Verification, by F. A. Herrmann, Jr.
		Report 2 Entrance Studies:
	Aug 1966	Section 1 Fixed-Bed Studies of South Jetty Rehabilitation, by F. A. Herrmann, Jr., and H. B. Simmons
	Nov 1966	Section 2 Fixed-Bed Studies of North Jetty Rehabilitation, by F. A. Herrmann, Jr., and H. B. Simmons
	Apr 1972	Section 3 Fixed-Bed Studies of Disposal Areas C and D, by F. A. Herrmann, Jr.
	Jul 1974	Section 4 Jetty A Rehabilitation, Jetty B, and Outer Bar Channel Relocation, by F. A. Herrmann, Jr.
		Report 3 40-Ft Channel Studies:
	Feb 1971	Section 1 Wauna-Lower Westport Bar, by F. A. Herrmann, Jr.
TR H-69-2	Feb 1969	Model Study of Galveston Harbor Entrance, Texas; Hydraulic Model Investigation, by H. B. Simmons and R. A. Boland
TR H-69-16	Nov 1969	Channel Improvement, Fire Inlet, New York; Hydraulic Model Investigation, by W. H Bobb and R. A. Boland
TR H-72-2		Grays Harbor Estuary, Washington:
	Apr 1972	Report 1 Verification and Base Tests; Hydraulic Model Investigation; by N. J. Brogdon, Jr.
	May 1973	Appendix A Supplementary Base Test Data; Hydraulic Model Investigation, by N. J. Brogdon, Jr., and G. M. Fisackerly
	Sep 1972	Report 2 North Jetty Study; Hydraulic Model Investigation, by N. J. Brogdon, Jr.
	Sep 1972	Report 3 Westport Small-Boat Basin Study; Hydraulic Model Investigation, by N. J. Brogdon, Jr.
	Sep 1972	Report 4 South Jetty Study; Hydraulic Model Investigation, by N. J. Brogdon, Jr.
	Oct 1975	Report 5 Maintenance Studies of 35-Ft.-Deep (MSL) Navigation Channel; Hydraulic Model Investigation, by N. J. Brogdon, Jr.
	Apr 1976	Report 6 45-Ft. MSL (40-Ft. MLLW) Navigation Channel Improvement Studies; Hydraulic Model Investigation, by N. J. Brogdon, Jr.
TR H-74-1	Mar 1974	Navigation Channel Improvements, Barnegat Inlet, New Jersey; Hydraulic Model Investigation, by R. A. Sager and N. W. Hollyfield
TR H-76-4		Improvements for Masonboro Inlet, North Carolina; Hydraulic Model Investigation, by W. C. Seabergh
	Apr 1976	Volume I
	Apr 1976	Volume II
TR H-77-21	Nov 1977	Improvements for Little River Inlet, South Carolina; Hydraulic Model Investigation, by W. C. Seabergh and E. F. Lane
TR H-78-4	Apr 1978	Improvements for Murrells Inlet, South Carolina; Hydraulic Model Investigation, by Maj. F. C. Perry, Jr., W. C. Seabergh, and E. F. Lane
TR HL-83-10	June 1983	Functional Design of Control Structures for Oregon Inlet, North Carolina; Hydraulic Model Investigation, by N. W. Hollyfield, J. W. McCoy, and W. C. Seabergh
	Mar 1985	Errata Sheet No. 1
TR HL-86-1	Jan 1986	Mississippi River Passes Physical Model Study; Report 2, Shoaling and Hydraulic Investigations in Southwest Pass; Hydraulic Model Investigation. By Howard A. Benson and Robert A. Boland
TR 2-711	Jan 1966	Matagorda Ship Channel Model Study, Matagorda Bay, Texas; Hydraulic Model Investigation, by H. J. Rhodes and H. B. Simmons
TR HL-88-16	July 1988	Advance Maintenance in Entrance Channels: Evaluation of Selected Projects; Hydraulic Model Investigation, by M. J. Trawle and J. A. Boyd
GITI 22	Feb 1982	Evaluation of Physical and Numerical Hydraulic Models, Masonboro Inlet, North Carolina, J. E. McTammany
TR HL-83-16		Columbia River Estuary Hybrid Model Studies
	Sep 1983	Report 1 Verification of Hybrid Modeling of the Columbia River Mouth, by W. H. McAnally, Jr., N. J. Brogdon, J. V. Letter, Jr., J. P. Stewart, and W. A. Thomas (Includes Appendixes A-G)
	Sep 1983	Report 4 Entrance Channel Tests, by W. H. McAnally Jr., N. J. Brogdon, and J. P. Stewart

Hydraulic Model Studies
I. A. 2. Estuaries, Bays and Rivers

Number	Date	Title
TR 2-694	Sep 1965	Hudson River Channel, New York and New Jersey; Plans to Reduce Shoaling in Hudson River Channel and Adjacent Pier Slips, by H. B. Simmons and W. H. Bobb
TR H-70-6	May 1970	Estuary Entrance, Umpqua River, Oregon; Hydraulic Model Investigation, by G. M. Fisackerly
TR H-72-9	Nov 1972	Navigation Channel Improvement, Gastineau Channel, Alaska; Hydraulic Model Investigation, by F. A. Herrmann, Jr.
TR H-74-12	Nov 1974	San Diego Bay Model Study; Hydraulic Model Investigation, by G. M. Fisackerly
TR HL-81-14	Dec 1981	Verification of the Chesapeake Bay Model, by N. W. Scheffner, L. G. Crosby, D. F. Bastian, A. M. Chambers and M. A. Granat
TR HL-82-3	Jan 1982	Low Freshwater Inflow Study, Chesapeake Bay Hydraulic Model Investigation, by D. R. Richards and L. F. Gulbrandsen
TR HL-82-5	Feb 1982	Baltimore Harbor and Channels Deepening Study; Chesapeake Bay Hydraulic Model Investigation, by M. A. Granat and L. F. Gulbrandsen

Number	Date	Title
TR HL-83-13	Jun 1983	Norfolk Harbor and Channels Deepening Study, Report 1, Physical Model Results, Chesapeake Bay Hydraulic Model Investigation, by D. R. Richards and M. R. Morton
TR HL-84-10	Dec 1984	Dimensions for Safe and Efficient Deep-Draft Navigation Channels; Hydraulic Model Investigation, by H. O. Turner, Jr.
TR HL-85-3	Apr 1985	Reverification of the Chesapeake Bay Model, by M. A. Granat, L. F. Gulbrandsen and V. R. Pankow
TR HL-86-1	Jan 1986	Mississippi River Passes Physical Model Study; Report 2, Shoaling and Hydraulic Investigations in Southwest Pass, by H. A. Benson and R. A. Boland, Jr.
MP HL-81-2	Jan 1981	Nanticoke River, Maryland Dye Dispersion Study, Chesapeake Bay Hydraulic Model Investigation, by D. R. Richards, S. R. River, and D. F. Bastian.
MP HL-86-7	Sep 1986	Estuary Model Test Evaluation, by N. J. Brogdon, Jr.

Hydraulic Model Studies
I. A. 3. Harbors

Number	Date	Title
TR 2-444	Apr 1957	Investigation for Reduction of Maintenance Dredging in Charleston Harbor, South Carolina; Summary Report of Model Investigation
	Apr 1957	Appendix 1 Subsidiary Model Tests
	Apr 1957	Appendix 2 Data Plots
	Apr 1957	Appendix 3 Flow-Pattern Photographs
TR 2-580		Savannah Harbor Investigation and Model Study:
		Volume III Results of Model Investigations:
	Oct 1961	Section 1 Model Verification and Results of General Studies
	Oct 1961	Section 2 Tests of Improvement Plans
	Nov 1963	Section 3 Results of Supplemental Tests
	Mar 1965	Section 4 Results of Tests of Increased Channel Dimensions, by H. J. Rhodes H. B. Simmons
TR 2-733	Jul 1986	Reduction of Shoaling in Charleston Harbor and Navigation Improvement of Cooper River, South Carolina; Hydraulic Model Investigation, by W. H. Bobb and H. B. Simmons
TR H-75-4		Los Angeles and Long Beach Harbors Model Study
	Jun 1975	Report 1 Prototype Data Acquisition and Observations, by E. B. Pickett, D. L. Durham, and W. H. McAnally, Jr.
	Jan 1975	Report 2 Observations of Ship Mooring and Movement, by L. G. Crosby and D. L. Durham
	Jul 1976	Report 3 Analyses of Wave and Ship Motion Data, by D. L. Durham, J. K. Thompson, D. G. Outlaw, and L. G. Crosby
	Feb 1977	Report 4 Model Design, by D. G. Outlaw, D. L. Durham, C. E. Chatham, and R. W. Whalin
	Feb 1978	Errata Sheet No. 1
	Sep 1975	Report 5 Tidal Verification and Base Circulation Tests, by W. H. McAnally, Jr. (includes Appendix A)
	Sep 1975	Appendix B Surface-Current Pattern Mosiacs, by W. H. McAnally, Jr.
	Aug 1979	Report 6 Resonant Response of the Modified Phase I Plan, by D. G. Outlaw
TR H-78-18	Nov 1978	Design for Harbor Entrance Improvements, Wells Harbor, Maine, Hydraulic Model Investigation, by R. R. Bottin, Jr.
TR HL-83-13		Norfolk Harbor and Channels Deepening Study:
	Jun 1983	Report 1 Physical Model Results; Chesapeake Bay Hydraulic Model Investigation, by D. R. Richards and M. R. Morton
	Mar 1985	Report 2 Sedimentation Investigation; Chesapeake Bay Hydraulic Model Investigation, by R. G. Berger, Jr., S. B. Heltzel, R. F. Athow, Jr., D. R. Richards, and M. J. Trawle (includes Appendix A)

Hydraulic Model Studies
I. A. 4. Dredging and Dredged Material Disposal

Number	Date	Title
TR 2-755	Jan 1967	Model Study of Hopper Dredges; Hydraulic Model Investigation, by J. J. Franco
TR H-72-5	Sep 1972	Plans for Reduction of Shoaling in Brunswick Harbor and Jekyll Creek, Georgia; Hydraulic Model Investigation, by F. A. Herrmann, Jr. and I. C. Tallant
TR H-72-8	Nov 1972	Disposal of Dredge Spoil; Problem Identification and Assessment and Research Program Development, by M. B. Body et. al.
TR H-73-12		Houston Ship Channel, Galveston Bay, Texas:
	Aug 1973	Report 1 Hydraulic and Salinity Verification; Hydraulic Model Investigation, by W. H. Bobb, R. A. Boland, Jr., and A. J. Banchetti
TR H-75-13		Mobile Bay Model Study:
	Sep 1975	Report 1 Effects of Proposed Theodore Ship Channel and Disposal Areas on Tides, Currents, Salinities, and Dye Dispersion, by R. J. Lawing, R. A. Boland, Jr., and W. H. Bobb (includes Appendixes A-B)
TR H-78-5		Effects of Depth on Dredging Frequency:
	May 1978	Report 1 Survey of District Offices, by M. J. Trawle and J. A. Boyd, Jr.
	Jul 1981	Report 2 Methods of Estuaring Shoaling Analysis, by M. J. Trawle
TR HL-84-6	Jul 1984	Agitation Dredging: Lessons and Guidelines from Past Projects, by T. W. Richardson (includes Appendixes A-B)

Hydraulic Model Studies
I. B. 1. Storm Surge Barriers

Number	Date	Title
Unnumbered		Model Study of Narragansett Bay:
	Feb 1957	Interim Report Protection of Narragansett Bay from Hurricane Tides; Hydraulic Model Investigation
	Jan 1959	Interim Report 2 Effects of Lower Bay Barriers on Salinities, Shoaling and Pollution in Narragansett Bay; Hydraulic Model Investigation
	Sep 1959	Interim Report 3 Effects of Fox Point Barrier on Water Temperatures
	Sep 1959	Interim Report 4 Effects on Cooling-Water Channel on Temperatures of Cooling Water for Power Stations
TR 2-636	Nov 1963	Effects on Lake Pontchartrain, Louisiana, of Hurricane Surge Control Structures and Mississippi River-Gulf Outlet Channel; Hydraulic Model Investigation
TR 2-662	Oct 1964	Protection of Narragansett Bay from Hurricane Surges; Summary Report; Hydraulic Model Investigation, H. B. Simmons
TR 2-663	Oct 1964	Discharge Characteristics of Hurricane Barriers, Wareham-Marion, Massachusetts; Hydraulic Model Investigation, by E. C. McNair, Jr., and J. L. Grace
TR 2-742	Oct 1966	Steady-flow Stability Tests of Navigation Opening Structures, Hilo Harbor Tusnami Barrier, Hilo, Hawaii; Hydraulic Model Investigation, by N. R. Oswalt and M. B. Boyd
TR 2-754	Jan 1967	Effects of Hurricane Barrier on Navigation Conditions in East Passage, Narragansett Bay, Rhode Island; Hydraulic Model Investigation, by J. G. Housley
TR H-69-12		Galveston Bay Hurricane Surge Study:
	Sep 1969	Report 1 Effects of Proposed Barriers on Hurricane Surge Heights; Hydraulic Model Investigation, by N. J. Brogdon, Jr.
	Mar 1973	Appendix A Calibration Tests; Hydraulic Model Investigation, by R. A. Sager and E. C. McNair, Jr.

Number	Date	Title
	Jul 1970	Report 2 Effects of Proposed Barriers on Tides, Currents, Salinities, and Dye Dispersion for Normal Tide Conditions, by W. H. Bobb and R. A. Boland, Jr.
	Jul 1970	Appendix A Dye Time-Concentration Curves
	Mar 1973	Appendix B Calibration Tests: Hydraulic Model Investigation, by R. A. Sager and E. C. McNair, Jr.
	Jul 1970	Report 3 Effects of Plan 2 Alpha and Plan 2 Gamma Barriers on Tides, Currents, Salinities, and Dye Dispersion for Normal Tide Conditions; Hydraulic Model Investigation, by W. H. Bobb and R. A. Boland, Jr.
	Jul 1970	Appendix A Dye-Time Concentration Curves
TR H-76-14	Sep 1976	Effects of Hurricane Surge Barrier on Hydraulic Environment, Jamaica Bay, New York; Hydraulic Model Investigation, by R. F. Athow, Jr.
TR H-76-16	Sep 1976	Hydraulic Characteristics of Rigolets Pass, Louisiana, Hurricane Surge Control Structures; Hydraulic Model Investigation, by R. C. Berger, Jr., and R. A. Boland, Jr. (Includes Appendix A)
TR HL-82-2		Lake Pontchartrain and Vicinity Hurricane Protection Plan:
	Jan 1982	Report 1 Prototype Data Acquisition and Analysis, by D. G. Outlaw (includes Appendixes A-E)
	Jun 1982	Report 2 Physical and Numerical Model Investigation of Control Structures and the Seabrook Lock; Hydraulic and Mathematical Model Investigation; by H. L. Butler, R. C. Berger, L. L. Daggett, and T. F. Berninghausen
	Oct 1983	Report 3 Numerical Model Investigation of Plan Impact on the Tidal Prism of Lake Pontchartrain, by H. L. Butler (includes Appendixes A-B)
MP H-72-1	Apr 1972	Physical Model Studies of Proposed Hurricane Surge Protection Schemes, by N. J. Brogdon and F. A. Herrmann, Jr.

Hydraulic Model Studies
I. C. 1. Saltwater Intrusion

Number	Date	Title
TM 2-310	Apr 1950	Salt Water Intrusion, Calcasieu River, Louisiana, and Connecting Waterways; Model Investigation.
TR HL-79-18	Nov 1979	Carquinez Strait, California, Salinity Barrier Calibration Study; Hydraulic Model Investigation, by R. C. Berger, Jr. (Includes Appendixes A-B)

Hydraulic Model Studies
I. C. 2. Sedimentation

Number	Date	Title
TR HL-82-15		The Atchafalaya River Delta:
	June 1988	Report 2 Field Data
		Section 1 Atchafalaya Bay Program Description and Data (2 volumes) by C. J. Coleman, A. M. Teeter, B. P. Donnell, G. M. Fisackerly, D. A. Crouse and J. W. Parman.
	Sep 1989	Section 2 Settling Characteristics of Bay Sediments by A. M. Teeter and W. Pankow.
	Jul 1982	Report 3 Extrapolation of Delta Growth, by J. V. Letter, Jr.
	Jan 1984	Report 4 Generic Analysis of Delta Development, by J. T. Wells, S. J. Chinburg, and J. M. Coleman (includes Appendixes A-B)
	Dec 1988	Report 5 The Atchafalaya River Delta Quasi-Two-Dimensional Model of Delta Growth and Impacts on River Stages, by W. A. Thomas, R. E. Heath, J. P. Stewart and D. G. Clark.
	Jul 1984	Report 6 Interim Summary Report of Growth Predictions, by W. H. McAnally, Jr., W. A. Thomas, J. V. Letter, Jr., and J. P. Stewart
	Sep 1985	Report 7 Analytical Analysis of the Development of the Atchafalaya River Delta
	Jan 1985	Report 9 Wind Climatology, by B. A. Ebersole
GITI 12	May 1977	A Case History of Port Mansfield Channel, Texas, by J. M. Kieslich

Hydraulic Model Studies
I. C. 3. Currents, Tides, Dispersion and Flushing

Number	Date	Title
TR 2-457	Jun 1957	Dispersion of Effluent in Delaware River from New Jersey Zinc Company Plant; Hydraulic Model Investigation
TR 2-767	Apr 1967	Magic Island Complex, Including Kewalo Basin and Ala Wai Boat Harbor, Honolulu, Oahu, Hawaii; Hydraulic Model Investigation, by C. W. Brasfeild and C. E. Chatham, Jr.
TR H-74-11	Nov 1974	Tillamook Bay Model Study; Hydraulic Model Investigation, by G. M. Fisackerly
TR HL-79-1		Newburport Harbor, Massachusetts:
	Feb 1979	Report 1 Design for Wave Protection and Erosion Control, by C. R. Curren and C. E. Chatham, Jr. (includes Appendix A)
TR HL-79-12		Mayport-Mill Cove Model Study:
	Jul 1979	Report 1 Hydraulic, Salinity, and Shoaling Verification; Hydraulic Model Investigation, by N. J. Brogdon, Jr.
	Aug 1979	Report 2 Mayport Naval Basin Study; Hydraulic Model Investigation, by N. J. Brogdon, Jr.
	Sep 1979	Report 3 Mill Cove Study; Hydraulic Model Investigation, by N. J. Brogdon, Jr. and J. W. Parman
TR HL-79-15	Sep 1979	San Juan National Historic Site, San Juan, Puerto Rico; Design for Prevention of Wave-Induced Erosion; Hydraulic Model Investigation, by R. R. Bottin, Jr. (includes Appendixes A-B)
TR HL-81-14	Dec 1981	Verification of the Chesapeake Bay Model; Chesapeake Bay Hydraulic Model Investigation, by N. W. Scheffner, L. G. Crosby, D. F. Bastian, A. H. Chambers, and H. A. Granat (includes Appendixes A-D)
TR HL-82-3	Jan 1982	Low Freshwater Inflow Study; Chesapeake Bay Hydraulic Model Investigation, by D. R. Richards and L. F. Gulbrandsen
	Mar 1982	Errata Sheet No. 1
TR HL-85-3	Apr 1985	Reverification of the Chesapeake Bay Model; Chesapeake Bay Hydraulic Model Investigation, by H. A. Granat, L. F. Gulbrandsen, and V. R. Pankow (includes Appendixes A-D)
MP 2-812	Apr 1966	Flushing Studies, Victoria Channel, Victoria, Texas; Hydraulic Model Investigation, by R. A. Boland
MP 2-912	Sep 1966	Effects of a Proposed 35-Foot Channel to Richmond on Currents and Salinities Over the Seed Oyster Beds in James River; Hydraulic Model Investigation, by W. H. Bobb, N. J. Brogdon, and H. B. Simmons
MP H-69-13	Dec 1969	Effects of Proposed Elizabeth River Dike on Tides, Currents, Salinities, and Shoaling; Hydraulic Model Investigation, by R. A. Boland and W. H. Bobb
MP H-72-8	Jun 1972	Effects of Proposed Extension of Craney Island Disposal Area on Tides, Currents, and Salinities; Hydraulic Model Investigation, by R. A. Boland
MP H-76-9	May 1976	Effects of 40-Foot Charleston Harbor Project on Tides, Currents, and Salinities; Hydraulic Model Investigation, by H. A. Benson
MP H-77-3	Mar 1977	Dispersion of Proposed Theodore Industrial Park Effluents in Mobile Bay; Hydraulic Model Investigation, by R. C. Berger, Jr., and M. J. Trawle

Number	Date	Title
MP H-78-6		Georgetown Harbor, South Carolina:
	Feb 1978	Report 1 Hydraulic, Salinity, and Shoaling Verification; Hydraulic Model Investigation, by M. J. Trawle
	May 1979	Report 2 Effects of Various Channel Schemes on Tides, Currents, and Shoaling; Hydraulic Model Investigation, by M. J. Trawle and R. A. Boland, Jr.
GITI 13	Aug 1977	Hydraulics and Stability of Tidal Inlets, by F. F. Escoffier
GITI 15	Nov 1977	Physical Model Simulation of the Hydraulics of Masonboro Inlet, North Carolina, R. A. Sager and W. C. Seaberg
GITI 16	Sep 1978	Hydraulics and Dynamics of North Inlet, South Carolina, 1975-76, D. Nummedal and S. M. Humphries
GITI 17	Feb 1979	An Evaluation of Movable-Bed Tidal Inlet Models, S. C. Jain and J. F. Kennedy
GITI GI 18	May 1980	Supplementary Tests of Masonboro Inlet Fixed-Bed Model: Hydraulic Model Investigation, W. C. Seabergh and R. A. Sager

Numerical Model and Analytical Study
II. A. 1. Hybrid Models

Number	Date	Title
TR H-73-16	Oct 1973	Enlargement of the Chesapeake and Delaware Canal; Hydraulic and Mathematical Model Investigation, by M. B. Body, W. H. Bobb, C. J. Huvall, and T. C. Hill
TR HL-83-16		Columbia River Estuary Hybrid Model Studies
	Sep 1983	Report 1 Verification of Hybrid Modeling of the Columbia River Mouth, by W. H. McAnally, Jr., N. J. Brogdon, J. V. Letter, Jr., J. P. Stewart, and W. A. Thomas (includes Appendixes A-C)
	Sep 1983	Report 4 Entrance Channel Tests, by W. H. McAnally Jr., N. J. Brogdon, and J. P. Stewart
TR HL-89-14	Jul 1989	Verification of the Hydrodynamic and Sediment Transport Hybrid Modeling System for Cumberland Sound and Kings Bay Navigation Channel, Georgia, by M. A. Granat, N. J. Brogdon, J. T. Cartwright and W. H. McAnally, Jr.
GITI 19	Oct 1981	Tidal Inlet Response to Jetty Construction, Kieslich, J. M.

Mathematical Model
II. A. 2. Studies

Number	Date	Title
TR H-78-22	Dec 1978	Numerical Simulation of the Coos Bay-South Slough Complex, by H. L. Butler
TR HL-87-1	Apr 1987	A Mathematical Study of the Impact on Salinity Intrusion of Deepening the Lower Mississippi River Navigation Channel, by B. H. Johnson, M. B. Boyd and G. H. Keulegan
TR HL-87-13	Sep 1987	Corpus Christi Inner Harbor Shoaling Investigation, by T. M. Smith, W. H. McAnally Jr. and A. M. Teeter
TR HL-88-8	Apr 1988	Lower James River Circulation Study, Virginia, Evaluation of Craney Island Enlargement Alternatives, by S. B. Heltzel and M. A. Granat
TR HL-88-24	Sep 1988	New Haven Harbor Numerical Model Study, by D. R. Richards and J. E. Clausner
TR HL-88-25	Sep 1988	I-664 Bridge-Tunnel Study, Virginia, Sedimentation and Circulation Investigation, by S. B. Heltzel
TR HL-89-3	Feb 1989	Effects of Cooper Rediversion Flows on Shoaling Conditions at Charleston Harbor, Charleston, South Carolina, by A. M. Teeter
TR HL-89-12	Jun 1989	Newport News Channel Deepening Study, Virginia; Numerical Model Investigation, by H. J. Lin and W. D. Martin
MP HL-87-2	Jun 1987 Sep 1988	A Numerical Model Analysis of Mississippi River Passes Navigation Channel Improvements, by D. R. Richards, et al (in four reports)
GITI 6	Jun 1977	Comparison of Numerical and Physical Hydraulic Models, Masonboro Inlet, North Carolina, Main text and Appendixes 1-4, D. L. Harris and B. R. Bodine
	Jun 1977	Appendix 1 Fixed-Bed Hydraulic Model Results, R. A. Sager and W. C. Seabergh
	Jun 1977	Appendix 2 Numerical Simulation of Hydrodynamics (WRE), F. D. Masch, R. J. Brandes and J. D. Reagan (in 2 Volumes)
	Jun 1977	Appendix 3 Numerical Simulation of Hydrodynamics (Tractor), R. J. Chen and L. A. Hembree, Jr.
	Jun 1977	Appendix 4 Simplified Numerical (Lumped Parameter) Simulation, C. J. Huval G. L. Wintergerst
TR CERC-83-2	Sep 1983	Mathematical Modeling of Three-Dimensional Coastal Currents and Sediment Dispersion: Model Development and Application, Y. P. Sheng

II. A. 3. Ship Simulation Studies

Number	Date	Title
TR HL-85-4	Jun 1985	Ship Simulation Study of John F. Baldwin (Phase II) Navigation Channel, San Francisco Bay, California, by C. Huval, B. Comes, and R. T. Garner III.
TR HL-87-5	May 1987	Ship Navigation Simulator Study; Savannah Harbor Widening Project, Savannah, Georgia, by J. C. Hewlett, L. L. Daggett and S. B. Heltzel

Hurricane Studies
II. B. 1. Storm Surge Height

Number	Date	Title
TR HL-79-2	Feb 1979	A Numerical Model for Tsunami Inundation, by J. R. Houston and H. L. Butler (includes Appendix A)
TR H-77-17	Sep 1977	Nearshore Numerical Storm Surge and Tidal Simulation, by J. J. Wanstrath
TR HL-82-15	Jan 1985	Report 8 Numerical Modeling of Hurricane-Induced Storm surge, by B. A. Ebersole
TR 76-3	Nov 1976	"Theory and Application," Storm Surge Simulation in Transformed Coordinates, Wanstrath, J. J., et. al.
	Nov 1976	"Program Documentation," Storm Surge Simulation in Transformed Coordinates, Wanstrath, J. J.
TR HL-80-18	Sep 1980	Type 19 Flood Insurance Study: Tsunami Predictions for Southern California, by J. R. Houston (includes Appendixes A-B)
CTH Technical Bulletin No. 21	Dec 1980	Evaluation of Numerical Storm Surge Models

Hydrodynamic Simulations
II. C. 1. Salt Water Intrusion

Number	Date	Title
WES Video File No. 88153	1988	Video Report - "Saltwater Intrusion Demonstration" by N. J. Brogdon, et al.

II. C. 2. Sedimentation Simulation

Number	Date	Title
TR 82-4	Oct 1982	Performance of a Sand Trap Structure and Effects of Impounded Sediments, Channel Islands Harbor, California, R. D. Hobson
TR HL-85-5	Sep 85	Spectral Analysis of River Columbia Estuary Currents, B. P. Donnell and W. H. McAnally, Jr.
GITI 5	Feb 1976	Notes on Tidal Inlets on Sandy Shores, M. P. O'Brien
GITI 12	May 1977	A Case History of Port Mansfield Channel, Texas, J. M. Kieslich

II. C. 3. Currents, Tides, Dispersion and Flushing

Number	Date	Title
TR H-69-9	Jun 1969	Theoretics in Design of the Proposed Crescent City Harbor Tsunami Model, by G. H. Keulegan, J. Harrison, and M. J. Mathews
TR H-78-11	Jun 1978	Numerical Simulation of Tidal Hydrodynamics, Great Egg Harbor and Corson Inlets, New Jersey, by H. L. Butler (includes Appendixes A-E; Appendix E is on microfiche only)
TR HL-80-3		Erosion Control of Scour During Construction:
	Sep 1984	Report 6 FINITE - A Numerical Model for Combined Refraction and Diffraction of Waves, by J. R. Houston and L. W. Chou (includes Appendix A)
	Sep 1984	Report 7 CURRENT - A Wave-Induced Current Model, by S. R. Vemulakonda (includes Appendix A)
TR CERC-84-2	Apr 1984	Numerical Simulation of Oregon Inlet Control Structures, Effects on Storm and Tide Elevations in Pamlico Sound, D. L. Leenknecht, J. A. Earickson, and H. L. Butler
GITI 14	Nov 1977	A Spatially Integrated Numerical Model of Inlet Hydraulics, W. N. Seelig, D. L. Harris and B. E. Herchenrodeer
SR 7	Feb 1981	Tides and Tidal Datums in the United States, D. L. Harris. (GPO Stock No. 008-022-00161-1)

Dredging Related Studies

II. D. 1. Dredged Material Disposal

Number	Date	Title
TR HL-87-12	Sep 1987	Technical Supplement to Dredged Material Disposal Study US Navy Home Port, Everett Washington, by S. A. Adamec, Jr., B. H. Johnson, A. M. Teeter and M. J. Trawle
TR HL-88-27	Nov 1988	San Francisco Bay: Modeling System for Dredged Material Disposal and Hydraulic Transport, by V. R. Pankow
TR HL-89-11	May 1989	Deposition and Erosion Testing on the Composite Dredged Material Sediment Sample from New Beford Harbor, Massachusetts, by A. M. Teeter and W. Pankow.
MP HL-86-1	Mar 1986	Alcatraz Disposal Site Investigation, Report 1, by M. J. Trawle and B. H. Johnson
MP HL-86-1	Oct 1986	Report 2, North Zone Disposal of Oakland Outer Harbor and Richmond Inner Harbor Sediments, by M. J. Trawle
MP HL-86-1	May 1987	Report 3, San Francisco Bay - Alcatraz Disposal Site Erodibility, by A. M. Teeter
MP HL-86-5	Aug 1986	Puget Sound Generic Dredged Material Disposal Alternatives, by M. J. Trawle and B. H. Johnson
TR EL-88-15	Dec 1988	New Bedford Harbor Superfund Project, Report 2, Sediment and Contaminant Hydraulic Transport Investigations, by A. M. Teeter

STORM SURGE ANALYSIS AND DESIGN WATER LEVEL DETERMINATIONS

Department of the Army
U.S. Army Corps of Engineers
April 1986

EDITORS NOTE

This section of our re-print volume dealing with coastal engineering problems is based on the Corps of Engineers manual EM 1110-2-1412, issued in 1986.

Storm surges in coastal areas are induced by high tides combined with wind-generated waves to produce abnormally high water levels and potential flooding. An understanding of this natural phenomenon is essential in order to plan control measures or to design structures which will not be seriously affected by the flooding.

The text offers a number of methods for predicting the size and frequency of storm surges due to hurricanes and abnormally high tides using statistical methods from recorded experience. Some sample problems are presented which relate storm waves, rainfall, wind and tides to storm intensity predictions.

While this manual does not directly involve design procedure, it does provide basic information which may be useful for implementing design decisions.

CHAPTER 1
INTRODUCTION

1-1. Purpose. This manual provides guidance for storm surge analysis and design water level determinations in coastal areas.

1-2. Applicability. this manual applies to all HQUSACE/COE elements and field operating activities (FOA) engaged in civil works function.

1-3. References.

a. ER 1110-2-1453

b. Shore Protection Manual (SPM), 4th ed., Vols I and II, U.S. Army Engineer Waterways Experiment Station, Coastal Engineering Research Center. Available from Superintendent of Documents, U.S. Government Printing Office, Washington, D.C. 20402.

1-4. Bibliography. Bibliographic items are cited in the text by numbers (item 1, 2, etc.) that correspond to items in Appendix A. Where any reference or bibliographic item contains information that conflicts with this manual, the provisions of this manual shall govern.

1-5. Units and Datums. The English system of units is generally used throughout this manual; however, the equivalent metric units are supplied in some cases. Unless otherwise noted, elevations of the seabed, land topography and water level elevations are based on the National Geodetic Vertical Datum (NGVD) of 1929.

1-6. Overview of Manual.

a. Coastal engineering studies often require estimation of surges induced by tropical storms and other accompanying water level changes in coastal regions. Accurate prediction of these abnormal water level rises during storm periods is essential for proper planning and design of coastal works, assessing the elevation and extent of coastal flooding and developing evacuation plans. Basic principles and estimating procedures pertaining to storm surges and related effects are presented.

b. Flood potential due to tropical storms is greater for coastal regions along the Atlantic and Gulf Coasts of the United States and storm surge analyses for these areas are emphasized. However, the methods and procedures presented are generally applicable to the Pacific Coast, Hawaiian Islands and the Great Lakes.

c. This manual is general in nature and therefore requires that good engineering judgment be exercised when applying the methods and procedures presented herein to actual storm surge problems. Although a complete understanding of the underlying theoretical concepts is not essential to performing storm surge estimates, a basic understanding of hydrodynamic processes, wave mechanics, statistics and computational hydraulics is needed to ensure proper application.

d. Four chapters are included in this manual. Chapter 1 provides an introduction to water level variations in coastal waters, storms originating over ocean areas, storm surge generation and its effects in coastal areas, and the theory of water motions applicable to storm surge analysis. Chapter 2 presents two different approaches for estimating storm surge. One approach involves prediction of the abnormal water level rises based on an analysis of historical data; and the other approach involves calculating the rises based on numerical computational procedures. Statistical techniques are presented in chapter 3 to provide a means for estimating the magnitude and frequency of occurrence of abnormal water levels in coastal regions when using either of the prediction approaches. Finally, Chapter 4 presents methods and procedures for including particular storm and nonstorm related effects in estimating the design water level.

e. Seven appendixes are also included in this manual. Appendix A contains a list of the references cited: and Appendix B lists the mathematical symbols used and their corresponding definitions. The remaining appendices provide information with regard to special computational procedures, example problems and tables. Also a glossary is provided at the end of the manual for the purpose of defining various terms used herein.

1-7. Nature of Tropical Storms. Many dangerous and destructive tropical storms have occurred along the Atlantic and Gulf Coast areas of the United States in this century alone. Some were extremely severe, others less severe, but all were destructive. Of these storms, the great storm of September 1900 stands above all others because it took the lives of more than 6,000 people, mostly on Galveston Island. Had major steps not been taken since 1900 with respect to storm warnings and deployment of coastal flood protection systems it is obvious the death toll would have been substantially higher than has occurred as a result of subsequent severe storms. In addition to the loss of lives in the past few decades, tropical storms have also caused property damages that ran into the billions of dollars. It has been estimated that Hurricane Carla (1961) caused damages in excess of $400 million (based on 1961 price levels) and flooded more than 1.5 million acres of

land. In many coastal areas a severe storm may raise the water level in excess of 15 feet above the normal level on the open coast and even higher in estuaries and other inland areas. The elevated coastal waters, due to surges, provide a higher level in which short period surface waves can propagate, thus subjecting beaches and structures to wave forces not ordinarily experienced. Surges coupled with the action of wind generated surface waves are responsible for the greatest damage to coastal areas. They can destroy or severely damage dwellings, business establishments, commercial properties and docking facilities, erode beaches, displace stones or concrete armor units on jetties, groins or breakwaters, undermine structures via scouring, cut new inlets through barrier beaches and shoal navigational channels. The latter shoaling problem can result in hazards to navigation thus impeding vessel traffic and hampering harbor operations.

1-8. Water Level Variations. The term "water level" is used herein to indicate the mean elevation of the water surface when averaged over a sufficient period of time (about 1 to 2 minutes) to eliminate the clearly distinguishable short period surface waves. Water level variations in coastal zones are produced by a number of distinct causes. These are identified as:

a. Storm Surge. A rise or possible fall of the normal water level in coastal waters due to the interaction between a storm and the underlying water surface.

b. Wave Setup. Superelevation of the water surface above the normal water level due to onshore mass transport of water by wave action alone.

c. Astronomical Tides. An almost periodic rising and falling of the water that results from gravitational attraction of the moon, sun and other astronomical bodies acting on the rotating earth.

c. Secular Fluctuations. Long term trends in sea level due to such causes as melting of the polar ice caps, large scale isostatic adjustments of the earth's crust and local subsidence.

e. Tsunamis. A long-period wave caused by an earthquake or underwater disturbance such as a volcanic eruption or a landslide. The spectrum of tsunamis covers a range of periods from several minutes to an hour.

f. Climatological Effects. Seasonal or long-term changes in the water level which result from seasonal heating or cooling of the water column or from seasonal variations in the mean wind fields.

g. Seiches. A standing wave oscillation in enclosed and semi-enclosed water bodies that can continue after the cessation of the originating force. Seiches are long period waves that can be induced in bays and some ocean basins by changes in atmospheric pressure or by winds. These standing waves are analogous to the sloshing back and forth in a bathtub once the water is disturbed. Energy of this wave is dissipated primarily by friction or by radiation to an adjacent sea in the case of a bay.

Although the focus in this manual is storm surge, the design engineer will need to consider such effects as wave setup in nearshore regions, astronomical tides and possible secular fluctuations, climatological changes and seiches in combination with storm surge to determine the total water level at a project site. Tsunamis may be disregarded in the determination of total water level during the passage of a storm. Astronomical tides can have a pronounced effect on the total water level rise in some coastal areas coincident with storm surge. Tides are a well documented phenomenon and can be predicted with considerable accuracy at locations where observations are available for one year or more. Because tide prediction methods have been published by a number of investigators applicable to coastal waters of the United States

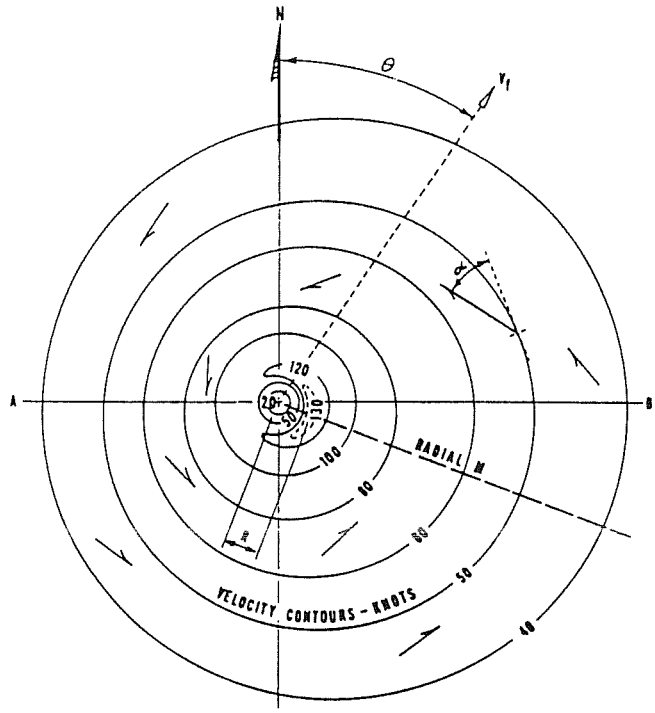

a. Wind isovel pattern and pertinent parameters

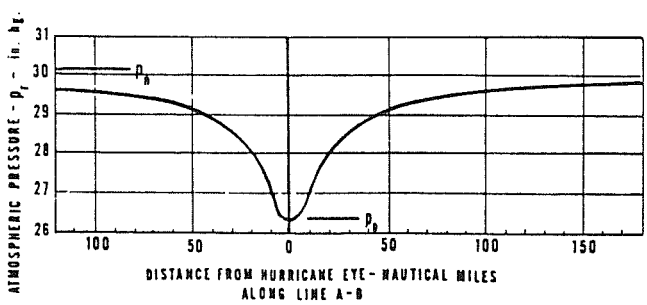

b. Pressure profile

FIGURE 1-1
Sketch showing hurricane parameters

(items 18, 24, 54, 59 of Appendix A) no attempt will be made for many coastal locations by the National Ocean Survey, National Oceanic and Atmospheric Administration (NOAA).

1-9. Storms.

a. A storm is an atmospheric disturbance characterized by one or more low pressure centers and high winds. These disturbances frequently are accompanied by precipitation of varying intensity. An important distinction is made in classifying storms: a storm originating in the tropics is called a "tropical storm;" a storm resulting from the interaction of a warm and a cold front is called an "extratropical storm". A severe tropical storm is referred to as a "hurricane" or "tropical cyclone" when the maximum sustained winds equal or exceed 75 miles per hour. Unlike extratropical storms and less severe tropical storms, hurricanes are well organized in respect to the wind patterns. The wind patterns of a hurricane are, more or less, circular with winds revolving counterclockwise (in the northern hemisphere) about the storm center or eye, not necessarily the geometric center. Winds in hurricanes blow spirally inward and not along a circle concentric with the storm

center. Wind isovel patterns and wind directions are illustrated as shown in Figure 1-1a. The eye is characterized as an area of low atmospheric pressure and light winds. Atmospheric pressure increases with distance from the eye to the periphery or outskirts of the hurricane. Highest wind speeds usually occur in the right quadrants of the hurricane at a distance varying from about 4 to 70 nautical miles from the center. However, in all directions outward from the eye of the hurricane, the wind speed increases rapidly to a maximum and then decreases with distance to the outskirts of the storm. The best single index for estimating the surge potential of a hurricane is the atmospheric pressure within the eye and if referred to as the "central pressure index" (CPI). In general, the lower the CPI, the higher the wind speeds. Other important parameters of a hurricane with regard to the surge potential are the "radius of maximum winds" (R) which is an index of the size of a storm, the speed of forward motion of a storm system (V_f) and the track direction (θ) in which a hurricane moves (measured clockwise from the north).

b. Pronounced water level changes due to tropical storms may occur anywhere along the gulf coast and anywhere from Cape Cod to the southern tip of Florida on the east coast of the United States. Occasionally the southern coast of California on the west coast experiences changes in water level as a result of tropical storms but these are usually small due to the narrow continental shelf in that region. Large changes in water level may occur along the northern part of the east coast of the United States as a result of extratropical storms in which strong winds blow in a north-easterly direction. These storms are commonly referred to as "Northeasters".

c. Northeasters are important from the standpoint of design considerations on the east coast. However, an acceptable technique for specifying the wind fields for design storms is not presently available. It is expected that such a technique will become available and be included in subsequent revisions of this manual.

d. In engineering studies hypothetical hurricanes are frequently used to assess the levels of flooding for a predetermined degree of severity. These storms are derived based on the specification of meteorological parameters R, V_f, P_o, P_n, θ, and α in which P_o is the central pressure, P_n is the peripheral pressure and α is the inflow angle (see Figure 1-1b). It has been the general practice to use invariant meteorological parameters for any given hypothetical hurricane prior to the storm making landfall. Thus such storms are classified as steady state hurricanes. Particular hypothetical hurricanes which have been used in some engineering investigations are referred to as the Standard Project Hurricane (SPH) and Probable Maximum Hurricane (PMH). The SPH is defined as a hurricane having a severe combination of values of meteorological parameters that will give high sustained wind speeds reasonable characteristic of a specified coastal location. A PMH, on the other hand, is defined as a hurricane having a combination of values of meteorological parameters that will give the highest sustained wind speed that can probably occur at a specified coastal location. Recurrence intervals for the SPH and PMH are not assigned due to the uncertainties involved in establishing their frequencies. The SPH is frequently used in the design of coastal works where a high degree of protection is required while the PMH is generally used solely in connection with the design of nuclear power generation plants sited in coastal areas.

e. Hypothetical hurricanes with more frequent recurrence intervals than the SPH may also be used to estimate the frequency and levels of flooding. The flood frequencies are established by calculating the water levels resulting from a rather large number of different hypothetical hurricanes and assessing the recurrence intervals by application of the joint probability method. Methodology is presented in Chapter 3 for determining flood frequencies.

1-10. Storm Surge Generation Processes. In shallow seas there are at least five distinct processes during passage of a storm which alter the water levels in the coastal zone (item 23 of Appendix A).

These processes are identified as:

a. direct wind effect
b. atmospheric pressure effect
c. effect of Earth's rotation
d. rainfall effect
e. wave setup effect

(1) Direct Wind Effect. The largest incremental change in water level, considering all contributing processes in storm surge generation, is attributed to the direct effects of wind. A wind blowing over the water surface exerts a horizontal force on the surface water and in shallow water induces a current in the general direction of the wind. The force exerted on the water by the wind is partly due to inequalities of air pressures on the upwind and downwind side of gravity waves and partly due to shearing stresses at the water surface. It is usually presumed that the wind stress is proportional to the square of the wind speed in which the coefficient of proportionality is usually assumed as a constant or assumed to vary with the wind speed. Variation of the coefficient is usually justified on the basis that the sea surface becomes increasingly rough with increasing wind speeds (see item 19 of Appendix A).

(2) Atmospheric Pressure Effect. Atmospheric pressure may vary significantly over the ocean during periods of severe tropical storms. Water levels rise in regions of low pressure and fall in regions of high pressure. Calculations of storm surge in the coastal zone have shown that atmospheric pressure differences can contribute as much as 2 to 3 feet to the peak surge.

(3) Earth's Rotation Effect. Due to the Earth's rotation a deflecting force, referred to as the Coriolis force, is produced which acts to the right of any current (at right angles to the velocity vector) in the Northern Hemisphere. The Coriolis force is purely a deflecting force and it cannot by itself change the speed of the water but only its direction. If the coast is to the right of the current, then this leads to an increase in the sea level at the coast and conversely a decrease in sea level if the coast is to the left of the current.

(4) Rainfall Effect. Observations from past storms reveal that large quantities of rainfall may occur when hurricanes move over the continental shelf and cross coastal areas. After landfall of a hurricane, a storm system or remnant hurricane may also dump large amounts of rainfall as it moves many miles inland. In general, rain falling on the open sea has minimal effect on the surge produced on the open coast due to the areal extent of the sea and mechanisms involved in establishing the gradient over the shelf. However, in bays, estuaries and in areas of low-rising water levels, rainfall can contributed significantly to the total rise. Also, the flood levels in these areas may be augmented as a result of rainfall runoff from adjacent land areas. An additional effect of rainfall on storm surge generation is caused by windblown raindrops striking the water surface. These wind-propelled raindrops exert a horizontal force on the water surface in the general direction of the wind due to their angle of entry at the air-sea interface.

(5) Wave Setup Effect. The sea level in nearshore regions may be increased due to the action of surfaced waves in the surf zone. When waves break offshore on a line more or less parallel to the beach, a significant quantity of water is transported shoreward causing a runup on the beach face. Water moved shoreward due to waves breaking cannot return

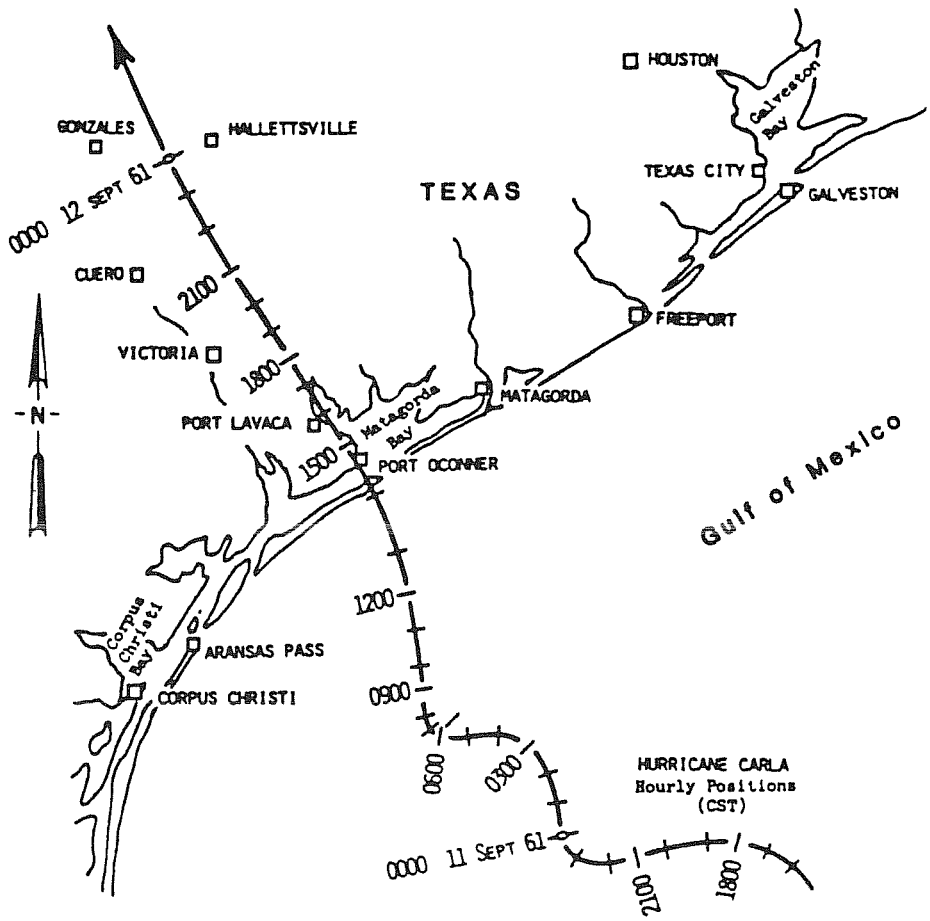

FIGURE 1-2
Hurricane Carla track, hourly positions, September 1961. (based on item 31 of Appendix A)

offshore as rapidly or effortlessly as it was brought shoreward. As a consequence of these differences in transport rates, water is piled up at the beach. A gradient is thus established which extends from where the waves break to the shore. This piling up of water near the shore is referred to as "wave setup".

1-11. Storm Surge on the Open Coast.

a. A tropical storm originates over the ocean and as the storm grows in size and intensifies a considerable amount of energy is transferred from the atmosphere to the water. In deep ocean areas most of the energy imparted to the water results primarily in the generation of surface waves, but when the storm moves into the shallower waters over the continental shelf a current is induced in the general direction of the wind. When wind blows shoreward, water is transported in the upper layers of the sea surface over the continental shelf to the coast, and water is returned seaward along the bottom layers above the seabed. Water returning seaward under the influence of gravity is slower and impeded by bottom friction, resulting in a gradient extending from the general vicinity of the edge of the continental shelf to the shoreline. At a state of equilibrium the gradient remains constant and thus the water brought shoreward is equal to the water returned seaward. The highest water level produced by a storm at any coastal location in the absence of astronomical tide effect is referred to as the "maximum surge" while the highest water level produced during the course of the storm is referred to as the "peak surge". For hurricanes moving on a path, more or less, perpendicular to a coast with offshore contours approximately parallel to the coast, the peak surge will normally occur at or near the point where the region of maximum winds intersects the shoreline--a distance approximately equal to R or the radius measured from the storm center to the region of maximum winds to the right of the storm center.

b. Abnormal water levels produced by storms on the open coast can persist over a period of several days and affect the water levels over hundreds of miles of coastline. These effects are demonstrated for Hurricane Carla (1961). The track of this severe tropical cyclone is shown in Figure 1-2 together with the hourly positions of the storm center. Figure 1-3a shows the duration in which water levels were affected on the open coast at Galveston, Texas, approximately 115 miles to the right of the storm track at the time of landfall. The total water level as depicted in Figure 1-3b shows only the storm surge which was obtained by subtracting the predicted tide from the total water level. Figure 1-4 shows the high water marks and extent of flooding based on a post-storm survey for Hurricane Carla.

1-12. Modification of Storm Surge. A disturbance on the continental shelf due to the passage of a storm will propagate into any estuary or bay on the coastline in a manner generally analogous to an astronomical tide. The amount of water transported from sea to estuary depends on the size of the opening (i.e., through the inlets or by overtopping low-lying land masses or barrier islands), difference in heads between the two water bodies and duration of the disturbance. The wind field over the embayment is primarily responsible for tilting the water surface across the estuary. Winds blowing inland will allow more water to enter the estuary and pile up water at the head of the estuary, while winds blowing seaward will

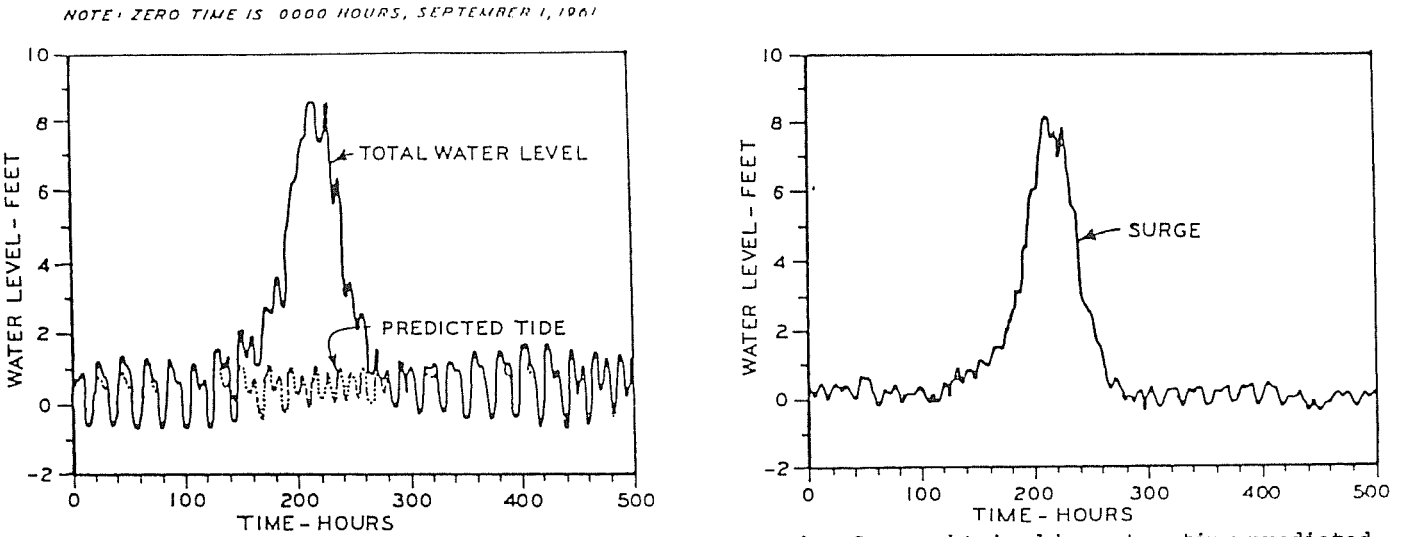

a. Observed total water level and predicted tide

b. Surge obtained by extracting predicted tide from total water level

FIGURE 1-3
Water level variations during Hurricane Carla (1961) at Pleasure Pier, Galveston, Texas.

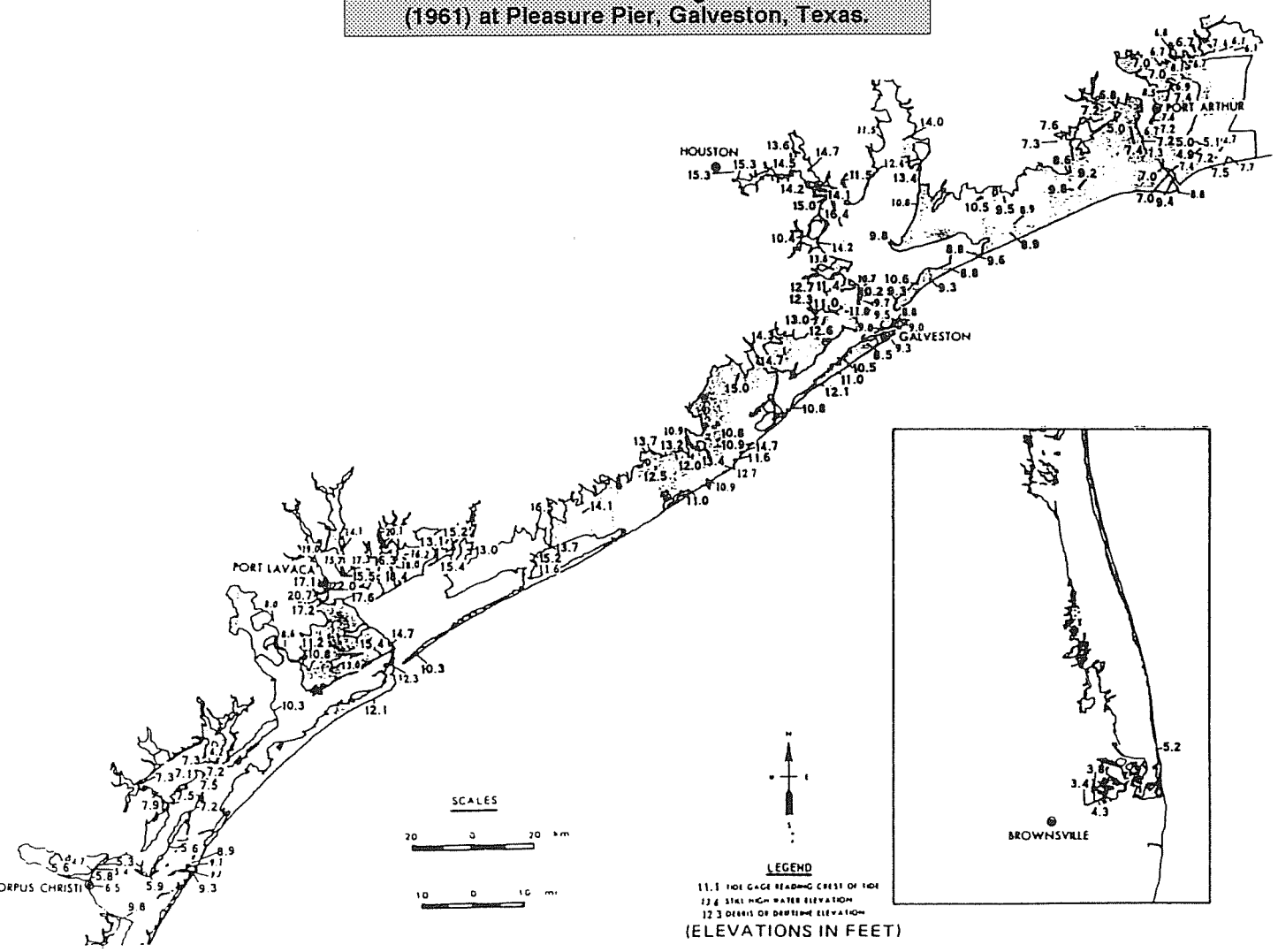

FIGURE 1-4
High water mark chart for Texas, Hurricane Carla 7-12 September 1961. (Shaded area indicates the extent of flooding.) (item 23 of Appendix A)

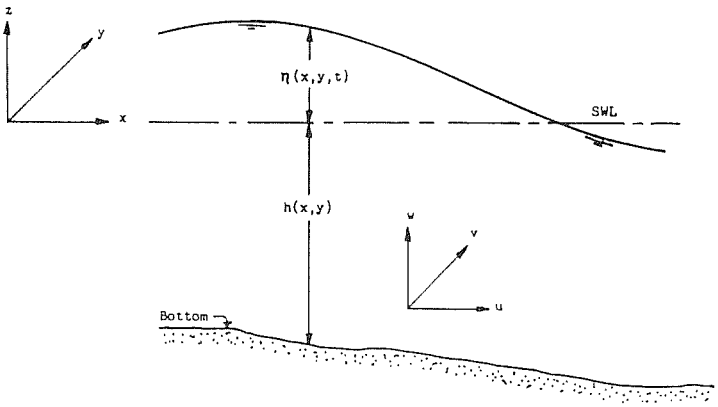

FIGURE 1-5
Reference frame

either restrict the flow of water from sea to estuary or transport water from estuary to sea depending on the slope of the water surface across the opening. In shallow estuaries, it is possible that the upwind side of the estuary will completely dry-up during a certain phase of the storm while piling water up at the downwind shore. The location of highest water levels in estuaries is usually constantly changing during the passage of a hurricane due to the circular wind patterns and storm motion. The rate and degree of change in water level depend on the track that the hurricane takes upon passing the embayment. Surge levels in estuaries can be considerably higher than those on the open coast when wind drives the water into a converging section of the estuary. Convergent sections are predominantly at those locations where streams empty into the estuary. In general, the increase in water surface elevation at any location in an estuary depends on the amount of water transferred from the sea, basin geometry, wind speed and direction, length of wind fetch, rainfall, rainfall runoff and possible water transported into the system by rivers. Surge levels are further modified when high water on the open coast or in estuaries flood onto adjacent low-lying land areas. At some locations the surge can cause water to move inland for considerable distances due to the flat coastal terrain. Vegetation and other obstacles in these areas cause extensive energy dissipation via turbulence and bottom friction; however, some energy is pumped back into the system by the wind.

1-13. Theoretical Considerations. The fundamental equations which describe water motions associated with storm surges, tides and other shallow water wave phenomena are presented in order to emphasize the underlying physical concepts and hydrodynamic processes involved. Also, these equations provide reference to the basic framework upon which mathematical models, as discussed in the following chapter, are formulated. The basic shallow water equations may be expressed in one, two, or three dimensions depending on the number of velocity components considered. Figure 1-5 shows the velocity components u, v and w for the x-, y- and z-directions, respectively. Computations performed with three-dimensional equations are exceptionally complex and, because the vertical velocity w is small compared to the horizontal velocities, it is usually justified to use two-dimensional equations. Further simplifications can be obtained by taking the equations in one horizontal dimension--a common practice prior to the introduction of high speed computers. However, one-dimensional equations can only provide limited information with regard to the water motions. For storm surge analysis it is, therefore, recommended that two-dimensional equations be used for calculating the water motions. In the presentation that follows, the three-dimensional expressions are given first and these are reduced to the two-dimensional expressions in order to demonstrate the approximations involved in the transformation.

a. Basic Equations. In theoretical studies of shallow water waves it is convenient to derive the "equations of motion" and the "equation of continuity" based on principles of conservation of momentum (Newton's second law) and the conservation of mass in terms of a column of fluid extending from the free surface to the sea bed. In embayments and shallow sea areas the flow is nearly horizontal and, thus, the vertical accelerations are negligible (ignoring short period surface waves and flow around obstacles). Additionally, it is usually assumed the water is of uniform density. Referring to the definitions in Figure 1-5, the three dimensional hydrodynamic equations (referred to as the Navier-Stokes equations) in the x-, y- and z- directions consistent with the previously stated assumptions are as follows:

$$\frac{\partial u}{\partial t} + u\frac{\partial u}{\partial x} + v\frac{\partial u}{\partial y} + w\frac{\partial u}{\partial z} - fv + \frac{1}{\rho}\left(\frac{\partial p}{\partial x} - \frac{\partial \tau_{xx}}{\partial x} - \frac{\partial \tau_{xy}}{\partial y} - \frac{\partial \tau_{xz}}{\partial z}\right) = 0 \quad [1\text{-}1]$$

$$\frac{\partial v}{\partial t} + u\frac{\partial v}{\partial x} + v\frac{\partial v}{\partial y} + w\frac{\partial v}{\partial z} + fu + \frac{1}{\rho}\left(\frac{\partial p}{\partial x} - \frac{\partial \tau_{xy}}{\partial x} - \frac{\partial \tau_{yy}}{\partial z} - \frac{\partial \tau_{yz}}{\partial z}\right) = 0 \quad [1\text{-}2]$$

$$\frac{\partial p}{\partial z} + \rho g = 0 \quad [1\text{-}3]$$

$$\frac{\partial u}{\partial x} + \frac{\partial v}{\partial y} + \frac{\partial w}{\partial z} \quad [1\text{-}4]$$

in which u, v, w are the velocity components in the x-, y- and z-directions, respectively; p is the pressure; t is time; g is the acceleration of gravity; f is the Coriolis parameter ($f = 2\omega \sin\phi$) is the angular velocity of the earth ($\omega = 2\pi/24$ radians/hour); ϕ is the geographical latitude; ρ is the water density; and τ_{xx}, τ_{xy}, etc., are the turbulent shear stresses. Equations [1-1] through [1-4] describe water motions in the vertical direction and two horizontal directions in which the first two relations are the equations of motion and the third relation is the hydrostatic pressure law derived from a simplification of vertical motions in accordance to the above stated assumptions. Equation [1-4] is an expression for the conservation of mass and is commonly referred to as the continuity equation. A more tractable form of these equations can be obtained by using particular transformation, boundary conditions and depth averaging. Equation [1-3] can be readily integrated to give the hydrostatic pressure distribution, hence

$$p - p_a = \rho g (\eta - z) \quad [1\text{-}5]$$

in which p_a is the atmospheric pressure (usually for simplicity assumed to be zero) and η is the elevation of the water surface above the mean water level. Equation [1-5] may be substituted into Equations [1-1] and [1-2] for defining p. Applying boundary conditions at the bottom z = h(x,y) and at the free surface $z = \eta(x,y,t)$, neglecting variations of u and v with z and integrating Equations [1-1], [1-2] and [1-4] over the total water depth, it is possible to write the hydrodynamic equations in two horizontal dimensions in the following form:

$$\frac{\partial u}{\partial t} + u\frac{\partial u}{\partial x} + v\frac{\partial u}{\partial y} = fv - g\frac{\partial}{\partial x}(\eta - \xi - \zeta) + \frac{1}{\rho D}(\tau_{sx} - \tau_{bx}) + \frac{W_x P}{D} + \epsilon_{xx}\frac{\partial^2 u}{\partial x^2} + \epsilon_{xy}\frac{\partial^2 u}{\partial y^2} \quad [1\text{-}6]$$

$$\frac{\partial v}{\partial t} + u\frac{\partial v}{\partial x} + v\frac{\partial v}{\partial y} = -fu - g\frac{\partial}{\partial y}(\eta - \xi - \zeta) + \frac{1}{\rho D}(\tau_{sy} - \tau_{by}) + \frac{W_y P}{D} + \epsilon_{yx}\frac{\partial^2 v}{\partial x^2} + \epsilon_{yy}\frac{\partial^2 v}{\partial y^2} \quad [1\text{-}7]$$

$$\frac{\partial \eta}{\partial t} + \frac{\partial (uD)}{\partial x} + \frac{\partial (vD)}{\partial y} = R \quad [1\text{-}8]$$

in which u, v are the depth-averaged velocities in the x, y directions; ξ is the atmospheric pressure deficit (see Appendix D), expressed as an equivalent head of water, ζ is the astronomical tide potential expressed as an equivalent head of water; W_x and W_y are the x, y- components, respectively, of the wind velocity taken at approximately 30 feet above the water surface; D is the total water depth ($D = \eta + h$); R is the rate at which water is either added to or lost from the system (i.e., as a result of precipitation, evaporation, etc.) expressed in depth per unit time; τ_{sc}, τ_{sy} are the s, y components of the surface shear stress due to the interaction between wind and water; τ_{bx}, τ_{by} are x, y components of bottom shear stress; ϵ_{xx}, ϵ_{xy}, etc. are the eddy viscosity coefficients, and P is the precipitation rate (depth/time). Generally, the wind shear stress components divided by the water density are taken in the form

$$\tau_{sx} = kW^2 \cos\theta$$
$$\tau_{sy} = kW^2 \sin\theta \qquad [1\text{-}9]$$

in which W = wind speed; θ = the angle between the velocity vector and the x-axis; and k is a nondimensional windstress coefficient (usually taken to be constant or presumed to be a function of the wind speed). In terms of the surface drag coefficient c_d (e.g., item 16), $k = D_c \rho_a/\rho$ where ρ_a, ρ are mass density of air and water respectively. The bottom shear stress components divided by the water density are normally taken as

$$\tau_{bx} = K u (u^2 + v^2)^{1/2}$$
$$\tau_{by} = K v (u^2 + v^2)^{1/2} \qquad [1\text{-}10]$$

in which K is a bottom shear stress coefficient usually expressed in accordance to either Manning's, Darcy-Weisbach's or Chezy's resistance law. Although the previous relations were written in terms of the depth integrated velocities, these relations may also be readily expressed in terms of the vertically integrated transport per unit width--a form of the equations preferred by a number of investigators. In this case the equations of motion and continuity become

$$\frac{\partial U}{\partial t} + \frac{U}{D}\frac{\partial U}{\partial x} + \frac{V}{D}\frac{\partial U}{\partial y} = fV - gD\frac{\partial}{\partial x}(\eta - \xi - \zeta) + \frac{1}{\rho}(\tau_{sx} - \tau_{bx}) + W_x P + \epsilon_{xx}\frac{\partial^2 U}{\partial x^2} + \epsilon_{xy}\frac{\partial^2 U}{\partial y^2} \qquad [1\text{-}11]$$

$$\frac{\partial V}{\partial t}) + \frac{U}{D}\frac{\partial V}{\partial x} + \frac{V}{D}\frac{\partial V}{\partial y} = -fU - gD\frac{\partial}{\partial y}(\eta - \xi - \zeta) + \frac{1}{\rho}(\tau_{sy} - T_{by}) + W_y P + \epsilon_{xy}\frac{\partial^2 V}{\partial x^2} + \epsilon_{yy}\frac{\partial^2 V}{\partial y^2} \qquad [1\text{-}12]$$

$$\frac{\partial \eta}{\partial t} + \frac{\partial U}{\partial x} + \frac{\partial V}{\partial y} = R \qquad [1\text{-}13]$$

in which U and V are the x and y components, respectively, of the volume transport per unit width. For this form of the equations, the wind shear stress components as given by Equation [1-19] are unchanged; however, the bottom shear stress components divided by the water density are given by:

$$\tau_{bx} = KU (U^2 + V^2)^{1/2} D^{-2}$$
$$\tau_{by} = KV (U^2 + V^2)^{1/2} D^{-2} \qquad [1\text{-}14]$$

b. Possible Alternate Forms of Basic Equations. The equations for motion and continuity given provide essentially a complete description of water motions associated with storm surges coupled with astronomical tides. There are a number of variations in which the basic equations may be expressed. Some of these variations are due to certain transformations made while others are due to simplifying the governing equations by neglecting the less important hydrodynamic processes. In conducting storm surge analysis it is sometimes possible to simplify the equations of motion while retaining sufficient accuracy of the estimates. Such simplifications can in some instances result in a substantial reduction in computational effort. For many problems it is possible to neglect the convective terms (i.e., the second and third terms on the left hand side of Equations [1-6] and [1-7] or Equations [1-11] and [1-12] due to their small contribution to the total processes involved. Omission of these terms make it impossible to compute circulation currents and horizontal eddies; however, such phenomena are not generally important in storm surge analysis since interest is primarily centered on the water level variations. In most cases, it is possible to neglect the eddy viscosity terms (i.e., the last two terms on the right hand side of Equation [1-6] and [1-7] or Equation [1-11] and [1-12] if the problem simulation time is only for a few days. These terms provide a mechanism whereby energy piling up at the smallest possible scale can be removed from the system as time elapses from the initial state. The energy buildup is gradual and the terms can become important if the simulation period is carried out over a period of several days. In the event that it is possible to neglect both the convective and eddy viscosity terms, it can be usually expected that the computational effort will be reduced by as much as 25 percent. The precipitation terms in the equations of motion are also frequently neglected in storm surge calculations because of their small contributions and the fact that in most instances there is insufficient knowledge to prescribe the precipitation over the system, particularly in open water areas. It is also possible to neglect the Coriolis terms when calculating the water motions in small coastal estuaries, but these terms should always be used when calculating storm surge on the open coast since their contributions can significantly affect the resulting water levels. Due to difficulties in specifying the proper forcing for astronomical tides, particularly in the open ocean, the tide potential is usually neglected in the basic relations and accounted for separately as a component that is added algebraically to the storm surge.

CHAPTER 2
APPROACH

2-1. General.

a. Two methods that are commonly used to estimate the frequency and levels of flooding in coastal waters are identified herein as the Historical Data approach and the Theoretical Approach. Each approach has certain advantages and disadvantages; however, the former approach generally has limited usage due to inadequacy of observed data while the latter is applicable to most problems. The historical data approach involves predicting the frequency and levels of flooding based on an analysis of past flood events, while the theoretical approach involves predicting the frequency and levels of flooding based on an analysis of past flood events, while the theoretical approach involves calculating the flood levels for numerous representative storms and the subsequent application of statistical procedures to determine the frequency of flooding. Statistical techniques for both approaches are presented in Chapter 3. In the use of the theoretical approach, a number of mathematical or numerical models have been developed for simulating the storm-induced water motions. Computer programs are used in conjunction with the models to perform the necessary calculations. The models, as generally discussed in this chapter, are formulated based on the governing hydrodynamic equations that were presented in Chapter 1.

b. In all future storm surge studies concerned with the design of coastal structures, it is required that the surge resulting from an SPH be evaluated except in the special case that the design is to be based on the PMH. The theoretical approach, of course, must be used for estimating both the SPH and PMH.

2-2. Historical Data Approach.

a. An accumulation of water level data from past storms over a span of many years at a given location may provide sufficient information for predicting design water level at that location. Rather long-period records of water level data are required to confidently predict the frequency and magnitude of flood levels by the historical data approach since the underlying assumption for this method is that past events are representative of future events. Obviously, there is no assurance that the assumption is completely satisfied; however, the longer the record, the more confidence one can have in the validity of the assumption.

b. Water level data recorded during storm periods may be obtained from a variety of sources. The principal source of recorded data is tide records of the National Ocean Survey (NOS). Other sources of recorded data are gages operated by the Corps of Engineers, U.S. Geological Survey and a few other organizations. High water marks also provide a means for obtaining maximum water levels; however they are inherently less reliable than measurements obtained from recording gages. Many sources are also available for obtaining high water marks such as those obtained by various government agencies, newspaper accounts, and private organizations. A principal source of high water marks is post storm reports prepared by U.S. Army Corps of Engineers District Offices. Maximum water levels from high water marks are usually established from such effects as debris accumulation and mudline discoloration. In open areas these marks generally reflect both the water level rise and the maximum amplitude of short period surface waves and possible wave runup. These are no reliable techniques establishing the true water level rise when surface wave effects are involved. The most preferable high water marks are those in which surface waves are filtered out, such as those obtained within buildings and other sheltered sites or from pipe gages designed specifically for recording the maximum water level.

c. Unfortunately, water level data are seldom available at the site for which the data are needed in connection with engineering studies. In the event there are sufficient and reliable water level data in the vicinity of the site, it may be possible to estimate the site data based on an adjustment to the existing data at nearby locations. Considerable care must be exercised in transposing the adjusted observed data to a nearby site since large discrepancies may result. Consideration must be given to the differences in flow processes and differences in physical characteristics (coastline shape, bathymetry, etc.) between the site under consideration and the sites of the known water level data. It will be necessary to extract the predicted astronomical tide from the observed water levels to obtain the surge component prior to transposing the data. Care has to be exercised in making such extractions since time of occurrence is unknown or difficult to assess. Also, it is necessary to predict the astronomical tide at the site under study so that an estimate can be made with regard to the total design water level. Because NOS is responsible for making tide predictions in the coastal zone, their services should be utilized in estimating the probably tidal oscillations at the project site. This information, coupled with rational engineering judgment with regard to storm surge behavior, can in some instances, provide sufficient basis for estimating the possible maximum storm surges at coastal locations other than at the gage locations. Transposition of adjusted historical data to other locations is generally applicable only to open coast sites rather than estuaries and other inland flooding areas. Transposing water level information inland of the open coast is not recommended due to the complex behavior of the water motions as a result of irregular basin geometry and uncertainties with regard to the effects of storm translation.

d. In application of the historical data approach it may be necessary to consider variations in mean sea level. A close examination of long-term tidal records reveals that the mean level of the sea is continually changing. This variation becomes apparent when comparing mean levels on a yearly basis at a given tidal station. In a study (item 23 of Appendix A) of monthly sea level at selected NOS tide stations for the East and Gulf Coast of the United States for the years 1919 to 1961, it was found there was as trend toward rising sea levels. In a more recent investigation, as discussed in item 24 of Appendix A, it was found that the trend for rising sea levels continues to evolve along these coasts. Variations in the annual cycle are believed to be predominately meteorological in origin and thus difficult to predict. Thus, correction of the gage records may be sometimes warranted to account for variations in the seasonal cycle and the secular trends in sea level.

e. The historical data approach has advantages over mathematical model simulation techniques from the standpoint that a study will usually require substantially less effort and cost. There are also disadvantages in using the historical data approach. These are identified as:

(1) Inadequate sample size.

(2) Uncertainties with regard to accuracy of data.

(3) Uncertainties with regard to data transposition.

(4) Inadequate spread of available data for the area in which interest is centered.

(5) Uncertainty if data sample is representative of the parent population.

(6) Provides no information with regard to the hydrodynamics.

(7) Generally inapplicable to coastal estuaries and low-lying land areas subject to flooding.

f. In summary, the decision whether to use or not to use the historical data approach will require careful consideration of the available data and the study site to be investigated.

2-3. Theoretical Approach. Solution schemes developed specifically for solving the governing partial differential equations for storm surge (i.e., Equations [1-6], [1-7] and [1-8] or Equations [1-11], [1-12] and [1-13] as presented in Chapter 1), including simplications made thereto, are referred to as mathematical models. Models of this sort are either analytical, if direct integration of the basic equations are involved or numerical, if the derivatives are approximated by finite differences. Due to inherent mathematical difficulties, the basic equations cannot be directly integrated unless many simplifications are introduced. As a consequence analytical models may only be applied to problems for very restrictive and simplified conditions, and thus solutions obtained are generally not acceptable in the resolution of practical problems. Although numerical integration procedures result in an approximate technique for integrating the basic differential equations, these procedures can produce reasonably accurate solutions in the simulation of water motions

2-4. Numerical Methods.

a. Most previous studies of transient storm surges in shallow seas and estuaries have used computational schemes based on a variety of finite difference methods. These schemes

are formulated by replacing the basic partial differential equations with an equivalent set of difference equations in which the latter equations are solved in finite increments of space Δx, Δy and finite increments of time Δt. This simply implies that algebraic equations are used to approximate the basic differential equations.

b. Finite difference methods may be classified as either explicit or implicit depending on the particular solution technique employed. Explicit methods consist of solving relatively simple algebraic expressions but suffer from the disadvantage of restricted numerical stability of the calculations. Numerical instability results in oscillations of the flow and elevations of the water surface which grow with time, resulting in invalid calculations. Implicit schemes, on the other hand, are unconditionally stable from a numerical point of view; however, this condition is obtained at the expense of algebraic complexity.

c. To insure numerical stability for an explicit scheme it is necessary to restrict how fast the solution is advanced in time--thus, the time step Δt must be restricted. An explicit scheme generally requires that

$$\Delta t \leq \frac{\Delta x \cdot \Delta y}{(\Delta x^2 + \Delta y^2)^{1/2} [(u^2 + v^2)^{1/2} + (gD)^{1/2}]_{max}} \quad [2\text{-}1]$$

in which Δx and Δy are constant over the entire grid and the subscript max signified that the value of the terms enclosed by the parenthesis is the maximum value expected anywhere in the system. For most problems the particle velocities u and v may be neglected because they are generally quite small in comparison to the shallow water wave speed $(gD)^{1/2}$. In the case that Δx and Δy are taken to be equivalent and the particle velocities are neglected, the numerical stability criterion reduces to

$$\Delta t \leq \frac{\Delta x}{(2gD_{max})^{1/2}} \quad [2\text{-}2]$$

in which D_{max} is the maximum depth anywhere in the system. The numerical stability criterion, as given by Equation [2-1], is called a "Courant-Friedrichs-Lewy condition". Although implicit schemes are unconditionally stable, the time step needs to be restricted from the standpoint of accuracy of the calculations. Generally, it is possible to advance the calculations about five times faster with the implicit scheme than with the explicit scheme. However, experience has shown that the solution can be advanced considerably faster with implicit schemes provided that the shallow water wave steepness is not too great.

c. Selection of either an explicit scheme or implicit scheme for application in storm surge analysis is left to the user's choice. Generally, the most suitable model for application is the one best understood by the user. It should be remarked, however, that any investigation requiring numerous simulations for a given coastal location can usually be performed more economically with a well formulated implicit scheme.

2-5. Grid Scheme Layout. In the application of finite difference storm surge models, representation of the modeled area is accomplished by superimposing a grid over a map of the study area in which the seaward and landward boundaries are usually taken approximately parallel with the shoreline along the open coast. As seen from the sea looking landward, the origin of the Cartesian coordinate is normally taken at the left-hand corner of the grid system. The positive x-axis is taken to the right in the along-shore direction and the positive y-axis in the landward direction. Various mesh configurations may be used for representing the elements or cells within the modeled area. Configurations that have been commonly used

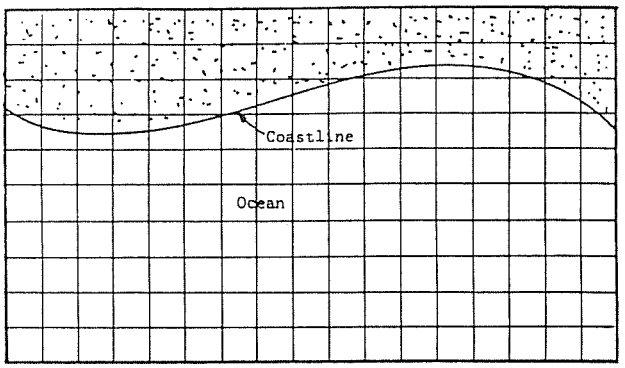

a. Grid layout of a coastal area.

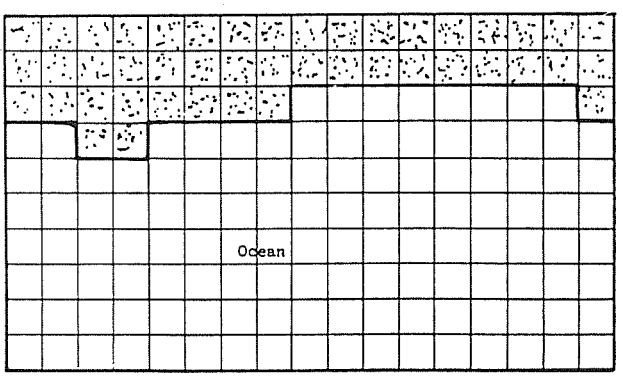

b. Model representation of coastline given in "a" above.

FIGURE 2-1
Schematic showing a coastal area using a grid with square mesh for actual and modeled systems.

are either constant rectangular, variable rectangular, orthogonal curvilinear, or unconstrained curvilinear. A constant rectangular mesh in which the spatial steps Δx and Δy are taken to be equal (i.e., a square mesh) over the entire grid is the simplest configuration (see Figure 2-1). A variable rectangular mesh (see Figure 2-2) makes allowance for varying both Δx and Δy in the representative x- and y- directions--a method suitable for obtaining higher resolution in those areas where interest is principally centered. In the use of both square and rectangular meshes, irregular coastlines are represented in a "stair step" fashion with possible convex and concave corners along the shoreline as shown in Figure 2-1. A curvilinear mesh, on the other hand, permits representing the coastline in a more realistic fashion as shown in Figure 2-3 for the physical plane. Also shown in the latter Figure is the transformed plane in which the physical plane grid is reduced to a grid with square mesh. The orthogonal curvilinear mesh uses the coast as the principal axis and normals to the coast offshore depth contours as the second principal axis in the physical plane. In the use of unconstrained curvilinear mesh the coast is also used as the principle axis; however, orthogonality of the mesh offshore is not required which results in a skewed Cartesian mesh resembling a mesh of parallelograms. The choice of a particular mesh for application to a certain study area depends on the physical characteristics of the system, the location in which interest is centered and the magnitude of the error that can be tolerated by using a simpler mesh. The simplest mesh, of course, is the square--both from the standpoint of effort and costs in performing the computations.

2-6. Numerical Representation of Prototype.

a. Implementation of the mathematical model to a study area is somewhat like that of the physical model. The

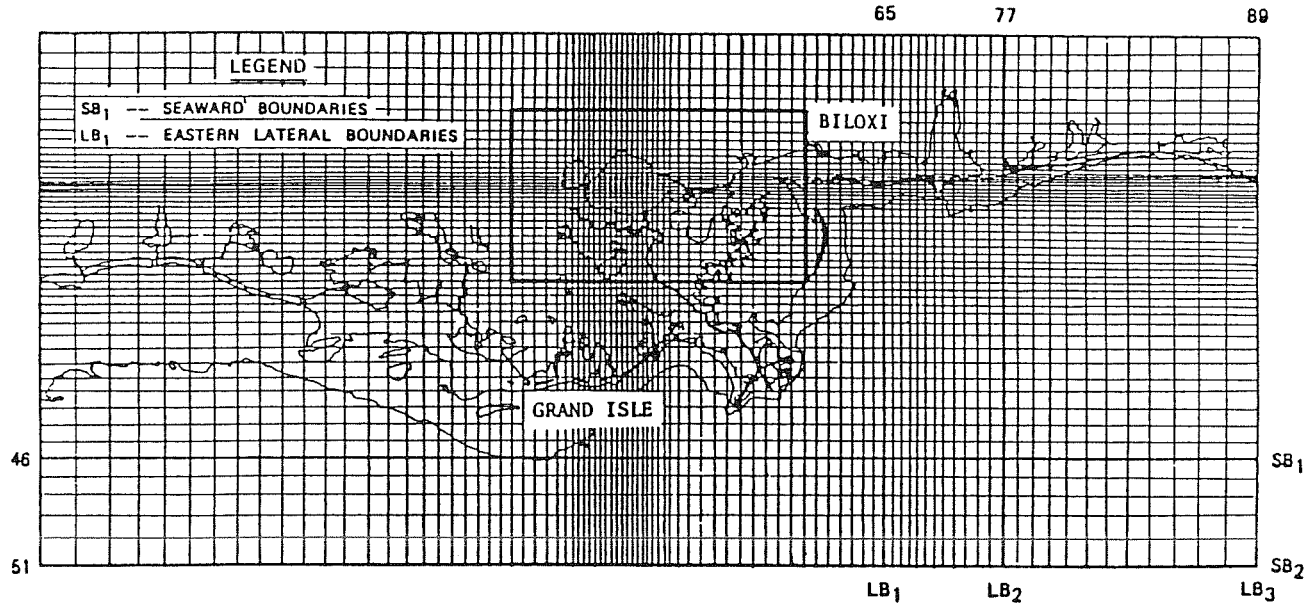

FIGURE 2-2
Computational grid for hurricane surge simulation in the vicinity of Lake Ponchartrain, LA (item 11 of Appendix A)

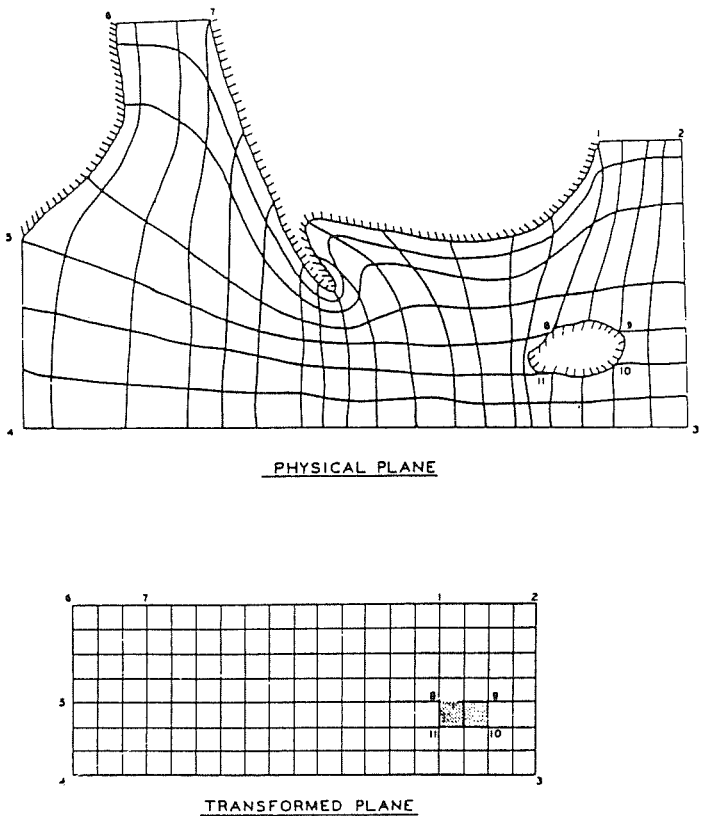

FIGURE 2-3
Example of coordinates generated in a field containing a jetty and an island. (item 61 of Appendix A)

mathematical model must be molded into a replica of the prototype, not with concrete or other materials but by numbers which represent the hydrography, topography and other physical features of the system. Unlike physical models, there is no need to distort the length scales in mathematical models since it is possible to use lengths that are identical to the prototype. It is, however, necessary to specify the elevations of the seabed and land at only discrete points within the system resulting in an approximation of the actual physical geometry.

b. Depths are usually specified at the mesh points or taken as an average over a cell as delineated by the mesh. Clearly, a smaller mesh size will result in a better description of the geometry for a given study area. However, decreasing the mesh size to better describe the physical system results in an increasing cost and effort in preparing the basic data and performing the computations.

c. Some available mathematical models have the capability of treating subgrid scale features such as narrow barriers and channels. The term subgrid scale feature implies that a barrier or channel is narrow compared to the mesh size. In the case of narrow barriers, allowance can be made for the barrier to block the flow or be overtopped depending on the stage on both sides of the barrier. Flow in a narrow channel may be computed from equations formulated in one horizontal dimension with provisions made for the channel to communicate with adjacent cells where two-dimensional flow is involved. These subgrid features are frequently important in treating estuarine problems.

2-7. Boundary Conditions.

a. The solution of the shallow water wave equations involves a boundary value problem which implies that any dependent variable specified on the boundary must be prescribed at every time level prior to advancing the solution. A variety of boundary conditions may be used in performing storm surge calculations. These conditions are required at the fixed boundaries which delineate the system, at moving boundaries and at boundaries prescribed internal to the system. For these boundaries it is necessary to specify either the velocities, flow rates or water levels.

b. Fixed boundaries at the limit of the system may either be open, if water is transported across the boundary, or closed if a water-land boundary exists. In the case of an open boundary it is usually necessary to estimate the flow or water level based on a knowledge of the water motions at a previous time step or based on known information. For a closed

boundary, the conditions are usually related to the normal component of flow at the boundary which simply implies that $u = 0$ or $v = 0$ at the water-land boundary.

c. Because low-lying terrain may alternately flood and dry up during the passage of a storm, provisions may be made for flooding of dry cells during rising stages and drying of the cells as the flood waters recede. Provisions for the moving boundary requires special checks to be made with regard to the elevation of the water surface at the junction of a flooded cell and an adjacent dry cell. Water from an inundated cell is allowed to flood an adjacent dry cell if the water elevation of the inundated cell exceeds the elevation of the bed of the dry cell.

d. Internal boundary conditions are required in the case that subgrid scale barriers or channels are incorporated into the model. Special flow computations are used in the case a barrier is overtopped or submerged during the progress of the storm. A broadcrested weir formula is usually used to establish the flow over the barrier. Also, special flow computations can be made in the case that water in a channel overtops its banks or water flows into the channel from adjacent areas.

2-8. Initial Conditions. To begin the calculations it is necessary to prescribe the initial values of the velocities and elevations of the water surface at every computational point in the system. If the calculations are started well in advance of the storm (usually about 24 hours), it is usually sufficient to begin with the system in a state of equilibrium in which u and v are taken to be zero and η is considered to be uniform over the entire system. Beginning the calculations in this manner minimizes the introduction of transient oscillations related to the starting conditions and allows the system to reach that state in which its response reflects only the effects of the forcing functions.

2-9. General Solution Procedures. Because of the variation in solution procedures used by available storm surge mathematical models, it is only possible to discuss these procedures in general terms. Input to these models includes such items as the system geometry, wind, initial conditions, rain, and possible discharges from rivers. Calculations are commenced at time $t_o + \Delta t$ in which t_o is the time at initial state. By sweeping the entire grid new values of u, v, and η are computed at all computational points based on the velocities and water levels at the initial state. In this sweep all cells are scanned for possible special computations related to moving and interior boundary conditions. Also, special computations are performed in the case of subgrid scale channels. The new values of u, v and η after the sweep is completed are set equal to current values and the time is advanced to $t_o + 2\Delta t$ and the sweep is again performed. This process is continued for a specified number if again performed. This process is continued for a specified number of time levels. Thus, the general solution procedure involves a marching process both with respect to space and time.

2-10. Calibration. Contrary to some claims otherwise, it is always necessary to adjust any mathematical model so that the water motions calculated respond in a manner similar to those occurring in nature. The necessity to calibrate a model stems from the fact that there is generally insufficient knowledge at the outset to properly account for frictional dissipation at the seabed. Bottom roughness may vary rather extensively over the modeled system, particularly when land areas are flooded during the storm. Also, basin geometry in the model is represented only at discrete locations and, thus, the modeled and prototype systems are not entirely identical. To overcome the lack of complete correspondence between model and prototype, the model must be adjusted so that the simulated water motions respond in a similar fashion as those that occur in the actual system. To account for the effects of both bottom roughness and lack of complete correspondence between model and prototype, models are usually calibrated by adjusting the coefficients for frictional dissipation although other adjustments are possible. Calibration of the model is achieved when calculated water levels are in reasonably good agreement with observed water levels from past occurrences. Both observed astronomical tides and past storms can be used in adjusting the model. Unfortunately, in many locations it will be necessary to place complete reliance on tidal observations for calibrating the model because of the lack of historical storm surge data.

2-11. Verification. A calibrated model should always be verified if historical storm surge data exist. Verification is a means of checking to see if an adjusted model can reasonably reproduce prototype observations obtained from a storm not used for calibration purposes. In the event that data exist for only a single storm, then calibration should be made with astronomical tide and a verification study should be made with the storm. However, in this case it may be necessary to further adjust the model based on the storm surge observations.

2-12. Wind Field Specification.

a. In the calculation of water motions induced by hurricanes it is necessary to specify the wind field over the sea. From the standpoint of storm surge calculations, proper wind field specification is of considerable importance due to the fact that wind has the greatest effect on storm surge generation. Many mathematical models have been proposed for studying the meteorological aspects of hurricanes. Wind field models that have been widely used in the United States are the Standard Project Hurricane (SPH) model, Probable Maximum Hurricane (PMH) model developed by the National Weather Service (item 36 of Appendix A) and the model developed more recently under contract with the Federal Emergency Management Agency (FEMA) as described in item 60 of Appendix A. Work is presently underway in the development of the so-called planetary boundary layer models for describing the wind field. The latter models appear to have considerable promise, but none has yet been critically tested.

b. The SPH and PMH wind field models have been used almost exclusively by the Corps of Engineers for performing storm surge calculations in the past. The SPH wind model has been used in the planning and design of various coastal projects while the PMH wind model has been used in the design of nuclear power generation plants sited in coastal areas. National Hurricane Research Report, No. 33 (item 22 of Appendix A) providing the first description of the SPH wind criteria, was subsequently revised in 1972 and published by the National Weather Service (NWS) as Memorandum HUR 7-120. Wind fields characteristic of the PMH were first described in NWS in 1979, the SPH and PMH windfields were refined based on longer periods of storm records and more recent technological advances. The results of the latter study were published in Technical Report NWS 23 (see item 58 of Appendix A).

c. Engineering Regulation 1110-2-1453 requires that all SPH and PMH wind fields be determined in accordance to the methods and procedures given in Technical Report NWS 23. The methodology for determining the SPH and PMH wind fields is summarized in Appendix C.

d. It is to be noted that the wind fields derived from the SPH and PMH wind field models will not necessarily result in a Standard Project Hurricane or Probable Maximum Hurricane. By definition these particular hypothetical

hurricanes are singular events and are responsible for producing the highest surge at a given coastal location based on a critical arrangement of the governing meteorological parameters. With the exception of the peripheral pressure, the SPH and PMH wind field models however consist of a range of values for the meteorological parameters and thus an analysis is required to select the proper values of the parameters for developing the SPH and PMH. Because of the range of meteorological parameters given for the SPH wind field model, it is possible to derive numerous hypothetical hurricanes. It is on this basis that the levels of flooding and associated frequencies can be determined via hydrodynamic computations and statistical analysis.

2-13. Remarks on Available Models.

a. In the past two decades a number of mathematical models have become available for calculating water motions in coastal waters in two horizontal dimensions. These models are sometimes classified as either open coast models or as embayment models since they were formulated to apply to one of these specific regions. However, some existing models were formulated such that they are applicable to problems both on the open coast and in embayments.

b. The first known two-dimensional model used for calculating storm surge on the open coast was introduced in 1963 (see item 45 of Appendix A). This numerical work was directed toward the reproduction of abnormal water levels inducted by Hurricane Carla (1961) along the Texas coast. Due to limitations in computer storage, at that time, it was necessary to use a grid with exceptionally coarse mesh, thus resulting in a rather crude estimate of the surge. However, as a consequence of this outstanding work many other models evolved. Computer capabilities have continually improved since the original application resulting in a better resolution of the modeled area.

c. In 1968, a numerical two-dimensional model was developed for calculating storm surge in an embayment as described in item 43 of Appendix A. Provisions were made in this model for simulating flooding and recession of a low-lying terrain (moving boundaries) and the flow over subgrid scale barriers. Application of the model was made to Galveston Bay, Texas for Hurricane Carla (1961) after calibrating the model with an experienced astronomical tide. The model was verified with Hurricane Cindy (1963). This particular model is referred hereafter as Surge I.

d. Both of the original models developed for calculating storm surge on the open coast and embayments were formulated with explicit finite difference solution schemes in which the water levels and flows were evaluated on a uniform mesh spacing for uniform time steps. A model worthy of note, although not developed specifically for storm surge calculations, is the implicit finite difference solution scheme formulated for simulating water motions in coastal areas as described in items 43 and 44 of Appendix A.

e. Subsequent to these original model developments many storm surge models have become available. Some of these were developed using different solution schemes while others are merely extensions or improvements to the original solution schemes. Discussions herein are limited to only a partial list of the currently available mathematical models for computing water motions in coastal areas. Models which are briefly discussed in the following paragraphs, are those that have been applied or can be readily applied by the U.S. Army Corps of Engineers.

f. Computer codes and guidance for application of these models are available at the Waterways Experiment Station (WES), Coastal Engineering Research Center (CERC). Critical evaluation of these models has been published by the Committee on Tidal Hydraulics (1980).

g. The available open coast and inland flooding storm surge models identified by the name assigned to these models are as follows:

Open Coast Models	Inland Flooding Models
SPLASH	SURGE I
SSURGE	SURGE II
TSURGE	WIFM
WIFM	TWO-D-SURGE
TWO-D-SURGE	SLOSH

It is to be noted that the models WIFM and TWO-D-SURGE are formulated such that they can be applied on either the open coast or inland flooding areas.

h. The model referred to as SPLASH is the result of the work carried out by the National Weather Service (see items 35, 36, 37, 38 and 39 of Appendix A). This model was developed for use in real time prediction of hurricane surge stemming from the need of the National Weather Service to make evacuation decisions in coastal areas during periods of these severe storms. The current version of SPLASH (item 40 of Appendix A) employs a curvilinear grid with variable mesh spacing in the onshore and offshore directions. A convenient feature of the model is the availability of prepared grid and bathymetry along the entire east and gulf coasts of the United States. This available information is an essential feature for real time use of the model along any coastal segment. A more recent model, referred to as SLOSH, has been developed by the National Weather service for addressing inland flooding problems. The latter model employs a polar coordinate grid and has been applied to a number of bays in the Gulf of Mexico.

i. The SSURGE model, originally developed under contract for CERC, (item 68 of Appendix A) was subsequently revised (items 69, 71, and 72 of Appendix A) at WES. This model, based on an explicit difference scheme, also employs a curvilinear grid with a variable mesh spacing which was formulated in a different manner than that of SPLASH.

j. The open coast storm surge model, developed under contract for the Federal Emergency Management Agency, is referred to as TSURGE (item 60 of Appendix A). This model is formulated with an explicit finite difference scheme and employs uniform square cells.

k. Both SSURGE and TSURGE models are discussed in a report by the Water Resources Council (1980). A comparison of results obtained from SPLASH and SSURGE for five historical storms is presented in item 34 of Appendix A. The TSURGE model has been reviewed in a special report published by the National Academy of Science Press (1983).

l. SURGE II and TWO-D-SURGE models are extensions of the SURGE I model. As discussed in item 56 of Appendix A, SURGE II was developed by modifying SURGE I model to include subgrid scale channels with possible levees on either side or both sides of a channel. A new algorithm was introduced to compute flows in the channel by the method of characteristics. Allowance was made for water in the overbank areas to communicate with the channel or vice versa by flowing over the banks or overtopping the adjacent levees. The SURGE I model also was modified in SURGE II to include a more realistic algorithm for computing flow over barriers. The TWO-D-SURGE model developed at CERC is generally similar to SURGE II except that the algorithm developed for channels is based on a finite difference scheme rather than the method of characteristics.

m. The WIFM model (items 8, 9 and 10 of Appendix A) developed at WES (presently with CERC at WES), employs an implicit solution scheme similar to the one given in item 43 of Appendix A. Basic features of this model include innudation simulation of low-lying terrain, treatment of subgrid scale barrier effects and an option for a variable rectangular grid. The model permits a selection of various

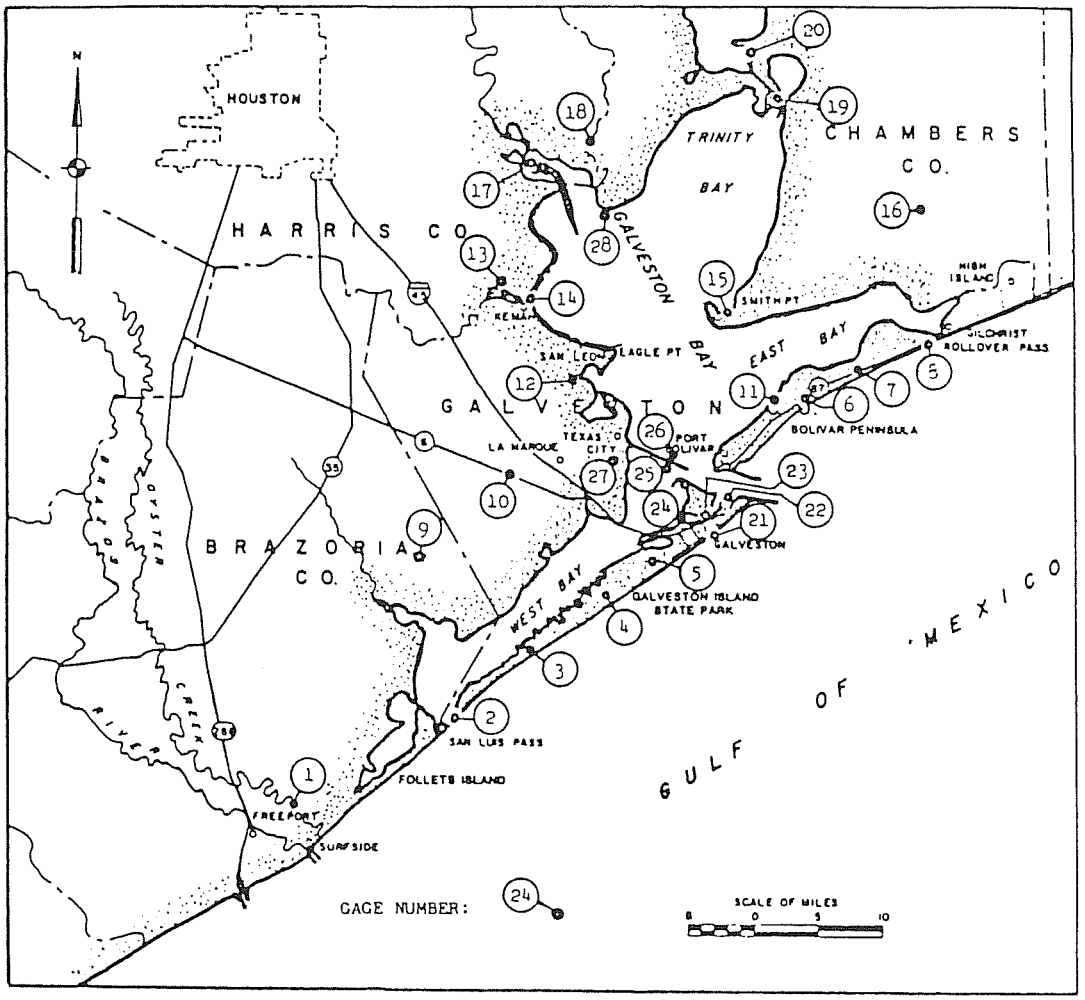

FIGURE 2-4
Locations where maximum water levels were observed during Hurricane Carla (1961)

difference formulations and can account for the convection of momentum and the Coriolis force. WIFM has been successfully applied to a wide range of shallow water wave problems.

n. A study has been made to compare the storm surge reproductions of the inland flooding models, SURGE II, TWO-D-SURGE and WIFM. This study involved simulating the surge induced by Hurricane Carla (1961) in Galveston Bay and vicinity. Numerical values (1 through 28) indicated on Figure 2-4 signify the locations at which maximum water levels were recorded during Hurricane Carla. Table 2-1 shows a comparison of the observed maximum water levels and those simulated by the three models at the locations where the maximum water levels were recorded (denoted by gage location). Also shown are the differences between the observed and computed values as well as the mean differences. It is not the be implied by this comparison that one model is more reliable than another since at other locations the mean difference may be different. The intent of this comparison is to only demonstrate the utility of these available storm surge models.

o. In addition to the mathematical model mentioned previously, the Corps has the proprietary rights of a model developed by the Danish Hydraulics Institute (item 1 of Appendix A). This model, referred to as S21MK8, utilizes an implicit scheme and is applicable to either open coast or estuary problems. This model has been verified and applied to a wide range of hydraulic problems. Information regarding this model is available at the U.S. Army Waterways Experiment Station, Coastal Engineering Research Center.

2-14. Comments With Regard to Model Application. The application of the mathematical model in conducting storm surge analyses is not difficult provided that one has a fundamental understanding of the model, its capabilities, input requirements and output options. A user's manual which outlines the operational procedures of the model is generally an essential document for proper application. Technological advances are continually evolving in mathematical modeling and it is, thus, necessary to keep abreast of any changes made to a model via communication with either the developer or custodian of the model. The U.S. Army Waterways Experiment Station, Coastal Engineering Research Center can provide guidance, training and consulting services for the models mentioned herein.

2-15. Physical Models. These models are used rather extensively in coastal engineering to study the effects of tides and short period surface waves in tide water regions. Although these models are effective tools for studying such phenomena, they are of limited use in modeling storm surge. Their ineffectiveness in the simulation of storm surge stems from the fact that the storm generation processes cannot be readily incorporated in the physical model. Processes which are

TABLE 2-1
Comparison of Highwater Levels at Selected Cage Locations Within and in the Vicinity Galveston Bay, Values in Feet

		WIFM				SURGE II			TWODSRG		
Gage Number	Gage Location	Observed	Computed	Difference	Time of Occurrence	Computed	Difference	Time of Occurrence	Computed	Difference	Occurrence
1	Oyster Creek	10.8	10.8	0.0	65.0	No Data	No Data	No Data	11.1	0.3	No Data
2	San Luis Pass	10.8	10.0	-0.8	74.0	9.1	-1.7	66.0	9.7	-1.1	74.5
3	Sea Isle Beach	12.1	10.0	-2.1	74.0	9.1	-3.0	75.0	9.6	-2.5	74.5
4	Bermuda Beach	10.5	9.8	-0.7	74.0	9.0	-1.5	75.0	9.5	-1.0	74.5
5	Scholes Field	8.5	9.6	1.1	67.5	7.2	-1.3	65.0	9.7	1.2	74.0
6	Bolivar Beach	9.3	9.3	0.0	74.5	7.5	-1.8	83.0	9.7	0.4	No Data
7	Crystal Beach	8.8	9.4	0.6	74.5	7.2	-1.6	85.0	9.7	0.9	No Data
8	Rollover Beach	9.6	9.3	-0.3	75.0	9.0	-0.6	75.0	9.4	-0.2	No Data
9	Halls Bayou	14.3	14.1	-0.2	77.0	14.7	0.4	77.0	15.1	0.8	81.5
10	Highway Six	12.6	12.7	0.1	77.0	11.7	-0.9	78.0	12.0	-0.6	76.5
11	Sievers Cove	10.6	9.3	-1.3	68.0	8.6	-2.0	79.0	9.6	-1.0	78.5
12	Dickinson Bayou	11.4	11.8	0.4	71.0	11.3	-0.1	80.0	12.0	0.6	79.25
13	Lakeside	10.4	13.1	2.7	80.0	13.1	2.7	80.0	13.8	3.4	80.5
14	Kemah	14.2	12.8	-1.4	80.8	12.4	-1.8	81.0	13.2	-1.0	79.5
15	Smith Point	9.8	10.4	0.6	79.0	10.3	0.5	82.0	11.1	1.3	No Data
16	Oyster Bayou	10.5	11.0	0.5	83.0	10.1	-0.4	86.0	11.3	0.8	No Data
17	Scott Bay	14.2	14.1	-0.1	81.0	13.7	-0.5	82.0	14.3	0.1	80.5
18	Baytown	11.5	14.4	2.9	81.0	13.1	1.6	81.0	14.7	3.2	80.5
19	Ananuac	12.4	12.7	0.3	81.0	12.5	0.1	82.0	12.8	0.4	No Data
20	Wallisville	14.0	14.0	0.0	82.0	13.8	-0.2	82.0	13.5	-0.5	No Data
21	Pleasure Pier	9.3	9.6	0.3	74.0	8.9	-0.4	74.0	9.4	0.1	74.5
22	Fort Point	9.0	9.5	0.5	67.0	8.9	-0.1	78.0	9.6	0.6	67.0
23	Pier 21	8.8	9.5	0.7	67.0	8.8	0.0	78.0	9.6	0.8	67.0
24	Pelican Bridge	9.0	9.4	0.4	67.0	8.9	-0.1	78.0	9.7	0.7	67.0
25	Texas City Dyke (South)	9.5	10.0	0.5	68.0	9.0	-0.5	79.0	10.2	0.7	67.75
26	Texac City Dyke (North)	9.7	10.0	0.3	68.0	9.4	-0.3	69.0	10.1	0.4	67.75
27	Carbide Docks	11.0	10.4	-0.6	69.0	9.7	-1.3	79.0	10.7	-0.3	75.75
28	Humble Docks	13.7	12.6	-1.1	80.0	12.6	-1.1	81.0	13.3	-0.4	80.0
Mean Absolute Difference from observed				.73			.98			.90	

extremely difficult to represent in the physical model are the temporal and spatial varying wind fields, atmospheric pressure variations over the water surface and the effects of earth's rotation. Although it may be possible to overcome these difficulties in the physical model, an undertaking of this sort would normally be prohibitive both from the standpoint of effort and cost. Inasmuch as physical models are impractical for simulating storm surge, they can be of use indirectly by supplying information with regard to the response of astronomical tides. This information can be beneficial in the application of either the historical data or mathematical model approaches, particularly at those coastal locations where tidal variations are unknown. In particular, such tidal information may aid in the calibration of a mathematical model for astronomical tide conditions. Only existing physical models should be used in simulating tide data. Construction of a physical model solely for the purpose of obtaining this information is not recommended.

CHAPTER 3
STATISTICAL METHODS

3-1. General.

a. This chapter presents method for predicting the magnitude and frequency of occurrence of storm-induced water levels coupled with the effects of astronomical tide in coastal regions. Generally, engineering studies concerned with predicting flood levels of coastal waters require that water level frequencies by determined in order to assess the risks and economics involved in project design.

b. Two different methods have been generally recognized for establishing abnormal water level frequencies: (a) historical and (b) synthetic. Historical methods consist of direct frequency analysis of the recorded water level data. Synthetic methods, on the other hand, consist of an indirect approach in which water level data are generated from a rather large ensemble of synthetic storms via numerical computations and flood frequencies are established based on an analysis of the computed water level data. In the application of the latter methods, a large variety of synthetic storms may be derived by utilizing various combinations of storm parameter probabilities that are characteristic of a given coastal location. Historical data of the individual storm parameters are used in the determination of the statistical distribution of the parameters. The statistical concept referred to as the "joint probability method" is used to determine the magnitude and frequency of occurrence of water levels when using the synthetic approach.

c. An underlying assumption in the use of historical methods is that the finite sample of recorded events is representative of all possible events or population at a particular coastal site. Obviously, there is no assurance that such an assumption is valid for any finite sample. It may only be inferred that for a larger sample there is usually a better chance that the sample is more representative of its parent population.

d. For coastal locations that have little or no historical water level data a synthetic method should be used. The primary advantage of this method is that a rather large data base can be generated based on various combinations of the storm parameters. Also, the storm parameters are reasonably well defined due to the technology available for describing meteorological aspects of hurricanes. In addition, computational hydraulics has advanced to the state that water levels can be computed with a reasonable degree of accuracy.

3-2. Historical Method.

a. In Chapter 2 the historical data approach was discussed

from the standpoint of the data base, applicability and its advantages and disadvantages. A subjective decision must be made with regard to whether the historical method should be used or not used for a given engineering study. This decision depends, of course, on the quantity and quality of data that are available as well as confidence that the sample data are representative of future events. With regard to the quantity of data, it has been suggested as a rule of thumb that at least N/2 years of data are required to confidently predict the annual percent chance of occurrence of an event with an average return interval of N years (item 4 of Appendix A). This simply implies that data recorded over a period of 50 years would be required to confidently predict the elevation of the water surface with a 1 percent chance of occurrence.

b. The historical method is considered applicable to various sites along the New England coast and other coastal areas where relatively long term water level records exist. In general this method has limited usage due to the lack of sufficient historical data.

c. From a statistical point of view, historical flood levels cannot always be regarded to be from the same population. This is due to the fact that the observed levels can be produced from either an extratropical storm, tropical storm, or severe tropical storm (hurricane) coincident with fluctuations caused by the astronomical tide. Consequently, mixed populations are always involved. As an approximation, however, it is generally considered appropriate to treat the entire water level record as a single population provided that the record is of sufficient length. In the event that a relatively short term record, 20 years or less, is to be analyzed, the predicted astronomical tide is to be extracted from the observed water levels and replaced with the mean high tide. The latter modification is recommended for the purpose of insuring that the tide component is of sufficient magnitude.

3-3. Series Selection. Data for frequency analysis may be obtained from recorded data by using either annual series or partial duration series. The annual series consist of using only one flood level or event per year while the partial duration series consist of all events above a predetermined base flood level of interest, regardless of the time of occurrence. More data can be incorporated into the analysis by using a partial duration series since all water levels exceeding an appropriate minimum base level in any given year can be taken into account. Additional information of this sort is advantageous provided that the magnitudes are such that they are useful in describing the less frequent events. In many instances such additional information may only provide a better description of the magnitudes for the more frequent events which are usually of little concern in most studies. Use of the partial duration series involves arbitrary selection of the base level which requires subjective decisions with regard to the independence of storm induced water levels and tide levels. It is, therefore, recommended that an annual series be utilized in frequency studies unless a partial series is needed to provide a more suitable description of those frequency levels that are of interest.

3-4. Adjustment of Data Base. Prior to performing any historical frequency analysis, all data should be examined for possible changes in the local mean sea level at the time the data were recorded in comparison to the present time. Chapter 2 noted that studies of sea level variations revealed that the sea level has continually risen over much of the present century. It should be assumed that this trend in sea level change has occurred over the past few centuries and all recorded and other historic data should be adjusted accordingly.

3-5. Frequency Curve - Graphical Method. In performing a frequency analysis the primary objectives are to determine the percent chance of exceedence of levels and possibly estimate the frequency of the water levels to some extent beyond the range in which recorded data are available. There are two methods that can be used in accomplishing these objectives, namely the graphical method and the analytical method. The latter method is discussed in the subsequent section. The graphical method consists of constructing a frequency curve in which the magnitude of the event (annual peak water level) is plotted against the estimated percent chance of exceedence on a suitable grid (usually a normal probability grid). A smooth curve drawn through the data points and extended somewhat beyond the data in the more infrequent range can thus define the frequency curve. In the development of the frequency curve it is necessary to arrange the recorded data according to the order of magnitude and approximate the plotting position based on a particular plotting formula. Various relations are available for defining the plotting positions; however, it is recommended that the mean frequency or Weibull plotting position formula be used in any graphical analysis. This formula is:

$$P = \frac{M}{N + 1} \qquad [3-1]$$

where P is the probability; M is the order of the event (events arranged in order of the magnitude) in which the largest event is ranked as 1; and N is the number of events. This is the formula generally recommended by the U.S. Interagency Advisory Committee on Water Data, (item 62 of Appendix A) for comparison purposes because it is analytically simple and intuitively easily understood (see items 12 and 72 also). In item 3 of Appendix A it was demonstrated that the Weibull plotting position expression is the best formula for economic and engineering design studies.

3-6. Frequency Curve - Analytical Method. There are many different theoretical frequency distributions available for studying water level frequencies on the open coast. Selection of a particular frequency distribution depends on how well the distribution fits the observed data and fulfills the goals and objectives of the study. It cannot be implied that in acceptance of a particular frequency distribution that the magnitude and frequency of occurrence are accurately described. In previous frequency studies of peak annual water levels on the New England coast it was found that the Pearson Type III distribution (without log transformation) provides a reasonable estimate of the water level frequencies. Based on these findings it is recommended that this frequency distribution be adopted for uniform design studies along the New England coastal areas.

a. Basic Equations. The probability density distribution of the Pearson Type III distribution is given by (item 41 of Appendix A)

$$P(x) = \frac{1}{\alpha\,\Gamma(\beta)}\left(\frac{x-\gamma}{\alpha}\right)^{\beta-1} \exp\left(-\frac{x-\gamma}{\alpha}\right) \qquad [3-2]$$

in which α, β and γ are parameters; r is the gamma function; and x is an event. Although there are various methods (moments, maximum likelihood, least squares and graphical) for estimating the parameters the method of moments is recommended. Based on the sample mean μ, standard deviation σ and the coefficient of skew G, to be defined, the parameters α, β and γ can be determined. By the method of moments it can be shown that

$$\beta = \left(\frac{2}{G}\right)^2 \qquad [3-3]$$

$$\alpha = \frac{\sigma}{\sqrt{\beta}} \qquad [3\text{-}4]$$

$$\gamma = \mu - \sigma\sqrt{\beta} \qquad [3\text{-}5]$$

The sample mean, standard deviation and the coefficient of skew are defined as follows:

$$\mu = \frac{\Sigma x}{N} \qquad [3\text{-}6]$$

$$\sigma = \left[\frac{\Sigma(x-\mu)^2}{N-1}\right]^{1/2} = \left[\frac{(\Sigma x^2) - (\frac{(\Sigma x)^2}{N})}{N-1}\right]^{1/2} \qquad [3\text{-}7b]$$

$$G = \frac{N\Sigma(x-\mu)^3}{(N-1)(N-2)\sigma^3} \qquad [3\text{-}8a]$$

$$= \frac{N^2(\Sigma x^3) - 3N(\Sigma x)(\Sigma x^2) + 2(\Sigma x)^3}{N(N-1)(N-2)\sigma^3} \qquad [3\text{-}8b]$$

in which
x = annual peak water surface elevation
N = number of items in data set
μ = arithmetic mean
σ = standard deviation
G = skew coefficient.

The standard deviation σ is a measure of dispersion of each of the observed events from the mean μ and the skew coefficient is numerical measure of the lack of symmetry of the frequency distribution. By integrating the right hand side of Equation [3-2] with respect to x, it can be shown after some manipulation that a general frequency relation can be expressed as (see item 41 of Appendix A for derivation).

$$x = \mu + K\sigma \qquad [3\text{-}9a]$$

or

$$\eta = \mu + K\sigma \qquad [3\text{-}9b]$$

in which x has been replaced by η to indicate that the water surface elevation is the event of interest in the present study. The coefficient K is a frequency factor that depends on the skew coefficient G for a given exceedence probability. Values of K can be obtained from tables provided in Appendix G or computed by the approximate method as given in item 41 of Appendix A. The latter method, convenient for computer applications, is based on the following relations:

$$K \simeq t + (t^2-1)\frac{G}{6} + \frac{1}{3}(t^3-6t)\left(\frac{G}{6}\right)^2$$

$$-(t^2-1)\left(\frac{G}{6}\right)^3 + t\left(\frac{G}{6}\right)^4 + \frac{1}{3}\left(\frac{G}{6}\right)^5 \qquad [3\text{-}10]$$

in which t is the standard normal deviate. An approximate expression for t when the cumulative probability P(t) is in the range $0 = <P(t) \leq 0.5$ is:

$$t \simeq w - \frac{C_0 + C_1 w + C_2 w^2}{1 + d_1 w + d_2 w^2 + d_3 w^3} \qquad [3\text{-}11]$$

in which

$C_0 = 2.515517$; $d_1 = 1.432788$

$C_1 = 0.802853$; $d_2 = 0.189269$

$C_2 = 0.010328$; $d_3 = 0.001308$

and

$$w = \left[\ln\frac{1}{P(t)^2}\right]^{1/2} \quad ; \quad P(t) \leq 0.5 \qquad [3\text{-}12a]$$

$$w = \left\{\ln\frac{1}{[1-P(t)]^2}\right\}^{1/2} \quad ; \quad P(t) > 0.5 \qquad [3\text{-}12b]$$

For values of P(t) greater than 0.5, it is necessary to change the sign of the calculated value of t.

b. Skew Coefficients for Small Samples. It is not possible to establish a reliable estimate of the skew coefficient from either Equations [3-8a] or [3-8b] when small samples are involved. It is impractical to base the skew coefficient to be used in a frequency study on a single record of annual peaks that is less than 100 years in length (item 2 of Appendix A). In performing water level frequency studies along the open coast it is recommended that reliance be placed on the skew coefficients determined from base stations with relative long term records for specifying the skew at subordinate stations with short term records. Depending on the situation that exists, the skew coefficient at a subordinate station can be either taken as equal to that of the base station or by interpolating the skew at a subordinate station based on the skew determined at adjacent base stations. In some cases it may be justified to specify the skew coefficient at a subordinate station based on weighted skew coefficients at the base stations to reflect the length of record.

c. Broken or Incomplete Record. In some cases it may be found that a continuous record was not maintained at a particular gaging station due to gage removal or other causes resulting in a broken record. For this situation the frequency study should be performed by considering the available record segments as a continuous record with the record length equal to the sum of the record segments. An incomplete record may result due to improper operation or gage failure during the period in which the highest annual stage was most likely to occur. In this case an attempt should be made of fill in the missing data based on known flood level information from nearby sites. If it is not possible to supply realistic information for completion of the record, the data should be treated in the same manner as described for a broken record.

d. Outliers. Data points which depart significantly from the trend of other data points are referred to as outliers. In the study of annual peak water level frequencies on the open coast, it is possible that outliers may be encountered. Because these outliers can significantly affect the resulting frequency analysis, especially for small samples, it is recommended that an outlier be treated as historic data as discussed int he subsequent section, provided that the period of record can be extended. If there is insufficient information to extend the historical period, then the high outlier should be treated as part of the systematic record. The detection of a high or low outlier can be determined from the following expression (item 62 of Appendix A)

$$\eta_H = \mu \pm K_N \sigma \qquad [3\text{-}13]$$

in which
η_H = threshold water level elevation;
μ = mean of the peak water level elevations excluding other outliers previously detected;
σ = standard deviation, excluding other outliers previously detected;
K_N = coefficient depending on the sample size as given in Table 3-1.

TABLE 3-1
Outlier Test K values

10 Percent Significance Level K Values
(From item 62 of Appendix A)

Sample size	K_N Value	Sample size	K_N Value	Sample size	K_N Value	Sample size	K_N Value
10	2.036	45	2.727	80	2.940	115	3.064
11	2.088	46	2.736	81	2.945	116	3.067
12	2.134	47	2.744	82	2.949	117	3.070
13	2.175	48	2.753	83	2.953	118	3.073
14	2.213	49	2.760	84	2.957	119	3.075
15	2.247	50	2.769	85	2.961	120	3.078
16	2.279	51	2.775	86	2.966	121	3.081
17	2.309	52	2.783	87	2.970	122	3.083
18	2.335	53	2.790	88	2.973	123	3.086
19	2.361	54	2.798	89	2.977	124	3.089
20	2.385	55	2.804	90	2.981	125	3.092
21	2.408	56	2.811	91	2.984	126	3.095
22	2.429	57	2.818	92	2.989	127	3.097
23	2.448	58	2.824	93	2.993	128	3.100
24	2.467	59	2.831	94	2.996	129	3.102
25	2.486	60	2.837	95	3.000	130	3.104
26	2.502	61	2.842	96	3.003	131	3.107
27	2.519	62	2.849	97	3.006	132	3.109
28	2.534	63	2.854	98	3.011	133	3.112
29	2.549	64	2.860	99	3.014	134	3.114
30	2.563	65	2.866	100	3.017	135	3.116
31	2.577	66	2.871	101	3.021	136	3.119
32	2.591	67	2.877	102	3.024	137	3.122
33	2.604	68	2.883	103	3.027	138	3.124
34	2.616	69	2.888	104	3.030	139	3.126
35	2.628	70	2.893	105	3.033	140	3.129
36	2.639	71	2.897	106	3.037	141	3.131
37	2.650	72	2.903	107	3.040	142	3.133
38	2.661	73	2.908	108	3.043	143	3.135
39	2.671	74	2.912	109	3.046	144	3.138
40	2.682	75	2.917	110	3.049	145	3.140
41	2.692	76	2.922	111	3.052	146	3.142
42	2.700	77	2.927	112	3.055	147	3.144
43	2.710	78	2.931	113	3.058	148	3.146
44	2.719	79	2.935	114	3.061	149	3.148

The positive sign in Equation [3-13] is for computing the threshold level for the high outlier and the negative sign is for computing the threshold level for the low outlier. A high outlier is detected if an observed water level elevation in the record exceeds the threshold value η_H and a low outlier is detected if the level is less than the threshold value.

e. Use of Historic Data. Authentic and adjusted historic events, antedating or intervening periods of systematic records, can be used to increase the accuracy of the frequency analysis. The use of any historic data in a frequency analysis should be thoroughly documented. Extension of a systematic record by use of historic data requires that Equations [3-6], [3-7], [3-8] and [3-9] be modified to account for the extended record. The modified expressions given herein are based on those presented in (item 62 of Appendix A) without log transformation. A weighting function is used for both the historic data and systematic record data. Historic data, including data for high outliers (low outliers not considered) are assigned the weight of 1.0, while the weight of systematic data is computed by

$$W = \frac{H - Z}{N} \qquad [3\text{-}14]$$

in which W is the weight; H is the number of years in the historical period; Z is the number of historic peak water levels including high outliers, and N is, as before, the number of events in the systematic record. The modified relations for the mean, standard deviation and skew coefficient are as follows:

$$\bar{\mu} = \frac{W \Sigma x + \Sigma x'}{H} \qquad [3\text{-}15]$$

$$\bar{\sigma} = \left[\frac{W \Sigma(x - \bar{\mu})^2 + \Sigma (x' - \bar{\mu})^2}{H - 1}\right]^{1/2} \qquad [3\text{-}16]$$

$$\bar{G} = \frac{H}{(H - 1)(H - 2)\bar{\sigma}^3}\left[\frac{W(N-1)(N-2)\sigma^3 G}{N} + 3W(N-1)(\mu - \bar{\mu})\sigma^2 + WN(\mu - \bar{\mu})^3 + \Sigma (x' - \bar{\mu})^3\right] \qquad [3\text{-}17]$$

in which x' is the magnitude of a historic peak or high outlier and the overbar signifies that the mean, standard deviation and skew coefficient are modified to reflect the historic data. The general frequency expression, Equation [3-9], is modified to read

$$\eta = \bar{\mu} + K\bar{\sigma} \qquad [3\text{-}18]$$

in which K is, as before, the frequency factor. When the data are plotted in accordance with the Weibull plotting position formula Equation [3-1] is modified, thus

$$p = \frac{\bar{m}}{H + 1} \qquad [3\text{-}19]$$

where

$$\bar{m} = E; \quad \text{when: } 1 \leq E \leq Z \qquad [3\text{-}20]$$

and

$$\bar{m} = WE - (W - 1)(Z + 0.5); \qquad [3\text{-}21]$$

when: $(Z + 1) \leq E \leq (Z + N)$

in which $\bar{m}$ is the historically adjusted order number of each event and E is the event number when events are ranked in order from greatest magnitude to smallest magnitude. The event numbers E will range from 1 to the number Z + N.

f. Confidence Limits. Frequency exceedence curves computed by the methods presented can only be considered as an estimate of the true population frequency curve since the computed curve is based only on a sample. Reliability of the computed frequency curve depends upon the sample size and accuracy of the theoretical distribution. A measure of the uncertainty of the estimated exceedence frequency curve can be established by computing the upper and lower confidence limits. The general frequency expression in Equation [3-9] can be modified to reflect the upper and lower confidence limits as follows:

$$\eta_\mu = \mu + \sigma K_u \qquad [3\text{-}22]$$

$$\eta_L = \mu + \sigma K_L \qquad [3\text{-}23]$$

in which η_u and η_L are the water levels for a given probability for the upper and lower confidence levels, respectively, and K_u and K_L are the frequency factors for the upper and lower confidence levels. The factors K_u and K_L are approximated by (item 62 of Appendix A):

$$K_u = \frac{K + (K^2 - ab)^{1/2}}{a} \qquad [3\text{-}24]$$

$$K_L = \frac{K - (K^2 - ab)^{1/2}}{a} \qquad [3\text{-}25]$$

in which

$$a = 1 - \frac{t^2}{2(N - 1)} \qquad [3\text{-}26]$$

$$b = K^2 - \frac{t^2}{N} \qquad [3\text{-}27]$$

and t is, as before, the standard normal deviate and K is the frequency factor used in deriving the estimated frequency curve. It is to be noted that K = t when the skew coefficient is zero in accordance with Equation [3-10]. The standard normal deviate can be obtained directly from the tables supplied in item 62 of Appendix A, for a given probability and zero skew for a given level of significance. When historic data are involved in the analysis the systematic record length N is considered to control the statistical reliability and is to be used for calculating the confidence limits. In all frequency studies the upper and lower confidence limits for levels of significance of 0.05 and 0.95 are to be included as a part of the analysis.

g. Expected Probability. Rather than using the exceedence probability in defining the frequency of water levels, it is generally considered more appropriate to use expected probability. According to item 62 of Appendix A, the expected probability is defined as the average of the true probabilities of all magnitude estimates for any specified flood frequency that might be made from successive samples of a specified size. For relatively large samples (150 or more) the expected probability is approximately equal to the exceedence probability but for small samples it may be significantly different. Equations given in item 62 of Appendix A for computing the expected probability P_N for a given exceedence probability P_∞ are as follows:

$$P_N = 0.0001 \left(1.0 + \frac{1600}{N^{1.72}}\right) \quad ; \text{ for } P_\infty = 0.0001 \qquad [3\text{-}28a]$$

$$= 0.001 \left(1.0 + \frac{280}{N^{1.55}}\right) \quad ; \text{ for } P_\infty = 0.001 \qquad [3\text{-}28b]$$

$$= 0.01 \left(1.0 + \frac{26}{N^{1.16}}\right) \quad ; \text{ for } P_\infty = 0.01 \qquad [3\text{-}28c]$$

$$= 0.05 \left(1.0 + \frac{6}{N^{1.04}}\right) \quad ; \text{ for } P_\infty = 0.05 \qquad [3\text{-}28d]$$

$$= 0.1 \left(1.0 + \frac{3}{N^{1.04}}\right) \quad ; \text{ for } P_\infty = 0.1 \qquad [3\text{-}28e]$$

$$= 0.3 \left(1.0 + \frac{0.46}{N^{0.925}}\right) \quad ; \text{ for } P_\infty = 0.3 \qquad [3\text{-}28f]$$

Because the expected probability is considered more representative of the true probability it is to be used in the determination of all water level frequencies in lieu of the exceedence probability.

3-7. Application of Historical Method. A problem is presented in Appendix F to illustrate the determination of the magnitude and frequency of occurrence of water levels at a station on the New England coast. Although the problem presented is performed by hand calculations a slightly modified version of a computer program available at the Hydrologic Engineering Center (HEC) may be used in carrying out the necessary computations. The existing program at HEC is based on the Log Pearson Type III frequency distribution and thus the method described therein requires removal of the log transformations.

3-8. Synthetic Method.

a. As discussed in section 3-1, the synthetic method for estimating the frequency of occurrence of combined astronomical and storm-induced tide of given level is particularly useful for regions where historical records of tides are non existent or not adequate. The method is commonly used in Federal Insurance Studies for coastal communities. For such studies, the historical method is used as a check.

b. The synthetic method is also commonly referred to as the joint probability method, because it employs probability information on storms to infer that of the surges associated with storms. In its simplest terms, the method simulates an extensive hypothetical record of surge events, for a given subregion of the coast, corresponding to a given storm climatology. The surge events, whose frequency of occurrence is determined from that of the storms, must then be combined in an appropriate statistical manner with known information on the astronomical tides for the subregion to yield a frequency of occurrence of given total water level. The statistical combination of historical surge data and tide data is an example of the joint probability method. Its real advantage is in the realistic evaluation of probabilities of rare events. The method requires a reliable storm surge model (see Chapter 2) by which to calculate the coastal surge profiles and their temporal evolution for each storm in the chosen ensemble of storms to be simulated.

c. The synthetic method owes its advantage to the fact that the climatological data base of storms for given subregion of the coastline can be determined with reasonable reliability by appropriate combination of information from a wider region, taking into account latitudinal and other trends of storm climatology. In other words, the statistics on storm intensity, horizontal scale and frequency of occurrence can be considered as slowly changing functions of coastal position, such that the entire ensemble of storm parameter information can be incorporated into a meaningful spatial pattern. In contrast, the statistics on water level are highly dependent upon location and local bathymetry, such that a merging of surge

data from different tide gages is not reliable as a means of broadening the data base for the direct historical method.

d. A disadvantage of the synthetic method is the amount of effort, both in terms of man-hours and computer time, required to carry out the simulated surge event calculations. The method is most useful for hurricane-induced surges, since hurricanes (and lesser tropical storms) can be characterized in terms of a few parameters whose statistics are amenable to analysis. Moreover, the wind field can be adequately estimated from these parameters in a manner similar to that of an SPH (see section 2-12).

3-9. Joint Probability Concept. An in-depth discussion of the underlying elements of the joint probability method is given in a recent National Research Council report (item 40 of Appendix A). The essential elements of the method are summarized here in the context of application to hurricanes.

a. Notation. Following the convention of the National Research Council report, capital letters are employed for random variables such as the hurricane parameters or storm surge; and lower case letters are employed for the arguments of probability density functions (pdf's). For convenience in denoting the used in other parts of the manual. The following notation will be adopted:

Physical Quantity	Random Variable	Argument
Central pressure deficit	D	d
Radius to maximum wind	R	r
Azimuth of storm track	θ	θ
Forward speed of storm	V	v
Distance to storm center	L	l
Peak surge elevation	S	s

More specifically, S denotes the peak surge for a given storm at some selected coastal site A and L denotes the minimum distance of the storm track from A (Figure 3-1). The latter definition avoids the necessity of distinguishing between landfalling and alongshore hurricanes in the treatment of the statistics, since for landfalling storms a given θ and L imply a given landfall point X, while for alongshore storms L is automatically the distance of the track offshore (or inshore, dependent on θ). The azimuth is taken in the direction of the storm heading, either in reference to north or in reference to the mean orientation of the coast in the vicinity of site A. The symbol D is employed for $P_n - P_o$ to avoid confusion with the probability notation P. Parameter D is the basic measure of storm intensity and the most important of all the parameters characterizing the storm. In most applications constant values of the hurricane parameters are employed along the path. A possible exception is that allowance for falling (decrease of D) can be made as the hurricane moves inland, in the case of land-falling storms.

b. Fundamental Relations.

(1) The underlying elements of the joint probability method for storm surges are three distinct probability functions. The first is the probability density for the surge at position A; this is denoted by $f_S(s)$. It is understood that this varies with position A. the probability that S at site A in a single random storm event exceeds s is given by

$$P(S > s) = \int_s^\infty f_S(s)ds \qquad [3-29]$$

This represents the exceedence probability for S and is the function which is sought.

(2) The second probability function is a joint (or multivariate pdf for the storm parameters. For compactness,

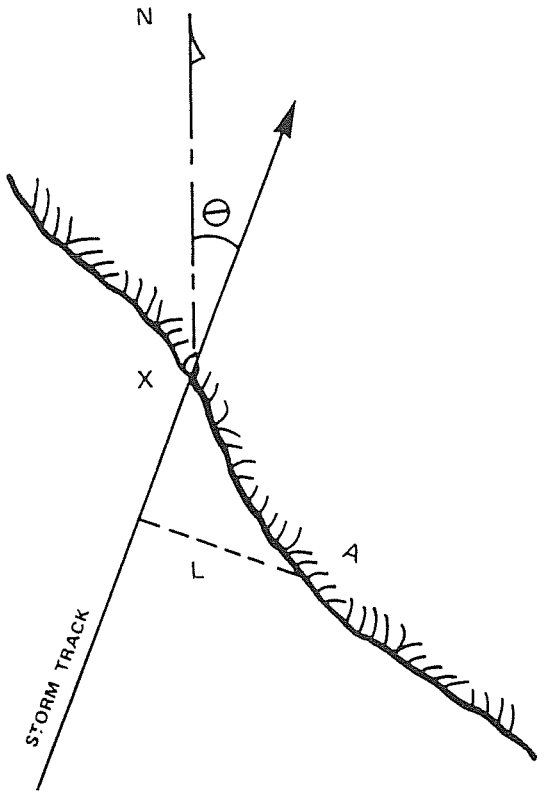

FIGURE 3-1
Schematic of landfalling storm and geometry parameters.

this is denoted by $f_{\underline{V}}(\underline{v})$, where $\underline{V}$ denotes the storm parameter vector (D,R,θ,V,L) and $\underline{v}$ is the counterpart argument vector. It is simply shorthand notation for

$$f_{\underline{V}}(\underline{v}) = F(d,r,\theta,v,l) \qquad [3-30]$$

This function must be determined from the storm climatology in the vicinity of site A.

(3) The third pdf is the conditional probability for S, given that $\underline{V} = \underline{v}$; it is denoted by $f_S(s \mid \underline{V} = \underline{v})$. This function is determined by the storm surge model and the offshore bathymetry in the vicinity of point A.

(4) Given the latter two pdf's, the fundamental relation for the surge probability function is

$$f_S(s) = \int f_S(s|\underline{V} = \underline{v})\ f_{\underline{V}}(\underline{v})\ d\underline{v} \qquad [3-31]$$

where the integration extends over all five dimensions of the storm parameter vector $\underline{V}$ (i.e., the entire domain of $\underline{v}$). The integral represents a convolution of the storm parameter pdf to yield the desired pdf for S, and is the basis for the joint probability method for deducing the surge statistics. In order to determine the pdf for total water level, including effects of astronomical tide and other variations of water level which are unrelated to storms, a further convolution of $f_S(s)$ is required; this is discussed later. The alternative is to include the astronomical tide in the surge calculation model, and include additional random parameters in $\underline{v}$, namely the amplitude and phase of the tide relative to that of the storm event.

c. Probability of Storm Occurrence.

(1) The occurrence of tropical cyclones (hurricanes and tropical storms) can be considered statistically as a Poisson process in the sense that during any given season the occurrence is random and unrelated to what has occurred

previously. The probability of exactly n storms occurring during a given year in a given region (i.e., a given geographical area or a given reach of coastline) is governed by a single parameter m which is the expected (mean) value of the yearly occurrence rate for the region:

$$P(N = n) = p_n = m^n \frac{\exp(-m)}{n!} \qquad [3\text{-}32]$$

The probability of at most n storms occurring in a given year is

$$P(N \leq n) = \sum_{j=o}^{n} p_j \qquad [3\text{-}33]$$

which approaches unity as n becomes much larger than m. both the mean and variance of the Poisson distribution are equal to m.

(2) As an example, during the period 1900 to 1972 inclusive, a total of 71 hurricanes ($D \geq 1$ inch H_g) crossed the gulf coast of the United States. From this sample we estimate m = 0.97 for this region. A detailed count f of the years having 0,1,2... hurricanes for this region during the period 1900 to 1972 (item 27 of Appendix A) shows the following results:

TABLE 3-2
Statistics for Hurricanes, Gulf of Mexico

n	f	73 p_n
0	30	28
1	21	27
2	16	13
3	6	4
4	0	1
Totals	73	73

The last column gives the expected count in 73 years as determined from the Poisson distribution with m = 0.97, after rounding to the nearest integer value. A chi-square test of the data in this table shows no significant difference of the sample from the Poisson distribution. In other words the differences are what one should expect for a sample this size.

d. Return Period for Storms. The average return period for storms in a given region is defined as 1/m. For the above gulf coast sample this is 1.03 years. Had the sample been limited to only those hurricanes crossing the Texas coast then the return period of hurricanes for that region is about 3.3 years (m = 0.30). The probability of no hurricane crossing the Texas coast in a given year is 74 percent, for one hurricane 22 percent, and for two or more hurricanes 4 percent.

e. Return Period for Surges. Suppose the joint probability approach for estimating the exceedence probability P(S > s) at site A has been applied to a region for which L has a range 0 to L_m and θ a range 0 to 360 deg. i.e, a circular region of radius L_m about A which contains all simulated hurricane tracks for which a significant response at A is expected. Let m be the mean yearly occurrence rate for this region for tropical cyclones having D greater than the minimum selection for the ensemble of storms being considered (e.g., if the ensemble is restricted to hurricanes then D should equal or exceed 1 inch of Hg and the corresponding m will be lower than if the ensemble includes all tropical cyclones). The expected yearly occurrence of surge levels s or greater is then m P (S > s) and the return period Q is simply the reciprocal of the above quantity. By plotting Q versus s, one can also determine the value of s for which Q has a certain value; the s values so determined are referred to as the Q--year surge (e.g., 50-year surge, 100-year surge, etc.). It must be borne in mind, however what the real meaning of such quantities are: namely that in a given year there is a probability of 1/Q that s will equal or exceed the Q-year surge. This is to be distinguished from P(S > s) which is the probability of exceedence for s given that a storm has occurred in the region in question.

3-10. Traditional Joint Probability Procedure. In the application of the above formal methodology, certain approximations are usually made with respect to the nature of the pdf functions and their representation for purposes of practical calculation. Normally the storm climatology is not sufficient to allow a definitive rendition of the five dimensional joint probability function $f_{\underline{V}}(v)$. However, the climatological data are generally sufficient, for most regions, to allow a reasonable rendition of the marginal distributions of each of the five storm parameters. The marginal distribution for a given parameter like d is the pdf for D regardless of the value of any of the other parameters.

a. Statistical Independence of Parameters. If the storm parameters are statistically independent then there joint probability density for the five dimensional set is simply the product of the marginal pdf's for the five parameters:

$$f_{\underline{V}}(\underline{v}) = f_D(d)\, f_R(r)\, f_\Theta(\theta)\, f_V(v)\, f_L(l), \qquad [3\text{-}34]$$

where $f_D(d)$ is the marginal pdf for D, etc. This simplification is attractive and is frequently employed as the basis for the subsequent analysis. The question of whether or not the approximation is justified is a constantly recurring one of these studies; it will be addressed in a later section along with a discussion of some typical marginal distribution function. The parameter L is one which is usually considered independent of the others. Moreover its marginal distribution is generally considered uniform over the region, i.e.

$$f_L(l) = \frac{1}{L_m} \qquad 0 < l < L_m$$

or

$$P(L < l) = 1 - \frac{l}{L_m} \qquad [3\text{-}35]$$

However there are exceptions even to the assumption of independence of L which may occur for complicated coastal regions. The New York bight is an example where storm intensity can be correlated with location of landfall and/or θ.

b. Discretization of Parameters. A second approximation frequently made is to treat the statistical distribution functions in a discrete (histogram) sense, where functions like $f_D(d)$ are replaced by partial probabilities for a finite number of selected bands (cells) of d, and assigned to the midpont value d_n of the band. For example let $p_D(d_n)$ represent the integral of $f_D(d)$ over the nth band of d centered at d_n; the approximation is to associate the probability $p_D(d_n)$ specifically with d_n. It is justified if $f_d(d)$ is linear in the vicinity of d_n, or if the band width of the cell is suitably small compared with the standard deviation of d from its mean. Thus the nature of the approximation lies in the degree of resolution (number of cells for each variable) and the range of the variable represented in the discretized ensemble of the storm parameter population. The most important parameter with respect to resolution and range is D. The important constraint, regardless of resolution, is of course that the sum of the partial probabilities over all cells for a given parameter equals unity. Example application of discretized distributions are given in the references cited in Section 3-15.

c. Ideal Model Assumption.

(1) A third approximation made in most, if not all applications, prior to 1983 is to consider the surge, for a given set of storm parameters, to be deterministic and equal to the value $z(\underline{v})$ computed from the adopted storm surge simulation model. This is tantamount to assuming that the storm surge model employed in the procedure is perfect. Given this (unlikely) assumption, it follows that the conditional pdf $f_S(s \mid \underline{V} = \underline{v})$ is a Dirac-delta function which is zero everywhere except for s equal to the value $z(\underline{v})$ dictated by the storm parameters. Since many different combinations of the parameters can produce a common s, this implies in turn that Equation [3-31] reduces to the following integral

$$f_S(s) = \int_A f_{\underline{V}}(\underline{v})\, dA(\underline{v}) \qquad [3\text{-}36]$$

evaluated over that "surface" of storm parameter space for which $s = z(\underline{v})$. Alternatively, using [3-29], this means that the exceedence probability for S is given by the sum of the probabilities for all those storms of the ensemble for which the computed surge $z(\underline{v})$ exceeds s.

(2) The implementation of the latter concept is facilitated by the discretization of the storm parameter probabilities discussed above and the assumption of statistical independence of parameters. For the discrete system, the probability of a simulated storm, having $d = d_n$, $r = r_n$, etc., is given by

$$p_n = p_D(d_n)\, p_R(f_n)\, p_\theta(\theta_n)\, p_r(v)\, p_L(1_n) \qquad [3\text{-}37]$$

and the surge associated with this storm is $s = s_n$. If there are N possible values for each parameter, then there exist N^5 possible combinations of the parameters (i.e., N^5 storms associated with s_n). The exceedence probability for s is then the sum of those p_n for which $s_n > s$.

d. Preliminary Comments on Accuracy.

(1) The accuracy of the synthetic method results heavily on that of the climatological base for storms and its application for a particular region. Also it rests heavily on the accuracy of the storm surge model, including the wind field parameterization employed to simulate the water level response at a particular location. Realistic application of the method should recognize that both the wind field parameterization as well as the storm surge model have their limitations. They collectively yield only an estimate of the storm surge for given storm parameters. Because of this it is imperative that the characterization of the model adopted for application to the synthetic method be known or established by special tests. Data requirements for such models evaluations are discussed in item 25 of Appendix A. In particular, verification of the model against storms of record, where reliable storm and storm surge information is available, is essential before one can accept the model for use in the synthetic method. In addition, calibration of the model in terms of observed tidal response should also be considered as standard practice.

(2) Two kinds of errors can exist in the model results: bias and random error. A reliable model is one without significant bias and for which the variance of the random error is reasonably close to the variance of observed highwater marks for a particular event and location. For such a model, the effect of random errors can be taken into account via Equation [3-31], so as to allow for realistic estimates of the exceedence probability for surges. This will be addressed by way of a specific example in a later section. For the Gulf of Mexico, allowance for the effect of random error in the model can be even more important than the astronomical tide.

(3) Errors related to treatment of the storm climatology can occur due to improper discretization of the storm parameters or because of the use of assumed statistical independence of parameters. The first of these points is addressed very thoroughly in the National Research Council report (item 40 of Appendix A). In particular an alternative to discretization of storm parameter distributions is discussed. The question of statistical dependence of D and R is discussed in that report and is also addressed here in a later section.

(4) Another source of error relates to the manner in which astronomical tide is taken into account. For large tide and surge, the hydrodynamics become nonlinear and simple linear superposition can introduce a bias error. Also the approximate methods of combining the two effects stochastically can introduce further error. Some of the approximate methods of combining the surge and tide statistics will be discussed but no attempt will be made to address the errors in a quantitative manner.

3-11. Statistical Distribution of Hurricane Parameters. Useful summaries and analyses of hurricane parameter data are given in items 27 and 57 of Appendix A. These sources give information on the frequency of occurrence of hurricanes and of tropical storms for various coastal regions of the United States. Marginal distributions of D (or alternatively of central pressure), R, θ, and V are given for certain broad regions. The latter statistics are restricted to hurricanes. Some sample illustrations are given here.

a. Frequency of Occurrence of Tropical Cyclones. Figure 3-2 is a reproduction of the adopted frequency of occurrence of tropical storms and hurricanes along the gulf and east coast of the United States. These are given as numbers per 100 years per 10 n. mi, although they may be interpreted as yearly occurrences per 1000 n. mi of coastline. The ratio of landfalling hurricanes to total number of landfalling hurricanes plus tropical storms is shown in Figure 3-3. As can be seen this ratio averages about 0.5 for the entire gulf and east coast. Exiting storms (not shown here) are limited mainly to the Florida peninsula and the east coast.

b. Central Pressure and Pressure Deficit. Figure 3-4 shows sample cumulative probability plots for the marginal distribution of central pressure (mb) for typical gulf coast and east coast positions. Dashed lines represent estimated extrapolation to 100 percent probability for the tropical storms ($P_o > 982$ mb.). In these plots the curves represent subjectively smoothed relations.

(1) An alternative is to fit some assumed parametric form to the distribution. Figure 3-5 shows data on pressure deficit D for the gulf coast derived from Table 1 of item 27 and plotted on log probability paper. The fitted straight line represents a log normal fit with slope consistent with the standard deviation of log D. In constructing this plot a value of 0.5 has been used for the ratio of hurricanes to total tropical cyclones. This type of plot (or a plot of the type employed in the historical method) allows a reasonable basis for extrapolation somewhat into the region of low probability of exceedence of D and also across the region of low D corresponding to tropical storms.

(2) The same data if plotted as log $P(D > d)$ versus D also yields a nearly straight line fit, at least for $P(D > d)$ less than 50 percent. This simple exponential type distribution will be found useful in later analysis.

c. Radius to Maximum Wind. Data on R for the gulf coast taken from Table 1 (in item 27 of Appendix A) has been analyzed in a manner similar to D and is presented in Figure 3-6. This shows a remarkably good representation of probability of exceedence of R as log normal:

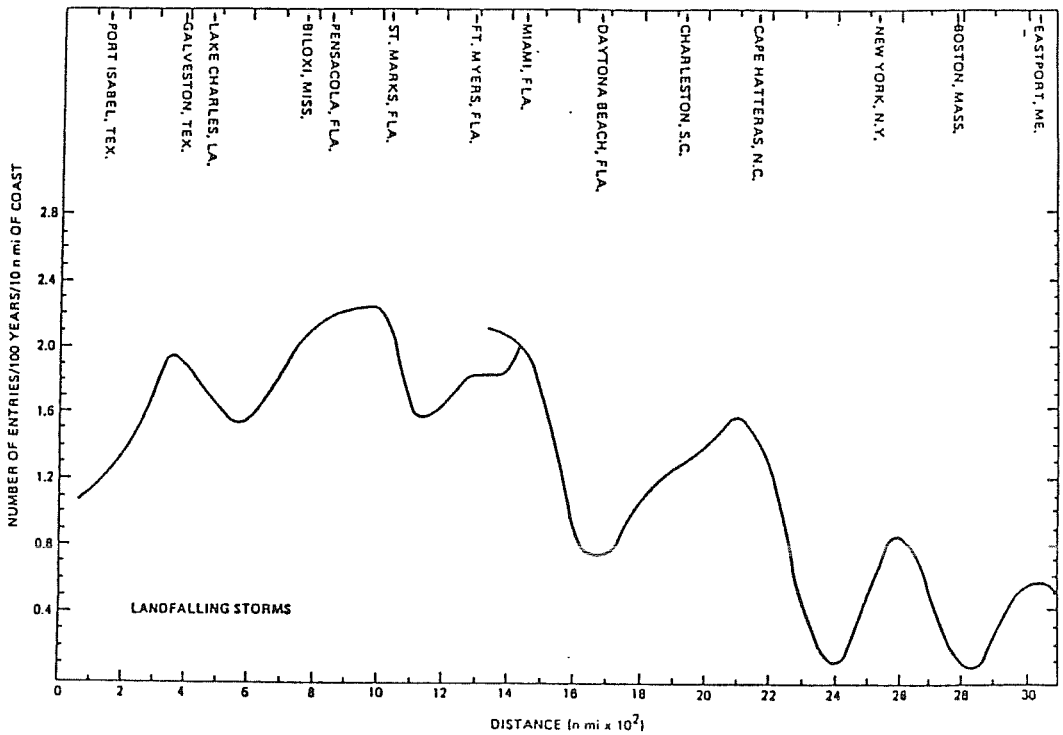

FIGURE 3-2
Adopted frequency of landfalling tropical stories and hurricanes (1871-1973) for the gulf and east coasts of the United States. (item 27 of Appendix A).

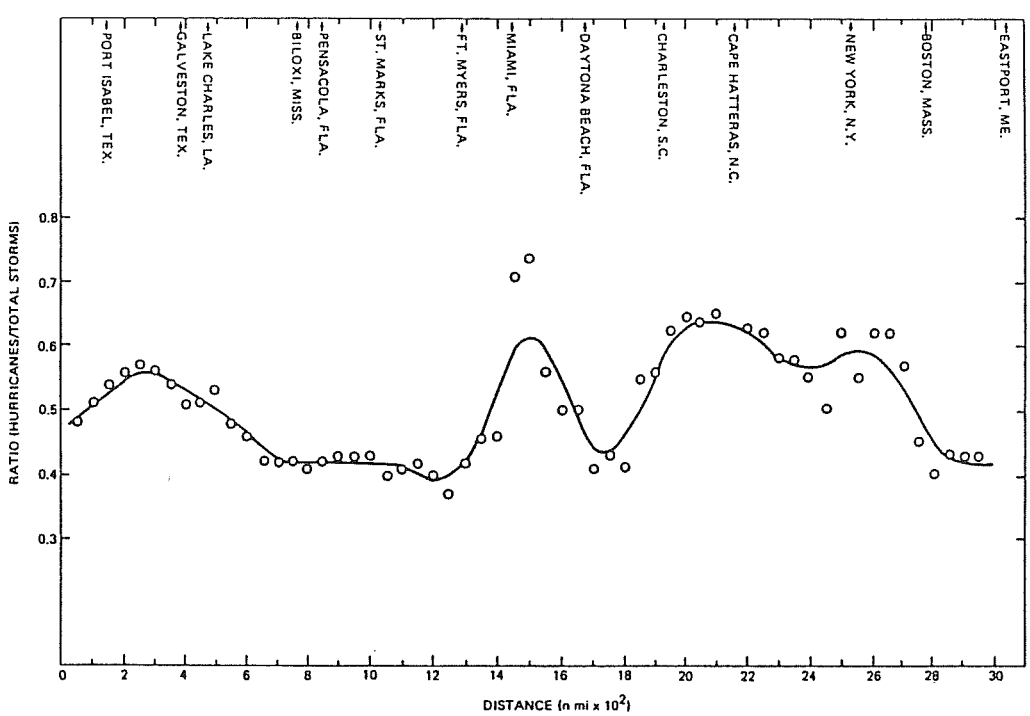

FIGURE 3-3
Ratio of landfalling hurricanes to total number of landfalling hurricanes and tropical storms (1886-1973). Based on counts in overlapping zones centered at 50-n.mi. intervals and objective smoothing along the coast. (item 27 of Appendix A)

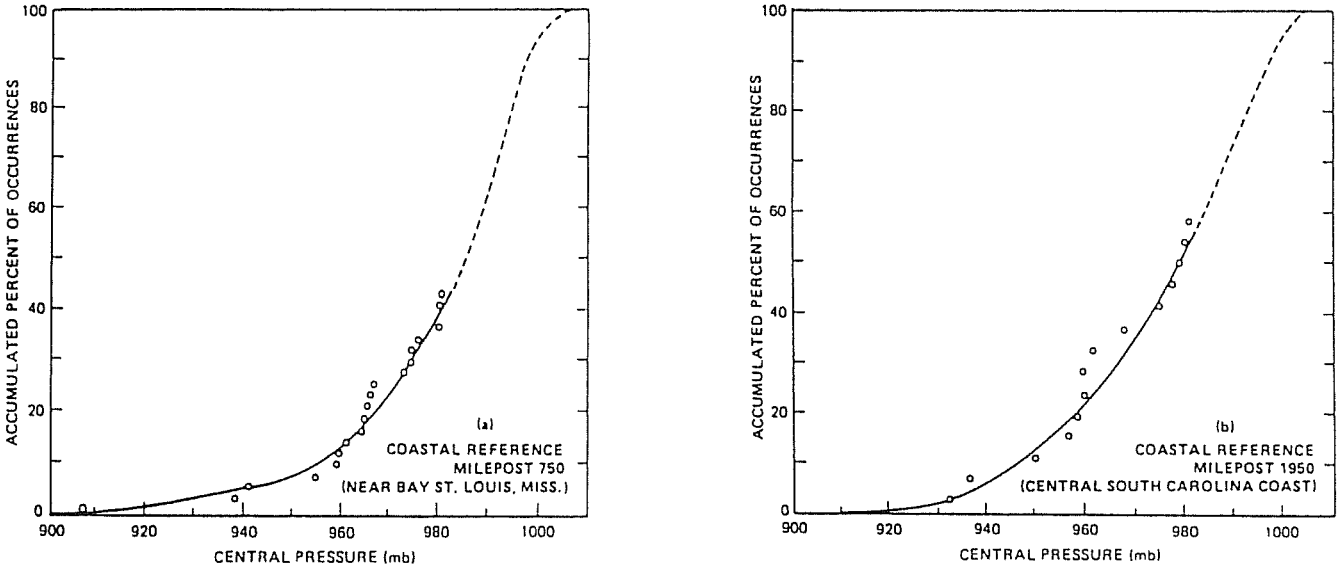

FIGURE 3-4
Graphs of central pressure versus cumulative percent of occurrences (a) Gulf of Mexico (milepost 750), near Bay St. Louis, MS., where Hurricane Camile went ashore and (b) east coast (milepost 1950) along central South Carolina coast. (item 27 of Appendix A).

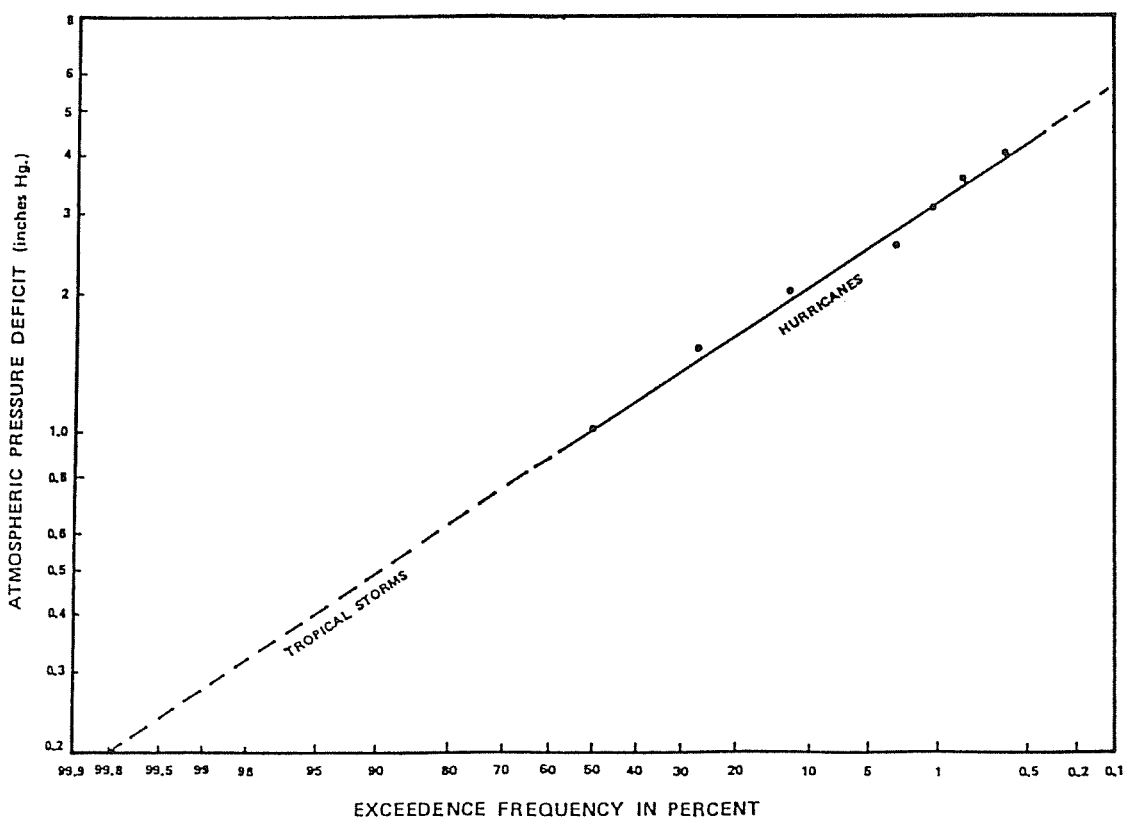

FIGURE 3-5
Exceedence probability of D for landfalling gulf coast hurricanes and tropical storms (estimated as 50 percent of total).

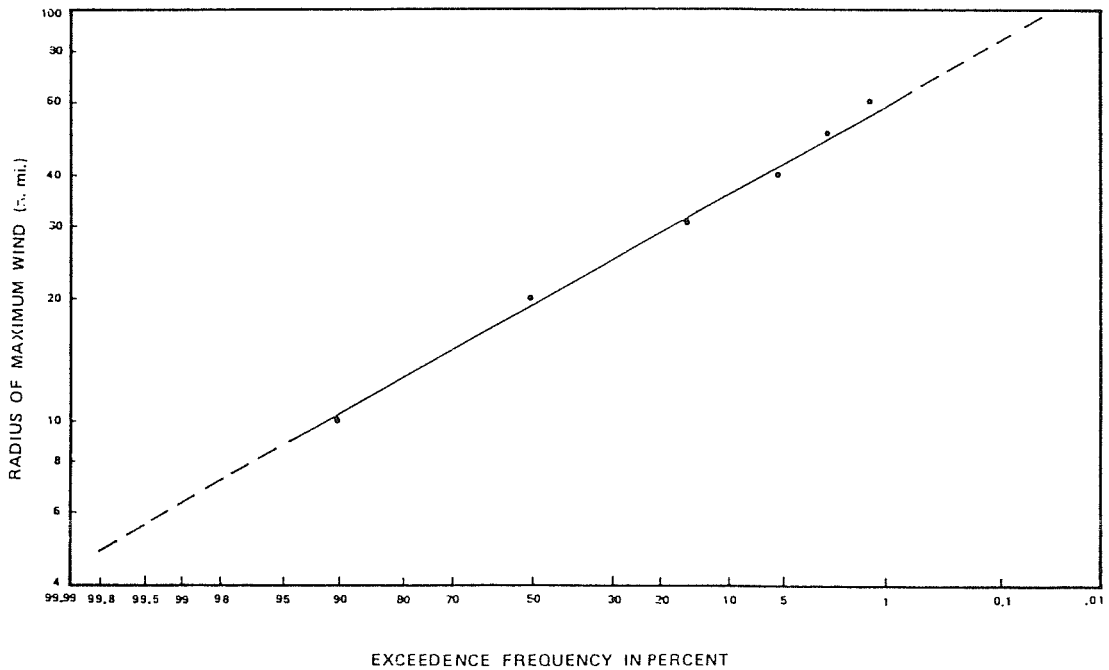

FIGURE 3-6
Exceedence probability of R for landfalling gulf coast hurricanes.

$$P(R > r) = \text{erfc}\left(\frac{\eta}{\sqrt{2}\sigma}\right) \qquad [3\text{-}38]$$

where $\eta = \log r$ and σ is the standard deviation of η. A similar relation applies to the representation for D in Figure 3-5.

d. Hurricane Propagation. Sample cumulative probability plots for forward speed and direction of hurricane propagation for the gulf and east coast are shown in Figures 3-7 and 3-8. It should be remarked that the latter reference contains generalized plots of the probability distributions for each storm parameter as a continuous function of position along the gulf and east coast (similar to Figures 3-2 and 3-3 but with contours of cumulative probability).

e. Question of Statistical Dependence of Parameters.

(1) This question is addressed by item 57 as well as in item 40 of Appendix a. Item 57, in particular, shows computed correlations among all combinations of parameters. These analyses support the concept of statistically significant negative correlation between R and D (or positive correlation for R and central pressure), but only marginally significant correlation among other hurricane parameters. There is a sound physical argument to support correlation between R and D, since conservation of angular momentum dictates that as a hurricane deepens and its maximum winds increase, the scale must shrink (assuming the total angular momentum is not changed). For any particular application the available data on hurricane parameters should be examined carefully to ascertain whether correlations exist for the region under consideration.

(2) The focus in this section is on possible relations between R and D. Figure 3-9 shows a scatter plot of R versus D for the gulf coast hurricane data derived from item 57 of Appendix A. Since it is restricted to hurricanes, a data void exists for $0 < D < 1$ inch. It is known however that the tropical storms in this range have R values which tend to exceed those of hurricanes. With this in mind, the visual inverse relation between r and D displayed in this figure is rather compelling.

(3) An important additional question to address is whether the existence of a correlation is important. The answer to this has been addressed in item 40 of Appendix A and is affirmative; results of special sensitivity tests presented in that report indeed show that if negative correlation is allowed in analysis of R and D statistics then the surge level for given return period Q is reduced by a small, but statistically significant amount. In other words by suppressing the possibility of combinations of large R with large D the probability of high surges is reduced. This is primarily due to the fact that for given D, the main effect of an increase in R is to increase the width of the coastal surge profile which thereby increases the probability of given surge height at a particular point. In addition, an increase of the peak surge height can occur due to an increase in R for given D.

(4) Given the importance of resolving the question of statistical dependency of R and D, it is pertinent to look to an alternative method of analysis of the R, D statistics. Figure 3-9 for the gulf coast data suggest an inverse relation such that log R and log D might be negatively correlated. Indeed an analysis of the latter shows a trend with a slope close to -1/2. This suggests replacing R by the following transform

$$Y = R\, D^{1/2} \qquad [3\text{-}39]$$

If the hypothesis is made that Y and D are statistically independent, then the covariance of log R and log D is negative and numerically equal to one-half the variance of log D. This is indeed verified (via an F-test) for both the gulf coast and east coast data.

(5) Figure 3-10 shows contours of Y superimposed on the same plot as in Figure 3-9. From this plot one can construct a contingency table (item 32 of Appendix A) for Y and D (Table 3-3). Entries are the number of hurricanes with Y and D values falling in the cells shown. Values in parentheses are the expected number which would exist in the cells if Y and D were truly independent and if the marginal distribution were the same as for the sample. These are simply the products of row totals times column totals divided by the total population,

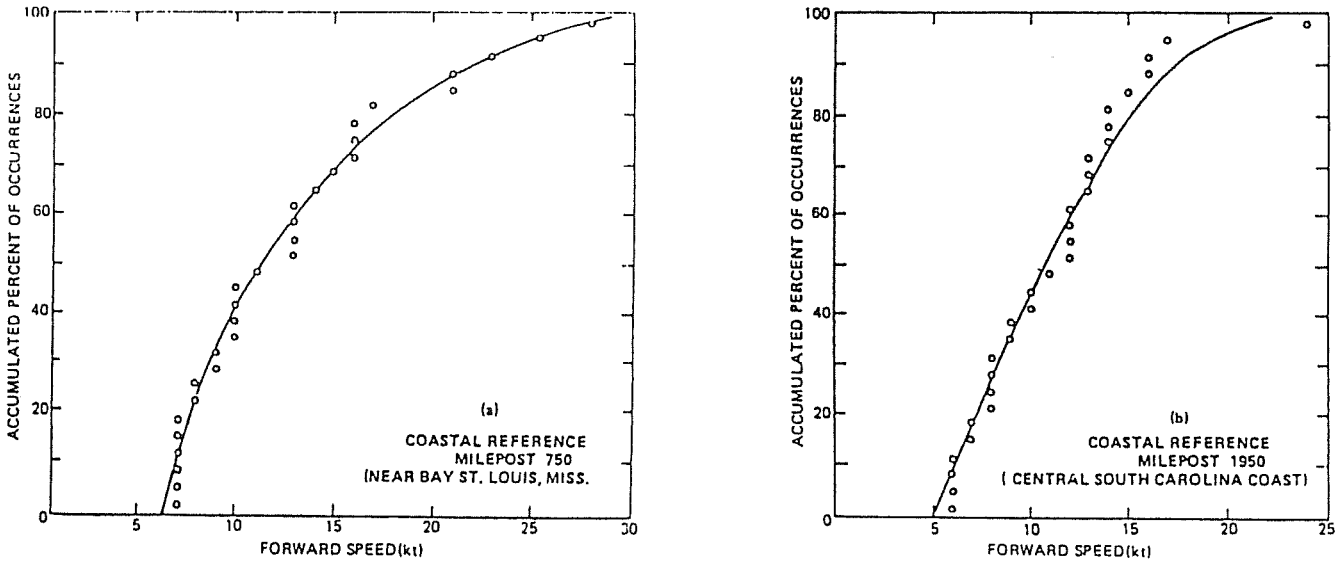

FIGURE 3-7
Landfalling hurricanes, forward speed versus cumulative percent of occurrences, (a) Gulf of Mexico (milepost 750) near Bay St. Louis, Miss., (b) east coast (milepost 1950) along central South Carolina coast. (item 27 of Appendix A)

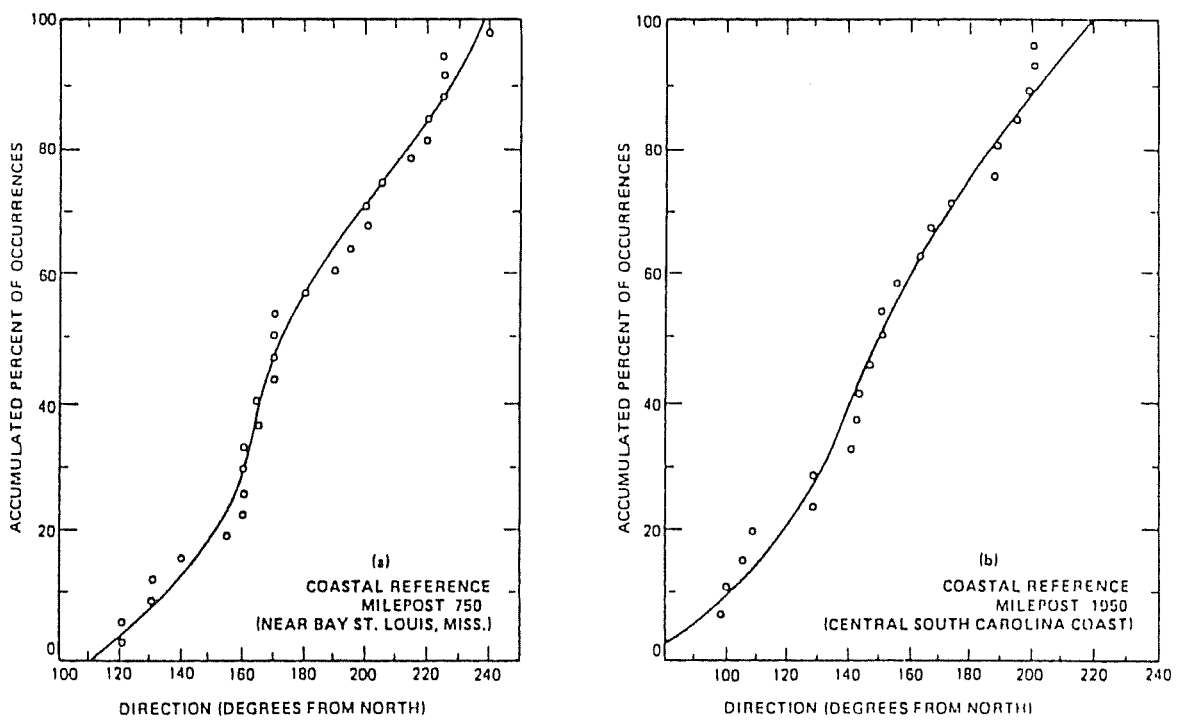

FIGURE 3-8
Landfalling hurricanes and tropical storms, direction of motion versus cumulative percent of occurrences, (a) Gulf of Mexico (milepost 750) near Bay St. Louis, Miss., (b) east coast (Milepost 1950) along central South Carolina coast. (item 27 of Appendix A)

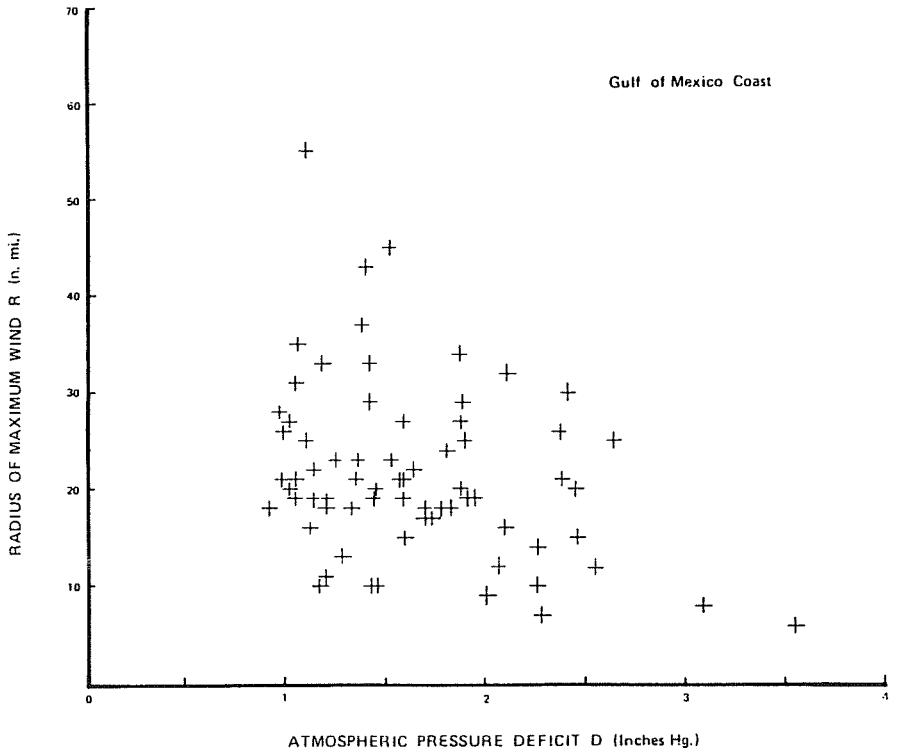

FIGURE 3-9
Scatter plot of R versus D for landfalling gulf coast hurricanes (1900 to 1977).

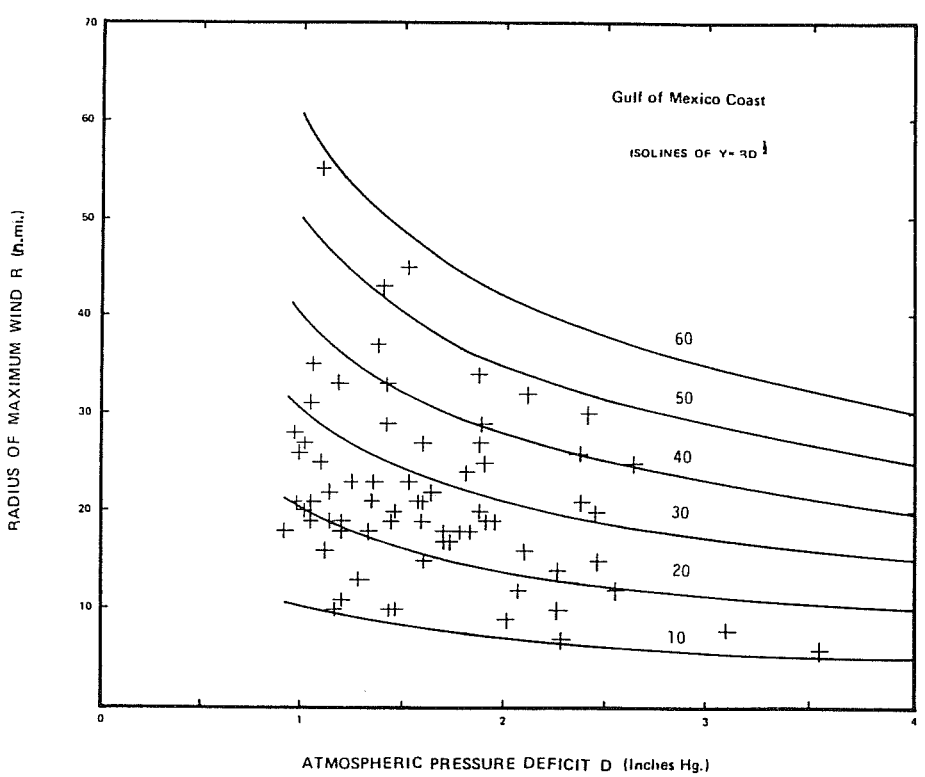

FIGURE 3-10
Contours of Y (= $RD^{1/2}$) on a R versus D plot with data points as in 3-9.

TABLE 3-3
Contingency Table for Y and D (Gulf Coast hurricane data)

D	0.9-1.5	1.5-2.0	2.0-4.0	Row Totals
Y				
40-60	3 (4)	3 (3)	3 (2)	9
30-40	5 (6)	4 (4)	3 (2)	12
20-30	16 (15)	13 (10)	3 (7)	32
0-20	9 (8)	2 (5)	6 (4)	17
Column Totals	33	22	15	70

TABLE 3-4
Contigency Table for R and D (Gulf coast hurricane data)

D	0.9-1.5	1.5-2.0	2.0-4.0	Row Totals
R				
31-60	6 (4)	2 (3)	1 (2)	9
25-31	6 (6)	4 (4)	2 (2)	12
17-25	15 (15)	14 (10)	3 (7)	32
0-17	6 (8)	2 (5)	9 (4)	17
Column Totals	33	22	15	70

R (n. mi.), D (inches Hg), $Y = R D^{1/2}$

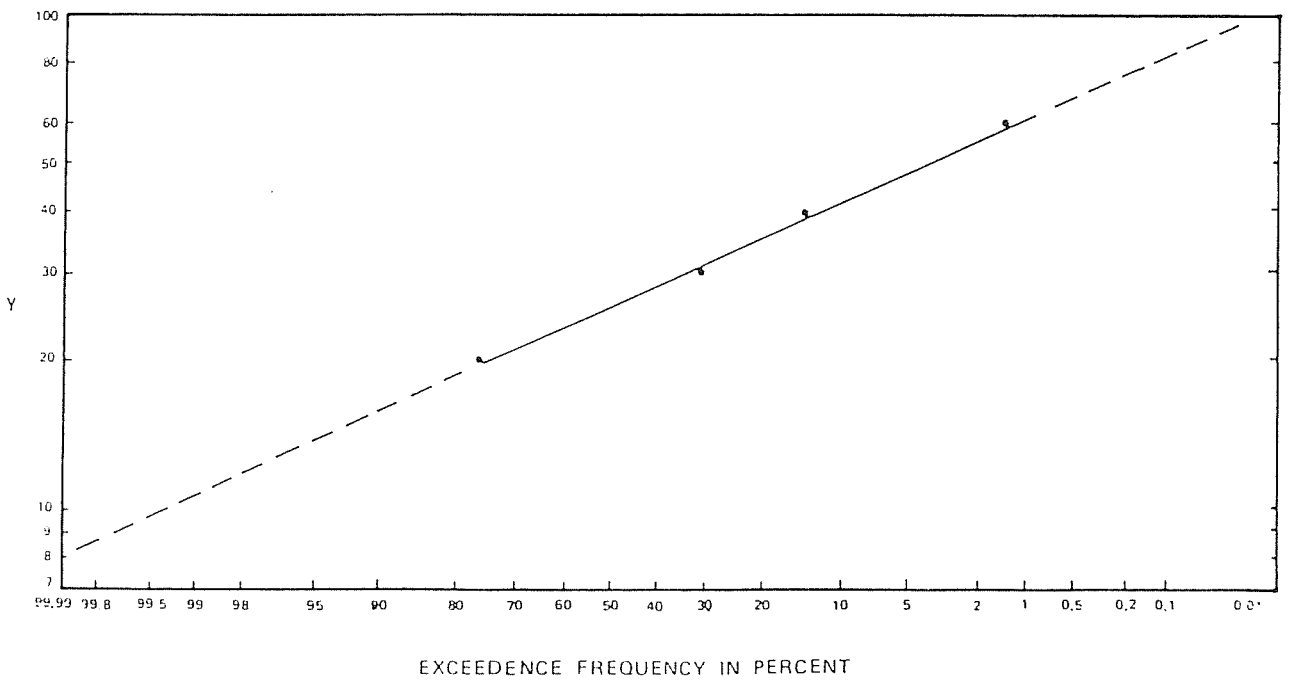

EXCEEDENCE FREQUENCY IN PERCENT

FIGURE 3-11
Exceedence probability of Y for landfalling gulf coast hurricanes. $Y = R D^{1/2}$ where R has units of n. mi. and D inches of Hg.

then rounded to the nearest whole number (e.g., for the upper left cell 9 x 33/70 = 4). A chi-square test with 3 x 4 - 6 = 6 degrees of freedom shows 25 percent probability that the differences are due to sampling variability. A similar contingency table for R and D (Table 3-4) can be constructed with 3 cells for D identical to those of Table 3-3 and 4 cells for R, such that the row totals are identical to those of Table 3-3. This permits a fair comparison with the Y and D analysis, since the values expected for independency of R and D (in parentheses) are identical to those of Table 3-3. The resulting chi-square value from Table 3-4 is nearly twice that of Table 3-3 and indicates that there is less than 5 percent probability that the differences are due to sampling variability. This supports the hypothesis that it is Y and D, rather than R and D, which are reasonably independent in a statistical sense.

(6) If one accepts the hypothesis of independent Y and D, then the role of R should be replaced by Y as a storm parameter, and the statistical independence concept retained to estimate the joint distribution. This requires the marginal distribution for Y rather than R in the calculations. For the gulf coast data, Y seems to be reasonably well represented by a log normal distribution (Figure 3-11). Where R is needed in the parameterized wind field, it is readily calculated from $Y D^{-1/2}$.

(7) In passing it is of interest to note that the maximum wind speed of W_m in the hurricane is proportional to $D^{1/2}$ (item 57 of Appendix A); hence Y is proportional to $W_m R$, which is the angular momentum per unit mass in the core of the hurricane. Thus the above hypothesis implies that the core angular momentum and the central pressure deficit are statistically independent.

(8) Before leaving this subject of possible R and D correlation it should be remarked that of all the storm parameters R is the most difficult to determine accurately. Indeed the evaluation of R depends on the choice of hurricane model. The analysis of this section employed the R data presently available. It is emphasized that the parameterization of hurricanes is an evolving one and that future studies may lead to more accurate methods of determining the scale parameter R, in which case the whole matter of R and D correlation must be readdressed.

3-12. Surge Simulation. In a reasonable well resolved application of the discretized joint probability method, the number of class values for D, R, θ, V and L might be taken as 8, 4, 5, 5 and 10 respectively. This corresponds to an ensemble of hypothetical storms with 8000 different combinations of parameters typical of hurricanes and tropical storms for the region in question. Actual simulation of the surge evolution for each of these 8000 storms using the adopted hydrodynamical surge model is normally cost prohibitive and in fact unnecessary.

a. Interpolational Procedure. A realistic approach in terms of cost effectiveness (without significant loss of accuracy) is to select a representative subsample of storms spanning the parameter space; by running simulations with the model for the subsample and estimating the surges for the remaining cases by an appropriate interpolational procedure, a considerable saving in computer effort can be realized if the subsample is much smaller than the total ensemble of storms. For example, previous experience shows that the peak surge elevation is very closely approximated by a linear function of D for a given site, other parameters being held fixed. This implies that the minimum number of D values in the subsample could be as low as two (preferably and lowest and highest of the original ensemble). However three values is preferable in order to allow some degree of nonlinearity. With respect to parameter L, the variations of the peak surge at fixed location is quite nonlinear and closely resembles the variation of peak surge profile with distance along shore (for the case of landfalling storms). Hence a large number of L values is generally required. Clearly one must exercise judgement in the selection of the subsample, depending on the range of parameters, coastline configuration, etc. Item 40 of Appendix A discusses an interpolational procedure which is based on a technique commonly employed in computer-contouring known as the inverse-square-distance interpolation. Another technique is the use of multidimensional cubic splines (items 15 and 17 of Appendix A).

b. Accuracy of Storm Surge Model. A comparison of existing numerical models of storm surges was carried out for the Office of Chief of Engineers by the Committee on Tidal Hydraulics (1980). Four different operational models were included in this test in which simulations of five hurricanes of record were carried out (Carla, 1961; Camille, 1969; Gracie, 1950; Hazel, 1954; and Eloise, 1972). Two of the models displayed a definite bias (one consistently overestimated and one consistently underestimated the peak surge). Such bias is readily minimized in terms of an appropriate adjustment in the associated wind field model employed (item 40 of Appendix A). However, even if such bias is minimized, there remains a substantial variance of the results compared with available observations. An analysis of the coastal profiles of peak surge elevations from model results and observational data shows an overall variance (after eliminating the bias) of about 6 ft^2, which corresponds to a root mean square error of about 2.5 ft. This is based upon 146 comparisons for the four models and the five hurricanes (about 7 comparisons from the coastal profile data per storm). The overall mean value of observed peak surge elevation in this comparison was 11.5 ft with a variance of about 28 ft^2 (standard deviation of 5.3 ft). Thus for individual storms the error variance after removal of bias is about 20 percent of the observed variance of peak level and the ratio of the rms error to the mean is similar (about 22 percent). This much error variance in model performance is difficult to ignore.

c. Provision for Model Variance.

(1) It is understood that in the above analysis of discrepancies between surge model results and observations that the astronomical tide has been subtracted, such that the error variance of the model (after removal of bias) is in fact more properly to be regarded as that variance of the observed surge which is not predicted by the model. Thus, unless one makes special provision in the methodology, the surge statistics emerging from simulations of storm response based on a typical model with valid climatological input will always have an associated variance which is too small. Moreover if there is a bias in the model, then a bias will also exist in the mean associated with the computed surge statistics. Clearly, the latter must be removed; the most effective method being to adjust the model so as to minimize any bias.

(2) With respect to the remaining unpredicted variance, it is not essential that attempts be made to refine the model so as to reduce the variance, as long as it does not exceed the value discussed in the previous section (which represents present state of the art). In fact any significant reduction is probably not feasible without expanding the model domain, including more physics in the hydrodynamic model, and increasing the degrees of freedom in the associated wind model. Three of the primary reasons for the unpredicted variance by the model are: incomplete information at the seaward boundary, lack of explicit allowance for wave set-up, and a wind model which is too idealized. The only way to remedy the lack of information at open boundaries is to employ a model encompassing a basin wide scale. To allow for wave set-up would require coupling a wave prediction model with the surge model; this would ultimately be desirable but is not presently a state of the art capability. To refine the wind model to make it more realistic would require more storm parameters; this in turn would require a re-analysis of the entire historical data base on hurricanes in order to establish the statistical characteristics for expanded parameterization, not to mention the additional quantum jump in the simulation costs.

(3) The alternative is to combine the estimated unpredicted variance (whatever the cause) with that predicted by the model simulations from known storm parameter climatology. The method for accomplishing this has already been identified via the fundamental relation in Equation [3-31]. In order to implement this, one needs an appropriate representation of the conditional probability function for S, given a specific set of storm parameters. a suggested candidate function is given in item 40 of Appendix A; this is simply the normal distribution function

$$f_S(s|\underline{V}=\underline{v}) = \frac{1}{\sqrt{2\pi}\,\sigma_s}\exp\left\{\frac{-[s-z(\underline{v})]^2}{2\sigma_s^2}\right\} \qquad [3\text{-}40]$$

where σ_s^2 is the variance of s about z and z is the value of s predicted by the model for given $\underline{v}$. For $\sigma_s \to o$ the above reduces to a Dirac-delta function. More generally σ_s^2 can be identified with the variance not accounted for by the model prediction. This relation pertains to unbiased models in the sense that an average of $z(\underline{v})$ over a given ensemble of parameters $\underline{v}$ corresponds closely to the average observed S associated with the same ensemble of $\underline{v}$.

(4) As an example illustration, suppose that σ_s is simply a constant for a given model (another logical possibility would be that $\sigma_s/z(\underline{v})$ is a constant for the model). As a further simplification suppose that the integral in Equation [3-31] can be replaced by an integral over the single dominant storm parameter d and that $z = \alpha d$ where α is a constant. This is equivalent to employing an integral over z with $f_d(d)$ replaced by $f_z(z)$. The latter being the pdf for S without allowance for the effect of σ_s. Finally the latter pdf is approximated by the exponential distribution

$$f_z(z) = \frac{1}{h}\exp\left(-\frac{z}{h}\right) \qquad [4\text{-}41]$$

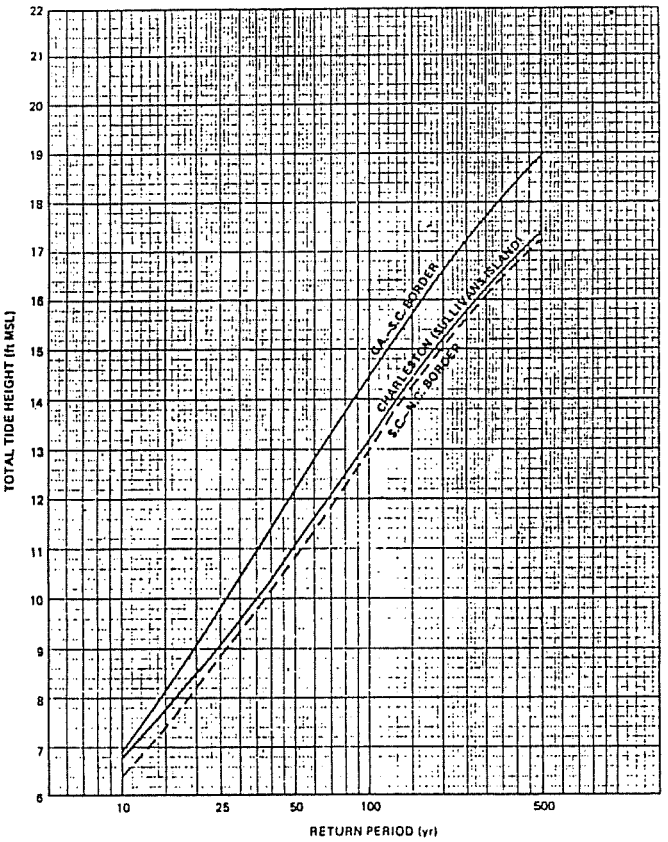

FIGURE 3-12
Tide frequencies at selected points on the South Carolina coast. (item 47 of Appendix A)

which implies an exceedance probability

$$P(Z > z) = \exp\left(-\frac{z}{h}\right) \qquad [3\text{-}42]$$

where h is a constant with the same dimensions as z. Examples of nearly exponential relations of this sort are shown in Figure 3-12, taken from an application (item 47 of Appendix A) of the joint probability method to the South Carolina coast. Here S is plotted versus log Q; note that $Q = (mP)^{-1}$. A true exponential distribution would be a straight line whose slope is proportional to h (h is the e-folding scale, i.e. the interval of S for which P and hence q changes by a factor of e).

(5) Under the foregoing restrictions, the pdf for S is given by the integral

$$f_S(s) = \frac{1}{\sqrt{2\pi}\, h\sigma_S} \int_0^\infty \exp\left[\frac{-(s-Z)^2}{2\sigma_S^2} - \frac{Z}{h}\right] dZ \qquad [3\text{-}43]$$

For values of $s >> \frac{\sigma_S^2}{h}$ this yields

$$f_S(s) = \frac{1}{h} \exp\left[-\frac{s}{h} + \frac{1}{2}\left(\frac{\sigma_S}{h}\right)^2\right] \qquad [3\text{-}44]$$

and hence

$$P(S > s) = \exp\left(-\frac{s'}{h}\right) \qquad [3\text{-}45]$$

where

$$s' = s - \frac{1}{2}\frac{\sigma_S^2}{h} \qquad [3\text{-}46]$$

Comparing this with Equation [3-42] we see that z and s' have identical exceedence probability; this implies that $s = z + 0.5\,\sigma_s^2/h$ for given exceedence probability. Hence the effect of the variance σ_s^2 is to increase all surge elevations by a constant amount $\sigma_s^2/2h$ over the values which would be obtained by ignoring the imperfections of the model. For the example of Figure 3-12 (upper curve), h = 3.0 ft based on the interval $10 < Q < 500$ years. Using $\sigma_s^2 = 6$ ft^2, as discussed earlier, gives $\sigma_s^2/2h$ of one ft., which implies that all S values should be increased by 1.0 ft. (i.e., a shift of the origin).

(6) Had the model contained bias, implying that the coefficient α in the relation $z = \alpha d$ is too low or too high, then it can be shown that the slope h is altered by the factor α/α_e where α is the model value and α_e is the expected or optimum value. Thus, while the random error in the model produces a simple shift of the S scale, bias produces a stretching or shrinking of the S scale. The effect of bias for large return periods therefore can be more serious than that of random error. This underscores the earlier statement that the error characteristics of the model must be known, via very thorough verification tests against hurricanes of record, if estimates of surge statistics having required tolerance are to be obtained. Moreover, it is preferable that bias be minimized in the model prior to its use in simulation runs, since it is difficult to correct after the fact for the general case.

(7) It is emphasized that the foregoing analysis involves a number of approximations. However it serves to illustrate the importance of considerations of model errors in the joint probability method. Moreover it contains the principles for more exact analysis in actual applications.

3-13. Distribution of Astronomical Tides. The astronomical tides represent an almost period, predictable part of the total water level variation. Some typical tide predictions for the Atlantic and Gulf of Mexico stations are shown in Figure 4-8, referenced to the local datum. As can be seen, the Atlantic coast tides are primarily semi-diurnal but with an inequality in the height of the two high tides per lunar day (24.84 hrs.). The tides in much of the Gulf of Mexico, from Pensacola westward, are dominantly diurnal but much smaller in range than those on the east coast. Tides along the west Florida shelf, like Key West, are mixed semi-diurnal and diurnal. All of the tidal regimes display a fortnightly modulation of amplitude, with highest tides at the time of new moon and full moon. Tidal amplitudes also vary from year to year with a period of about 19 years (the metonic cycle). In addition to the short period semi-diurnal and diurnal tides, longer period oscillations exist in mean sea level, the largest being that associated with the annual tide (which also includes effects of seasonal heating/cooling and changes in the general circulation). All of these known variations for a given station can and should be included in the joint probability method for establishing the combined surge and tide statistics for that station.

a. Statistics of Tides.

(1) Item 24 of Appendix A is an excellent reference on tides, tidal datums and tidal statistics for application in the joint probability method. This report gives tables and graphs of the cumulative probability for hourly astronomical tide, high and low tides, and extreme monthly high and low tides (all referenced to local mean sea level) for all primary and some secondary National Ocean Survey tide gage locations of the United States. The astronomical tides have a distinct upper and lower bound which can be realized at least once during a given 19 year period.

(2) An example of tidal statistics for Sandy Hook, New Jersey (item 24 of Appendix A) is shown in Figure 3-13; this includes a sample hourly tide sequence. The tidal heights in feet can be obtained by noting that the mean range (4.67 ft. for this station) is equal to the interval MHW-MLW. The parameter σ on the elevation scale is the standard deviation of

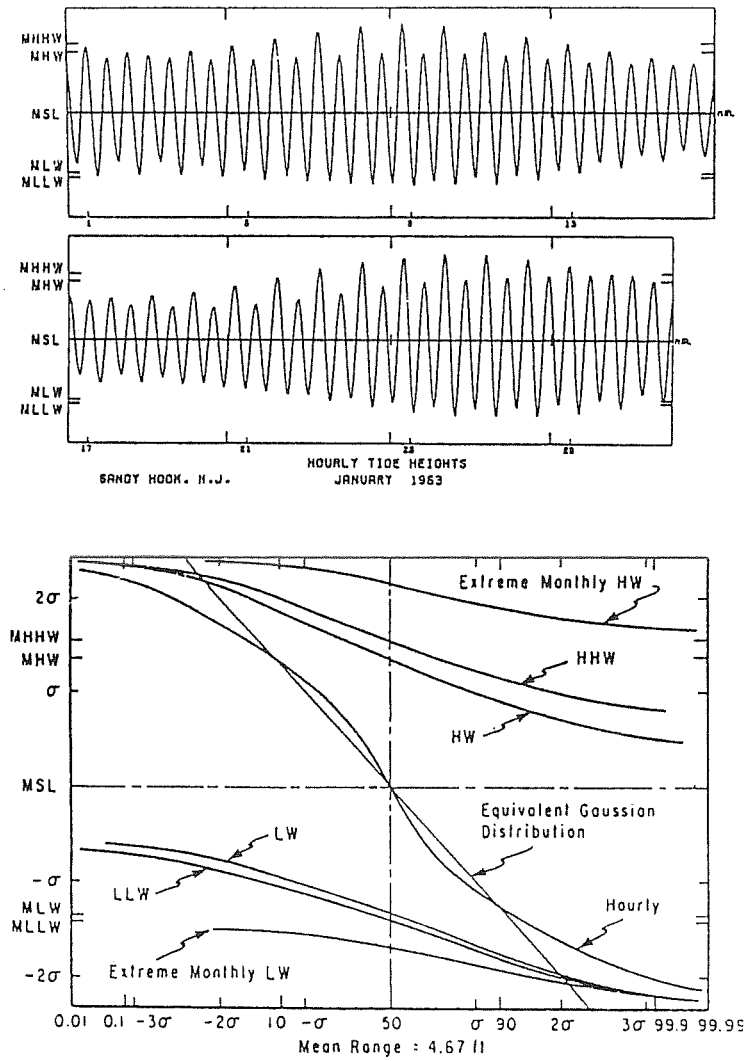

FIGURE 3-13
Cumulative probability for hourly tide, high water HW, low water LW, diurnal high HHW, diurnal low LLW, extreme monthly high, and extreme monthly low for Sandy Hook, New Jersey (lower panel); sample hourly tides (upper panel). (item 24 of Appendix A)

all hourly heights for the station over a 19 year period; for Sandy Hook $\sigma = 1.70$ ft., implying a variance of 2.89^2. The 19 year extreme high is 4.2 ft. and the extreme low is -4.0 ft.; these are the upper and lower bounds of the plot. The points σ, 2σ, 3σ on the abscissa indicate the positions on the probability scale corresponding to these elevations, for an equivalent Gaussian (normal) distribution of hourly values. The absicissa scale is such that a normal distribution would be a straight line. This example, which is typical, emphasizes that the statistics of hourly tides departs significantly from that of a normal distribution.

b. Long Period Variations of Tide.

(1) In addition to the predictable seasonal variation in mean sea level, there exist variations from year to year in mean sea level at most stations. The latter consists of a long term trend of the order of a foot per hundred years, upwards in mid-latitude stations along mainland U.S.A. but downwards for high latitude stations like Yakutat, Alaska (item 24 of Appendix A). Superimposed on this mean trend are unpredictable variations from year to year or decade to decade, having a variance of the order of a few tenths of a foot.

(2) The trend in sea level is perhaps best taken into account by allowing for an increase of mean sea level datum at least equal to that which would occur during the life expectancy of a given coastal structure.

(3) The seasonal variations likewise should be taken into account deterministically by allowing for the mean sea level which is expected during the mid part of the storm season.

3-14. Combination of Surge and Tide. The total tide is a combination of the astronomical and storm induced changes in water level. As remarked earlier, the most desirable approach would be to include the astronomical tide within the hydrodynamical model with appropriate forcing. This is not feasible for two reasons, one technical and the other practical. To include the astronomical tide in the model requires appropriate forcing at the open sea boundary, in such a way as to yield the correct tidal response along the coast. The accuracy with which the resulting tides can be reproduced in state of the art models, is perhaps better than that of surges, but only at the cost of considerable additional preliminary efforts in tuning the forcing to yield the correct response for a given region. While such extra efforts to solve this technical problem are not out of the question, the cost required in routine runs of the combined surge and tide can be increased by an order of magnitude. The reason for this is that an extra random parameter (the amplitude and phase of the tide relative to the surge) must be introduced, such that for each storm to be simulated, a separate run must be made for the selected number of amplitude and phases of the tide during a representative fortnightly period. The alternative is to add the effects of tides to the surge assuming that the two effects are linearly superimposable. This is a compromise between cost and accuracy. There are various approximate methods for combining the surge and tide in a appropriate stochastic manner. These are discussed in the next several sections starting with the most accurate. An important point to be borne in mind in the selection of a given approximate method is that of consistency with the error of tolerance which one is willing to accept.

a. Basic Method.

(1) It must be stressed that the focus of interest in tide statistics is on maximum water level associated with the combined tide and surge during a given storm event. Thus for a given storm of the chosen ensemble, one predicts the surge at given site A from the model. Such predictions give a surge hydrograph versus time at site A. If the absolute time of peak surge were known, as in the case of a storm of record, then the hourly predicted tide for the period of the surge can be added to the surge hydrograph to yield a resultant total tide from which the maximum water level for the event can then be determined. Since the surge hydrograph and the tide have different shapes and time scales there is no simple method of determining the maxima of the two components other than adding the hour by hour values and searching for the maximum.

(2) For probability studies, obviously the time of occurrence of the peak surge is a random variable. The peak surge can occur at any hour of the day, any day during the storm season, and any year of the metonic cycle of the tide.Thus even for a single storm event there is a large ensemble of possible realizations of combined tide and surge. If one employs time steps of 1 hour (somewhat coarse for the semi-diurnal tide) by which to progressively shift the surge relative to the tide, then in order to cover all possible realizations for storm seasons of 120 days out of every year for 19 years requires 54,720 combinations (from which the same number of maximum water levels are deduced). Remember, this is for one storm event. If 8000 storm events are to be considered, this leads to

over 4 x 10^8 such combinations for one site! Now multiply this by the number of sites to be studied. Obviously one must seek some practical compromise between accuracy and computer effort even for this linear superposition problem. Before addressing the various approximations of this basic method it should be noted that the exceedence probability for total tide is obtained the same way as for surge alone. Specifically, the entire ensemble of maximum combined tide, for all storm events and all tidal phasing, is ordered by elevation and the fraction exceeding a given level yields the probability of exceedence for a single storm event.

b. Approximation A. The most accurate of the approximate methods is to carry out the above type of combination of tide with the simulated surge hydrograph, for given storm and given site, for a restricted sample of the astronomical tide. Specifically one can employ a typical tide regime corresponding to a lunar month (two fortnightly cycles) with given extreme monthly high and low tide.

This requires 28 x 24 = 672 combinations using a progressive one hour shift. In order to account for the variation of extreme monthly range of the tide, the latter can be discretized into say 5 bands of equal probability, using statistical information similar to that of Figure 3-13 for the site in question (but perhaps based on data only for the storm seasons during 19 years). This would imply a total of 672 x 5 = 3360 combinations per storm event, which represents a reduction in effort of over 16 fold over that of the basic method, but with comparable accuracy. A variation of this method has been employed in studies discussed in item 59 of Appendix A. Another possibility is to employ a typical year of tide regime (one for which the nodal factor for each constituent has its average value); use of a single average node factor does not distort the statistics greatly.

c. Approximation B.

(1) The second method of approximation is applicable to tidal regimes which are predominately semi-diurnal (as along the east coast of the United States). This involves adding the surge hydrograph at selected phases to a simple cycle of the tide for given high water elevation (HW) and given low water (LW), but allowing a discrete set of the latter with known probabilities similar to those of Figure 3-13. Generally in the application of this method about 10 HW, LW combinations together with 20 tide phases are employed for each storm event. This reduces the effort to 200 combinations per storm event. However its accuracy is less than that of Approximation A since a sinusoidal tide is employed to combine with the surge. It is therefore not recommended for mixed tide regimes.

(2) This method has been applied in a number of studies by the National Weather Service (NWS), an example of which is given in NWS report 16 (item 47 of Appendix A). A further approximation in the NEW methodology is to parametrize the surge hydrograph as a Gaussian curve characterized by three parameters: height S, standard deviation τ (or an alternate measure of temporal scale) and the time of the peak surge, τ_m relative to the tide of high tide. Thus the approximate surge hydrograph Z(t) is

$$Z(t) = S \exp\left[-\frac{(t-t_m)^2}{2\tau^2}\right] \qquad [3\text{-}47]$$

while a typical astronomical tide cycle is given by

$$A(t) = H \cos \omega t \qquad [3\text{-}48]$$

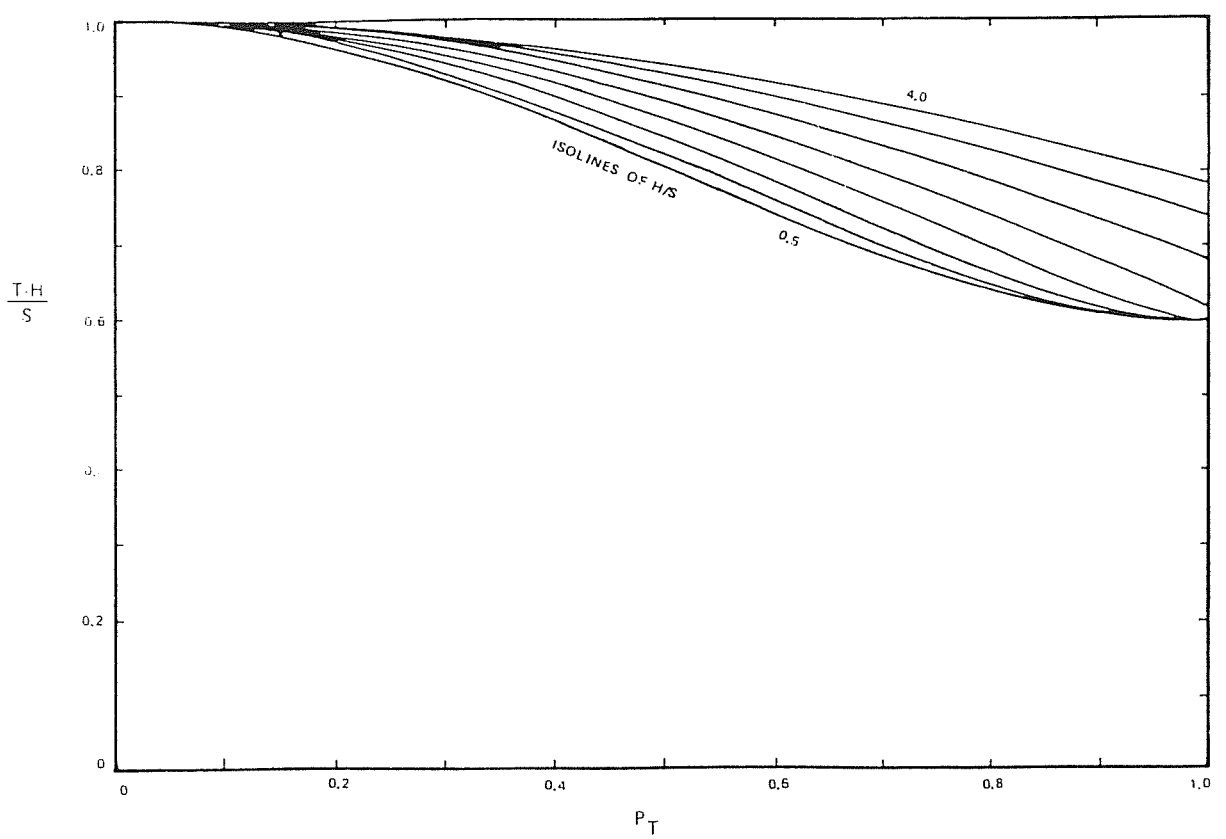

FIGURE 3-14
Exceedence probability of (T-H)/S = 0.2 and selected values of $\omega\tau$ in steps 0.5 from 0.5 to 4.0

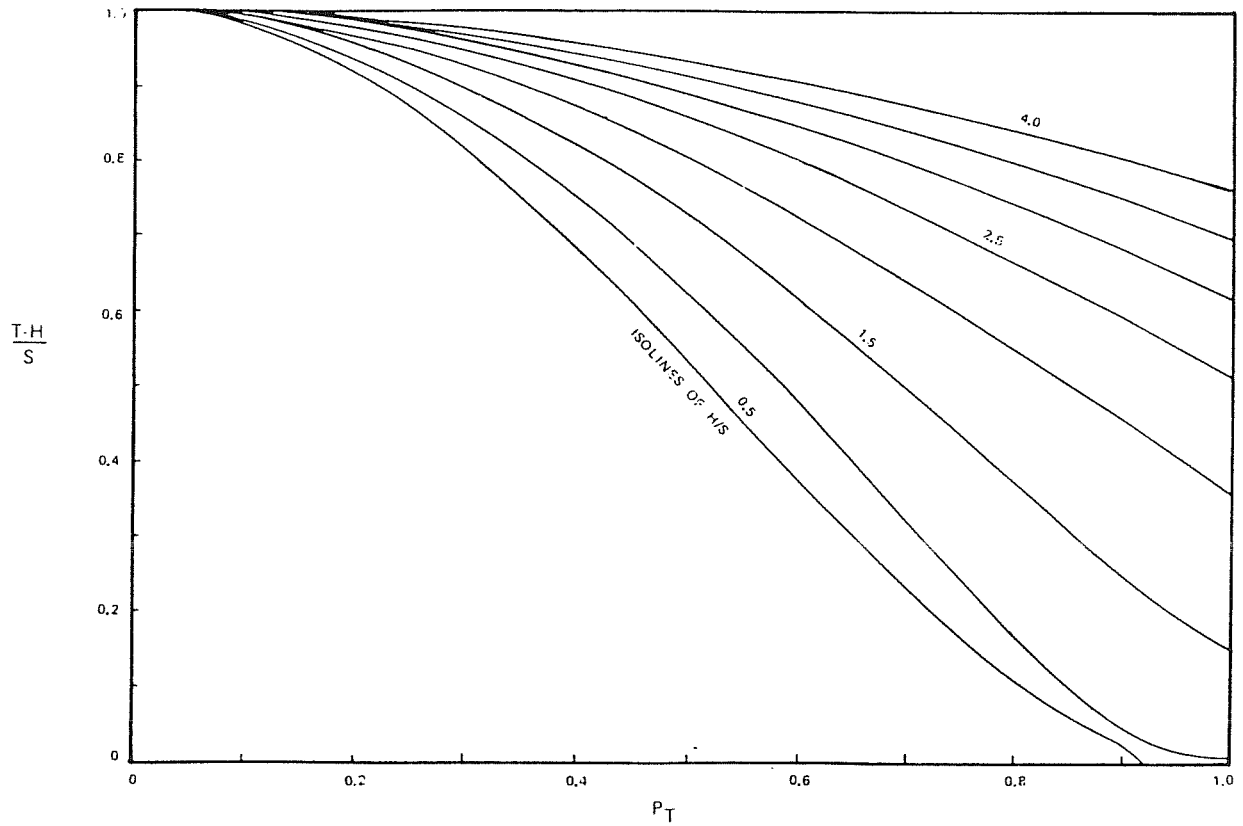

FIGURE 3-15
Exceedence probability of (T-H)/S for H/S = 0.5 and selected values of $\omega\tau$ in steps 0.5 from 0.5 to 4.0.

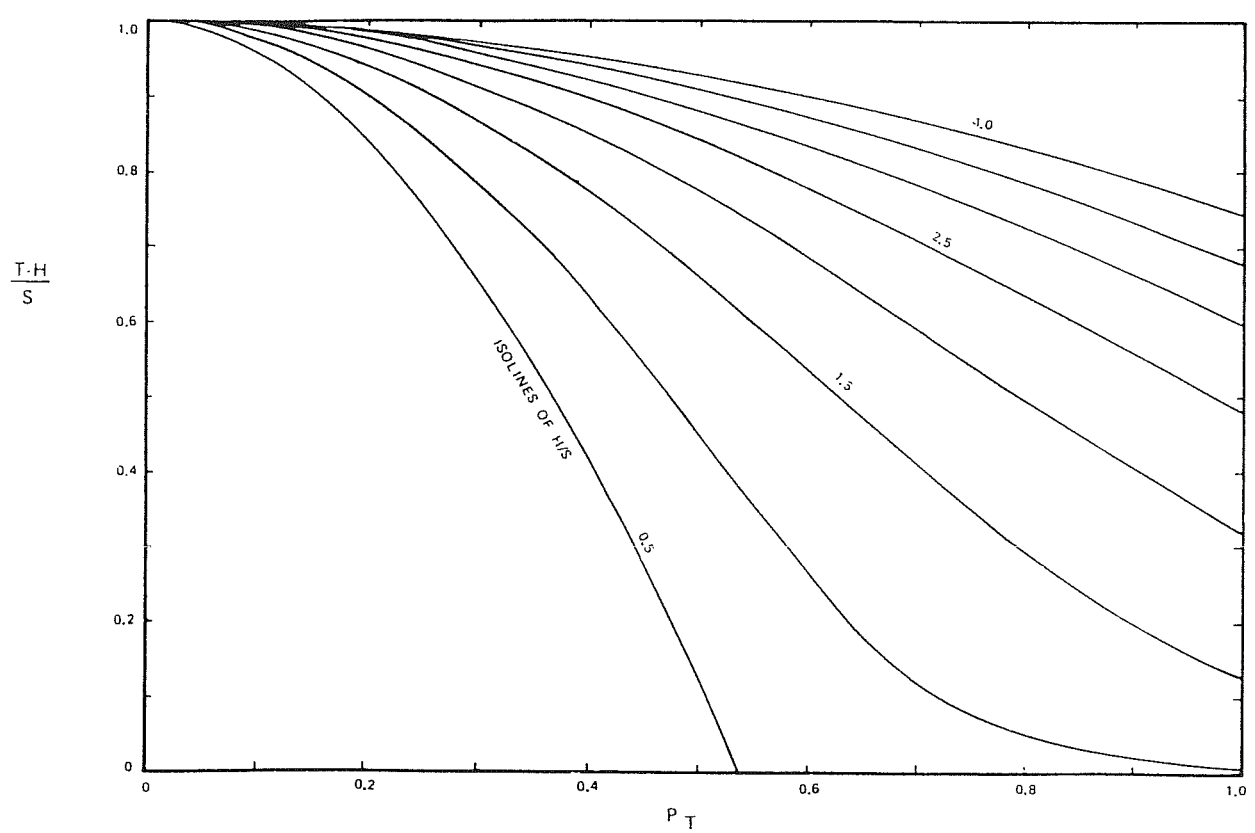

FIGURE 3-16
Exceedence probability of (T-H)/S for H/S = 1.0 and selected values of $\omega\tau$ in steps 0.5 from 0.5 to 4.0.

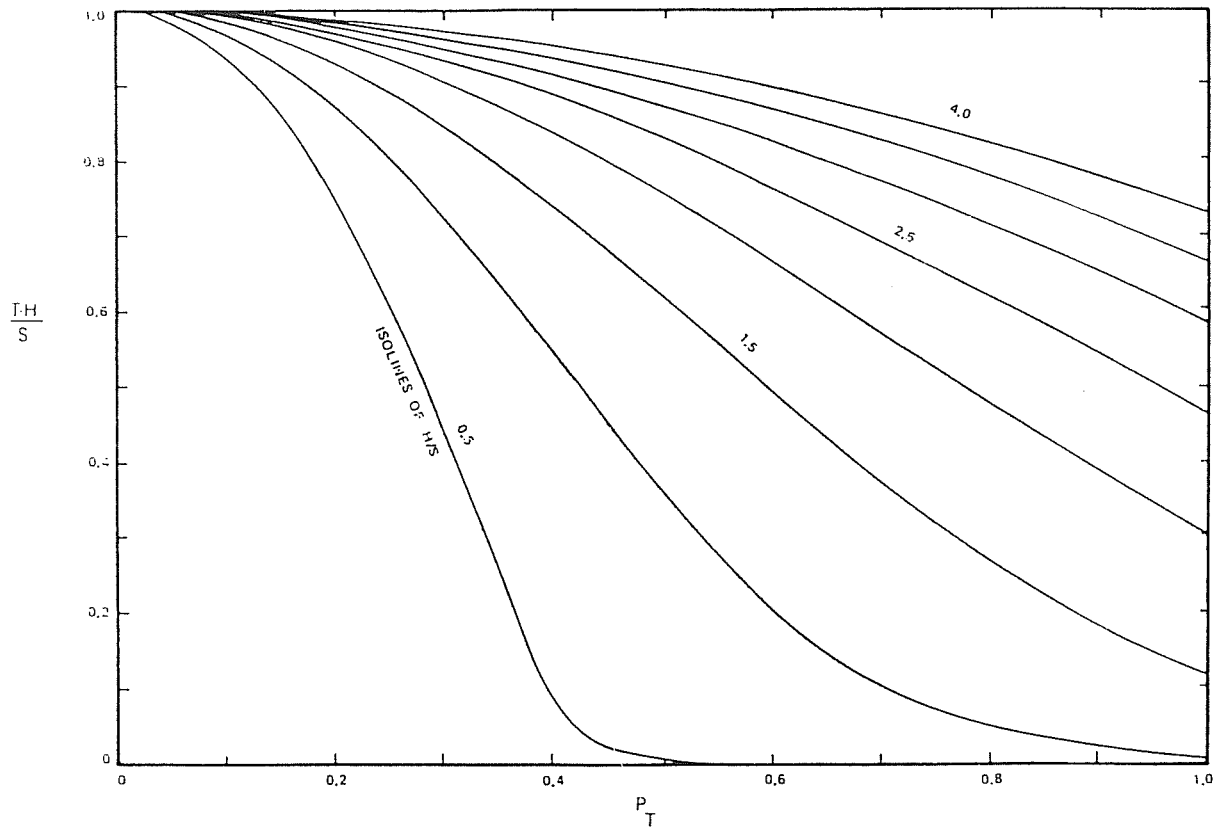

FIGURE 3-17
Exceedence probability of (T-H)/S for H/S = 2.0 and selected values of $\omega\tau$ in steps 0.5 from 0.5 to 4.0.

where H is the amplitude and ω the frequency (2π/period) of the tide. In this approximation H = (HW - LW)/2.

(3) Each of the parameters S, τ, t_m and H are to be regarded as stochastic: s, τ, t_m being realizations for a random storm and H a high water realization for a randomly selected tidal cycle. However for particular combinations of S, τ, H one can evaluate the maximum combined tide T = 0 Max [A(t) + Z(t)] as a function of ωt_m. But since ωt_m is random with uniform probability in the interval 0 to π (or $-\pi$ to 0), the variable $\omega t_m/\pi$ is a measure of the probability for T. Hence it is possible to construct plots of exceedence probability P_T for selected values of the dimensionless parameters H/S and $\omega\tau$. Moreover, since T must fall in the range H to H + S, a convenient non-dimensional scale for plotting of T is the transform (T - H)/S, which has the range 0 to 1. Figures 3-14 to 3-17 show the latter quantity versus the exceedence probability P_T for selected H/S and selected $\omega\tau$. As an example, Figure 3-16 shows that for the case of H//S = 1 and $\omega\tau$ = 0.5, (T - H)/S can be expected to exceed 0.85 with a probability of 20 percent. It is emphasized that this is for given S, τ and H.

(4) Two extreme cases are of interest. For $\omega\tau >> 1$ and H/S > 1

$$T = H + S \exp\left[-0.5 \left(\frac{\pi P_T}{\omega\tau} \right)^2 \right] \quad ; \qquad [3\text{-}49]$$

while for $\omega\tau < 1$ and H/S << 1

$$T = S + \cos(\pi P_T) \quad . \qquad [3\text{-}50]$$

The first case corresponds to a relatively small surge of several days duration superimposed on a large amplitude semi-diurnal tide; this is typical of the situation for winter storms on the northeast coast of the United States. The curve for $\omega\tau$ = 4 in Figure 3-17 (H/S = 2) is represented well by relation in Equation [3-49]. The second case corresponds to a combination of large surge of short duration and small diurnal tide; the case of hurricane Camille landfalling on the northern gulf coast is an example. The curve for $\omega\tau$ = 0.5 in Figure 3-14 is represented well by relation in Equation [3-50].

(5) For the general case, Figures 3-14 to 3-15 indicate a wide variation in the relationship between (T - H)/S and P_T for different relative time scales for surge and relative tidal amplitude H/S. Bear in mind that the exceedence probability P_T is for fixed S, τ, and H. To get the exceedence probability for given S and τ but randomly selected tidal regime, the above probability must be appropriately combined with that of H (the high water statistics) as discussed earlier. Finally the exceedence probability for T with the storm and the tidal regime selected at random is a further convolution with the statistics of S and τ.

d. Approximation C.

(1) For the case of small $\omega\tau$ and low amplitude tides (compared with surge), the approximation B can be generalized to the form

$$T = S + A(t) \quad . \qquad [3\text{-}51]$$

The exceedence probability for T - S for given S is the same as that of the hourly tides, an example of which was given in figure 3-13. This implies that in order to obtain the exceedence probability for T, a simple convolution of the exceedence probability for S with the pdf for hourly tides is sufficient.

Moreover, if the further approximation is made that the hourly tides have a Gaussian distribution with standard deviation σ and that the surge statistics are exponential, as in Equation [3-42], then an analysis similar to that of section 3-12 shows that the exceedence probability of T is the same as that of S + $\sigma^2/2h$.

(2) This very simple approximation may be justifiable for gulf coast studies where σ is typically small. A comparison of this kind of approximation with the much more exact method A is given in item 59 of Appendix A for application to Naples, Florida. For this location S = 0.94 ft (item 24 of Appendix A, Table 7) and h = 2.9 ft. (determined from Figure 4.3, item 59 of Appendix A). This yields a value of $\sigma 2/sh$ of 0.23 ft, which compares very favorably to the difference between the curves for T and S for low exceedence probability determined by the more exact procedure.

(3) While method C is a rough approximation, and of course, limited to small σ, the resulting small differences between T and S for given exceedence probability is such that the effort required by a more exact method is not warranted.

3-15. Concluding Remarks on the Synthetic Method.

a. This lengthy tutorial on the synthetic method has emphasized the principles of the methodology and some features which have not previously been addressed explicitly, such as the effect of errors in the surge model and the concept of nonlinear transformation of the storm parameters to achieve a set which is statistically independent. Detailed applications of the method are beyond the scope of this manual. Numerous applications exist in the literature. For details, the reader is referred to the following example applications: items 26, 27, 29, 30, 46 and 47 of Appendix A.

b. It should be remarked that in some of the studies carried out by the National Weather Service account is made of the correlation of R and D by employing a conditional probability of R for given D, which favors lower R for high D (see for example item 28 of Appendix A). It should also be noted that in most applications, the adopted surge levels for a given return period at a given site are checked against historical data for the site. If differences exist at the low return periods (where the historical records are most reliable) then adjustments can be made in the final curves to reflect effects possibly not included in the analysis, such as normal weather regimes or underidentified seasonal or year to year changes.

c. Finally it should be pointed out that while linear superposition of surge and tide may be justifiable for open coast situations, it is generally not sufficient for estuaries. For the latter situation a more realistic approach is discussed in item 52 of Appendix A.

CHAPTER 4
RELATED EFFECTS

4-1. General. This chapter presents methods and procedures for estimating the effects of direct rainfall, direct surface runoff, fluvial inflows, astronomical tide, initial water level and wave setup in water level determinations. Direct surface runoff is defined herein as the rainfall excess that drains off the land (non channelized) into the adjacent water body. Rainfall and wave setup effects were identified in Chapter 1 as two of the processes associated with storm surge generation, however, all of these effects can contribute to the total rise of water level in coastal waters during storm periods. The total rise at maximum stage is, of course, of paramount importance since it is this water level that is used in planning and design of coastal projects.

4-2. Direct Rainfall and Direct Surface Runoff.

a. As previously indicated, rain falling on the open sea usually has a minimal effect on the surge produced along the open coast. However, in estuaries and in areas where low-lying terrain landward from the coast is flooded, rain may cause a rather substantial rise in the local water level. Water levels may be increased either from direct rainfall over the water body or inundated area, or as a result of direct surface runoff from adjacent land areas. Prediction of probable rainfall amounts and their distribution is thus essential in estimating design water levels for many coastal regions. Rainfall information is also important in design of pumping facilities and gravity drainage structures in connection with hurricane flood protection projects.

b. Rainfall associated with severe landfalling tropical storms has been studied by a number of investigators. Item 13 of Appendix A (published in 1926) was among the first studies concerned with mapping the areal distribution of hurricane rainfall. This study revealed that in a moving hurricane rainfall was asymmetrically distributed with the heaviest amount being in front (60 to 80 miles) and to the right of the storm center. It was also found that relatively little rain falls to the rear of the storm. Furthermore, it was noted that when the storm motion ceases the rainfall pattern becomes more symmetrical with respect to the storm center. Subsequent investigations of hurricane rainfall have in general substantiated these findings.

c. The methodology presented for estimating rainfall associated with hurricanes is based on a study conducted in 1968 as discussed in item 21 of Appendix A. In this study, frequency and areal distributions of rainfall were developed from 46 tropical storms that crossed the Gulf Coast between Apalachicola, Florida and Brownsville, Texas. Unfortunately, no investigation similar to the latter has been carried out for the Atlantic Coast of the United States. Inasmuch as the methodology presented is strictly applicable to the coastal region in the Gulf of Mexico, it is possible to estimate the tropical rainfall along the east coast of the United States by using a modified version. The necessary modification to the methodology is discussed later in this section.

d. Although item 21 of Appendix A provides frequency and areal distributions of rainfall in zones from 25 miles offshore to 100 miles inland, only one zone (Zone A) is considered herein. It extends from the coastline to 25 miles inland--an area that is usually of primary concern in storm water level determinations. Point rainfall depth for a given frequency and a given distance from the left or right of the storm track is considered to vary uniformly along the coast for any given storm. Also, the rainfall depths are considered uniform, along any line parallel to the storm track extending across the 25 mile wide zone. Point rainfall for selected frequency levels at either 6 and 12 hour intervals before landfall and after landfall is shown in Figures 4-1 to 4-6. Hours indicated as negative values in the figures signify hours before landfall. Figure 4-7 is used to transform point rainfall for 6 and 12-hour intervals for the various frequency levels to area rainfall (areas up to 1000 square miles).

e. For design purposes, the rainfall duration within the selected zone is presumed to be a function of the speed at which the tropical storm moves through the zone. At a given point within the zone, rainfall duration is assumed to be directly related to the forward speed of the storm, regardless of the path prescribed for landfalling storms. It is further assumed that rainfall duration is related to the storm translation speeds in accordance to the Standard Project Hurricane Criteria as high translation speed (HT), moderate speed (MT) and slow speed (ST). On this basis the rainfall duration for a HT storm is taken as 12-hours (6-hours before landfall and 6-hours after landfall), for a MT storm 24-hours (12 hours before landfall and

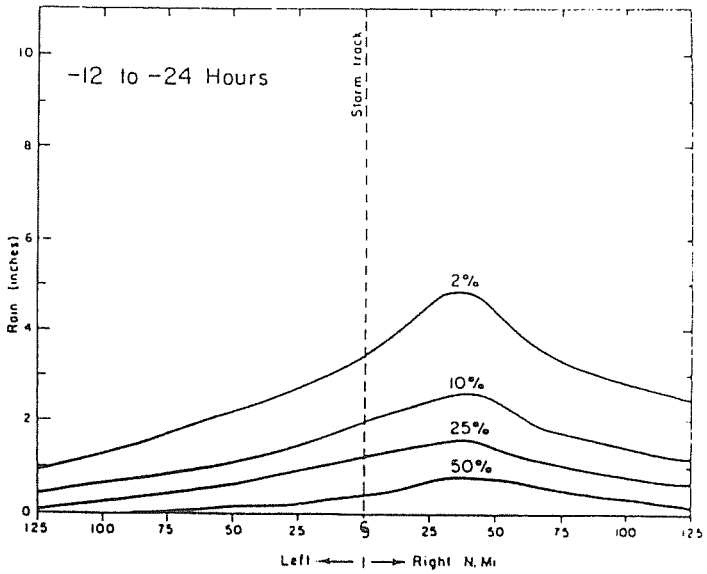

FIGURE 4-1
Rainfall for selected frequency levels for 12 to 24 hours before landfall. (item 21 of Appendix A)

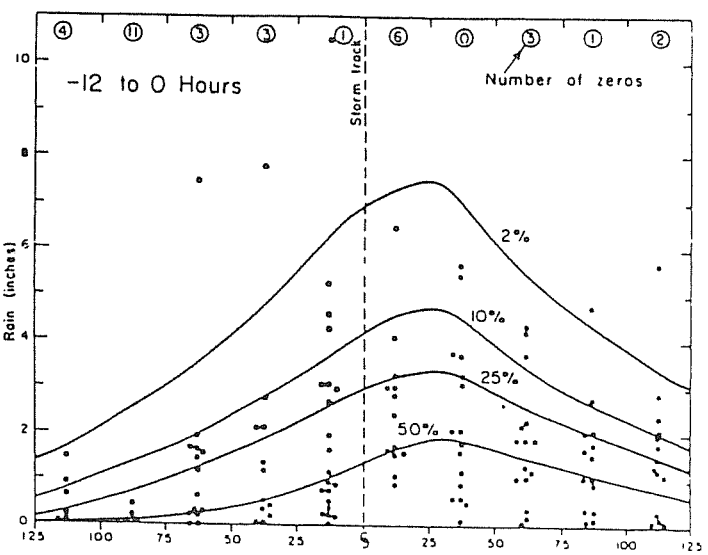

FIGURE 4-2
Rainfall for selected frequency levels for 12 hours before landfall. (item 21 of Appendix A)

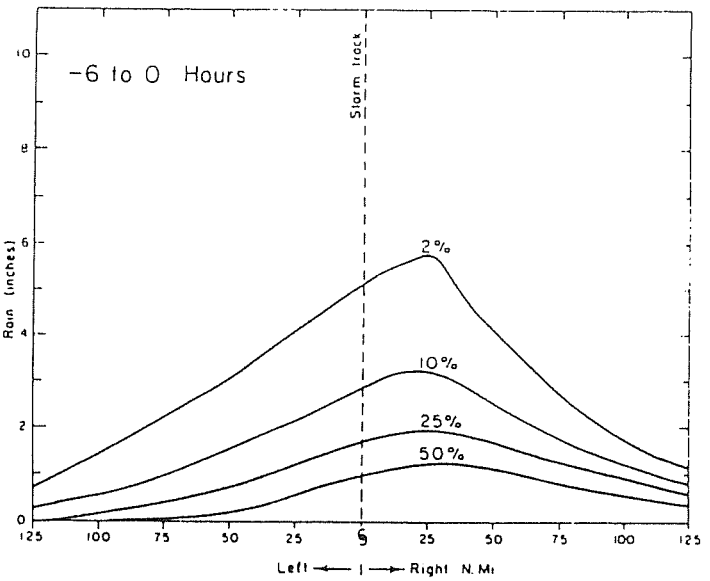

FIGURE 4-3
Rainfall for 6-hour period preceding landfall for selected frequency levels. (item 21 of Appendix A).

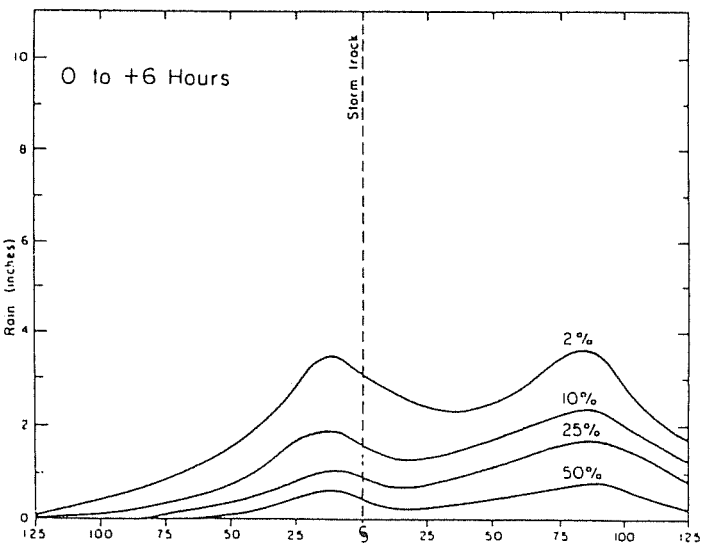

FIGURE 4-4
Rainfall for 6-hour period after land fall for selected frequency levels. (item 21 of Appendix A).

12-hours after landfall) and for ST storm 48-hours (24-hours before landfall and 24-hours after landfall). The basis for the later assumption is that a high speed storm will pass over the zone rather rapidly while a slow speed storm will subject the zone to a much longer rainfall duration.

f. Point rainfall data as exhibited in Figures 4-1 to 4-6 depict curves for the 2-, 10-, 25- and 50-percent levels of occurrence. The 2-percent curve implies that 98 percent of the expected rainfall depths on the average corresponds to the curve or below and 2-percent are above for a given period and distance from the storm track. Because the 2-percent curve will usually provide a conservative estimate of the rainfall, it is recommended for approximating the design rainfall.

g. The following problem will illustrate the procedures required to determine the average expected rainfall coincident with a tropical storm moving over a coastal zone.

EXAMPLE PROBLEM

Given: A moderate speed design hurricane enters a coast and moves over the zone along a path perpendicular to the coast.

Find: The average rainfall expected over an area of 500 square miles centered 50 miles to the right of the projected storm path.

Solution: Because the storm is moving at a moderate speed, the point rainfall must be determined 12-hours before landfall and 12-hours after landfall. From Figure 4-2 the point rainfall depth 12-hours before landfall is about 6.1 inches at the distance 50 miles to the right of the storm track; and according to Figure 4-5 the point rainfall 12-hours after landfall is about 6.3 inches. The adjustment ratio from Figure

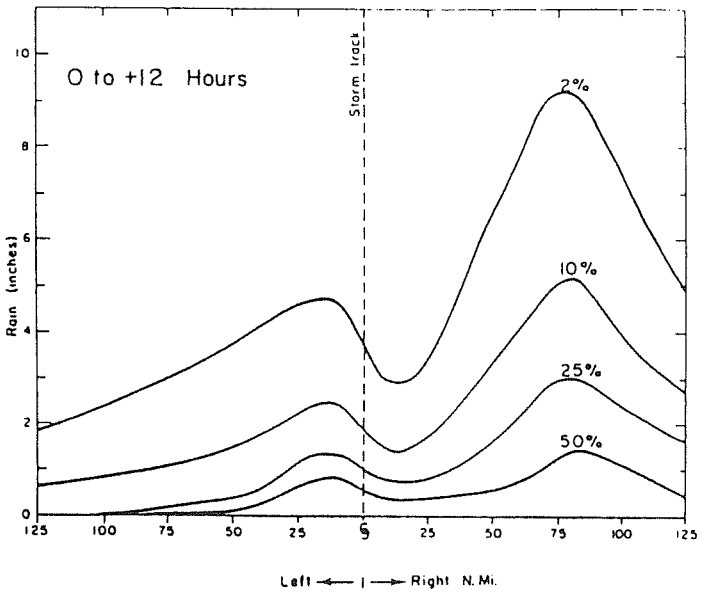

FIGURE 4-5
Rainfall for the first 12-hour period after landfall for selected frequency levels. (item 21 of Appendix A).

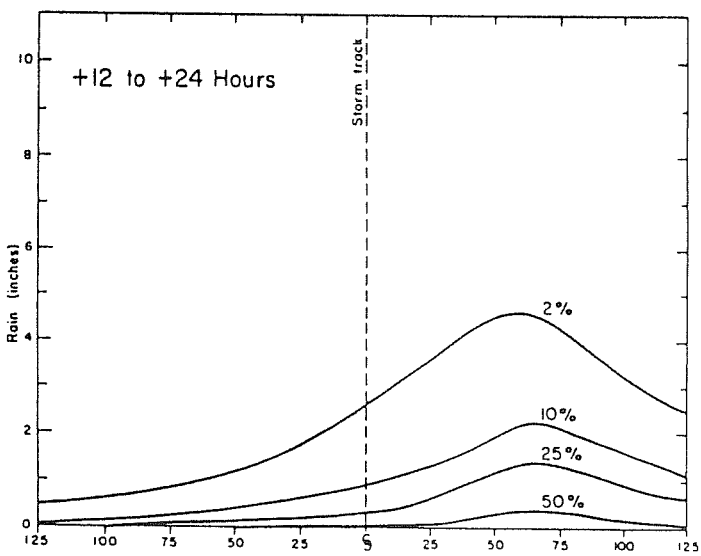

FIGURE 4-6
Rainfall for the second 12-hour period after landfall for selected frequency levels. (item 21 of Appendix A).

4-7 for a 500 square mile area and a 12-hour rainfall period is approximately 0.82. Upon multiplying the ratio times the point rainfall amounts, it is found that the average rainfall in the period 12-hours before landfall is about 5 inches and 12-hours after landfall about 5.2 inches.

****

h. With a knowledge of the rainfall rates, it is possible to include this effect directly as part of the mathematical model simulations via the continuity relation in Equation [1-8]. Thus by using an appropriate interpolation procedure, it is possible to add a quantity of rainfall at each time step. This applies to both direct rainfall over water bodies and inundated areas and rainfall runoff from adjacent land areas. Provisions for including surface runoff in the model require that the model be

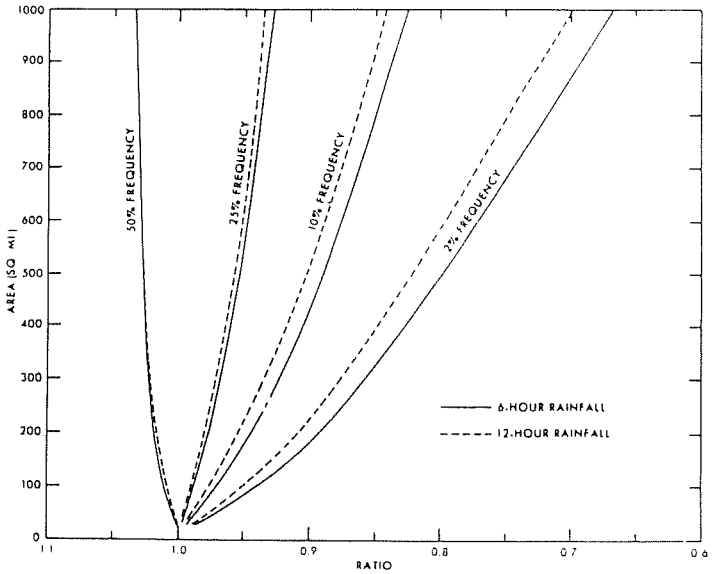

FIGURE 4-7
Ratios of areal rainfall for selected frequency levels. (item 21 of Appendix A).

formulated such that moving boundaries can be treated and the adjacent land areas are incorporated into the modeled system. Direct surface runoff amounts prescribed will require adjustment to account for the effects of initial losses and infiltration during the course of the storm.

i. The problem of accounting for direct rainfall and rainfall surface runoff from adjacent land areas was first treated in connection with studies of storm surges in Galveston Bay (item 54 of Appendix A).

j. The method described for specifying rainfall over coastal areas along the Gulf Coast of the United States is considered applicable to the Atlantic Coast provided that the point rainfall depths are adjusted to reflect the probable depths characteristic of the region under consideration. These expected rainfall amounts can be estimated based on those tropical storms that have occurred in the study area and general vicinity. In applying the method to the Atlantic Coast, it is assumed that the distribution of the rainfall and area correction factors as given on figure 4-7 are identical to those estimated for the Gulf Coast.

4-3. Fluvial Inflows.

a. Large quantities of water may be dumped into embayments and other flooded areas along the coast during tropical storm periods as a result of inflow from rivers or other streams. These inflows can also be responsible for increasing the water levels in coastal regions. This effect, like rainfall and direct surface runoff may also be included in the numerical computations provided that the discharges are known or can be prescribed at a given location with the modeled system throughout the simulation period. Inflow into the system is taken to occur at the boundary which delineates the modeled area and at a given cell or embedded channel reach which corresponds to the location of the prototype stream. To account for the influx of water due to river inflow, an additional term may be added to the right hand side of Equation [1-8] or [1-13]. This term is simply the discharge Q at any time t divided by the water surface area A for a given cell.

b. In many instances it may be advantageous to account for direct surface runoff in the form of channelized flow at the landward boundaries of the system rather than incorporating those contributing areas into the modeled system. Enlarging the system to be modeled solely for the purpose of including

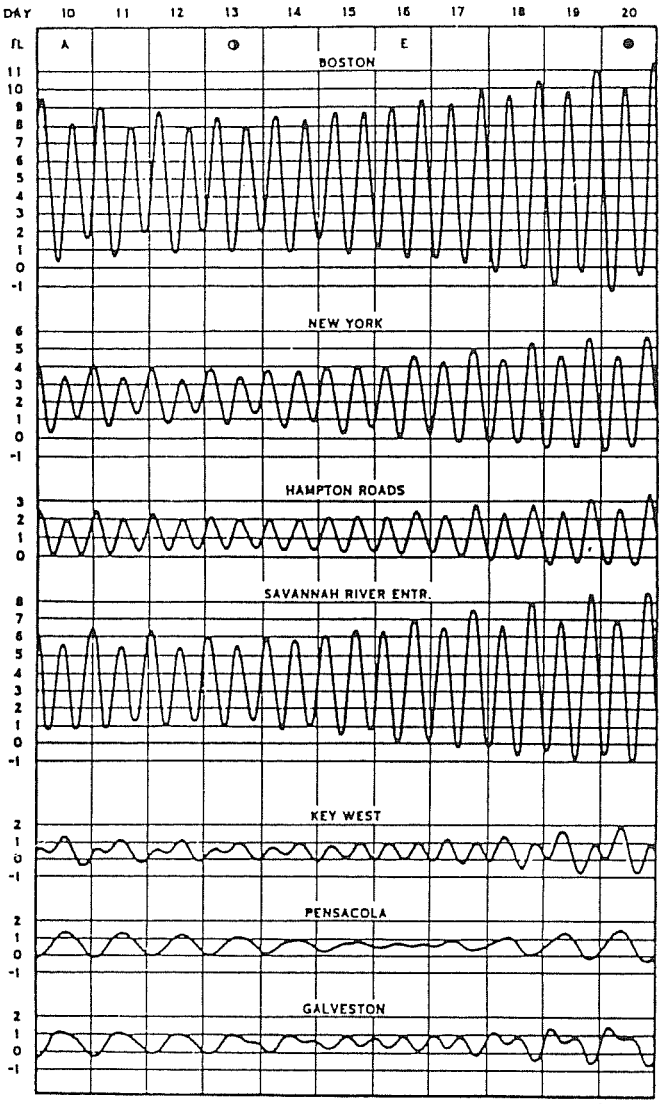

(from National Ocean Survey, NOAA, Tide Tables)

FIGURE 4-8
Typical tide curves along Atlantic and Gulf coasts.

such areas can increase the computational costs significantly and thus such as approach should usually be avoided.

c. Prediction of direct surface runoff from contributing areas external to the modeled system will require a separate hydrologic study based on the estimated rainfall amounts and distribution as included herein. Provided that interest is only centered on the maximum water levels produced during the tropical storm period, surface runoff needs only to be considered for those areas that will contribute to the maximum water levels. Thus contributing areas sufficiently far removed from an embayment or flooded area may not need to be considered due to the extensive travel time involved.

d. In design studies it is necessary to estimate a representative discharge from major streams that occur coincident with a tropical storm. Increasing the normal flow by 20-percent should generally provide a conservative estimate of the water entering the system. The justification for increasing the normal flow is based on the fact that the discharge will be increased to some extent as a result of rain falling in the lower part of the watershed upstream of the modeled area and to provide for possibly higher flows than the normal due to prior rains in the upper part of the watershed and possibly releases from an upstream reservoir. In some design studies it may be justified to conduct detailed hydrologic and hydraulic investigations to determine the inflow from rivers.

4-4. Astronomical Tide.

a. On an annual basis the principal causes of water-level variations with respect to the mean sea level datum are the astronomical tide and wind driven surge. During tropical storm periods, tide fluctuations may be responsible for increasing or decreasing the total water rise except at those times when tidal slack water exists. The magnitude of maximum rise and fall of water levels due to the tide depends on the particular coastal location. Typical tide curves for specific locations along the Atlantic and Gulf Coasts of the United States are shown in figure 4-8. These curves demonstrate the relatively large differences in tidal oscillations that may occur along these coasts. Tides propagated into coastal regions are modified as a result of frictional dissipation and basin geometry in the same manner as storm surge. Such modifications are thus responsible for the large differences in tides occurring along the coasts.

b. The effects of tide coincident with storm surge where shown in Figure 1-2 for the case of Hurricane Carla (1961) on the open coast at Galveston, Texas. As indicated in Figure 4-8, tides for this location are quite small compared to other locations. In some coastal locations the tide component may be as great or greater than the surge component at the time at which the tide is at maximum amplitude.

c. Although astronomical tide and storm surge components are induced by two physically independent causes, there is an interaction between these components during storm periods. Basic shallow water theory which is applicable to both tide and surge indicates that both effects are depth dependent and thus any change in depth caused by one of the components affects the other.

d. As a result of this interaction, the propagational speed of the tide is altered. This causes a phase lag between any predicted tide and the actual tide. As a consequence phase errors are introduced when the surge component is determined by extracting the predicted tide from the total water level as was done in the case of Hurricane Carla at Galveston (Figure 1-2). Phase errors of this sort, particularly when the tide range is large, can result in a surge component that oscillates at the same frequency as the tide.

e. Prediction of the total rise in water level is complicated when considering synthetic storms because it is necessary to combine the effects of both surge and astronomical tide. The tide potential can be computed along with the surge according to Equations [1-6] and [1-7] or [1-11] and [1-12] provided that the tide can be prescribed as the storm moves over the coastal area. However, to do so requires information on the spatial and temporal variations of the tide as well as phasing of the tide with respect to the storm. Such information is, of course, unavailable for design studies and it is thus necessary to resort to an approximate technique for including the effects of tide. A technique was presented in Chapter 3 for including the tide in the water level determinations by the synthetic storm surge approach.

f. In most previous studies of SPH surge it has been the practice to add an additional rise to the design water level to account for the astronomical tide effect. Although this is a simple approach to a complex problem, it appears to be reasonable in the absence of a more suitable technique. It is therefore recommended that for design purposes that the mean value of the tidal amplitude be used for increasing the SPH final design water level. This increase will general provide a conservative estimate of the total rise.

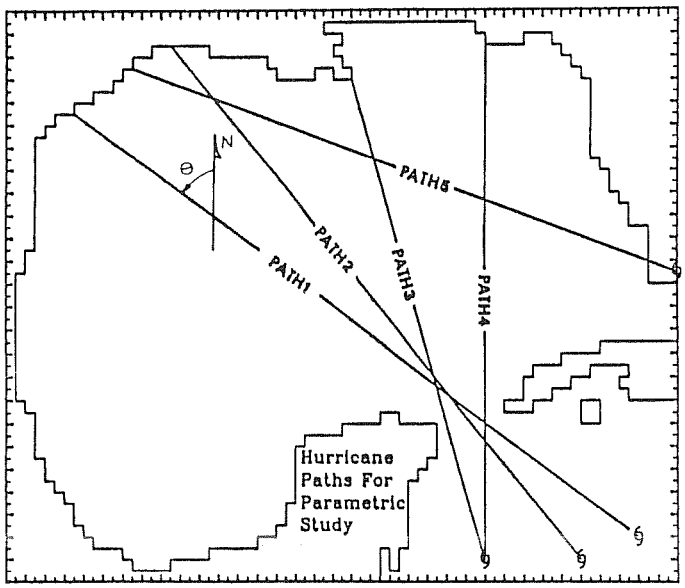

FIGURE 4-9
Selected paths for synthetic storms employed in the parametric study and definition of θ. (Based on item 7 of Appendix A).

4-5. Initial Water Level.

a. In studies of storm surge and associated effects it is necessary to estimate the elevation of the water surface at initial state for a given coastal area. The starting elevation is important since it affects the final water level estimates. In advance of a tropical storm it is, of course, possible that the initial water level is equal to, above or below the normal water level. Departure of the sea level from the normal level prior to the storm can be attributed to a number of different causes. Such causes were identified in Section 1-8 as storm surge, wave setup, astronomical tide, secular fluctuations, tsunamis, climatological effects and seiches. Generally, it will be only necessary to consider the effects of surge and astronomical tide in estimating the initial water level. Because the effect of tide is treated separately it is assumed for simplicity that slack tide exists at initial state. Prior to a tropical storm, an extratropical storm may generate surge in coastal areas resulting in an increase or decrease in water level depending on whether the wind is blowing in the onshore or offshore direction. Surge generated in this manner is sometimes referred to as "presurge". To account for the possibility that presurge can result in an increase in water level in advance of the tropical storm, an additional rise of 0.5 feet above the normal water level is recommended for establishing the initial water level for design purposes along the East Coast of the United States.

b. Along the Gulf Coast of the United States there is observational evidence of a hurricane-induced presurge anomaly (or forerunner) which is manifested in the form of a slow rise in water level which can commence several days prior to the primary surge (see Figure 1-3) as an example for Carla (1961). Because of its importance to surge prediction in the Gulf of Mexico, a Corps of Engineers' funded project, as discussed in item 7 of Appendix A, was carried out to study the cause and behavior of the Gulf forerunners. Some of the important aspects of the approach and results are summarized here.

c. The Gulf forerunner study (item 7 of Appendix A) employed a numerical model encompassing the entire Gulf of Mexico and part of the Cayumen Sea; the grid resolution was 15 minutes of latitude and longitude, which is sufficient to provide a reasonable rendition of the bathymetry. The model also allows for Coriolis acceleration, but is quasilinear (only the bed friction is nonlinear). After verification of the model for hurricanes Carla (1961) and Allen (1980), a series of runs were carried out using a parameterized hurricane model (item 57 of Appendix A). This parametric study employed five paths (See Figure 4-9), two radii to maximum wind, three forward speeds and three central pressures in various combination. The model was forced by both wind stress and atmospheric pressure gradient. At the open boundaries (Florida Strait and the seaward boundaries of the Cayman Sea) the water level was taken equal to the inverted barometer term (i.e., the local atmospheric pressure deficit relative to normal, expressed as an equivalent head of water).

d. The results indicate that, aside from usual local effects in the shallow water areas of the continental shelf, a gulf-wide volume mode of response can occur which is nearly uniform in amplitude over the Gulf and nearly everywhere in-phase (except near the ports). Moreover the initial rise of water level associated with this mode can commence as the hurricane center enters the Gulf. This mode (denoted H_g) can be quantified (from the model runs) in terms of the spatial average of the water level anomaly over the whole Gulf (excluding astronomical tide). The first positive peak in H_g can be regarded as the forerunner surge. The signal H_g is a dynamic response to the combined hurricane forcing over the basin system and exhibits oscillations with an average period of about 28 hours. The latter is identified as the natural Helmholtz period of the gulf, which is excited to varying degree, dependent upon the hurricane path and parameters. Long period oscillations also occur in H_g. However, during the first few days of the hurricane transit across the Gulf, a rough approximation of the gulf-wide H_g response is that it is a combination of a sustained mean rise and an oscillatory Helmholtz mode whose amplitude is about equal to the mean rise. The behavior is similar to the response of a spring scale when a weight is suddenly added and it oscillates between the initial zero value and twice the final equilibrium value.

e. It is emphasized that the forced gulf-wide H_g mode, which is responsible for the forerunner, is an oscillatory mode in time and is superimposed (like the astronomical tide) on the locally-induced wind effect in shallow water. Thus, it is not the initial peak of H_g which is important, but the subsequent value of H_g which happens to occur at the time of the dominant local peak surge. Thus the relative phasing of the local surge and H_g is very important.

f. Along the Texas coast, for typical hurricane events entering the Gulf at Yucatan Channel, the H_g model can produce a small peak forerunner surge of order 0.5 m or less preceding the primary surge by a day or so (depending upon the storm speed). For hurricanes running northward through the Yucatan Channel, parallel to and near the west Florida shelf edge an H_g mode is produced, but may be masked by the tendency of draw-down of water level near shore associated with offshore winds preceding the hurricane eye. Thus all hurricanes in the gulf can produce an oscillatory gulfwide volume mode, but not all paths produce an obvious positive forerunner. Nevertheless the H_g mode can still influence the value of the peak surge at shore as discussed earlier.

g. An approximate formula which yields a reasonable fit in the first few cycles of the H_g time sequences (as deduced from the model parametric study) is given below. The study employed straight paths of given: azimuth θ (measured in radians counterclockwise from the north), radius to maximum wind R (km), central pressure deficit Δp (mb) and starting position. In the following relation H_g is in meters, t is the elapsed time in hours from the entry of the hurricane eye into the Gulf of Mexico and τ is the time in hours to the first peak value of H_g (refer to Figure 4-10:

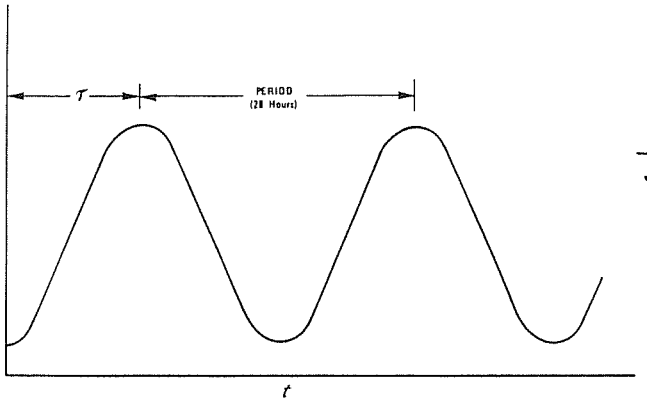

FIGURE 4-10
Schematic if H_g time sequence (t - elapsed time from entry of hurricane eye into Gulf)

$$H_g = A \left(\frac{R}{30}\right)^{0.9} \frac{\Delta p}{80} [1-B \cos (1.6\,\theta)] \left[1-\cos \frac{2\pi}{28} (t - \tau)\right] . \qquad [4-1]$$

For hurricanes which enter the Gulf from the Cayman Sea:

$$A = 0.22 \quad , B = 0.40$$

and

$$\tau = 24 - 14 \cos (1.6\,\theta) \quad . \qquad [4-2a]$$

For hurricanes with westerly paths, entering the Gulf from the Atlantic Ocean north of Cuba:

$$A = 0.10 \quad , B = 0$$

and

$$\tau = 24 \quad . \qquad [4-2b]$$

It is emphasized that while the forward speed of the storm does not enter explicitly in the above relations, it is important in determining whether a given peak in H_g is coincident with the arrival of the hurricane (and hence the peak surge) at shore.

h. The above relations allow one to include (by linear superposition) the approximate effect of the gulf-wide H_g mode in limited area models. However it is stressed that the relations do over-simplify the actual H_g response for any given hurricane, particularly in respect to the accuracy of the magnitude and time of successive peaks in H_g. The first peak is rendered most accurately by relation Equation [4-1]; the following peaks are less accurate in both magnitude and phase. In fact there is a slow decay in the magnitude, such that after about five days the H_g signal is essentially gone. As always one must exercise proper engineering judgment in application of such simplified relations. But as with the Gulf tides, the amplitude of H_g is rather modest.

4-6. Wave Setup.

a. In Chapter 1 it was indicated that water can pile up in nearshore regions as a result of waves breaking offshore. Although short period surface waves are responsible for very little transport in the direction of wave propagation in open water, they may, upon breaking, be responsible for significant transport near shore. Water propelled shoreward due to the breaking wave action occurs rather rapidly but the water returned seaward under the influence of gravity is slower. This difference in transport rates in the onshore and offshore directions results in a pileup of water near shore referred to as wave setup.

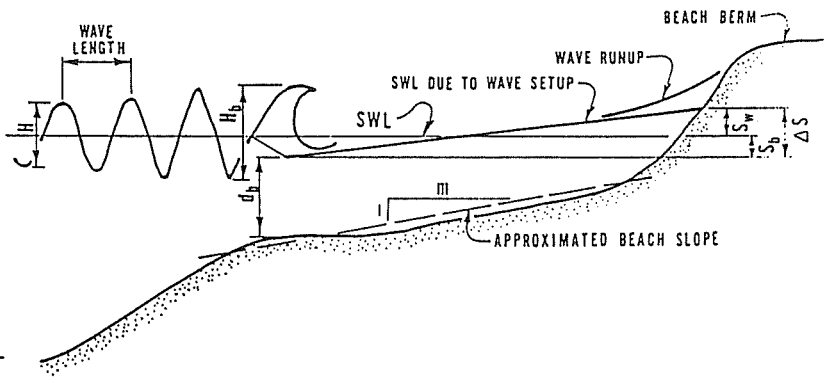

FIGURE 4-11
Definition sketch of wave setup.

b. In a laboratory study (item 56 of Appendix A) it was found that when waves break on a slope there is a decrease in the mean water level or setdown at the point of breaking; and from this point the mean water level sloped upward to the point of intersection with the shore. Figure 4-11 shows schematically the setdown and wave setup and definitions used in calculating the wave setup. Also shown is wave runup, an effect which is not to be confused with wave setup.

c. To estimate the rise in water level near shore due to wave setup requires a knowledge of the incoming wave field. A method is presented in Appendix E for calculating hurricane generated surface waves in the nearshore region. Also presented is an example problem to clarify the computational procedures involved.

d. Wave characteristics determined in the near shore area provide the necessary information for estimating wave setup in the nearshore region. The method given herein for calculating the wave setup is based on the method presented in the Shore protection manual (1977). The rise in water level above the still water level due to wave setup can be estimated by

$$S_w = \left[0.15\, d_b - \frac{g^{1/2}\, H'^{2}_{o}\, T}{64\,\pi\, d_b^{3/2}}\right] \cos \alpha \qquad [4-3]$$

in which S_w is the wave setup; d_b is the depth of water at the breaker point; g is gravity; H'_o is the equivalent unrefracted deepwater significant wave height; T is the wave period; and α is the angle between the wave crest at breaking and shore. The first term in the parenthesis on the right hand side of the equation is total rise in water level at shore above the setdown at the breaker point or as shown in Figure 4-11, and the second term is S_b or the amount of setdown below the normal water level. The water depth at breaking is given by

$$d_b = \frac{H_b}{b - \frac{aH_b}{gT^2}} \qquad [4-4]$$

in which H_b is the breaking wave height and factors a and b are (approximately)

$$a = 43.75\,(1 - e^{-19m}) \qquad [4-5]$$

$$b = \frac{1.56}{1 + e^{-19.5m}} \qquad [4-6]$$

where m is the estimated effective beach slope. The approximate breaking wave height may be determined from

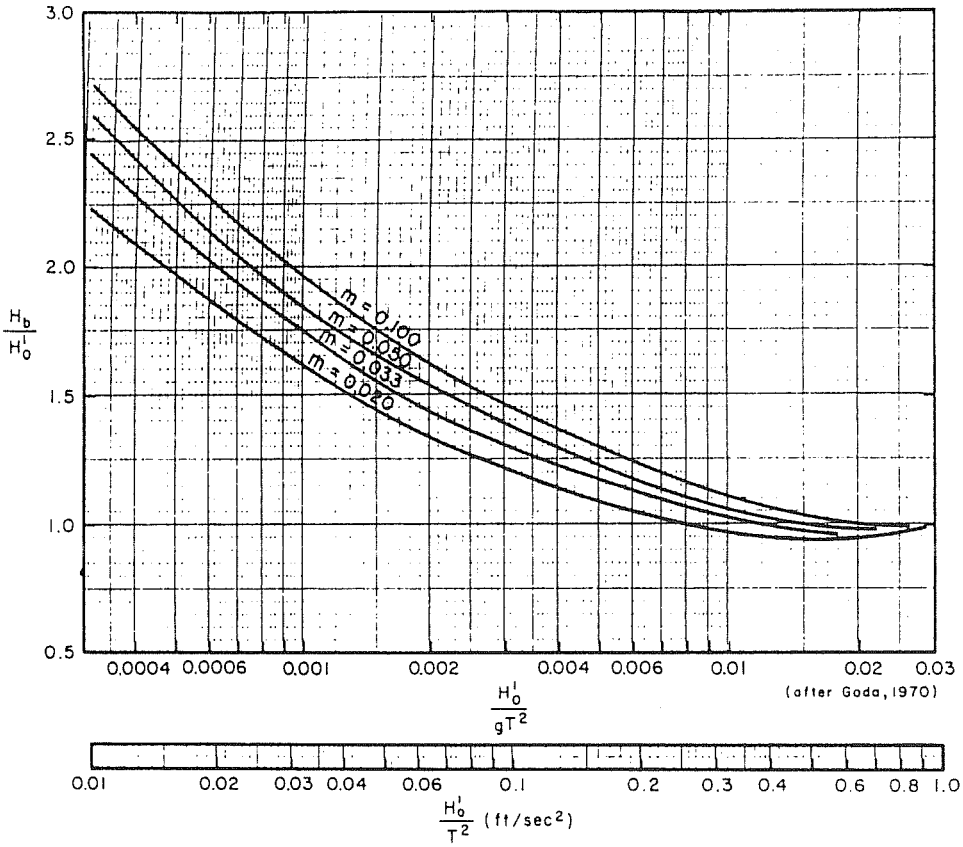

FIGURE 4-12
Breaker height, index, H_b/H'_o versus deep water steepness H'_o/gT^2.
(after item 20 of Appendix A).

Figure 4-12 when the unrefracted deepwater significant wave height, corresponding wave period and beach slope are known.

EXAMPLE PROBLEM

Given: From an analysis of a wave field associated with a hurricane it was found that the unrefracted deepwater significant wave height H'_o was 20 feet and the corresponding wave period T was 10 seconds at a point where the total water depth is 25 feet. The net rise in water level about NVGD due to storm surge and astronomical tide is 10 feet. Wind is blowing in a direction normal to the shore at the point and time in which the wave characteristics were estimated. Also the beach area shoreward of the point has an effective beach slope of 1:20 and the depth contours are more or less parallel to the shoreline.

Find: The maximum water level rise at shore and the wave setup that would be expected if the waves approached at an angle of 30 degrees to the coastline.

Solution: Based on m = 0.05, and using Figure 4-12 it is found that

$$\frac{H_b}{H'_o} = 1.17 \quad .$$

Thus the breaking wave height is

$$H_b = 23.4 \text{ feet} \quad .$$

In accordance to Equations [4-5] and [4-6]

$$a = 43.75 \left[1 - e^{(-19)(0.05)} \right] = 26.83$$

$$b = \frac{1.56}{1 + e^{(-19.5)(0.05)}} = 1.333 \quad .$$

The depth of breaking, as evaluated by Equation [4-4], is

$$d_b = \frac{23.4}{1.133 - \frac{(26.83)(23.4)}{(32.2)(100)}} = 24.9 \text{ feet} \quad .$$

The wave setup according to Equation [4-3] is

$$S_w = 0.15\ (24.0) - \frac{(32.2)^{1/2}\ (20)^2\ 10}{64\pi\ (24.9)^{3/2}}$$

$$\simeq 3.74 - 0.91 \simeq 2.83 \text{ feet} \quad .$$

Thus the total rise at shore is about 13 feet above NVGD. If the wave crest had approached at an angle of 30 degrees to the shore, then the wave setup at the shore, according to Equation [4-3], would have been approximately 2.5 feet.

APPENDIX A
BIBLIOGRAPHY

1. Abbott, M. B. 1979. Computational Hydraulics, Elements of the Theory of Free Surface Flows, Pitman, London.

2. Beard, L. R. 1962. "Statistical Methods in Hydrology", U.S. Army Corps of Engineers, Civil Works Investigation Project CW-151.

3. Benson, M. A. 1962. "Plotting Positions and the Economics of Engineering Planning, Proc. ASCE, Vol. 88, No. HY6, pp 57-72.

4. Borgman, L. E., and Resio, D. T. 1977. "External Statistics in Wave Climatology." Ports 77, Vol. 1.

5. Bretschneider, C. L. 1954. "Modification of Wave Height Due to Bottom Friction, Percolation, and Refraction," TM 4-45, U. S. Army Corps of Engineers, Beach Erosion Board, Washington, DC.

6. Bretschneider, C. L. 1959. "Hurricane Design-Wave Practices," Trans. Amer. Society of Civil Engineers, Vol. 124, Paper No. 2965.

7. Bunpapong, M., Reid, R.O., and Whitaker, R. E. 1985. "An Investigation of Hurricane-Induced Forerunner Surge in the Gulf of Mexico," Technical Report CERC-85-5, U. S. Army Engineer Waterways Experiment Station, Vicksburg, MS.

8. Butler, H. L. 1978 (June). "Numerical Simulation of Tidal Hydrodynamics, Great Egg Harbor and Corson Inlets, New Jersey," Technical Report H-78-11, U. S. Army Engineer Waterways Experiment Station, CE, Vicksburg, MS.

9. Butler, H. L. 1978 (Aug - Sept). "Coastal Flood Simulation in Stretched Coordinates," Proceedings of the Sixteenth Coastal Engineering Conference, American Society of Civil Engineers, Vol. 1, p 1030.

10. Butler, H. L. 1970. "Evolution of a Numerical Model for Simulating Long-Period Wave Behavior in Ocean-Estuarine Systems," Estuarine and Wetland Processes, with Emphasis on Modeling, P. Hamilton and K. B. MacDonald, Eds., Proceedings, Symposium on Estuarine and Wetland Processes and Water Quality Modeling, New Orleans, LA., p 147.

11. Butler, H. L. 1982 (Mar). "Finite Difference Numerical Model for Long-Period Wave Behavior: With Emphasis on Storm Surge Modeling," Seminar on Two-Dimensional Flow Modeling, Hydrologic Engineering Center, Davis, CA.

12. Chow, V. T. 1964. Handbook of Applied Hydrology, McGraw-Hill Book Co., New York, pp 8-28 and 8-29.

13. Cline, I. M. 1926. Tropical Cyclones, McMillan Co., New York, p 301.

14. Committee on Tidal Hydraulics. 1980. "Evaluation of Numerical Storm Surge Models," Technical Bulletin No. 21, Office, Chief of Engineers, U.S. Army, Washington, DC.

15. Courant, R., Friedrichs, K. O. and Lewy, H. 1928. "Uber die partiellen differenzengleichungen der mathematischen Physik", Math. Ann., 100, p 32.

16. de Boor, c. 1978. "A Practical Guide to Splines," Applied Math. Sci. 27, Springer-Verlag, New York.

17. de Boor, C. 1979. "Efficient Computer Manipulation of Tensor Products," ACM Trns. Math. Software, Vol. 5 (2): 173-182.

18. Doodson, A. T., and Warburg, H. D. 1941. Admiralty Manual of Tides, Her Majesty's Stationery Office, London, p 270.

19. Garrat, J. R. 1977. "Review of Drag Coefficients over Oceans and Continents," Monthly Weather Review 105, p 915-929.

20. Goda, Y. 1970. "A Synthesis of Breaker Indices," Transactions of the Japanese Society of Civil Engineers, Vol. 2, Part 2.

21. Goodyear, H. V. 1968. "Frequency and Areal Distributions of Tropical Storm Rainfall in the United States Coastal Region on the Gulf of Mexico," ESSA Technical Report, WB-7.

22. Grahanm, H. E., and Nunn, D. E. 1959. "Meteorological Considerations Pertinent to Standard Project Hurricane, Atlantic and Gulf Coasts of the United States," Report 33, National Hurricane Research Project, U.S. Department of commerce, Washington, DC.

23. Harris, D. L. 1963. "Characteristics of the Hurricane Storm Surge," Technical Paper No. 48, U. S. Weather Bureau, Washington, DC.

24. Harris, D. L. 1981 (Feb). "Tides and Tidal Datums in the United States," Special Report 7, Coastal Engineering Research Center, U.S. Army Corps of Engineers.

25. Harris, D. L. 1982. "Data Requirements for the Evaluation of Storm Surge Models," U. S. Nuclear Regulatory Commission, Washington, DC.

26. Ho, F. P. 1974 (Sept). "Storm Tide Frequency Analysis for the Coast of Georgia," NOAA Tech Memo NWS HYDRO-19, National Weather Service.

27. Ho, F. P., Schwerdt, R. W., and Goodyear, H. V. 1975 (May). "Some Climatological Characteristics of Hurricanes and Tropical Storms, Gulf and East Coasts of the United States," NOAA Technical Report, NWS 15.

28. Ho, F. P. 1975 (May). "Storm Tide Frequency Analysis for the Coast of Puerto Rico," NOAA Tech Memo NWS HYDRO-23, National Weather Service.

29. Ho, F. P., and Myers, V. A. 1975 (Nov). "Joint Probability Method of Tide Frequency Analysis Applied to Apalachicola Bay and St. George Sound, Florida," NOAA Tech Report NWS 18, National Weather Service.

30. Ho, F. P., Tracey, R. J. 1975 (May). "Storm Tide Frequency Analysis for the Coast of North Carolina, South of Cape Lookout," NOAA Tech Memo NWS HYDRO-21, National Weather Service.

31. Ho, F. P. and Miller, J. F. 1982 (Aug). "Pertinent Meteorological and Hurricane Tide Data for Hurricane Carla," NOAA Technical Report, NWS 32.

32. Hoel, P. G. 1947. Introduction to Mathematical Statistics, John Wiley and Sons, Inc., New York.

33. Hubertz, J. M. and Wanstrath, J. J. 1979. "A Comparison of Two Numerical Storm Surge Prediction Models," Proceedings of Symposium on Long Waves in the Ocean, Marine Sciences Directorate Manuscript Rpt. Series No. 53, Department of Fisheries and the Environment, Ottawa, Ontario.

34. Jelesnianski, C. P. 1965 (Jun). "A Numerical Calculation of Storm Surges Induced by a Tropical Storm Impinging on the Continental Shelf," Monthly Weather Review, Vol. 93, No. 6, p 343-358.

35. Jelesnianski, C. P. 1966 (Jun). "Numerical Computations of Storm Surges without Bottom Stress," Monthly Weather Review, Vol. 94, No. 6, p 379-394.

36. Jelesnianski, C. P. 1967 (Nov). "Numerical Computations of Storm Surge with Bottom Stress," Monthly Weather Review, Vol. 95, No. 11, p 749-756.

37. Jelesnianski, C. P. 1972 (Apr). "SPLASH (Special Program to List Amplitudes of Surges from Hurricanes); Part I: Landfall Storms," NOAA Technical Memorandum NWS TDL-46, National Weather Service, Silver Spring, MD.

38. Jelesnianski, C. P. 1974 (Mar). "SPLASH (Special Program to List Amplitudes of Surges from Hurricanes); Part II: General Track and Variant Storm Conditions," NOAA Technical Memorandum NWS TDL-52, National Weather Service, Silver Spring, MD.

39. Jelesnianski, C. P. 1976 (Jul). "A Sheared Coordinate System for Storm Surge Equations of Motions with a Mildly Curved Coast," NOAa Technical Memorandum NWS TDL-62, National Weather Service, Silver Spring, MD.

40. Jennings, F. D. 1983. "Evaluation of the FEMA Model for Estimating Potential Coastal Flooding from Hurricanes and its Application to Lee County, Florida," Committee on Coastal Flooding From Hurricanes, Advisory Board on the Built Environment, National Research Council. National Academy Press, Washington, DC.

41. Kite, G. W. 1978. Frequency and Risk Analysis in Hydrology, Water Resources Publications, Fort Collins, CO.

42. Leenderste, J. J. 1967. "Aspects of a Computational Model for Long-Period Water Wave Progagation," The Rand Corporation, Santa Monica, CA.

43. Leenderste, J. J. 1970 (Feb). "A Water-Quality Simulation Model for Well-Mixed Estuaries and Coastal Seas, Vol. I, Principles of Comutation," RM-6230-rc, Rand Corp., Santa Monica, CA.

44. Miyazaki, M. 1963. "A Numerical Computation of the Storm Surge of Hurricane Carla 1961 in the Gulf of Mexico," Technical Report 10, Department of Geophysical Sciences, University of Chicago, Chicago, IL.

45. Myers, V. A. 1954. "Characteristics of United States Hurricane Pertinent to Levee Design for Lake Okeechobee, Florida," Hydrometeorological Report No. 32. U. S. Weather Bureau, Department of Commerce and U. S. Army Corps of Engineers, Washington, DC., p 106.

46. Myers, V. A. 1970 (Apr). "Joint Probability Method of Tide Frequency Analysis Applied to Atlantic City and Long Beach Island, NJ." ESSA Tech WBTM HYDRO 11.

47. Myers, V. A. 1975 (Jun). "Storm Tide Frequencies on the South Carolina Coast," NOAA Tech Report NWS 16, National Weather Service.

48. National Oceanic and Atmospheric Administration. 1972. "Revised Standard Project Hurricane Criteria for the Atlantic and Gulf Coasts of the United States," Memorandum HUR 7-120, National Weather Service, Silver Spring, MD.

49. National Oceanic and Atmospheric Administration. 1979. "Tide Tables, 1980 High and Low Water Predictions, West Coast of North and South America Including the Hawaiian Islands," National Ocean Survey, Rockville, MD.

50. National Oceanic and Atmospheric Administration. 1979. "Tide Tables, 1980 High and Low Water Predictions, East Coast of North and South America Including Greenland," National Ocean Survey, Rockville, MD.

51. Neumann, C. J., and Cry, G. W. 1978 (Jun). "Tropical Cyclones of the North Atlantic 1871-1977," NOAA National Weather Service, Environmental Data Service, Superintendent of Documents, U. S. Government Printing Office, Washington, DC. 20402, Stock No. 003-017-00425-2.

52. Overland, J. E., and Myers, V. A. 1976. "Model of Hurricane Tide in Cape Fear Estuary," Journal of Waterways and Coastal Engineering Division, ASCE, Vol. 102, WW No. 4.

53. Pillsbury, G. B. 1956 (May). "Tidal Hydraulics," U. S. Army Corps of Engineers, Washington, DC.

54. Reid, R. O., and Bodine, B. R. 1968. "Numerical Model for Storm Surges in Galveston Bay," Journal of Waterways and Harbors Division, No. WWI, p 33-57.

55. Reid, R. O., Vastano, A. C., and Reid, T. J. 1977 (Nov). "Development of Surge II program with Application to the Sabine-Calcasieu Area for Hurricane Carla and Design Hurricanes," Technical Report No. 77-13, U. S. Army Coastal Engineering Research Center, CE, Fort Belvoir, VA.

56. Saville, T., Jr. 1961. "Experimental Determination of Wave Setup," Proceedings, Second Technical Conference on Hurricanes, National Hurricane Research Project, Report No. 50, p 242-252.

57. Schwerdt, R. W., Ho, F. P., and Watkins, R. R. 1979. "Meteorological Criteria for Standard Project Hurricane and Probable Maximum Hurricane Windfields, Gulf and East Coasts of the United States," Technical Report NWS 23, National Oceanic and Atmospheric Administration, U. S. Department of Commerce, Washington, DC.

58. Schureman, P. 1941. "Manual of Harmonic Analysis and Prediction of Tides," Special Publication No. 98. U. S. Department of Commerce, Coast and Geodetic Survey, Washington, DC.

59. Tetra Tech, Inc. 1981. "Coastal Flooding Storm Surge Model," Parts 1, 2, and 3, Prepared for the Federal Emergency Management Agency.

60. Thompson, J. R. 1983. "A Boundary-Fitted Coordinate Code for General Two-Dimensional Regions with Obstacles and Boundary Instrusions," Technical Report E-83-8, prepared by Mississippi State University, Mississippi State, MS, for the U. S. Army Engineer Waterways Experiment Station, CE, Vicksburg, MS.

61. U. S. Army Corps of Engineers. 1977. "Shore Protection Manual," Vol. 1, 2, and 3, Third Edition, Coastal Engineering Research Center, Fort Belvoir, VA.

62. U. S. Interagency Advisory Committee on Water Data. 1981. "Guidelines for Determining Flood Flow Frequency," Bulletin No. 178, Published by U. S. Geological Survey, Reston, VA.

63. U. S. Water Resources Council. 1980. "An Assessment of Storm Surge Modeling," Washington, DC.

64. U. S. Weather Bureau. 1959. "Relations Between SPH Isovel Patterns and Probable Maximum Events for Lower New England Area." Memorandum HUR 7-59 Department of Commerce, Washington, DC.

65. U. S. Weather Bureau. 1959. "Relations Between SPH Isovel Patterns and Probable Maximum Events for the New Orleans Area." Memorandum HUR 7-61 Department of Commerce, Washington, DC.

66. Vreugdenhil, C. B. and Voogt, J. 1976 (Sep). "Hydrodynamic Transport Phenomena in Estuaries and Coastal Waters: Scope of Mathematical Models," Symposium on Modeling Techniques, Waterways and Harbors Division of ASCE.

67. Wanstrath, J. J., Whitaker, R. E., Reid, R. O., and Vastano, A. C. 1976 (Nov). "Storm Surge Simulation in Transformed Coordinates, Vol. I and II," U. S. Army Corps of Engineers, Coastal Engineering Research Center, Technical Report No. 76-3.

68. Wanstrath, J. J. 1977 (Sep). "Nearshore Numerical Storm Surge and Tidal Simulation," Technical Report H-77-17, U. S. Army Engineer Waterways Experiment Station, CE, Vicksburg, MS.

69. Wanstrath, J. J., Butler, H. L., Vincent, C. L., Resio, D. T., and Whalin, R. W. 1977 (Oct) "Use of Numerical Models for Computation of Coastal Water Levels," Preprint 3070 ASCE Fall Convention and Exhibit, San Francisco, CA.

70. Wanstrath, J. J. 1978 (Feb). "An Open-Coast Mathematical Storm Surge Model with Coastal Flooding for Louisiana; Theory and Application," Miscellaneous Paper H-78-5, Report 1, U. S. Army Engineer Waterways Experiment Station, CE, Vicksburg, MS.

71. Wanstrath, J. J. 1978 (Feb). "An Open-Coast Mathematical Storm Surge Model with Coastal Flooding for Louisiana; Theory and Application," Miscellaneous Paper H-78-5, Report 2, U. S. Army Engineer Waterways Experiment Station, CE, Vicksburg, MS.

72. Yevjevich, Vujica. 1972. Probability and Statistics in Hydrology, Water Resources Publications, Fort Collins, CO.

APPENDIX B
ENGINEERING SYMBOLS

Symbol	Units	Term
a	--	factor depending on beach slope Equation [4-5]
	--	parameter used in calculation of confidence limits Equation [3-26]
A	--	storm parameter space

Symbol	Units	Term
A(t)	ft	amplitude of tide as a function of time
b	--	factor depending on beach slope Equation [4-6]
	--	parameter used in calculation of confidence limits Equation [3-27]
C_d	--	water surface drag coefficient
CPI	in of Hg	central pressure index
C_0 C_1 C_2	--	constants used in approximating the standard normal deviate Equation [3-11]
d	ft	local depth of water
	in of Hg	argument of central pressure deficit D
d_b	ft	depth of water at which significant waves break offshore
$\bar{d}_t$	ft	average water depth for two successive reach intervals (used in estimating hurricane waves)
d_1 d_2 d_3	--	constants used in approximating the standard normal deviate Equation. 3-11]
D	ft	total water depth at position x, y and at time t
	in of Hg	atmospheric pressure deficit
D_{max}	ft	maximum depth of water to be expected anywhere in the system (numerical stability consideration)
e	--	2.71828 ....., $e^x = \exp(x)$
erfc(x)	--	complementary error function of x
E	--	event number when events rank from the greatest to smallest magnitude Equations [3-20] and [3-21]
f	rad/sec	Coriolis parameter, $f = 2\omega \sin\phi$
f_f	--	bottom friction factor (used in connection with short period wave dissipation)
F_e	ft	effective wave fetch length
F'_e	ft	the effective wave fetch length at the previous computational step as used in the marching procedure for estimating hurricane waves
g	ft/sec	acceleration due to gravity
G	--	skew coefficient
$\bar{G}$	--	skew coefficient when historic and/or outliers are considered
h	ft	seabed elevation relative to datum (usually referenced to NGVD)
H	ft	height of short period surface wave
H	ft	tidal amplitude
H	--	number of years in a historical period Equation [3-14]
H_b	ft	height of short period breaking wave
H_i	ft	height of short period surface wave in particular spatial segment (used in the computation of hurricane waves)
H_o	ft	height of deepwater significant wave
H'_o	ft	equivalent unrefracted deepwater significant wave height
HW	ft	high water tidal elevation
k	--	wind stress coefficient (non-dimensional)
	--	surface friction coefficient Equation [C-8]
K	--	bottom stress coefficient (used in conjunction with shallow water waves)
	--	frequency factor
	--	coefficient that is inversely proportional to the square root of the air density just above the water surface Equation [D-2]
K_f	--	short period surface wave decay factor
K_N	--	coefficient depending on sample size Equation [3-13]
K_L	--	frequency factor for lower confidence level Equation [3-25]
K_S	--	shoaling coefficient
K_u	--	frequency factor for upper confidence level Equation [3-24]
l	ft	argument of distance from storm center L
L	ft	short period surface wave length
	n mi, mi	distance from storm center
L_o	ft	short period surface wave length in deep water
LW	ft	low water tidal elevation
m	ft/ft	beach slope
		expected mean value Equation [3-32]
$\bar{m}$	--	order of the event when historic data and/or high outliers are included (events arranged in order of magnitude in which the largest event is ranked as 1)
M	--	order of the event (events arranged in the order of magnitude in which the largest event is ranked as 1)

Symbol	Units	Term
n	--	number of storms Equations [3-32] and [3-33]
N	--	a statistical term denoting the number of events
NGVD	--	National Geodetic Vertical Datum of 1929
p	in of Hg, lb/ft²	pressure
p_j	--	probability of a storm in a given year Equation [3-33]
pdf's	--	probability density functions
p_a	in of Hg	atmospheric pressure
p_n	in of Hg	atmospheric pressure at the outskirts of a storm
p_o	in of Hg	atmospheric pressure in the eye of a hurricane
p_r	in of Hg	atmospheric pressure at a point located at a radial distance r from the storm center
P	--	probability
	ft/sec	precipitation rate (depth/time)
P_N	--	expected probability
P_T	--	exceedence probability of tide
Q	--	reciprocal of m, P(S < s)
r	mi, n mi	radial distance from storm center
	mi, n mi	argument of radius to maximum wind R
R	mi, n mi	radial distance from storm center to region of maximum winds
	ft/sec	rate at which water is gained or lost at the air-sea interface
s	ft	argument of peak surge elevation S
S	ft	peak surge elevation
S_b	ft	setdown or decrease in water level from the mean water level at the location where waves break offshore
S_w	ft	wave setup due to waves breaking offshore
t	sec	time
	--	standard normal deviate
	hr	residence time in which the eye of a hurricane is in the Gulf of Mexico
t_m	hr	time of peak surge relative to the time of high tide
T	sec	short period surface wave period
	ft	tide elevation
T_o	sec	deepwater significant wave period
T_o'	sec	equivalent unrefracted deepwater significant wave period
u	ft/sec	x-component water particle velocity
	ft/sec	x-component vertically integrated velocity
U	ft²/sec	x-component of volume transport (per unit width)
v	ft/sec	y-component of water particle velocity
	ft/sec	y-component vertically integrated velocity
	mi/hr, knots	argument of the forward speed of storm V
$\underline{v}$	--	counterpart argument of the storm parameter vector
V	ft²/sec	y-component of volume transport (per unit width
V	mi/hr, knots	used to denote forward speed of storm
V_f	mi/hr, knots	storm translation speed
V_o	--	conversion factor for selected units Equations [C-5] through [C-7]
V_{gx}	mi/hr	maximum gradient wind speed 10 meters (33 feet) above water surface
V_k	mi/hr, knots	reduced wind speed due to frictional resistance
V_r	mi/hr, knots	wind speed at a point that is located at the radial distance r from the hurricane center
V_s	mi/hr, knots	wind speed at a point in a stationary hurricane that is located at a radial distance r from the hurricane center
V_{xm}	mi/hr, knots	maximum sustained windspeed in a moving hurricane
V_{xs}	mi/hr, knots	maximum sustained windspeed in a stationary hurricane
$\underline{V}$	--	storm parameter vector
w	ft/sec	z-component water particle velocity
	--	parameter used in approximating the standard normal deviate Equation [3-12]
W	mi/hr, knots	wind speed 10 meters (33 feet) above the water surface
W	--	weight factor Equation [3-14]
W_m	mi/hr, knots	maximum sustained surface wind speed
W_x , W_y	mi/hr, knots	x and y-components of wind speed 10 meters (33 feet) above surface
x	--	horizontal Cartesian coordinate

Symbol	Units	Term
	ft	implies statistical event (water level in this manual)
x'	ft	magnitude of historic or high outlier annual peak water level
Y	--	horizontal Cartesian coordinate
Y	knots(in of Hg)$^{1/2}$	product of the radius of maximum wind and square root of the atmospheric pressure deficit
z	--	vertical Cartesian coordinate
Z	ft	water level at the edge of continental shelf
	--	number of historic peaks including high outliers
Z(t)	ft	elevation of surge as a function of time
α	deg	angle between wave crest at breaking and shore
	--	parameter used in probability density distribution Equation [3-2]
	deg	wind inflow angle in a hurricane (see Figure 1-1a)
β	--	parameter used in probability density distribution Equation [3-2]
	deg	angle between the x-axis and the radial line extending outward from the storm center
β	deg	angle between a hurricane track and the maximum wind surface vector
γ	--	parameter used in probability density distribution Equation [3-2]
Γ	--	gamma function
ΔF	ft	incremental distance along wave fetch
Δp	in of Hg	difference in pressure at the periphery of a hurricane and the central pressure within the eye.
ΔS	ft	difference in the water level due to wave setup and the mean water level
Δt	sec	time interval (or time step) between successive calculations
Δx	ft	spatial step in x-direction
Δy	ft	spatial step in y-direction
ϵ_{xx} , ϵ_{xy}	--	eddy viscosity coefficients Equation [1-6]
ϵ_{yx} , ϵ_{yy}	--	eddy viscosity coefficients Equation [1-7]
ζ	ft	astronomical tide potential
η	ft	water level elevation relative to the water level

Symbol	Units	Term
η	ft	annual peak water
η_H	ft	threshold elevation for a high or low outlier Equation [3-13]
η_u , η_L	ft	water level elevations for the upper and lower confidence levels, respectively
κ	--	coefficient depending on the forward speed of a hurricane and the increase in effective fetch due to storm motion
μ	--	sample mean (statistical term)
$\bar{\mu}$	--	sample mean for data that includes either historic data and/or high outliers
Θ	deg	azimuth of the storm track
θ	deg	argument of the azimuth of the storm track Θ
θ	deg	angle between velocity vector and the x-axis (see Equation [1-9]
ξ	ft	atmospheric pressure deficit
π	--	3.14159.....
ρ	lb-sec^2/ft^4	water density
ρ_a	lb-sec^2/ft^4	air density
σ	--	standard deviation
$\bar{\sigma}$	--	standard deviation when either historic data and/or high outliers are included
Σ	--	denotes a summation
τ	hr	time to first positive peak of the fore runner surge after entry of hurricane eye into Gulf of Mexico
τ_{bx} , τ_{by}	lb/ft^2	x and y-components of bottom stress
τ_{sx} , τ_{sy}	lb/ft^2	x and y-components of surface stress
τ_{xx} , τ_{xy} , τ_{xz}	lb/ft^2	turbulent shear stresses Equation [1-1]
τ_{yy} , τ_{xy} , τ_{yz}	lb/ft^2	turbulent shear stresses Equation [1-2]
ϕ	deg	earth's latitude
ω	rad/sec	angular velocity of earth ($\omega = 2\pi/24$ rad/hr)
	rad/sec	tidal frequency (2π/period)
∞	--	signifies infinity

APPENDIX C
CRITERIA FOR DETERMINING SPH AND PMH WIND FIELDS

C-1. General. This appendix summarizes the necessary meteorological criteria presented in Technical Report NWS 23 (item 57 in Appendix A) for developing wind fields in connection with a Standard Project Hurricane (SPH) and the Probable Maximum Hurricane (PMH). Details and justification for adopting the various criterions as presented herein are omitted; however, such information can be found in the original report.

C-2. Meteorological Parameters.

a. The various meteorological parameters used for describing hurricane wind fields are identified as:

peripheral pressure (p_n)
central pressure (p_o)
radius of maximum winds (R)
forward speed (V_f)
track direction (θ)
inflow angle (α)

which were presented in Chapter 1. In defining wind fields it is also necessary to consider wind speed distribution and the limits of rotation of the wind.

b. All of the parameters, with the exception of the peripheral pressure p_n and the inflow angle α, generally vary along the Gulf and East Coasts of the United States. As a consequence the National Weather Service developed a standard chart with distances along the abscissa with mileposts beginning (mile 0) at the United States-Mexico border and ending at United States-Canada border. These mileposts are adopted for all storm surge studies conducted by the Corps of Engineers.

c. The meteorological parameters are to be determined as follows:

(1) Peripheral Pressure. For the SPH and PMH the peripheral pressure p_n or the sea-level pressure at the outskirts of the hurricane is to be taken as 29.77 in. (100.8 kPa) and 30.12 in. (102.0 kPa), respectively. (It is noted that atmospheric pressure given herein in units of inches (in.) implies inches of mercury.)

(2) Central Pressure. The lowest sea-level pressure p_o at the hurricane center is determined from Figures C-1 and C-2 for the SPH and PHM for a given coastal location.

(3) Radius of Maximum Winds. Figures C-3 and C-4, respectively, show the radial distances from the hurricane center to the regions of maximum winds R for SPH and PMH. It is to be noted that R can vary in a range between the upper and lower limits specified.

(4) Forward Speed. The range of translation speed V_f of the hurricane center for the SPH and PMH is shown in Figures C-5 and C-6.

(5) Track Direction. the permissible range of track directionn θ for the SPH and PMH is shown in Figures C-7 and C-8, respectively. Categories A, B, and C indicated in thee figures refer to forward speed V_f of the hurricanes. These speed categories are defined in Table C-1.

C-3. Pressure Distribution. The mathematical expression for defining the pressure distribution (item 45 of Appendix A) within a SPH and a PMH is:

$$\frac{p - p_o}{p_n - p_o} = e^{R/r} \qquad [C\text{-}1]$$

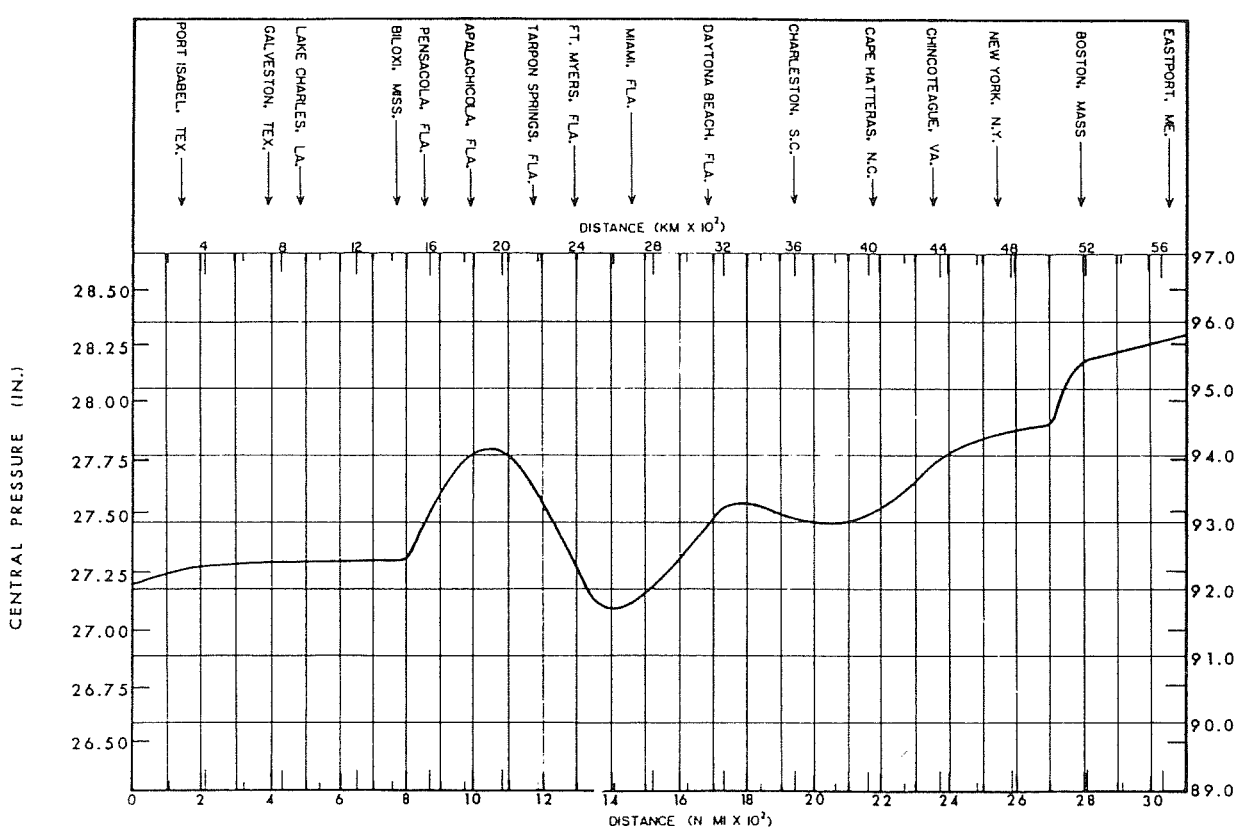

FIGURE C-1
Plot showing the SPH p_o. (item 57 of Appendix A).

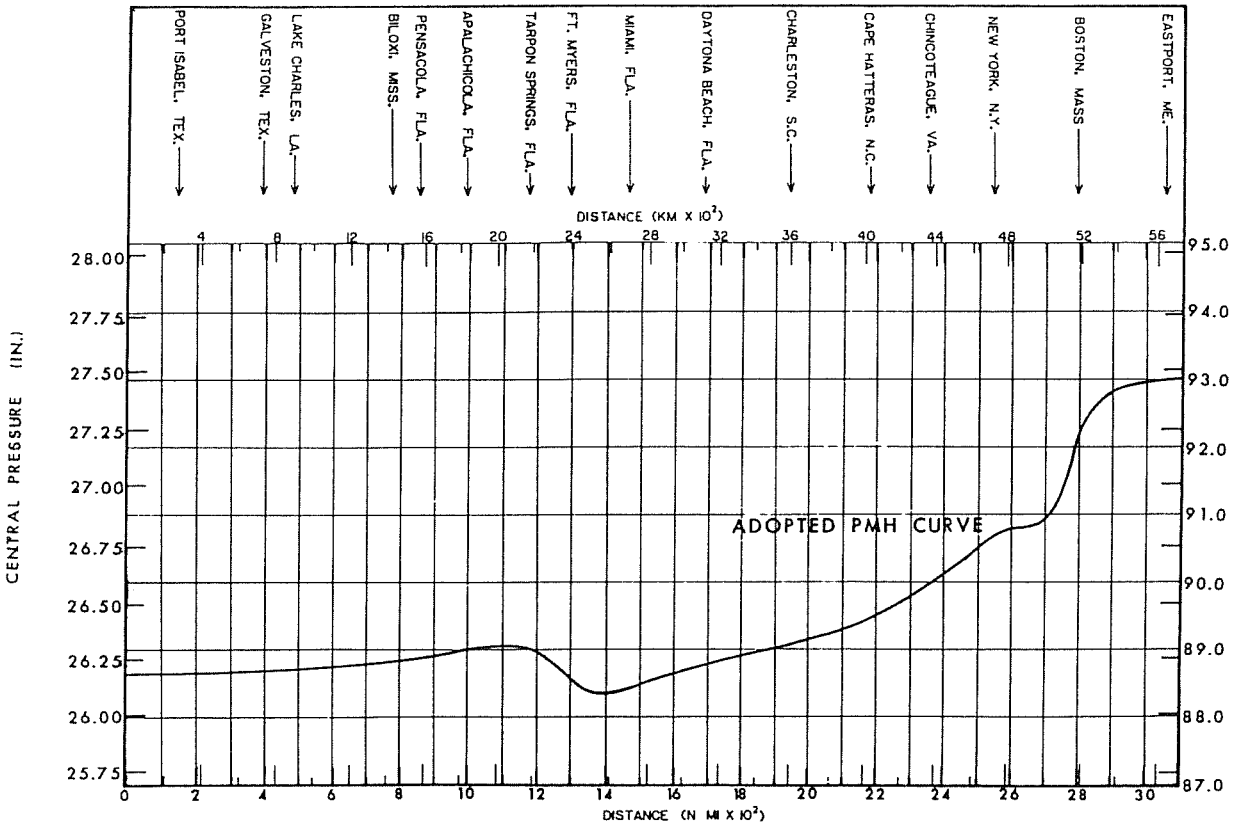

FIGURE C-2
Plot showing the PMP p_o (item 57 of Appendix A)

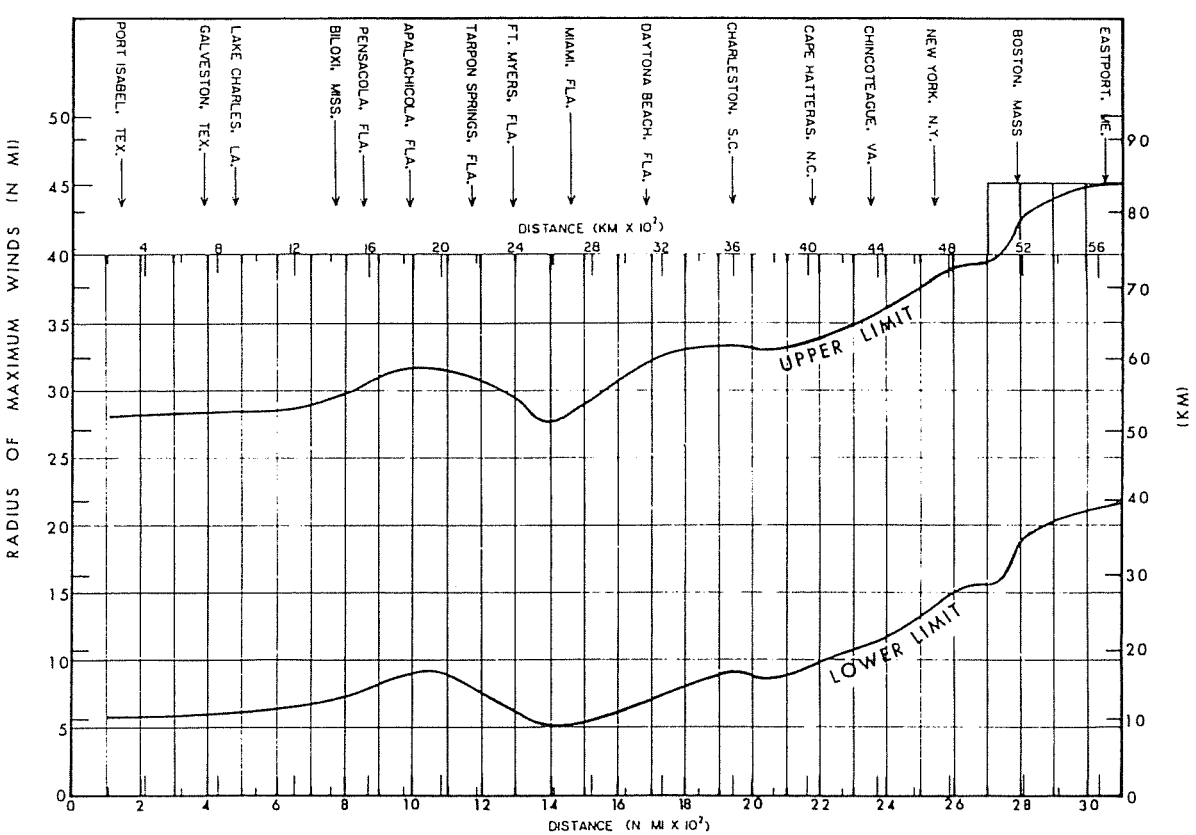

FIGURE C-3
Upper and lower limits of radius to maximum winds for the SPH. (item 57 of Appendix A)

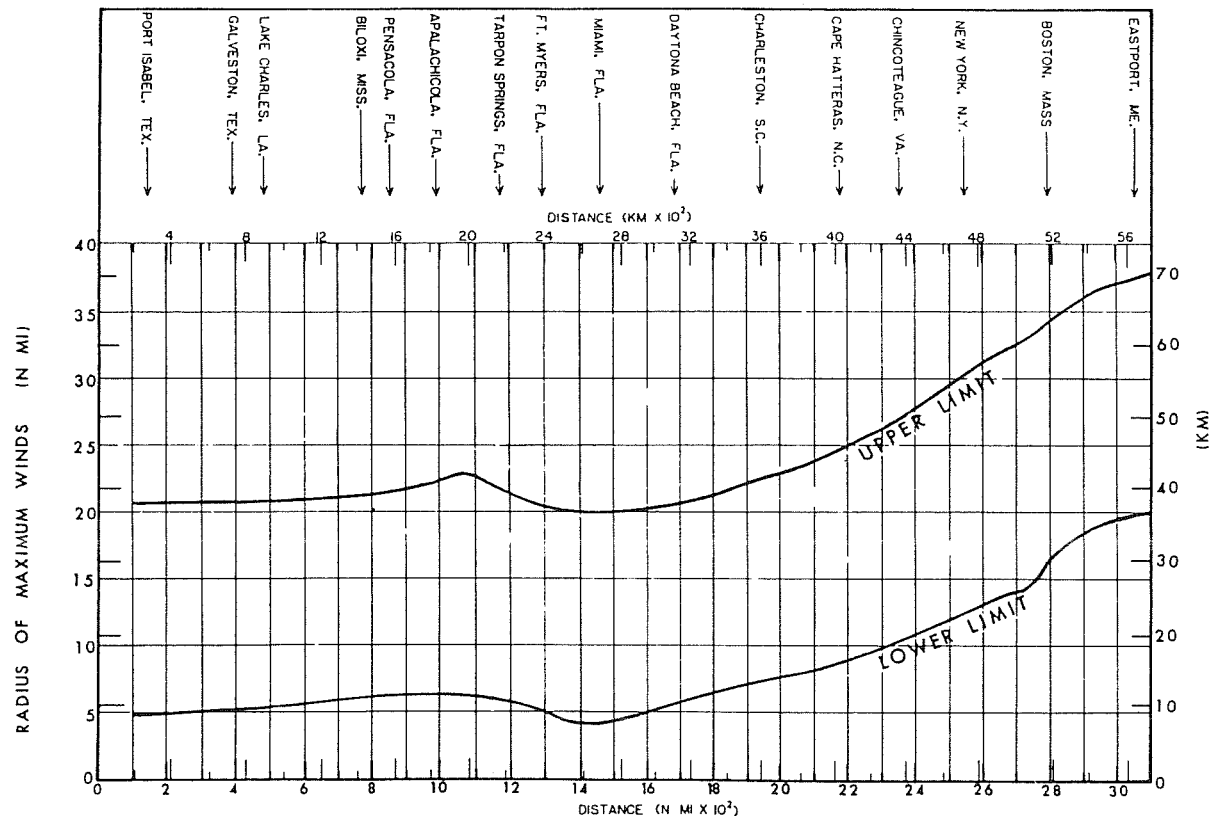

FIGURE C-4
Upper and lower limits of radius to maximum winds for the PMH. (item 57 of Appendix A)

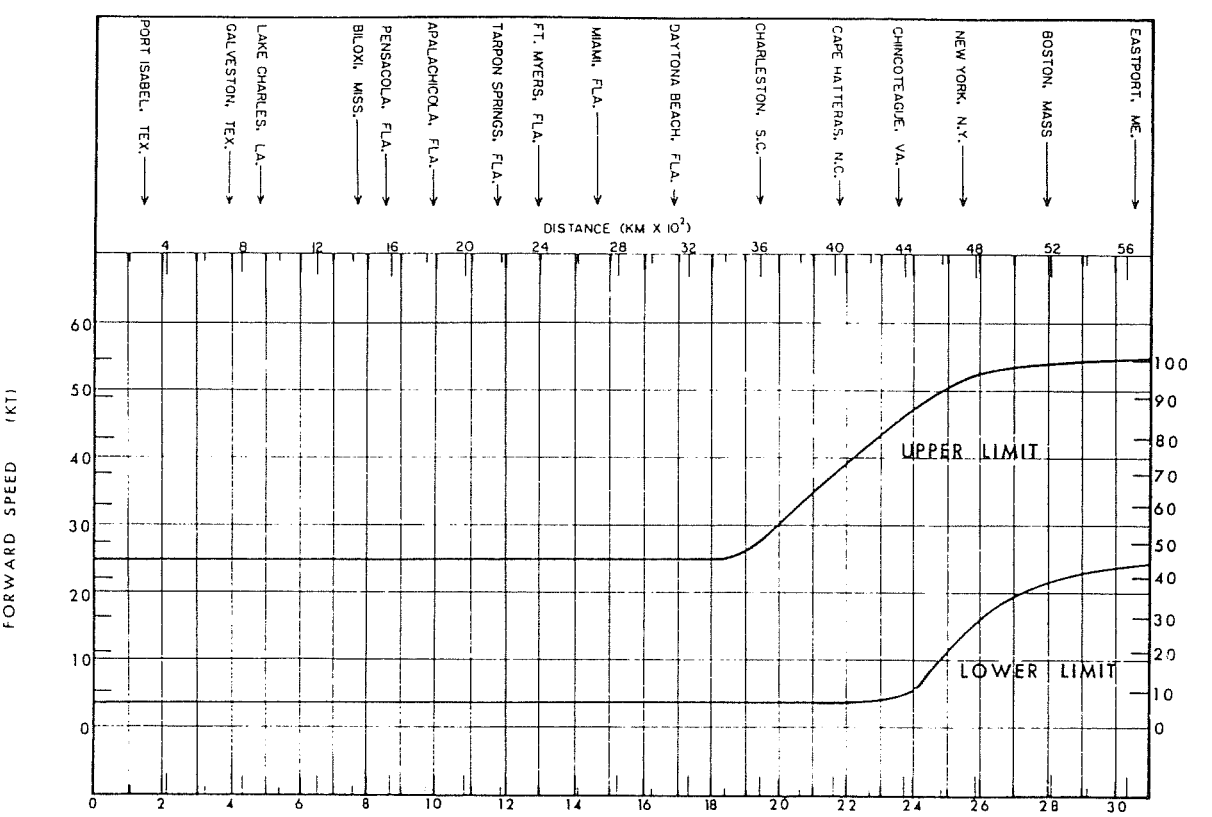

FIGURE C-5
SPH upper and lower limits of V_f. (item 57 of Appendix A)

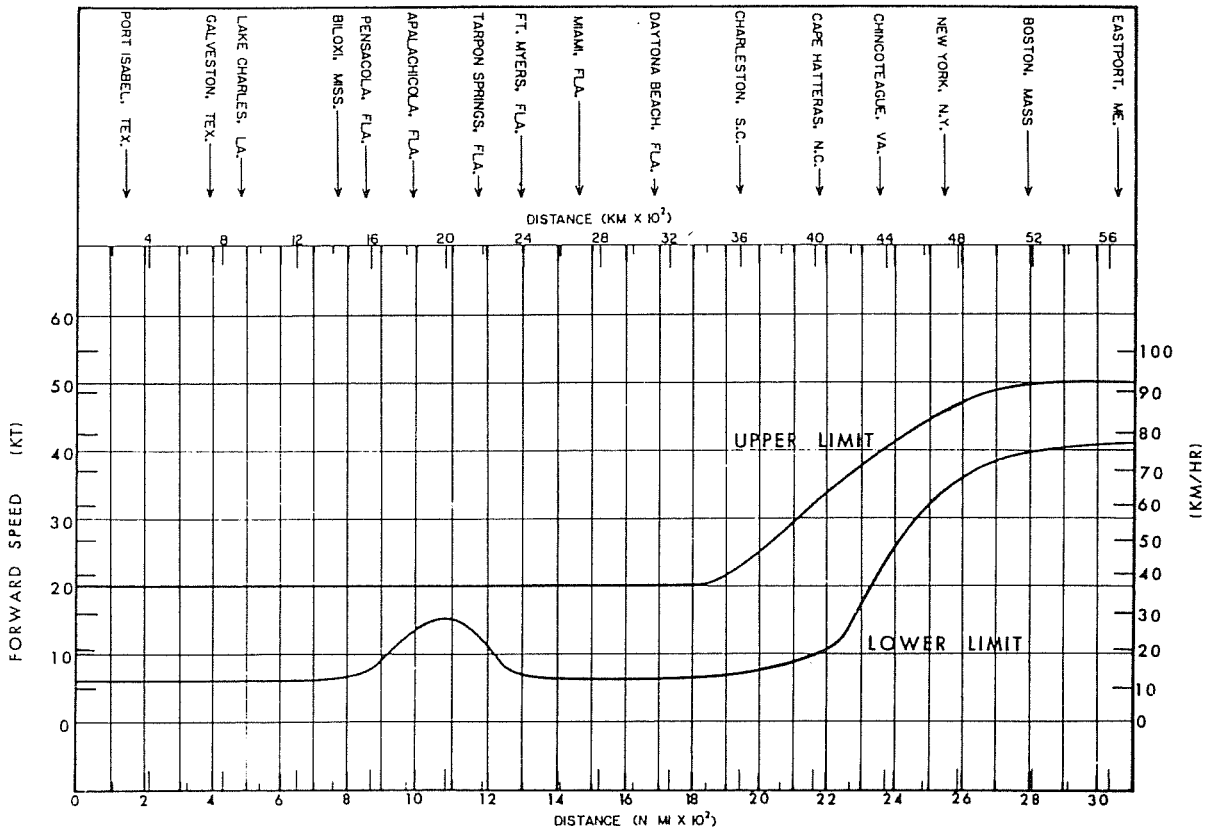

FIGURE C-6
PMH upper and lower limits of V_f.
(item 57 of Appendix A)

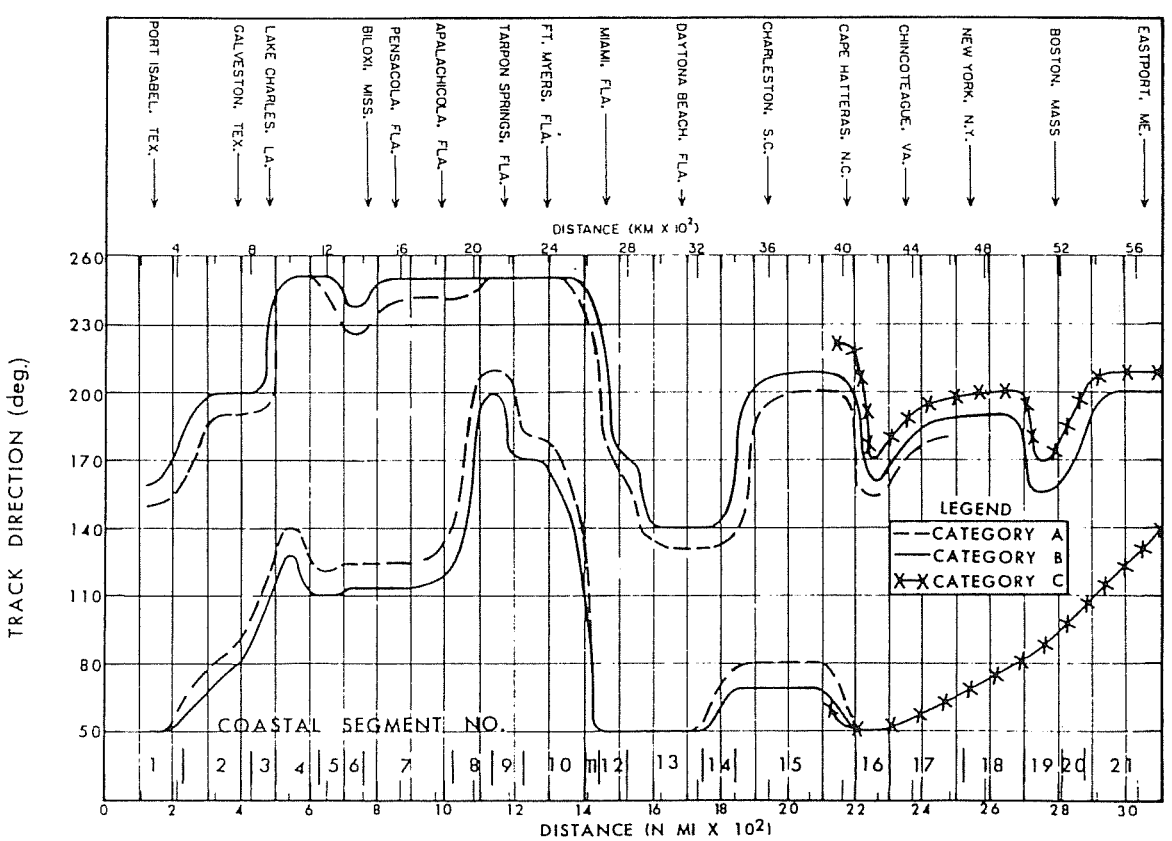

FIGURE C-7
Maximum allowable range of SPH θ.
(item 57 of Appendix A)

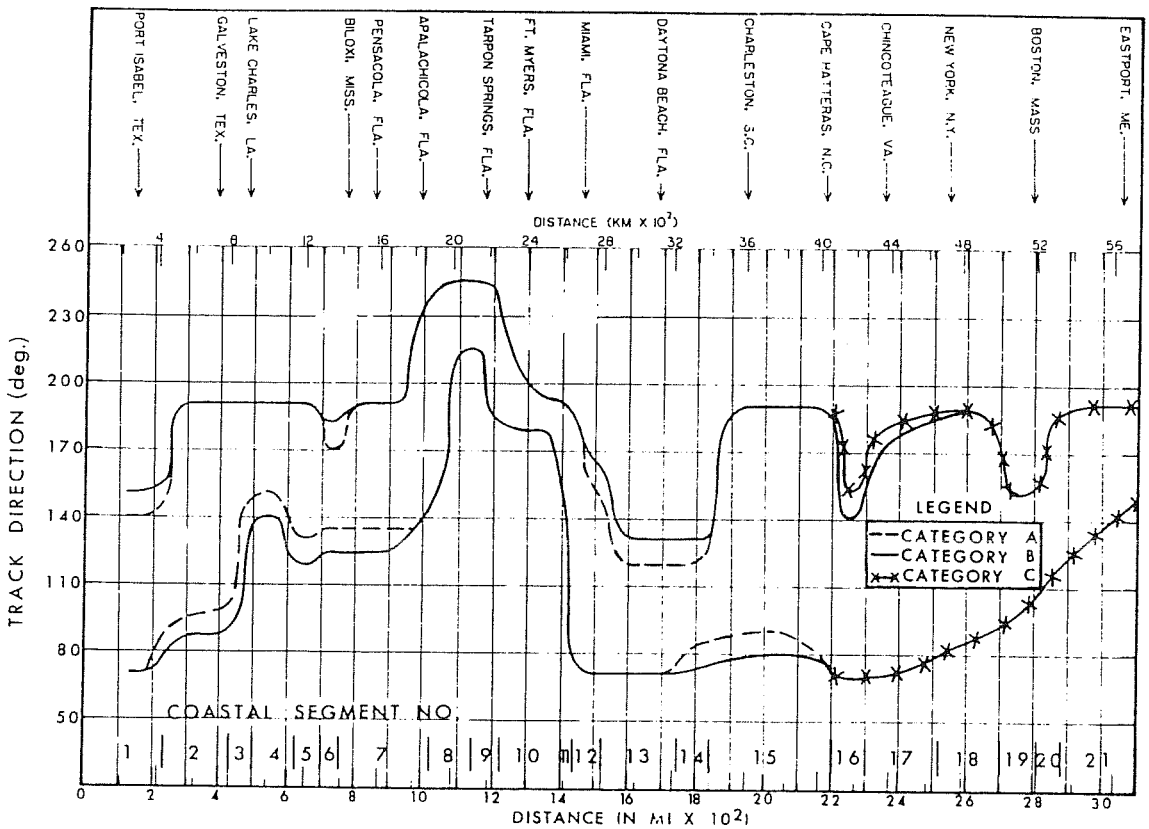

FIGURE C-8
Maximum allowable range of PMH θ.
(item 57 of Appendix A)

TABLE C-1
Speed Categories Used in Determining the Relation Between V_f and θ.

Speed Category		Forward Speed
SPH	A	6kt ≤ V_f ≤ 10 kt
	B	10 kt ≤ V_f ≤ 36 kt
	C	V_f ≤ 36 kt
PMH	A	4 kt ≤ V_f ≤ 10 kt
	B	10 kt F V_f ≤ 36 kt
	C	V_f > 36 kt

in which p is the sea-level pressure at the radial distance r from the hurricane center. This expression is used to develop the maximum gradient wind speed as given in the subsequent section. In addition, this expression is used to develop a relation for evaluating the pressure setup which is covered in Appendix D.

C-4. Wind Field Specification. This section is concerned with estimating the winds 10m (32.8 ft.) above the water surface and the modification of wind when the rotating wind crosses overland areas.

a. Overwater Maximum Gradient Winds. The maximum gradient winds (V_{gx}) are the peak hurricane winds blowing parallel to the isobars under conditions of circular motion. An expression for this wind (see Chapter 12, NWS 23 (item 57 of Appendix A) for derivation) is

$$V_{gx} = K\,(p_n - p_o)^{1/2} - \frac{Rf}{2} \qquad [C\text{-}2]$$

in which f is the Coriolis parameter and K is a coefficient that is inversely proportional to the square root of the air density just above the water surface. Because air density is influenced by sea-surface temperatures K is dependent on the earth's latitude. Figures C-9 and C-10 show the relation between the coefficient K and latitude for three units of measurement for the SPH and PMH, respectively.

b. Overwater Maximum Winds in a Stationary Hurricane. The maximum 10-m, 10-minute averaged winds for a hurricane at rest (V_{xs}) have been found from observations to be a fixed fraction of the maximum gradient winds V_{gx}. The adopted empirical relations for defining the maximum wind is

$$V_{xs} = 0.9\ V_{gx}\ ,\ \text{for SPH} \qquad [C\text{-}3]$$

and

$$V_{xs} = 0.95\ V_{gx}\ ,\ \text{for PMH}\ . \qquad [C\text{-}4]$$

c. Overwater Maximum Winds in a Moving Hurricane.

(1) An asymmetry factor must be added to the maximum winds in a stationary hurricane to account for a moving hurricane. For a moving hurricane, the maximum wind V_x, for the SPH is:

$$V_{xm} = 0.9\ V_{gx} + 1.5\ (V_f^{0.63})\ (V_{fo}^{0.37})\ \cos\beta \qquad [C\text{-}5]$$

and for the PMH

$$V_{xm} = 0.95\ V_{gx} + 1.5\ (V_f^{0.63})\ (V_{fo}^{0.37})\ \cos\beta \qquad [C\text{-}6]$$

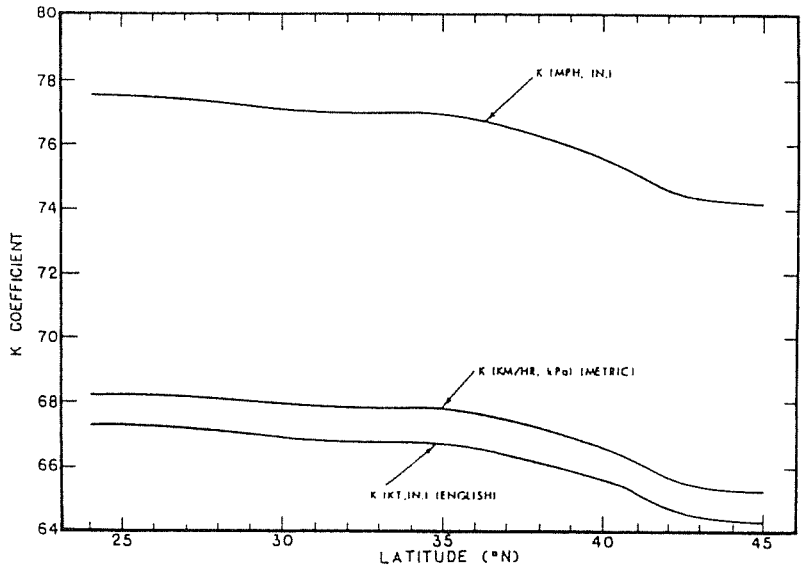

FIGURE C-9
Values of the latitude - dependent K coefficient for three units of measurement for the SPH. (item 57 of Appendix A)

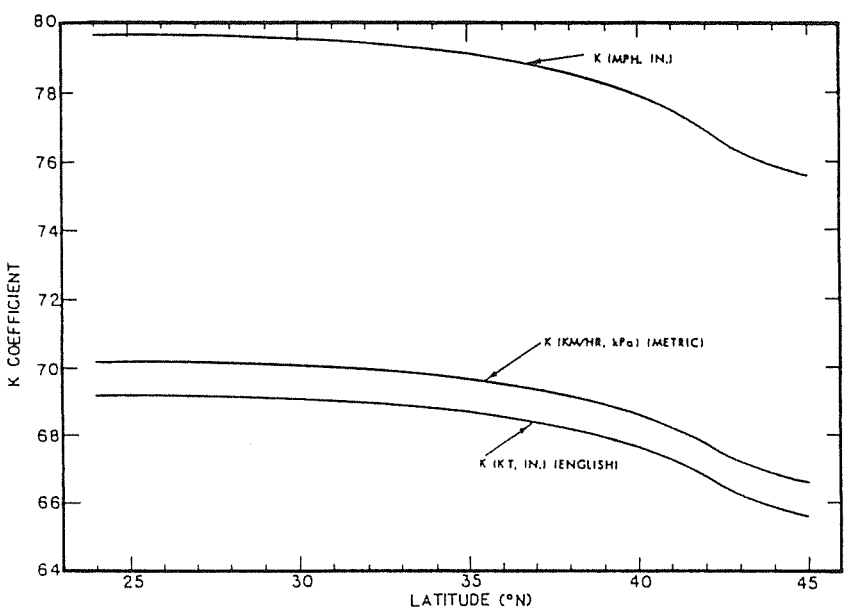

FIGURE C-10
Values of the latitude - dependent K coefficient for three units of measurement for the PMH. (item 57 of Appendix A)

in which V_{fo} = 1 when units are in knots, 0.514791 when units are meters per second, 1.853248 when units in kilometers per hour, and 1.51556 when units are in miles per hour. The angle β is the angle between the hurricane track and the maximum surface wind vector. At a particular position in the right rear quadrant of a hurricane the maximum wind can blow in a direction parallel to the track direction, and in this case β=0 and cos β=1. However, the region of maximum winds are allowed to occur at any position between 0 degrees and 180 degrees clockwise from the track direction. The latter limits of rotation of the wind fields were adopted based on observations from past hurricanes.

(2) In previous discussions, the wind relations given provide estimates of the maximum winds. A general expression for estimating the wind speed V_r at any radial distance r from the hurricane center is

$$V_r = V_s + 1.5\,(V_f^{0.63})\,(V_{fo}^{0.37})\cos\beta \qquad [C\text{-}7]$$

in which V_s is the wind speed in stationary hurricane at radius r. Figure C-11 shows the relative wind speed ratio V_s/V_{xs} versus the distance r outward from R for various radii R. Figure C-12, on the other hand shows the speed within the radius of maximum winds.

d. Wind Inflow Angle. As indicated in Chapter 1, winds blow spirally inward toward the hurricane center. The angle between a tangent line on an isovel circle and the associated wind vector is defined as the wind inflow angle α. The inflow

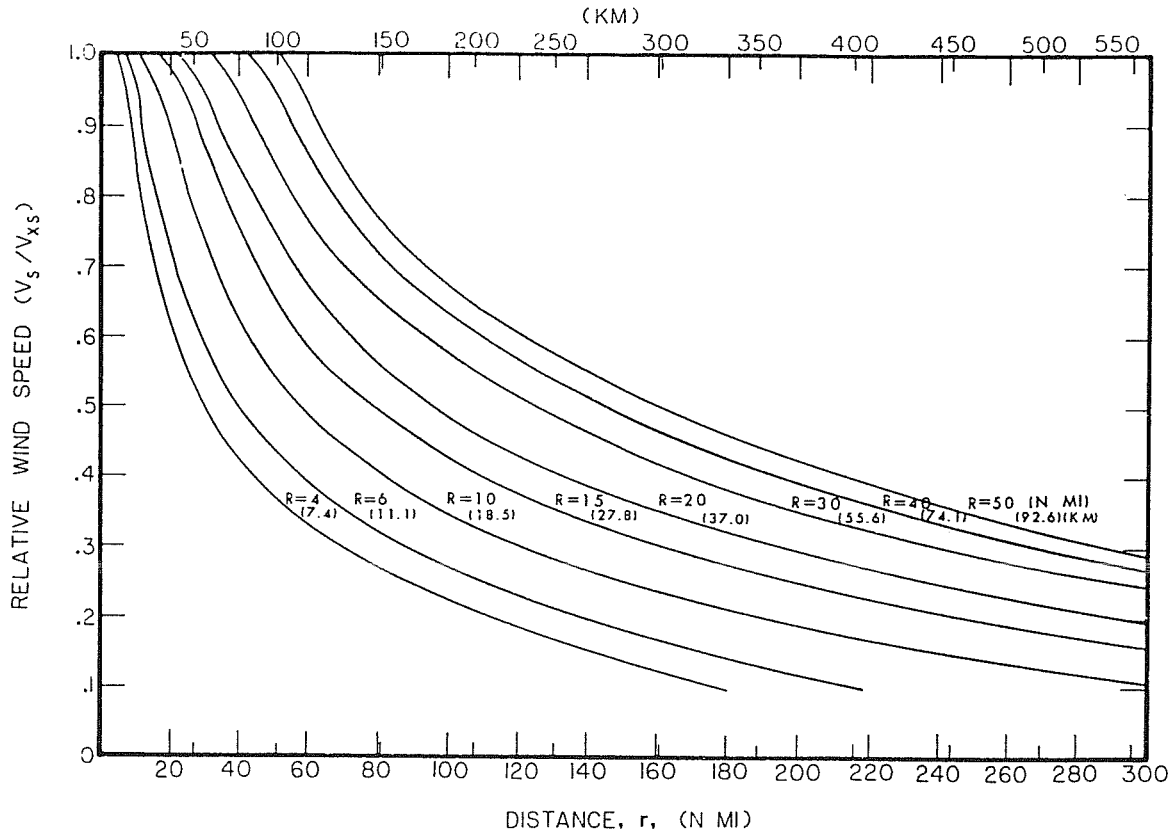

FIGURE C-11
Standardized wind profiles outward from R for the stationary SPH and PMH.
(Item 57 of Appendix A)

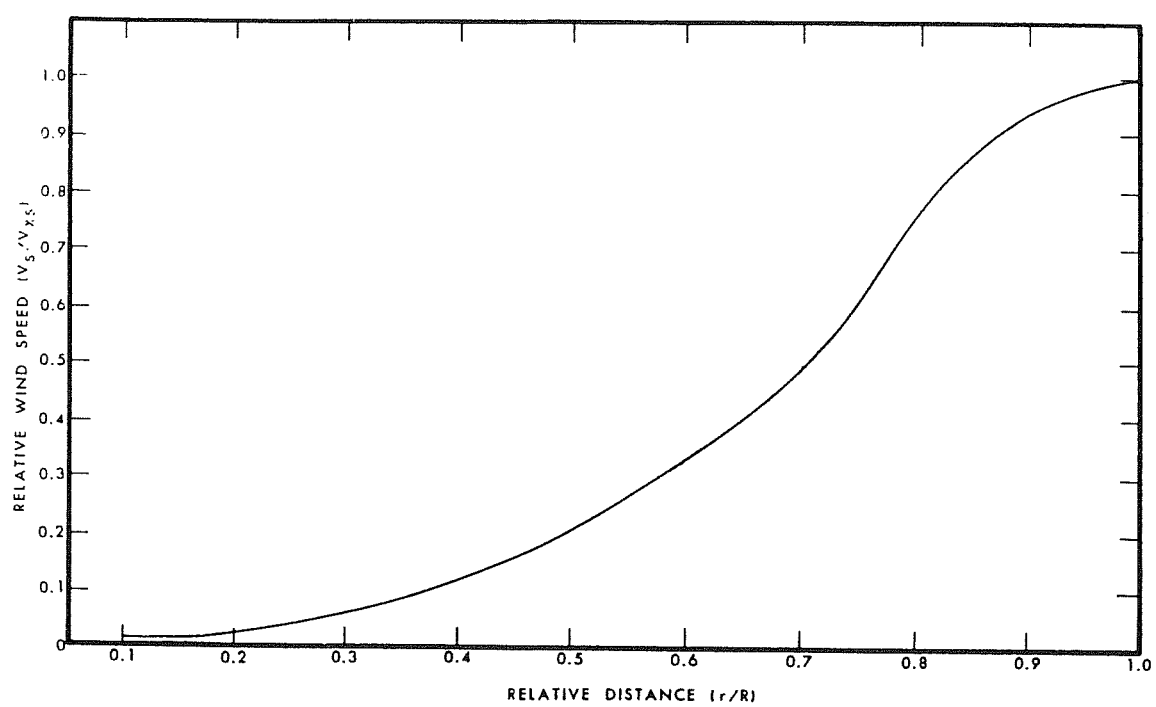

FIGURE C-12
Variation of relative wind speed with relative distance within the radius of maximum winds for the stationary SPH and PMH.

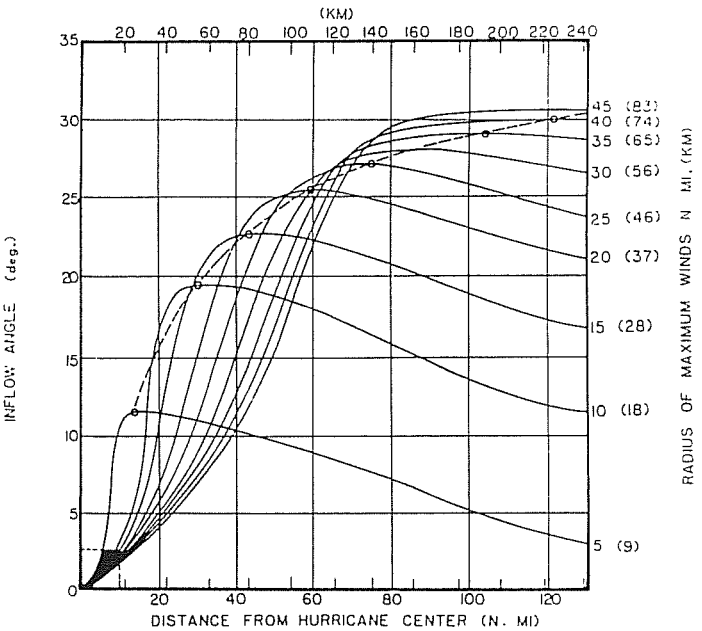

FIGURE C-13
Adopted SPH inflow angles versus distance from the hurricane center at selected R values. Open circles denote maximum inflow angle at each R. (item 57 of Appendix A)

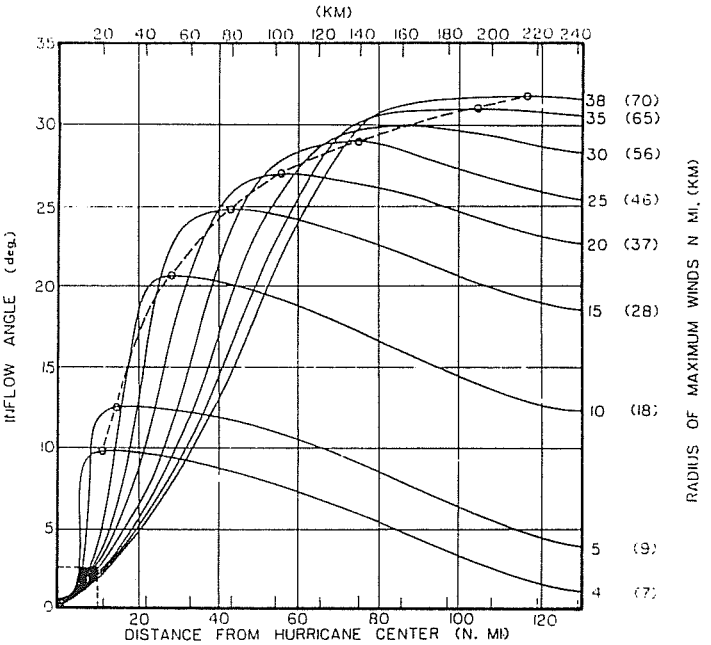

FIGURE C-14
Same as Figure C-13 except for the PMH. (item 57 of Appendix A)

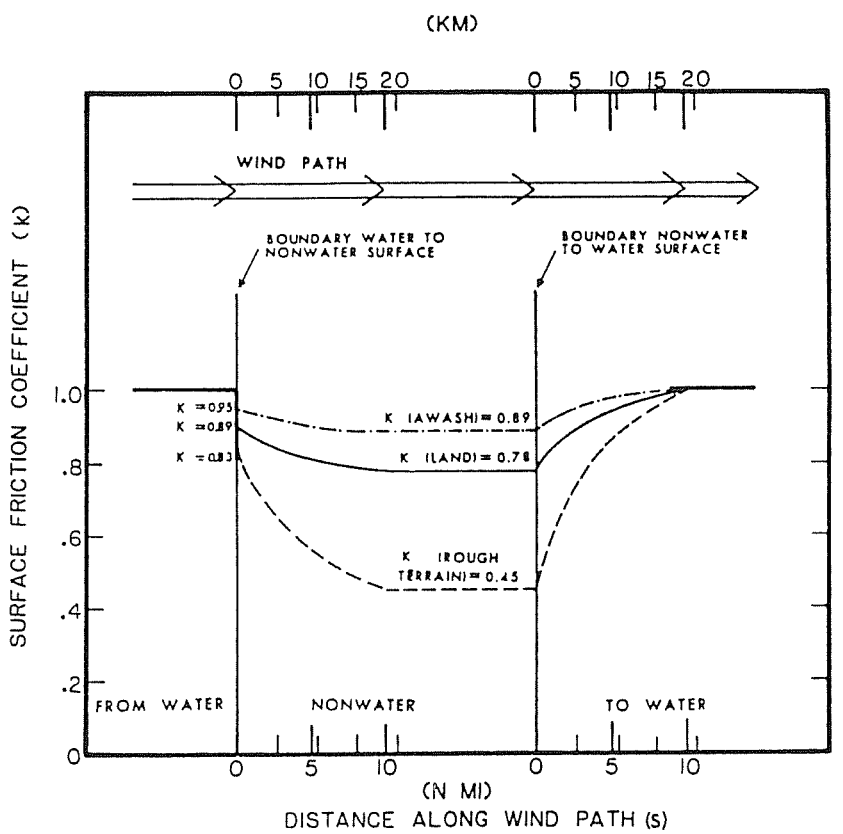

FIGURE C-15
Schematic of near shore frictional adjustments. (item 57 of Appendix A)

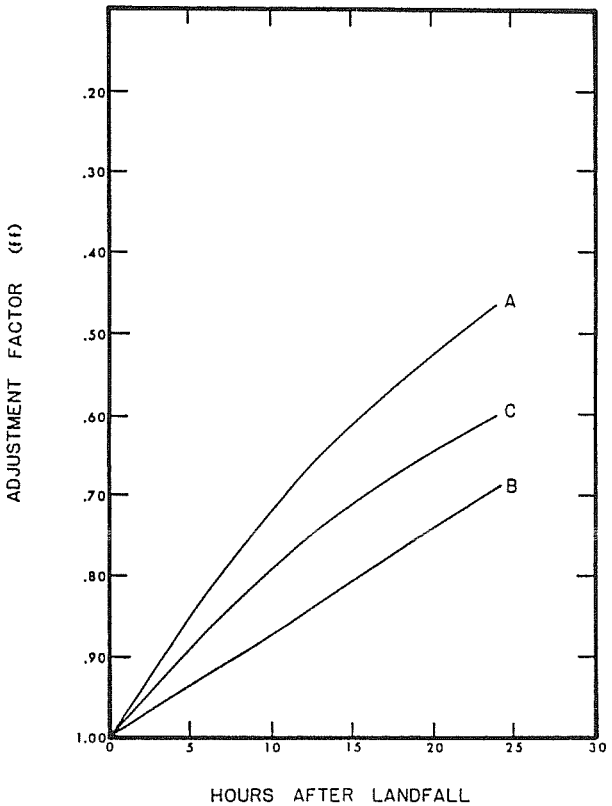

FIGURE C-16
Smoothed adjustment factor curves for reducing hurricane wind speeds when center is overland for three geographic regions defined in Figure C-17. (item 57 of Appendix A)

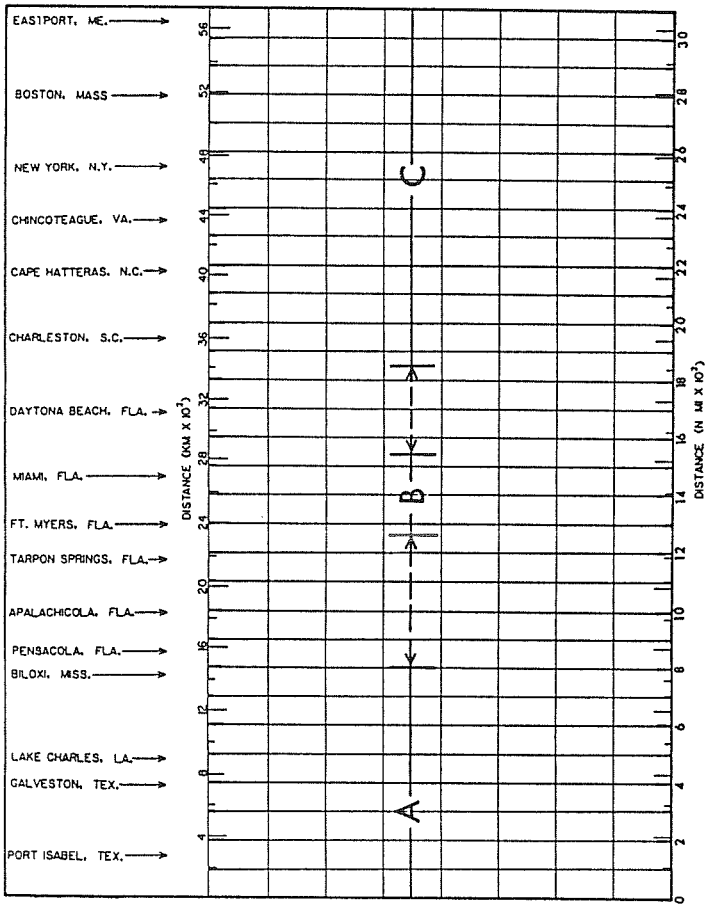

FIGURE C-17
Limits of three geographic regions (A, B, and C). Dashed lines delineate where linear interpolation should be used to develop intermediate curves in Figure C-16. (item 57 of Appendix A)

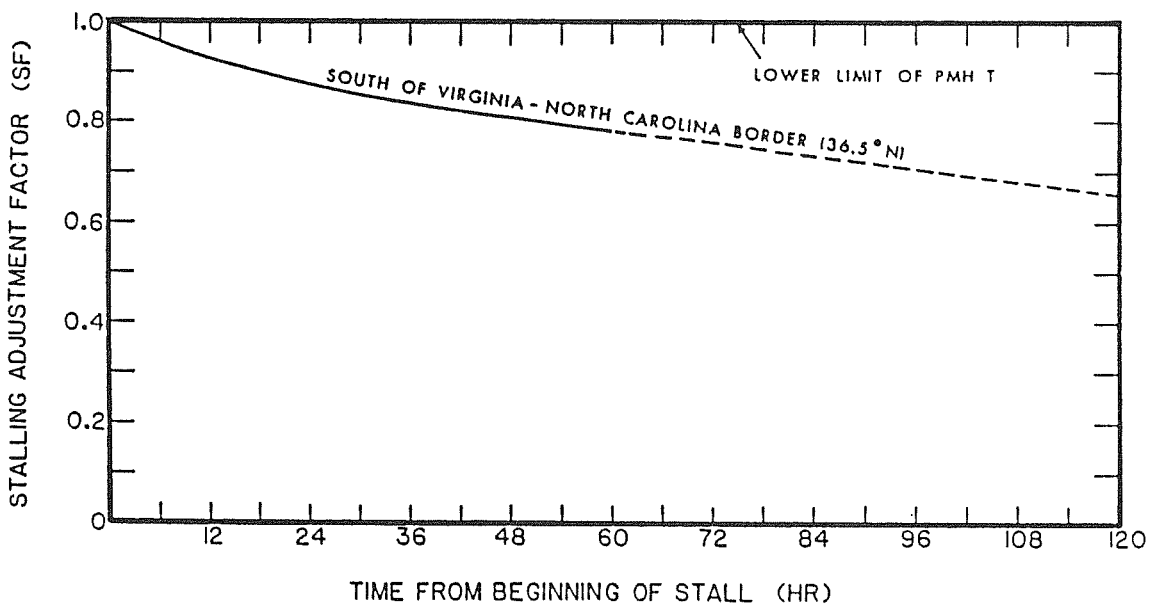

FIGURE C-18
Stalling adjustment factor curve for the PMH to be used south of the Virginia - North Carolina border (36.5° N). (item 57 of Appendix A)

angle in degrees versus the distance from the hurricane center is shown in Figures [C-13] and [C-14] for the SPH and PMH, respectively, for various radii R.

e. Wind Modification Due to Frictional Effects. When revolving hurricane winds begin to sweep over inundated coastal terrain the winds lose speed due to increased surface friction. At the coast there is an abrupt decrease in wind speed and as the wind continues to blow overland the wind speed is further reduced until finally an approximate state of equilibrium is reached where no further reduction occurs. After the wind circles back over the ocean, or encounters a water body such as an embayment, the wind speed begins to increase and if the wind travels over the water surface for a sufficient distance it is essentially restored to its full strength. In general, the reduction of wind speed in inundated lowlying land areas due to frictional effects can be determined from

$$V_k = k\, V_r \qquad [C\text{-}8]$$

where V_k is the wind speed adjusted for frictional resistance and k is the surface friction coefficient. Figure C-15 shows the variation of k with distance along the wind path for four different roughness categories which are designated as over water, awash, and rough terrain. According to technical Report NWS 23, awash is defined as normally dry ground with tree or shrub growth, hill dunes, which are noninundated; land--relatively flat noninundated terrain or buildings; rough terrain--major urban areas, dense forest, and mountains with abrupt changes in elevation over short distance. It is to be noted from Figure C-15 that the surface friction coefficient k varies only over a distance of 10 nautical miles when wind blows from water to nonwater areas or from nonwater areas to water areas.

g. Adjustment of Wind Speed for Filling Overland. When the hurricane center or eye crosses the coast and moves into inundated land areas the winds speed decrease due to filling. This weakening of the hurricane may be approximated by reducing the overwater SPH and PMH wind speed values by an adjustment factor. This factor has been derived for three separate geographic regions A, B, and C. The adjustment factor for these regions are shown in Figure C-16 and the geographic regions are shown in Figure C-17.

f. The Stalled PMH. A slow moving PMH is defined as being stalled when the forward speed $V_f < 5$ knots (9km/hr). Wind speeds decrease with time after stall provided that the forward speed is maintained in the stalled range. The percentage decrease in the winds for a PMH with time after stall is shown in Figure C-18. The curve provided in this figure is applicable along the gulf and east coasts south of Virginia-North Carolina border (milepost 2260).

APPENDIX D
ATMOSPHERIC PRESSURE SETUP

In Chapter 1, it was noted that atmospheric pressure variations over the sea cause the water level to rise in areas of low pressure and fall in areas of high pressure. This appendix is concerned with estimating the amount of rise attributed to the decrease in atmospheric pressure associated with hurricanes. A rise in water due to the pressure effect is commonly referred to as "pressure setup". The response of the water to pressure is like that of an inverted barometer and thus also frequently is referred to as the "inverted barometer effect". An expression for the atmospheric pressure in a hurricane was given in Appendix C (see Equation [C-1]) as

$$p = p_o + (p_n - p_o)\, e^{-R/r} \qquad [D\text{-}1]$$

in which p is the pressure at a radial distance r from the hurricane center; p_o is the central pressure; p_n is the peripheral pressure; and R is the radius of maximum winds. Equation [D-1] may be readily written in terms of the rise in water level at any distance r from the hurricane center, or specifically

$$\xi = 1.14\, (p_n - p_o)\, (1 - e^{-R/r}) \qquad [D\text{-}2]$$

in which ξ is, as before (Chapter 1), an equivalent head of water in feet when the pressures p_n and p_o have units of mercury. A certain lapse of time is required for the water to respond to a change in sea-level pressure, thus pressure setup is a time dependent process which requires that water in higher pressure areas be transported to the lower pressure area. As a consequence, Equation [D-2] is considered more valid for slow moving hurricanes and in regions where the water depth is relatively deep. In shallow coastal areas the equilibrium pressure setup, as predicted by the expression given, would be seldom reached due to the effects of bottom friction. Generally, the pressure setup effect can be neglected in shallow bays and estuaries. The gradient pressure setup which appears in the equations of motion as given in Chapter 1 can be expressed from Equation [C-2] as:

$$\frac{\partial \xi}{\partial x} = 1.14\, (p_n - p_o)\, \frac{R}{r^2}\, e^{-R/r} \cos\beta \qquad [D\text{-}3]$$

$$\frac{\partial \xi}{\partial y} = 1.14\, (p_n - p_o)\, \frac{R}{r^2}\, e^{-R/r} \sin\beta \qquad [D\text{-}4]$$

in which β is the angle between the x-axis and the radial line from the storm center to the point in which the pressure setup is to be evaluated.

APPENDIX E
HURRICANE GENERATED SURFACE WAVES

E-1. General. In the prediction of short period surface waves generated by hurricane winds, the determination of the wave fetch and duration from a wind field is more difficult than for more normal weather conditions. Difficulties arise because hurricane winds blow spirally inward toward the center as the storm system moves over the ocean. Fetch areas in which the wind speed and direction remain approximately constant are always small and a fully arisen sea would seldom be realized. A mathematical model developed for estimating wave characteristics in a hurricane is described in the Shore Protection Manual (1977). This model provides a reasonable approach for predicting hurricane waves provided that the model is modified to account for the more recent SPH wind field criteria that were presented in Appendix C. The original model together with the necessary modifications are described herein and an example problem is given to illustrate the computational procedures for predicting hurricane waves.

E-2. Prediction Method. For a moving hurricane, the following expressions can be used to obtain an estimate of the deep water significant wave height and period at the point of maximum wind:

$$H_o = 16.5 \exp\left(\frac{R\,\Delta p}{100}\right)\left(1 + \frac{0.208\,\kappa\, V_f}{V_{xm}^{1/2}}\right) \qquad [E\text{-}1]$$

$$T_o = 8.6 \exp\left(\frac{T\,\Delta p}{200}\right)\left(1 + \frac{0.104\,\kappa\, V_f}{V_{xm}^{1/2}}\right) \qquad [E\text{-}2]$$

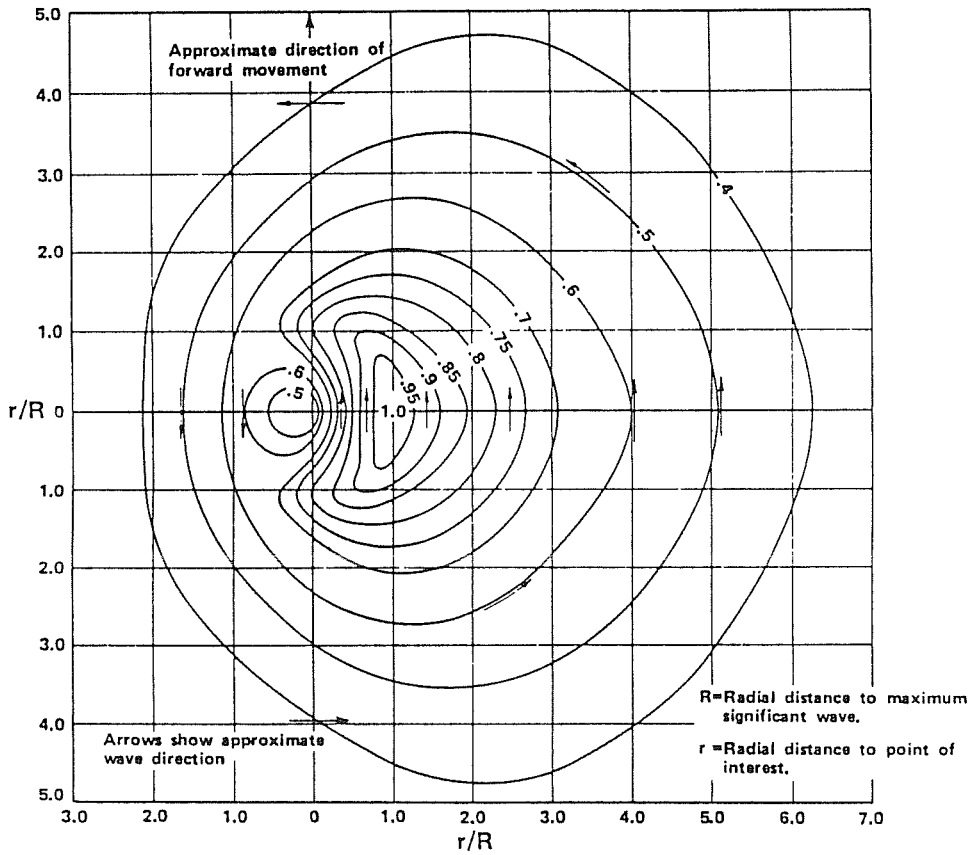

FIGURE E-1
Isolines of relative significant wave height for slow-moving hurricane.

where

$\exp(x)$ = e^x, in which e = 2.71828 ...

H_o = deep water significant wave height in feet

T_o = the corresponding significant wave period in seconds

R = radius of maximum winds in nautical miles

Δp = $p_n - p_o$ in inches of mercury in which p_n is the peripheral pressure and p_o is the central pressure

V_f = forward speed of hurricane in knots

V_{xm} = maximum sustained wind speed in knots at radius R.

$$V_{xm} = 0.9\ V_{gx} + 1.5\ V_f^{0.63} \cos \beta \qquad [E-3]$$

and for the PMH

$$V_{xm} = 0.95\ V_{gx} + 1.5\ V_f^{0.63} \cos \beta \qquad [E-4]$$

β = angle between the hurricane track direction and the maximum surface wind direction

V_{gx} = maximum gradient wind speed, see Equation [C-2]

$$V_{gx} = K\ (\Delta p)^{1/2} - \frac{Rf}{2} \qquad [E-5]$$

K = a coefficient that depends on the air density just above the sea surface and can be obtained from either Figure C-9 or C-10 for the SPH and PMH, respectively

f = Coriolis parameter = 2 ω sin ϕ in which ϕ is the

ω = $2\pi/24$ radians per hour

κ = a coefficient depending on the forward speed of the hurricane and the increase in effective fetch due to the hurricane translation. For a slow moving hurricane it is suggested that $\kappa = 1.0$.

a. After determination of H_o for the point of maximum wind it is possible to obtain the approximate deepwater wave height H_o for other points within the hurricane by use of Figure E-1. A sufficient approximation of the deepwater significant wave period can be obtained from

$$T_o = 2.13\ H_o^{1/2} \qquad [E-6]$$

in which H_o is in feet. The latter expression is derived from empirical data which show that the wave steepness H/T^2 will be about 0.22.

EXAMPLE PROBLEM

Given: Consider a SPH at latitude 37 degrees N situated over the ocean (mile post about 2300 n mi.) with R = 34 nautical miles and V_f = 26 knots.

Find: The deepwater significant wave height and period.

Solution: The Coriolis parameter is given by

$$f = 2\ \omega \sin \phi = 2\left(\frac{2\pi}{24}\right) \sin 37 = 0.315\ .$$

For a SPH, P_n = 29.77 inches.

At the mile post given the central pressure p_o, according to Figure C-1, is approximately 27.65 inches. Therefore,

$$\Delta p = 29.77 - 27.65 = 2.12 \text{ inches.}$$

TABLE E-1
Computation Of Wind Waves Over Continental Shelf

1	2	3	4	5	6	7	8	9	10	11	12	13	14	15	16
X	d_1	d_2	$\bar{d}_t$	F_e	H_o	T_o	$\frac{\bar{d}_t}{L_o}$	$\frac{f_f H_o \Delta X}{(d_t)^2}$	K_f	H_o'	F_e'	T_o'	$\frac{d_2}{L_o'}$	K_s	H
65	1004	504	754	107.4	54.0	15.7	0.597	0.029	1.000	54.0	107.4	15.7	0.399	0.9758	52.7
60	504	194	349	107.4	54.0	15.7	0.277	0.135	0.985	53.2	104.2	15.5	0.158	0.9130	48.6
55	194	158	176	107.4	54.0	15.7	0.139	0.530	0.930	50.2	92.9	15.1	0.135	0.9156	46.0
50	158	122	140	97.9	51.6	15.3	0.117	0.800	0.900	46.4	79.2	14.5	0.113	0.9239	42.9
45	122	116	119	84.2	47.8	14.7	0.108	1.026	0.850	40.6	60.8	13.6	0.123	0.9192	37.3
40	116	116	116	65.8	42.3	13.9	0.118	0.956	0.890	37.6	52.1	13.1	0.133	0.9161	34.4
35	116	110	113	57.1	39.4	13.4	0.123	0.938	0.880	34.7	44.3	12.5	0.136	0.9154	31.8
30	110	88	99	49.3	36.6	12.9	0.116	1.135	0.870	31.8	37.3	12.0	0.119	0.9209	29.3
25	88	78	83	42.3	33.9	12.4	0.105	1.496	0.830	28.1	29.1	11.3	0.119	0.9209	25.9
20	78	68	73	34.0	30.4	11.7	0.103	1.734	0.810	24.6	22.3	10.6	0.120	0.9204	22.6
15	68	62	65	27.3	27.2	11.0	0.106	1.957	0.790	21.5	17.0	9.9	0.124	0.9189	19.8
10	62	52	57	22.0	24.4	10.5	0.101	2.283	0.750	18.3	12.3	9.1	0.123	0.9192	16.8
5	52	44	48	17.3	21.7	9.9	0.095	2.863	0.720	15.6	9.0	8.4	0.121	0.9200	14.4
0	44	36	40	14.0	19.4	9.4	0.088	3.686	0.650	12.6	5.9	7.6	0.122	0.9196	11.6

The coefficient K found from Figure c-9 is about 66.6 knots-inches. Using Equation E-5

$$V_{gx} = K\,\Delta p^{1/2} - \frac{rf}{2} = 66.5\,(2.12)^{1/2} - \frac{35(0.315)}{2} = 91.3 \text{ knots.}$$

Using Equation [E-3] and assuming that the maximum wind is blowing in a direction parallel to the hurricane path ($\beta = 0$), then

$$V_{xm} = 0.9\,(91.3) + 1.5\,(26)^{0.63}\,(1)$$
$$= 93.9 \text{ knots.}$$

Assume for simplicity that $\kappa = 1$. Using Equation [E-1]

$$H_o = 16.5 \exp\left(\frac{R\,\Delta p}{100}\right)\left(1 + \frac{0.208\,\kappa\,V_f}{V_{xm}^{1/2}}\right)$$

$$H_o = 16.5 \exp\left[\frac{35(2.12)}{100}\right]\left[1 + \frac{0.208\,(1)\,(26)}{(93.9)^{1/2}}\right]$$

$$\simeq 54.0 \text{ feet.}$$

Using Equation [E-2]

$$T_o = 8.6 \exp\left(\frac{R\,\Delta p}{200}\right)\left(1 + \frac{0.104\,\kappa\,V_f}{V_{xm}^{1/2}}\right)$$

$$T_o = 8.6 \exp\left[\frac{(35)\,(2.12)}{200}\right]\left[1 + \frac{0.104\,(1)\,(26)}{(93.9)^{1/2}}\right]$$

$$= 15.9 \text{ sec .}$$

Using Equation [E-6]

$$T_o = 2.13\,(H_o)^{1/2} = 2.13\,(54)^{1/2} = 15.7 \text{ sec}$$

which shows that the latter simple relation is of sufficient accuracy and will be used in subsequent calculations. With a knowledge of the deepwater significant wave height and period it is possible to determine the changes in these wave characteristics as the hurricane moves over the continental shelf. In order to make this determination it is necessary to account for the combined effects of bottom friction, refraction, the continued action of the wind and the forward speed of the hurricane. It is necessary to use relatively short wind fetch length due to the revolving winds and thus a numerical integration procedure must be utilized. When waves refract over the bottom contours, it will be also necessary to use appropriate refraction diagrams as presented in the Shore Protection Manual (1984). In the use of the numerical procedure, an effective fetch length F_e is required which is given by

$$F_e = \left(\frac{H_o}{0.0555\,V_{xm}}\right)^2 . \qquad [E-7]$$

for the preceding example problem

$$F_e = \left[\frac{54.0}{(0.555)(93.9)}\right]^2 = 107.4 \text{ n mi.}$$

The deepwater significant wave height H_o can be evaluated by using a modified version of Equation [E-7] as given by

$$H_o = 0.0555\,V_{xm}\,(F'_e + \Delta F)^{1/2} \qquad [E-8]$$

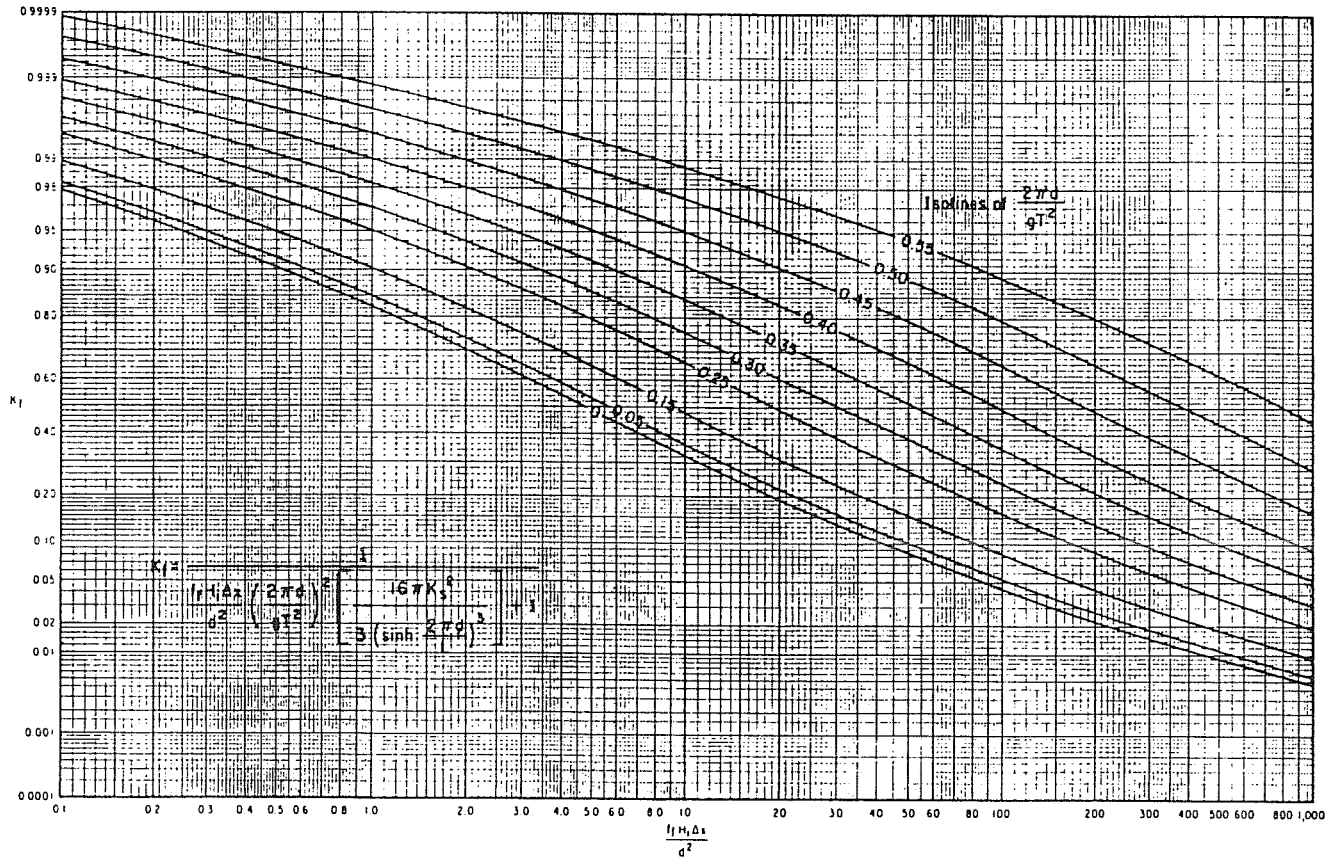

FIGURE E-2
Relationship for friction loss over a bottom of constant depth. (item 5 of Appendix A)

in which F'_e is defined in the procedures outlined below and ΔF is a specified fetch length interval used in the numerical integration technique. The procedure for calculating the surface waves over the continental shelf is illustrated by using a bottom profile seaward of the Chesapeake Bay entrance (profile taken from the 1977 Shore Protection Manual) and the hurricane taken from the previous example. The water depths used are assumed to include the storm surge and astronomical tide over the shelf area. Refraction is neglected in this example. The result of the computations are shown in Table E-1. Explanation of the computations are as follows:

Column 1 of Table E-1 is the distance in nautical miles measured seaward from the entrance to Chesapeake Bay, using increments of 5 n mi. for each section.

Column 2 is the depth d_1 at the beginning of each section.

Column 3 is the depth d_2 at the shoreward end of each section.

Column 4 is $\bar{d}_t$ the average of Columns 2 and 3 to the nearest foot.

Column 5 is the effective fetch F_e in nautical miles, and is determined for the first step directly from Equation [E-7]. For successive steps, $F_e = F'_e + \Delta F \leq 54.9$ n mi. where F'_e is given in Column 12 one line above in each case, and $\Delta F = 5$ n mi.

Column 6 is the deepwater significant wave height H_o and is obtained from Equation [E-1] on the first step and Equation [E-8] for the succeeding steps.

Column 7 is the deepwater significant wave period and is obtained by Equation [E-6].

Column 8 is the average water depth $\bar{d}_t$ divided by the deepwater wave length L_o where

$$\frac{\bar{d}_t}{L_o} = \frac{2\pi\,\bar{d}_t}{gT_o^2} \quad .$$

Column 9 is the parameter in Figure e-2

$$\frac{f_f\,H_i\,\Delta X}{d^2} = \frac{f_f\,H_o\,\Delta X}{(\bar{d}_t)^2}$$

in which friction factor f_f is assumed to be 0.01 $\Delta X = 5$ (6080) = 30,400 feet.

Column 10 is the friction factor K_f which is obtained from Figure E-2 using column 8 and column 9.

Column 11 is the equivalent deepwater wave height H'_o and is obtained from $H'_o = K_f H_o$ (the products of column 6 and 10).

Column 12 is the equivalent effective length F_e and is obtained from Equation [E-7] by replacing H_o by H'_o or

$$F'_e = \left(\frac{H'_o}{0.0555\ V_{xm}}\right)^2 \quad .$$

Column 13 is the equivalent deepwater wave period T_o in seconds and computed by

$$T'_o = 2.13\ (H'_o)^{1/2} \quad .$$

Column 14 is the depth d_2 divided by the equivalent deep water wave length

$$L_o = 5.12\ (T'_o)^2 \quad .$$

Column 15 is the shoaling coefficient K_s which can be obtained from Table C-1, Appendix C of the Shore Protection Manual in which $H/H'_o = K_s$ as a function of d_2/L_o (column 14).

Column 16 is the significant wave height H in which

$$H = K_s H'_o$$

or the products of Columns 11 and 15.

After completing the computations for the first row, the computations are commenced on the second row etc., until the table is completed.

APPENDIX F
APPLICATION OF HISTORICAL FREQUENCY METHOD

The following problem illustrates the computational procedures involved in calculating the magnitude and frequency of occurrence of water levels at the State Pier, Providence, Rhode Island based on the formula and procedures discussed in Chapter 3. The basic and ordered annual peak water level data are given in Table F-1. The last two rows in the basic data, columns 3 and 4, shows historic water elevations of 18 feet for years 1635 and 1638. Historic data for these years are not considered a part of the more recent systematic record. By ignoring the historic record for the present, it is found by summing columns 4, 5, and 6 that:

$$\Sigma x = 269.1; \qquad \Sigma x^2 = 1908.95$$

and

$$\Sigma x^3 = 16{,}352.259 \quad .$$

For the systematic record (N = 43) the mean, standard deviation, and skew coefficient according to Equations [3-6], [3-7b], and [3-8b] are:

$$\mu = \frac{\Sigma x}{N} = \frac{269.1}{43} = 6.2581$$

$$\sigma = \left[\frac{(\Sigma x^2) - \frac{(\Sigma x)^2}{N}}{N-1}\right]^{1/2} = \left[\frac{1908.95 - \frac{(269.1)^2}{43}}{43-1}\right]^{1/2} = 2.3143$$

$$G = \frac{N^2(\Sigma x^3) - 3N(\Sigma x)(\Sigma x^2) + 2(\Sigma x)^3}{N(N-1)(N-2)\sigma^3}$$

$$= \frac{(43)^2(16352.259) - 3(43)(269.1)(1908.95) + 2(269.1)^3}{43(43-1)(43-2)(2.3143)^3} = 3.2053$$

Use Equation [3-13] to test for high outlier.

$$\eta_H = \mu + K_N \sigma$$

From Table 3-1, $K_N = 2.71$ for N = 43, thus

$$\eta_H = 6.2581 + (2.71)(2.3143) = 12.5 \text{ feet} \quad .$$

A review of the systematic record reveals that the peak elevation of 16.0 feet in 1938 and the peak elevation of 14.9 feet in 1954 exceed the threshold value of 12.5 feet. Due to the fact that the systematic record is extended considerably as a result of the historic events, only the 1938 event will be used as a high outlier and the 1954 event will be considered as part of the systematic record. Because of the high outlier the statistics of the systematic record are re-evaluated as follows:

$$\Sigma x = 269.1 - 16 = 253.1$$

$$\Sigma x^2 = 1908.95 - 256 = 1652.95$$

$$\Sigma x^3 = 16{,}352.259 - 4096 = 12256.259 \quad .$$

Thus for N = 42

$$\mu = \frac{\Sigma x}{N} = \frac{253.1}{42} = 6.0262$$

$$\sigma = \left[\frac{(\Sigma x^2) - \frac{(\Sigma x)^2}{N}}{N-1}\right]^{1/2} = \left[\frac{1652.95 - \frac{(253.1)^2}{42}}{42-1}\right]^{1/2} = 1.7650$$

$$G = \frac{N^2(\Sigma x^3) - 3N(\Sigma x)(\Sigma x^2) + 2(\Sigma x)^3}{N(N-1)(N-2)\sigma^3}$$

$$= \frac{(42)^2(12256.259) - 3(42)(253.1)(1652.95) + 2(253.1)^3}{(42)(42-1)(42-2)(1.765)^3}$$

$$= 3.5209 \quad .$$

Adjustment of the statistics is required to account for the historic data including the high outlier. The weight factor W according to Equation [3-14] with a historic period from 1635 through 1975 or 341 years is:

$$W = \frac{H - Z}{N} = \frac{341 - 3}{42} = 8.0476 \quad .$$

The sum of the historic water levels is:

$$\Sigma x' = 18 + 18 + 16 = 52 \quad .$$

By Equation [3-15]

$$\bar{\mu} = \frac{W(\Sigma x) + \Sigma x'}{H} = \frac{(8.0476)(253.1) + 52}{341} = 6.126 \quad .$$

Based on the adjusted mean, $x - \bar{\mu}$ is computed as shown in column 11, $(x - \bar{\mu})^2$ in column 12 and $(x' - \bar{\mu})^3$ in column 13.

The sums are:

$$\Sigma (x - \bar{\mu})^2 = 128.03$$

$$\Sigma (x' - \bar{\mu})^2 = 379\ 48$$

$$\Sigma (x' - \bar{\mu})^3 = 4310.949 \quad .$$

By use of Equation [3-16] it is found that

$$\bar{\sigma} = \left[\frac{W\Sigma(x - \bar{\mu})^2 + \Sigma(x' - \bar{\mu})^2}{H-1}\right]^{1/2}$$

$$= \left[\frac{(8.0476)(128.03) + 379.48}{341-1}\right]^{1/2}$$

$$= 2.0363 \quad .$$

From Equation [3-17]

$$\bar{G} = \frac{H}{(H-1)(H-2)\sigma^3}\left[\frac{W(N-1)(N-2)\sigma^3 G}{N} + 3W(N-1)(\mu - \bar{\mu})\sigma^2 + WN(\mu - \bar{\mu})^3 + \Sigma(x' - \bar{\mu})^3\right]$$

$$\bar{G} = \frac{341}{(340)(339)(2.0363)^3}\left[\frac{(8.0476)(41)(40)(1.765)^3(3.5209)}{42}\right.$$

TABLE F-1
Annual Peak Water Levels, State Pier Providence, R.I.

BASIC DATA							ORDERED DATA				HISTORICAL DATA INFORMATION	
1	2	3	4	5	6	7	8	9	10	11	12	13
MO	DAY	YEAR	x ELEV (FT)	x^2	x^3	RANK	YEAR	x ELEV (FT)	PLOTTING POSITION	$x - \bar{\mu}$	COLUMN 11 SQUARED	COLUMN 11 CUBED
10	11	1931	4.2	17.64	74.088	1	1635	18.0	.0029	11.874	140.992	1555.251
11	30	1932	5.3	28.09	148.877	2	1638	18.0	.0058	11.874	140.992	1555.251
1	27	1933	6.0	36.00	216.000	3	1938	16.0	.0058	9.874	97.496	957.419
1	16	1934	4.5	20.25	91.125	4	1954	14.9	.0220	8.774	76.983	
9	15	1935	4.3	18.49	79.507	5	1944	10.1	.0455	3.974	15.793	
10	1	1936	5.6	31.36	175.616	6	1960	8.0	.0691	1.874	3.512	
10	23	1937	5.0	25.00	125.000	7	1963	7.9	.0926	1.774	3.147	
9	21	1938	16.0	256.00	4096.000	8	1974	7.0	.1161	0.874	0.764	
4	2	1939	5.5	30.25	166.375	9	1950	7.0	.1397	0.874	0.764	
11	27	1940	5.2	27.04	140.608	10	1953	6.7	.1632	0.574	0.329	
5	11	1941	4.9	24.01	117.649	11	1942	6.6	.1867	0.474	0.225	
3	3	1942	6.6	43.56	287.496	12	1970	6.4	.2102	0.274	0.075	
3	6	1943	5.7	32.49	185.193	13	1972	6.3	.2338	0.174	0.030	
9	14	1944	10.1	102.01	1030.301	14	1966	6.3	.2573	0.174	0.030	
11	22	1945	6.3	39.69	250.047	15	1945	6.3	.2808	0.174	0.030	
11	10	1946	5.0	25.00	125.000	16	1951	6.1	.3044	-0.026	0.001	
3	3	1947	5.9	34.81	205.379	17	1933	6.0	.3279	-0.126	0.016	
12	20	1948	5.1	26.01	132.651	18	1973	5.9	.3514	-0.226	0.021	
10	22	1949	5.6	31.36	175.616	19	1947	5.9	.3750	-0.226	0.021	
11	25	1950	7.0	49.00	343.000	20	1962	5.9	.3985	-0.226	0.021	
2	7	1951	6.1	37.21	226.981	21	1943	5.7	.4220	-0.426	0.181	
10	0	1952	4.8	23.04	110.592	22	1958	5.7	.4456	-0.426	0.181	
11	7	1953	6.7	44.89	300.763	23	1971	5.7	.4691	-0.426	0.181	
8	31	1954	14.9	222.01	3307.949	24	1968	5.6	.4926	-0.526	0.277	
10	16	1955	5.6	31.36	175.616	25	1936	5.6	.5162	-0.526	0.277	
3	16	1956	5.0	25.00	125.000	26	1955	5.6	.5397	-0.526	0.277	
2	15	1957	4.8	23.04	110.592	27	1949	5.6	.5632	-0.526	0.277	
4	3	1958	5.7	32.49	185.193	28	1964	5.5	.5867	-0.626	0.392	
12	29	1959	5.2	27.04	140.608	29	1939	5.5	.6103	-0.626	0.392	
9	12	1960	8.0	64.00	512.000	30	1975	5.4	.6338	-0.726	0.527	

TABLE F-1 (Continued)
Annual Peak Water Levels, State Pier
Providence, R.I.

BASIC DATA						ORDERED DATA				HISTORICAL DATA INFORMATION		
1	2	3	4	5	6	7	8	9	10	11	12	13
MO	DAY	YEAR	x ELEV (FT)	x^2	x^3	RANK	YEAR	x ELEV (FT)	PLOTTING POSITION	$x - \bar{\mu}$	COLUMN 11 SQUARED	COLUMN 11 CUBED
1	16	1961	5.3	31.36	148.877	31	1969	5.3	.6573	-0.826	0.682	
12	6	1962	5.9	34.81	205.379	32	1932	5.3	.6809	-0.826	0.682	
11	30	1963	7.9	62.41	493.039	33	1961	5.3	.7044	-0.826	0.682	
11	20	1964	5.5	30.25	166.375	34	1959	5.2	.7279	-0.926	0.857	
12	29	1966	6.3	39.69	250.047	35	1940	5.2	.7515	-0.926	0.857	
11	12	1968	5.6	31.36	175.616	36	1948	5.1	.7750	-1.026	1.053	
12	11	1969	5.3	28.09	148.877	37	1937	5.0	.7985	-1.126	1.268	
3	3	1970	6.4	40.96	262.144	38	1956	5.0	.8221	-1.126	1.268	
3	1	1971	5.7	32.49	185.193	39	1946	5.0	.8456	-1.126	1.268	
11	26	1972	6.3	39.69	250.047	40	1941	4.9	.8691	-1.226	1.503	
4	4	1973	5.9	34.81	205.379	41	1957	4.8	.8926	-1.326	1.758	
12	2	1974	7.0	49.00	343.000	42	1952	4.8	.9162	-1.326	1.758	
4	3	1975	5.4	29.16	157.464	43	1934	4.5	.9397	-1.626	2.643	
8	15	1635	18.0			44	1935	4.3	.9632	-1.826	3.334	
8	3	1638	18.0			45	1931	4.2	.9868	-1.926	3.709	

TABLE F-2
Frequency Curve and Confidence Limits

EXCEEDENCE FREQUENCY CURVE				CONFIDENCE LIMITS								
1	2	3	4	5	6	7	8	9	10	11	12	13
P	K	$K\bar{\sigma}$	η(FT)	K^2	b	ab	$(K^2 - ab)$	$\frac{K_U}{a}\left(K+\frac{Col.8}{a}\right)$	$\frac{K_L}{a}\left(K+\frac{Col.8}{a}\right)$	η(FT) .05 LIMIT	η(FT) .96 LIMIT	η(FT) EXPECTED PROBABILITY
.002	6.64627	13.5337	19.5	44.1729	44.1085	42.6529	1.2329	8.1481	5.5981	22.6	17.5	21.7
.005	5.25291	10.6965	16.8	27.5930	27.5286	26.6202	0.9863	6.4521	4.4122	19.2	15.1	18.2
.010	4.22473	8.6028	14.7	17.8483	17.7839	17.1970	0.8071	5.2035	3.5343	16.7	13.3	15.7
.020	3.22641	6.5699	12.7	10.4097	10.3433	10.0020	0.6385	3.9968	2.6762	14.2	11.6	13.3
.040	2.26862	4.6120	10.7	5.1466	5.0822	4.9145	0.4818	2.8443	1.8480	11.9	9.9	11.1
.100	1.09552	2.2308	8.4	1.2002	1.1358	1.0983	0.3192	1.4630	0.8028	9.6	7.8	8.5
.200	0.32171	0.6551	6.8	0.1035	0.0391	0.0378	0.2563	0.5977	0.0676	7.4	6.3	6.8
.500	-0.41253	-0.8400	5.3	0.1702	0.1058	0.1023	0.2606	-0.1571	-0.6961	5.8	4.7	5.3
.800	-0.56242	-1.1453	5.0	0.3163	0.2519	0.2436	0.2696	-0.3028	-0.8604	5.5	4.4	5.0
.900	-0.57035	-1.1614	5.0	0.3253	0.2620	0.2534	0.2681	-0.3126	-0.8671	5.5	4.4	5.0
.950	-0.57130	-1.1633	5.0	0.3264	0.2620	0.2534	0.2702	-0.3114	-0.8702	5.5	4.4	5.0
.990	-0.57143	-1.1636	5.0	0.3265	0.2621	0.2535	0.2702	-0.3115	-0.8704	5.5	4.4	5.0

NOTE: $\bar{G} = 3.5$

$\bar{\sigma} = 2.0363$

$\bar{\mu} = 6.126$

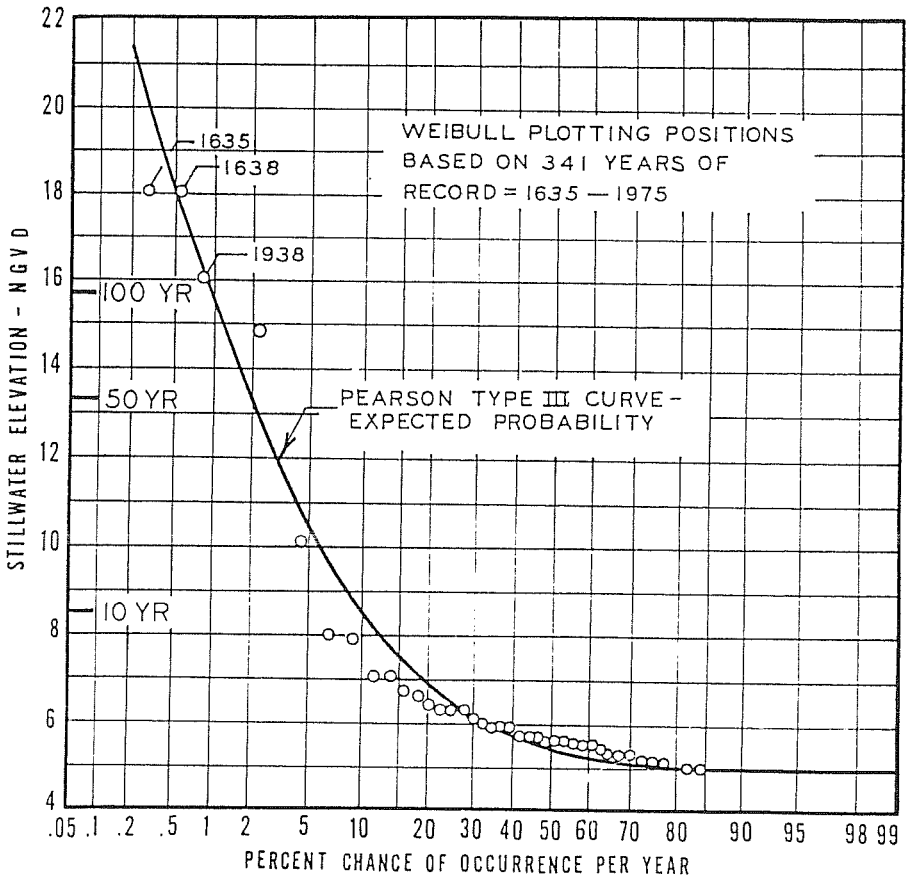

FIGURE F-1
Frequency of water levels at the State Pier, Providence, R.I.

$$+ 3(8.0476)(41)(6.0262 - 6.126)(1.765)^2$$

$$+ (8.0476)(42)(6.0262 - 6.126)^3 + 4310.949\Big] .$$

$$\bar{G} = 3.5341, \text{ say } 3.5 .$$

Table F-2 shows summaries of the exceedence frequency curve. The first column is a tabulation of the prescribed exceedence probabilities and column 2 shows the corresponding frequency factors for $\bar{G} = 3.5$. (The K values can be found in Bulletin No. 17b.) Column 3 shows the frequency factor times the standard deviation and column 4 is the solution of Equation [3-18], or

$$\eta = \bar{\mu} + \bar{\sigma}K .$$

The upper and lower confidence limits for levels of significance of .05 and .95 are computed as follows:

The standard normal deviate t at confidence level 0.05 is 1.64485 as found in Bulletin No. 17b for zero skew. From Equations [3-26] and [3-27] it is found that

$$a = 1 - \frac{t^2}{2(N-1)} = 1 - \frac{(1.64485)^2}{2\,(42-1)} = 0.967$$

$$b = K^2 - \frac{t^2}{N} = K^2 - \frac{(1.64485)^2}{42} = K^2 - .0644174172 .$$

The values of K^2 are shown in column 5 in Table F-2 and the values of b are shown in column 6. The solutions of Equation [3-24] and [3-25] are shown in columns 9 and 10. The upper and lower confidence limits for the water levels according to Equations [3-22] and [3-23] are shown in columns 11 and 12, respectively. The water level elevations corresponding to the expected probabilities are shown in column 13. These are determined by using Equation [3-28] through [3-28f], interpolation of the intermediate expected probabilities and plotting the resulting frequency curve. Figure F-1 shows the expected probability curve derived together with the observed peak water levels.